

METRIC

MIL-HDBK-1211(MI)
17 July 1995

MILITARY HANDBOOK

MISSILE FLIGHT SIMULATION

PART ONE

SURFACE-TO-AIR MISSILES



This handbook is for guidance only. Do not
cite this document as a requirement.

AMSC N/A

FSC 14GP

DISTRIBUTION STATEMENT A. Approved for public release; distribution is unlimited,

FOREWORD

1 This military handbook is approved for use by all activities and agencies of the Department of the Army and is available for use by all Departments and Agencies of the Department of Defense.

2. This handbook is for guidance only. This handbook cannot be cited as a requirement. If it is, the contractor does not have to comply.

3. Surface-to-air missiles are designed to defend a land area against an aerial threat. The size of the defended area and the capabilities of the threat have great influence on the speed, maneuverability, and lethality requirements of the missile system. Simulation of the missile flight path can provide valuable information about these requirements. A missile flight simulation is a computational tool that calculates the flight of a missile from launch until it engages the target. The simulation is based on mathematical models of the missile, target and environment. This military handbook provides guidance for the preparation of these mathematical models to simulate the flight of a surface-to-air missile.

4. Beneficial comments (recommendations, additions, and deletions) and any pertinent data that may be of use in improving this document should be addressed to Commander, U.S. Army Missile Command, ATTN: AMSMI-RD-SE-TD-ST, Redstone Arsenal, AL 35898-5270, by using the Standardization Document Improvement Proposal (DD Form 1426) appearing at the end of this document, or by letter.

CONTENTS

FOREWORD	ii
LIST OF ILLUSTRATIONS	xii
LIST OF TABLES	xiii
LIST OF ABBREVIATIONS AND ACRONYMS	xiv

CHAPTER 1
INTRODUCTION

1-1 BACKGROUND	1-1
1-1.1 DESCRIPTION OF A MISSILE FLIGHT SIMULATION	1-1
1-1.2 PURPOSE OF A MISSILE FLIGHT SIMULATION	1-2
1-1.3 IMPLEMENTATION OF A MISSILE FLIGHT SIMULATION	1-2
1-2 PURPOSE OF THE HANDBOOK	1-3
1-3 SCOPE OF THE HANDBOOK	1-4
1-4 ORGANIZATION OF THE HANDBOOK	1-4
REFERENCES	1-4
BIBLIOGRAPHY	1-4

CHAPTER 2
MISSILE SYSTEM DESCRIPTION

2-0 LIST OF SYMBOLS	2-1
2-1 INTRODUCTION	2-1
2-2 MISSILE	2-2
2-2.1 SEEKER	2-3
2-2.1.1 Optical Seekers	2-3
2-2.1.1.1 Reticle	2-5
2-2.1.1.2 Pseudoimaging	2-8
2-2.1.1.3 Imaging	2-8
2-2.1.2 Radio Frequency Seekers	2-8
2-2.1.2.1 Pulse Radar	2-10
2-2.1.2.2 Continuous Wave Radar	2-10
2-2.1.2.3 Pulse Doppler Radar	2-10
2-2.1.3 Angle Tracking Methods	2-10
2-2.1.3.1 Sequential Lobing	2-12
2-2.1.3.2 Conical scanning	2-12
2-2.1.3.3 Monopulse Tracking	2-12
2-2.2 AUTOPILOT	2-12
2-2.3 CONTROL	2-12
2-2.3.1 Lateral Acceleration	2-13
2-2.3.2 Canard Control	2-14
2-2.3.3 Tail Control	2-15
2-2.3.4 Wing Control	2-15
2-2.3.5 Control Servomotor	2-15
2-2.4 WARHEAD AND FUZE	2-15
2-2.4.1 Warhead	2-15
2-2.4.1.1 Shaped Charge	2-18
2-2.4.1.2 Continuous Rod	2-18
2-2.4.1.3 Fragment	2-18
2-2.4.2 Fuze	2-18
2-2.4.3 Lethality	2-19
2-2.5 PROPULSION	2-20
2-2.5.1 Motor	2-20
2-2.5.1.1 Boost Glide	2-21

2-2.5.1.2 Boost Sustain	2-21
2-2.5.1.3 Specific Impulse	2-21
2-2.5.1.4 Temperature Effects	2-22
2-2.5.2 Tube Launch Ejection	2-22
2-2.5.3 Propulsion Design and Operational Implications	2-22
2-2.6 AIRFRAME	2-23
2-2.6.1 Typical Configurations	2-23
2-2.6.2 Static Stability	2-23
2-3 GUIDANCE	2-24
2-3.1 GUIDANCE IMPLEMENTATION	2-25
2-3.1.1 Ground Guidance and Tracking	2-25
2-3.1.1.1 Command	2-25
2-3.1.1.2 Track via Missile	2-25
2-3.1.1.3 Command to Line of Sight	2-27
2-3.1.1.4 Target Illuminators	2-27
2-3.1.2 (Inboard Guidance and Tracking	2-27
2-3.1.2.1 Active	2-27
2-3.1.2.2 Semiactive	2-27
2-3.1.2.3 Passive	2-27
2-3.2 GUIDANCE LAWS	2-27
2-3.2.1 Intercept Point Prediction	2-28
2-3.2.2 Pursuit	2-28
2-3.2.3 Beam Rider	2-28
2-3.2.4 Proportional Navigation	2-28
2-3.2.5 Optimal Guidance	2-30
2-4 LAUNCHER	2-31
2-4.1 SOURCE OF INITIAL CONDITIONS	2-31
2-4.2 LAUNCHER POINTING DIRECTION	2-31
REFERENCES	2-31
BIBLIOGRAPHY	2-31

CHAPTER 3

MISSILE SIMULATION OVERVIEW

3-0 LIST OF SYMBOLS	3-1
3-1 INTRODUCTION	3-1
3-2 MISSILE SIMULATION OBJECTIVES	3-2
3-2.1 MISSILE SIMULATION PERSPECTIVE	3-2
3-2.1.1 Establishing Requirements	3-2
3-2.1.2 Designing and Optimizing Missiles	3-3
3-2.1.3 Assessing Missile Performance	3-3
3-2.1.4 Training	3-4
3-2.2 OBJECTIVES OF SIMULATIONS ADDRESSED IN THIS HANDBOOK	3-4
3-3 ESSENTIALS OF MISSILE SIMULATIONS	3-4
3-3.1 SIMULATING MISSILE GUIDANCE AND CONTROL	3-4
3-3.1.1 Guidance	3-5
3-3.1.2 Autopilot and Control	3-5
3-3.2 SIMULATING MISSILE AND TARGET MOTION	3-5
3-3.2.1 Gravitational Force	3-5
3-3.2.2 Propulsive Force	3-6
3-3.2.3 Aerodynamic Force	3-6
3-3.2.4 Airframe Response	3-7
3-3.3 ROLE OF COORDINATE SYSTEMS	3-8
3-3.4 COMPUTATIONAL CYCLE	3-10
3-4 LEVEL OF SIMULATION DETAIL	3-12
3-4.1 MODELING TO MATCH SIMULATION OBJECTIVES	

3-4.2 MODEL SOPHISTICATION REQUIRED TO SATISFY HANDBOOK OBJECTIVES	3-13
REFERENCES	3-13
BIBLIOGRAPHY	3-14

CHAPTER 4 MISSILE DYNAMICS

4-0 LIST OF SYMBOLS	4-1
4-1 INTRODUCTION	4-3
4-2 NOMENCLATURE AND CONVENTIONS	4-4
4-3 BASIC EQUATIONS	4-6
4-3.1 NEWTON'S SECOND LAW OF MOTION	4-6
4-3.2 ROTATING REFERENCE FRAMES	4-7
4-3.2.1 Time Derivative of a Vector	4-8
4-3.2.2 Acceleration in a Rotating Frame	4-9
4-4 FORCES AND MOMENTS	4-10
4-4.1 AERODYNAMIC FORCES AND MOMENTS	4-10
4-4.2 THRUST FORCE AND MOMENT	4-12
4-4.2.1 Variable Mass	4-12
4-4.2.2 Moment Due to Thrust	4-14
4-4.3 GRAVITATIONAL FORCE	4-14
4-4.3.1 Newtonian Gravitation	4-14
4-4.3.2 Gravity in Rotating Earth Frame	4-14
4-5 EQUATIONS OF MOTION	4-16
4-5.1 TRANSLATIONAL EQUATIONS	4-16
4-5.2 ROTATIONAL EQUATIONS	4-18
4-5.2.1 Rotational Accelerations	4-20
4-5.2.2 Gyroscopic Moments	4-20
4-5.2.3 Rate of Change of Euler Angles	4-21
4-6 APPLICATION OF EQUATIONS OF MOTION	4-21
REFERENCES	4-22
BIBLIOGRAPHY	4-22

CHAPTER 5 MISSILE AERODYNAMICS

5-0 LIST OF SYMBOLS	5-1
5-1 INTRODUCTION	5-2
5-2 AERODYNAMIC COEFFICIENTS	5-3
5-2.1 APPLICATION OF AERODYNAMIC COEFFICIENTS	5-3
5-2.1.1 Dynamic Pressure Parameter	5-3
5-2.1.2 Force COefficient	5-4
5-2.1.2.1 Effect of Mach Number	5-4
5-2.1.2.2 Effect of Reynolds Number	5-4
5-2.1.3 Reference Area	5-4
5-2.1.4 Components of Forces and Moments	5-5
5-2.1.5 Linearity Assumption	5-6
5-2.2 DRAG COEFFICIENTS	5-6
5-2.3 LIFT COEFFICIENTS	5-9
5-2.4 MOMENT COEFFICIENTS	5-9
5-3 AERODYNAMIC STABILITY DERIVATIVES	5-12
5-3.1 LIFT CURVE SLOPE	5-12
5-3.2 STATIC PITCH STABILITY DERIVATIVE	5-13
5-3.3 DYNAMIC STABILITY DERIVATIVES	5-13
5-3,4 ROLL STABILITY DERIVATIVES	5-14
5-4 DETERMINATION OF AERODYNAMIC COEFFICIENTS	5-14
5-4.1 ANALYTICAL PREDICTION	5-15

5-4.2	WIND TUNNEL TESTING	5-16
5-4.3	FLIGHT TESTING	5-17
5-5	ATMOSPHERIC PROPERTIES	5-17
5-6	MISSILE AERODYNAMIC FORCE AND MOMENT EQUATIONS	5-18
5-6.1	FORCES AND MOMENTS	5-18
5-6.2	COEFFICIENTS	5-19
5-6.3	SIMPLIFICATIONS	5-20
5-7	ROLLING AIRFRAME CONSIDERATIONS	5-20
5-7.1	ROLLING REFERENCE FRAMES	5-21
5-7.2	NEGLECTING LOW ROLL RATES	5-21
5-7.3	AVERAGING AERODYNAMIC COEFFICIENTS	5-21
5-7.4	MAGNUS EFFECT	5-22
5-7.5	MODULATION OF FIN DEFLECTION ANGLE	5-22
	REFERENCES	5-23
	BIBLIOGRAPHY	5-23

CHAPTER 6

MISSILE PROPULSION

6-0	LIST OF SYMBOLS	6-1
6-1	INTRODUCTION	6-1
6-2	TYPES OF PROPULSION	6-1
6-2.1	SOLID PROPELLANT ROCKET MOTOR	6-1
6-2.2	AIR-AUGMENTED ROCKET MOTOR	6-2
6-2.3	LIQUID PROPELLANT ROCKET MOTOR	6-2
6-2.4	TURBOJET ENGINE	6-2
6-2.5	RAMJET ENGINE	6-2
6-3	SIMULATION OF THRUST AND MASS PARAMETERS	6-2
6-3.1	GRAIN TEMPERATURE	6-2
6-3.2	REFERENCE CONDITIONS	6-3
6-3.3	MASS CHANGE	6-3
6-3.4	TUBE LAUNCH	6-3
6-4	PROPULSION FORCE AND MOMENT VECTORS	6-3
	REFERENCES	6-5

CHAPTER 7

MISSILE AND TARGET MOTION

7-0	LIST OF SYMBOLS	7-1
7-1	INTRODUCTION	7-4
7-2	COORDINATE SYSTEMS	7-4
7-3	MISSILE MOTION	7-4
7-3.1	INITIAL CONDITIONS	7-4
7-3.2	MISSILE FLIGHT	7-5
7-3.2.1	Six Degrees of Freedom	7-5
7-3.2.1.1	Translational Equations	7-5
7-3.2.1.1.1	Aerodynamic Force	7-5
7-3.2.1.1.2	Propulsive Force	7-6
7-3.2.1.1.3	Gravitational Force	7-7
7-3.2.1.1.4	Translational and Angular Rates	7-7
7-3.2.1.1.5	Mass	7-7
7-3.2.1.2	Rotational Equations	7-7
7-3.2.1.2.1	Aerodynamic Moment	7-8
7-3.2.1.2.2	Propulsive Moment	7-9
7-3.2.1.2.3	Moments of Inertia	7-10
7-3.2.1.3	Euler Angles	7-10
7-3.2.2	Five Degrees of Freedom	7-10

7-3.2.3 Three Degrees of Freedom	7-10
7-3.2.3.1 Aerodynamic Force	7-10
7-3.2.3.1.1 Instantaneous Response	7-10
7-3.2.3.1.2 Second-Order Response	7-13
7-3.2.3.2 Propulsive Force	7-13
7-3.2.3.3 Gravitational Force	7-13
7-4 TARGET MOTION	7-14
7-4.1 STRAIGHT, CONSTANT-SPEED FLIGHT	7-14
7-4.2 MANEUVERING FLIGHT	7-14
7-4.2.1 Load Factor	7-15
7-4.2.2 Horizontal Turns	7-15
7-4.2.3 Weaves in Horizontal Plane	7-16
7-4.2.3.1 Cosine Weave	7-16
7-4.2.3.2 Circular-Arc Weave	7-16
7-4.2.4 Roll Attitude	7-17
7-5 RELATIVE MISSILE-TARGET GEOMETRY	7-17
7-5.1 RELATIVE POSITION	7-17
7-5.2 RELATIVE ATTITUDE	7-17
7-5.3 MISS DISTANCE	7-18
REFERENCES	7-21
BIBLIOGRAPHY	7-21

CHAPTER 8

GUIDANCE AND CONTROL MODELING

8-0 LIST OF SYMBOLS	8-1
8-1 INTRODUCTION	8-2
8-2 GUIDANCE MODELING	8-3
8-2.1 SEEKER MODELING	8-3
8-2.1.1 Perfect Seeker	8-3
8-2.1.2 Accurate Tracking With Time Lag	8-5
8-2.1.3 Intermediate-Fidelity Seeker Model	8-6
8-2.2 GUIDANCE PROCESSOR MODELING	8-8
8-2.2.1 Perfect Guidance	8-8
8-2.2.2 Practical proportional Navigation	8-9
8-2.2.2.1 Missiles With RF Seekers	8-9
8-2.2.2.2 Missiles With IR Seekers	8-10
8-2.3 AUTOPILOT MODELING	8-11
8-2.3.1 Six Degrees of Freedom	8-11
8-2.3.2 Five Degrees of Freedom	8-13
8-2.3.3 Three Degrees of Freedom	8-13
8-2.4 GROUND-BASED GUIDANCE MODELING	8-13
8-2.4.1 Semiactive Homing	8-14
8-2.4.2 Command	8-14
8-2.4.3 Beam Rider and Command to Line of Sight	8-14
8-2.4.4 Track Via Missile	8-16
8-3 CONTROL SYSTEM MODELING	8-17
8-4 HARDWARE SUBSTITUTION	8-18
8-4.1 DESCRIPTION OF MISSILE HARDWARE SUBSTITUTION	8-18
8-4.1.1 Substituting Missile Hardware	8-18
8-4.1.1.1 Missile-Seeker-in-the-Loop Simulation	8-19
8-4.1.1.2 Missile-Seeker-Electronics-in-the-Loop Simulation	8-19
8-4.1.2 Positioning Missile Hardware	8-20
8-4.1.3 Closing the Loop With Missile Hardware	8-20
8-4.2 SEEKER HARDWARE SUBSTITUTION	8-23
8-4.3 AUTOPILOT HARDWARE SUBSTITUTION	8-23

8-4.4 CONTROL HARDWARE SUBSTITUTION	8-23
REFERENCES	8-23
BIBLIOGRAPHY	8-24

CHAPTER 9 SCENE SIMULATION

9-1 INTRODUCTION	9-1
9-2 SCENE ELEMENTS	9-1
9-2.1 TARGET	9-1
9-2.1.1 Electro-Optical Signatures	9-2
9-2.1.2 Radio Frequency Signatures	9-3
9-2.2 SCENE BACKGROUND	9-4
9-2.3 COUNTERMEASURES	9-4
9-2.3.1 Signature Suppression	9-4
9-2.3.2 Evasive Maneuvers	9-4
9-2.3.3 Jamming	9-4
9-2.3.4 Decoys	9-4
9-2.4 ATMOSPHERIC AND RANGE EFFECTS	9-5
9-3 METHODS OF SCENE SIMULATION	9-5
9-3.1 MATHEMATICAL SCENE SIMULATION	9-6
9-3.2 PHYSICAL SCENE SIMULATION	9-6
9-3.2.1 Electro-Optical	9-6
9-3.2.2 Radio Frequency	9-6
9-3.3 ELECTRONIC SCENE SIMULATION	9-7
9-4 EQUIPMENT FOR SCENE SIMULATION	9-7
9-4.1 ELECTRO-OPTICAL SCENES	9-7
9-4.1.1 Ultraviolet-Infrared Scene Generator (UVIRSG)	9-7
9-4.1.1.1 Components and Operation	9-7
9-4.1.1.2 Targets	9-9
9-4.1.1.3 Decoys	9-9
9-4.1.2 Target Image Simulator	9-9
9-4.1.2.1 Components and Operation	9-9
9-4.1.2.2 Iterative Modeling	9-9
9-4.1.2.3 Updating on the Fly	9-10
9-4.1.3 Unique Decoy Generator	9-10
RADIO FREQUENCY SCENES	9-10
9-4.2.1 Simulation Equipment	9-10
9-4.2.2 Levels of Fidelity	9-11
REFERENCES	9-12
BIBLIOGRAPHY	9-12

CHAPTER 10 IMPLEMENTATION

10-0 LIST OF SYMBOLS	10-1
10-1 INTRODUCTION	10-1
10-2 SELECTION OF COMPUTERS	10-2
10-2.1 ASSESSING COMPUTER PROCESSING SPEED (BENCHMARKS)	10-4
10-2.2 EXAMPLE SIMULATION COMPUTER FACILITY	10-4
10-2.3 SECONDARY CONSIDERATIONS	10-5
10-3 SELECTION OF COMPUTER LANGUAGES	10-6
10-4 TECHNIQUES	10-7
10-4.1 NUMERICAL SOLUTION OF DIFFERENTIAL EQUATIONS	10-8
10-4.1.1 Explicit Methods	10-8
10-4.1.1.1 Euler Method	10-8

10-4.1.1.2 Runge-Kutta Method	10-9
10-4.1.2 Implicit Methods	10-10
10-4.1.2.1 One-Step Processes	10-10
10-4.1.2.1.1 Improved Euler Method	10-10
10-4.1.2.1.2 Modified Euler Method	10-11
10-4.1.2.2 Multistep Processes	10-11
10-4.1.2.2.1 Milne Method	10-11
10-4.1.2.2.2 Adams Methods	10-12
10-4.1.3 Modern Numerical Integration Methods	10-13
10-4.1.4 Applications	10-13
10-4.2 DIGITAL SOLUTION OF TRANSFER FUNCTIONS	10-14
10-4.2.1 The Tustin Method	10-14
10-4.2.2 Root-Matching Method	10-16
10-4.3 SPECIAL INSTRUCTIONS FOR HARDWARE-IN-THI-LOOP SIMULATIONS	10-19
REFERENCES	10-19
BIBLIOGRAPHY	10-20

CHAPTER 11

VERIFICATION AND VALIDATION

11-1 INTRODUCTION	11-1
11-2 VERIFICATION	ii-1
11-3 VALIDATION	11-2
11-3.1 LEVELS OF CONFIDENCE	11-2
11-3.2 COMPARISON WITH TEST RESULTS	11-3
11-3.2.1 Statistical Methods	11-3
11-3.2.2 Nonstatistical Methods	11-4
11-3.2.3 Model Calibration	13-4
11-3.2.4 Neighborhood of Validity	11-4
11-3.3 SCENE VALIDATION	11-4
11-4 ACCREDITATION	11-4
11-5 SELECTION OF METHODS	11-5
REFERENCES	11-5
BIBLIOGRAPHY	11-5

CHAPTER 12

SIMULATION SYNTHESIS

12-0 LIST OF SYMBOLS	12-1
12-1 INTRODUCTION	12-4
12-2 EXAMPLE SIMULATION	12-4
12-2.1 SCENARIO	12-4
12-2.2 OBJECTIVES	12-4
12-2.3 PROGRAM STRUCTURE	12-5
12-2.4 INPUT DATA	12-6
12-2.4.1 Mass	12-6
12-2.4.2 Propulsion	12-6
12-2.4.3 Aerodynamics	12-6
12-2.4.4 Seeker	12-7
12-2.4.5 Autopilot and Controls	12-7
12-2.4.6 Program Control	12-7
12-2.4.7 Constants	12-7
12-2.5 INITIALIZATION	12-7
12-2.6 FIRE CONTROL	12-7
12-2.7 ATMOSPHERE	12-8
12-2.8 RELATIVE POSITION AND VELOCITY	12-9
12-2.9 TEST CLOSING SPEED	12-9

12-2.10	SEEKER	12-9
12-2.11	GUIDANCE AND CONTROL	12-10
12-2.11.1	Test for Active Guidance	12-10
12-2.11.2	Autopilot	12-10
12-2.11.3	Control System	12-11
12-2.11.4	Autopilot and Control System Lag	12-12
12-2.11.5	Fin Angle of Incidence	12-12
12-2.12	AERODYNAMICS	12-13
12-2.12.1	Lift and Drag	12-13
12-2.12.2	Axial Force and Normal Force	12-13
12-2.12.3	Aerodynamic Moments	12-14
12-2.13	PROPULSION	12-15
12-2.14	GRAVITY	12-15
12-2.15	EQUATIONS OF MOTION	12-16
12-2.15.1	Rotation, Translation, and Euler Angles	12-16
12-2.15.2	Missile Position	12-17
12-2.15.3	Target Position	12-18
12-2.16	UPDATE	12-18
12-2.17	TEST FOR MAXIMUM TIME OR CRASH	12-19
12-2.18	SUBROUTINES	12-19
12-2.18.1	RK4	12-19
12-2.18.2	DERIVS	12-20
12-2.18.3	MISDIS	12-20
12-2.18.4	TBE	12-21
12-2.18.5	TEB	12-21
12-2.19	RESULTS	12-21
REFERENCE	12-26

APPENDIX A COORDINATE SYSTEMS

A-0	LIST OF SYMBOLS	A-1
A-1	INTRODUCTION	A-1
A-2	COORDINATE SYSTEM CONVENTIONS	A-1
A-3	COORDINATE SYSTEM DEFINITIONS	A-2
A-3.1	EARTH COORDINATE SYSTEM	A-2
A-3.2	BODY COORDINATE SYSTEM	A-2
A-3.3	WIND COORDINATE SYSTEM	A-3
A-3.4	GUIDANCE COORDINATE SYSTEM	A-3
A-3.5	TRACKER (SEEKER) COORDINATE SYSTEM	A-3
A-3.6	TARGET COORDINATE SYSTEM	A-3
A-4	COORDINATE SYSTEM TRANSFORMATIONS	A-3
A-4.1	BODY TO EARTH	A-4
A-4.2	WIND TO BODY	A-4
A-4.3	GUIDANCE TO EARTH	A-4
A-4.4	TRACKER (SEEKER) TO BODY	A-4
A-4.5	TARGET TO EARTH	A-5
A-5	QUATERNIONS	A-5
REFERENCE	A-5
BIBLIOGRAPHY	A-5

APPENDIX B ATMOSPHERIC MODELING

B-0	LIST OF SYMBOLS	B-1
B-1	INTRODUCTION	B-1
B-2	SOURCES OF ATMOSPHERIC DATA	B-1

B-3 ATMOSPHERIC PROPERTIES	B-1
B-4 MODELING ATMOSPHERIC PROPERTIES	B-1
REFERENCES	B-3
GLOSSARY	G-1
INDEX	I-1
SUBJECT TERM LISTING	ST-1

LIST OF ILLUSTRATIONS

1-1	Missile Flight Simulation	1-2
1-2	Spectrum of Methods for Determining Missile Performance	1-3
2-1	Guidance and Control Terminology	2-2
2-2	Major Component Sections of a Homing Missile	2-3
2-3	Attenuation of Optical Radiation	2-4
2-4	Distribution of IR Radiation from a Typical Target	2-4
2-5	Basic Reticle Tracker	2-5
2-6	Typical Conical-Scan Reticle Seeker Assembly	2-5
2-7	Projection of Tracking Error on Reticle Plane	2-6
2-8	Generic Reticle Patterns	2-7
2-9	Rosette Scan Pattern	2-8
2-10	Typical Radar Seeker	2-9
2-11	Attenuation of RF Radiation by Atmosphere and Rain	2-9
2-12	RF Tracking	2-11
2-13	Function of the Autopilot	2-12
2-14	Acceleration Required to Change Direction of Flight	2-13
2-15	Aerodynamic Lift	2-13
2-16	Moment Produced by Thrust Vector Control	2-14
2-17	Aerodynamic Moment Reduced by Control-Surface Deflection	2-14
2-18	Torque Balance Servo Configuration	2-16
2-19	Warhead Fragment Patterns	2-17
2-20	Fuze and Warhead Relationships	2-19
2-21	Typical Solid propellant Rocket Motor	2-20
2-22	propellant Grain Configurations	2-21
2-23	Typical Boost-Glide and Boost-Sustain Histories	2-22
2-24	Effect of Temperature on Thrust History	2-23
2-25	Guidance Loop	2-24
2-26	Command Guidance	2-26
2-27	Track-via-Missile Guidance	2-26
2-28	Beam-Rider Guidance	2-29
2-29	Proportional Navigation Guidance	2-29
3-1	Coordinate Systems	3-9
3-2	Typical Top-Level Flow Diagram for a Flight Simulation	3-11
4-1	Forces, Velocities, Moments, and Angular Rates in Body Reference Frame	4-4
4-2	Euler Angle Rotations	4-5
4-3	Velocity Vector in Body-Frame and Earth-Frame Coordinates	4-6
4-4	Time Rate of Change of Vector B	4-8
4-5	Aerodynamic Force in Body- and Wind-Frame Coordinates	4-11
4-6	Relationship Between Gravitational Mass Attraction and Gravity Experienced by an Observer on a Rotating	4-15
5-1	Comparison of Dragon a Disk and an Aerodynamic Shape	5-7
5-2	Effect of Rocket Plume on Base Drag	5-8
5-3	Zero-Lift Drag Coefficient	5-9
5-4	Drag Polar	5-9
5-5	Coefficient of Lift Versus Angle of Attack	5-9
5-6	Moment Coefficient Versus Angle of Attack	5-10
5-7	Spring Analogy for Stability	5-13
5-8	Fin Rotation Relative to Plane of Missile Maneuver	5-22
6-1	Thrust Force and Moment	6-4
7-1	Forces and Accelerations in Horizontal, 2-g Turn	7-15
7-2	Relative Attitude of Target	7-18
7-3	Miss Distance Vector Diagram	7-19
7-4	Typical Dependence of P_z on Miss Distance	7-20

8-1	Relationship Between Range Vector and Line of Sight to Tracking Point	8-4
8-2	Response of First-Order Seeker to Step Command	8-6
8-3	Tracking Point of Centroid Tracker	8-6
8-4	Typical Discriminator Gain and Seeker Weighting Functions	8-7
8-5	Effect of Rate Bias	8-8
8-6	Navigation Ratio Achieved by Typical IR Missile Design	8-10
8-7	System Gain for Typical IR Missile	8-10
8-8	Numbering Convention for Control Surfaces	8-12
8-9	Convention for Direction of Control-Surface Rotation	8-12
8-10	Guidance Error for Beam Rider or Command to Line of Sight	8-15
8-11	Control System Block Diagrams	8-17
8-12	Examples of Production Hardware Employed in Simulation	8-19
8-13	Flight Simulation Employing Actual Missile Seeker in the Loop	8-21
8-14	Flight Simulation Employing Seeker Electronics in the Loop	8-22
9-1	Size of Target Relative to Reticule Pattern	9-2
9-2	Typical Radar Cross Section in Azimuth Plane of Target	9-3
9-3	Ultraviolet-hfkared Scene Generator Configuration	9-8
9-4	Typical RF Scene Simulation Configuration	9-11
10-1	Truncation Error in Euler Method	10-9
10-2	Response of First-Order 'Transfer Function to Step Input Calculated by Tustin Method	10-15
10-3	Response of First-Order Transfer Function to Step Input Calculated by Root-Matching Method	10-17
10-4	Response of Second-Order Transfer Function to Step Input Calculated by Root-Matching Method	10-18
11-1	Validation-Building a Pyramid of Confidence	11-2
11-2	Effect of Model Validity Level on Benefit-to-Cost Ratio	11-3
12-1	Typical Top-Level Flow Diagram for a Flight Simulation	12-5
12-2	Top View of Simulated Engagement	12-22
12-3	Side View of Simulated Engagement $x_e z_e$ -Plane	12-22
12-4	Missile Speed History	12-22
12-5	Seeker-Kead Angular Rate Histories	12-23
12-6	Lateral Acceleration Command Histories	12-23
12-7	Deflection Angle Histories	12-24
12-8	Missile Rotational Moment Histories	12-24
12-9	Angle-of-Attack and Angle-of-Sideslip Histories	12-25
12-10	Total Angle-of-Attack History	12-25
12-11	Missile Rotational Rate Histories	12-25
A-1	Coordinate System Conventions	A-2

LIST OF TABLES

4-1	Nomenclature for Forces, Moments, and Motion	4-4
4-2	Acceleration due to Gravity at Earth Surface	4-15
5-1	Selected Flight-Test Parameters for Estimating Aerodynamic Characteristics	5-17
B-1	Properties of US Standard Atmosphere (1976)	B-2

LIST OF ABBREVIATIONS AND ACRONYMS

AAFTD = Aerodynamic Analysis of Flight-Test Data	IR = infrared
ADI = Applied Dynamics International	MFLOPS = millions of floating point operations per second
ACM = arithmetic computation module	MIPS = millions of instructions per second
AD RTS = Applied Dynamics Real-Time Station	MISDIS = miss distance
AGC = automatic gain control	MPU = missile-positioning unit
AIM= analog interface module	MTI = moving target indicator
AM = amplitude modulation	NACA = National Advisory Committee for Aeronautics
APSE = Automatic Programming and Scaling of Equations	NASA = National Aeronautics and Space Administration
CCM = counter-countermeasures	NOPS = normalized operations per second
CE= Compute Engine	PGS = Program Generation System
COP = Communications Processor	PIM = processor interface module
CPU = central processing unit	PIR = Parallel Intelligent Resource
CRT = cathode-ray tube	RCSA = radar cross section
CSSL = Continuous System Simulation Language	RFSS = Radio Frequency Simulation System
CVND = circular variable neutral density	RAM= radar-absorbent materials
CW = continuous wave	RCS = radar cross section
DAP = digital autopilot	RF= radio frequency
DIAC = Digitally Implemented Analog Computer	SE = Starlight Executive
DIM = digital interface module	SESL = Starlight Interactive Simulation Language
DoD = Department of Defense	TIS = target image simulator
EAI = Electronic Associates, Incorporated	TVM= track-via-missile
ECSSL = Extended Continuous System Simulation Language	UNDEGE = unique decoy generator
ECM = electronic countermeasures	US = United States
ELOS = elevation line of sight	UV = ultraviolet
EO = electro-optical	UVKRSR = ultraviolet-infkamd scene generator
FM= frequency modulation	VAMP = VME Ancillary Multiprocessor
FOV = field of view	VIM= VME bus Interact Manager
GPSS = General-Purpose Simulation System	VME= Versa Module Eurocad
GUI = graphical user interface	

CHAPTER 1

INTRODUCTION

Background information is finished regarding the need for missile flight simulations, and brief descriptions are given of their character, purpose, and implementation. The purpose, scope and organization of the handbook are described.

1-1 BACKGROUND

Surface-to-air missile systems are developed to meet specified operational requirements. In a broad sense these requirements include the size of the defended area and lethality. In addition, the conditions under which the missile system is to operate are specified to include the environment and characteristics of the threat (target). The defended area and threat characteristics determine the missile range and altitude requirements. The speed and maneuverability of the target influence the speed and maneuverability required of the missile. The target signature-emitted or reflected electromagnetic radiation-and the operational environment influence the design of the missile guidance system, and likely threat countermeasures are particularly important in establishing guidance system characteristics. The required lethality, generally expressed as kill probability, translates to requirements for missile guidance accuracy, dynamic airframe maneuver characteristics, counter-countermeasures capability, and fuzing and warhead characteristics. The kill probability requirements are usually stated as the probability of achieving specific levels of damage to the target under specified engagement conditions.

Department of Defense (DoD) procedures for acquiring and supporting missile systems establish key milestones at which both program management and technical decisions must be made. From the initial formulation of the concept for a new missile system to the end of the life cycle of the missile, there is a continuous need to predict the performance of alternative designs of the missile that meet changing operational requirements and to introduce improvements that meet the evolving threat (Refs. 1, 2, and 3). An increasingly important source of information for decision makers is missile flight simulation. The major missile system performance measures, kill probability and size of area to be defended, can be predicted by modeling how the missile approaches the target (missile flight) and how the warhead fragments impact the vulnerable components of different target types under all dynamic and environmental conditions. Most missile system evaluators choose to simplify the evaluation process by modeling missile flight separately, with its own performance measure. As described later in this handbook, many missile development and evaluation objectives can be satisfied by considering only missile flight. One of the principal objectives of modeling missile flight is to predict how close the missile will approach the target under varying dy-

amic and environmental conditions. Miss distance is often used as a measure of missile system performance. In general, the smaller the miss distance, the greater the probability of killing the target. The mathematical analysis of missile flight is complex and involves nonlinearities, logic sequences, singular events, and interactions among multiple subsystems. Computer simulation techniques are ideally suited to this task.

1-1.1 DESCRIPTION OF A MISSILE FLIGHT SIMULATION

A missile flight simulation is a computational tool that calculates the flight path and other important parameters of a missile as it leaves the launcher and engages a target. A simulation is based on mathematical models of the missile, target and environment, and these mathematical models consist of equations that describe physical laws and logical sequences. The missile model includes factors such as missile mass, thrust aerodynamics, guidance and control, and the equations necessary to calculate the missile attitude and flight path. The target model is often less detailed but includes sufficient data and equations to determine the target flight path, signature, and countermeasures. The model of the environment contains, at a minimum, the atmospheric characteristics and gravity. Clouds, haze, sun position, and terrain or sea surface characteristics are included if they are important to the purpose of the simulation. Sometimes breadboarded components or actual missile hardware is used instead of mathematical models of certain missile subsystems.

The physical laws in the simulation are those governing the motion of the missile and target and those affecting any simulated subsystems. For example, the equations of motion of the missile determine the acceleration, velocity, and position resulting from the forces due to gravity, thrust, and aerodynamics. Other equations governing physical processes may be required to simulate subsystems such as the target tracking system or the missile control system.

The simulation logic controls conditional events. Examples of time-related, conditional events are initiation of target maneuvers, decoy deployment, and changes in guidance phases. Examples of events that depend on other events are the action to be taken if the commanded missile maneuver exceeds the specified limits set for the missile and termination of the simulation when the missile reaches its closest approach to the target.

The inputs and outputs of a missile flight simulation are shown in Fig. 1-1. Inputs are data needed by the mathematical models that may change from one computer run to the next. Examples of inputs are initial conditions such as the positions and velocities of the missile and target at the instant the simulation begins, programmed target maneuvers, and countermeasure control parameters. If the target model is a general one, target signature data are treated as inputs. Data that seldom or never change are usually built into the models. For example, a simulation of a specific type of missile usually has descriptive data built into the missile model, but simulations of generic missiles or missiles not yet completely defined may be arranged so that parameters subject to change are inputs. Environmental conditions, e.g., atmospheric density as a function of altitude, are usually built into the simulation; however, a nonstandard atmosphere or other variable environmental conditions can be selected by an appropriate choice of input. Typical missile flight simulation outputs include the missile flight-path history and the resulting miss distance. Depending on the needs of the user, the time histories of many different missile functions and responses may be outputs, such as fin deflection angles, missile translational and rotational rates and accelerations, seeker function, and control system function.

1-1.2 PURPOSE OF A MISSILE FLIGHT SIMULATION

The performance of a missile system is determined by the interaction of all of its subsystems. Each subsystem component must perform its own function properly, and the integration of all subsystems into a whole missile must be balanced and tuned for best performance. Very small variations in any component can unbalance the system and result in unacceptable missile performance. Missile designers and evaluators use a variety of methods to obtain information on the performance of alternative missile configurations. These include analytical estimates, computer simulations, laboratory tests, and flight tests as shown in Fig. 1-2. Simple analytical techniques provide estimates of missile performance characteristics, such as maximum range and time of flight, but the detailed interactions of subsystems are difficult or impossi-

ble to predict accurately by simple analytical means. The most credible means is flight testing, but it is also the most costly. Laboratory testing also provides credible information, but it is restricted mainly to subsystem evaluation. Between the extremes of low-cost, low-credibility analytical methods and high-cost, high-credibility testing methods is a gap filled by computer simulation (Ref. 1). Clearly, this is a wide gap that leaves room for wide variation in the sophistication of missile simulations depending on whether the simulation user's needs fall closer to analytical estimates or to flight-test results. For example, a very simple simulation could determine the general size and shape of the area that could be defended by a surface-to-air missile with a given weight and thrust history. If the effects of seeker range limits, gimbal angle limits, and tracking rate limits on the size of the defended area are of concern, these functions must be modeled in the simulation. If the contributions of various missile design characteristics to miss distance are of interest, the functions contributing to miss distance must be included in the model, particularly those that relate to missile response times and maneuver limitations. If emphasis is to be placed on target tracking and guidance and control, more detailed missile function models are required, even to the point of using actual missile hardware in the simulation and generating scenes for the hardware seeker to view. In general, as the information needs of the user become more detailed and require greater precision, the simulation must become more complex, refined, and detailed (Ref. 2).

1-1.3 IMPLEMENTATION OF A MISSILE FLIGHT SIMULATION

The performance characteristics of the first guided missiles were analyzed by using analog computers. The physical simulation consisted of patchboards with hundreds of wires making the electrical component connections required in the computer to solve the differential equations that described missile behavior. Today, except for some very specialized applications, analog computers have been replaced by digital computers. A digital simulation consists physically of lines of computer instructions, usually stored magnetically on disks or tape. Hard copy (printed on paper) and cathode-ray

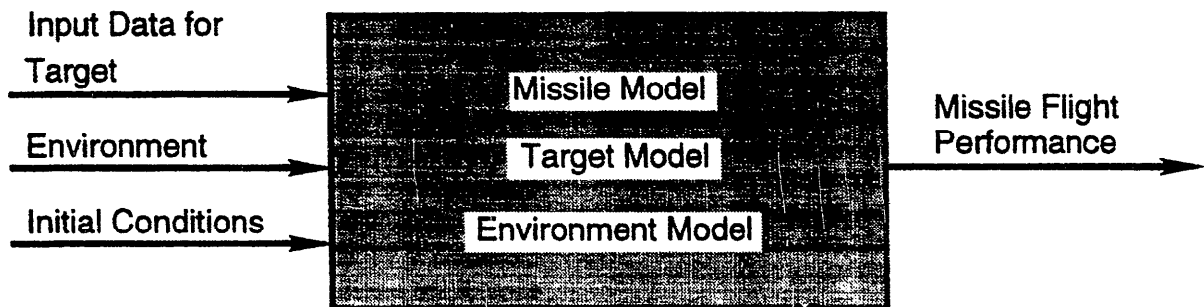


Figure 1-1. Missile Flight Simulation

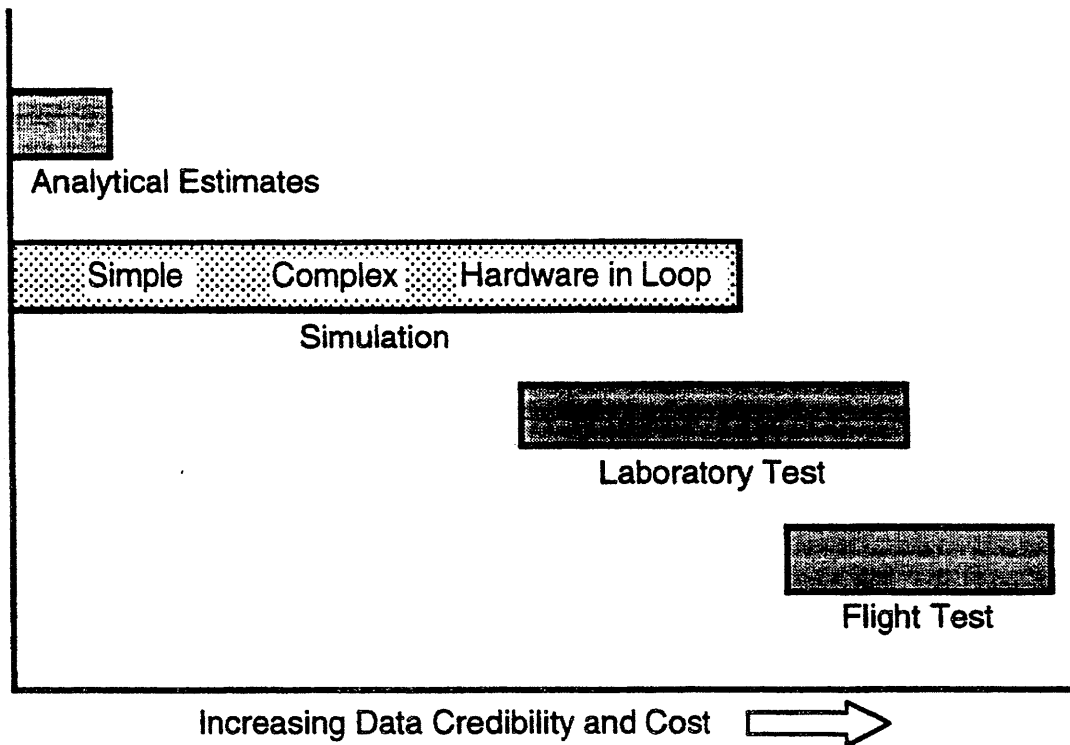


Figure 1-2. Spectrum of Methods for Determining Missile Performance

tube (CRT) displays of the lines of instruction are readily available to simulation users and programmers to be used in analyses and to understand what the simulation does. Inputs or changes to the simulation are easily made by typing them into the computer using a keyboard.

Some hybrid simulations are basically digital but use analog computers with analog-to-digital (A/D) converters to generate certain simulated functions. Typically, 'hybrids' are used in applications that require the outputs in real time and in which the simulated functions contain high-frequency spectral components that would be difficult or impossible to produce with current digital equipment alone.

The need for real-time computation is usually the result of using actual missile hardware in the simulation, which, of course, must run in real time (Refs. 2, 3, and 4). In this case the physical simulation consists of lines of instruction for the digital portion, wired patchboards for the analog portion, and the actual hardware components (the seeker, for example). The equipment needed to run a hybrid simulation that includes actual seeker hardware is a digital computer, an analog computer, and a seeker scene generator. Less complex simulations may require only a digital computer.

1-2 PURPOSE OF THE HANDBOOK

Many Government agencies and contractors use missile flight simulations. These simulations are continually being revised and improved as user needs change, as missile designs change, and as better simulation hardware becomes

available. New simulations are developed as the need arises. There is a relatively small core of individuals who have the knowledge and experience to maintain these simulations and to develop new ones. Scattered documentation exists on various aspects of missile simulation, and most simulations have some form of documentation that describes them. Many of the pragmatic techniques used to produce the desired results within the limitations of cost, time, and current hardware, however, exist only in the minds of the specialists in this field.

The objective of this handbook is to document methods of missile flight simulation to preserve current knowledge and to provide a consolidated source of information. Specifically, the purposes of this handbook are to (1) present the fundamental elements, equations, and techniques necessary to develop missile flight simulations, (2) describe the typical computational equipment used for missile flight simulation and the specialized equipment used to generate the target scene, and (3) present the methodology for certifying that a missile flight simulation provides an accurate representation of missile performance.

The intended users of this handbook are (1) Army design engineers with many years of experience, (2) recently graduated engineers with limited knowledge of the principles of missile simulation, (3) specialists in particular fields of Army materiel design with superficial knowledge in the field of missile simulation, and (4) engineers employed by contractors.

1-3 SCOPE OF THE HANDBOOK

Guided missile technology embraces almost all of the physical sciences, and missile flight simulation can simulate almost any missile function to whatever degree of realism is required or affordable. To cover all aspects with all degrees of simulation complexity in a single volume would clearly be impractical. Therefore, in the interests of practicality and utility, this handbook is limited to flight simulations of surface-to-air missiles used by the US Army. Because many functions are basically common to a wide variety of missile types, however, this information will also be useful to those interested in other types of missiles.

A broad range of model sophistication is covered in the handbook because it is important that the level of sophistication of a simulation model be matched to the specific purposes of the simulation. For some applications it is unnecessary to calculate the missile rotational behavior directly from the aerodynamic characteristics. For these applications, equations of motion with three translational degrees of freedom are adequate. In cases in which the missile rotational behavior is critical and simplified methods are not acceptable, the equations of motion must contain at least two, and sometimes three, additional degrees of freedom. The equations and methods for both three- and six-degree-of-freedom models are presented. Very simple and moderately complex mathematical seeker models are given, and the use of actual flight hardware or breadboard hardware in the simulation is described.

Very specialized missile system component simulation techniques are beyond the scope of this handbook. Representative examples of modeling topics that are beyond the scope are detailed seeker signal processing, propellant grain burning dynamics, detailed servo system component simulation, complex aerodynamic cross coupling, airframe deflection and flutter, and fuze and warhead operation.

Equations and simulation methodology are given for all the major subsystems of surface-to-air missiles. The basic simulation equations can be implemented by either digital or analog means; however, since by far the greatest proportion of current flight simulations uses digital computation, digital methods are emphasized.

1-4 ORGANIZATION OF THE HANDBOOK

Chapter 2 describes a missile system to include its hardware components and its tracking and guidance functions. Chapter 3 contains an overview of the subject of missile simulation. Chapters 4 through 9 expand on individual topics in greater depth and present techniques used to simulate the components and functions of the missile system. Chapter 10 discusses methods of implementing the simulation model that include selection of the most appropriate computer hardware, the applicability of different computer languages, and various computational techniques. Chapter 11 addresses

methods of verifying and validating the simulation model to ensure that the simulation program correctly represents the intended mathematical model and that the model adequately represents the actual missile. Chapter 12 brings together the methods described in previous chapters in the form of an example simulation showing proper sequencing and interfacing among the various simulation components.

In addition to covering a range of levels of simulation sophistication for different users, the handbook describes the use of simplified equations to reduce computational time in order to preserve the real-time aspects of hardware-in-the-loop operation. Individual chapters present appropriate equations and methods of simplifying them, and the need for simplification is discussed in detail in Chapter 10.

REFERENCES

1. M. M. Rea, A. M. Baird et al, Missile System Simulation at the Advanced Simulation Center, Technics! Report RD-82-11, Systems Simulation and Development Directorate, Advanced Simulation Center, US Army Missile Laboratory, US Army Missile Command, Redstone Arsenal, AL, 25 January 1982.
2. F. M. Belrose and A. M. Baird, The Role of Simulation in High-Technology Missile Applications, Technical Report RD-CR-83-23, US Army Missile Command, Redstone Arsenal, AL, April 1983.
3. H. L. Pastrick C. M. Will et al, "Recent Experience in Simulating Missile Flight Hardware in Terminal Homing Applications", Proceedings of Society of Photo-Optical Instrumentation Engineers, Optics in Missile Engineering, Vol. 133, Los Angeles, CA, January 1978, Society of Photo-Optical Instrumentation Engineers, Bellingham, WA.
4. P. C. Gregory, "Guidance Simulation Techniques", Guidance and Control for Tactical Guided Weapons With Emphasis on Simulation and Testing, AGARD-LS-101, Advisory Group for Aerospace Research and Development North Atlantic Treaty Organization, Neuilly sur Seine, France, May 1979.

BIBLIOGRAPHY

- H. L. Pastrick, C. M. Will et al, Hardware-in-the-Loop Simulations: A Guidance System Optimization Tool, Paper No. 74-929, American Institute of Aeronautics and Astronautics Mechanics and Control of Flight Conference, Anaheim, CA, August 1974, American Institute of Aeronautics and Astronautics, Washington, DC.
- H. L. Pastrick et al, "System Performance Prediction by Modeling Test Data in Digital Simulations", Journal of Spacecraft and Rockets (March 1974).
- W. Read and J. Sheehan, "AMRAAM System Simulation, A Detailed Design and Performance Evaluation Tool", Electronic Progress 22.4 (Winter 1980).

CHAPTER 2

MISSILE SYSTEM DESCRIPTION

Understanding missile flight simulations requires a knowledge of what is being simulated—the missile. This chapter describes in general terms the missile subsystems and functions that are important to the simulation of missile flight. These include in par. 2-2 the subsystems of the physical missile—seeker autopilot, control, warhead and fuze propulsion, and airframe; in par. 2-3 the various types of guidance; and in par. 2-4 specific considerations of missile launch that are applicable to missile flight simulation.

2-0 LIST OF SYMBOLS

- D** = aerodynamic drag force vector, N
- F_p** = thrust force vector, N
- L** = aerodynamic lift force vector, N
- L** = magnitude of aerodynamic lift force vector L, N
- l_{cm}** = lever arm, m
- P₁, P₂** = pneumatic servo nozzle pressures, Pa
- V** = relative air velocity, m/s
- ΔH** = radio frequency lobe difference signal, V
- Δt** = computation time step ($t_{n+1} - t_n$), s
- ε** = tracking error angle (angle between line-of-sight to target and seeker boresight axis), rad
- Σ** = radio frequency lobe sum signal, V

2-1 INTRODUCTION

Surface-to-air missile systems are designed to meet specified operational requirements. The variety of requirements leads to different missile sizes and fictional arrangements. Many of the differences among missile systems are the results of variations in tracking implementations and guidance concepts. The purpose of a surface-to-air missile system is to destroy threatening airborne targets. The system includes the missile flight vehicle and supportive equipment such as a launcher, any ground-based missile and/or target trackers, and any ground-based guidance processors. As a target approaches the missile launch site, a tracking system measures target motion relative to the missile. A fire control function determines the time and direction to launch, and the missile is propelled from the launcher by a propulsion system, usually a rocket motor. As the tracking system continues to measure relative motion, a guidance processor derives missile maneuver commands to guide the missile to intercept the target. The maneuver commands are transformed into missile control-surface deflection commands by an autopilot and a control system supplies the actuator power to rotate the control surfaces. Aerodynamic lift on the missile generated by control-surface deflections produces maneuvers that are responsive to guidance commands. An explosive warhead is detonated on impact or upon proximity with the target. Missile flight performance depends on the mechanizations of and the interactions among the various missile subsystems and the guidance concept.

Surface-to-air missile systems are the Army's primary defense against airborne threats. Their objective is to deny enemy aircraft access to friendly resources. Army air defenses consist of several layers of defensive capability, each with different missile system requirements. Long-range, high-altitude systems are required for widespread coverage of the field army and military bases. Medium-range systems with low- and medium-altitude capability are used to cover forward-deployed combat units and the rear areas of divisions and corps. Short-range systems, with the capability to destroy low-level threats, are used to defend airfields, depots, frontline armor, and moving columns. Man-portable systems, also with a capability against low-level threats, are used for close-in defense (Ref. 1).

The size of the missile flight vehicle is dictated largely by the distance it is required to fly (range) and the weight of its payload (warhead). The payload weight in turn depends on the expected miss distance, and miss distance depends on guidance accuracy. Different guidance implementations result in different potential accuracies. Missile size and configuration design requires that tradeoffs be made among all of these factors.

Current US Army surface-to-air missiles range in mass from about 8 to 900 kg. The smallest missiles are hunched from man-portable launch tubes; after launch they are guided by an onboard guidance system. The largest missiles fly to long range and high altitude and are supported by radars and guidance computers on the ground that interact with the onboard guidance system.

An individual surface-to-air missile system is called a fire unit. In general, a fire unit consists of the equipment and personnel to transport the system from one launch site to another; to search for, identify, and track airborne targets; to launch and guide missiles; and to reload launchers. A given fire unit can engage only those targets that come within range of the missile. Even a target that is within range sometimes cannot be engaged successfully because its position is such that the line of sight from the missile to the target rotates into angular positions, or angular rates, that exceed the capabilities of the tracking sensor. The locus of possible positions of the target at the time of missile launch that are within range and within tracking limitations establishes the missile system kinematic launch boundary. The kinematic launch boundary of any given missile system depends on tar-

get speed and flight path. The actual launch boundary is often smaller than the kinematic launch boundary because of additional limitations that depend on the sensitivity of the tracking sensor to radiation from the target and the geometric distribution of the spectral and intensity characteristics of radiation from the target (target signature). Also effective countermeasures employed by the target greatly decrease the size and shape of the launch boundary.

Fire units are located with overlapping launch boundaries at sites suited to defending friendly resources. Alerts (warning that a potential target is in the general area) and cues (giving the direction in which to look) maybe communicated among the fire units and centralized surveillance systems. As an enemy aircraft penetrates to within range of the search system of a given fire unit it is detected, identified as unfriendly, and the tracking sensor is locked on the target. The missile fire control system monitors target position and provides an indication of the time when the target enters the launch boundary. The fire control system also provides the azimuth and elevation angles needed to point the launcher.

The missile is launched by a switch operated by the fire unit crew. The missile propulsion system rapidly generates thrust and propels the missile along the launcher and into the air. Until the missile speed is sufficient for aerodynamic control, it flies ballistically. The tracking system continues to track the target and provide information on the position and motion of the target relative to the missile. The missile guidance system interprets this information and generates guidance commands that tell the missile how to maneuver to intercept the target. These maneuver commands are determined by the application of logic (guidance law) to the relative missile and target motion. The autopilot and control systems in the missile flight vehicle convert the guidance commands into aerodynamic control surface deflections that cause the missile flight path to turn. This process continues from the time guidance is initiated until the time of intercept.

Because of inaccuracies, limitations, and time lags, however, the missile does not always impact the target but may fly close to it. The distance separating the missile and target at the closest approach of the missile to the target is the miss distance. The objective of guidance and control is to cause the miss distance to be as small as possible.

As the missile approaches the target, the fuze senses the presence of the target and detonates the warhead. If the miss distance is small enough and the fuze operates at precisely the right moment, the warhead explosion disables the target. If observation by the fire unit crew indicates that the missile was ineffective and the target is still within the launch boundary, another missile may be launched.

All surface-to-air missile systems are not alike. The major difference is various approaches to missile guidance. All include some form of target tracking; some tracking sensors are large and located on the ground, whereas others are small and are carried onboard the missile. Different tracking systems sense different bands of the electromagnetic spectrum. Some guidance processors employ ground-based computers; others are small and simple enough to be located in the missile. Some guidance laws are more easily implemented with one arrangement of guidance system components than with other arrangements. Design of the guidance system has a significant impact on the design of the missile flight vehicle.

2-2 MISSILE

Major subsystems that may be included in the flight vehicle are guidance and control fuze and warhead, motor, and airframe. The guidance and control system is often subdivided into individual subsystems as shown in Fig. 2-1. If a missile has a seeker, the onboard guidance system usually is composed of the seeker and autopilot Fig. 2-2 is a longitudinal cross section of a typical surface-to-air missile having all of these subsystems onboard.* If a missile does not have a seeker, the only onboard guidance components may be an-

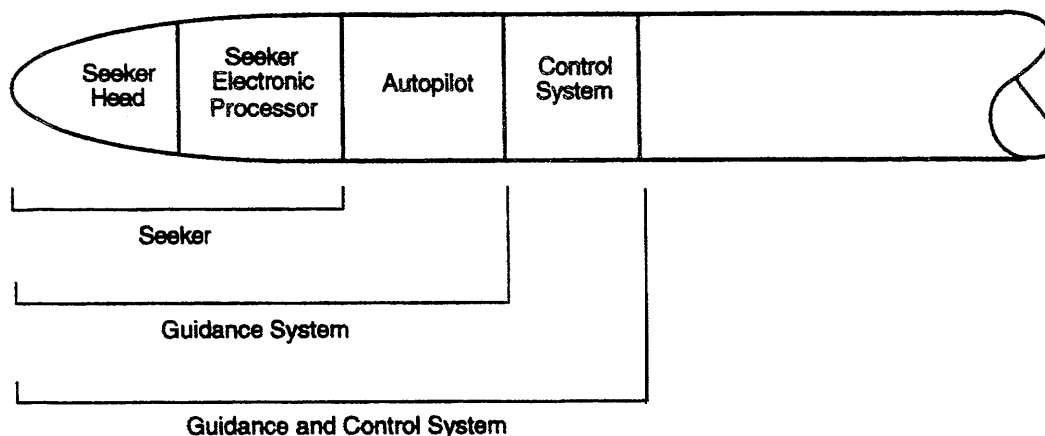


Figure 2-1. Guidance and Control Terminology

*A given missile may not contain all of the subsystems described. For example, some missiles do not contain seekers, and some particularly accurate missiles do not have proximity fuzes.

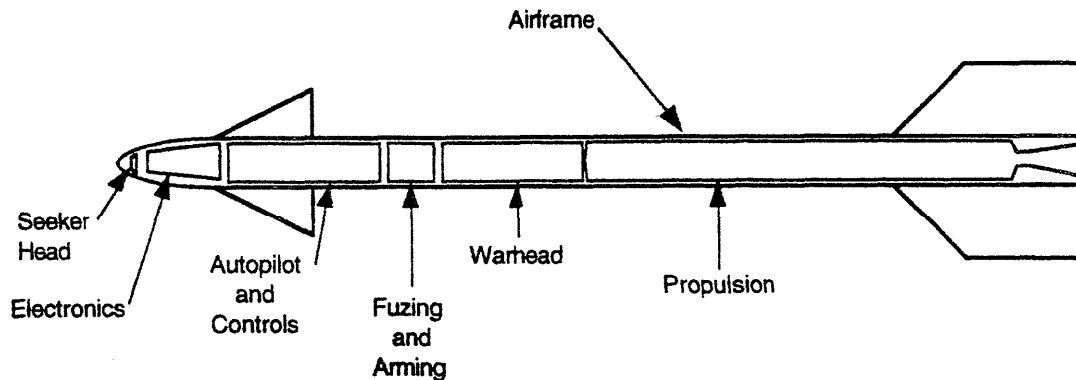


Figure 2-2. Major Component Sections of a Homing Missile

tennas for receiving information from the ground-based guidance components and an autopilot to translate guidance information into control commands.

2-2.1 SEEKER

A missile seeker is composed of a seeker head to collect and detect energy from the target, a tracking function to keep the seeker boresight axis pointed toward the target, and a processing function to extract useful information from the detection and tracking circuits.

The seeker usually is mounted in the nose of the missile where it can have an unobstructed view ahead. The seeker antenna or optical system is usually mounted on gimbals to permit its central viewing direction (boresight axis) to be rotated in both azimuth and elevation relative to the missile centerline (Ref. 2). The limits of the angular viewing direction (gimbal angle limits) are typically about ± 40 to ± 60 deg relative to the centerline axis of the missile. If the angle between the missile centerline and the line of sight to the target exceeds the gimbal angle limits, the seeker is physically constrained by the gimbal stops and can no longer track the target.

The gimballed portion of the seeker head usually is stabilized to keep it pointing in a fixed direction regardless of perturbing angular motions of the missile body. The two most prevalent means of stabilization are to spin a portion of the gimballed components so that they act as a gyro and to use actuators to hold the seeker in a stabilized direction using control signals from gyros mounted on the gimbal frames. In either case, signals from the tracking circuitry are required to change the pointing direction of the seeker.

The two common seeker types are optical and radio frequency (RF). The methods and equipment used to sense signals in the optical and RF bands are different so they lead to different implementations of the two types of seekers.

2-2.1.1 Optical Seekers

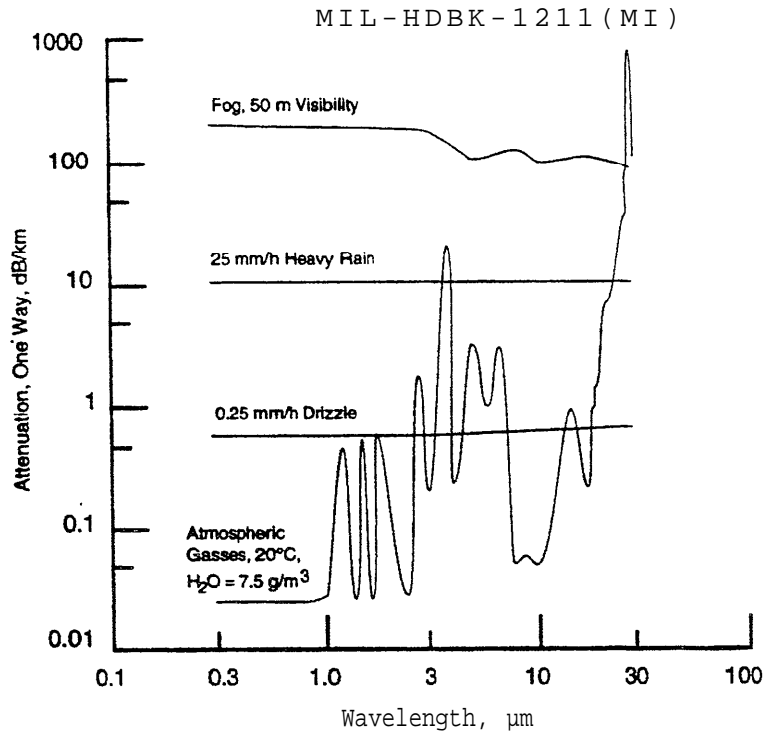
Seekers that sense radiation in the ultraviolet (UV), visual, and infrared (IR) portions of the electromagnetic spectrum are classed as optical seekers. The radiation is transmitted through the atmosphere from the target. Not all target radia-

tion directed toward the seeker will reach it because of attenuation. Optical radiation is attenuated by the geometrical distance from the source (inverse range squared); by absorption and scattering by the atmosphere; by clouds, haze, rain, and snow, and by other obscurants such as smoke and dust. The amount of attenuation is influenced by the wavelength of the radiation. For example, there are atmospheric transmission windows (relatively lower attenuation) at wavelengths of 1-3 μm , 3-5 μm , and 8-12 μm in the IR spectral region (Fig. 2-3). IR radiation outside these windows is attenuated so severely by the atmosphere that only these windows are used for IR sensors. The 1-3 μm band was used by early IR seekers, which were not cooled. The 3-5 μm band is the most applicable to current cooled IR seekers. Little of the radiation from the target exhaust plume is contained in the 8-12 μm band; thus this band is less desirable for surface-to-air missiles. The visible spectrum is transmitted through a window from 0.4 to 0.8 μm , and an ultraviolet window exists from 0.34 to 0.39 μm (Ref. 3). Some seekers are designed to use more than one optical band to discriminate between targets and decoys.

Sources of optical radiation that can be used by seekers are the engine exhaust plume, hot metal, and aerodynamic heating. In the visible portion of the spectrum, reflected sunlight can be used. UV radiation is transmitted to the seeker from the background scene. The target blocks out UV radiation and provides contrast with the background. A laser seeker would of course use reflected laser radiation. The distribution of IR radiation from a typical target is shown in Fig. 2-4. When the target exhaust plume is used as the primary source of radiation being sensed by the seeker, it is necessary to bias the guidance ahead of the plume for crossing (other than head-on or tail-on) engagements; otherwise, the missile will pass through the plume behind the target.

Optical seekers contain a telescope used to view the target. The instantaneous field of view is conical, and the cone axis coincides with the optics axis of the telescope. The telescope forms an optical image of the target and background.

Accurate target tracking requires that the seeker boresight axis be pointed continuously toward the target. The angle between the boresight axis and the line of sight to the target is



NOTE: Each curve indicates attenuations independent of the other curves.

Figure 2-3. Attenuation of Optical Radiation (Adapted from Ref. 3)

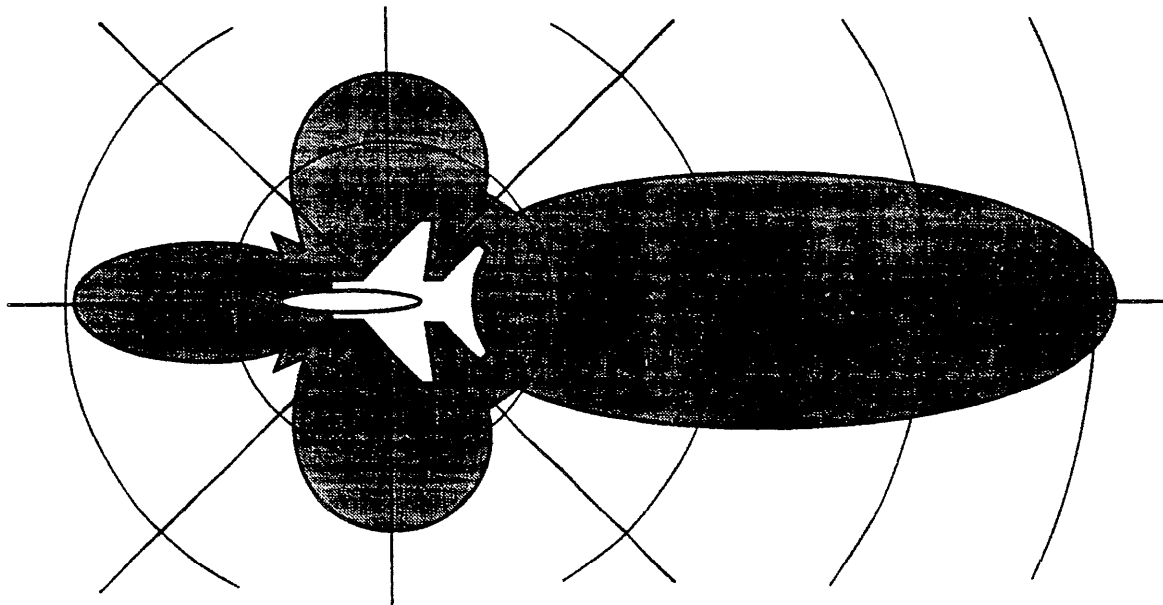


Figure 2-4. Distribution of IR Radiation from a Typical Target

the tracking error. As the line of sight to the target changes because of relative target motion, the pointing direction of the seeker must be changed to follow it. The information necessary to determine the magnitude and direction of the tracking error is contained in the telescope image. Different methods of extracting the target error have been developed. AH employ photoelectric devices, called detectors, to con-

vert information contained in the optical telescope image into an electrical signal suitable for processing.

There are three types of optical seekers based on the different techniques used to process the optical image. These methods are reticle, pseudoimaging, and imaging. Each method is discussed in the paragraphs that follow.

2-2.1.1.1 Reticle

The simplest form of optical seeker directs the entire telescope image onto a single detector. This image contains the sum of the radiant power from the background scene and from the target. One approach to extracting the tracking error from the image is to pass the image through an optical device (reticle) designed to encode the tracking error.

The basic arrangement of the reticle tracker is illustrated in Fig. 2-5. A cross-sectional view of a typical reticle seeker and the optical ray paths through the telescope are shown in Fig. 2-6. The telescope collects optical radiation and focuses an image of the field of view on the reticle. The reticle, located between the telescope and the detector, contains a spatial pattern of varying optical transmission. Some parts of the

pattern block that portion of the image that is focused upon them; other parts allow the image to pass through to the detector. The transparent and opaque areas are arranged so that the modulation (passing and blocking of energy) encodes the position of the small sources relative to the boresight axis and discriminates against larger sources in the background. The modulated radiation is collected and deposited on the detector, which produces an electrical signal proportional to the amount of incident radiant power. The seeker electronics amplify this detector signal and demodulate it to recover an error signal that represents the tracking error. The error signal is fed back to point the telescope such that the error is reduced.

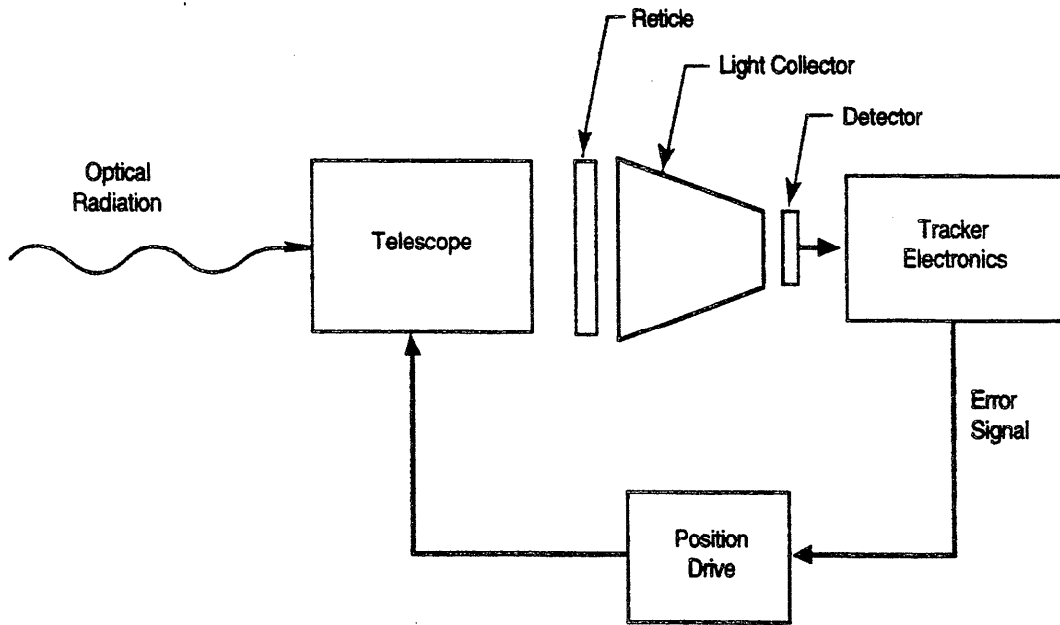


Figure 2-5. Basic Reticle Tracker (Adapted from Ref. 4)

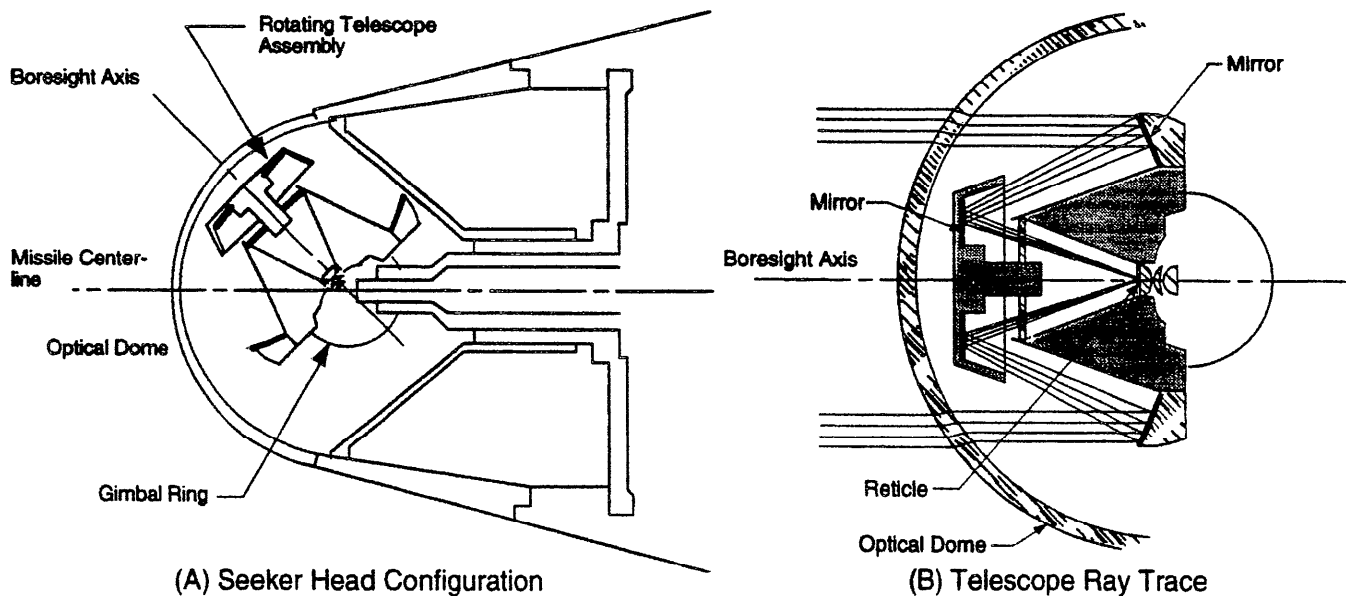


Figure 2-6. Typical Conical-Scan Reticle Seeker Assembly (Adapted from Ref. 5)

To measure the tracking error, the position of the target is projected on the plane of the reticle as shown in Fig. 2-7. (Details of the reticle pattern and the ray paths through the telescope are omitted for clarity.) The tracking error is represented by a vector in the reticle plane. Its origin is at the reticle center (boresight axis), and its tip is at the intersection of the target line of sight and the reticle plane. This vector is quantified by its polar angle, which is relative to an arbitrary reference, and its magnitude, which is proportional to the angular tracking error. The tracking error magnitude is measured as a radial distance on the reticle. The minimum information required for tracking is the polar angle. For proportional control, it is necessary also to have a signal indicating the radial component.

The passing and "blocking of target energy requires relative motion between the reticle and the target image. There are two common methods used to provide this motion. One is spinning the reticle about the boresight axis (spin scan). The other is employing a stationary reticle and conically rotating (nutating) the telescope optical axis about the boresight axis (conical scan). When a spin-scan seeker is tracking perfectly, the target appears at the center of the field of view, and the target image is focused on the center of the reticle.

Tracking by a conical scan seeker causes the target image to rotate in a circle because of the coning motion of the telescope. Perfect tracking causes the target circle to be concentric with the reticle pattern, which is centered on the boresight axis.

In spin-scan seekers the reticle rotation produces a signal consisting of pulses as the target image is chopped by the reticle pattern. Fig. 2-8(A) shows an example of a spin-scan reticle. This reticle pattern is asymmetric, which results in a pulse-burst when the target-sensing sector of the pattern rotates over the target image and in a steady signal when the phasing sector covers the target image. The transmission of the phasing sector is 0.5, which matches the average transmission of the target-sensing sector and thereby minimizes the signal modulation caused by background objects of moderate size such as clouds. The phase of the modulated signal envelope encodes the polar angle of the tracking error vector. The magnitude of the tracking error vector can be encoded if the reticle pattern has radial bands, each with different numbers of image interrupters. This pattern gives a variable number of pulses in the pulse burst that depends on the magnitude of the tracking error vector. Thus the number of pulses per pulse burst is a measure of the magnitude of the angular tracking error.

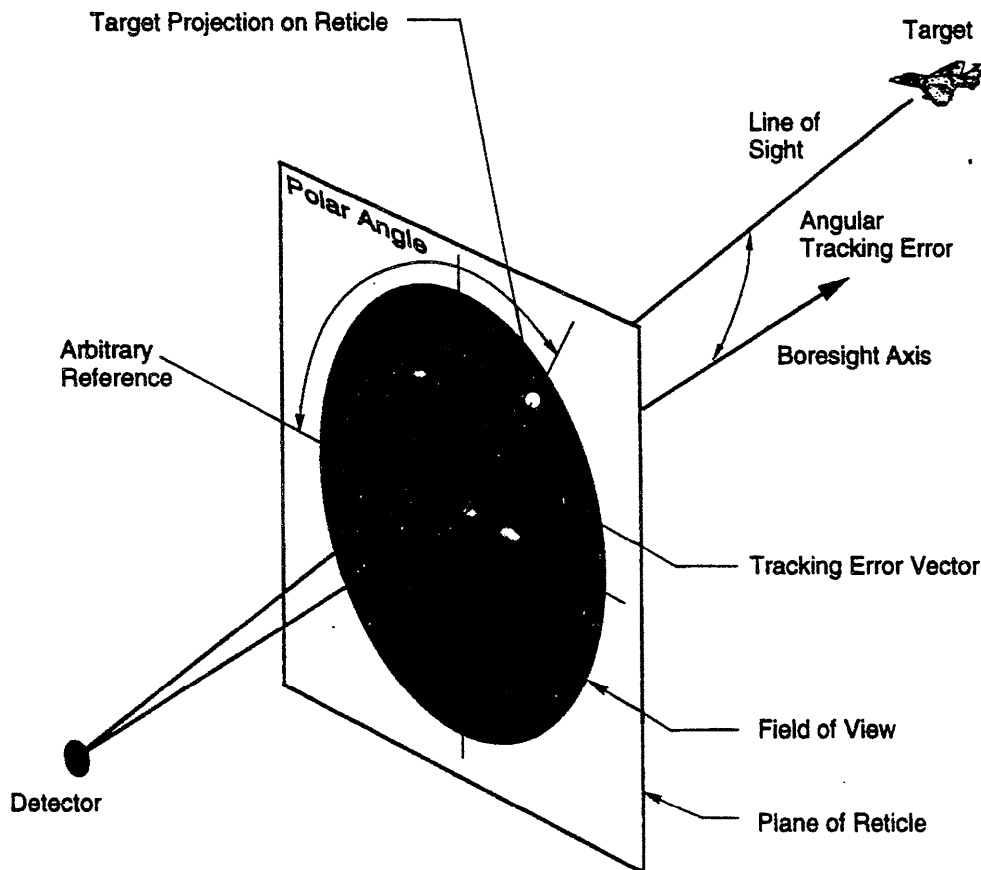


Figure 2-7. Projection of Tracking Error on Reticle Plane

-  Transparent
-  Opaque
-  50% Transmission

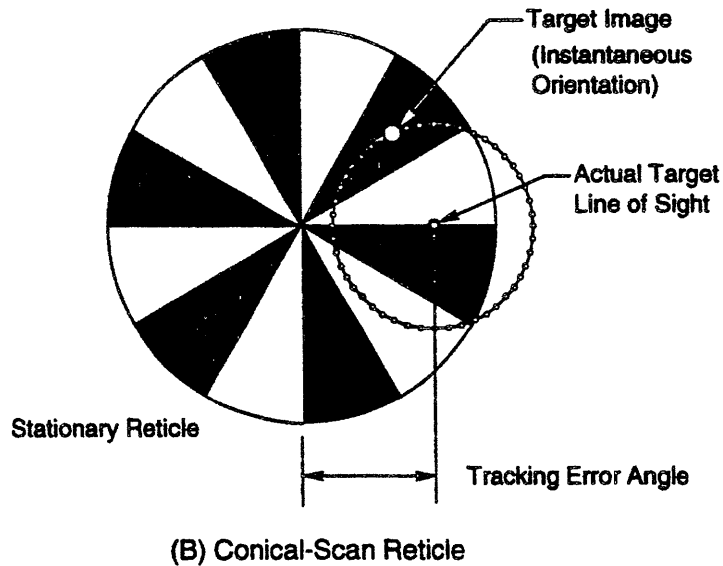
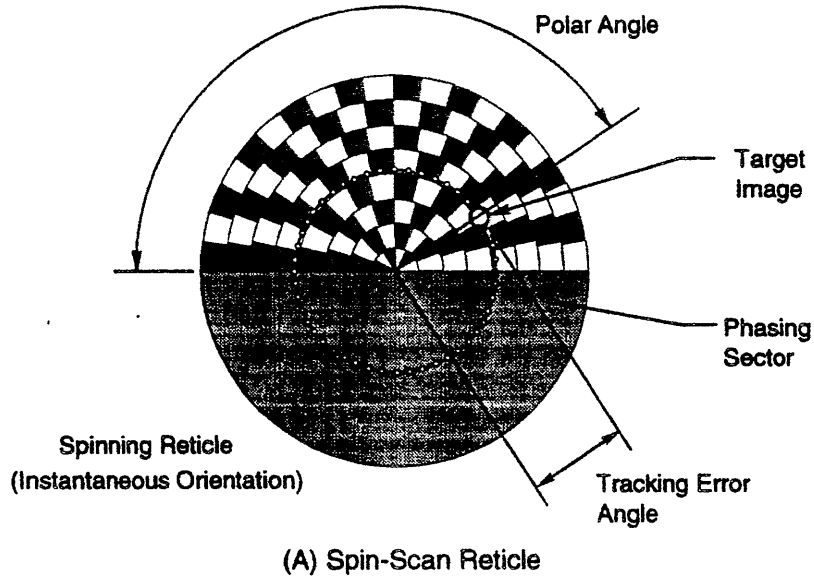


Figure 2-8. Genetic Reticle Patterns (Adapted from Ref. 4)

A major limitation of spin-scan trackers is that the carrier signal is lost when the tracking error is near zero; thus low tracking precision results. This limitation is overcome by conical scan trackers. In this case, a constant frequency signal is generated when the tracking error is near zero because the target image traces a circular path concentric with the reticle pattern. As the target position moves off-axis, as shown in Fig. 2-8(B), the circular path of the target image is no longer concentric with the reticle pattern. Thus a phased

modulation is produced that accurately indicates the target polar and radial position components in the field of view.

If the target image path on the reticle passes over pattern regions of uniform width, as in the spin-scan pattern of Fig. 2-8(A), an amplitude modulation (AM) demodulator is used to process the signal. If the target image passes over varying widths of reticle pattern, as in the conical scan pattern of Fig. 2-8(B), a frequency modulation (FM) demodulator is used.

2-2.1.1.2 Pseudoimaging

The continuing search for better methods of discriminating the background from the target and for discriminating between decoys and targets led to the development of pseudoimaging seekers. These seekers provide some of the advantages of fully imaging seekers (such as television cameras) but with less complexity. Although some of the features of the scene can be derived electronically, a full image is not developed. The tracking system used in pseudoimaging seekers is in the general class called scanning trackers (Ref. 4). In general, scanning trackers incorporate one or more detectors that have instantaneous fields of view that are small fractions of the total field of view. These detectors scan the total field of view repeatedly and thereby transform the scanned scene into a set of detector signals. Reference signals are also generated, derived from the scan motion, that represent the instantaneous position of each detector field of view within the total field of view. The signal processor identifies the target signal in the detector outputs, usually by a thresholding process, and samples the reference signals at that time to determine the target position in the field of view. These position signals are then used to point the seeker so that the target is centered within the total field of view.

Pseudoimaging seekers have numerous performance advantages over reticle seekers. The instantaneous field of view of each detector is smaller than that of reticle seekers, so it gives smaller background signals. On the other hand, pseudoimaging seekers do not lend themselves to optical spatial filtering, as afforded by reticles, to suppress large background objects. The burden of background rejection for pseudoimaging seekers is transferred to the signal processor. With relatively small instantaneous fields of view, pseudoimaging seekers preserve more of the scene information in the detector signals than reticle seekers. This permits resolution of multiple targets and selection of the desired target based upon observable criteria. For extended targets, i.e., larger than the instantaneous field of view of a detector, the signal processor can be designed to track a particular point on the target, such as the centroid, an edge, or some other identifiable point. Pseudoimaging seekers naturally lend themselves to the use of digital signal processing since the signal processors for this class of systems usually contain a substantial number of logic functions.

The rosette pattern, illustrated in Fig. 2-9, is an important scan pattern for pseudoimaging seekers. The rosette scan seeker uses a single detector with a scan pattern that contains a number of loops, or petals, emanating from a common center. A rosette scan is easily mechanized by means of two counterrotating optical elements, each of which deflects incoming rays by the same angle. The deflection elements can be optical prisms, tilted mirrors, or off-centered lenses. At any given instant only one point from the scene is focused on the detector. The relative positions of features in the scene can be determined since the relative pointing direction within the rosette scan is known at the moment each feature is detected.

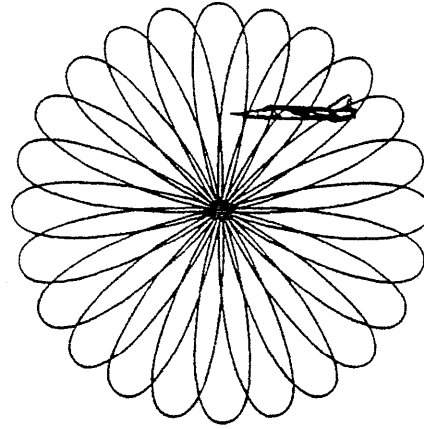


Figure 2-9. Rosette Scan Pattern (Adapted from Ref. 4)

2-2.1.1.3 Imaging

An imaging seeker uses either single or multiple detectors that produce video signals by means of a raster scan of the target scene (Ref. 4). Imaging sensors generally preserve more scene information than nonimaging sensors; thus imaging seekers can discriminate between objects by various criteria. This feature satisfies performance requirements beyond the capabilities of most nonimaging seekers. The primary advantages of an imaging seeker are its resistance to countermeasures, its discrimination of background and its contributions to fuzing logic.

Examples of imaging sensors are television cameras and focal plane array devices. A focal plane array is a pattern of individual detectors for the purpose of imaging. There are two basic methods of imaging with detector arrays. One is to focus the entire scene optically on a two-dimensional array and sample each element electronically by using a raster scan to produce scene images. The other method is to scan the scene mechanically to generate image data from a relatively small number of detectors (Ref. 3).

Systems that image only a portion of the total field of view on the focal plane array and move this instantaneous field of view about to cover the total field of view operate in a scanning mode. Systems that image the total field of view on the focal plane array operate in a staring mode.

One current approach to image processing is to couple a focal plane array with a microprocessor containing a pattern recognition algorithm to recognize and identify targets automatically.

2-2.1.2 Radio Frequency Seekers

An RF seeker is essentially a radar in which the antenna is employed to collect RF radiation reflected from the target. The RF power may be generated by systems onboard the target, by a target illuminator on the ground or by a transmitter onboard the missile. A passive RF seeker receives radiation generated by the target. A semiactive seeker receives reflected target echoes of radiation originally generated by a ground-based illuminator. An active seeker receives target

echoes of radiation originally generated and transmitted from onboard the missile. Various transmitted waveforms and processing methods are used to exact information. Seeker radar antennas take various physical forms, but the most common are parabolic dish or planar array antennas (Ref. 6) mounted on gimbals. A typical radar seeker employing a gimballed planar array is shown in Fig. 2-10.

Two-way attenuation of RF radiation by atmospheric effects is shown in Fig. 2-11 as a function of radiation frequency. Scattering losses caused by fog, drizzle, and rainfall are not significant y greater than they are for the standard atmosphere at frequencies below 3 GHz, but they rapidly become significant at frequencies greater than 10 GHz.

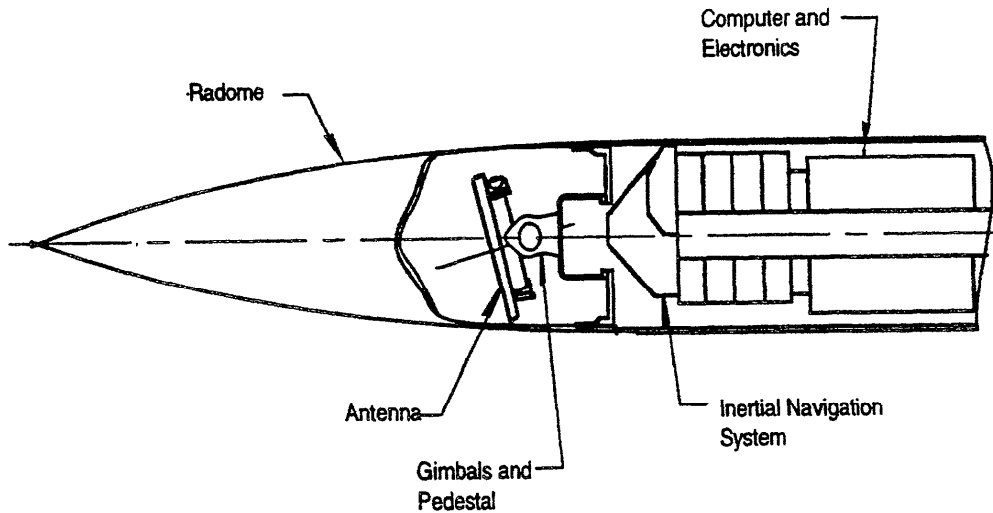
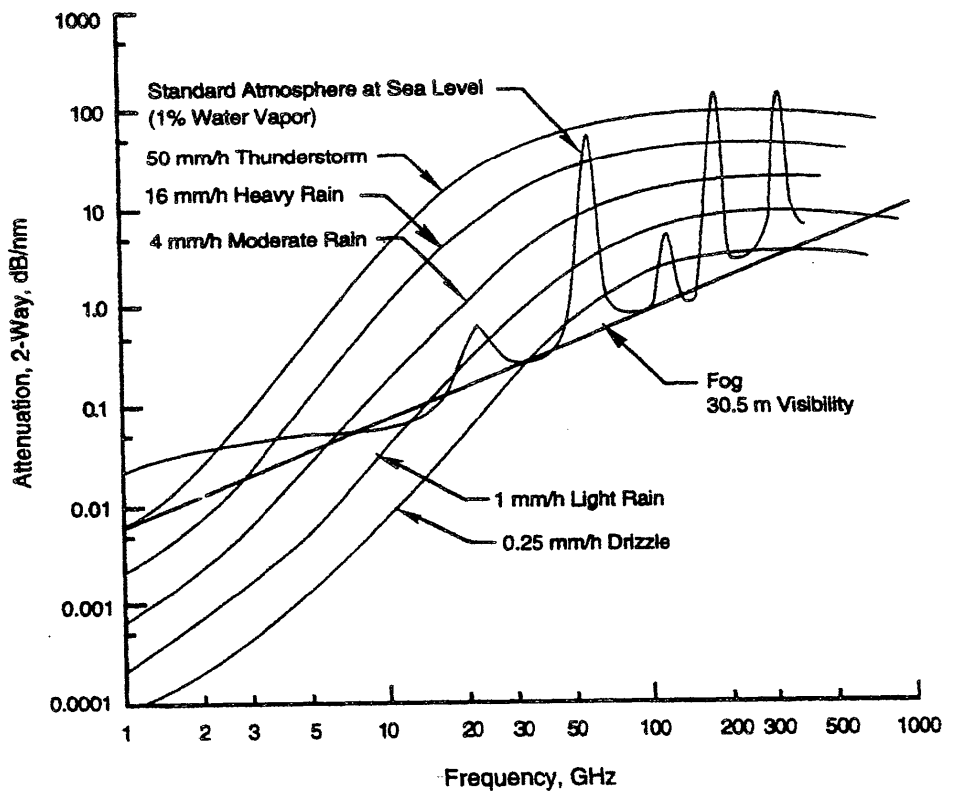


Figure 2-10. Typical Radar Seeker (Ref. 3)



NOTE: Each curve indicates attenuations independent of the other curves.

Reprinted with permission. Copyright © by Artech House, Inc.

Figure 2-11. Attenuation of RF Radiation by Atmosphere and Rain (Adapted from Ref.7)

Passive techniques are being employed in the design of new aircraft to decrease their RF signatures. Sophisticated electronic countermeasures (ECM) equipment is carried on-board aircraft to produce clutter or to introduce deceptive or confusing signals into the signal processors of the RF seeker. RF expendable decoys with signatures greater than the signature of the target have the potential to attract RF missiles away from the target. Missile seeker counter-countermeasures (CCM) techniques include Doppler and range tracking and sophisticated signal processing.

The basic radar types applicable to surface-to-air missiles are pulse radars, continuous wave (CW) radars, and pulse Doppler radars (Ref. 8). Seekers employing these radar types can be active, semiactive, or passive.

2-2.1.2.1 Pulse Radar

A pulse radar transmits a relatively short burst of electromagnetic energy, and the receiver listens for the echo. The antenna is designed to receive energy in one or more relatively narrow (pencil) beams (also called lobes). The echo received from targets in these beams is used to track the target. Range to the target can also be determined by observing the time it takes for the pulse to return.

2-2.1.2.2 Continuous Wave Radar

A continuous wave (CW) radar transmits continuously rather than by pulses, and as a result it cannot determine the range to the target without some additional modulation. The change in frequency between the transmitted signal and the echo, caused by the Doppler effect, can be used to determine the component of relative target velocity along the line of sight. This is useful for discriminating the moving target from stationary clutter or from decoys that have velocities different from that of the target. CW radars have two major disadvantages. One is the inability to measure range; the second is the transmitter signals leak directly into the receiver, a disadvantage that requires excellent system stability and large dynamic range to give good performance.

2-2.1.2.3 Pulse Doppler Radar

Pulse Doppler radar combines the pulse operation with the use of Doppler from the CW radar to measure directly both range and range rate or radial velocity of targets. The Doppler principle makes it possible for a CW radar to detect a moving target, and it permits a pulse radar to detect a weak signal from a moving target in the presence of strong clutter signals. By using Doppler shift and special filters, the return from a moving target can be detected by pulse Doppler radar. This is referred to as moving target indicator (MTI).

This type of radar transmits pulses just as the pulse radar does and can, therefore, use time to determine range. Also, when the signal is received, its frequency can be compared with the transmitter frequency to determine radial velocity based on the frequency (Doppler) shift. Use of Doppler filters permits tracking the target in velocity, a useful discriminant against some types of countermeasures. Because the

bandwidth of the pulses is large relative to Doppler frequency shifts, the signal must be coherent in order to measure velocity. A coherent signal is one in which the phase is consistent from one pulse to the next, as if each pulse had been cut from a single continuous wave. Another useful feature of coherent pulse Doppler radars is that they are better able to discriminate against noise than noncoherent radars.

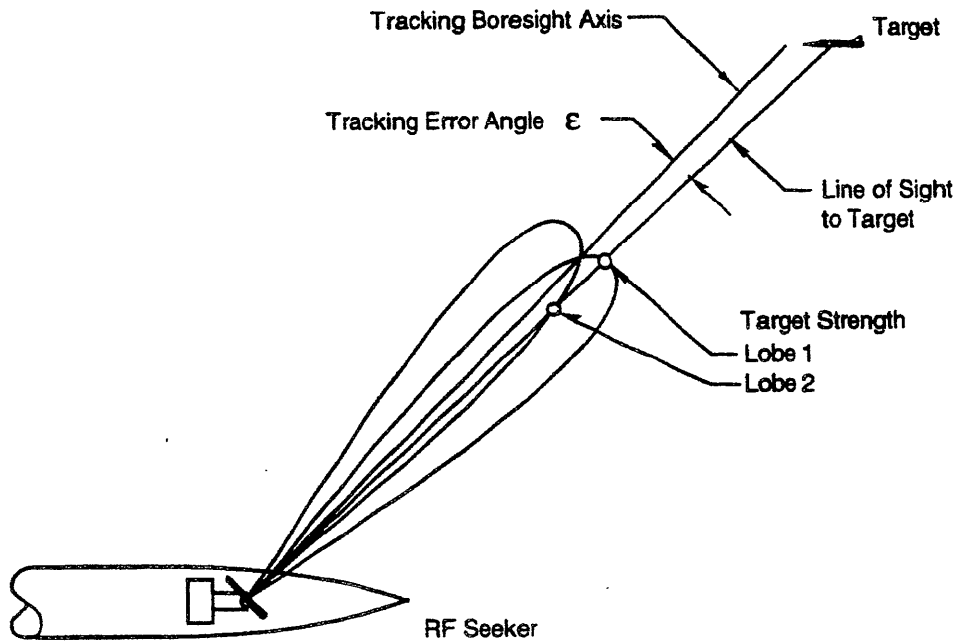
Use of the Doppler effect to discriminate clutter makes possible a reliable capability of looking down against the earth background under certain engagement conditions. Tracking in frequency (velocity gating) and range (range gating) is a powerful tool used to discriminate against decoys.

2-2.13 Angle Tracking Methods

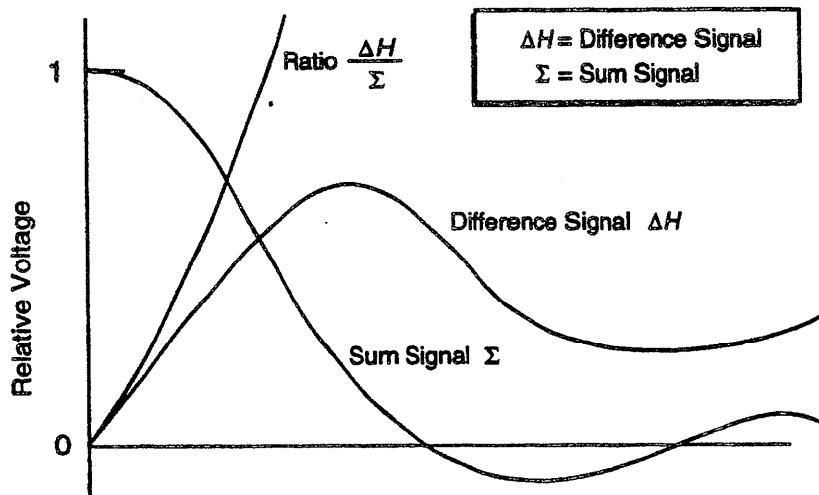
Several methods are used to detect angular errors in tracking a target with radar. Among these are sequential lobing, conical scanning, and two forms of monopulse tracking (Ref. 8). All of these methods are based on the same general principles but are implemented in slightly different ways. They all make use of the fact that the magnitude (or phase) of the target return signal depends on the angle between the line of sight to the target and the axis of the radar antenna lobe pattern. When the target is located exactly on the lobe axis, the magnitude of the target return signal is greatest. Other factors, however, also affect the magnitude of the target signal, such as target radar cross section, aspect angle, and range. Therefore, a single lobe is not sufficient to determine the magnitude of the angular tracking error. Also the radial direction of the tracking error cannot be determined from a single lobe because of lobe symmetry about its axis.

Tracking usually is implemented by using two separate tracking channels—one corresponds to the azimuth plane and the other to the elevation plane (Ref. 6). At least two lobes in each plane are required to determine the components of the tracking error (Fig. 2-12(A)). In a given plane the axes of the two lobes are separated from each other by a small angle and are symmetric about the boresight axis of the tracker. Target strength is measured in each lobe and converted to a voltage. The voltage difference between the two lobes is a measure of the tracking error. A target line of sight coincident with the tracker boresight axis (zero tracking error) forms equal angles with each of the radar lobe axes, and the voltage difference between the signals from the lobes is zero, which indicates zero tracking error. As the target moves off the tracking boresight axis, it moves away from one lobe and toward the other and creates a voltage difference between the lobes, as shown in Fig. 2-12(A). For small tracking errors this difference is approximately proportional to the magnitude of the tracking error as shown in Fig. 2-12(B). In practice, the voltage difference normalized by the voltage sum Σ is used to indicate the magnitude and direction of the tracking error.

The reflection of RF radiation from the target is not uniform; it varies in magnitude and phase depending on the aspect angle (azimuth and elevation relative to the target) and



(A) RF Tracking Lobes



Reprinted with permission. Copyright © by Artech House, Inc.

Figure 2-12. RF Tracking (Adapted from Ref. 6)

on the particular target surface from which it is reflected. Because of the complex geometry of the target surface, glint points occur and disappear as the aspect changes. An RF seeker integrates the signals from all glint points within the field of view, resulting in an erratic track which contributes to miss distance. Under some circumstances the track point may be located completely off the physical target.

Another phenomenon contributing to RF seeker tracking errors is the refraction of the received radiation by the aerodynamic shape of the radome of the seeker. The degree of re-

fraction changes as the angular attitude of the missile changes. The component of guidance commands resulting from this change in refraction angle can couple with the airframe dynamics and produce oscillations in the missile flight path that increase miss distance. To make the radome hemispherical in order to eliminate refraction, however, is impractical because the radar antenna (and, therefore, the radome in which it is housed) must have an aperture as large as possible, and the aerodynamic drag from a large hemispherical missile nose would be unacceptable.

2-2.1.3.1 Sequential Lobing

An early technique used for radar tracking is sequential lobing, which is switching the antenna boresight from one side of the tracked target to the other. The amplitudes of the returns will be equal when the target is centered between the switched positions of the antenna. If the target is not centered, the amplitudes will differ; this difference is the tracking error signal. A major disadvantage of sequential lobing is that the target signal strength can fluctuate during the short interval required to switch lobes, which introduces errors into the estimate of the tracking error.

2-2.1.3.2 Conical Scanning

Conical scanning is implemented by scanning the axis of a single beam around the surface of a cone with the cone apex at the radar and the cone axis coincident with the boresight axis of the tracker. Once each revolution the beam appears on either side of the cone axis in a given plane. Target return signals are measured and compared for these two lobe positions for each tracking channel in order to estimate tracking error. The disadvantage of target fluctuations between lobes also is inherent in conical scanning.

Although it is similar to sequential lobing, conical scan is preferred in most applications since it suffers less loss of signal strength and the antenna systems are usually less complex.

2-2.1.3.3 Monopulse Tracking

As its name implies, monopulse tracking forms the two lobes per tracking plane with a single pulse. That is, both lobes are formed at the same time; thus the problem of target fluctuation between lobes is eliminated. One implementation of monopulse tracking uses amplitude comparison of the target return signals to estimate the tracking error, as in sequential lobing and conical scanning. The other implementation makes use of the fact that the phase difference between the two returns is proportional to the angular tracking error.

Monopulse radar provides a better tracking technique than the other types of radars, but in many applications in which the ultimate in performance is not needed, the conical-scan radar is used because it is less costly and less complex.

2-2.2 AUTOPILOT

Typically, the output from the seeker or ground-based guidance components is an electrical signal that contains information on the direction of the current heading error of the

missile and some relative measure of the magnitude of the error. The autopilot converts the steering error signals into control surface deflection commands (Fig. 2-13) to correct the course of the missile.

The autopilot is a link between the function that indicates a change of heading is needed (guidance processor) and the mechanism that can change the heading (control system). The guidance processor—which may be located on the ground or contained in the seeker signal processor, autopilot, or both—must accurately implement some prescribed guidance law to ensure that the control commands it develops will guide the missile close to the target.

The autopilot translates the commands produced by the guidance processor into a form suitable for driving the control actuators and limits the commands as necessary to maintain flight stability and airframe integrity (Ref. 3). The design of the autopilot depends on the aerodynamics of the missile airframe and the type of controls employed. Since some guided missiles must perform over extreme ranges of flight conditions, the autopilot may be designed to compensate for some of the nonlinearities in the aerodynamics in order to ensure a stable system. If the missile design requires roll control, the autopilot may sense roll position or roll rate and issue appropriate control commands. Some missiles require control to compensate for the acceleration due to gravity; in this case the autopilot receives the necessary sensor data and determines the direction and magnitude of the commands required to compensate for gravity. The autopilot may introduce airframe damping to prevent large overshoots in response to maneuver commands or to compensate for dynamic instabilities. It may contain amplifiers, integrators, and mixing circuits that send signals to the proper control surface actuators. In some applications missile maneuver commands may be produced solely on the basis of the seeker output.

2-2.3 CONTROL

Once the guidance processor has determined the magnitude and direction of the error in the missile flight path and the autopilot has determined the steering command, the missile control system must adjust the control surfaces to produce the acceleration required to correct the flight path. This corrective acceleration is applied in a lateral direction (perpendicular to the missile flight path) to change the direction of the missile velocity vector (Fig. 2-14). Intentional acceleration along the flight path to correct the magnitude of the

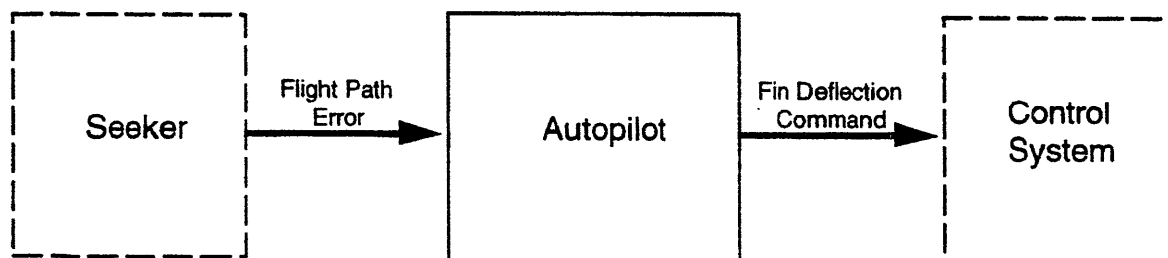


Figure 2-13. Function of the Autopilot

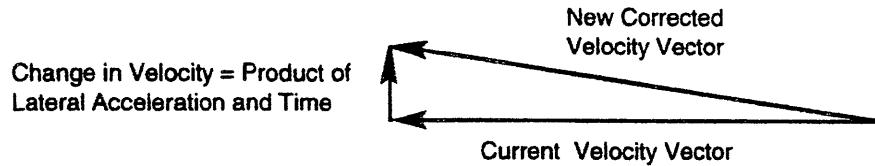


Figure 2-14. Acceleration Required to Change Direction of Flight

velocity vector (for early or late arrival) is a potentially useful concept, but it is not presently used to guide surface-to-air missiles because of the complexity of throttling solid propellant motors.

2-2,3.1 Lateral Acceleration

Lateral acceleration of a missile requires a lateral force. The force required to alter the flight of a missile can be generated by different methods; however, the method currently employed in most United States (US) Army surface-to-air missiles is development of aerodynamic lift in a direction perpendicular to the flight path.

in an airplane, lift is produced primarily by the flow of air over the wing, as shown schematically in Fig. 2-15(A). As the angle of attack-the angle between the chord of the airfoil and the velocity vector-is increased, the magnitude of the lift force is increased to the point at which stall occurs. Aerodynamic lift on a missile is analogous to lift on an airplane. Although the missile usually has very small wings or none at all it may have fins, and when the missile body comb-

ined with its fins is inclined by an angle of attack as shown in Fig. 2-15(B), lift is produced. Lift force is approximately proportional to the square of the speed. Thus the relatively high speed of a missile is sufficient to achieve lateral accelerations many times the acceleration due to gravity (many g's), even though the area--body plus fins-on which the aerodynamic pressure acts is relatively small.

For aerodynamic lift to be generated, the missile must achieve an angle of attack-angle between the missile centerline and the missile velocity vector. The steering command from the autopilot calls for a lateral acceleration to correct the error in the missile heading. This command may be a direct acceleration command, or it may be an indirect command, such as calling for fin deflection angles or fin actuator torques. In any case, it is a lateral acceleration that is to be achieved, and it is the task of the control system to cause the missile to assume an angle of attack that will produce that acceleration.

A moment, i.e., a force multiplied by a lever arm, is required to cause a missile to rotate to achieve an angle of at-

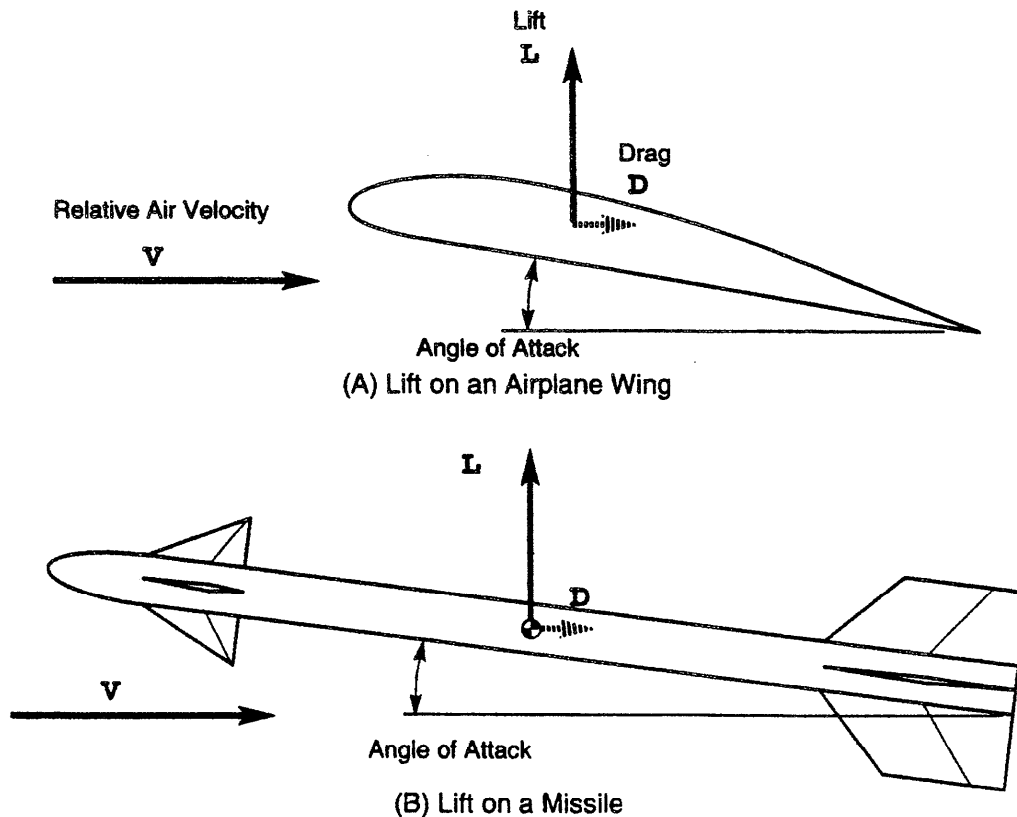


Figure 2-15. Aerodynamic Lift

tack. This moment can be developed by several means, but the methods currently used in US Army surface-to-air missiles are thrust vector control and aerodynamic fin deflection. The latter is predominating. In thrust vector control the exhaust gases from the propulsion system are deflected laterally by a small angle so that the resultant thrust vector is no longer aligned with the center of mass of the missile (Ref. 3). This misalignment causes a moment in addition to the translational force of the thrust. In Fig. 2-16 the thrust force F_P acts at a lever arm ℓ_{arm} to produce a moment on the missile. In aerodynamic fin deflection the airflow over the deflected control surfaces produces an aerodynamic moment on the missile that causes the missile to rotate relative to its velocity vector and thus achieve an angle of attack. Fig. 2-17 illus-

trates the production of an aerodynamic moment on the missile for two different locations of the control surfaces.

2-2.3.2 Canard Control

Fig. 2-17(A) shows how an aerodynamic moment is generated when the control surface is a canard fin (located at the front of the missile). With the canard fin rotated as shown, a lift L (similar to that on an airplane wing) is developed on the fin itself. This lift, acting on the lever arm ℓ_{arm} relative to the missile center of mass, produces a nose-up moment when the fin is deflected as shown. The magnitude of the aerodynamic moment is proportional to the lift L that acts on the control surface. The lift in turn is dependent on the deflection angle of the control surface. Thus the control system can control

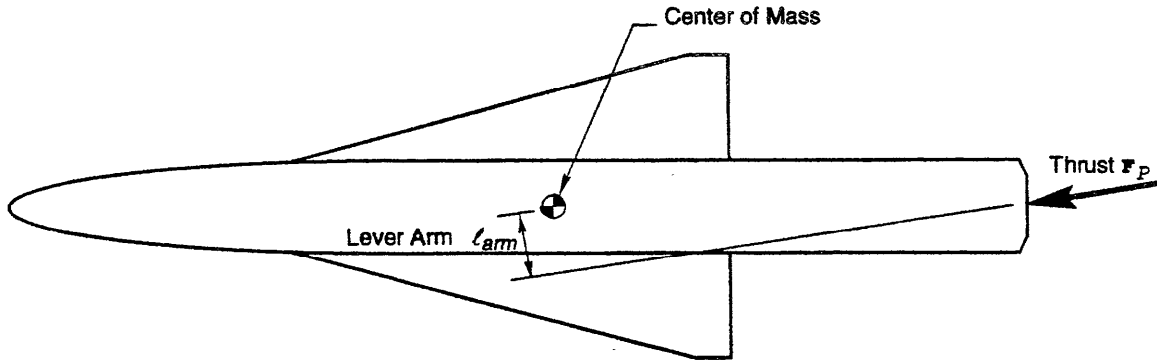


Figure 2-16. Moment Produced by Thrust Vector Control

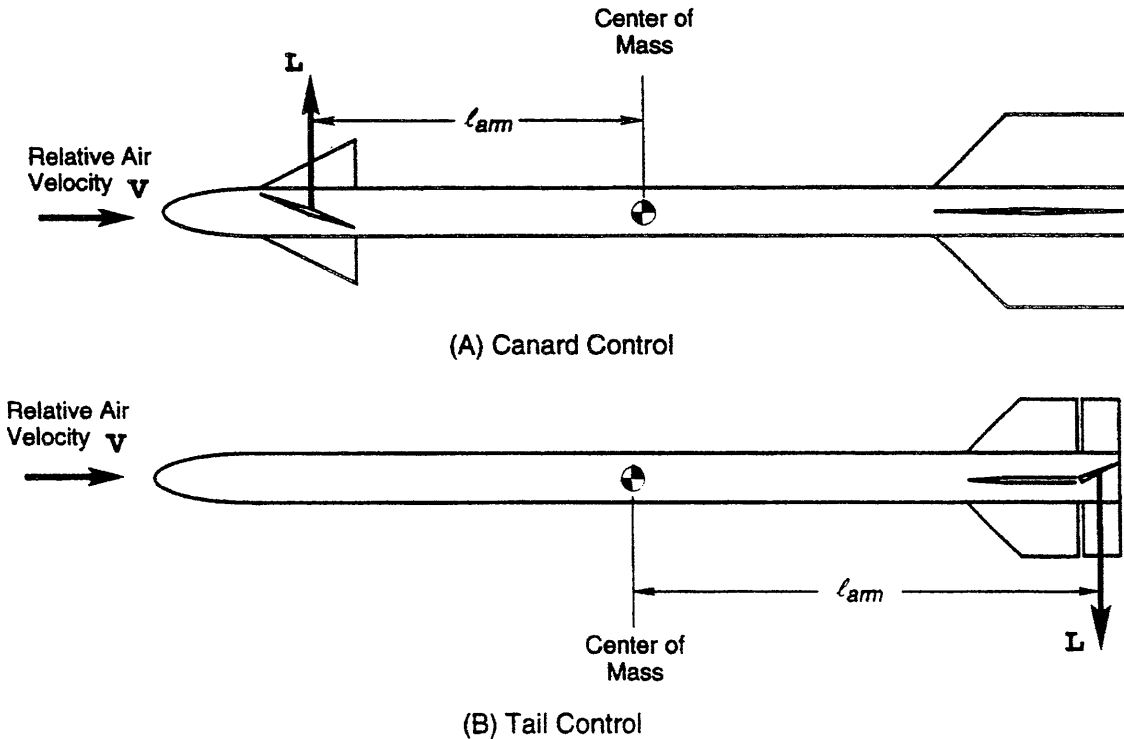


Figure 2-17. Aerodynamic Moment Produced by Control-Surface Deflection

the magnitude of the aerodynamic moment by controlling the angle of rotation of the control surface.

When the missile has a finite angle of attack, a restoring moment is generated by aerodynamic lift on the tail surface. Since the tail surface is located behind the center of mass of the missile, this restoring moment is in a direction opposing the control moment generated by the canard fins. The magnitude of the restoring moment is approximately proportional to the magnitude of the angle of attack therefore, as the angle of attack increases-as a result of fin deflection-the restoring moment increases. When the angle of attack reaches the point at which the restoring moment equals the control moment, a balanced condition-called the trim condition-is achieved. When the fins are initially deflected, a missile has a transient response that depends on the magnitudes of the moments, the moment of inertia of the missile, and the aerodynamic damping characteristics of the missile; the steady state result of the fin deflection is the trim angle of attack.

The fact that the lever arm l_{arm} is relatively long results in a large aerodynamic control moment that rotates the missile with a high angular rate to the desired angle of attack. Fast response of the missile to maneuver commands is a very important characteristic for engaging maneuvering targets.

2-2.3.3 Tail Control

Fig. 2-17(B) shows the use of tail surfaces for control. Either the entire tail fin is only the trailing edge is hinged as shown. With tail control the lift on the control surface is in the direction opposite to the desired lateral acceleration of the missile so that the lift on the control surface subtracts from the overall missile lift (Ref. 3). This can result in slightly decreased lateral accelerations and slightly increased response time. Another disadvantage of tail control is that long electric and hydraulic connections are required from the guidance package near the nose of the missile to the tail control actuators. Also downwash flow from the body and fins forward of the tail control surfaces changes rapidly with changes in the angle of attack and thus makes the trim angle of attack difficult to predict.

2-2.3.4 Wing Control

Some missiles have small wings located near the center of mass of the missile. When these wings are used as the control surfaces, the lift on the wing-which may be a substantial portion of the overall missile lift-can be developed very quickly without having to rotate the entire missile to an angle of attack. Wing control is not presently used in US Army surface-to-air missiles.

2-2.3.5 Control Servomotor

The device that converts a control command horn the autopilot into a control surface deflection is called a servomotor, often shortened to servo. A control servo usually includes amplification of the commanded steering signal, application of the amplified signal to a solenoid-operated con-

troller, application of controlled high-pressure hydraulic or pneumatic fluid to an actuator, and mechanical actuation (rotation) of the control surface.

Various types of auxiliary power supplies have been used to provide hydraulic or pneumatic pressure. The type most often used is a hot gas system in which propellant-type fuel is converted into high-pressure gas in a combustion chamber. This gas is then used to drive a hydraulic pump that provides power to hydraulic actuators, or the hot gas is used directly to power pneumatic actuators. The amount of fuel available to power the control system is limited; when the fuel is exhausted, the missile becomes uncontrollable.

In the operation of a pneumatic servo (Ref. 9) gas flows continuously from the supply source and exhausts through the pneumatic servo nozzles with pressures P_1 and P_2 . The exhaust flow is regulated by a flapper-nozzle valve. By decreasing the gas flow through one nozzle and increasing the flow through the other nozzle, the pressure is increased on one of the actuator pistons and reduced on the other. This pressure difference causes one piston to move down and the other to move up and thereby controls the deflection angle of the control surface. The control surface may be aerodynamically unbalanced about the hinge point such that a restoring torque is produced (aerodynamic hinge moment). The resulting deflection angle of the control surface is determined by the balance point between the aerodynamic hinge moment and the hinge moment generated by the actuator torque. This type of servo is called a torque-balance servo. A torque-balance servo provides a torque on the control surface that is proportional to the steering command signal. The angular deflection of the control surface is a function of the aerodynamic hinge moment acting on the surface and the power of the actuator. Large hinge moments require large, powerful actuators. Atypical mechanization of a torque-balance servo is illustrated in Fig. 2-18.

The angular position of the control surface maybe sensed and returned to the amplifier to form a feedback loop. This type of control servo produces a control surface deflection that is proportional to the input steering command signal.

2-2.4 WARHEAD AND FUZE

The ultimate objective of a guided missile is to disable or destroy the target. Warheads containing high explosives are typically used as the disabling or destroying mechanism. For most guided missiles the guidance accuracy is such that the missile will not always actually impact the target but will usually pass close to it. Near misses can be converted to successful intercepts by the use of proximity fuzes that sense the approach of the missile to the target and initiate a warhead detonation command.

2-2.4.1 Warhead

A bare high-explosive charge produces a high-pressure shock wave that radiates spherically from the burst point. The overpressure (pressure above ambient), the dynamic pressure (related to the air density and particle velocity be-

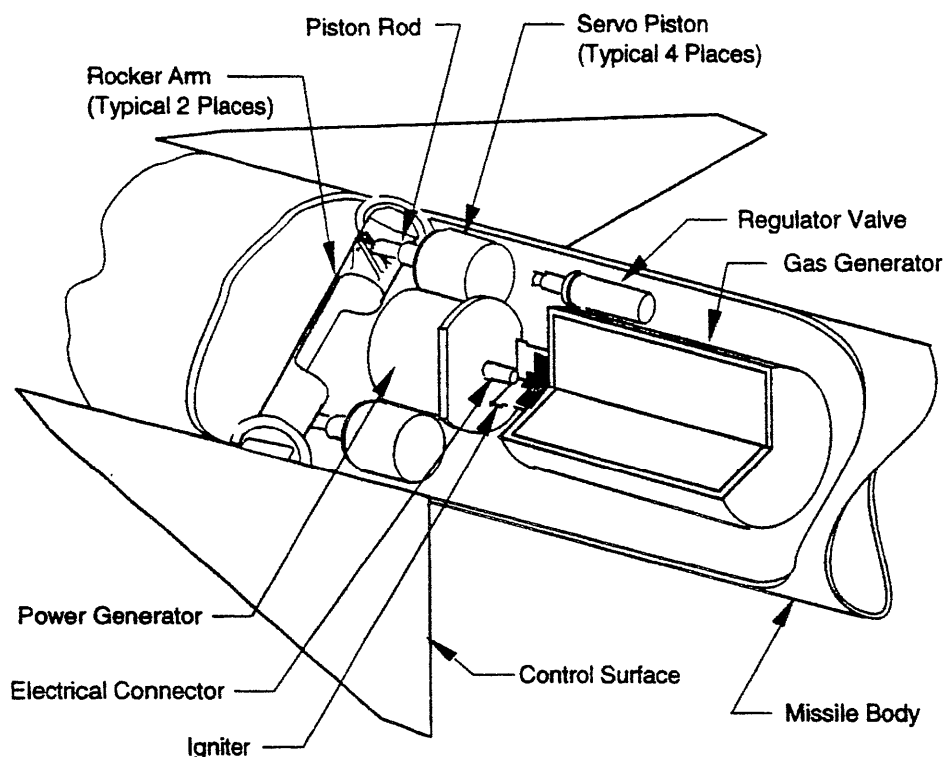


Figure 2-18. Torque Balance Servo Conjunction (Ref. 5)

hind the shock wave), and the time variation of these pressures interact with the target structure to cause damage. This damage mechanism is called Mast. The relationship between the magnitude of blast damage and the radial distance from the burst point to the structural surface of the target depends on the weight and type of the high-explosive charge, the ambient atmospheric air density, and the design of the target structure. The ability of blast effects to cause target damage falls off sharply with increased range from the burst so sharply in fact that blast is not an effective damage mechanism unless the miss distance is very small or the high-explosive charge is very large.

To increase the radius in which significant target damage can be achieved, the explosive charge is enclosed in a metal case. On detonation of the charge the case breaks into fragments with high kinetic energy that carries them greater distances from the burst point. Fragments create damage by imparting energy and momentum to the impacted target structure and internal components. The effectiveness of fragments depends on their mass, velocity, material, and areal density (number of fragments per unit area of target surface). Fragment velocity falls off rapidly with range from the burst point, caused by aerodynamic drag (slowdown), and areal density decreases with range because at greater distances the

same number of fragments cover a larger area. Thus the ranges at which fragments are effective are also limited but not as limited as the ranges for blast effects. If the warhead energy is distributed isotropically (equal distribution of energy in all directions from the burst point), the radius of warhead effectiveness is much less than it would be if the energy were focused. Because of their limited range of effectiveness, warheads with isotropic energy distributions are never used. Many different warhead concepts have been developed to focus the available warhead energy into preferred directions at the expense of other directions.

Usually warhead energy is directed into a relatively narrow spherical sector approximately perpendicular to the missile axis. In a static firing as in a warhead test arena across section through the sector swept out by fragments appears as fragment beams, illustrated by the static pattern in Fig. 2-19(A). In an actual engagement the perpendicular velocity of any given fragment caused by the warhead detonation is added vectorially to the velocity of the missile at the time of detonation, giving the velocity of the fragment relative to the atmosphere. The result is a sweeping forward of the fragment beams. Subtracting the target velocity vector gives the velocity of the fragment relative to the target as shown by the dynamic pattern in Fig. 2-19(B).

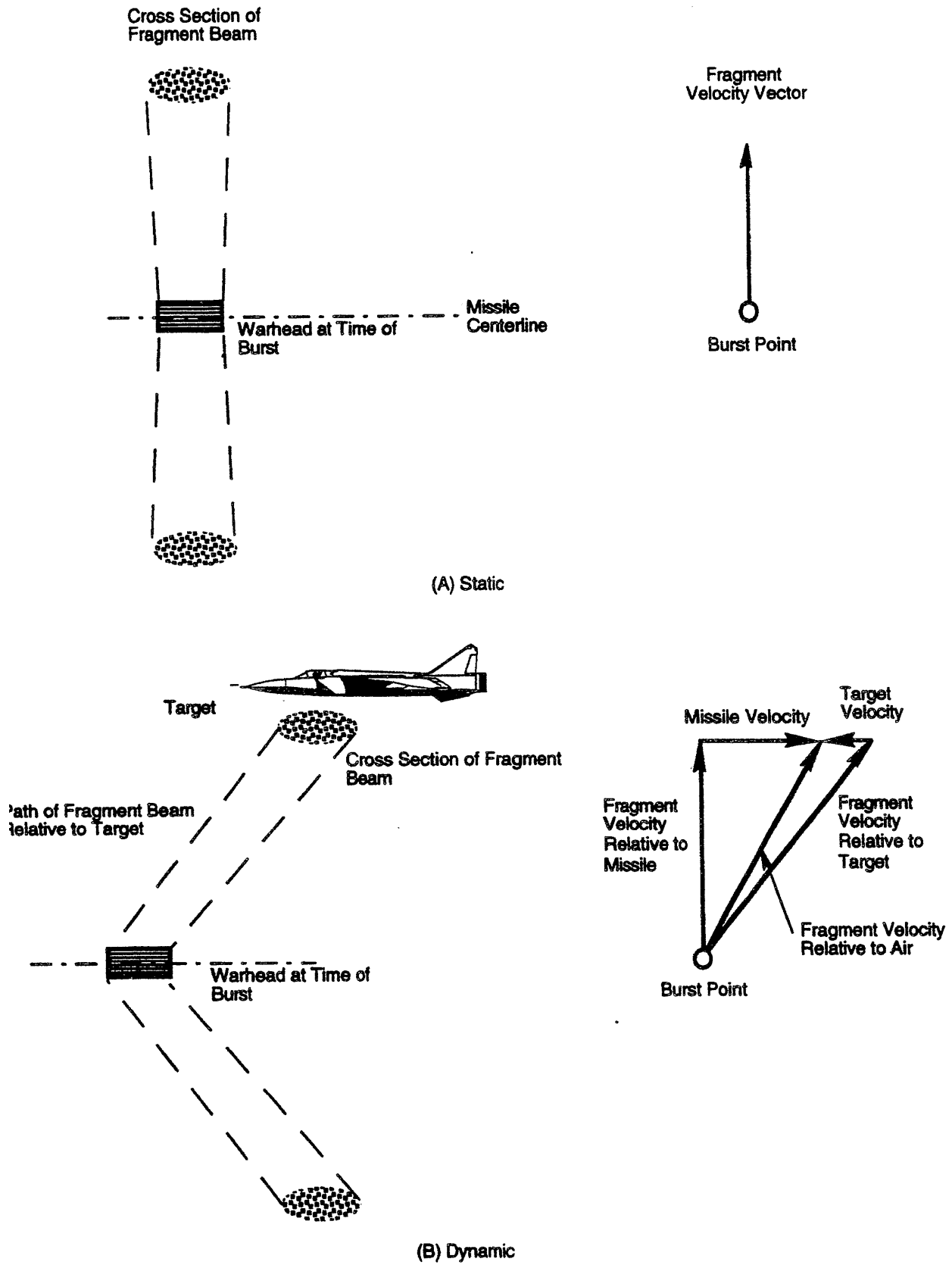


Figure 2-19. Warhead Fragment Patterns

2-2.4.1.1 Shaped Charge

One concept that dramatically focuses the warhead energy is the shaped-charge warhead. This warhead is composed of many shaped charges directed radially outward from the centerline of the missile. Each shaped charge expels hypervelocity particles of a metallic liner into a very narrow, concentrated beam. The extremely high velocity of the fragments adds another damage mechanism, called the vaporific effect, which resembles the effect of an explosion occurring inside the target structure. Inspection of structures damaged by this mechanism shows aircraft skins peeled outward rather than the inward deformation that would be typical of slower fragments and external blast. In addition, between the shaped-charge spokes are areas of enhanced external blast effects, which reach to much greater ranges than blast effects from isotropic warheads.

2-2.4.1.2 Continuous Rod

Continuous rod warheads are designed with a cylindrical casing composed of a double layer of steel rods. The rods are welded in such a way that each end of a rod is connected to an end of a neighboring rod. As the rods are blown out radially by the explosion, they hang together forming a continuous circle. The objective of the continuous rod warhead is to cut long slices of target skins and stringers and thus weaken the structure to the point at which aerodynamic loads will destroy it. When the continuous ring of rods reaches its maximum diameter, it breaks up, and the lethality drops off markedly.

Continuous rod warheads are effective in tail chase engagements in which they can slice halfway through the fuselage of a small- to medium-sized target. Engagements from the forward hemisphere are less effective because the rod breaks up on impact with the leading edge structure of the wing.

2-2.4.1.3 Fragment

Most surface-to-air missiles use blast-fragment warheads. Although damage is caused primarily by the fragments, a bonus is obtained from coincident blast effects if the miss distance is small enough.

The approximately cylindrical metal warhead casing is fabricated by scoring or other means so that the explosion of the charge breaks the casing into many discrete fragments of uniform shape and size. These fragments fly out radially, approximately perpendicular to the centerline of the missile, and form a circular band of fragments that expands in diameter (Fig. 2-19).

Fragments are not very effective in causing target structural damage except at close miss distances at which a high density of fragments can be applied. Fragments are very effective, however, against target components such as a pilot, fuel cells, wiring, plumbing, electronic control equipment, electronic armament equipment, and engine peripheral equipment. Even though the fragments are focused into a relatively narrow beam, the expanding radius increases the area containing fragments and reduces the number of fragments

per unit area. Given that the fragment beam intercepts a vulnerable component of the target, the probability of at least one fragment impacting the component depends on the areal density of fragments at the range of intercept.

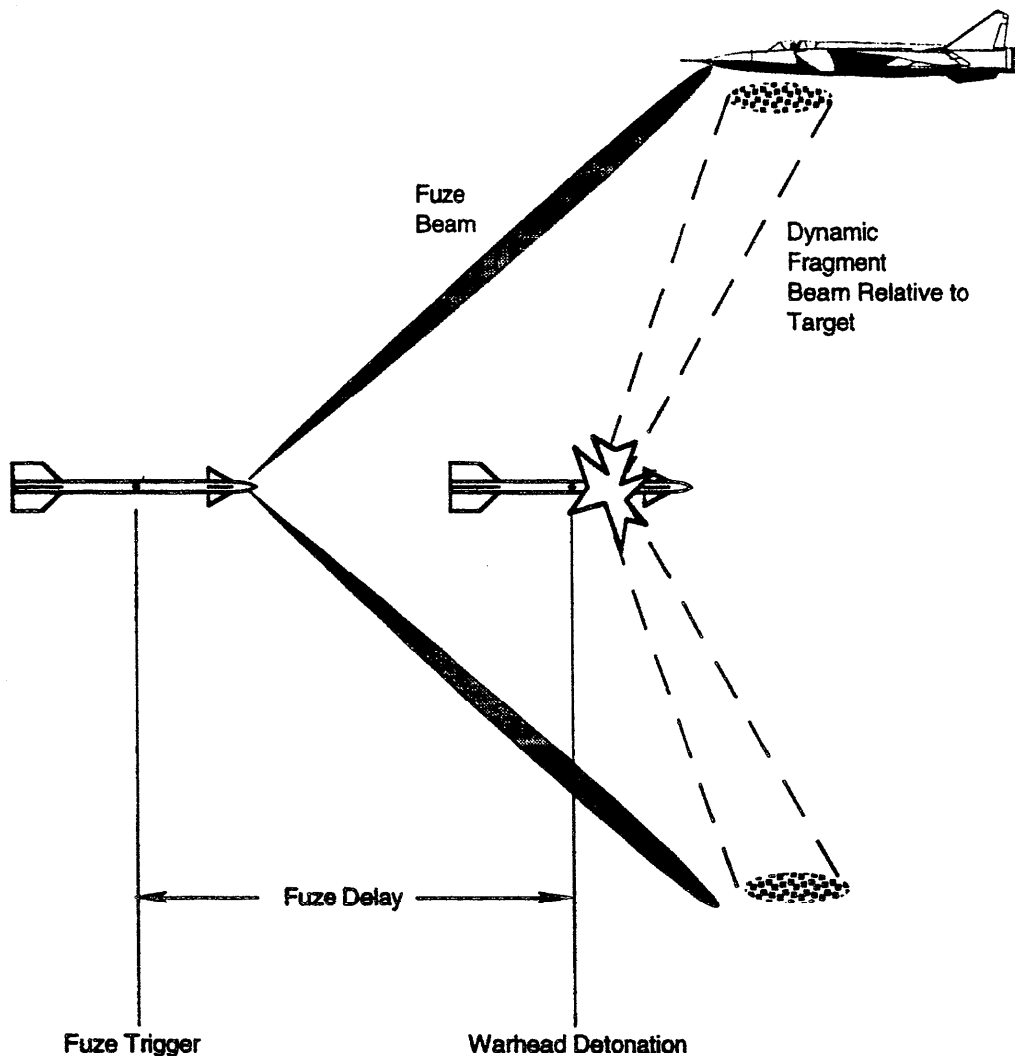
In the design of a fragment warhead there is a tradeoff to be made involving the size (weight) of individual fragments. If the fragments are made very small (2 g (30 grains)), the fragment beam is composed of thousands of fragments, which produces a high areal density. But small fragments slow down in the air more quickly than huge fragments, and the number of target components that are vulnerable to small, slow-speed fragments is significantly less than for larger, faster fragments. Different warhead designs cover the spectrum from small fragments to large, rod-shaped fragments weighing several hundred grains.

2-2.4.2 Fuze

The fuze is the device that initiates the signal to detonate the warhead. Most surface-to-air missiles contain two fuzes—an impact fuze that is triggered by impact with the target and a proximity fuze that is triggered by a close approach to the target.

Focusing the warhead energy into a narrow beam increases its radius of effectiveness (lethal radius), but it does so at the cost of increased sensitivity to the timing of the detonation. To be effective, a warhead must be detonated at a time when its expanding fragment beam will intercept a vulnerable part of the target. In a typical nose-on engagement the time during which a detonation will result in fragment impacts on the target is approximately 12 ms. The fuze must sense the approach to the target and initiate the firing signal so that detonation occurs within that period. Often the fuze beam is swept forward at a greater angle than that of the anticipated dynamic fragment beam, allowing a short delay time between fuze triggering and actual warhead detonation as illustrated in Fig. 2-20. For a fixed Fuze beam angle the optimum fuze delay varies considerably for different engagement velocities and aspect angles because of the variation in the angle of the dynamic fragment beam. Various schemes have been devised to estimate closing velocity as a basis for adaptively setting the fuze delay time (adapting to the situation in real time), but to reduce costs and complexity, often a delay time is selected that is a compromise among all anticipated engagement conditions.

A number of different types of fuzes have been developed. Early radio proximity fuzes had poorly shaped fuze beams that changed shape (in the wrong direction) when the relative velocity changed. Modern fuzes have well-formed, narrow, fixed beams. They may be active, i.e., RF or laser energy is transmitted and echoes from the target are received, or they may be passive, i.e., sensing IR energy radiated from the target or exhaust plume. Sometimes signals from the seeker can be used to arm the fuze. A new generation of fuzes is being developed that takes advantage of onboard microprocessors and imaging seekers to determine the optimum fuze delay time based on relative velocity, aspect angle, and target size.



Missile and warhead motions shown are relative to the airplane.

Figure 2-20. Fuze and Warhead Relationships

Fuzes usually are designed with some fixed maximum range that corresponds approximately to the lethal radius of the warhead to prevent fuzing on terrain, foliage, or sea waves in low-altitude engagements. A major consideration in the design of modern fuzes is the reduction of the effectiveness of potential countermeasures against them.

2-2.4.3 Lethality

The lethality of a missile system is the ultimate measure of its effectiveness; however, reliable estimates of kill probability are difficult to obtain. The most reliable means of estimating kill probability is to flight-test a missile with live warheads against drone targets. Uncertainties arise even with flight testing because high-confidence results require many tests and testing is extremely expensive. In addition, it is difficult to reproduce combat conditions and environments in a controlled test on a test range. Different aircraft have differ-

ent vulnerabilities, and enemy aircraft are not available for use as drone targets.

Static tests in warhead test arenas provide data on warhead patterns and energy distributions, and on the vulnerabilities of various target components to the different damage mechanisms; however, dynamic and high-altitude effects are difficult to obtain without flight testing. Fuze tests are performed in the laboratory and in dynamic test arenas to provide data on fuze performance, but the proximity to disturbing factors such as the ground, target support structures, and instrumentation introduces uncertainty into the results. Arena testing alone cannot provide estimates of the kill probability of a missile system, but arena test results do provide valuable data on which to base computer simulations of the terminal engagement phase.

Terminal engagement simulations are used in studies of warhead and fuze design requirements, in studies of aircraft

vulnerability, and to estimate the kill probability of a given missile design against a given target. Terminal engagement simulations typically contain very detailed data and calculations on warhead and fuze characteristics and on target components and their vulnerabilities. Kill probability simulations use the final outputs of missile flyout simulations as input data to establish relative positions, velocities, and attitudes between the missile and target in the endgame (terminal phase).

2-2.5 PROPULSION

A rocket motor is the usual source of missile propulsion. Some of the early US Army surface-to-air missiles used liquid propellants; there have been studies of and proposals for using ram-air-augmented solids in current missiles. Some foreign missiles as well as older US Navy surface-to-air missiles use ram-jet motors. All current US Army surface-to-air missiles, however, use solid propellant rocket motors for propulsion.

2-2.5.1 Motor

Fig. 2-21 illustrates a typical solid propellant rocket motor. The solid propellant grain contains a fuel and an oxidizer, which burn inside the combustion chamber to create high-pressure, gaseous combustion products. The gas is exhausted through a converging-diverging nozzle at supersonic speed. If the incremental pressures acting on the inside and outside surfaces of the combustion chamber and nozzle are integrated (summed), the result is a net force acting along the axis of the rocket motor. This force is called the thrust. A more convenient method of calculating and analyzing rocket motor thrust is based on the principle of conservation of momentum. The momentum imparted to the exhaust gases must be equal and opposite in direction to the momentum imparted to the missile; the force that acts against the missile in one direction and against the exhaust gas in the opposite direction is equal to the mass rate of flow multiplied by the velocity of the gas (rate of change of momentum) relative to the vehicle. The thrust is composed of the force that results from momentum change minus a pressure imbalance, which results from

the fact that ambient atmospheric pressure cannot exert a force on the missile in the region of the nozzle exit area. Both views, (1) integration of pressures and (2) momentum rate plus atmospheric pressure imbalance, predict the same values of thrust applied to the missile. These considerations are discussed further in Chapter 4.

The time history of the thrust of a solid propellant rocket motor depends on the design of the propellant grain. If the grain surface area that is exposed to combustion is large, the rate of generating and exhausting gases is high, and the resulting thrust is high. Conversely, a low thrust for a longer duration can be obtained with a given propellant if the exposed burning area is small. The size of the burning area depends on the original shape of the propellant grain and on the application of inhibitors to surfaces on which burning is to be prevented. Inhibitors are composed of materials that are essentially inert or that burn very slowly.

A cylindrical solid grain with all surfaces inhibited except one end, as shown in Fig. 2-22(A), burns at a uniform rate. At any given time the burning surface is the cross-sectional area of the cylinder. This provides a constant level of thrust from ignition to burnout; however, the thrust level is low because of the relatively small burning area on the end of the propellant grain. A grain configuration that gives a higher thrust level is a cylinder with a cylindrical port (hole) along its axis and other surfaces inhibited as shown in Fig. 2-22(B). The grain surface area in the port is larger and thus gives a larger thrust. As the propellant surrounding the port is consumed, the port diameter grows and increases the burning area with time. As the burning area—and therefore also the gas production rate and chamber pressure—increases, the thrust increases with time. A rocket motor whose thrust increases with time is said to have progressive burning characteristics. A more neutral burning characteristic is obtained when the cross section of the port is shaped like a star, as illustrated in Fig. 2-22(C). A solid cylindrical grain with no inhibited surfaces has regressive burning characteristics, i.e., the thrust level decreases with time. Many different grain designs have been developed in order to produce different shapes of the thrust history curve.

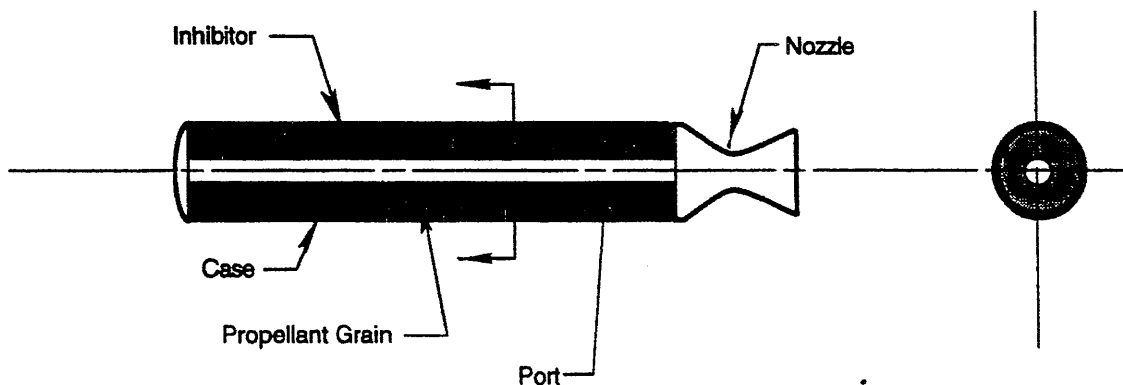


Figure 2-21. Typical Solid Propellant Rocket Motor

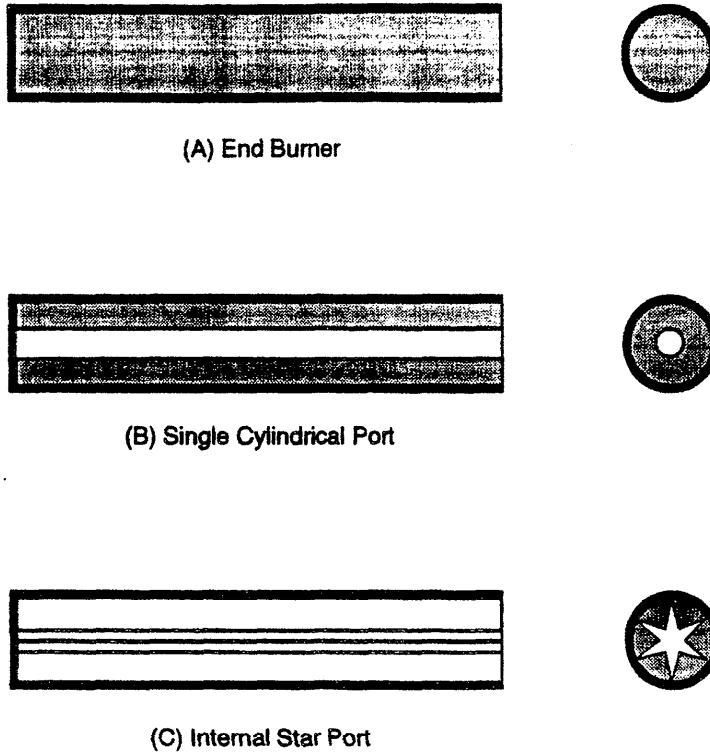


Figure 2-22. Propellant Grain Configurations

2-2.5.1.1 Boost Glide

Some rocket motors are designed to provide their total impulse near the beginning of the flight. The motor burns out and provides no more thrust, so the missile glides on to the target. A propulsion system of this type is called a boost-glide system. A typical boost-glide thrust history and the corresponding missile velocity history are shown in Fig. 2-23(A).

2-2.5.1.5.2 Boost Sustain

When a small thrust is provided to continue after the main boost thrust has ended the propulsion system is called a boost-sustain system. A typical boost-sustain thrust history and the resulting missile velocity history are shown in Fig. 2-23(B). The drastic change in thrust levels from boost to sustain can be accomplished in different ways. In a two-stage propulsion system the missile contains two different rocket motors, a boost motor and a sustain motor, often mounted in tandem. The boost motor is ignited first and the missile is accelerated. When the boost motor burns out it is separated and drops away from the missile. The sustainer motor is then ignited to maintain the missile speed. Other boost-sustain designs use the same rocket nozzle for both thrust phases, with the change in thrust level being accomplished by the grain configuration and the arrangement of the combustion chamber.

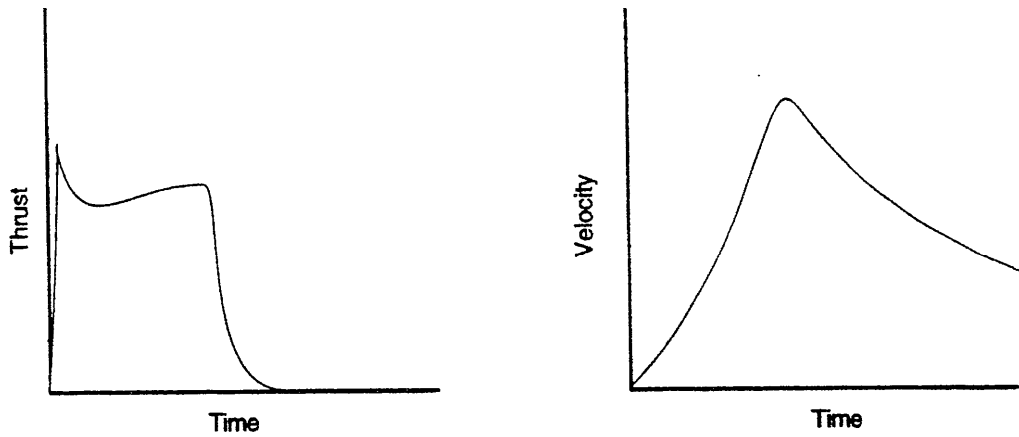
2-2.5.1.3 Specific Impulse

Specific impulse is one of the most important parameters used to describe the performance of a rocket motor (Ref. 10).

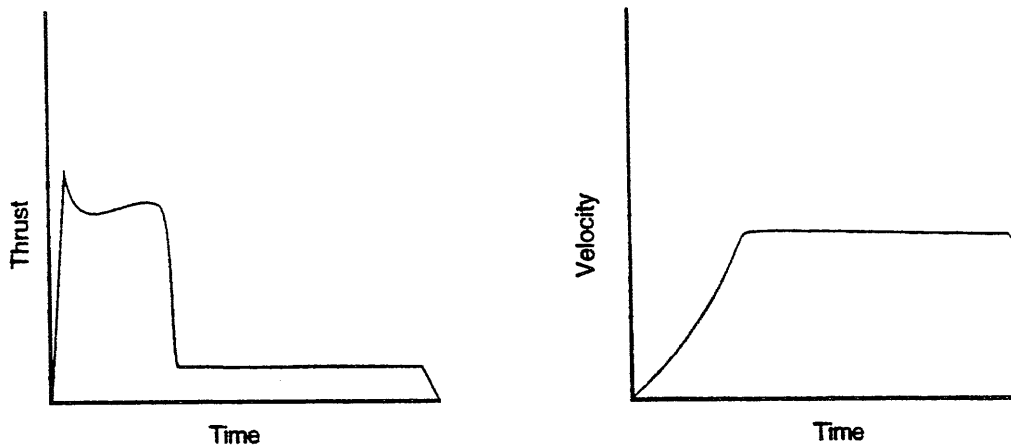
It can be defined as the thrust that can be obtained per unit of gas flow rate. For simulation purposes an equivalent but more useful definition is the amount of impulse (integration of thrust with respect to time) that can be obtained with a unit of mass of propellant. Specific impulse is important to missile performance because performance is extremely sensitive to missile weight, and the propellant contributes such a large fraction of missile weight. With a given missile configuration a small increase in propellant specific impulse can markedly improve missile performance. Conversely, a missile designed to deliver a given performance can be smaller and lighter if a propellant with greater specific impulse is used.

The published specific impulse for a propellant is usually given on the basis of an ideal nozzle and specified nozzle exit pressure, grain temperature, and chamber pressure. Delivered specific impulse is the specific impulse actually achieved by a rocket motor under the conditions of the test, and it may differ significantly from the standard published value for the propellant.

Typical values of delivered, sea level specific impulse for solid propellant motors vary from 1570 to 2350 N·s/kg, depending on the composition of the propellant and motor design. In a boost-sustain configuration using a single nozzle for both thrust levels, the design is usually optimized for the boost phase; thus the specific impulse for boost is often higher than for sustain.



(A) Boost Glide



(B) Boost Sustain

Figure 2-23. Typical Boost-Glide and Boost-Sustain Histories

2-2.5.1.4 Temperature Effects

The burning rate and the total impulse of a rocket motor are affected by the initial propellant grain temperature. Fig. 2-24 shows typical effects of grain temperature on thrust history. Variation of total impulse, i.e., the area under the thrust history curve, is only about $\pm 3\%$ over the range of temperature extremes between -57° and 76°C (Ref. 5). For a given missile firing, the grain temperature is not always easy to determine because it depends on the environmental conditions surrounding the missile over several hours before firing.

2-2.5.2 Tube Launch Ejection

Missiles that are shoulder fired must be designed to prevent the rocket plume from causing injury to the firer. These missiles are ejected from the tube by using an ejection charge that bums out within the tube. After exit from a tube, the ejection charge casing drops away from the missile, and if an internal acceleration switch is closed—indicating successful

ejection—the boost motor is ignited at a safe distance from the firer.

2-2.5.3 Propulsion Design and Operational Implications

The selection of a particular propulsion system configuration for a new missile system is strongly influenced by the design tradeoffs and operational requirements of the design. For example, ejection system requirements for shoulder-fired missiles are dictated by launch crew safety. Tradeoffs among the advantages and disadvantages of boost-glide and boost-sustain configurations involve interrelations among many factors. Boost-glide is the most straightforward and simple propulsion system, but the speed is either increasing rapidly during boost or decreasing rapidly during glide, and speed changes (accelerations) make guidance more difficult. Also, to achieve enough speed during boost to carry the missile to a long range during glide may require a peak speed so high that aerodynamic heating of the radome or optical dome

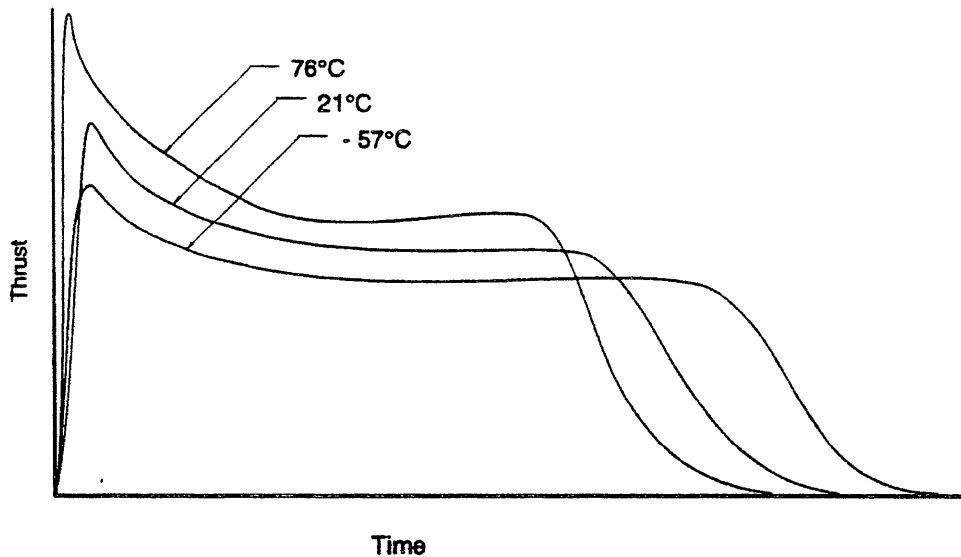


Figure 2-24. Effect of Temperature on Thrust History (Ref. 5)

could cause structural problems or interfere with signal transmission. The guidance law used in the missile design combined with the shape of the thrust history determine the flight path of the missile relative to the target. Undesirable flight paths (resulting from certain thrust histories) can cause loss of seeker lock because of gimbal angle constraints.

A decision to use boost-sustain propulsion requires further decisions regarding how to mechanize it. Among the choices are the use of two stages with stage separation after boost, the use of two combustion chambers with a single, nonoptimum nozzle, or alteration of the nozzle conjunction between boost and sustain.

Many of these considerations relate to design simplicity, cost, and efficiency. Other considerations apply to operational and performance factors such as man-portability, launch crew safety, preventing falling boost stages from striking friendly troops, maximum missile range, and guidance accuracy.

2-2.6 AIRFRAME

The airframe consists of the structural and aerodynamic components of a missile. For purposes of missile simulation, the important features of the airframe are its configuration, weight and moments of inertia.

2-2.6.1 Typical Configurations

A typical surface-to-air missile airframe is a cylindrical tube structure that houses all the missile subsystems and supports the control fins, stabilizing fins, and wings (if any). The tube typically consists of sections, containing different subsystems, attached end-to-end. The cylindrical frame may be an integral part of the section it houses. The method of control influences the airframe configuration. Configurations with canard control, tail control, and wing control are discussed in subpar. 2-2.3. Airframe deflection, i.e., aeroelastic effect, is an important consideration in missile design but is beyond the scope of this handbook.

The front end (nose) of the missile is usually a radome or optical dome to house the seeker. Radomes, housing RF seekers, have pointed noses to minimize drag under supersonic flow conditions. Optical domes, housing optical seekers, are usually hemispherical to avoid optical ray diffraction, and the contribution to drag is acceptable because they can be made small. The rocket nozzle exit usually forms the tail end of the airframe, and there are usually stabilizing fins located near the tail to provide static stability.

2-2.6.2 Static Stability

Static stability of a missile is defined as the inherent tendency of the missile to return to its trimmed (steady state) angle of attack if it is displaced from this angle by an outside force. Without static stability a small perturbation from the trimmed angle of attack would continue to increase in magnitude and cause the missile to tumble. The aerodynamic shape of the airframe of a missile and the location of its center of mass determine its static stability.

The resultant of all the aerodynamic pressures on the missile acts through a point called the center of pressure, the location of which is determined by the aerodynamic shape. A measure of the static stability is the distance from the center of mass to the center of pressure. The static margin is this distance normalized by a reference dimension, which is often the missile diameter (Ref. 11). When the center of mass is located ahead of the center of pressure, the missile is said to be statically stable. Large stabilizing fins at the tail of the missile give a large static margin.

The static stability of the missile opposes any angle of attack; therefore, an aerodynamic moment produced by control fin deflection must overcome the restoring moment resulting from the static stability of the missile. The greater the static stability, the greater the control moment required to achieve a maneuver. Increasing the stability of a given configuration will always reduce the amount of maneuverability for given control surface deflections. It is important that stat-

ic stability be maintained overall flight conditions, but small static margins are desirable because they result in faster response and greater angles of attack-and, therefore, greater lateral accelerations-for given control fin deflections.

The magnitude of the static margin changes during missile flight because pressure distributions over the missile change with Mach number, which shifts the center of pressure and because the center of mass of the missile also shifts as propellant is burned. One of the challenges in missile design is to provide a static margin as small as possible and yet ensure that the configuration will remain stable throughout missile flight.

Typically, the center of mass shifts forward as the propellant burns. This increases the static margin and therefore decreases maneuverability in the later portions of the flight. In contrast, the rotational inertia of the missile is reduced as the propellant grain burns and thus permits faster response to control commands.

In the interest of quick response, some very high-performance missiles are designed to be statically unstable; autopilot control is used to maintain stability. Current US Army surface-to-air missiles are statically stable and have small static margins.

2-3 GUIDANCE

Guidance is a generic term that describes the hardware, the functions, and the processes used to steer a missile to intercept a target. Steering a missile to a target is analogous to steering any other vehicle, e.g., an automobile. The driver visually senses the continuously changing position of the automobile relative to a target, e.g., the garage doorway. This stream of visual information is passed to the driver's brain where it is processed and used to generate control signals that are transmitted to his arms and hands for positioning the steering wheel. If the steering wheel is turned too much or too little, the changing scene reveals the error, and revised control signals are transmitted.

Continuing the analogy and for the moment restricting the discussion to a missile with a seeker, the eyes of the missile are the seeker head its brain is the combination of the seeker

electronics processor and the autopilot, and its nerve system (muscle control) and muscles are contained in its control system (Ref. 2). Any such process in which the error is continuously observed, i.e., measured, and corrections are made to reduce the observed error is a closed loop process. In this application the process is described by the guidance loop illustrated in Fig. 2-25.

Referring to Fig. 2-25, the sequence of events in guiding a missile begins when the seeker (intercept error sensor) senses the scene and determines the instantaneous intercept error. The guidance processor then determines the appropriate maneuver command, based on the guidance law, to reduce the error. The autopilot in turn determines the control that is needed to achieve this command and transmits the control signals to the control system actuators to deflect the control surfaces. The control surfaces aerodynamically change the heading of the missile in a direction to reduce the heading error. The loop is closed as the intercept error sensor determines the new instantaneous intercept error.

The distinction among the various components of the guidance and control system is often blurred by the very close relationships and interactions among their functions. For example, in some missiles the autopilot function-to translate the steering error signal into a control command-is handled entirely by the steering signal amplifier and the valve that regulates the pressure on the fin actuators; is no separate box or component called "autopilot".

As in all aspects of missile design, there are tradeoffs and compromises to be made in selecting a guidance system. Some of the factors to be considered are

1. Larger sensors are generally more accurate, but space and weight allowances onboard a missile are extremely limited.
2. Sensors operating at short range are more accurate. Therefore, a sensor on the missile becomes more accurate as the missile approaches the target, but a sensor on the ground becomes less accurate as the missile flies farther away from it.
3. Sensors are costly and those onboard the missile are expended with every launch.

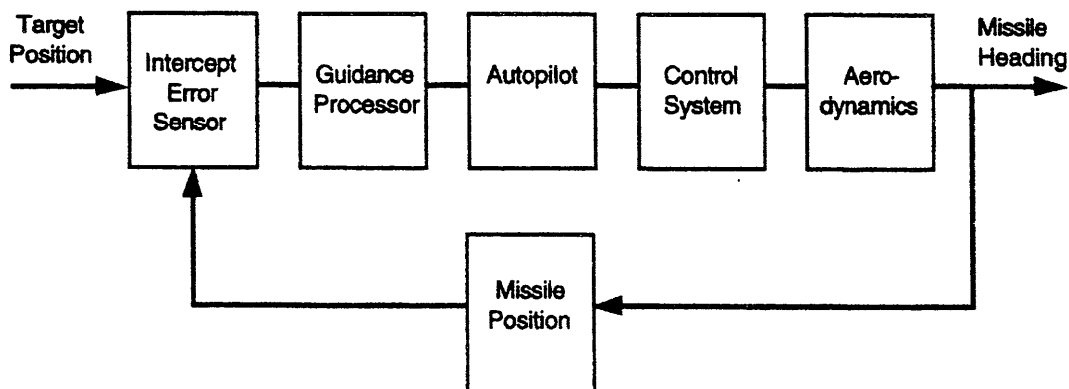


Figure 2-25. Guidance Loop

4. Different sensors are subject to different types of countermeasures. For example, active radars are subject to detection and jamming, whereas passive optical seekers provide no detectable signal to the enemy but have their own susceptibilities to countermeasures.

5. Some types of sensors penetrate adverse atmospheric conditions better than others.

6. Certain RF sensors measure range accurately but measure angular position of the target much less accurately. Optical sensors measure angle accurately but do not measure range at all.

As a result of tradeoffs among these and other considerations, several different guidance schemes have been used for surface-to-air missiles. Some of the basic concepts are described in the next subparagraph.

2.3.1 GUIDANCE IMPLEMENTATION (Ref. 12)

In the analogy given earlier the eyes of a missile were represented by the seeker head, located at the front of the missile, and the guidance processing was done onboard the missile. There are other possible configurations, however. For example, a sensor could be located on the ground rather than on the missile, and the guidance processor also could be on the ground. In this case missile steering commands must be relayed from the ground to the missile.

The various configurations for implementing surface-to-air guidance systems are broadly grouped into two categories: those in which guidance processing is located on the ground and those in which it is located on the missile. When guidance information is relayed from the ground to the missile, it is called command guidance. When the target tracker and guidance processing are onboard the missile, it is called homing guidance. Some guidance system configurations have sensors both on the missile and on the ground. These are more difficult to fit into an orderly grouping, but in general, when flight path correction commands are transmitted to the missile from the ground, some type of command guidance is implied. Guidance implementations using sensors and processors on the ground and implementations using onboard guidance and tracking are described in the subparagraphs that follow.

2-3.1.1 Ground Guidance and Tracking

Long-range missiles may require very large target-tracking sensors, too large to be carried onboard the missiles. Also very sophisticated high-speed computations involved in guidance processing and countermeasures rejection have in the past required computation equipment that is too bulky and heavy to be carried onboard the missiles. For these reasons missile systems have been developed with sensors and computers located on the ground. Another reason for ground-based sensors and computation, even for short-range missiles with relatively simple guidance processors, is simply to keep the expendable flight hardware as simple and low in cost as possible.

Three forms of guidance implementation--command, track-via-missile, and command-to-line-of-sight--that use sensors and processors located on the ground are currently being used by US Army surface-to-air systems.

2-3.1.1.1 Command

Command guidance receives its name from the fact that guidance commands are generated by a guidance processor that is not a part of the missile (Ref. 11). For a surface-to-air system these commands usually are determined by a guidance processor located at the missile launch point and transmitted to the missile. The measurement system consists of a target-track and a missile-track radar located at the launch point as shown in Fig. 2-26. Measured position data for the target and missile are fed into a computer also located on the ground. The computer calculates the guidance commands, and they are transmitted to the missile where they are carried out by the autopilot and control system of the missile.

One problem associated with command guidance is that measurements made when the missile is in the critical terminal phase of flight are the least accurate. (The missile is at the greatest distance from the sensor.) At typical engagement ranges of surface-to-air, command-guided missiles, these measurements contain such large errors that large miss distances result. One method used to overcome this difficulty is to use a very large warhead that is effective even when it is detonated at a large miss distance from the target. This of course requires that the missile be very large in order to transport the heavy warhead to the target.

Examples of command guided vehicles are the early Soviet surface-to-air missiles (Ref. 7) and the US Army Nike Ajax, Nike Hercules, Sprint, and Spartan missiles. No current US Army surface-to-air missiles use this type of command guidance in the terminal phase. Command guidance, however, is useful for the midcourse phase (defined in subparagraph 2-3.1.1.2) of long-range missiles, prior to the initiation of terminal guidance. In the midcourse phase the range from the missile to the target exceeds the capability of small onboard sensors, and the demand for accuracy in the midcourse phase is less severe.

2.3.1.1.2 Track via Missile

More accurate guidance than command guidance is possible by placing a sensor on the missile so that as the missile approaches the target, the error produced by the inherent angular tracking inaccuracy is diminished by the shortened range from the missile to the target. In addition, the position of the target is directly measured relative to the missile. This eliminates the error that would have been produced by a ground sensor that estimates both the missile position and the target position and calculates the difference. If the measurements made by the onboard sensor are transmitted to a guidance processor on the ground, the system is called a track-via-missile (TVM) guidance system. This system is illustrated in Fig. 2-27. Since the onboard sensor must be relatively small, it may not be able to track the target at long

range during the early and midportions of the flight. In this case, a large ground-based sensor is used to measure target and missile positions during the early and midportions of the flight when great accuracy is not required. This is called

midcourse command guidance. When the range from the missile to the target becomes short enough, the onboard sensor locks onto the target, and the terminal guidance phase using TVM begins (Ref. 13).

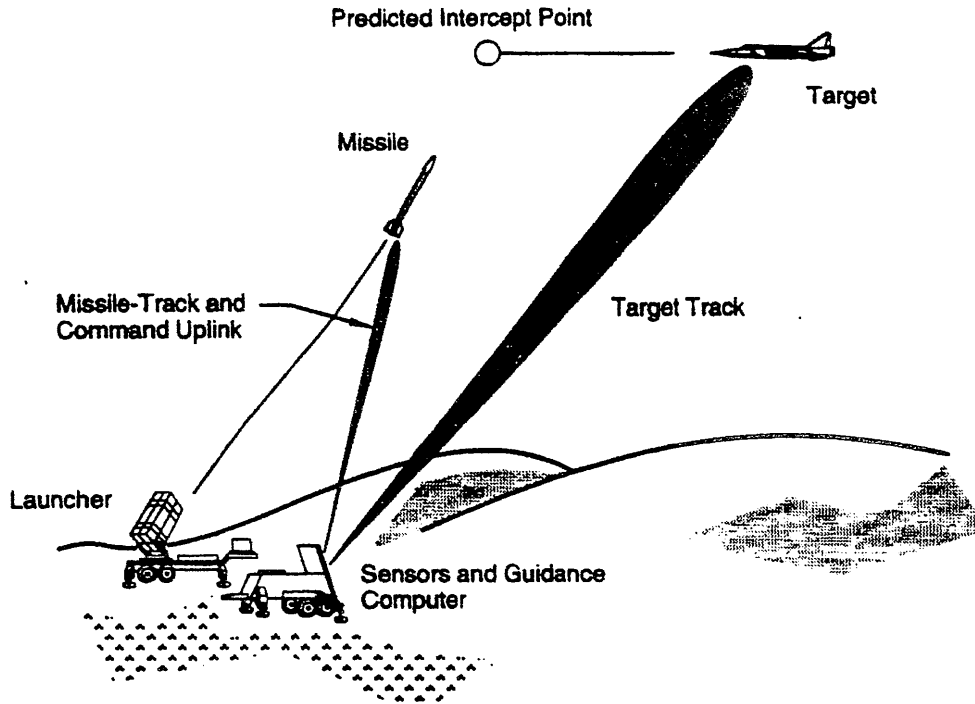


Figure 2-26. Command Guidance

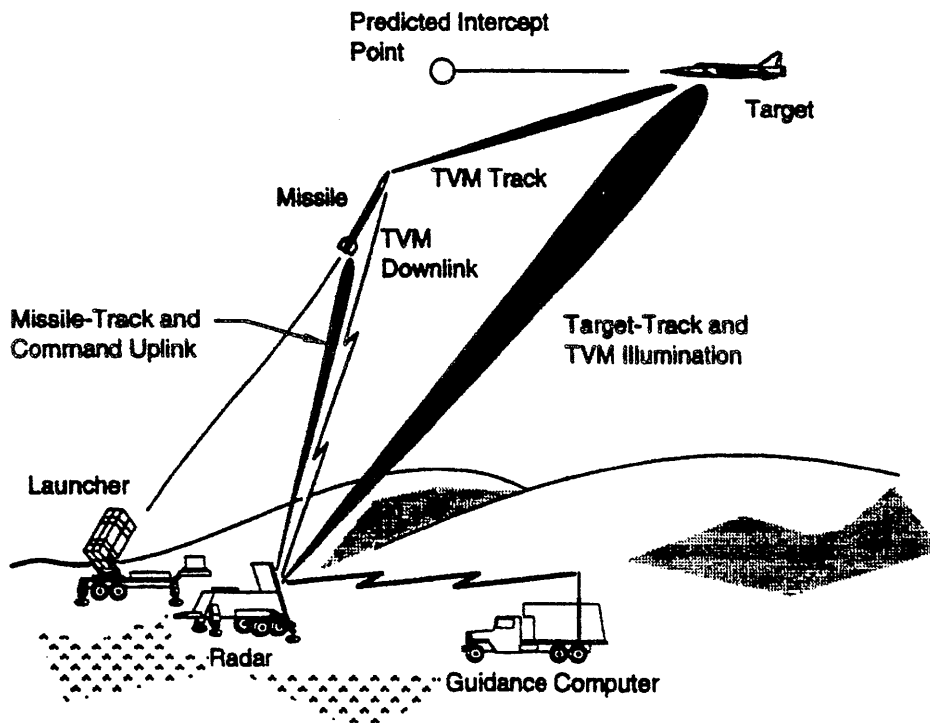


Figure 2-27. Track-via-Missile Guidance

2-3.1.1.3 Command to Line of Sight

One way to implement guidance with a single ground-based sensor is to track the target and keep the missile within the target-track beam. Slight movement of the missile away from the center of the beam is sensed by the ground-based sensor, and correction commands are transmitted to the missile to bring it back to the center of the beam. This is called command-to-line-of-sight guidance. In a different implementation that cannot be classified as command guidance, the missile itself senses its position within the beam and develops its own guidance commands. This is called beam-riding guidance and is discussed in subpar. 2-3.2.3.

2-3.1.1.4 Target Illuminators

Sometimes ground-based target trackers are used in conjunction with homing guidance. The purpose of the ground-based tracker is simply to illuminate the target with electromagnetic energy. The onboard seeker tracks the target by using energy that originated at the illuminator and is reflected from the target. Thus the onboard system does not need to generate and transmit energy, so the cost, weight, and complexity of a missile are considerably reduced. Guidance implementations that use target illuminators are called semiactive systems and are discussed further in subpar. 2-3.1.2.2.

2-3.1.2 Onboard Guidance and Tracking

To achieve truly small miss distances-permitting a minimal warhead and therefore a small missile--requires that a target tracker (seeker) be onboard the missile. With the seeker onboard, sensor measurements become more accurate at the time accuracy is most needed, i.e., during final approach to the target.

Homing guidance usually implies that the guidance processing, as well as the seeker, is onboard the missile--although TVM (subpar. 2-3.1.1.2) is a form of homing guidance--with the guidance processing performed on the ground.

Current applications of homing guidance usually measure only the angular rate of the line of sight from the missile to the target. This is the only measurement necessary to support a very powerful guidance law, i.e., proportional navigation (subpar. 2-3.2.4). Implementation to measure the line-of-sight rate is relatively easy. In optical seekers part of the seeker head typically spins as a gyro. A torque is required to cause the seeker head to change its orientation in space to track the target. The voltage required to produce this torque is proportional to the angular rate of the line of sight to the target. In RF seekers the usual practice is to mount small gyros directly on the gimballed antenna platform to sense the angular rate of the antenna as it is driven to track the line of sight to the target. The outputs from these gyros are used as a measure of the line-of-sight angular rate.

Guidance employing onboard seekers can be implemented as active, semiactive, or passive systems. Each system is described in the subparagraphs that follow.

2-3.1.2.1 Active

An active guidance system generates radiant power onboard the missile and transmits it in the direction of the target (Ref. 11). Power reflected from the target is received and tracked by the onboard system. An active system has the potential to measure relative bearing and range from the missile to the target angular rate of the line of sight to the target, and the rate of range change (range rate) for use in determining guidance commands. Some of these measurements may not be used in a given missile design. A disadvantage of an active system is that the flight vehicle is burdened with the weight and space required by the power generation system. Also emissions from an active system may alert the target that a missile has been launched and give the target an opportunity to activate countermeasures.

2-3.1.2.2 Semiactive

In a semiactive guidance system the power used to illuminate the target is generated on the ground (Ref. 11). The ground-based system not only must acquire the target initially but also must continue to track the target throughout the engagement to provide power for the onboard seeker to track. This is a disadvantage since it ties up ground-based resources and prevents them from being applied to other targets and other missile launches. Another disadvantage is that, like the active system emissions from a semiactive system can alert the target that a missile has been launched.

A semiactive seeker has the potential to measure the bearing of the target relative to the missile and the angular rate of the line of sight from the missile to the target but it has no means of measuring range. If the guidance implementation has a rear-facing antenna on the missile to receive the direct illuminating signal as a reference, it can measure the Doppler frequency, and range rate can be derived from the Doppler frequency. The use of range rate can be important--not so much to guide the missile but to discriminate the target from clutter and countermeasures.

2-3.1.2.3 Passive

A passive guidance system transmits no-power (Ref. 3). The power tracked by the onboard seeker is either generated by the target itself (RF or IR), is reflected power generated by a natural source (solar), or is background power blocked by the target (UV). Once a passive seeker is locked onto the target and launched, there is no more need for support from the ground-based launch system. This gives rise to the concept of "fire and forget", which permits the ground-based system to turn its attention to new targets and new launches. Passive seekers have the potential to measure relative bearing and the angular rate of the line of sight; they cannot, however, measure range or range rate.

2-3.2 GUIDANCE LAWS

A guided missile engagement is a highly dynamic process. The conditions that determine how close the missile comes to the target are continuously changing, sometimes at a very

high rate. A guidance sensor measures one or more parameters of the path of the missile relative to the target. A logical process is needed to determine the required flight path corrections based on the sensor measurements. This logical process is called a guidance law. The objective of a guidance law is to cause the missile to come as close as possible to the target. Guidance laws usually can be expressed in mathematical terms and are implemented through a combination of electrical circuits and mechanical control functions.

The two basic criteria on which guidance laws are based are that the guidance must (1) be effective under anticipated conditions of use and (2) be able to be implemented using the particular sensor configuration selected. A number of different schemes and their many variations have been used for missile guidance, chief among which are intercept point prediction, pursuit, beam-rider, proportional navigation, and methods based on modern control theory.

2-3.2.1 Intercept Point Prediction

Ideally, a missile could be guided simply by projecting the target position ahead by an amount corresponding to the time of flight of the missile and steering the missile to that point. In reality this is not an easy task. First, the target is not likely to cooperate by flying a predictable path. Second, the missile time of flight cannot be predicted accurately. Even the future velocity history of the missile is uncertain it is affected by unpredictable variations in motor thrust, atmospheric drag (which is caused partly by the very control commands that are to be determined), and the wind. Since predictions cannot be made accurately, the engagement conditions must be assessed continuously and the guidance commands updated based on current information. The accuracy of guidance using intercept point prediction depends largely on the accuracy of sensor measurements.

Intercept point prediction is applicable only when missile and target positions and velocities are both available. Command guidance systems meet these requirements.

2-3.2.2 Pursuit

One of the most obvious and primitive guidance laws is pursuit guidance, in which the missile velocity vector is directed toward the position of the target at any instant in time (Ref. 3). Pursuit guidance has been labeled "hound and hare" guidance because, presumably, it is the guidance law used by a dog chasing a rabbit. Anyone who has observed such an engagement however, can testify that even a dog knows that leading the target i.e., anticipating its future position, improves the chances of intercept. A variation of pursuit guidance that introduces the concept of leading the target is deviated pursuit guidance. In this form of guidance, the angle between the missile velocity vector and the line of sight to the target is held constant. Both the pursuit and deviated pursuit guidance laws require a very high missile turning rate close to the time of intercept. Since there are physical limits on the turning rate that can be achieved by a missile, the result is the missile misses the target. The magnitude of the

miss can be small for slow targets or for near-tail-chase engagements, but in general, pursuit guidance is not effective in the surface-to-air role and is not used.

2-3.2.3 Beam Rider

If a surface-to-air missile system is being used to defend a relatively small area the intercept ranges can be short enough that the accuracy from a ground-based sensor is acceptable, thus the cost and complexity of an onboard target sensor are eliminated. The missile system can be simplified further by eliminating the ground-based missile tracker; however, such elimination leaves only one way to keep track of the missile and that is to keep it within the target-track sensor beam. As the missile begins to move away from the beam, this movement is sensed either by the ground sensor or by antennas on the missile, and control commands are provided to hold the missile in the beam (Ref. 11). This is called beam-rider guidance and is illustrated in Fig. 2-28. As the target moves, the target-track beam follows it, and the missile flies up the beam. With no tracking error and perfect missile maneuver response to the control commands, the missile would eventually intercept the target. In reality, however, the miss distance depends on how well these functions are performed.

A disadvantage of beam-rider guidance is that, although some target lead is inherent in the system, not enough lead is provided early in the flight, which results in an inefficient flight path. In some crossing geometries, the case in which a missile crosses the target *this places a severe maneuver requirement on the missile near its terminal phase, which may exceed the maneuvering capability of the missile.

A number of surface-to-air missiles developed by the Soviets and a few developed in Western Europe use some form of beam-rider guidance. The only US Army surface-to-air missile using an adaptation of beam-rider guidance is RO-UND, which was developed in Europe.

2-3.2.4 Proportional Navigation

The guidance scheme that has proven to be extremely effective is proportional navigation. In proportional navigation the missile is steered so as to cause the angular rate of the missile flight path to be proportional to the angular rate of the line of sight from the missile to the target (Ref. 11). The proportionality factor, called the navigation ratio, is usually set between 3 and 5, i.e., the turn rate of the missile is three to five times the angular rate of the line of sight. The result is that the angular line-of-sight rate is driven toward zero, and the missile is steered to a flight path in which the bearing angle to the target tends to remain constant as shown in Fig. 2-29. One basic tenet of ship piloting is that "constant bearing means collision". It can be shown that under the conditions of constant target velocity and constant missile velocity, proportional navigation does indeed lead to an intercept. Furthermore, the missile flight path that results from proportional navigation guidance is efficient in the sense that any launch-direction errors are steered out early in the flight

and leave only minimal corrective maneuvers to be required near the terminal phase in which flight path corrections are critical. For the stated conditions (constant velocities) pro-

portional navigation has the same effect as predicting an intercept point and steering the missile to that point, but without the need to measure range or positions.

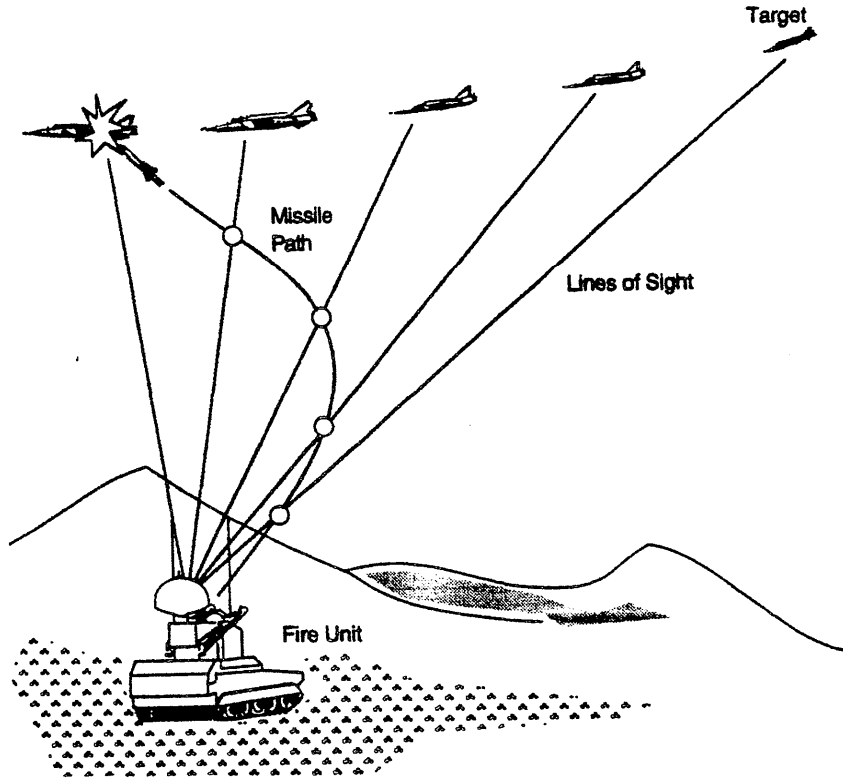


Figure 2-28. Beam- Rider Guidancet

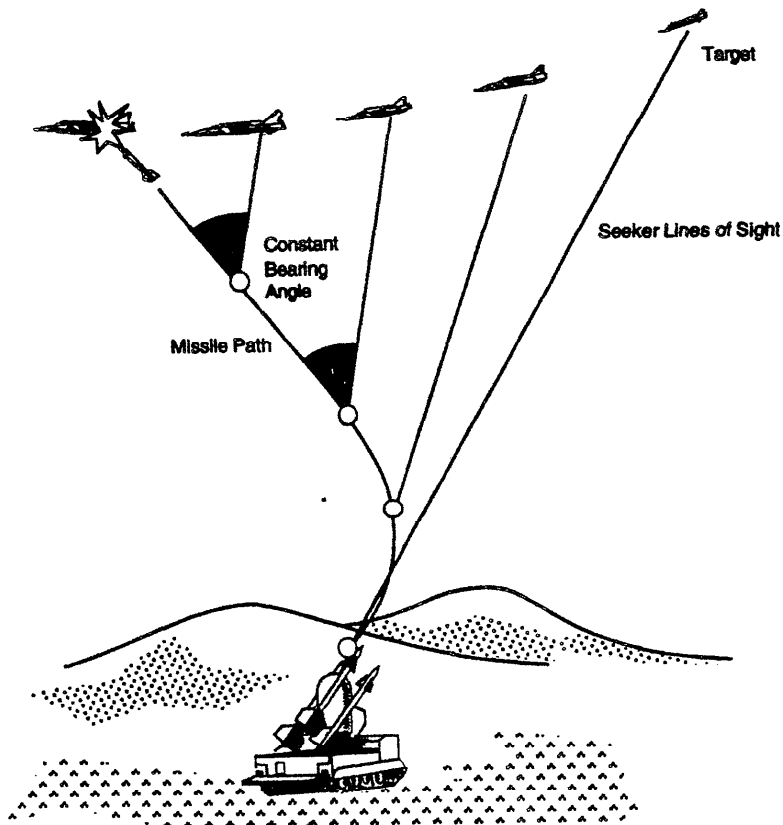


Figure 2-29. Proportional Navigation Guidance

In actual engagements neither the target velocity nor the missile velocity is constant; therefore, the basic premise on which proportional navigation is based is not valid. Proportional navigation is so robust, however, that acceptable miss distances can be achieved even against targets that perform relatively severe evasive maneuvers if the missile response time is short enough and if the missile is capable of sufficient acceleration in a lateral maneuver. Any target or missile accelerations in the early or midportions of the flight are sensed by the seeker as a change in line-of-sight direction. This leads to steering commands that soon null the perturbations produced by the accelerations. If the accelerations are continuous, such as during missile boost or when the target is performing a continuous turn, the steering commands cause the missile "fright path to change continuously to keep up with the changing situation with only a small lag. The magnitude of this lag combined with the limits on the ability of a missile to maneuver determine the magnitude of the miss distance.

For proportional navigation to be used in its strictest sense, a measure of missile speed is required because the acceleration of the maneuver necessary to produce the desired flight path turn rate depends on missile speed. Since the effectiveness of proportional navigation is relatively insensitive to the navigation ratio, approximations can be made without seriously affecting its usefulness as a guidance premise. For example, a small error in the estimation of the acceleration of the maneuver is equivalent to a small change in the navigation ratio. Since missile speed is usually not available, closing velocity (if available) or some other approximation of missile velocity can be used to determine the acceleration of the required maneuver. In fact in practice an acceptable approximation to proportional navigation is simply to make the magnitude of the fin deflection proportional to the angular line-of-sight rate. The actual lateral acceleration achieved--and thus the navigation ratio achieved--depends on the missile configuration, Mach number, and air density. The ratio of achieved acceleration to angular line-of-sight rate is called the system gain.

In the early part of the missile boost phase, the missile speed is relatively low. Proportional navigation guidance does not anticipate that the speed will soon be much greater but provides guidance commands based only on the current seeker angular rate. This puts the missile on a course with a large lead angle consistent with the current speed. The lead angle, however, is much too large as the missile speed increases and requires a flight path correction back to a smaller lead angle. To prevent this unnecessary maneuvering, the navigation ratio is sometimes intentionally shaped, i.e., its magnitude is changed with time. A low value of navigation ratio early in the flight slows down the missile response to early misleading guidance commands, whereas a high ratio as the missile approaches the target permits fast response to target evasive maneuvers.

Proportional navigation is particularly applicable to pas-

sive homing guidance implementations because the line-of-sight angular rate is the only necessary input. Some form of proportional navigation (sometimes with the addition of biases) is employed in essentially all Army missiles that have seekers. Because of its simplicity and effectiveness, proportional navigation is also sometimes used in midcourse command guidance. Future missile guidance processors will take advantage of the greatly increased onboard computational power to integrate modem control and optimization techniques.

2-3.2.5 Optimal Guidance

Aircraft and pilot support systems are being developed with the capability to maneuver with very high lateral accelerations. With the development of these highly maneuverable targets, the usefulness of classical guidance laws, such as proportional navigation, is becoming marginal (Ref. 2). In addition, countermeasures techniques are becoming increasingly sophisticated in their ability to introduce noise and deceptive data into the missile guidance processor. Consequently, there is a need to improve surface-to-air missile capability to meet these threats. Missiles are being designed presently with improved capabilities that include guidance laws that can deal more effectively with target evasive maneuvers and noisy, deceptive guidance data. These guidance law improvements have been made possible by several recent technological advancements.

Modern estimation and control theory provides the framework for the development of guidance laws that are closer to optimum. These modem advancements in control theory were developed in the late 1950's and early 1960s. Modem estimation and control theory is based on a time-domain approach that uses state variables to describe the condition of the system being controlled and incorporates optimal estimators such as the Kalman filter. In theory these methods allow "optimal" separation of the target signal from the noise by using a priori information about the missile and target dynamics and noise covariances. Missile and target states other than line-of-sight rate can be estimated even when not measured, provided they are mathematically observable.

During the late 1960s and early 1970s, a few missile designers examined the possibility of applying these advanced techniques in missile guidance. They concluded that except in the most simplistic and unrealistic cases, the mechanization of such algorithms in real time onboard a small missile was not feasible because the calculations involved procedures that could not be accomplished efficiently with the techniques that were then available.

Several things have changed since that time to make implementation of guidance laws based on modem optimal control techniques possible (Ref. 2). New theories have appeared, and old ones have been extended and refined. Several new numerical techniques for solving complex equations have been developed. Finally, and most important, the microcomputer has been developed. These advances now make

implementation of improved guidance laws practical, and future generations of missiles are expected to be able to address the problem of noisy data, with some data being of higher quality than others, and the problem of uncertainty in factors such as future target maneuvers. Refs. 2 and 14 review optimal estimation and control theory with applications to optimal guidance.

2-4 LAUNCHER

A missile is supported and guided by its launcher through the first few centimeters of motion after motor ignition. Man-portable missile launchers are in the form of tubes; fixed and mobile launchers can be in the form of rails or tubes.

2-4.1 SOURCE OF INITIAL CONDITIONS

The importance of the launcher (any kind) to a missile flight simulation is that it establishes the initial conditions from which missile flight calculations begin. The initial missile velocity simulated is in the direction in which the launcher points and has a magnitude that represents the actual missile speed when it leaves the constraints of the launcher. If the launcher is being slewed at the time of launch, the angular slewing rate is imparted to the missile, and this is included in the initial conditions of the missile simulation. As the missile travels forward out of the tube or off the rail, the front part of the missile becomes unsupported first Gravity begins to accelerate the missile nose downward while the rear of the missile is still supported and thus gives the missile a small nose-down angular rate. This is called tip-off (Ref. 15) and is taken into account in flight simulations with varying degrees of reality, depending on their importance to the objectives of the simulation.

2-4.2 LAUNCHER POINTING DIRECTION

The pointing direction of the launcher at the moment of launch is established by some fire control rule or algorithm. Typically the missile is launched in a direction ahead of the target. The angle ahead of the target is called the lead angle. If the target is at low altitude, the launcher may be positioned at an elevation angle that is higher than the target to prevent the missile from striking the ground. This is called super elevation. The fire control algorithms used to determine the amount of lead and super elevation are usually supplied by the missile manufacturer.

REFERENCES

1. "Army Weaponry and Equipment", Army, 436-41 (October 1986).
2. 3. Gonzalez, "New Methods in the Terminal Guidance and Control of Tactical Missiles", Guidance and Control for Tactical Guided Weapons With Emphasis on Simulation and Testing, AGARD-LS-101, Advisory Group for Aerospace Research and Development, North Atlantic Treaty Organization, Neuilly sur Seine, France, May 1979.

3. R. J. Heaston and C. W. Smoots, Introduction to Precision Guided Munitions, Vol. I: Tutorial, GACIAC HB-83-01, Guidance & Control Information Analysis Center, IIT Research Institute, Chicago, IL, May 1983.
4. W. L. Wolfe and G. J. Zissis, The Infrared Handbook, Infrared Information and Analysis Center, Environmental Research Institute of Michigan, prepared for the Office of Naval Research, Department of the Navy, Washington, DC, 1978.
5. W. G. Younkin, Studies of the Sidewinders IC Aeromechanics, Part 2, Dynamics, NAVWEPS Report 6596, Part 2, NOTS TP 2482, US Naval Ordnance Test Station, China Lake, CA June 1964.
6. S. A. Hovanessian, Radar System Design and Analysis, Artech House, Inc., Dedham, MA, 1984.
7. D. C. Schleher, Introduction to Electronic Warfare, Artech House, Inc., Dedham, MA, 1986.
8. M. I. Skolnik Introduction to Radar Systems, Second Edition, McGraw-Hill Book Co., Inc., New York, NY, 1980.
9. M. Hobbs, Basics of Missile Guidance and Space Techniques, Vol. 1, John F. Rider Publisher, Inc., New York, NY, 1959.
10. G. P. Sutton, Rocket Propulsion Elements, Second Edition, John Wiley & Sons, Inc., New York, NY, 1956.
11. J. J. Jerger, "Systems Preliminary Design", Principles of Guided Missile Design, G. Merrill, Ed., D. Van Nostrand Co., Inc., Princeton, NJ, 1950.
12. A. S. Locke, "Guidance", Principles of Guided Missile Design, G. Merrill, Ed., D. Van Nostrand Co., Inc., Princeton, NJ, 1955.
13. "Patriot-the Air Defense System for the 80s", Armada International 4, No. 3, (1980).
14. W. Hofmann and D. Joos, "Missile Guidance Techniques" Guidance and Control for Tactical Guided Weapons With Emphasis on Simulation and Testing, AGARD-LS-101, Advisory Group for Aerospace Research and Development NATO, Neuilly sur Seine, France, May 1979.
- M. C. W. Besserer, "Missile Engineering Handbook", Principles of Guided Missile Design, G. Merrill Ed., D. Van Nostrand Company, Inc., Princeton, NJ, 1958.

BIBLIOGRAPHY

CONTROL (CLASSICAL)

- R. N. Clark Introduction to Automatic Control Systems, John Wiley & Sons, Inc., New York, NY, 1964.
- V. Del Toro and S. R. Parker, Principles of Control Systems Engineering, McGraw-Hill Book Co., Inc., New York, NY, 1960.
- B. Etkin, Dynamics of Flight-Stability and Control, John Wiley & Sons, Inc., New York, NY, 1982, pp. 211-92.

H. S. Seifert and K. Brown, Ballistic Missile and Space Vehicle Systems, John Wiley & Sons, Inc., New York, NY, 1961, pp. 345-471.

CONTROL (MODERN)

B. D. O. Anderson and J. B. Moore, Optimal Filtering, Prentice-Hall, Inc., Englewood Cliffs, NJ, 1979.

W. L. Brogan, Modern Control Theory, Second Edition, Prentice-Hall, Inc., Englewood Cliffs, NJ, 1985.

A. Gelb, Ed., Applied Optima/ Estimation, The MIT Press, Massachusetts Institute of Technology, Cambridge, MA, 1986.

GUIDANCE

R.R. Bennett and W. E. Matthews, Analytical Determination of Miss Distances for Linear Homing Navigation Systems, TM-260, Hughes Aircraft Company, March 1952.

G. Desloovere, "Guiding Tactical Missiles," Space/Aeronautics (November 1965).

J. Geddes, "Phoenix Missile System", Interavia 12 (1982).

A. Ivanov, "Semiactive Radar Guidance", Microwave Journal (September 1983).

J. E. Kain and D. J. Yost Command to Line-of-Sight Guidance-A Stochastic Optimal Control Problem, Paper No. 76-1956, AIAA Guidance and Control Conference, 1976.

J. Long and A. Ivanov, "Radar Guidance of Missiles", Electronic Progress XVI No. 3 (Fall 1974).

H. Maurer, "Trends in Radar Missile Guidance", International Defense Review 9 (1980).

C. F. Price, Advanced Concepts for Guidance & Control of Tactical Missiles, TR-170-5, 'The Analytic Sciences Corporation, Reading, MA June 1973.

PROPULSION

C. W. Besserer, "Missile Engineering Handbook", Principles of Guided Missile Design, G. Merrill, Ed., D. Van Nostrand, Co., Inc., Princeton, NJ, 1958, pp. 287-95.

E. A. Bonney et al, "Aerodynamics, Propulsion. Structures. and Design Practice", Principles of Guided Missile Design, G. Merrill, Ed., D. Van Nostrand Co., Inc., Princeton, NJ, 1956, pp. 332-97.

A.E. Puckett and S. Ramo, Guided Missile Engineering, McGraw-Hill Book Co., Inc., New York, NY, 1959, pp. 70-119.

H.S. Seifert and K. Brown, Ballistic Missile and Space Vehicle Systems, John Wiley & Sons, Inc., New York, NY, 1961, pp. 15-53,77-89.

W. G. Younkin, Studies of the Sidewinder IC Aeromechanics, Part 2, Dynamics, NAVWEPS Report 6596, Part 2, NOTS TP 2482, US Naval Ordnance Test Station, China Lake, CA, June 1964, pp. 18-21.

RADAR

M. I. Skolnik Introduction to Radar Systems, McGraw-Hill Book Co., Inc., New York, NY, Second Edition, 1980.

M. L Skolnik, Radar Handbook, McGraw-Hill Book Co., Inc., New York, NY, 1970.

D. K. Barton and H. R. Ward, Handbook of Radar Measurement, Artech House, Inc., Dedham, MA, 1984.

D. K. Barton, Modern Radar System Analysis, Artech House, Inc., Norwood, MA, 1988.

R. F. Russell and R. H. Garlough, Active RF Seekers for Land Combat Seekers, Technical Report No. RE 81-19. US Army Missile Command, Redstone Arsenal, AL, April 1981.

SERVOS

H. Chestnut and R. W. Mayer, Servomechanism and Regulating System Design, Vol. 1, John Wiley & Sons, Inc., New York, NY, 1951.

WARHEAD AND FUZE

G. Merrill, H. Goldberg, and R. H. Helmholtz, "Operations Research, Armament, Launching," Principles of Guided Missile Design, G. Merrill, Ed., D. Van Nostrand Company, Inc., Princeton, NJ, 1956, pp. 251-65,287-313.

CHAPTER 3

MISSILE SIMULATION OVERVIEW

An overview of missile flight simulation is given in this chapter. The four primary objectives of flight simulations—establishing requirements, designing and operating missiles, assessing missile performance, and training—are discussed. The essentials of simulating missile guidance and control and the motions of the missile and target are described; a discussion of the role of coordinate systems is included. Appropriate levels of simulation detail, to match simulation objectives, are discussed.

3-0 LIST OF SYMBOLS

a	= translational acceleration, m/s^2
C_F	= general aerodynamic force coefficient, dimensionless
C_M	= general aerodynamic moment coefficient, dimensionless
d	= aerodynamic reference length of body, m
F	= force acting on a particle or body, N
F_A	= aerodynamic force, N
I	= moment of inertia of a body, $kg \cdot m^2$
M	= moment acting on a body, N·m
M_A	= aerodynamic moment, N·m
M_N	= Mach number, dimensionless
m	= mass of a particle or body, kg
p_a	= atmospheric pressure, Pa
Q	= dynamic pressure parameter, Pa
S	= aerodynamic reference area, m^2
V	= magnitude of velocity of air relative to a body, airspeed, m/s
ρ	= atmospheric density, kg/m^3
$\dot{\omega}$	= angular acceleration, rad/s^2

3-1 INTRODUCTION

A missile flight simulation is a tool that implements models of the various missile components and their interfaces with each other and the environment. The simulation provides a time sequence of the dynamic events describing the operation and flight of the missile. Inputs to the simulation are parameters likely to change from one computer run to the next, i.e., from one simulated missile flight experiment to the next. Examples of inputs are the initial conditions at the time of missile launch, target signature characteristics, and target flight-path control parameters. Outputs typically are missile and target positions and attitudes and parameters that describe missile subsystems operation throughout the simulated flight.

If the time required by a computer to solve the mathematical equations and perform the logic functions to simulate a

missile is different from the actual operating time of the real missile, the simulation is said to be operating in nonreal time. Some applications require that the flight simulation be run in real time, i.e., that the timing of the sequence of events in the simulated flight be the same as that in the actual flight being simulated. The amount of computer processing time required to evaluate the mathematical equations of the simulation model depends on the computer used and on the characteristics of the model itself, such as the time intervals established in the model between computational steps.

There are many different uses for missile flight simulations, and different uses require different simulation approaches. The levels of sophistication of missile flight simulations vary greatly depending on the application. These levels range from unsophisticated two-dimensional flyout models to very detailed six-degree-of-freedom models that include hardware-in-the-loop and seeker scene simulations. The applications and corresponding simulation objectives are discussed in par. 3-2, the essential ingredients that make up a simulation are discussed in par. 3-3, and the level of detail of these ingredients required to meet simulation objectives is discussed in par. 3-4.

Flight simulations provide a means of obtaining data that are significantly more detailed and complete and that cover a broader range of environments and scenarios than it is possible to obtain by using traditional system test methods and at far less cost. For a short-range missile 3000 to 10,000 engagements can be simulated with the funds needed to fire only one missile on the range (Ref. 1). A simulation operated in a controlled emission environment allows covert evaluation of foreign systems and jammers as well as development and test of sensitive programs that could not be performed by flight testing without risk of compromise (Ref. 2).

It is extremely difficult and expensive to test critical performance factors of modern airborne guidance systems in actual missile flight tests; consequently, implementation of extensive flight-test programs is essentially impossible for this purpose. High-performance, multiple targets, including decoys, cannot be provided repeatedly to collect performance statistics on guidance system capabilities under controlled and measurable conditions (Ref. 3). Even if such flight-test programs could be implemented, the cost of enough tests to be statistically significant would be prohibi-

live. Missile flight simulation provides a solution to this predicament. Simulation is a way to find answers to questions about missile performance that are impractical or impossible to find by direct experimentation or analytical solution (Ref. 4).

Early missile simulations were used to understand and evaluate missile systems from a purely technical standpoint. Simulations are now performed for both technical and managerial reasons (Ref. 2). In acquiring complex weapon systems, the Department of Defense (DoD) establishes compressed schedules and key milestones at which programmatic and technical decisions must be made. Careful and methodical procedures have been set up to evaluate each phase of weapon system acquisition and to ensure that a sound basis of technology is available (Ref. 5). Acquisition and operation of high-quality, affordable, and high-technology weapons require effective test and evaluation over the entire life cycle of a weapon system (Ref. 6). Projects compete for funding, and poor performance is frequently used to terminate projects. This places heavy emphasis on the success of highly visible flight demonstrations. Flight-test success rates of better than 95% have been achieved through careful preparation and planning by using flight simulations to verify the missile design before flight test and to predict the results of each test (Ref. 5).

In this environment missile flight simulation has prospered and is becoming an increasingly important and valuable source of reliable information that assists designers, program managers, evaluators, and decision makers. Preparation of a hierarchy of flight simulations to aid in various phases throughout the life cycle of a missile system is now considered to be indispensable (Ref. 5).

3-2 MISSILE SIMULATION OBJECTIVES

The objectives of a given missile flight simulation are actually the objectives of the intended users. As discussed in Chapter 1, these objectives are to obtain knowledge and understanding of various aspects of the performance of a missile for any of the many different purposes encountered in the analysis, development, procurement, and operation of missile systems. These purposes are amplified and placed in perspective in subpar. 3-2.1, and the specific uses for simulations addressed in this handbook are discussed in subpar. 3-2.2.

3-2.1 MISSILE SIMULATION PERSPECTIVE

There are four basic applications of missile flight simulations: (1) to establish missile performance requirements, (2) to design and optimize missile systems, (3) to assess missile system performance, and (4) to teach users the correct use of the missile in battlefield situations. These four applications, in the order in which they are listed, generally reflect the life cycle of a missile system although there may be overlaps. The level of sophistication of a simulation varies widely depending on which application is the objective of the simulation.

3-2.1.1 Establishing Requirements

The evolution of weapons technology is accelerating. Even before a weapon designed with current technology has been fielded, the development of countermeasures against it has begun. Counter-countermeasures are developed during weapon improvement programs, and the cycle repeats itself. There are continuous efforts by the DoD, the military services, and their contractors to integrate these developments into tactical operational planning and to establish requirements for future weapon systems, for improvements in current weapon systems, and for improvements in the employment and tactics of operational systems. Not only are technical requirements established, but determinations are made of the number of each type of weapon that will be needed in the national arsenal. All of these requirements are developed through many kinds of studies and analyses. Operations analysis techniques and models are an important contribution to decisions on weapon systems requirements. These models cover the spectrum from one-on-one engagements between a weapon and a target to many-on-many engagements between a multitude of weapons of different kinds against a multitude of targets of different kinds.

Large war game models, e.g., operations models and campaign models, provide an understanding of the interactions of a mix of weapon systems and command-and-control systems in combat environments. In the operation of these models the overall result is often the battle being won by one side or the other, but what is more important is that the particulars of the battle are made visible so that the factors that drive the outcome can be evaluated. Some of these factors are the quantities and locations of fire units and command-and-control units, target search and detection system characteristics, weapons launch doctrines, fire unit reaction times, number of missiles per fire unit, reload times, kill assessment times, defended area coverage, missile flyout times, counter-countermeasure capabilities, and kill probabilities. Many of these factors are affected by the performance capabilities of the missile flight vehicles. These large campaign models are run iteratively with variations in the inputs to find gaps or deficiencies in tactics and in weapon system capabilities and to test alternative solutions. The consequence is a better understanding of the improvements needed in existing systems and of the requirements for new systems.

These large war game models rely on missile flight simulations for data on the performance capabilities of the various missiles under the conditions and in the environments being analyzed. Sometimes missile flight simulations are included within the war game models, but more often the flight simulations are run independently to build up a database, such as defended area diagrams and kill probabilities, for use as inputs to the war game models. In these requirements the overall missile size, configuration, and performance characteristics are key factors, and modeling should be designed to highlight them but not to obscure them with unnecessary detail. The level of detail needed in missile flight simulations to be used to establish requirements varies depending on the

main interest underlying the applications of the simulations. For example, if the emphasis is on defended area coverage, relatively simple flight simulations are adequate; however, if the reaction of the missile seeker to specific countermeasures techniques is emphasized, more detailed seeker simulations may be required, even to the inclusion of actual seeker hardware. Since war game models account for multiple, simultaneous engagements and are run repeatedly with variations in input parameters, a large amount of computer processing time can be required. To reduce computer time, missile flight simulations that are embedded in war game models are usually highly simplified. Flight simulations that are run off-line to produce aggregated data for input to warfare models, however, generally take on whatever degree of sophistication is required to meet the objectives.

3-2.12 Designing and Optimising Missiles

The objectives of missile simulations to be used in the design and development of missile systems can be categorized as optimizing the Performance of a preliminary design, testing new approaches to the solution of design problems, forecasting flight-test results, and studying flight-test anomalies. The models are constructed in a way that allows attributes of subsystems that interact and Meet overall system performance to be varied for parametric studies. Simulations often account for the random nature of the various performance parameters so that statistical information can be gathered.

Experience in missile system development has shown that each new system has unique characteristics that place different requirements on simulations. In the development of a new system, the best use of simulation resources is made when simulation capabilities evolve in conjunction with the development process of the missile system. The simulation realism necessary to predict flight-test results cannot be achieved instantaneously, nor are the requirements for simulation realism the same throughout the life cycle of the missile system. During the early development stages-when concept formulation, proof of concept and source selection are dominant issues-relatively simple simulations are often appropriate. During full-scale development and initial procurement when system performance under adverse combat conditions must be demonstrated, much more complex simulated environments and missile response characteristics are needed (Ref. 2).

The general progression of the hierarchy of missile flight simulations usually starts in the initial phase of missile development with simplified, linearized models based on estimated aerodynamic parameters. The simulations are used as a guide by the system analyst to assist in assessing mechanization tradeoffs and missile configuration designs, selecting optimum types of equipment and investigating the outer bounds or limits of performance capability. From there, the modeling evolves into nonlinear, six-degree-of-freedom digital simulations based on aerodynamic data obtained from wind tunnel tests. Designers need these more complex, detailed simulations on which to base their section of appro-

prate guidance laws, control logic, and autopilot designs; to establish equipment specifications; and to evaluate system and subsystem performance (Ref. 7). Competitive selection issues are resolved in a common test bed-the simulation. After the decision has been made to proceed with a given missile design, a hardware-in-the-loop simulation is developed (Ref. 8). The missile hardware components commonly used in simulations are the autopilot, terminal guidance seeker, and controls. Finally, the six-degree-of-freedom simulation may be developed more fully to analyze the effectiveness of the fuze and warhead and to predict the probability of killing targets.

One of the important objectives of missile flight tests is to validate the simulation model. During flight testing, measured data are obtained for missile component performance variables under the influence of the actual flight environment actual aerodynamic characteristics, and random system errors. The simulation output data are compared with flight-test measurements, and model aerodynamic coefficients and other parameters are adjusted as necessary to match flight-test results. In the validation process postflight simulation runs are made to duplicate the conditions of the actual missile test flights as closely as possible, to include using the best estimates of actual system errors evident during testing and of measured environmental data. The model is fully validated when the output of the simulation is in reasonable agreement with the observed flight-test data over the entire range of operating conditions (Ref. 8).

3-2.1.3 Assessing Missile Performance

The ability of simulations to predict flight performance accurately not only enhances future flight successes but also permits exhaustive investigation of missile performance under extreme tactical conditions with a high degree of confidence in the results (Ref. 8). Using simulations to reduce the number of flight tests significantly reduces overall missile system development time and cost Preflight simulations are used to select only the most important engagement scenarios for use in flight tests. During these preflight studies, system deficiencies are frequently exposed and remedied before flight tests. Postflight simulations are used to exploit flight-test data to their full potential. Development time is reduced by providing extensive experimentation by using simulations rather than many costly and time-consuming flight tests. Major decisions, such as whether or not a missile system is ready to be advanced from one acquisition phase to the next are based largely on simulation results. Both Government and contractor manpower is saved as a result of the improved efficiency realized by eliminating false starts, exposing deficiencies early, and correctly resolving complex technological issues (Ref. 2).

Missile simulations used to assess missile performance in lieu of multitudes of flight tests are often extremely detailed and sophisticated; thus they provide the ultimate tool-short of flight testing itself (Ref. 7).

Although considerable confidence can be placed in a ma-

ture and validated flight simulation, complete confidence should never be placed in a simulation. No matter how detailed the simulation, the possibility always remains that the actual missile flight environment contains some phenomena--phenomena that have not been considered in the design of the simulation and that have not been encountered in limited flight testing--which cause the actual flight to differ significantly from the simulated flight. Therefore, when simulation is used as a management tool in lieu of flight testing, the risk of erroneously judging the adequacy of the missile must be weighed against the cost of additional flight testing.

3-2.1.4 Training

Simulation plays an important role in many aspects of modern military training. On combat training ranges computer simulations of missile flight provide realistic practice and assessment of crew performance without the expenditure of actual missile hardware. Thus large numbers of training exercises can be performed at a small fraction of the cost of live firings. Training in an operational environment involves simultaneous engagements of multiple airborne targets, including countermeasures, by multiple surface-to-air fire units and attendant command-and-control functions. In this environment a major cause of unsuccessful guided missile engagements is launching of the missile at a moment when the combination of target position and velocity parameters is not within acceptable launch limits. When a launch crew actuates the firing switch in a training exercise with simulated missiles, the launch parameters are provided to the computer simulation. Actual target position is measured by test range instrumentation and is input to the simulation in near-real time. The computer calculates the missile flight that would have resulted had an actual missile been fired. The simulation provides the training instructor with information on the predicted outcome of the engagement as well as on the causes of unsuccessful engagements.

In developing a missile flight simulation for training purposes, the missile involved normally will be one that has been fully developed and has performance characteristics that are well known through previous, more detailed simulating and testing. For this reason the detailed performances and interrelationships among missile subsystems are of low importance in simulations for training; therefore, many shortcuts and methods to aggregate the simulation details are applied to enable the simulation to operate in realtime. Realtime execution is necessary when troops undergoing training are stimulated with battlefield events that require launch decisions in real time.

3-2.2 OBJECTIVES OF SIMULATIONS ADDRESSED IN THIS HANDBOOK

The US Army uses missile flight simulations to establish requirements for missile systems and to develop, procure, and operate those systems. These applications require esti-

mates of missile flight performance in one form or another, and the primary sources of those estimates--short of actual flight testing--are missile flight simulations.

Among the US Army's objectives in using missile flight simulations are to (1) predict missile performance for proposed or conceptual missile system designs, (2) plan flight tests and analyze flight-test results, (3) aid in acceptance testing of missile system designs, (4) determine missile performance to augment flight testing, (5) evaluate missile performance against countermeasures, and (6) develop new countermeasures that Army aircraft could use against surface-to-air threats. These objectives are included in the overall objective of assessing missile performance. The simulation methods described are intended to apply to specific Army requirements, but because of the general nature of the methods, they could apply to other objectives as well.

3-3 ESSENTIALS OF MISSILE SIMULATIONS

Forces applied to a missile cause translational and rotational accelerations, velocities, and displacements. In a surface-to-air guided missile these forces include aerodynamic forces that are controlled in order to direct the missile flight path toward an intercept with a target. If the missile is stable, the result is a smooth, predictable trajectory through the atmosphere. The motion of a missile along its flight path is predicted in a flight simulation by application of the laws of physics in a mathematical model of the missile and the environment. The model must simulate the guidance and control and account for all of the forces and inertial characteristics of the missile in order to calculate its motion. A simulation uses various coordinate systems, each of which is defined to facilitate simulation of different missile functions.

3-3.1 SIMULATING MISSILE GUIDANCE AND CONTROL

The guidance routines in a flight simulation contain algorithms that model the guidance functions; these include tracking the target and application of the guidance law. The guidance routines calculate a missile maneuver command (a guidance command) in response to the relative missile and target motion as perceived by the target tracker. The maneuver command is passed into the autopilot routine; there a mathematical model of the autopilot (or autopilot hardware) transforms the guidance command into control commands, which are passed to the control system routine. The control system model calculates control surface deflections in response to these commands, and the aerodynamic simulation model calculates the aerodynamic forces and moments on the airframe, which result from the surface deflections. The aerodynamic moments are input to an airframe response model that calculates the achieved angle of attack. The angle of attack produces aerodynamic lift forces that cause the missile flight path to change.

3-3.1.1 Guidance

The model of the target tracker requires target signature data and characteristics of other sources in the target scene, such as background, decoys, and jammers. The target signature, at the aspect angle defined by the line of sight from the missile, is obtained from input tables or algorithms. The line-of-sight vector, its angular rate, and other characteristics of the target scene are processed by the model of the target tracker or by a hardware tracker viewing a simulated scene to determine the instantaneous pointing direction of the target tracker. The target track data are applied to the guidance law contained in the guidance processor model to determine the guidance commands.

3-3.1.2 Autopilot and Control

If detailed autopilot and control system interactions with other missile functions are critical to the purpose of the simulation, it may be necessary to develop high-fidelity simulation subroutines for these subsystems or to substitute actual hardware in place of simulating them. In applications in which the detailed responses of these subsystems are not critical or the response characteristics are known, they are simulated by appropriate transfer functions with gains and time constants selected to match a priori data. The outputs of the control system model (or transfer function) are the fin deflections. In less complex simulations in which fin deflections are not calculated, the function of the autopilot and control system models is to transform the guidance command directly into a commanded angle of attack. The autopilot and control system models allow an appropriate simulated time delay between the guidance command and the airframe response and apply limits as appropriate on fin deflection angles or on angle of attack and/or lateral maneuver acceleration.

3-3.2 SIMULATING MISSILE AND TARGET MOTION

Computer models that simulate the motion of missiles and those that simulate the motion of airplanes are based on the same physical principles: application of propulsive, aerodynamic, and gravitational forces and the responses of the respective airframes to those forces. In general, however, missile flight simulations are much more concerned with the details of the missile flight than with the motion of the target aircraft. In most missile flight simulations, the motion of the target is precalculated and its time sequence is input as a table; or very general algorithms (e.g., straight lines, circular arcs, and sinusoids; or simplified responses to maneuver commands) are employed to calculate the target flight path. Therefore, although the discussion that follows is equally applicable to the simulation of missiles and aircraft, the emphasis is on missiles.

A mathematical model of the motions of the missile and target is based on Newton's second law. At each instant of time a force acting on a rigid body (missile or target) results in an instantaneous acceleration of the center of the mass of

the body. The acceleration is directly proportional to the force; the proportionality constant is the reciprocal of the mass of the body. If the force vector passes through the center of mass of the body, a pure translation results. If the force vector does not pass through the center of mass, a combination of translation and rotation results. The instantaneous rotational acceleration of the body is proportional to the moment of the force acting about an axis through the center of mass. In this case the proportionality constant is the reciprocal of the moment of inertia of the body about that axis. These concepts are expressed mathematically as the familiar equations

$$F = ma, \text{ N} \quad (3-1)$$

and

$$M = I \dot{\omega}, \text{ N}\cdot\text{m} \quad (3-2)$$

where

- F = force acting on a particular body, N**
- m = mass of a particle or body, kg**
- a = translational acceleration, m/s²**
- M = moment acting on a body, N·m**
- I = moment of inertia of a body, kg·m²**
- $\dot{\omega}$ = angular acceleration, rad/s².**

Specific requirements of the laws in the form shown are that the mass be constant and that the accelerations be calculated with respect to an absolute reference frame fixed in inertial space, i.e., a reference frame rigidly associated with the fixed stars (those heavenly bodies that do not show any appreciable change in relative position from century to century) (Ref. 9). It is often convenient to use reference frames that move relative to inertial space; in which case it is necessary to modify the equations to account for the motion of the reference frame. These modifications and the method of handling the variable mass of the missile are presented in Chapter 4.

Three basic types of forces act on a missile and are included in almost all flight simulations—the forces of gravity, propulsion, and aerodynamics. In addition, the gyroscopic moments of internal rotors (or the rotating airframe itself) are sometimes included in simulations; these are discussed in Chapter 4.

3-3.2.1 Gravitational Force

According to Newton's law of gravitation, every particle in the universe attracts every other particle with a force that varies directly as the product of the two masses and inversely as the square of the distance between them. This gravitational mass attraction is directed along the line connecting the masses. For systems of particles, such as a missile and the earth, the resultant gravitational mass attraction is the vector sum of the forces on individual particles. Although the non-spherical mass distribution of the earth affects the magnitude and direction of the resultant attractive force on bodies such

as missiles, the nonspherical components are usually small enough to be neglected in surface-to-air missile applications. For missiles that operate at altitudes between sea level and 30,000 m, the change in the radial distance affects the gravitational mass attraction by less than 1%; however, the correction for changes in altitude is so simple that it is usually applied in flight simulations.

The force of gravity observed in a rotating earth reference frame is the vector sum of the force due to gravitational mass attraction force and a "pseudoforce" called centrifugal force (Refs, 10 and 11). Centrifugal force on a body in a rotating frame is called a pseudoforce because it does not exist under Newton's law in a nonrotating inertial tie of reference. Since there is no centrifugal force at the poles, the observed gravitational force is equal to the gravitational mass attraction force, and it decreases at lower latitudes to a minimum at the equator. This variation of the observed gravitational force with latitude has only small significance in missile flight simulation because the maximum variation is only about 0.5%. If the simulation is to match actual flight-test results, however, the effect of centrifugal force at the latitude of the test range is usually considered.

Since the effects of earth curvature, angular rate, and direction of the gravity vector have an insignificant impact on the dynamics of the missile during its relatively short flight, it is possible to assume a Cartesian coordinate system fixed to the surface of a nonrotating earth. Usually (as defined in subpar. 3-3.3) the x- and y-axes of this earth coordinate system define a plane tangent to the earth at the simulated launch point. Assumptions about the gravitational vector in this coordinate system allow simplifications to be made in the equations of motion. The direction of the gravitational force vector is assumed to be perpendicular to the plane tangent to the surface of the earth. All gravity vectors are assumed to be parallel rather than to converge toward the center of the earth and the magnitude of the gravity vector contains the centrifugal correction.

3-3.2.2 Propulsive Force

The force of propulsion (thrust) applied to the missile usually is supplied by a rocket motor. The resulting thrust vector usually is designed to pass through the center of mass of the missile so as not to contribute unwanted rotational moments. Provisions are made in some simulations to study the effects of small thrust misalignment errors (Ref. 7). In simulating missiles that use thrust-vector control, the direction of the thrust vector is responsive to missile control commands.

For applications that use solid propellant rocket motors, the magnitude of the missile thrust is independent of all parameters that change during the flight except time and atmospheric pressure. Thus the magnitude of the thrust is supplied to the simulation born a table of thrust as a function of time at a specified reference pressure. At each time advancement

within the simulation, the appropriate value of thrust is selected from the table, Interpolation is used when the simulated time falls between the times tabulated. As the simulated missile changes altitude and, therefore, ambient atmospheric pressure, the magnitude of the thrust is corrected by an algorithm in the simulation that accounts for the difference between the reference pressure and the pressure at the current altitude. If the effects of rocket propellant grain temperature on thrust are simulated, they are usually included in the thrust table and require no special algorithms within the simulation.

For missiles that use other types of propulsion, simulation of the thrust maybe more complicated. For example, the effects of missile speed and ambient atmospheric air conditions must be included in the simulation of the thrust of ram jets or air-augmented rockets.

3-3.2.3 Aerodynamic Force

The magnitudes of aerodynamic forces and moments on a missile of given configuration are a function of the Mach number at which the missile travels and the ambient atmospheric pressure or, equivalently, speed and atmospheric density. The methods of dimensional analysis (Refs. 12 and 13) show that the aerodynamic forces F_A and moments M_A are functionally related to these parameters as expressed by

$$F_A = Q C_F S, N \quad (3-3)$$

$$M_A = Q C_M S d, N \cdot m \quad (3-4)$$

where

C_F = general aerodynamic force coefficient, dimensionless

C_M = general aerodynamic moment coefficient, dimensionless

d = aerodynamic reference length of body, m

F_A = aerodynamic force, N

M_A = aerodynamic moment, N·m

Q = dynamic pressure parameter, Pa.

The force and moment coefficients C_F and C_M , respectively, are functions of Mach number M_N and vehicle configuration, which includes any control-surface deflections. The dynamic pressure parameter Q is defined as

$$Q = 0.7 p_a M_N^2, Pa \quad (3-5)$$

or the equivalent form

$$Q = 0.5 \rho V^2, Pa^* \quad (3-6)$$

where

M_N = Mach number, dimensionless

P_a = atmospheric pressure, Pa

V = magnitude of velocity of air relative to a body, airspeed, m/s

ρ = atmospheric density, kg/m³.

These equations are evaluated within the simulation at each computational time step. The term $C_p S$ represents the aerodynamic force per unit of dynamic pressure, and $C_m S d$ represents the aerodynamic moment per unit of dynamic pressure parameter. Reference area S and reference length d are related to missile size; they are constants for any given missile. A complete statement of an aerodynamic coefficient for use as data includes the value of the coefficient plus the reference area and reference length, where applicable, on which the coefficient is based. For surface-to-air missiles the reference area is usually the cross-sectional area of the missile body, and the reference length is usually the diameter of the missile body; however, any other representative area-planform area, wing area, surface area-or length-body length or wing mean aerodynamic chord-may be used. The reference area on which aerodynamic force coefficient data are based must always be specified; otherwise, the data are incomplete and unusable. Likewise, the reference length, in addition to the reference area, for any aerodynamic moment coefficient data must be specified. Care must be taken to ensure that the reference area and reference length used in the simulation are consistent with those on which the aerodynamic data are based. The dependence of the aerodynamic forces and moments on the aerodynamic shape of the missile is described by the coefficients C_p and C_m . At subsonic speeds the coefficients are relatively constant with Mach number, but at transonic and supersonic speeds they are strongly influenced by Mach number. These coefficients are estimated or derived from wind tunnel or flight tests and are supplied to the simulation in the form of tables as functions of Mach number and control-surface deflection. The moment coefficient C_m also depends on the location of the center of mass of the missile, and this dependency must be taken into account in the simulation.

Aerodynamic coefficients also depend on the Reynolds number, which represents the ratio of inertial forces to viscous forces in the fluid flow under consideration. This dependency is relatively weak within the range of Reynolds numbers experienced by most surface-to-air missiles and can sometimes be neglected. However, since the Reynolds num-

ber varies with altitude, as well as with missile speed and size for simulations of missiles that reach high altitude, it may be necessary to supply tables of aerodynamic coefficients also as functions of altitude.

3-3.2.4 Airframe Response

A missile or an airplane, considered a rigid body in space, is a dynamic system in six degrees of freedom. Its motion in space is defined by six components of velocity, i.e., three translational and three rotational. Simplifications are sometimes made in missile flight simulations by approximating-or neglecting altogether-the degree of freedom that represents missile roll; this results in a five-degree-of-freedom model. Simulations that are further simplified by approximating all three rotational degrees of freedom but that retain the three translational degrees of freedom, are three-degree-of-freedom models.

In simulations with five or six degrees of freedom, the fins are deflected at each computational time step in response to commands from the autopilot. Aerodynamic moments are calculated on the basis of the fin deflections, and solution of the rotational equations of motion yields the missile angle of attack.

In simulations with three degrees of freedom, the difference between six-degree-of-freedom models is that the simulated missile directly assumes an angle of attack corresponding to the lateral acceleration commanded by the guidance model. The calculations of fin deflections and aerodynamic moments are bypassed thus the transient behavior of the missile in developing an angle of attack does not meet all the detailed nonlinear response characteristics that can be included when aerodynamic moments are calculated by using tabular aerodynamic moment data. For many applications in which missile transient response characteristics are known or can be assumed, sufficient simulation fidelity is obtained by employing a transfer function in place of a detailed simulation of the aerodynamic response. The commanded angle of attack is the input to the transfer function, and the achieved angle of attack is the output. For example, employing a transfer function that corresponds to a second-order dynamic system permits adjusting the time required for the simulated missile to respond to commands and the amount the achieved angle of attack overshoots the commanded angle of attack. (These parameters are important to missile miss distance.) By adjusting these parameters, the missile response characteristics are calibrated to match flight-test data or the results of more sophisticated simulations.

*It is common usage, almost universal, to call Q the "dynamic pressure". This usage is strictly correct only in the subsonic flow region. In the transonic and supersonic flow regions, the actual measurable dynamic pressure is equal to the dynamic pressure parameter multiplied by a compressibility factor however, the parameter is commonly referred to as dynamic pressure.

3-3.3 ROLE OF COORDINATE SYSTEMS

Many of the factors used in mathematical analyses of missile performance can be expressed as vectors in three-dimensional space, i.e., they have the attributes of magnitude and direction. The vectors used in missile flight simulations represent factors such as forces, accelerations, velocities, positions, moments, angular accelerations, and angular rates. For the direction of a vector to have meaning, it must be described relative to some frame of reference. Right-handed, orthogonal coordinate systems are commonly used as frames of reference. A vector is described by its three components on the axes of a coordinate system.

A number of different coordinate systems may be used in a given missile flight simulation. Coordinate systems are characterized by the positions of their origins, their angular orientations, and their motions relative to inertial space or relative to other specified systems. A given vector can be described by its coordinates in any of the coordinate systems. If the coordinates of a vector are given in one reference frame, the coordinates of that vector in any other reference frame can be determined if the position and orientation of one reference frame relative to the other is known.

The reason for using different coordinate systems is a matter of mathematical convenience. For example, a coordinate system fixed in inertial space is required for calculating absolute accelerations, a coordinate system aligned with the vehicle velocity vector facilitates aerodynamic calculations, and a coordinate system aligned with the principal axes of the body simplifies calculation of angular accelerations.

A long-standing convention for coordinate systems for airplanes is that the x-axis of a coordinate system points forward, the y-axis is toward the right wing, and the z-axis is toward the floor of the airplane. This general convention has been retained in missile applications and is employed in this handbook. In applications to rolling symmetrical missiles, however, it is sometimes difficult to define which is the right wing and which direction is toward the floor; obviously, this requires a more detailed definition of the coordinate system.

Although coordinate systems located at any arbitrary position and with any arbitrary orientation and motion are feasible, only certain well-defined systems are ordinarily used. The most common systems used in flat-earth simulations are the earth, body, wind, guidance, tracker, and target coordinate systems illustrated in Fig. 3-1. A given simulation may not contain all of these coordinate systems, and additional coordinate systems may be used for special applications. Brief discussions of the common coordinate systems follow, and more detailed definitions, as well as methods used to transform vectors from one coordinate system to another, are given in Appendix B.

1. *Earth Coordinate System* (x_e, y_e, z_e). In a flat-earth simulation the earth is usually assumed to be fixed in space, i.e., neither translating nor rotating. In this case, absolute accelerations can be measured with respect to any coordinate

system fixed to the earth. Such a system is called an earth coordinate system and is commonly used as a basis for measuring accelerations, velocities, and positions of a missile, target, and decoys.

2. *Body Coordinate System* (x_b, y_b, z_b). The body coordinate system is fixed to the missile and aligned with the principal axes of the missile. Thus the system is particularly useful for calculations of angular rates because the equations of motion contain no terms involving the products of the moments of inertia and the moments of inertia about the reference frame axes are independent of missile attitude. By definition, the body coordinate system is considered to be rigidly attached to the missile so that in flight the coordinate axes translate, yaw, pitch, and roll with the missile. In some simulations the roll of the missile is not explicitly taken into account, or it can be calculated by other means and thus eliminates the need for the body axes to roll with the missile. In these applications the body coordinate system translates, yaws, and pitches with the missile but does not roll.

3. *Wind Coordinate System* (x_w, y_w, z_w). The movement of undisturbed air relative to the missile (relative wind) is tangent to the missile flight path. The wind coordinate system is viewed as being aligned with the relative wind to simplify the calculation of aerodynamic forces and moments. By definition, the aerodynamic drag and lift vectors are aligned with wind system axes.

4. *Guidance Coordinate System* (x_g, y_g, z_g). The guidance coordinate system is aligned with the initial line-of-sight vector from the missile to the target. Its origin is fixed to the missile and translates with it, but the system does not rotate. Since the system does not rotate, it is an appropriate coordinate system for use in calculating absolute angular accelerations and rates of the seeker head. Also, since an axis is aligned with the initial line-of-sight vector, angular variations of the line of sight from the axis are often small. This permits use of small-angle approximations in calculations.

5. *Tracker Coordinate System* (x_s, y_s, z_s). The tracker coordinate system is used for modeling the target tracker, which may be either an onboard seeker or a tracker located on the ground. The alignment of this coordinate system is with the central tracker viewing axis, and the system contains a plane that is parallel with the reticle plane of an infrared (IR) seeker, the focal plane of an imaging seeker, or the planar array of a radio frequency (RF) antenna. This arrangement simplifies calculations of tracker functions for some applications. The origin of the tracker coordinate system is at the location of the target tracker, which may be either on the missile or on the ground. In using the tracker coordinate system for an onboard seeker, the system is assumed to be rigidly attached to the seeker except in roll; thus the coordinate system translates and rotates with the seeker but does not roll. The coordinate system for ground-based trackers does not translate, but it does rotate in azimuth and elevation with the tracker and does not roll.

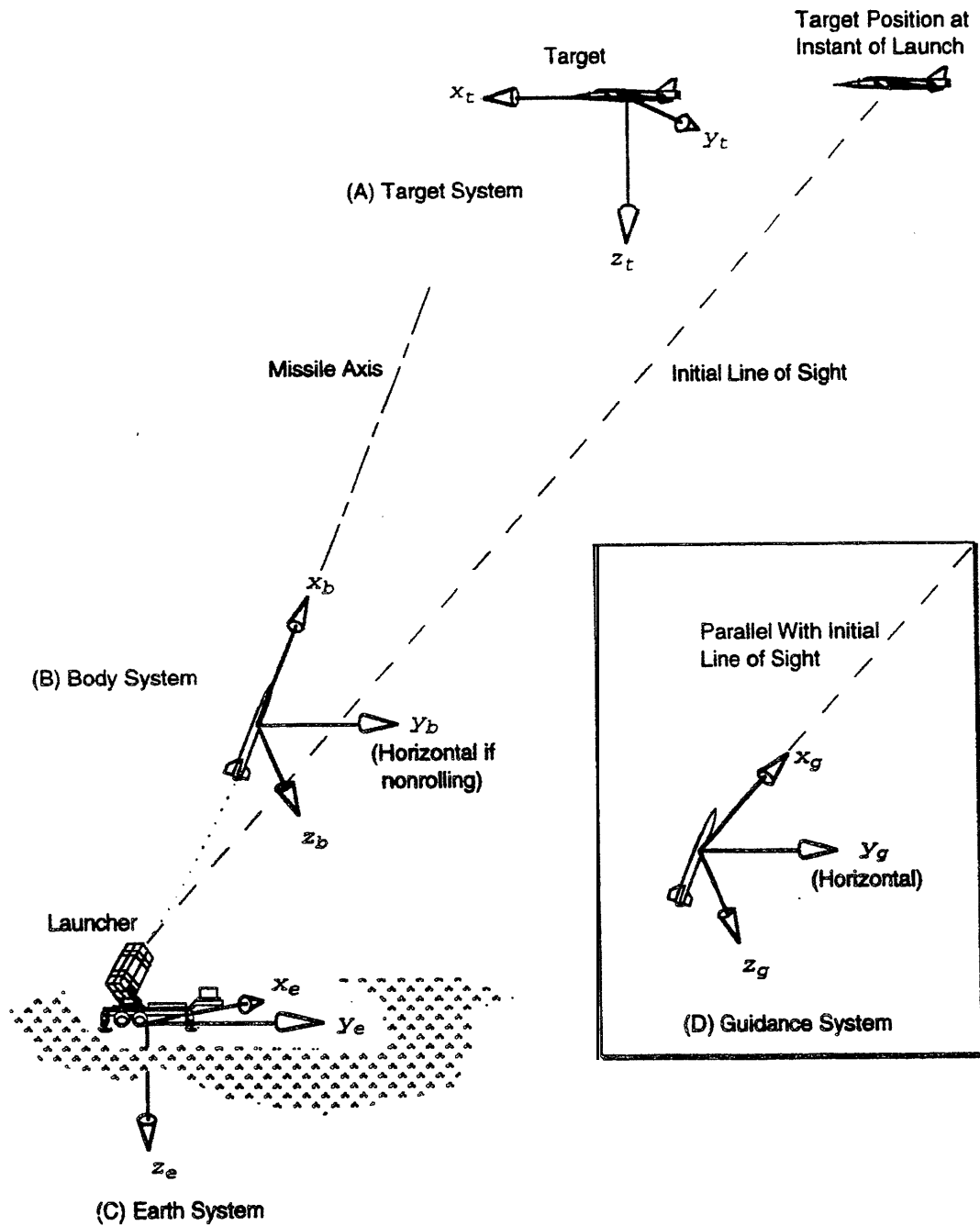


Figure 3.1. Coordinate Systems

(cont'd on next page)

6. Target Coordinate System (x_t, y_t, z_t) . Target signature data usually are supplied as a function of azimuth and elevation aspect angles. These angles are defined in the target coordinate system. Not all target signature data are based on the same coordinate system definition; therefore, the simulation user must transform the signature data if they are not

supplied in the coordinate system used by his/her simulation. A standard coordinate system for aircraft is similar to the body coordinate system defined for the missile. The target coordinate system is viewed as being rigidly attached to the target; therefore, it translates, pitches, yaws, and rolls with the target.

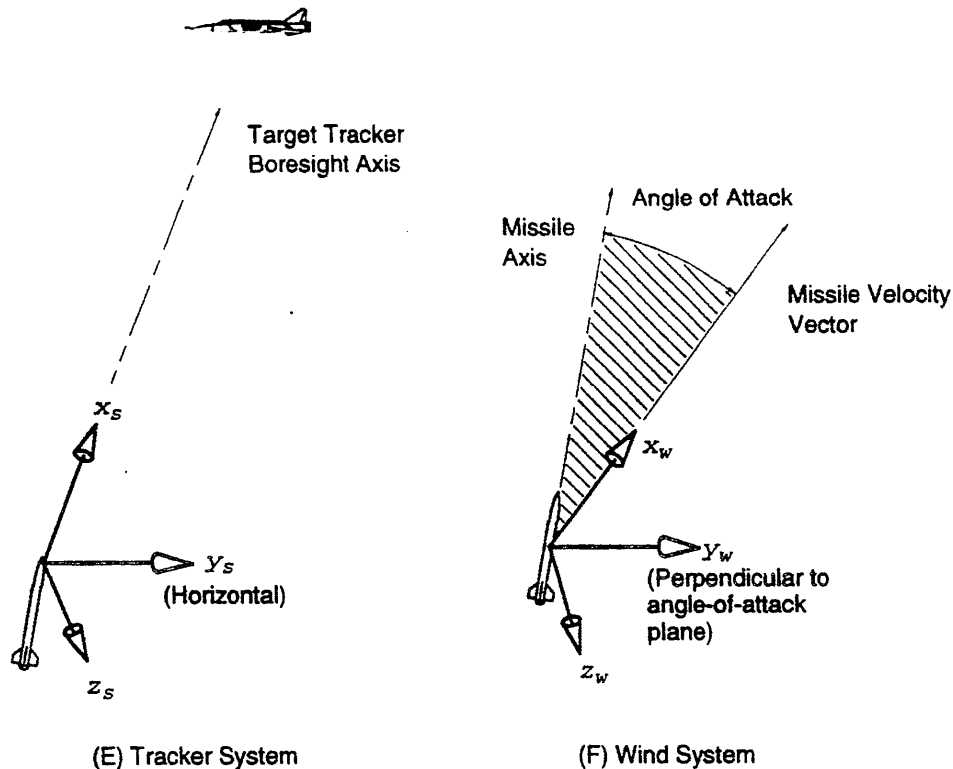


Figure 3-1. (cont'd)

3-3.4 COMPUTATIONAL CYCLE

In a computer program the computation proceeds, or flows, from one processing task to the next. In a missile flight simulation each task generally represents calculations or logic processing to simulate some function of the actual missile operation or some interaction between the missile and its environment. In a digital simulation the processing is done in discrete time steps, the size of which must be carefully considered to ensure faithful representation of the highest frequency components of the simulated missile system. At any given time step the processing proceeds through each task and calculates any changes that occur within that time increment. After completion of all tasks appropriate to that time increment, the program steps to the next time increment and repeats the cycle.

Computer programs are described by flow diagrams that show the flow of processing from one task to the next. Typically, flow diagrams are developed at different levels of aggregation. In a top-level diagram the tasks are very aggregated and thus permit a big-picture view of the interactions of major subroutines. Lower level diagrams contain additional details until, at the lowest level, every processing operation is represented.

Fig. 3-2 shows a top-level flow diagram for a typical missile flight simulation. Each block in the diagram represents a major function, or group of functions, or a major logic process in the computer program. The direction of processing flow is indicated by arrows. One cycle through the flow diagram represents an incremental time step.

Progressing through Fig. 3-2, the program starts by reading input data that describe the initial conditions and other parameters that change from one computer run to the next. Typical initial conditions include target initial position, velocity, and attitude vectors and missile launcher position if other than the origin of the coordinate system. Inputs describing the target include target signature data, target maneuver parameters, and countermeasures parameters. Environmental inputs could include standard or nonstandard atmosphere, sun position, and atmospheric transmission parameters. If the design of the missile being simulated is not frozen, any of many different missile parameters could be treated as inputs. These might include seeker performance parameters, guidance law parameters, aerodynamic coefficient data, propulsion data, mass, moments of inertia, and dynamic time constants.

Initialization includes calculating such factors as launcher pointing direction and slewing rate and initial seeker pointing direction. If the initial target position is beyond the target sensor range, the program may proceed until the target is within range before missile launch.

A table lookup procedure accesses the atmospheric data tables to determine atmospheric pressure, density, and speed of sound at the altitude of the missile. These parameters are used to calculate missile Mach number and dynamic pressure parameter based on missile speed.

Missile and target position and velocity vectors are used to calculate the relative position and velocity vectors with respect to the target. A test is performed to determine whether

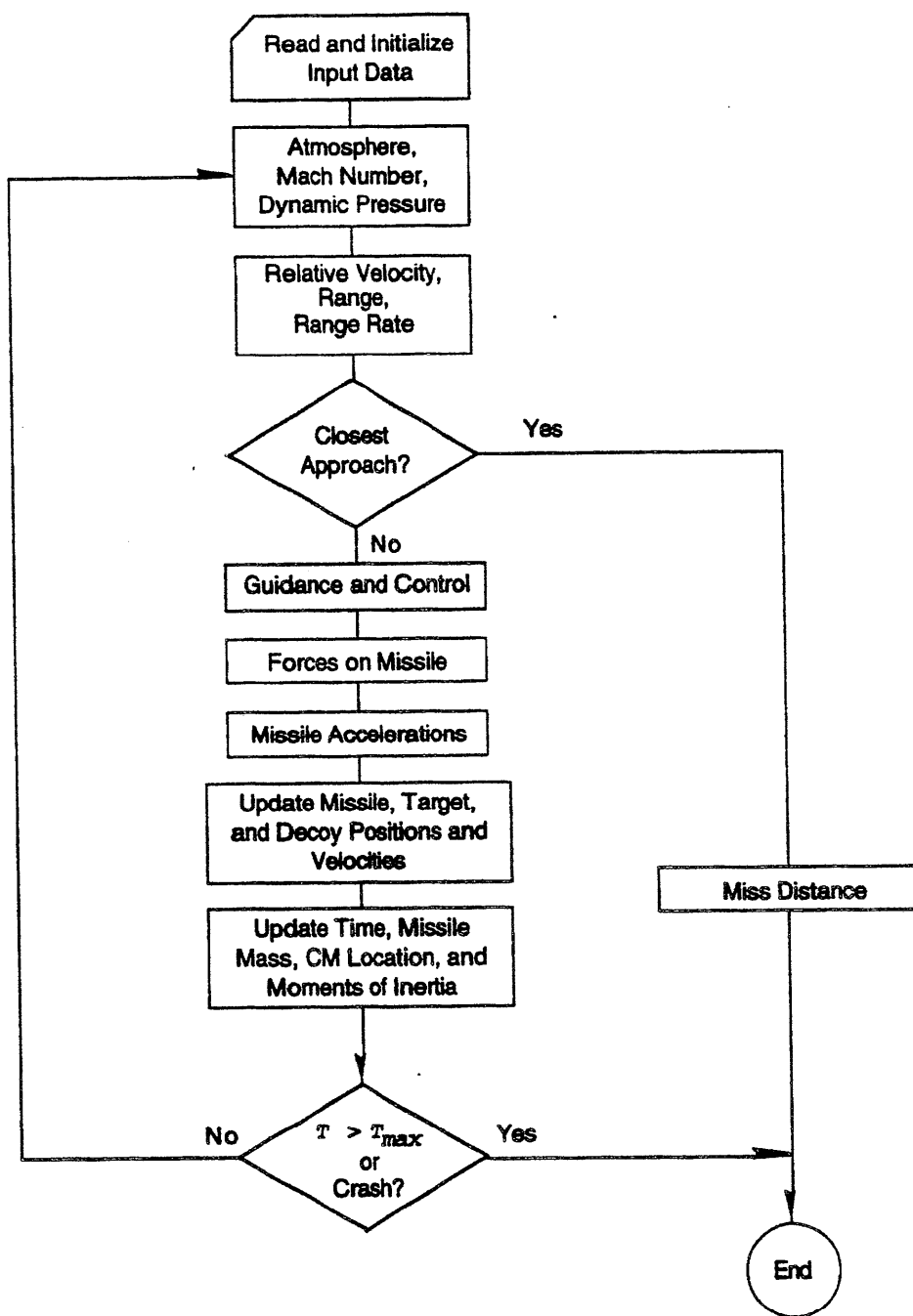


Figure 3-2. Typical Top-Level Flow Diagram for a Flight Simulation

the missile has reached its closest approach to the target, which of course will not occur until the end of the engagement. If the test shows that the closest approach has been reached, the program sequence is diverted to a routine that calculates miss distance and the program ends. Otherwise, the program continues into the guidance routine.

The guidance section of the program calculates the aspect angles of the target relative to the line-of-sight vector and uses these to determine the target signature as viewed by the target tracker. The line-of-sight vector and the target signature are passed into the target tracker routine (or to the phys-

ical target scene simulator if a hardware seeker is used). The tracker routine (or seeker hardware) determines the tracking error and the response of the tracker in terms of a new tracker pointing direction. The guidance processing routine applies the tracker output to the guidance law to determine the missile guidance maneuver command, and this command is processed by the autopilot and control routines or hardware components to determine control-surface deflections.

Aerodynamic forces and moments on the missile are calculated based on the current velocity vector, missile attitude, control-surface deflections, Mach number, and dynamic

pressure parameter. Thrust is determined from the thrust data as a function of current program time and corrected for ambient pressure.

The equations of motion are used to calculate the components of missile acceleration. Parameters required for substitution into these equations are the forces and moments, missile mass and moments of inertia, missile angular rates, and the gravitational acceleration vector.

Missile accelerations are integrated to determine translational and rotational velocity and position vectors at the end of the current computation interval. The target attitude, velocity, and position are updated-usually by using relatively simple equations. If decoys have been deployed, their velocities and positions are calculated.

Missile mass is reduced by an amount proportional to the momentum component of thrust during the computational interval, and moments of inertia and the location of the center of mass are appropriately adjusted.

At this point all parameters have been updated to the end of the current computational interval. The time is now incremented to the beginning of the next interval in preparation for the next computation cycle. If the new time exceeds the input value of maximum simulated flight time (e.g., time of seeker coolant depletion or self-destruct) or if the missile altitude is less than the terrain altitude, the program ends. Otherwise, the program returns to the atmosphere routine to start the next computation cycle.

3-4 LEVEL OF SIMULATION DETAIL

The various levels of simulations needed for missile development and the diversity of simulations used for related analyses require a wide range of simulation approaches. Basically, these approaches differ in terms of the degree of fidelity in simulating the target track sensor and in simulating the transient control and maneuver response of the missile. For example, methods used to simulate target sensors range from the very simple assumption that tracking is performed perfectly to the use of real-time simulations using actual-flight hardware seekers that view simulated target scenes that radiate physical electromagnetic energy. Also methods used to simulate missile motion range from the use of simple two-degree-of-freedom formulations to very sophisticated six-degree-of-freedom models. (See subpar. 3-3.2.4.)

A major consideration is whether the simulation should be designed to operate in real time. Certain simulated events, such as control-surface deflections and seeker signal processing, contain high-frequency spectral components that require very small computational time steps to simulate. Because of the small time steps, the time to calculate these events may be considerably longer than the time it would take for them to happen in actual missile flight. When actual missile hardware components are substituted for some of the mathematical equations in the simulation, it is necessary that the model be constrained to run in real time to mesh with the

real-time operation of the hardware. Various techniques are used to achieve real-time simulation. These techniques include the use of analog computers to simulate functions with high-frequency components, very high-speed digital equipment, and computational approximations.

As previously stated, the level of detail to be included in a simulation very much depends on the objectives of the user. An important part of the development of a missile flight simulation is planning the levels of detail to be included based on an assessment of user objectives. Including unnecessary detail can have serious consequences. It increases the chances for subtle program errors that may never be found and that could mask important simulation results, it decreases the general visibility of the interactions within the simulation program and complicates the interpretation of simulation results, and it reduces the utility of a simulation because it increases development time and computer setup and run times. Conversely, omitting detail that is important to the objectives of the user of the simulation can invalidate the simulation for its intended purpose or, worse, lead unsuspecting users to wrong conclusions.

3-4.1 MODELING TO MATCH SIMULATION OBJECTIVES

The different levels of model sophistication or detail needed to satisfy different simulation objectives are best illustrated by examples. In the examples that follow, several different sets of simulation objectives are cited, and each is followed by comments on the level of simulation detail required to meet those objectives.

1. Example No. 1:

a. Objective. A simulation to provide the flyout characteristic, e.g., range as a function of time, for different missile configurations to use in preliminary design studies.

b. Level of Simulation Detail. Accurate thrust and drag model is required, but seeker can be assumed to be perfect. Missile response characteristics can be instantaneous. Modeling missile rotations is not required; two degrees of freedom may be adequate. Simple Euler numerical solution of equations of motion is adequate; modeling of target motion is not required.

2. Example No. 2:

a. Objective. A simulation to provide general defense coverage diagrams for different missile configurations for use in air defense system studies.

b. Level of Simulation Detail. Seeker gimbal angle limits, tracking rate limits, and missile lateral maneuver acceleration constraints should be added. Any minimum closing velocity requirements (for fuzing) or minimum missile velocity (for controllability) should be included. At least a three-degree-of-freedom simulation is required, but more than three degrees are probably not necessary. Seeker lock-on range limits can be included in the simulation, but often these limits are superimposed on the simulation results off-line.

3. Example No. 3:

a. Objective. A simulation to evaluate generic missile performance against maneuvering targets.

b. Level of Simulation Detail. Missile response characteristics become important, but it may be possible to aggregate missile response into one or more time constants rather than to simulate the dynamic response in detail. Three degrees of freedom plus a technique to calculate dynamic angle of attack is usually sufficient for a generic missile.

4. Example No. 4:

a. Objective. A simulation to determine the response characteristics of a specific missile design.

b. Level of Simulation Detail. The dynamics of the missile autopilot, control system, and airframe angular rates must be simulated. This requires modeling forces and moments with at least five degrees of freedom. If the missile roll rate is rapid enough to affect missile performance significantly, six degrees of freedom may be required, or techniques for treating rolling airframes in nonrolling coordinate frames may be used.

5. Example No. 5:

a. Objective. A simulation to determine the response of generic seekers to countermeasures.

b. Level of Simulation Detail. Generic seeker response to signals within the field of view must be simulated. This could be accomplished by using tabular input data that describe the static gain curves if IR seekers are simulated or that describe the sum and difference curves that result from the antenna patterns if RF seekers are simulated. Three degrees of freedom are often adequate for studying generic seeker response characteristics.

6. Example No. 6

a. Objective. A simulation to determine the response of a specific seeker to countermeasures.

b. Level of Simulation Detail. A very detail model of seeker dynamics and signal processing is required. An alternative is to substitute actual seeker hardware into the tracking loop and to generate a scene for the seeker to view. At least five degrees of freedom are required to support hardware-in-the-loop and may also be required to support a very detailed mathematical seeker model.

7. Example No. 7:

a. Objective. A simulation to evaluate aerodynamic cross-coupling effects, airframe vibration and deflection effects, and wing flutter.

b. Level of Simulation Detail. Very detailed modeling of these effects is required. Six degrees of freedom are required for these very sophisticated simulations. The methods used to model these effects are beyond the scope of this handbook because they require complicated and specialized techniques.

3-4.2 MODEL SOPHISTICATION REQUIRED TO SATISFY HANDBOOK OBJECTIVES

The discussion of simulation techniques here is oriented toward satisfying the handbook objectives discussed in sub-

par. 3-2.2. Consequently, the following general levels of detail are addressed:

1. Three, five, or six degrees of freedom

2. The level of sophistication of aerodynamic modeling depends primarily on the number of degrees of freedom. When body rotation rates are not calculated explicitly (three degrees of freedom), aerodynamic moment coefficients are not required. When fin deflections are not calculated explicitly, the dependence of aerodynamic coefficients on fin deflection is neglected. (Coefficients are input as functions only of Mach number and angle of attack if trim conditions are assumed.) For five- or six-degree-of-freedom simulations, aerodynamic force coefficients are functions of Mach number, angle of attack, and fin deflection; in addition, moment coefficients are functions of the location of the center of mass of the missile. For missiles that reach high altitude, these coefficients also may be functions of Reynolds number.

3. Motor thrust for missiles powered by solid rocket propellant is input as a function of time for some reference altitude. Variations in thrust caused by temperature are handled by adjusting the input thrust table, and variations in thrust relative to altitude are calculated within the simulation.

4. The seeker is modeled by assuming that it has the capability to track perfectly (with gimbal angle and rate limits), by using static gain curves (for infrared seekers) or sum and difference curves (for radio frequency seekers), or by substituting actual seeker hardware-in-the-loop. When mathematical seeker modeling is used, the dynamic characteristics are represented by an approximate transfer function, by a detailed mathematical model (including modeling the gyro), or by a combination of a transfer function and certain portions of the hardware components.

5. Autopilot and control dynamics are handled by transfer functions or by use of actual autopilot and control hardware-in-the-hop.

REFERENCES

1. N. A. Kheir, "A Validation Procedure for Missile Systems Simulation Models", Proceedings of the Seventh Annual Pittsburgh Conference, Modeling and Simulation, Vol. 7, Part 1, Pittsburgh, PA April 1976.
2. M. M. Rea et al, Missile System Simulation at the Advanced Simulation Center, Technical Report RD-82-11, Systems Simulation and Development Directorate, Advanced Simulation Center, US Army Missile Laboratory, US Army Missile Command, Redstone Arsenal, AL, 25 January 1982.
3. P. C. Gregory, "Testing of Missile Guidance and Control Systems", Guidance and Control for Tactical Guided Weapons With Emphasis on Simulation and Testing, AGARD-LS-101, Advisory Group for Aerospace Research and Development, North Atlantic Treaty Organization, Neuilly sur Seine, France, May 1979.

4. W. Read and J. Sheehan, "AMRAAM System Simulation, A Detailed Design and Performance Evaluation Tool", *Electronic Progress* 22,4 (Winter 1980).
5. P. C. Gregory, "Guidance Simulation Techniques", *Guidance and Control for Tactical Guided Weapons With Emphasis on Simulation and Testing*, AGARD-LS-101, Advisory Group for Aerospace Research and Development, North Atlantic Treaty Organization, Neuilly sur Seine, France, May 1979.
6. F. M. Belrose and A. M. Baird, *The Role of Simulation in High-Technology Missile Applications*, Technical Report RD-CR-83-23, US Army Missile Command, Redstone Arsenal, AL, April 1983.
7. H. L. Pastrick et al, "Monte Carlo Model Requirements for Hardware-in-the-Loop Missile Simulations", *Proceedings of the 1976 Summer Computer Simulation Conference*, Washington, DC, 1976.
8. T. R. Driscoll and H. F. Eckenroth, "Flight Test Validation of the Patriot Missile Six-Degree-of-Freedom Aerodynamic Simulation Model", *Automatic Control Theory and Applications* 7, 1 (January 1979).
9. A. Miele, *Flight Mechanics, Volume 1, Theory of Flight Paths*, Addison-Wesley Publishing Company, Inc., Reading, MA, 1962.
10. R. C. Duncan, *Dynamics of Atmospheric Entry*, McGraw-Hill Book Company, Inc., New York, NY, 1962.
11. A. E. Puckett and S. Ramo, *Guided Missile Engineering*, McGraw-Hill, New York, NY, 1959.
12. R. S. Shevell, *Fundamentals of Flight*, Prentice-Hall, inc., Englewood Cliffs, NJ, 1983.
13. E. A. Bonney et al, "Aerodynamics, Propulsion, Structures and Design Practice", *Principles of Guided Missile Design*, G. Merrill, Ed., D. Van Nostrand Company, Inc., Princeton, NJ, 1956.
- A. C. Jolly, "On An Application of Hardware-in-the-Loop Simulation to Missile System Performance Evaluation", *Proceedings 7th Annual Southeastern Symposium on System Theory*, Tuskegee, AL, IEEE Catalog Number: 75CH0968-8C, 20-21 March, 1975, Institute of Electrical and Electronics Engineers, Inc., New York, NY.
- R. J. Kochenburger, *Computer Simulation of Dynamic Systems*, Prentice-Hall, Inc., Englewood Cliffs, NJ, 1972.
- R. D. Lewis and C. H. Horgen, "Optical Sensor System Evaluation", *Proceedings of the Society of Photo-Optical Instrumentation Engineers, System Aspects of Electro-Optics*, SPIE Vol 187, May 1979, Society of Photo-Optical Instrumentation Engineers, Bellingham, WA.
- C. T. Maney, "Tactical Missile Performance Requirements, A Methodology for Development", *Guidance and Control for Tactical Guided Weapons With Emphasis on Simulation and Testing*, AGARD-LD-101, Advisory Group for Aerospace Research and Development North Atlantic Treaty Organization, Neuilly sur Seine, France, May 1979.
- P. Manville, "Weapon Delivery and Its Evaluation", *Guidance and Control for Tactical Guided Weapons With Emphasis on Simulation and Testing*, AGARD-LS-101, Advisory Group for Aerospace Research and Development North Atlantic Treaty Organization, Neuilly sur Seine, France, May 1979.
- G. A. Mihram, *Simulation: Statistical Foundations and Methodology*, Academic Press, New York, NY, 1972.
- T. H. Naylor, Ed., *The Design of Computer Simulation Experiments*, Duke University Press, Durham, NC, 1969.
- T. Naylor et al, *Computer Simulation Techniques*, John Wiley & Sons, Inc., New York, NY, 1966.
- H. L. Pastrick et al, "System Performance Prediction by Modeling Test Data on Digital Simulations", *Journal of Spacecraft and Rockets* (March 1974).
- H. L. Pasterick et al, "Real-Time Hybrid Hardware-in-the-Loop Simulation of a Terminal Homing Missile", *Proceedings of the 1973 Summer Computer Simulation Conference*, Montreal, Canada July 1973.
- J. Reitman, *Computer Simulation Applications*, Wiley Interscience, New York, NY, 1971.
- R. E. Shannon, *Systems Simulation, The Art and Science*, Prentice-Hall, Inc., Englewood Cliffs, NJ, 1975.
- E. Sisle and E. D. McCarthy, "Hardware-in-the-Loop Simulation for an Active Missile", *Simulation* 39, 5 (November 1982).

BIBLIOGRAHY SIMULATION

- T. A. Atherton, "A Missile Flight Simulator for Infrared Countermeasures Investigations", *Proceedings of the Society of Photo-Optical Instrumentation Engineers, Optics in Missile Engineering*, SPIE Vol 133, Los Angeles, CA, January 1978, Society of Photo-Optical Instrumentation Engineers, Bellingham, WA.
- D. N. Chorafas, *Systems and Simulation*, Academic Press, New York, NY, 1965.

CHAPTER 4

MISSILE DYNAMICS

Chapters 1 through 3 provide general information on missile systems and missile simulations; Chapter 4 begins development of the specific mathematical techniques employed in missile flight simulations. The approach discussed in the previous chapters includes calculating the forces and moments acting on the missile and substituting them into the equations of motion to yield vehicle accelerations. Chapter 4 expands on this approach by beginning with a more general statement of Newton's second law of motion and proceeds through development of equations for translational and rotational motions, for expressing these equations relative to rotating reference frames, and for handling the gyroscopic moments of internal rotors.

4-0 LIST OF SYMBOLS

<p>\mathbf{A} = aerodynamic axial force vector, N</p> <p>\mathbf{A}_g = acceleration vector due to gravitational mass attraction between earth and.. a free-falling object m/s^2</p> <p>\mathbf{A}_{inrtl} = absolute acceleration vector of a particle, i.e., relative to an inertial frame, m/s^2</p> <p>\mathbf{A}_{rot} = acceleration vector of a particle relative to (as viewed by an observer in) a rotating reference frame, m/s^2</p> <p>A = magnitude of aerodynamic axial force vector A, N</p> <p>A_e = rocket nozzle exit area, m^2</p> <p>\mathbf{B} = arbitrary general vector</p> <p>$\dot{\mathbf{B}}_{inrtl}$ = rate of change of general vector B relative to inertial reference frame</p> <p>$\dot{\mathbf{B}}_{rot}$ = rate of change of general vector B relative to (as viewed by an observer in) a rotating reference frame</p> <p>B = magnitude of general vector B</p> <p>\mathbf{D} = aerodynamic drag force vector, N</p> <p>D = magnitude of aerodynamic drag force vector D, N</p> <p>dm = infinitesimal mass, kg</p> <p>\mathbf{F} = vector sum of forces acting on a particle or body, N</p> <p>\mathbf{F}_A = resultant aerodynamic force vector, N</p> <p>\mathbf{F}_g = gravitational force vector including effects of earth rotation, N</p> <p>\mathbf{F}_p = total instantaneous thrust force vector, N</p> <p>\mathbf{F}_{ext} = vector sum of external forces F_A, F_g, and pressure thrust (This variable does not include the force of momentum thrust which is internal to the closed system defined as the missile flight vehicle plus rocket exhaust gases.), N</p>	<p>F = magnitude of sum of forces acting on the body, N</p> <p>$F_{Ax_b}, F_{Ay_b}, F_{Az_b}$ = components of aerodynamic force vector F_A expressed in the body coordinate system N</p> <p>F_G = magnitude of the mutual force of gravitational mass attraction between two masses, N</p> <p>F_g = magnitude of gravitational force vector F_g weight of body, N</p> <p>$F_{gx_b}, F_{gy_b}, F_{gz_b}$ = components of gravitational force vector F_g expressed in the body coordinate system N</p> <p>$F_{px_b}, F_{py_b}, F_{pz_b}$ = components of thrust vector F_p expressed in the body coordinate system, N</p> <p>F_x, F_y, F_z = general components of force expressed in the body coordinate system (same as</p> <p>$F_{x_b}, F_{y_b}, F_{z_b}$ = components of total force vector F expressed in the body coordinate system, N</p> <p>G = universal gravitational constant, $6.673 \times 10^{-11} m^3/(kg \cdot s^2)$</p> <p>$\mathbf{g}$ = vector of acceleration due to gravity at altitude of the body, m/s^2</p> <p>\mathbf{g}_0 = vector of acceleration due to gravity at earth surface, m/s^2</p> <p>g = magnitude of acceleration-due-to-gravity vector g, m/s^2</p> <p>g_0 = magnitude of the acceleration due to gravity at the earth surface vector g, m/s^2</p> <p>\mathbf{h} = angular momentum vector of a particle or body, $N \cdot m \cdot s$</p> <p>$\dot{\mathbf{h}}$ = rate-of-change vector of angular momentum h, $N \cdot m$</p> <p>$\dot{\mathbf{h}}_{inrtl}$ = rate-of-change vector of angular mo-</p>
--------------------------------------------------------------------------------------------------------------------------------------------------------------------------------------------------------------------------------------------------------------------------------------------------------------------------------------------------------------------------------------------------------------------------------------------------------------------------------------------------------------------------------------------------------------------------------------------------------------------------------------------------------------------------------------------------------------------------------------------------------------------------------------------------------------------------------------------------------------------------------------------------------------------------------------------------------------------------------------------------------------------------------------------------------------------------------------------------------------------------------------------------------------------------------------------------------------------------------------------------------------------------------------------------------------------------------------------------------------------------------------------------------------------------------------------------------------------------------------------------------------------------------------------------------------------------------------------------------------------------------------------------------------------------------------------------------------------------------------------------------------------------------------------------------------------------------------------------------------------------------------------------------------------------------------------------------------------------------------------------------	----------------------------------------------------------------------------------------------------------------------------------------------------------------------------------------------------------------------------------------------------------------------------------------------------------------------------------------------------------------------------------------------------------------------------------------------------------------------------------------------------------------------------------------------------------------------------------------------------------------------------------------------------------------------------------------------------------------------------------------------------------------------------------------------------------------------------------------------------------------------------------------------------------------------------------------------------------------------------------------------------------------------------------------------------------------------------------------------------------------------------------------------------------------------------------------------------------------------------------------------------------------------------------------------------------------------------------------------------------------------------------------------------------------------------------------------------------------------------------------------------------------------------------------------------------------------------------------------------------------------------------------------------------------------------------------------------------------------------------------------------------------------------------------------------------------------------------------------------------------------------------------------------------------------------------------------

- momentum h relative to inertial reference frame, $N \cdot m$
- \dot{h}_{rot} = rate-of-change vector of angular momentum h relative to (as viewed by an observer in) a rotating reference frame, $N \cdot m$
- h' = angular momentum vector of all rotors, $N \cdot m \cdot s$
- h = altitude above sea level, m
- \dot{h}_{rot} = magnitude of the rate-of-change vector of angular momentum h relative to (as viewed by an observer in) a rotating reference frame, $N \cdot m$
- h'_x, h'_y, h'_z = components of rotor angular momentum vector h expressed in the body coordinate system, $N \cdot m \cdot s$
- $[I]$ = inertia matrix of a body, $kg \cdot m^2$
- $\dot{[I]}$ = rate of change of inertia matrix, $kg \cdot m^2/s$
- $[I']$ = inertia matrix of a rotor relative to the body coordinate system, $kg \cdot m^2$
- I'_x, I'_y, I'_z = diagonal elements of rotor inertia matrix $[I]$ relative to body axes, $kg \cdot m^2$
- I_x, I_y, I_z = moments of inertia (diagonal elements of inertia matrix when products of inertia are zero), $kg \cdot m^2$
- I_{xx}, I_{yy}, I_{zz} = moments of inertia (diagonal elements of inertia matrix in the general case where products of inertia are not necessarily zero), $kg \cdot m^2$
- I_{xy}, I_{xz}, I_{yz} = products of inertia (off-diagonal elements of inertia matrix), $kg \cdot m^2$
- i_b, j_b, k_b = Unit vectors in directions of x_b -, y_b - and z_b -axes (body coordinate system), respectively, dimensionless
- i_e, j_e, k_e = unit vectors in directions of x_e -, y_e - and z_e -axes (earth coordinate system), respectively, dimensionless
- L = aerodynamic lift force vector, N
- L, M, N = components of total vector M expressed in body coordinate system (roll, pitch, and yaw respectively), $N \cdot m$
- L_A, M_A, N_A = components of aerodynamic moment vector MA expressed in body coordinate system (roll, pitch, and yaw, respectively), $N \cdot m$
- L_p, M_p, N_p = components of propulsion moment vector M_p expressed in body coordinate system (roll, pitch, and yaw, respectively), $N \cdot m$
- magnitude of aerodynamic lift force vector L , N
- M = total moment vector acting on a particle or body, $N \cdot m$
- m = instantaneous mass of a particle or body, kg
- \dot{m} = rate of change of missile mass m ($\dot{m}_e = -\dot{m}$), kg/s
- \dot{m}_e = mass rate of flow of exhaust gas ($\dot{m}_e = -\dot{m}$), kg/s
- m_{earth} = mass of earth, 5.977×10^{24} kg
- m_1, m_2 = masses of bodies, kg
- N = aerodynamic normal force vector, N
- N = magnitude of aerodynamic normal force vector N , N
- P = instantaneous position vector of a particle or point (may be expressed in any coordinate system), m
- \dot{P}_{inertl} = rate of change of position vector P relative to inertial reference frame, m/s
- \dot{P}_{rot} = rate of change of position vector P relative to (as viewed by an observer in) a rotating reference frame, m/s
- p = linear momentum vector of a particle or body, $N \cdot s$
- p_f = "final" total system momentum at end of time interval, $N \cdot s$
- p_i = "initial" total system momentum at beginning of time interval, $N \cdot s$
- p, q, r = components of angular rate vector ω expressed in body coordinate system (roll, pitch, and yaw, respectively), rad/s (deg/s)
- $\dot{p}, \dot{q}, \dot{r}$ = components of angular acceleration $\dot{\omega}$ expressed in body coordinate system (roll, pitch, and yaw, respectively), rad/s^2 (deg/s²)
- p', q', r' = components of rotor rate vector expressed in body coordinate system (roll, pitch, and yaw, respectively), rad/s (deg/s)
- p_a = ambient atmospheric pressure, Pa
- p_e = average pressure across rocket nozzle exit area, Pa
- R_{cm} = vector from earth center to body mass center, m
- R_e = radius vector from earth center to point on earth surface, m
- R_{cm} = distance between the centers of masses of two bodies, m
- R_e = radius of the earth, m
- t = time, s
- t = simulated time since launch (ignition), s

$\mathbf{u}_{R_{cm}}$	= unit vector directed from center of earth toward body, dimensionless	x_e, y_e, z_e	= coordinates of earth coordinate system
\mathbf{u}_{ve}	= unit vector in direction of relative exhaust velocity V_{re} , dimensionless	x_w, y_w, z_w	= coordinates of the wind coordinate system
u, v, w	= components of absolute linear velocity V expressed in body coordinate system, m/s	α	= angle of attack in pitch plane, rad (deg)
$\dot{u}, \dot{v}, \dot{w}$	= components of linear (translational) acceleration expressed in body coordinate system, m/s^2	α_T	= total angle of attack, rad (deg)
\mathbf{V}	= absolute linear velocity vector of a body, m/s	β	= angle of sideslip, rad (deg)
$\dot{\mathbf{V}}$	= absolute acceleration vector of center of mass of a body, m/s^2	Δm_e	= mass of exhaust gases expelled from missile during time increment Δt , kg
\mathbf{V}_e	= absolute velocity vector of expelled exhaust gas, m/s	θ	= Euler angle rotation in elevation (pitch angle), rad (deg)
$\dot{\mathbf{V}}_e$	= rate of change of V_e , m/s^2	$\dot{\theta}$	= rate of change of θ , rad/s (deg/s)
$\dot{\mathbf{V}}_{inrtl}$	= acceleration vector of a body relative to an inertial reference frame, m/s^2	ϕ	= Euler angle rotation in roll (roll angle), rad (deg)
\mathbf{V}_{re}	= velocity vector of expelled exhaust gas relative to center of mass of missile, m/s	$\dot{\phi}$	= rate of change of ϕ , rad/s (deg/s)
\mathbf{V}_{rot}	= velocity vector of a body relative to (as viewed by an observer in) a rotating reference frame, m/s	ψ	= Euler angle rotation in azimuth (heading angle), rad (deg)
$\dot{\mathbf{V}}_{rot}$	= acceleration vector of a body relative to (as viewed by an observer in) a rotating reference frame, m/s^2	$\dot{\psi}$	= rate of change of Euler rotation in azimuth rad/s (deg/s)
\dot{V}	= magnitude of absolute acceleration of center of mass, m/s^2	Ω	= angular rate vector of the rotor relative to the body coordinate system, rad/s (deg/s)
$\dot{V}_{xb}, \dot{V}_{yb}, \dot{V}_{zb}$	= components of absolute acceleration of center of mass expressed in body coordinate system, m/s^2	ω	= angular rate vector of rotating reference frame relative to inertial frame, rad/s (deg/s)
V_{xe}, V_{ye}, V_{ze}	= components of absolute velocity vector V expressed in earth coordinate system, m/s	$\dot{\omega}$	= angular acceleration vector of the body, rad/s^2 (deg/s ²)
x, y, z	= coordinate axes in right-handed coordinate system	ω_e	= absolute (sidereal) angular rate of the earth, rad/s (deg/s)
x_b, y_b, z_b	= coordinates of the body coordinate system	ω	= magnitude of angular rate of rotating frame relative to inertial frame, rad/s (deg/s)
x_b, y_b, z_b	= subscripts indicating component is in direction of indicated axis of body coordinate system		
x_{b0}, y_{b0}, z_{b0}	= orientation of the body coordinate frame before Euler rotations (aligned with the earth reference frame)		
x_{b1}, y_{b1}, z_{b1}	= intermediate orientation of the body coordinate frame after the first Euler rotation		
x_{b2}, y_{b2}, z_{b2}	= intermediate orientation of the body coordinate frame after the second Euler rotation		

INTRODUCTION

Missile flight simulation models are based on mathematical equations that describe the dynamic motions of missiles that result from the forces and moments acting upon them. The mathematical tools employed are the equations of motion, which describe the relationships between the forces acting on the missile and the resulting missile motion. The purpose of considering missile dynamics in flight simulation is to understand these mathematical relationships.

Three-degree-of-freedom models employ translational equations of motion; six-degree-of-freedom models employ, in addition, rotational equations of motion. The inputs to the equations of motion are the forces and moments acting on the missile; the outputs are the missile accelerations that result from the applied forces and moments.

The forces and moments are produced by aerodynamics, propulsion, and gravity. Aerodynamic forces and moments are generated by the flow of air past the missile; they depend on the missile speed, configuration, and attitude, as well as on the properties of the ambient air. Propulsive thrust is usually designed to act through the missile center

of mass and thus produces no moment about the center of mass. Although gravitational force is affected by a number of factors, the generally accepted standard value—sometimes corrected for latitude and altitude—is usually sufficiently accurate for surface-to-air missile flight simulation. Gravity is assumed to act through the center of mass of the missile and produces no moment about the center of mass.

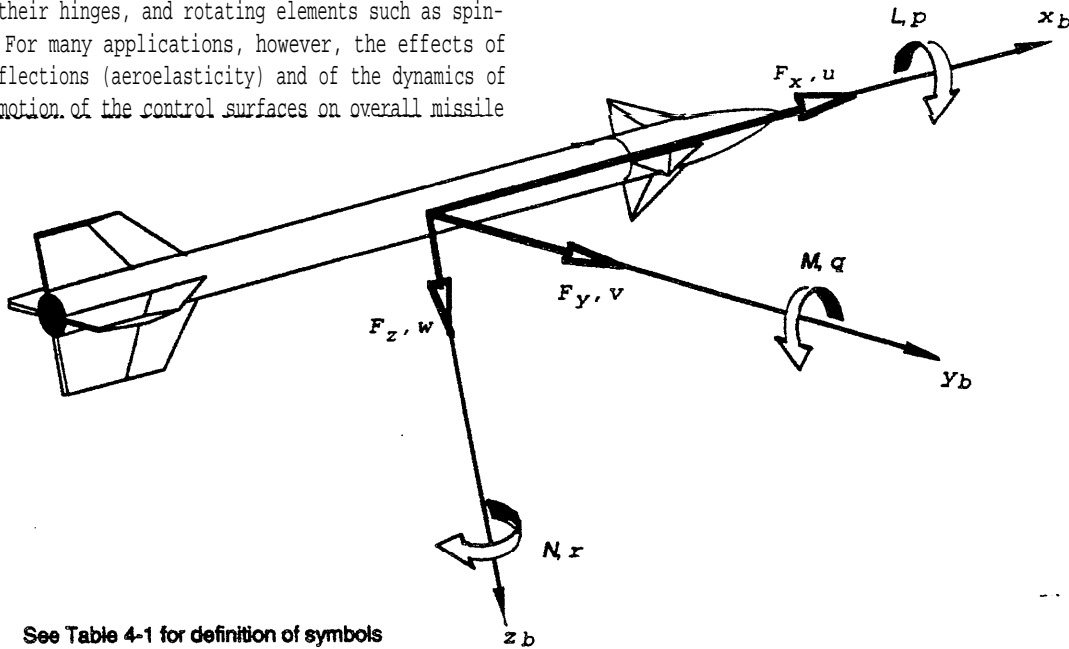
The equations of motion are based on Newton's laws of motion, which apply only to nonaccelerating reference frames. Calculations of rotational missile motion are greatly facilitated however, if they are expressed in the body reference frame, which rotates. Therefore, the equations of motion must be modified to adapt Newton's laws to rotating frames. The equations of motion, modified to make them applicable to calculations expressed in the body reference frame are summarized in Eqs. 4-37 and 4-46. If the missile has an inertial rotor, additional gyroscopic moments must be taken into account as in Eqs. 4-50.

A missile in flight is a complicated dynamic system composed of elastic structural components, control surfaces that rotate about their hinges, and rotating elements such as spinning rotors. For many applications, however, the effects of structural deflections (aeroelasticity) and of the dynamics of the relative motion of the control surfaces on overall missile

dynamics can be neglected. In such cases the analysis of missile dynamics is based on the equations of motion for a single rigid body.

4-2 NOMENCLATURE AND CONVENTIONS

Typically, the forces and moments on a missile are resolved into components in either the body coordinate system or the wind coordinate system. In this handbook, the use of the body coordinate system is emphasized because it causes principal body rotational axes to be aligned with coordinate frame axes. Fig. 4-1 shows the components of force, moment velocity, and angular rate of a missile resolved in the body coordinate system. The six projections of the linear and angular velocity vectors on the moving body frame axes are the six degrees of freedom. In aeronautics the nomenclature and conventions for positive directions have become informally standardized (Refs. 1-5). Current usage is shown in Fig. 4-1 and Table 4-1.



See Table 4-1 for definition of symbols

Figure 4-1. Forces, Velocities, Moments, and Angular Rates in Body Reference Frame

Table 4-1. NOMENCLATURE FOR FORCES, MOMENTS, AND MOTION

AXIS	FORCE ALONG AXIS	MOMENT ABOUT AXIS	LINEAR VELOCITY	ANGULAR DISPLACEMENT	ANGULAR VELOCITY	MOMENT OF INERTIA
x	F_x	L	u	ϕ	p	I_x
y	F_y	M	v	θ	q	I_y
z	F_z	N	w	ψ	r	I_z

The position of the mass center of the missile is given by its Cartesian coordinates expressed in an inertial frame of reference, such as the fixed-earth frame (x_e, y_e, z_e) . The angular orientation of the missile is given by three rotations $\Psi, \theta,$ and ϕ relative to the inertial frame of reference. These are called Euler rotations, and the order of the successive rotations is important. Starting with the body coordinate frame aligned with the earth coordinate frame, the generally accepted order is (1) rotate the body frame about the z_b -axis through the heading angle Ψ , (2) rotate about the y_b -axis through the pitch angle θ , and (3) rotate about the x_b -axis through the roll angle ϕ as shown in Fig. 4-2. In this figure

sub-subscripts are employed to indicate the intermediate orientations of the body-frame axes. Sub-subscript 0 indicates the starting orientation aligned with the earth frame; sub-subscript 1 shows the orientation after the first Euler rotation; and so on to the final orientation in which the sub-subscript is omitted.

The missile velocity vector is expressed in both earth-frame and body-frame coordinates in Fig. 4-3. For this purpose, the origins of the two frames are superimposed on the center of mass of the missile. The total inertial velocity V has components $u, v,$ and w on the body frame axes, and $V_{x_e}, V_{y_e},$ and V_{z_e} on the earth-frame axes.

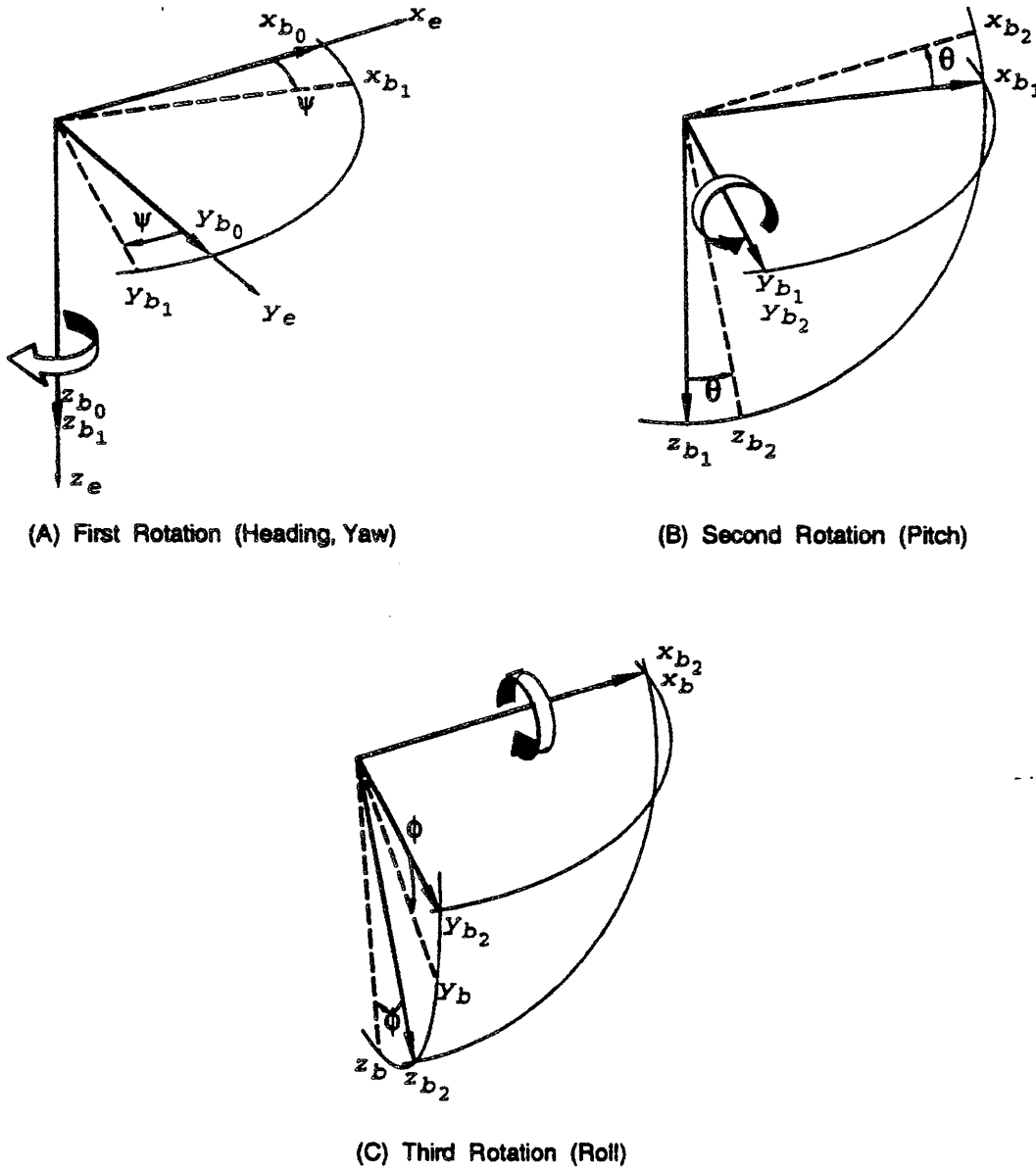


Figure 4-2. Euler Angle Rotations

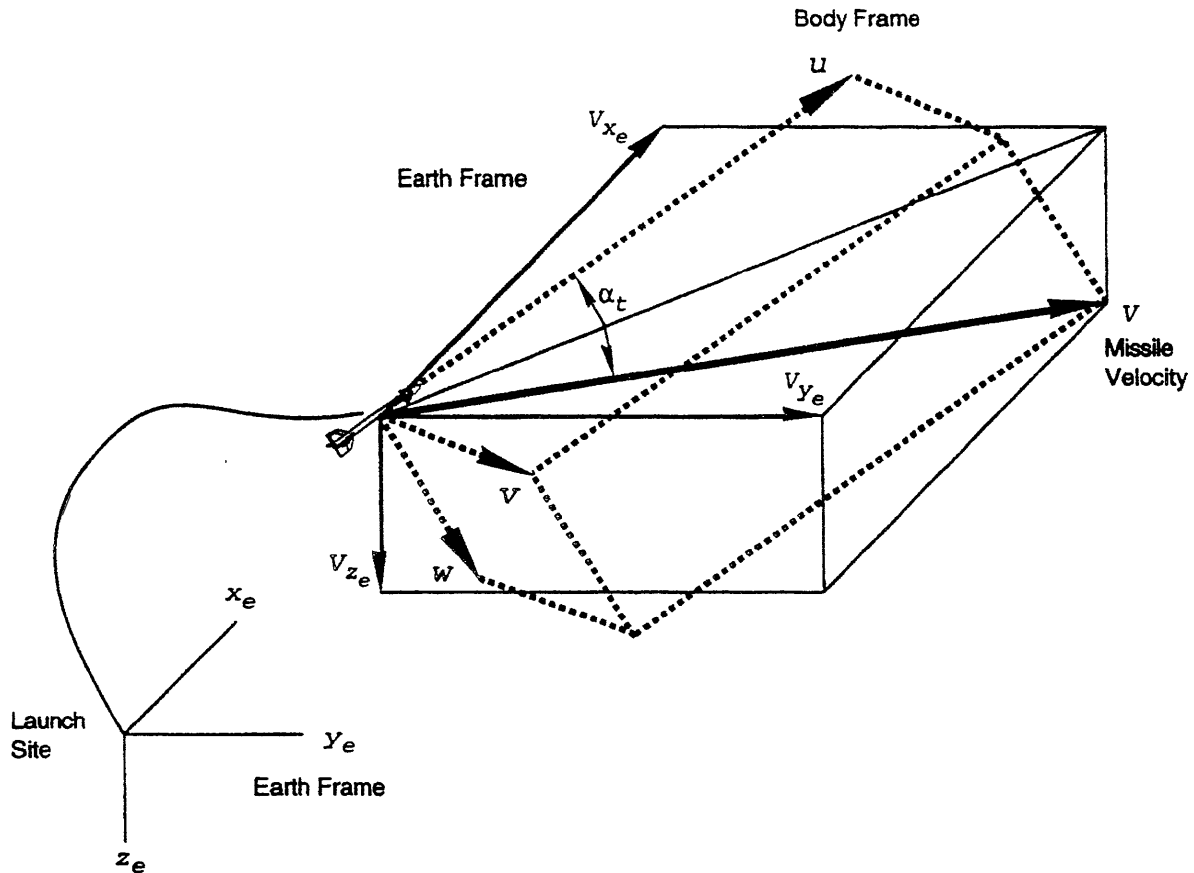


Figure 4-3. Velocity Vector in Body-Frame and Earth-Frame Coordinates

4-3 BASIC EQUATIONS

Equations describing the motion of a body relative to time are fundamental to a quantitative analysis of dynamic motion. The equations presented here are based entirely on Newtonian mechanics. In their most direct application Newton's equations apply only when the velocities and accelerations are measured in an inertial reference frame. Other names given to inertial reference frames are absolute, fixed, or Newtonian reference frames. In six-degree-of-freedom situations—which include missile rotations—equations of motion expressed in an inertial reference frame are unwieldy because as the body rotates the moments of inertia about the inertial axes vary and derivatives of the moments of inertia must appear in the equations (Ref. 2). This is a serious complication that can be avoided by employing moving (or Eulerian) axes that are fixed to the missile (Ref. 1). Eulerian axes rotate with the missile so that the moments of inertia about the respective reference axes are not affected by missile rotation. This use of rotating axes is not entirely without penalty, however, since they introduce the complication that rates of change, i.e., velocities and accelerations, measured with respect to these axes are not the absolute rates of change required by the Newtonian laws. Equations for the absolute rates of change entail additional

mathematical terms in the equations of motion. These additional terms are much to be preferred to the variable inertia coefficients required when the problem is analyzed entirely in an inertial reference frame. The necessary additional terms are discussed in subpar. 4-3.2.

4-3.1 NEWTON'S SECOND LAW OF MOTION

Newton's second law of motion maybe considered equivalently as a fundamental postulate or as a definition of force and mass (Ref. 6). Newton's laws are basic and cannot be derived because they are simply the result of observation. Their validity can be accepted on the basis of 300 yr of fruitless attempts to find them fallacious, at least for velocities that are small compared to the speed of light (Ref. 7). For a single particle the correct and most fundamental form of Newton's second law of motion is

$$\mathbf{F} = \frac{d\mathbf{p}}{dt}, \text{ N} \quad (4-1)$$

and a direct extension of this law to rotational motion gives

$$\mathbf{M} = \frac{d\mathbf{h}}{dt}, \text{ N}\cdot\text{m} \quad (4-2)$$

where

- F** = vector sum of forces acting on the particle, N
h = angular momentum vector of the particle,
 N·m·s
M = total moment (torque) vector acting on the
 particle, N·m
p = linear momentum vector of the particle, N·s
t = time, s.

Eq. 4-1 states that the force acting on a particle in a given direction equals the time rate of change of the momentum of the particle in that direction. Eq. 4-2 states that the moment of force (torque) on a particle about a given axis equals the time rate of change of the angular momentum of the particle about that axis. In the application of these laws, the linear and angular rates of momentum must be measured relative to an inertial reference frame.

Rigid bodies are composed of individual particles that do not move relative to each other. The equations of motion for a rigid body are developed by summing (integrating) the equations for individual particles (or incremental masses) over all the constituent particles. Performing the differentiation indicated in Eqs. 4-1 and 4-2 and integrating over all particles in the body yields the equations of motion of a rigid body as given in scalar form in Eqs. 3-1 and 3-2 and repeated here in vector form:

$$\mathbf{F} = m\dot{\mathbf{V}}, \mathbf{N} \quad (4-3)$$

$$\mathbf{M} = [I] \dot{\boldsymbol{\omega}}, \mathbf{N}\cdot\mathbf{m} \quad (4-4)$$

where

- F** = vector sum of forces acting on the body, N
[I] = inertia matrix of the body relative to the axis
 of rotation (See subpar. 4-5.2.), kg·m²
M = total moment vector acting on the body, N·m
m = mass of the body, kg
 $\dot{\mathbf{V}}$ = absolute acceleration vector of center of
 mass of a body, m/s²
 $\dot{\boldsymbol{\omega}}$ = absolute angular acceleration vector of the
 body, rad/s².

To qualify the variables of Eqs. 4-3 and 4-4 further, **F** is the vector sum of all forces acting on the missile, **M** is the vector sum of all moments acting on the missile, $\dot{\boldsymbol{\omega}}$ is the angular rate of the missile about an axis through the center of mass, and the moment of inertia matrix **[I]** is taken with respect to the axis of rotation. The vectors in Eqs. 4-3 and 4-4 can be expressed as components in any reference frame, but the accelerations represented by $\dot{\mathbf{V}}$ and $\dot{\boldsymbol{\omega}}$ must be measured relative to an inertial frame.

Derivation of Eqs. 4-3 and 4-4 is based on the assumption

that the mass *m* and the inertia matrix **[I]** are constants, but these parameters are not constant in a missile during the operation of the propulsion system because of the consumption of propellant. Fortunately, as is shown in subpar. 4-4.2.1, a derivation that rigorously takes into account the change in mass arrives at the same result given in Eq. 4-3, i.e., Eq. 4-3 is also applicable to a missile that has variable mass due to the burning of propellant. Rigorous accounting for a variable moment of inertia is not easy, but as discussed in subpar. 4-5.2, the time rate of change of the moment of inertia due to the burning of propellant is usually small enough that terms expressing this rate can be neglected. By this assumption, Eq. 4-4 also is applicable to missile flight simulations. In a simulation the values of *m* and **[I]** substituted into the equations are continuously updated during the time propellant is being consumed.

These equations of motion are expanded in the paragraphs that follow to account for rotating reference frames and moments of inertia that are specified relative to the axes of reference frames rather than the specific axis of rotation.

4-3.2 ROTATING REFERENCE FRAMES

In considering rotating reference frames, it is important to make a clear distinction between two different relationships that exist between a vector and a reference frame. The first is that a vector can have components expressed in any given reference frame; the second relationship is that a vector can change in magnitude and direction over the relative to the given reference frame. These changes can result from changes in the vector, from motion of the reference frame, or both. Vector components in the first relationship are easily transformed from one reference frame to another, however, considerations of vector rates of change in the second relationship are more complicated. Any given vector can be resolved into components in any reference frame, i.e., it can be expressed in terms of the unit vectors that define the axes of any reference frame. Thus the same vector can be expressed in either a rotating reference frame or an inertial reference frame, but its rate of change with respect to time as viewed by observers in the two systems is very different. A vector resolved in a given reference frame is said to be "expressed" in that frame (some authors use the term "referred to" (Ref. 4)). The rate of change of a vector, as viewed by an observer fixed to and moving with a given reference frame, is said to be "relative to" or "with respect to" that reference frame. These terms are used many times in this chapter with the very specific meanings given here. Many references do not emphasize the distinction between these terms; this leads to confusion on the part of the reader. The point to be made here, and by the example in par. 4-3.2.1, is: to be applied to Newton's equations of motion, the rate of change of a vector must be relative to an inertial reference frame, but it can be expressed in any reference frame.

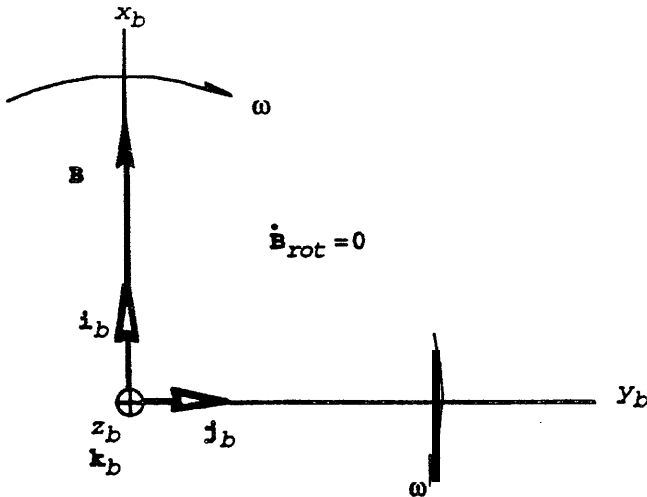
4-3.2.1 Time Derivative of a Vector

An instantaneous vector, for example, a force on the missile, can be transformed between inertial and rotating frames by application of the transformation equations in Appendix A. In such a transformation the vector is unchanged; only its components are changed. Great care must be taken, however, when any vector representing the rate of change of a vector is transferred between reference frames.

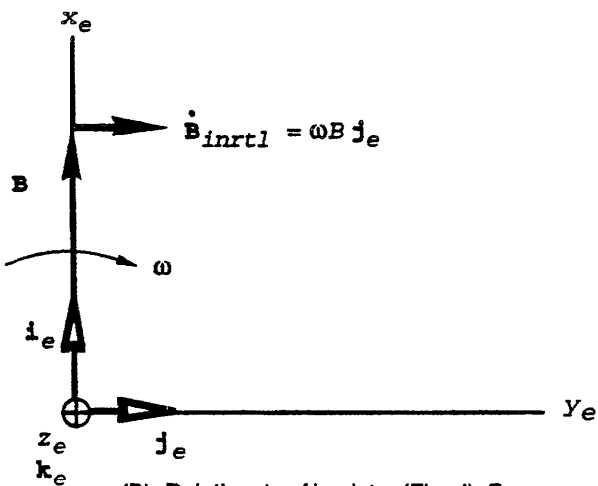
To illustrate, consider an example in which some arbitrary vector B has constant magnitude B and is always directed along the x_b -axis of the body reference frame as shown in Fig. 4-4(A). The vector B is expressed in the body coordinate frame by

$$B = Bi_b + 0j_b + 0k_b \quad (4-5)$$

where



(A) Relative to Rotating Body Frame



(B) Relative to Absolute (Fixed) Frame

Figure 4-4. Time Rate of Change of Vector B

B = magnitude of general vector B

i_b, j_b, k_b = unit vectors along the $x_b, y_b,$ and z_b -axes, respectively, of the body frame, dimensionless.

Assume that the body frame is rotating about the Z_b -axis at a rate of ω rad/s, but to simplify the example, assume that at a given instant of time the angular orientation of the rotating body coordinate frame happens to coincide with that of the fixed-earth (inertial) coordinate frame as shown in Fig. 4-4(B). At that instant the coordinates of B expressed in the earth frame are the same as the coordinates in the rotating the by the assumption that $i_b, j_b,$ and k_b momentarily coincide with $i_e, j_e,$ and $k_e,$ respectively

$$B = Bi_e + 0j_e + 0k_e \quad (4-6)$$

where

B = arbitrary general vector

B = magnitude of general vector B

i_e, j_e, k_e = unit vectors along the $x_e, y_e,$ and z_e - axes, respectively, of the earth coordinate system, dimensionless.

However, when we consider the absolute rate of change of vector B , we also must consider the rate of change of the rotating reference frame. Since we have assumed that B has constant magnitude and always points along the x_b -axis, the rate of change of B with respect to the rotating body frame is zero. That is

$$\left(\frac{dB}{dt}\right)_{body} = 0i_b + 0j_b + 0k_b \quad (4-7)$$

where

B = arbitrary general vector

i_b, j_b, k_b = unit vectors along the $x_b, y_b,$ and z_b - axes, respectively, of the body frame, -dimensionless

t = time, s.

But, from elementary mechanics, as shown in Fig. 4-4(B), the rate of change of B with respect to the fixed-earth (inertial) frame at that instant is

$$\left(\frac{dB}{dt}\right)_{earth} = 0i_e + \omega B j_e + 0k_e \quad (4-8)$$

where

ω = magnitude of angular rate of rotating frame relative to inertial frame, rad/s (deg/s).

In general, when the derivative (or incremental change) of a vector is calculated using components in a given reference frame, the resulting rate of change of the vector is rela-

tive to that particular reference frame. If that reference frame is not an inertial one, the rate of change is not an absolute one as required by Newton's laws. In the example the rate of change of B calculated by finding the rates of change of its components in the rotating frame (zero) is not an absolute rate of change. A mathematical procedure is required to convert the rate-of-change vector to one that is relative to an inertial frame. The general mathematical equation for calculating the rate of change of any vector relative to an inertial frame when the rate of change of that vector is known relative to a rotating frame is (Ref. 8)

$$\left(\frac{dB}{dt}\right)_{inrtl} = \left(\frac{dB}{dt}\right)_{rot} + (\omega \times B) \quad (4-9)$$

(expressed in any frame)

where

B = any vector

$\left(\frac{dB}{dt}\right)_{inrtl}$ = time rate of change of B relative to inertial frame

$\left(\frac{dB}{dt}\right)_{rot}$ = time rate of change of B relative to rotating frame

ω = angular rate vector of rotating frame relative to inertial frame, rad/s (deg/s).

Here $\omega \times B$ represents the difference between the time derivative of the vector as measured in an inertial reference frame and its time derivative as measured in the rotating reference frame. It is important to note that B is the same vector in both the inertial and the rotating reference frames, but the vector representing the time rate of change of B as seen by an observer in the moving system is not the same as the vector representing the absolute time rate of change.

By applying Eq. 4-9 to the example, $(dB/dt)_{rot}$ is zero, and $\omega \times B$ has magnitude and is in the direction of the y_z -axis. Substitution into Eq. 4-9 yields the vector $(dB/dt)_{inrtl}$ expressed in the rotating frame. The final result is identical with Eq. 4-8 and shows that the general equation gives the same result as the analysis based on elementary mechanics (Fig. 4-4) as expected.

4-3.2.2 Acceleration in a Rotating Frame

We now extend the discussion of rotating reference frames to include the handling of acceleration vectors and to consider the motion of particles or bodies located at positions other than the origin of the rotating frame. Applications could be, for example, the motion of a mechanical linkage within the missile as the missile experiences rotational motion or the motion of an object with respect to the rotating earth. Although most applications of this type are beyond the scope of this handbook the equations are presented in this paragraph (1) as a basis for discussion in subpar. 4-4.3 of the acceleration due to gravity and (2) to reinforce the understanding that the equations employed in subpars. 4-5.1 and 4-5.2 are a subset of the overall analysis

of rotating reference frames.

Let P be the instantaneous position vector of a particle (or a point), and let ω be the absolute angular rate of a rotating reference frame. Given the rate of change of position relative to the rotating frame P_{rot} , the rate of change of position of the particle relative to an inertial frame P_{inrtl} is obtained by substituting P for B in Eq. 4-9

$$\dot{P}_{inrtl} = \dot{P}_{rot} + \omega \times P, \text{ m/s} \quad (4-10)$$

where

P = instantaneous position vector of a particle or point, m

\dot{P}_{inrtl} = rate of change of position vector P relative to inertial reference frame, m/s

\dot{P}_{rot} = rate of change of position vector P relative to (as viewed by an observer in) a rotating reference frame, m/s

ω = angular rate vector of rotating reference frame relative to inertial frame, rad/s.

In the same way the rates of change of velocity with respect to the two reference frames are related by

$$\dot{V}_{inrtl} = \dot{V}_{rot} + \omega \times V, \text{ m/s}^2 \quad (4-11)$$

where

V = absolute linear velocity vector of a body, m/s
(It is equivalent to P_{inrtl} in Eq. 4-10.)

\dot{V}_{inrtl} = acceleration vector of a body relative to an inertial reference frame, m/s^2

\dot{V}_{rot} = acceleration vector of a body relative to (as viewed by an observer in) a rotating reference frame, m/s^2

ω = angular rate vector of rotating reference frame relative to inertial frame, rad/s.

Substituting Eq. 4-10 into 4-11 leads to the general expression that yields the acceleration of a particle with respect to an inertial reference frame for a given position and motion of the particle measured with respect to a rotating reference frame (Ref. 4)

$$\mathbf{A}_{inrtl} = \mathbf{A}_{rot} + \omega \times \mathbf{P} + 2\omega \times \mathbf{V}_{rot} + \omega \times (\omega \times \mathbf{P}), \quad (4-12)$$

m/s^2

where

\mathbf{A}_{inrtl} = absolute acceleration vector of a particle, i.e., relative to an inertial reference frame, m/s^2

\mathbf{A}_{rot} = acceleration vector of a particle relative to (as viewed by an observer in) a rotating reference frame, m/s^2

P = instantaneous position vector of a particle or point, m

\mathbf{V}_{rot} = velocity vector of a body relative to (as viewed

by an observer in) a rotating reference frame,
In/s

$\dot{\omega}$ = angular acceleration vector of a body, rad/s²

ω = angular rate vector of rotating reference frame
relative to inertial frame, rad/s.

Eq. 4-12 gives the absolute acceleration of a particle as a function of the position, velocity, and acceleration of the point in a rotating reference frame for a given angular rate and angular acceleration of the rotating frame. The term on the left A_{inert} is the acceleration appropriate for use in Newton's equations. The first term on the right A_{rot} is the acceleration of the particle as viewed by an observer in the rotating frame. The variable V_{rot} is the velocity of the particle as viewed by an observer in the rotating frame. The second term on the right $\dot{\omega} \times P$ results from the angular acceleration of the rotating frame; this term vanishes when the rotating frame rotates at a uniform rate, such as a frame fixed to the rotating earth. The negative of the third term on the right $-2\omega \times V_{\text{rot}}$ is called the Coriolis acceleration, and the negative of the last term $-\omega \times (\omega \times P)$ is called the centrifugal acceleration.

Multiplication of Eq. 4-12 by the mass of the body and setting the result equal to the sum of forces on the body is a way of applying Newtonian mechanics to a rotating reference frame. After multiplication by mass, the various terms in Eq. 4-12 have the units of force, and indeed, to an observer in a rotating reference frame, objects behave as if they have been acted upon by forces even when no external forces have been applied. This behavior is explained by the fact that bodies in motion relative to inertial space retain that motion until acted upon by an external force (Newton's first law), and points on the rotating reference frame accelerate away from the steady, straight-line path of the body. To an observer located on the rotating frame, this relative acceleration produces the appearance that some force is acting on the body to cause the relative acceleration. Furthermore, the observed relative motion can be accurately predicted by introducing forces called pseudoforces (or inertia forces) into Newton's equations of motion. The pseudoforces are so named because they cannot be associated with any particular body or agent in the environment of the body on which they act (Ref. 9). When multiplied by mass, the Coriolis and centrifugal acceleration terms in Eq. 4-12 become pseudoforces and are respectively called the Coriolis force and the centrifugal force. When viewed from an inertial reference frame, the pseudoforces disappear. These pseudoforces simply provide a technique that permits the application of Newtonian mechanics to events that are viewed from an accelerating reference frame.

Thus for mechanical problems dealing with rotational motion, there are two choices: (1) select an inertial frame as a reference frame and consider only "real" forces, i.e., forces that can be associated with definite agents in the

environment or (2) select a noninertial frame as a reference frame and consider not only the "real" forces but also suitably defined pseudoforces. Although the first alternative leads to a clearer understanding of the problem, the second is often employed because other aspects of the problem cause it to be the simplest approach, especially in the treatment of moments of inertia. Both approaches are completely equivalent, and the choice is a matter of convenience (Ref. 9).

4-4 FORCES AND MOMENTS

Solution of the equations of motion requires knowledge of the sum of the forces and the sum of the moments acting on the missile. These forces consist of the aerodynamic forces, propulsive thrust, and gravitational force. The moments are aerodynamic moments and any moment caused by misalignment of the thrust vector. Gravity is assumed to produce no moment.

4-4.1 AERODYNAMIC FORCES AND MOMENTS

The magnitudes of aerodynamic forces and moments depend on ambient air conditions and on missile configuration, attitude, and speed. Missile configuration includes the configuration of the body plus any fixed fins and the control surfaces. If the missile and surrounding air mass are considered components of a single closed system the forces that develop between the air and the missile produce equal but opposite changes in the momentums of the two systems; thus the momentum of the total system is conserved in conformance with Newton's laws, as discussed further in Chapter 5.

The resultant (total) aerodynamic force F_a on the missile can be resolved in any coordinate frame to give three orthogonal components. Often the most convenient reference frame for calculating aerodynamic forces is the wind coordinate system. If the wind coordinate system is defined as shown in Fig. 3-1(F), the total angle of attack α , and the resultant aerodynamic force F_a lie in the x_z -plane, as shown in Fig. 4-5; there is no side force and no sideslip angle β in this system. The component of F_a on the x -axis is called the drag force D , and the component on the z -axis is called the lift force L . The term "lift" implies a force directed upward to oppose the force due to gravity; however, in missile aerodynamics lift is applied in whatever direction is needed to control the flight path of the air vehicle.

The wind coordinate system is not always defined precisely as shown in Fig. 3-1(F) with the y -axis perpendicular to the plane of the total angle of attack. In the more general case, the xz -planes for the two coordinate systems are not necessarily aligned, and the resultant aerodynamic force F_a does not necessarily lie in the x_z -plane. In such systems sideslip angles and side force components must be taken into account,

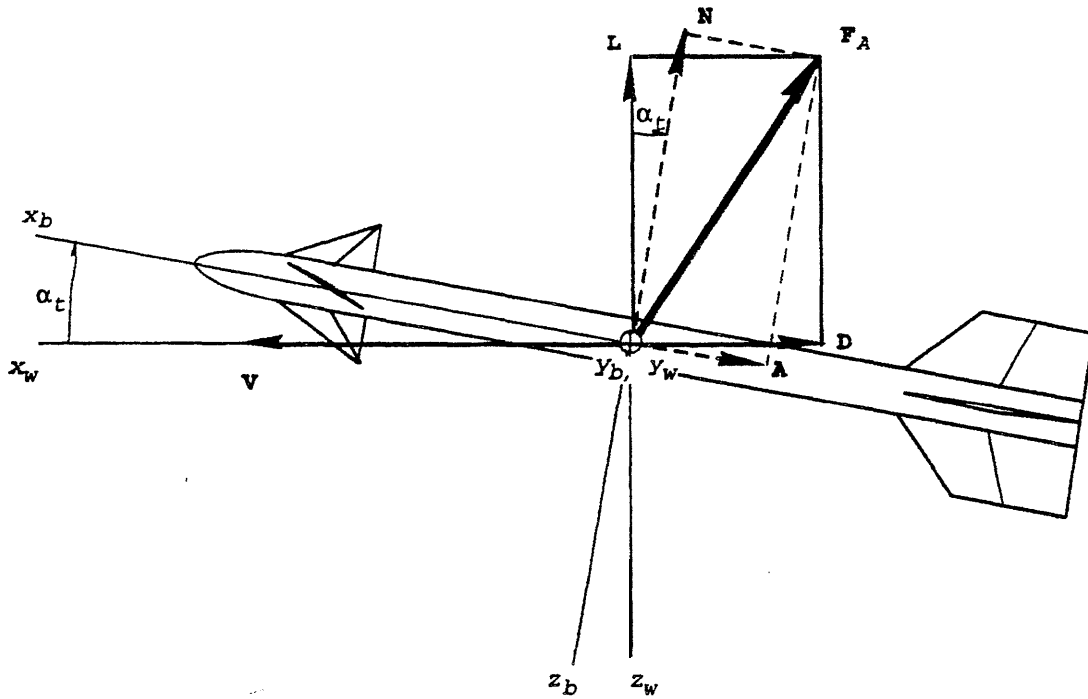


Figure 4-5. Aerodynamic Force in Body and Wind-Frame Coordinates

If aerodynamic forces are calculated in the wind system, they must be transformed to the body system for use in equations expressed in the body system. When F_A is expressed in the body system, its component on the x_b -axis is called the axial force A (parallel with the missile longitudinal axis, as shown in Fig. 4-5). The component on the z_b -axis is called the normal force N (normal to the missile longitudinal axis).

The lift L and drag D can be transformed to the normal force N and axial force A by

$$A = D \cos \alpha_t - L \sin \alpha_t, N \quad (4-13)$$

$$N = D \sin \alpha_t + L \cos \alpha_t, N \quad (4-14)$$

where

A = magnitude of aerodynamic axial force vector
A, N

D = magnitude of aerodynamic drag force vector
D, N

L = magnitude of aerodynamic lift force vector
L, N

N = magnitude of aerodynamic normal force vector
N, N

α_t = total angle of attack, rad.

When missile rotational motion is not calculated explicitly in a simulation (three degrees of freedom), the aerodynamic force components can be transformed from the wind or body system to an absolute reference frame-earth sys-

tem when the earth is assumed to be nonrotating-and substituted directly into Eq. 4-3 along with the nonaerodynamic forces on the missile, i.e., thrust and gravity, to solve for missile translational motion. When missile rotational motion is included in a simulation aerodynamic (and other) forces are substituted into the equations of motion for the rotating body frame, to be presented in Eqs. 4-37.

If the resultant aerodynamic force, i.e., the sum of all the aerodynamic forces acting on the missile body, fixed fins, and control surfaces, does not pass through the center of mass of the missile, an aerodynamic moment results. The magnitude of the moment is equal to the product of the resultant aerodynamic force and a lever arm defined as the perpendicular distance from the resultant aerodynamic force vector to the center of mass of the missile.

A steady state (trimmed) condition exists when the moments generated by the forces on the control surfaces are exactly balanced by moments in the opposite direction generated by forces on the body and fixed fins, as discussed in subpar. 2-2.6.2.

In three-degree-of-freedom simulations trimmed conditions are assumed, and aerodynamic moments need not be calculated. In that case, the transition between different trimmed conditions is calculated by means of a simple transfer function as described in Chapter 7. In five- or six-degree-of-freedom simulations the aerodynamic moments are calculated by the method described in Chapter 5 by using equations of the form of Eq. 3-4. There is no practical application for a four-degree-of-freedom simulation.

If aerodynamic moments are calculated in other than the body reference frame, they are transformed to it. The com-

ponents in the body frame of the vector representing the sum of all aerodynamic moments are L_x , M_x , and N_x along the x_b , y_b , and z_b axes, respectively.

4-4.2 THRUST FORCE AND MOMENT

The total thrust produced by a rocket motor is composed of two parts—the momentum thrust and the pressure thrust. As the rocket propellant burns, the products of combustion are exhausted through the rocket nozzle at high velocity. The force that propels these exhaust gases has an equal and opposite reaction on the missile. The momentum imparted to the gases in the rearward direction is balanced by the momentum imparted to the missile in the forward direction and thus conserves the momentum within the closed system. The portion of the total thrust attributed to this momentum change has magnitude $\dot{m}_e V_{re}$ where \dot{m}_e is the mass rate of flow of the exhaust gases and V_{re} is the velocity of the exhaust gases relative to the missile.

The average pressure p_e of the expanding exhaust gases at the exit plane of the rocket nozzle acts over the exit area A_e of the rocket nozzle. The remainder of the missile is surrounded by the ambient atmospheric pressure p_a . This imbalance of pressure constitutes the pressure thrust, which has magnitude $(p_e - p_a)A_e$. Combining the two thrust portions in vector form, the total thrust force on the missile is given by

where

- A_e = rocket nozzle exit area, m^2
- \mathbf{F}_p = total instantaneous thrust force vector, N
- \dot{m}_e = mass rate of flow of exhaust gas ($\dot{m}_e = -\dot{m}$), kg/s
- p_a = ambient atmospheric pressure, Pa
- p_e = average pressure across rocket nozzle exit area, Pa
- \mathbf{u}_{ve} = unit vector in direction of relative exhaust velocity V_{re} , dimensionless
- \mathbf{V}_{re} = velocity vector of expelled exhaust gas relative to center of mass of missile, m/s.

Momentum thrust is by far the major portion of the total thrust. Since the pressure portion of the thrust acts over part of the base area of the missile—the nozzle exit area, it is possible to include it within the overall definition of the aerodynamic base drag; in this case, however, it cannot also be included in the thrust.

4-4.2.1 Variable Mass

As pointed out in subpar. 4-3.1, Eq. 4-3, $\mathbf{F} = m\dot{\mathbf{V}}$, was originally derived on the assumption of constant mass, but this same equation is obtained also when the effects of mass variation due to propellant burning are taken into account. A

frequent error in the application of Newton's equations of motion to systems with variable mass is to assume that the rate of change of linear momentum is given by (Ref. 8)

$$\mathbf{F} = \frac{d(m\mathbf{V})}{dt} = m\dot{\mathbf{V}} + \mathbf{V}\dot{m}, \text{ N (wrong)} \quad (4-16)$$

where

- \mathbf{F} = vector sum of forces acting on the missile, N
- m = instantaneous mass of missile (includes mass of unburned propellant), kg
- \dot{m} = rate of change of missile mass ($\dot{m}_e = -\dot{m}$), kg/s
- t = time, s
- \mathbf{V} = absolute linear velocity vector of missile, m/s
- $\dot{\mathbf{V}}$ = absolute acceleration vector of center of mass of missile, m/s^2 .

The correct rate of change of momentum of the system must take into account the fact that not all mass particles in the system have the same velocity. In the case of a missile, the missile itself (including unburned propellant) has absolute velocity \mathbf{V} , and the exhaust gases have absolute velocity \mathbf{V}_e or relative velocity \mathbf{V}_{re} with respect to the center of mass of the missile.

In order to employ Newton's second law, Eq. 4-1, the system under consideration must be defined as one of constant mass. This is accomplished by assuming a total, closed system that consists of the missile flight vehicle plus the rocket exhaust gases expelled during an incremental time interval Δt (Ref. 9).

Although this total, closed system has constant mass, parts of the system have an interchange of mass. During the time interval Δt the missile body mass is reduced by the mass of the expelled gases Δm_e . At the end of the time interval, the mass of the missile is $(m - \Delta m_e)$, the mass of the ejected gases is Δm_e , and the momentum acquired by the gases is equal and opposite to the momentum acquired by the missile. The momentum thus acquired by the missile is due to the momentum component of thrust. (See subpar. 4-22.)

In the absence of forces external to this total, closed system, the overall momentum of the system would be conserved. However, in reality, external forces are applied to the system, and the resulting change in momentum is given by Eq. 4-1. To emphasize that the applied forces must be external to the total, closed system, the subscript ext is added to \mathbf{F} . This addition gives

$$\mathbf{F}_{ext} = \frac{d\mathbf{p}}{dt}, \text{ N} \quad (4-17)$$

where

- \mathbf{F}_{ext} = vector sum of external forces applied to the total system, N

\mathbf{p} = linear momentum vector of the total system,
N•s

Since the momentum component of thrust is developed internally to the total system, as defined, it does not contribute to the forces F_{ext} . For a missile the external forces F_{ext} consist of aerodynamic forces, the pressure component of thrust, and gravity. These external forces are applied directly to the missile body; therefore, they affect only the portion of the total system momentum attributable to the missile. For rocket motors operating within the atmosphere, atmospheric interactions cause external forces to be applied also to the exhaust gases; however, these forces do not affect the missile and therefore can be disregarded.

From Eq. 4-17 an appropriate result for the time interval Δt can be written as

$$\mathbf{F}_{ext} \approx \frac{\Delta \mathbf{p}}{\Delta t} = \frac{\mathbf{p}_f - \mathbf{p}_i}{\Delta t}, \mathbf{N} \quad (4-18)$$

where

\mathbf{p}_i = initial total system momentum at beginning of time interval, N•s

\mathbf{p}_f = final total system momentum at end of time interval, N•s.

The values of the momentum of the total system at the beginning and end of the time interval are given by

$$\left. \begin{aligned} \mathbf{p}_i &= m\mathbf{V}, \mathbf{N}\cdot\mathbf{s} \\ \mathbf{p}_f &= (m - \Delta m_e)(\mathbf{V} + \Delta \mathbf{V}) + \Delta m_e \mathbf{V}_e, \mathbf{N}\cdot\mathbf{s} \end{aligned} \right\} \quad (4-19)$$

where

m = missile mass at beginning of time interval, kg

Δm_e = mass of exhaust gases expelled from missile during time interval, kg

\mathbf{V} = absolute velocity of missile at beginning of time interval, m/s

$\Delta \mathbf{V}$ = change in missile velocity during time interval, m/s

\mathbf{V}_e = absolute velocity of exhaust gases, m/s.

Substitution of Eqs. 4-19 into Eq. 4-18 gives

$$\mathbf{F}_{ext} = \frac{(m - \Delta m_e)(\mathbf{V} + \Delta \mathbf{V}) + \Delta m_e \mathbf{V}_e - m\mathbf{V}}{\Delta t} \quad (4-20)$$

If Δt approaches zero, i.e., $\Delta t \rightarrow 0$, then

$$\left. \begin{aligned} \frac{\Delta \dot{\mathbf{V}}}{\Delta t} &\rightarrow \frac{d\mathbf{V}}{dt} = \dot{\mathbf{V}} \\ \frac{\Delta m_e}{\Delta t} &\rightarrow \frac{dm_e}{dt} = \dot{m}_e \\ \frac{\Delta m_e \Delta \mathbf{V}}{\Delta t} &\rightarrow 0 \end{aligned} \right\} \quad (4-21)$$

Substitution of Eqs. 4-21 into Eq. 4-20 gives

$$\mathbf{F}_{ext} = m\dot{\mathbf{V}} + (\mathbf{V}_e - \mathbf{V})\dot{m}_e, \mathbf{N} \quad (4-22)$$

Letting $\mathbf{V}_{re} = \mathbf{V}_e - \mathbf{V}$ gives

$$\mathbf{F}_{ext} = m\dot{\mathbf{V}} + \mathbf{V}_{re}\dot{m}_e, \mathbf{N} \quad (4-23)$$

where

\mathbf{F}_{ext} = vector of sum of external forces applied to the total system, N

m = missile mass at beginning of time interval, kg

\dot{m}_e = mass rate of flow of exhaust gas, kg/s

$\dot{\mathbf{V}}$ = absolute acceleration vector of center of mass of a body, m/s²

\mathbf{V}_{re} = velocity vector of expelled exhaust gas relative to center of mass of missile, m/s.

The last term on the right side of Eq. 4-23 (product of relative exhaust velocity and the mass rate of flow) is the momentum component of thrust as in Eq. 4-15.

As previously stated the vector sum of forces external to the total, closed system F_{ext} consists of the aerodynamic force F_A , the pressure force $(p_e - p_a)A_e(-\mathbf{u}_{ve})$, and the gravitational force F_g . Substituting these terms for F_{ext} in Eq. 4-23 and moving the momentum thrust term to the left side of the equation gives

$$\mathbf{F}_A - \dot{m}_e \mathbf{V}_{re} + (p_e - p_a)A_e(-\mathbf{u}_{ve}) + \mathbf{F}_g = m\dot{\mathbf{V}}, \mathbf{N} \quad (4-24)$$

where

A_e = rocket nozzle exit area, m²

\mathbf{F}_A = resultant aerodynamic force vector, N

\mathbf{F}_g = gravitational force vector including effects of earth rotation, N

m = instantaneous mass of a particle or body, kg

\dot{m}_e = mass rate of flow of exhaust gas, kg/s

p_a = ambient atmospheric pressure, Pa

p_e = average pressure across rocket nozzle exit area, Pa

\mathbf{u}_{ve} = unit vector in direction of relative exhaust velocity \mathbf{V}_{re} , dimensionless

$\dot{\mathbf{V}}$ = absolute acceleration vector of center of mass of a body, m/s^2

\mathbf{V}_{rc} = velocity vector of expelled exhaust gas relative to center of mass of missile, m/s .

Substituting Eq. 4-15 (the definition of F_p), which includes both the pressure and momentum components of thrust, into Eq. 4-24 gives

$$\mathbf{F}_A + \mathbf{F}_p + \mathbf{F}_g = m\dot{\mathbf{V}}, \text{N} \quad (4-25)$$

and finally, setting F equal to the sum of forces acting directly on the missile ($F_A + F_p + F_g$) allows one to write

$$\mathbf{F} = m\dot{\mathbf{V}}, \text{N} \quad (4-3)$$

the familiar form of Newton's equation.

In summary, F consists of F_{ext} plus the momentum component of thrust $-m_e V_{rc}$. F_{ext} is the sum of forces that are external to the total, closed system, which includes a portion of the exhaust gases, whereas F is the sum of forces that are external to a new system defined to include only the missile. The rate of change of mass, which was used incorrectly in Eq. 4-16, has been correctly absorbed into the momentum component of thrust (in terms of its negative m_e). Thus it is shown that a missile with a rocket motor is analyzed in the same way as any problem having constant mass except that the value of m to be used in Eq. 4-3 is a function of time (Ref. 8).

4-4.2.2 Moment Due to Thrust

If the thrust vector F_p passes through the center of mass of the missile, no rotational moment is generated by the thrust. When the thrust vector does not pass through the center of mass, either by design or error, the resulting moment on the missile is equal to the product of the magnitude of the thrust and the perpendicular distance between the thrust vector and the center of mass (Fig. 2-16). The equations used to describe this moment are presented in Chapter 6.

4-4.3 GRAVITATIONAL FORCE

The force of gravity observed on the earth is the result of two physical effects—the Newtonian gravitational mass attraction and the rotation of the earth about its axis.

4-4.3.1 Newtonian Gravitation

The law of gravitation, defined by Newton, that governs the mutual attraction between bodies is

$$F_G = \frac{Gm_1m_2}{R_{cm}^2}, \text{N} \quad (4-26)$$

where

F_G = magnitude of the mutual force of gravitational mass attraction between two masses, N

G = universal gravitational constant, $6.673 \times 10^{-11} \text{ m}^3/(\text{kg}\cdot\text{s}^2)$

m_1, m_2 = masses of bodies, kg

R_{cm} = distance between centers of masses of two bodies, m .

Gravitational attraction is exerted on a missile by all planets, stars, the moon, and the sun. It is a force that pulls the vehicle in the direction of the center of mass of the attracting body. Within the immediate vicinity of the earth, the attraction of the other planets and bodies is negligible compared to the gravitational force of the earth.

In the absence of forces other than gravity, all objects, regardless of mass, that are allowed to fall at a given position on the earth will have the same acceleration A_g . This can be seen by combining Eqs. 4-3 and 4-26 and canceling the term representing the mass of the falling object. This combination gives

$$A_g = \frac{Gm_{earth}}{R_{cm}^2} (-\mathbf{u}_{R_{cm}}), \text{m/s}^2 \quad (4-27)$$

where

A_g = acceleration vector due to gravitational mass attraction between earth and a free-falling object, m/s^2

G = universal gravitational constant, $6.673 \times 10^{-11} \text{ m}^3/(\text{kg}\cdot\text{s}^2)$

m_{earth} = mass of earth, $5.977 \times 10^{24} \text{ kg}$

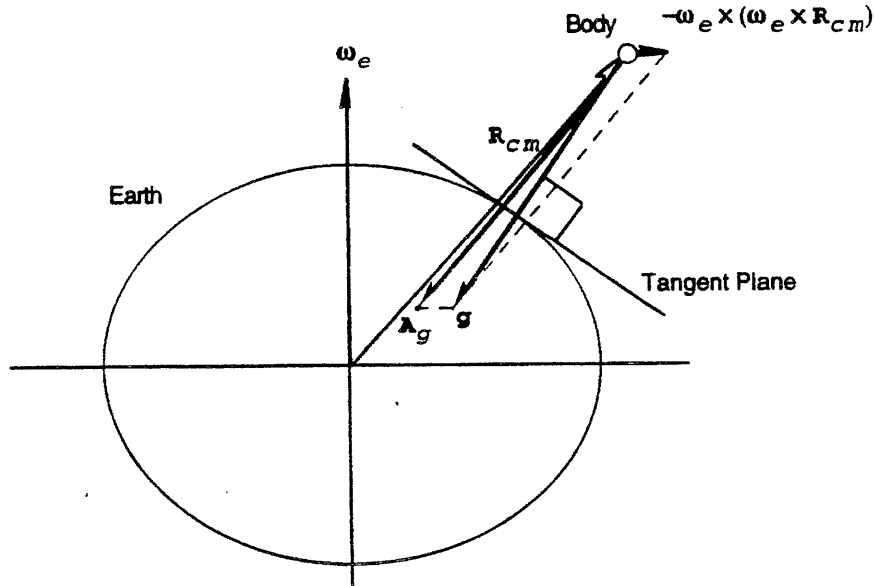
R_{cm} = distance from earth center to body mass center, m

$\mathbf{u}_{R_{cm}}$ = unit vector directed from center of earth toward body, dimensionless.

Eq. 4-27 is based on the assumption that the earth is spherical. The nonspherical characteristics of the earth can be taken into account by adding empirical terms to the previous equations (Refs. 10 and 11). In this case, as shown in Fig. 4-6, the vectors A_g and R_{cm} are not precisely aligned.

4-403.2 Gravity in Rotating Earth Frame

The acceleration calculated by Eq. 4-27 is the acceleration of a body that would be measured with respect to an inertial reference frame; therefore, A_g is the absolute acceleration. Because the earth rotates, the acceleration of a freely falling body as measured relative to the earth is slightly less than the absolute value. The acceleration due to gravity g experienced by an observer on the rotating earth includes the acceleration caused by the gravitational mass attraction plus the effect of the rotating reference frame as shown in Fig. 4-6. The effect of the rotating reference frame on the acceleration due to gravity is determined by use of Eq. 4-12. For a body that is stationary relative to the earth and located at the surface of the earth, the terms in Eq. 4-12



Earth oblateness is exaggerated.

Figure 4-6. Relationship Between Gravitational Mass Attraction and Gravity Experienced by an Observer on a Rotating Earth

take values as follows: $\dot{\omega} = 0$, $\mathbf{V}_{rot} = 0$, $\mathbf{P} = \mathbf{R}_{cm} = \mathbf{R}_e$, $\mathbf{A}_{inrtl} = \mathbf{A}_g$, $\mathbf{A}_{rot} = \mathbf{g}_0$; and $\omega = \omega_e$. Substituting these values into Eq. 4-12 and solving for g , gives

$$\mathbf{g}_0 = \mathbf{A}_g - \omega_e \times (\omega_e \times \mathbf{R}_e), \text{ m/s}^2 \quad (4-28)$$

where

- \mathbf{A}_g = acceleration vector due to gravitational mass attraction between earth and a free-falling object m/s^2
- \mathbf{g}_0 = vector of acceleration due to gravity at earth surface, m/s^2
- \mathbf{R}_{cm} = vector from earth center to body mass center, m
- \mathbf{R}_e = radius vector from earth center to point on earth surface, m
- ω_e = absolute (sidereal) angular rate of the earth, rad/s

The first term on the right side of Eq. 4-28 is the absolute acceleration produced by mass attraction as given in Eq. 4-27. The second term on the right is the centrifugal acceleration. The Coriolis term in Eq. 4-12 is zero in Eq. 4-28 because Coriolis acceleration is a function of velocity, and g_0 is defined for a body that is momentarily stationary relative to the earth.

Both A_g and R_e are slightly affected by the oblateness of the earth. To account for both the centrifugal acceleration and the oblateness of the earth, the values of g_0 (the magnitude of g) at various latitudes are given in Table 4-2.

TABLE 4-2. ACCELERATION DUE TO GRAVITY AT EARTH SURFACE

LATITUDE, deg	ACCELERATION g_0 , m/s^2
0	9.780
10	9.782
20	9.787
30	9.793
40	9.802
50	9.811
60	9.819
70	9.826
80	9.830
90	9.832

The standard value that has been accepted internationally for gravitational acceleration relative to the rotating earth at sea level and at a latitude of 45 deg is 9.80665 m/s^2 .

The proximity of large land masses and the variations in the density of the crust of the earth also influence the local value of the acceleration due to gravity by a small but detectable amount. These gravity anomalies are negligible in almost all applications of surface-to-air missile simulations.

The variation of the acceleration due to gravity with altitude is primarily the result of the R_e^2 term in Eq. 4-27. The centrifugal term in Eq. 4-28 also depends on the distance from the center of the earth; however, for altitudes within the atmosphere of the earth, that variation is so small that it can usually be neglected. If the acceleration due to gravity at the surface of the earth g_0 is known, the acceleration at any altitude h is given to close approximation by

$$g = g_0 \left[\frac{R_e^2}{(R_e + h)^2} \right], \text{ m/s}^2 \quad (4-29)$$

where

- g = magnitude of acceleration-due-to-gravity vector g , m/s^2
- g_0 = magnitude of the acceleration due to gravity at the earth surface vector g_0 , m/s^2
- h = altitude above sea level, m
- R_e = radius of the earth, m .

In missile flight simulations the desired output is motion relative to the earth. If the assumption of a spherical (or oblate) rotating earth is made, calculations of missile motion usually are performed relative to an inertial reference frame by using Eq. 4-27 for gravitational acceleration, and the position of the missile relative to the earth is calculated after calculating the appropriate rotational position of the earth. Surface-to-air missile simulations, however, usually are based on the assumption of a flat, nonrotating earth. In this case the motion of the missile relative to the earth is best approximated by employing the gravitational acceleration g . Generally, the international standard value of g or a value selected from Table 4-2 for the appropriate latitude is considered sufficiently accurate for the acceleration due to gravity at the surface of the earth. Although the correction for altitude (Eq. 4-29) is small for altitudes within the atmosphere, the correction is such a simple calculation that it is often incorporated in the model.

Gravitational force F_g is calculated by substituting the acceleration due to gravity into Newton's equation:

$$F_g = mg, \text{ N} \quad (4-30)$$

where

- F_g = magnitude of gravitational force vector F_g , weight of body, N
- g = magnitude of acceleration-due-to-gravity vector g , m/s^2
- m = mass of the body, kg .

The term F_g is commonly called the weight of the object. Thus Eq. 4-30 is the defining equation for the term weight. The gravitational force vector F_g has magnitude F_g and is

directed locally downward (in the direction of g in Fig. 4-6).

For surface-to-air missile simulations gravity is assumed to act with equal force on every element of mass in the missile. Thus no rotational moment is generated, and gravity is considered to be acting through the center of mass of the missile. Actually, some mass elements of the missile are slightly farther from the center of the earth than others, and the elements closer to the center of the earth are attracted more strongly. The result is that the center of gravitational attraction is not located exactly at the center of mass (Ref. 12). This effect is employed in the stabilization of certain satellites.

4-5 EQUATIONS OF MOTION

The equations of motion provide the means by which to calculate missile accelerations when forces on the missile are given. Par. 4-3 describes the mathematical basis of the equations of motion developed directly from Newton's equations, and par. 4-4 describes the forces and moments that are included in the equations of motion. We are now prepared to develop the equations of motion in the body reference frame, which rotates relative to inertial space.

4-5.1 TRANSLATIONAL EQUATIONS

The basis of the translational equations of motion is

$$F = m\dot{V}, \text{ N} \quad (4-3)$$

where it is understood from the discussion in subpar. 4-4.2.1 that F includes the sum of the external forces-aerodynamic, pressure thrust, and gravitational-and the internally generated momentum thrust and that the variable mass has been correctly taken into account.

In a missile flight simulation the usual procedure used to solve the translational equation of motion, Eq. 4-3, is to calculate the summation of forces F based on aerodynamic, propulsive, and gravitational data, substitute F into the equation, and solve for the absolute acceleration V . Expressing Eq. 4-3 in body frame coordinates and solving for the components of absolute acceleration give

$$\left. \begin{aligned} (\dot{V}_{x_b})_{inrtl} &= \frac{F_{x_b}}{m}, \text{ m/s}^2 \\ (\dot{V}_{y_b})_{inrtl} &= \frac{F_{y_b}}{m}, \text{ m/s}^2 \\ (\dot{V}_{z_b})_{inrtl} &= \frac{F_{z_b}}{m}, \text{ m/s}^2 \end{aligned} \right\} \quad (4-31)$$

where

$$F_{x_b}, F_{y_b}, F_{z_b} = \text{components of total force vector } F$$

expressed in the body coordinate system, N

m = instantaneous mass of particle or body, kg

$\dot{V}_{xb}, \dot{V}_{yb}, \dot{V}_{zb}$ = components of absolute acceleration of center of mass expressed in body coordinate system relative to an inertial frame, m/s^2 .

If accelerometers, which measure nongravitational acceleration relative to inertial space, were aligned with each of the body frame axes, they would measure the acceleration components given by Eqs. 4-31 less the acceleration due to gravity (Ref. 4). Even though Eqs. 4-31 represent components of absolute acceleration, that acceleration vector is expressed in the rotating coordinates of the body reference frame.

The objective at this point is to calculate the absolute velocity V of the center of mass of the missile. V is the integral of the terms on the left side of Eqs. 4-31; however, the fact that the reference frame is rotating must be taken into account in performing the integration. For example, if the absolute acceleration in Eqs. 4-31 is integrated directly in the rotating reference frame, the result is a velocity expressed in the rotating reference frame, but it is not the absolute velocity. Eq. 4-9 must be employed to find the absolute velocity when the integration is performed in rotating coordinates. Substituting V for B in Eq. 4-9 and rearranging give

$$\dot{V}_{rot} = \dot{V}_{inertl} - (\omega \times V), m/s^2 \quad (4-32)$$

where

V = absolute linear velocity vector of a body, m/s

\dot{V}_{inertl} = acceleration vector of a body relative to an inertial reference frame, m/s^2

\dot{V}_{rot} = acceleration vector of a body relative to (as viewed by an observer in) a rotating reference frame, m/s^2

ω = angular rate vector of rotating reference frame relative to inertial frame, rad/s.

Eq. 4-32 can be expressed in any reference frame. The acceleration terms are relative to a rotating frame and an inertial frame, respectively, as indicated by the subscripts. The angular rate of the rotating frame relative to the inertial frame is represented by ω . The absolute acceleration V_{inertl} is equivalent to the applied-force-to-mass ratio, as given by Eqs. 4-31. If the integration is performed in the rotating coordinates, V_{rot} is the vector that must be integrated to yield the absolute velocity V (with respect to the inertial frame). To integrate Eq. 4-32, it must be expressed in the coordinates of the chosen reference frame, in this case, the

body frame. The first term on the right side of Eq. 4-32 is already expressed in body coordinates by Eqs. 4-31. The vectors w and V are expressed in body coordinates by

$$\omega = p i_b + q j_b + r k_b, \text{ rad/s} \quad (4-33)$$

$$V = u i_b + v j_b + w k_b, \text{ m/s}, \quad (4-34)$$

and the cross product is given by

$$\omega \times V = (qw - rv)i_b + (ru - pw)j_b + (pv - qu)k_b, m/s^2 \quad (4-35)$$

where

i_b, j_b, k_b = unit directions of $x_b, y_b,$ and z_b -axes (body coordinate system), respectively, dimensionless

p, q, r = components of the angular rate vector ω expressed in body coordinate system (roll, pitch, and yaw, respectively), rad/s

u, v, w = components of absolute linear velocity vector V expressed in body coordinate system m/s

V = absolute linear velocity vector of a body, m/s

ω = angular rate Vector of rotating reference frame relative to inertial frame, rad/s.

Substituting Eqs. 4-31 and 4-35 into Eq. 4-32 and substituting w for (V_{zb}) for $(V_{xb})_{rot}$ and v for $(V_{yb})_{rot}$ give

$$\left. \begin{aligned} \dot{u} &= \frac{F_{x_b}}{m} - (qw - rv), m/s^2 \\ \dot{v} &= \frac{F_{y_b}}{m} - (ru - pw), m/s^2 \\ \dot{w} &= \frac{F_{z_b}}{m} - (pv - qu), m/s^2 \end{aligned} \right\} \quad (4-36)$$

where

$F_{x_b}, F_{y_b}, F_{z_b}$ = components of total force vector F expressed in the body coordinate system, N

$\dot{u}, \dot{v}, \dot{w}$ = components of linear (translational) acceleration expressed in body coordinate system, m/s^2 .

Eqs. 4-36 are the translational equations of motion expressed in the body reference frame, which rotates. With the exception of the assumption that the missile is a rigid

body, these equations are perfectly general, i.e., no simplifying assumptions have been used in their derivation. Integration yields the absolute velocity V expressed in body coordinates as u , v , and w .

To use V to calculate the missile path relative to the earth, V must be transformed to earth frame coordinates. Multiplication of V by the appropriate transformation matrix from Appendix A transforms the expression of the absolute velocity from rotating to earth coordinates. The absolute velocity in inertial (fixed-earth) coordinates can then be integrated directly without using the cross-product terms of Eq. 4-9 to obtain the missile translational displacement in inertial coordinates.

Another method used to obtain missile velocity and displacement is to transform the absolute acceleration to inertial coordinates before integration. This is done by multiplying the vector determined by Eqs. 4-31, i.e., the absolute acceleration expressed in body coordinates, by the appropriate transformation matrix from Appendix A. Once the acceleration is expressed in inertial coordinates, it is integrated twice without any cross-product terms to yield absolute velocity and translational displacement directly in inertial coordinates. The disadvantage of this method is that the velocity so obtained must then be transformed back to body coordinates for aerodynamic force and moment calculations.

The individual forces are substituted into Eqs. 4-36 to give the final translational equations of motion.

Let

- F_{Ax_b} = x component in the body frame of the sum of aerodynamic forces on the missile, N
- F_{Px_b} = x component in the body frame of the sum of propulsive forces on the missile, N
- F_{Gx_b} = x component in the body frame of the sum of gravitational forces on the missile, N

and let similar symbols with subscripts y and z represent, respectively, the y and z components of the sums of the forces.

Then

$$\left. \begin{aligned} \dot{u} &= \frac{F_{Ax_b} + F_{Px_b} + F_{Gx_b}}{m} - (qw - rv), \text{ m/s}^2 \\ \dot{v} &= \frac{F_{Ay_b} + F_{Py_b} + F_{Gy_b}}{m} - (ru - pw), \text{ m/s}^2 \\ \dot{w} &= \frac{F_{Az_b} + F_{Pz_b} + F_{Gz_b}}{m} - (pv - qu), \text{ m/s}^2 \end{aligned} \right\} \quad (4-37)$$

where

- $F_{Ax_b}, F_{Ay_b}, F_{Az_b}$ = components of aerodynamic force

in the body coordinate system, N

- $F_{Gx_b}, F_{Gy_b}, F_{Gz_b}$ = components of gravitational force vector F_g expressed in the body coordinate system, N

- $F_{Px_b}, F_{Py_b}, F_{Pz_b}$ = components of thrust vector F_p expressed in the body coordinate system, N

- p, q, r = components of angular rate vector ω expressed in body coordinate system (roll, pitch, and yaw respectively), rad/s

- u, v, w = components of absolute linear velocity vector V expressed in body coordinate system, m/s

- $\dot{u}, \dot{v}, \dot{w}$ = components of linear (translational) acceleration expressed in body coordinate system, m/s^2 .

4-5.2 ROTATIONAL EQUATIONS

Eq. 4-2 expresses the basic relationship for rotational motion of a particle in an inertial (absolute) reference frame. This equation is extended to rigid bodies by summing over all the particles (or incremental masses) of the body. If the moments acting on the missile are given, Eq. 4-2 is used to calculate the angular rate w of the missile. The angular rate is contained within the angular momentum vector h . In the general case with no constraints on the axis of rotation, the relationship between h and ω involves the inertia matrix (also called the inertia tensor) $[I]$. That relationship is given by

$$h = [I]\omega, \text{ N}\cdot\text{m}\cdot\text{s} \quad (4-38)$$

where

$$[I] = \begin{bmatrix} I_{xx} & -I_{xy} & -I_{xz} \\ -I_{xy} & I_{yy} & -I_{yz} \\ -I_{xz} & -I_{yz} & I_{zz} \end{bmatrix}, \text{ kg}\cdot\text{m}^2$$

$$I_{xx} = \int (y^2 + z^2) dm \quad I_{xy} = \int (xy) dm$$

$$I_{yy} = \int (z^2 + x^2) dm \quad I_{xz} = \int (xz) dm$$

$$I_{zz} = \int (x^2 + y^2) dm \quad I_{yz} = \int (yz) dm$$

x, y, z = coordinates of infinitesimal masses of the body, m

dm = infinitesimal mass, kg.

I_{xx}, I_{yy} and I_{zz} are called moments of inertia, and I_{xy}, I_{xz} , and I_{yz} are called products of inertia. A particular orientation of the reference frame axes relative to the body can always be chosen for which the products-of-inertia terms vanish,

giving

$$[I] = \begin{bmatrix} I_x & 0 & 0 \\ 0 & I_y & 0 \\ 0 & 0 & I_z \end{bmatrix}, \text{ kg}\cdot\text{m}^2 \quad (4-39)$$

Since the double subscript is required only when products of inertia are involved, single subscripts are sufficient when the reference frame that causes products of inertia to vanish is selected. This particular orientation is such that the reference frame axes are aligned with the principal axes of the body and is true for any rigid body, not only symmetrical ones. Selecting this particular reference frame greatly simplifies the equations of motion. Since the body frame axes meet this selection criterion, i.e., they are aligned with the principal axes of the body, there is considerable motivation to express the rotational equations of motion in the body frame. The mass distribution of a missile about its y-axis is often essentially the same as that about its z-axis. Therefore, the further simplification of setting I_y equal to I_z is often possible; however, the distinction is retained here for generality.

In some applications there may be other considerations that lead to selection of a reference frame other than the body frame, e.g., the wind coordinate frame. In that case the products-of-inertia terms are, in general, nonzero, and they must be retained in the development of the rotational equations of motion. The result is a very complex set of rotational equations of motion (Ref. 3). Even in that case, however, some of the products-of-inertia terms vanish if mass symmetries exist in the body about either the xz-plane or the xy-plane. In this handbook the body frame is selected, permitting use of the simpler diagonalized inertia matrix, i.e., all matrix elements are zero except on the diagonal.

Substituting Eq 4-38 into Eq. 4-2 and taking the derivative with respect to time give

$$\dot{\mathbf{h}} = [I] \dot{\boldsymbol{\omega}} + [\dot{I}] \boldsymbol{\omega}, \text{ N}\cdot\text{m} \quad (4-40)$$

where

$\dot{\mathbf{h}}$ = rate-of-change vector of angular momentum \mathbf{h} ,
N·m

$[I]$ = inertia matrix of a body, $\text{kg}\cdot\text{m}^2$

$[\dot{I}]$ = rate of change of inertia matrix, $\text{kg}\cdot\text{m}^2/\text{s}$

$\boldsymbol{\omega}$ = angular rate vector of rotating reference frame
relative to inertial frame, rad/s

$\dot{\boldsymbol{\omega}}$ = angular acceleration vector, rad/s^2 .

If Eq. 4-40 were evaluated in an inertial reference frame, the moments of inertia about the frame axes would change as the body experienced rotational motion and result in non-zero values of $[\dot{I}]$. However, if a reference frame fixed to the body were employed, the inertia matrix would not be changed by body motion and thus would provide another

motivation to select the body frame. During the operation of the propulsion system of a missile, there is another source of change in the moments of inertia that is not related to body motion. As the propellant mass is expelled from the missile, the moments of inertia change. This change in the value of $[I]$ is usually updated continuously in a flight simulation, but the time rate of change $[\dot{I}]$ is usually small enough to be neglected in Eq. 4-40. Thus selecting the body frame and assuming that the time rates of change of the moments of inertia caused by propellant expulsion are small cause $[\dot{I}]$ in Eq. 4-40 to vanish.

Since the angular momentum \mathbf{h} is a vector quantity, its time rate of change relative to an inertial reference frame (as required by Eq. 4-2) is different from its rate of change relative to a rotating reference frame. Again, this difference is taken into account by employing Eq. 4-9. Substituting \mathbf{h} for \mathbf{B} in Eq. 4-9 gives

$$\dot{\mathbf{h}}_{inertl} = \dot{\mathbf{h}}_{rot} + \boldsymbol{\omega} \times \mathbf{h}, \text{ N}\cdot\text{m} \quad (4-41)$$

where

\mathbf{h} = angular momentum vector of a body, $\text{N}\cdot\text{m}\cdot\text{s}$

$\dot{\mathbf{h}}_{inertl}$ = rate-of-change vector of angular momentum \mathbf{h}
relative to inertial reference frame, $\text{N}\cdot\text{m}$

$\dot{\mathbf{h}}_{rot}$ = rate-of-change vector of angular momentum \mathbf{h}
relative to (as viewed by an observer in) a rotating
reference frame, $\text{N}\cdot\text{m}$

$\boldsymbol{\omega}$ = angular rate vector of rotating reference frame
relative to inertial frame, rad/s .

Then, from Eq. 4-2

$$\mathbf{M} = \dot{\mathbf{h}}_{rot} + \boldsymbol{\omega} \times \mathbf{h}, \text{ N}\cdot\text{m} \quad (4-42)$$

where

$\dot{\mathbf{h}}_{rot}$ = magnitude of the rate-of-change vector angular
momentum \mathbf{h} relative to (as viewed by an
observer in) a rotating reference frame, $\text{N}\cdot\text{m}$

\mathbf{M} = total moment vector acting on the body, $\text{N}\cdot\text{m}$.

If $[I]$ is calculated relative to the body frame axes and $\boldsymbol{\omega}$ is expressed in the body frame, the time rate of change of angular momentum relative to that frame (the first term on the right side of Eq. 4-42) is given by

$$\dot{\mathbf{h}}_{rot} = [I] \dot{\boldsymbol{\omega}}, \text{ N}\cdot\text{m}. \quad (4-43)$$

The second term on the right side of Eq. 4-42 is

$$\boldsymbol{\omega} \times \mathbf{h} = qr(I_z - I_y) \mathbf{i}_b + pr(I_x - I_z) \mathbf{j}_b + pq(I_y - I_x) \mathbf{k}_b, \text{ N}\cdot\text{m}. \quad (4-44)$$

Substituting Eqs. 4-43 and 4-44 in Eq. 4-42 and rearranging give

$$\left. \begin{aligned} \dot{p} &= [L - qr(I_z - I_y)] / I_x, \text{ rad/s}^2 \\ \dot{q} &= [M - pr(I_x - I_z)] / I_y, \text{ rad/s}^2 \\ \dot{r} &= [N - pq(I_y - I_x)] / I_z, \text{ rad/s}^2 \end{aligned} \right\} \quad (4-45)$$

where

I_x, I_y, I_z = moments of inertia (diagonal elements of inertia matrix when products of inertia are zero), $\text{kg}\cdot\text{m}^2$

L, M, N = components of total moment vector M expressed in body coordinate system (roll, pitch, and yaw, respectively), $\text{N}\cdot\text{m}$

p, q, r = components of angular rate vector w expressed in body coordinate system (roll, pitch, and yaw, respectively), rad/s

$\dot{p}, \dot{q}, \dot{r}$ = components of angular acceleration \dot{w} expressed in body coordinate system (roll, pitch, and yaw, respectively), rad/s^2

Eqs. 4-45 are the rotational equations of motion expressed in body frame coordinates. Integration of Eqs. 4-45 yields the inertial angular rate w of the missile expressed in rotating body coordinates p, q, r .

4-5.2.1 Rotational Accelerations

Eqs. 4-45 give the absolute angular acceleration of the missile about its center of mass, expressed in the body reference frame. These equations are used to calculate the angular acceleration when the moments on the missile are given. If the moment terms L, M , and N in Eqs 4-45 are separated into aerodynamic and propulsion components, this equation becomes

$$\left. \begin{aligned} \dot{p} &= [L_A + L_p - qr(I_z - I_y)] / I_x, \text{ rad/s}^2 \\ \dot{q} &= [M_A + M_p - rp(I_x - I_z)] / I_y, \text{ rad/s}^2 \\ \dot{r} &= [N_A + N_p - pq(I_y - I_x)] / I_z, \text{ rad/s}^2 \end{aligned} \right\} \quad (4-46)$$

where

L_A, M_A, N_A = components of aerodynamic moment vector M_A expressed in body coordinate system (roll, pitch, and yaw, respectively), $\text{N}\cdot\text{m}$

L_p, M_p, N_p = components of propulsion moment vector M_p expressed in body coordinate system (roll, pitch, and yaw, respectively), $\text{N}\cdot\text{m}$.

4-5.2.2 Gyroscopic Moments

To evaluate the angular momentum vector h (Eq. 4-38) it is assumed that the missile is a single rigid body. If some portions of the missile mass are spinning relative to the body reference frame, e.g., spinning rotors, the additional angular momentum may be significant enough to be considered in the equations of rotational motion. Each spinning mass has an angular momentum relative to the body axes. This can be computed from Eq. 4-38 by interpreting the moments of inertia and products of inertia as those of the rotor with respect to axes parallel to the body axes and origin at the rotor mass center. For this application the angular velocity in Eq. 4-38 is interpreted as that of the rotor relative to the body axes. Let the resultant relative angular momentum of all rotors be h' , assumed to be constant. It can be shown that the total angular momentum of a missile with spinning rotors is obtained simply by adding h' to the h previously obtained

$$\mathbf{h} = [I]\boldsymbol{\omega} + \mathbf{h}', \text{ N}\cdot\text{m}\cdot\text{s} \quad (4-47)$$

where

\mathbf{h} = angular momentum vector of body, $\text{N}\cdot\text{m}\cdot\text{s}$

\mathbf{h}' = angular momentum vector of all rotors, $\text{N}\cdot\text{m}\cdot\text{s}$

$[I]$ = inertia matrix of a body, $\text{kg}\cdot\text{m}^2$

$\boldsymbol{\omega}$ = angular rate of rotating reference frame relative to inertial frame, rad/s .

As a result of adding h' terms to the angular momentum equation (Eq. 4-38), certain extra terms, known as gyroscopic couples (Ref. 2), appear in the rotational equations of motion. After adding these terms and solving for the angular rate components, the rotational equations of motion for a missile with spinning rotors are

$$\left. \begin{aligned} \dot{p} &= [L - qr(I_z - I_y) - qh'_z + rh'_y] / I_x, \text{ rad/s}^2 \\ \dot{q} &= [M - pr(I_x - I_z) - rh'_z + ph'_y] / I_y, \text{ rad/s}^2 \\ \dot{r} &= [N - pq(I_y - I_x) - ph'_z + qh'_y] / I_z, \text{ rad/s}^2 \end{aligned} \right\} \quad (4-48)$$

where

h'_x, h'_y, h'_z = components of rotor angular momentum vector h' expressed in the body coordinate system, $\text{N}\cdot\text{m}\cdot\text{s}$.

The angular momentum of a given rotor is

$$\mathbf{h}' = [I']\boldsymbol{\Omega}, \text{ N}\cdot\text{m}\cdot\text{s} \quad (4-49)$$

where

$[I']$ = inertia matrix of a rotor relative to the body coordinate system, $\text{kg}\cdot\text{m}^2$

Ω = angular rate vector of the rotor relative to the body coordinate system, $p'i_b + q'j_b + r'k_b$, rad/s.

For the general case the inertia matrix [I] for a rotor will include the rotor products of inertia; however, if the rotor axis is aligned with a missile body axis, the rotor products of inertia will vanish. The rotational equations of motion for a missile with a single rotor, and with the rotor axis aligned with a body axis, become

$$\left. \begin{aligned} \dot{p} &= [L - qr(I_z - I_y) - qr'I'_z + rq'I'_y] / I_x, \\ &\text{rad/s}^2 \\ \dot{q} &= [M - pr(I_x - I_z) - rp'I'_x + pr'I'_z] / I_y, \\ &\text{rad/s}^2 \\ \dot{r} &= [N - pq(I_y - I_x) - pq'I'_y + qp'I'_x] / I_z, \\ &\text{rad/s}^2 \end{aligned} \right\} \quad (4-50)$$

where

I'_x, I'_y, I'_z = diagonal elements of rotor inertia matrix relative to body axes, $\text{kg}\cdot\text{m}^2$

p', q', r' = components of rotor rate vector expressed in body coordinate system (roll, pitch, and yaw, respectively), rad/s

L, M, N = components of total moment vector M expressed in body coordinate system (roll, pitch, and yaw, respectively, N-m)

p, q, r = components of the angular rate vector ω expressed in body coordinate system (roll, pitch, and yaw, respectively), rad/s

I_x, I_y, I_z = moments of inertia (diagonal elements of inertia matrix when products of inertia are zero), $\text{kg}\cdot\text{m}^2$.

Note that in Eqs. 4-50 if a hypothetical internal rotor has inertial and rotational rate components that are identical to those of the airframe without the rotor, i.e., primed terms = unprimed terms, the terms representing the rotor are identical with the terms representing the airframe without the rotor, as expected. This observation serves only to give an understanding of the additional rotor terms and to add credi-

bility to them.

4-5.2.3 Rate of Change of Euler Angles

As discussed in par. 4-2 and shown in Fig. 4-2, the orientation of the body reference frame is specified by the three Euler angles, Ψ , θ , and ϕ . As the missile changes its orientation in space, the Euler angles change. The rates of change of the Euler angles are related to the angular rate ω of the body frame. This relationship is given in terms of the components of ω in the body reference frame (p, q, and r) by Ref. 2

$$\left. \begin{aligned} \dot{\phi} &= p + (q \sin \phi + r \cos \phi) \tan \theta, \text{ rad/s} \\ \dot{\theta} &= q \cos \phi - r \sin \phi, \text{ rad/s} \\ \dot{\Psi} &= (q \sin \phi + r \cos \phi) / \cos \theta, \text{ rad/s} \end{aligned} \right\} \quad (4-51)$$

where

θ = Euler angle rotation in elevation (pitch angle), rad (deg)

$\dot{\theta}$ = rate of change of θ , rad/s

ϕ = Euler angle rotation in roll (roll angle), rad (deg)

$\dot{\phi}$ = rate of change of ϕ , rad/s

$\dot{\Psi}$ = rate of change of Euler rotation in azimuth, rad/s.

The angular orientation of the missile at any time t is obtained by integrating Eqs. 4-51 from launch to time t and adding to the initial orientation angles at launch.

4-6 APPLICATION OF EQUATIONS OF MOTION

The dynamic motion of a missile is calculated by using the equations of motion given in this chapter. The methods used to calculate the aerodynamic and propulsive forces and moments are given in Chapters 5 and 6, respectively. The gravitational force is determined from Table 4-1 or Eq. 4-29. At each computational time step these forces and moments are substituted into Eqs. 4-37 and 4-46, respectively, to yield the translational and rotational accelerations of the missile. These are absolute accelerations expressed in the rotating body coordinates. Integration of these accelerations gives the translational and rotational absolute velocity components expressed in the rotating coordinates. These velocities are transformed to the fixed-earth (inertial) system by using the transformation equations in Appendix A. The resulting absolute velocities are integrated in earth coordinates to yield missile position in earth coordinates. The attitude of the missile in earth coordinates is obtained by integration of Eqs. 4-51.

REFERENCES

1. C. D. Perkins and R. E. Hage, *Airplane Performance Stability and Control*, John Wiley & Sons, Inc., New York, NY, 1949.
2. B. Etkin, *Dynamics of Flight—Stability and Control*, John Wiley & Sons, Inc., New York, NY, 1982.
3. *Dynamics of the Airframe*, BU AER Report AE-61-4 H, Bureau of Aeronautics, Navy Department, Washington, DC, 1952.
4. P. N. Jenkins, *Missile Dynamics Equations for Guidance and Control Modeling and Analysis*, Technical Report RG-84-17, Guidance and Control Directorate, US Army Missile Laboratory, US Army Missile Command, Redstone Arsenal, AL April 1984.
5. R. W. Kolk *Modern Flight Dynamics*, Prentice-Hall, inc., Englewood Cliffs, NJ, 1961.
6. H. Goldstein, *Classical Mechanics*, Addison-Wesley Publishing Company, Inc., Reading, MA, 1965.
7. M. Rauscher, *Introduction to Aeronautical Dynamics*, John Wiley & Sons, Inc., New York NY, 1953.
8. J. L. Meriam and L. G. Kraige, *Engineering Mechanics, Volume 2, Dynamics*, Second Edition, John Wiley & Sons, Inc., New York, NY, 1986.
9. D. Halliday and R. Resnick, *Physics, Parts I and II*, John Wiley & Sons, Inc., New York, NY, 1967.
10. R. c. Duncan, *Dynamics of Atmospheric Entry*, McGraw-Hill Book Company, Inc., New York, NY, 1982.
11. R W. Wolverton, *Flight Performance Handbook for Orbital Operations*, John Wiley & Sons, Inc., New York NY, 1963.
12. K. R. Symon, *Mechanics*, Third Edition, Addison-Wesley Publishing Company, Inc., Reading, MA 1971.

BIBLIOGRAPHY

EQUATIONS OF MOTION

- E. A. Bonney, M. J. Zucrow, and C. W. Besserer, "Aerodynamics, Propulsion, Structures and Design Practice", *Principles of Guided Missile Design*, G. Merrill, Ed., D. Van Nostrand Company, Inc., Princeton, NJ, 1956.
- J. E. Cochran, Jr., and J. R. Beaty, *Simulation of the Flight of a Short-Range Air Defense System Rocket Before Radar Acquisition*, Final Report US Army Research Office, Engineering Experiment Station, Auburn University, Auburn, AL, April 1977.
- A. B. Markov, *A Nonlinear Six-Degree-of-Freedom Ballistic Aerial Target Simulation Model*, Vol. 1, Theoretical Development, Suffield Memorandum No. 1081, PCN No. 2IV10, Defense Research Establishment Suffield Ralston, Alberta, Canada, February 1984.
- G. P. Sutton, *Rocket Propulsion Elements*, Second Edition, John Wiley & Sons, Inc., New York NY, 1956.

GRAVITY

- R. K. Burkard, *Geodesy for the Layman*, Geophysical and Space Sciences Branch, Chart Research Division, Aeronautical Chart and Information Center, St. Louis, MO, February 1968, p. 41.

RIGID BODY DYNAMICS

- D. P. LeGalley and J. W. McKee, Eds., *Space Exploration*, McGraw-Hill Book Company, New York, NY, 1964, p. 74.

CHAPTER 5

MISSILE AERODYNAMICS

As stated in Chapters 3 and 4, simulation of missile flight requires calculation of the forces and moments that act on the missile. The particular forces and moments contributed by aerodynamics are addressed in detail in this chapter. The various sources of aerodynamic data are discussed; representation of aerodynamic data in the form of force and moment coefficients is presented; and stability derivatives are defined. Methods and equations for employing the data in the calculation of the aerodynamic force vector F_a and the aerodynamic moment vector M_a are described. Effects of atmospheric properties—density, pressure, viscosity, and speed of sound—and of airflow parameters—Mach number and Reynolds number—on the aerodynamic forces and moments are discussed. Methods used to simplify the calculations are presented and special methods applicable to rolling airframes are described.

5-0 LIST OF SYMBOLS

- C_b = general aerodynamic coefficient based on body cross-sectional area, dimensionless
- C_D = aerodynamic drag coefficient, dimensionless
- C_{D_0} = zero-lift drag coefficient, dimensionless
- C_{D_s} = slope of curve formed by C_D versus δ , rad^{-1} (deg^{-1})
- C_F = general aerodynamic force coefficient, dimensionless
- C_L = aerodynamic lift coefficient, dimensionless
- C_{L_a} = slope of curve formed by lift coefficient C_L versus angle of attack a , rad^{-1} (deg^{-1})
- C_{L_δ} = slope of curve formed by lift coefficient C_L versus control-surface deflection δ , rad^{-1} (deg^{-1})
- C_l = aerodynamic roll moment coefficient about center of mass, dimensionless
- C_{lp} = roll damping derivative, rad^{-1} (deg^{-1})
- C_{l_δ} = slope of curve formed by roll moment coefficient C_l versus effective control-surface deflection δ , rad^{-1} (deg^{-1})
- C_n = general aerodynamic moment coefficient, dimensionless
- C_m = aerodynamic pitch moment coefficient about center of mass, dimensionless
- C_{m_q} = pitch damping derivative relative to pitch rate q , rad^{-1} (deg^{-1})
- $C_{m_{ref}}$ = pitch moment coefficient about reference moment station, dimensionless
- C_{m_a} = slope of curve formed by pitch moment coefficient C_m versus angle of attack a , rad^{-1} (deg^{-1})
- C_{m_α} = pitch damping derivative relative to angle of attack rate \dot{a} (slope of curve formed by C_m versus \dot{a}), rad^{-1} (deg^{-1})
- C_{m_δ} = slope of curve formed by pitch moment coefficient C_m versus control-surface deflection δ , rad^{-1} (deg^{-1})
- C_{N_y} = coefficient corresponding to component of normal force on y_b -axis, dimensionless
- C_{N_z} = coefficient corresponding to component of normal force on z_b -axis, dimensionless
- C_n = aerodynamic yaw moment coefficient about center of mass, dimensionless
- C_{n_r} = yaw damping derivative relative to yaw rate r , rad^{-1} (deg^{-1})
- $C_{n_{ref}}$ = yawing moment coefficient about reference moment station, dimensionless
- C_{n_β} = slope of curve formed by yawing moment coefficient C_n versus angle of sideslip β , rad^{-1} (deg^{-1})
- $C_{n_{\dot{\beta}}}$ = yaw damping derivative relative to angle-of-sideslip rate $\dot{\beta}$, rad^{-1} (deg^{-1})
- C_{n_δ} = slope of curve formed by yaw moment coefficient C_n versus effective control-surface deflection δ , rad^{-1} (deg^{-1})
- C_w = general aerodynamic coefficient based on wetted area, dimensionless
- D = magnitude of aerodynamic drag force vector D , N
- \bar{d} = aerodynamic reference length of body, m
- F_A = resultant aerodynamic force vector, N
- F = general force (aerodynamic), N
- F_A = magnitude of resultant aerodynamic force vector F_A , N
- I_x, I_y, I_z = moments of inertia of missile including any rotors (diagonal elements of inertia matrix $[I]$ when products of inertia are zero), $\text{kg}\cdot\text{m}^2$
- I_x, I_y, I_z = diagonal elements of rotor inertia matrix $[I]$ relative to body axes, $\text{kg}\cdot\text{m}^2$
- $J = I_y = I_z$ for symmetrical missile, $\text{kg}\cdot\text{m}^2$
- k = constant depending on body shape and flow regime, dimensionless
- L, M, N = components of total moment vector M expressed in body coordinate system (roll, pitch, and yaw, respectively), $\text{N}\cdot\text{m}$
- L_x, M_x, N_x = components of aerodynamic moment vector M_a expressed in body coordinate system (roll, pitch, and yaw, respectively), $\text{N}\cdot\text{m}$
- L = magnitude of aerodynamic lift force vector L , N

M_A = aerodynamic moment vector, N·m
 M_N = Mach number, dimensionless
 p, q, r = components of the angular rate vector ω expressed in body coordinate system (roll, pitch, and yaw, respectively), rad/s (deg/s)
 $\dot{p}, \dot{q}, \dot{r}$ = components of the angular acceleration of the missile measured with respect to the x_b -, y_b -, and z_b -axes, respectively, rad/s² (deg/s²)
 p', q', r' = components of rotor rate vector expressed in body coordinate system (roll, pitch, and yaw, respectively), rad/s (deg/s)
 p_a = ambient atmospheric pressure, Pa
 p_r = constant or nearly constant roll rate of missile, rad/s (deg/s)
 Q = dynamic pressure parameter, Pa
 S = aerodynamic reference area, m²
 S_b = cross-sectional area of body, m²
 S_w = wetted area of body, m²
 V = speed of a body, speed of air relative to a body, magnitude of velocity vector V , m/s*
 V_s = speed of sound in fluid, m/s
 α = exponent depending on body shape and air-flow regime, dimensionless
 x_{cm} = instantaneous distance from missile nose to center of mass, m
 x_{ref} = distance from missile nose to reference moment station, m
 α = angle of attack in pitch plane, rad (deg)
 $\dot{\alpha}$ = angle of attack rate, rad/s (deg/s)
 β = angle of sideslip (angle of attack in yaw plane), rad (deg)
 δ = general or effective angular deflection of control surface relative to a body, rad (deg)
 δ_p = angle of effective control-surface deflection in the pitch direction, rad (deg)
 δ_{peak} = peak control-surface deflection during revolution of missile, rad (deg)
 δ_r = effective control-surface deflection angle corresponding to roll, rad (deg)
 δ_y = angle of effective control-surface deflection in the yaw direction, rad (deg)
 δ_{yavg} = average component of control-surface deflection in y-direction, rad (deg)
 θ = missile pitch angle (Euler angle rotation in elevation), rad (deg)
 μ = atmospheric dynamic viscosity, kg/(m·s)
 ν = atmospheric kinematic viscosity, m²/s
 ρ = atmospheric density, kg/m³
 ϕ = missile roll angle (Euler angle rotation in roll), rad (deg)
 Ω = angular rate vector of rotor relative to body coordinate system, rad/s (deg/s)

ω = angular rate vector of simulated missile, rad/s (deg/s)
 ω = angular rate, rad/s (deg/s)

5-1 INTRODUCTION

Aerodynamic flow over a body has different characteristics, depending on the speed of the air relative to the body. The aerodynamic coefficients in turn depend on these characteristics of the flow. The different flow characteristics are grouped into five basic flow regimes based on Mach number M_N . These regimes are described as incompressible subsonic, compressible subsonic, transonic, supersonic, and hypersonic. Commonly accepted ranges of Mach number that define these flow classifications are

1. Incompressible subsonic flow: $0 < M_N < 0.5$
2. Compressible subsonic flow: $0.5 \leq M_N < 0.8$
3. Transonic flow: $0.8 \leq M_N < 1.2$
4. supersonic flow: $1.2 \leq M_N < 5$
5. Hypersonic flow: $5 \leq M_N$

There are two general types of aerodynamic forces on a body: normal (or pressure) forces and tangential (or shearing) forces (Ref. 1). Pressure forces can act only normal to the surface of the body. The tangential (shearing) forces result from the viscous shearing stress between successive layers of fluid molecules adjacent to the surface of the body. These tangential forces are commonly called friction forces. In addition to causing friction forces, viscous effects can also influence the flow pattern around the body and thus affect the pressure force. The pressure forces are affected also by shock waves and expansion waves, which are formed about the body when the flow is supersonic (Ref. 1). The total pressure force on the body is the vector sum of all the aerodynamic forces normal to the various surfaces of the body. Similarly, the total friction force is the vector sum of all the tangential forces. The combination of these two types of forces at any instant of time determines the total aerodynamic force and moment on the body.

If the incremental pressures and tangential forces on the missile could be predicted within a missile flight simulation, they could be integrated over the entire surface of the missile to yield directly the aerodynamic forces and moments. Although methods of analyzing fluid flow to calculate these incremental pressures and incremental tangential forces on arbitrary bodies are fundamental in the study of aerodynamics, these methods are only now becoming feasible on the largest and fastest computers. The computational task required to use this approach directly in a flight simulation would be prohibitive.

The classical method used to determine aerodynamic forces and moments on a body is by experiments in which the integrated forces and moments on a model of the body are measured in a wind tunnel. (See subpar. 5-4.2 for a dis-

*The symbol V represents the speed of a body, such as a particle, missile, or target. In this handbook the speed of the air relative to a body is equivalent to the speed of the body because the effects of atmospheric winds are not treated. Where it is important to distinguish between missile and target speeds, appropriate subscripts M or T are used. General aerodynamic equations are written without these subscripts.

cussion of wind tunnel s.) For an airborne vehicle these measurements are made under various conditions of flow and with various vehicle attitudes relative to the flow. These measurements provide a large body of data covering essentially all anticipated flight conditions for that vehicle. When such model data are available for a missile configuration, they can be scaled up to be applicable to the full-scale missile.

Analytical equations and data for estimating aerodynamic forces and moments have been developed based partially on theory and partially on wind tunnel measurements on great numbers of different model configurations and flow conditions. Although these analytical methods are generally not as accurate as actual wind tunnel measurements for a given missile configuration, they are a means of calculating force and moment estimates when wind tunnel data for a missile configuration are not available.

Much of the effort of the National Advisory Committee for Aeronautics (NACA)-predecessor to the National Aeronautics and Space Administration (NASA)--was dedicated to investigation of aerodynamic forces and moments. This work included extensive wind tunnel testing and analytical studies aimed at providing methods of evaluating the variation of forces and moments with changes in the type of flow and changes in vehicle configurations (Ref. 2). The outputs from most of these tests and studies are in the form of aerodynamic coefficients associated with very detailed descriptions of the geometry and motion of the vehicle and of the flow conditions. An aerodynamic force coefficient is a practical means of lumping the many necessary considerations into a manageable parameter that can be used to calculate aerodynamic forces under specific conditions.

5-2 AERODYNAMIC COEFFICIENTS

In missile flight simulations the aerodynamic forces and moments on the missile must be calculated at each computation time of the simulation. Regardless of whether aerodynamic forces and moments are determined by wind tunnel measurements or by analytical predictions, they are expressed mathematically by means of dimensionless aerodynamic coefficients, such as C_F in Eq. 3-3 and C_M in Eq. 3-4. The dimensionless aerodynamic coefficients, which are independent of the missile size for a given configuration, are the standard means of converting data obtained from wind tunnel models to data that are applicable to full-scale missiles (Ref. 3).

5-2.1 APPLICATION OF AERODYNAMIC COEFFICIENTS

For high-fidelity flight simulations nonlinear aerodynamic coefficients are input to the simulation by means of extensive tables or function generators covering all the anticipated variations in the applicable parameters. However, the coefficients are often approximately linear in the

regions of most interest, and simulations are often based on linearity assumptions, which permit acceptable fidelity to be achieved using greatly simplified data as input. The input tables can then be reduced to much smaller tables containing only the values of the slopes of the linearized coefficient curves. These slopes, or derivatives, of the curves have been used extensively in aerodynamic stability analyses and are therefore called stability derivatives.

When stability derivatives are used, instantaneous aerodynamic coefficients are calculated in the simulation by multiplying the appropriate derivative by the instantaneous value of the applicable variable (subpar. 5-2.1.5). If it is necessary to include nonlinearities, they can be approximated by adding terms involving powers of the parameters. Coefficient and derivative data for aerodynamic moments are based on specified locations of the center of mass of the missile. When the instantaneous center of mass differs from the one on which the input data are based, the moment coefficients must be corrected Eqs. 5-12).

To apply test data or empirical methods in a flight simulation, it is necessary that the factors affecting aerodynamic forces and moments be presented in their proper relationship. This relationship has been determined by the method of dimensional analysis (Refs. 1 and 4) and confirmed by one-dimensional fluid mechanics theory, by potential theory (Ref. 1), and by wind tunnel and flight testing. For aerodynamic forces this relationship is given by the familiar form of the aerodynamic force equation employed extensively in aerodynamics:

$$F = 0.5\rho V^2 C_F S, N \quad (5-1)$$

where

- C_F = general aerodynamic force coefficient, dimensionless
- F = general force (aerodynamic), N
- S = aerodynamic reference area, m²
- V = speed of a body, speed of air relative to a body, magnitude of velocity vector V , m/s
- ρ = atmospheric density, kg/m³.

In practice F and C_F are always expressed in terms of specific components, e.g., drag force D and coefficient of drag C_D (subpar. 5-2.1.4).

5-2.1.1 Dynamic Pressure Parameter

The term $0.5\rho V^2$ is a very important quantity, known as the dynamic pressure parameter, which was discussed in subpar. 3-3.2.3. The dynamic pressure parameter is equal to the kinetic energy per unit volume of air. Two equivalent forms of the dynamic pressure parameter were presented in Chapter 3 as

$$Q = 0.7p_a M_N^2, Pa \quad (3-5)$$

$$Q = 0.5\rho V^2, \text{ Pa} \quad (3-6)$$

where

- M_N = Mach number, dimensionless
- P_a = ambient atmospheric pressure, Pa
- Q = dynamic pressure parameter, Pa.

Whenever a fluid passes around an object there is a point at which the flow divides—part goes one way and part the other. This point of division is called the stagnation point because, theoretically, the molecules of fluid at this point are brought to rest relative to the object. At the stagnation point the rise in pressure, caused by the loss of all kinetic energy of the fluid is called the dynamic pressure, which in incompressible flow is equal to the dynamic pressure parameter Q . Thus in incompressible flow the force on the body per unit area at the stagnation point is equal to the dynamic pressure parameter.

Although the dynamic pressure actually acts only at the stagnation point, Eq. 5-1 shows that the total aerodynamic force F on the entire body is proportional to the dynamic pressure parameter.

In compressible flow the actual dynamic pressure is larger than the dynamic pressure parameter (Ref. 3); nevertheless, accepted practice is to use the dynamic pressure parameter to characterize both incompressible and compressible flows. The difference is taken into account by the dependency of the force coefficient on Mach number.

5-2.102 Force Coefficient

The force coefficient C_f is a dimensionless coefficient that accounts for all the factors that affect aerodynamic force except those included explicitly in Eq. 5-1. Force coefficients usually are based on tests and are defined as the ratio of the measured force to the product of the dynamic pressure parameter and the reference area, as shown by solving for the force coefficient in Eq. 5-1. The force coefficient can be viewed as a proportionality between the actual aerodynamic force on a body and a reference force. The reference force is the force that would result from applying a pressure equal to the dynamic pressure parameter to the reference area.

The value of the aerodynamic force coefficient for a given body configuration is affected primarily by the shape of the body (including any control-surface deflections), the orientation of the body within the flow (angle of attack), and the flow conditions. For the types of flow generally encountered in surface-to-air flight simulations, the flow conditions can be specified by two parameters: the Mach number and the Reynolds number.

5-2.1.2.1 Effect of Mach Number

As previously defined, the Mach number is the ratio of the missile speed, i.e., the relative speed of fluid flow, to the speed of sound in the ambient air. As the missile speed approaches and exceeds the speed of sound, the compress-

ibility characteristics of the air have a pronounced effect on the aerodynamic forces and moments. Shock waves are formed that affect the pressures and the distribution of pressures on the surface of the vehicle. These compressibility effects are taken into account in aerodynamic force and moment equations by including them in the aerodynamic coefficients. The compressibility effects are so important that aerodynamic force and moment coefficients for missiles are always given as functions of Mach number.

5-2.122 Effect of Reynolds Number

Another fluid-flow property that affects the values of the aerodynamic force and moment coefficients is characterized by the Reynolds number. The Reynolds number is a measure of the ratio of the inertial properties of the fluid flow to the viscous properties. Reynolds number is given by

$$\text{Reynolds number} = \frac{\rho V d}{\mu}, \text{ dimensionless (5-2)}$$

where

- d = aerodynamic reference length of body, m
- V = speed of a body, speed of air relative to a body, magnitude of velocity vector V , m/s
- μ = atmospheric dynamic viscosity, kg/(m-s)
- ρ = atmospheric density, kg/m³.

The reference length d is a scale factor that accounts for the effect of the size of the missile on the flow characteristics. The missile diameter is often selected as the reference length, but the length of the missile body is also commonly used. Force coefficients are functions of Reynolds number. When a force coefficient is given, the Reynolds number upon which it is based must also be given; in addition, the missile dimension used as a reference length for the Reynolds number must be specified.

Although Reynolds number varies as the missile changes speed and altitude, the effect on the aerodynamic force coefficients is generally small over the major portion of the flight of a typical surface-to-air missile. For this reason the variation of the force coefficients with Reynolds number is often neglected in missile flight simulation, except to ensure that the force coefficient data correspond to the general range of Reynolds numbers typical of full-scale missile flight. The variation of force coefficients with Reynolds number becomes important for missiles that fly to very high altitudes, greater than about 15 km, and in the interpretation of wind tunnel data based on small-scale models.

5-2.1.3 Reference Area

Aerodynamic pressures and tangential forces per unit area must be integrated over the surface area of the body to yield the force on the body. This dependence on area is represented in Eq. 5-1 by the reference area S which is actu-

ally a scaling factor, rather than a specific area acted on by a specific pressure. The reference area accounts for the relative size of the body in aerodynamic force calculations. Under similar flow conditions, the aerodynamic forces on geometrically similar bodies are proportional to the respective reference areas of the bodies. For geometrically similar bodies, the proportionality is constant, regardless of which area of the bodies is selected as the reference area. For a given body and flow, the product of the force coefficient and the reference area $C_f S$ must not vary with different choices for the reference area; therefore, the value of the force coefficient depends on which area of the body is used as the reference area.

Although the selection of the particular area of the body to be employed as the reference area S is completely arbitrary, common practice is to use the wing planform area for airplanes and the body cross-sectional area for missiles. Other areas are sometimes used for specific applications. For example, the body wetted area, i.e., total surface exposed to the air, is used for calculations of viscous friction forces; however, when these viscous components are combined with the pressure forces, a single reference area is needed. A coefficient based on wetted area is converted to the body cross-sectional area by

$$C_b = C_w \frac{S_w}{S_b}, \text{ dimensionless} \quad (5-3)$$

where

- C_b = general aerodynamic coefficient based on body cross-sectional area, dimensionless
- C_w = general aerodynamic coefficient based on wetted area dimensionless
- S_b = cross-sectional area of body, m^2
- S_w = wetted area of body, m^2 .

When coefficients based on other reference areas are encountered, they can be converted to any desired reference area by equations of the form of Eq. 5-3 based on the equivalence of the product $C_f S$.

An aerodynamic coefficient determined for a subscale model of a missile is directly applicable to the full-scale missile under similar flow conditions when used in Eq. 5-1, in which the corresponding reference area of the full-scale missile is used.

5-2.1.4 Components of Forces and Moments

The resultant aerodynamic force F_A is always considered in terms of its components, either lift and drag or normal force and axial force, as discussed in subpar. 4-4.1. Therefore, values for a total aerodynamic force coefficient C_f of a body are never used. The relationships among drag, axial force, lift, and normal force were given by Eqs. 4-13 and 4-

14. These equations show that under conditions of zero lift, i.e., angle of attack = 0, drag and axial force are identical and lift and normal force are identical. In the general case in which the angle of attack $\neq 0$, the resultant aerodynamic force can be resolved into either lift/drag components or normal-force/axial-force components, and given aerodynamic data tables may be encountered in either or both sets of coordinates. For purposes of flight simulation, working with lift/drag components has the advantage that these force components produce accelerations perpendicular to and along the path of the vehicle. Therefore, discussions in the following paragraphs emphasize the use of lift and drag components.

The drag coefficient C_D and the lift coefficient C_L are typically used in Eq. 5-1 in place of C_f to define the respective components of the resultant aerodynamic force F_A . The expressions for D and L are

$$D = 0.5\rho V^2 C_D S, N \quad (5-4)$$

$$L = 0.5\rho V^2 C_L S, N \quad (5-5)$$

where

- C_D = aerodynamic drag coefficient dimensionless
- C_L = aerodynamic lift coefficient, dimensionless
- D = magnitude of aerodynamic drag force vector D , N
- L = magnitude of aerodynamic lift force vector L , N
- S = aerodynamic reference area, m^2
- V = speed of a body, speed of air relative to a body, magnitude of velocity vector V , m/s
- ρ = atmospheric density, kg/m^3 .

In calculations and discussions these components are handled as separate but related forces.

Theory and experiment show that the equation to calculate aerodynamic moments is analogous to that for aerodynamic forces but with the addition of a characteristic length term d as indicated previously by Eq. 3-4. For missiles this reference length is usually taken as the body diameter. As with aerodynamic forces, aerodynamic moments are always considered in terms of their components. The aerodynamic rolling moment i.e., the moment about the x-axis in the body reference frame, is calculated by substituting the rolling moment coefficient C_l into Eq. 3-4 in place of the general term C_m . In a like manner, the aerodynamic moments about the other two axes are given by similar equations using the pitching moment coefficient C_m and the yawing moment coefficient C_n . Expressions for the aerodynamic moment components about the coordinate axes are

$$L_A = 0.5\rho V^2 C_l S d, N \cdot m \quad (5-6)$$

$$M_A = 0.5\rho V^2 C_m S d, \text{ N}\cdot\text{m} \quad (5-7)$$

$$N_A = 0.5\rho V^2 C_n S d, \text{ N}\cdot\text{m} \quad (5-8)$$

where

C_i = aerodynamic roll moment coefficient about center of mass, dimensionless

C_m = aerodynamic pitch moment coefficient about center of mass, dimensionless

C_n = aerodynamic yaw moment coefficient about center of mass, dimensionless

d = reference length of body, m

L_A, M_A, N_A = components of aerodynamic moment vector M_A expressed in body coordinate system (roll, pitch, and yaw, respectively), N-m

S = aerodynamic reference area, m²

V = speed of a body, speed of air relative to a body, magnitude of velocity vector V , m/s

ρ = atmospheric density, kg/m³

For missiles in a mature state of development, very detailed force and moment coefficient data maybe available as a function of Mach number, altitude, angle of attack, and sometimes control-surface deflection. In this case the most accurate use of these data in a simulation is through direct tabular data inputs with interpolation among the tabular values rather than by use of the stability derivatives, which are discussed in subpar. 5-2.1.5 and par. 5-3.

5-2.1.5 Linearity Assumption

Aerodynamic coefficients are typically plotted as functions of parameters such as angle of attack control-surface deflection angle, and missile roll position. In general, these are not linear over all values of the parameters. The most applicable portion of the curves, however, are often approximately linear, and advantage has been taken of this fact in classical aerodynamic analyses. The assumption of linearity allows the behavior of a given aerodynamic coefficient relative to a given parameter to be described by specifying only the slope, or derivative, of the curve. The value of the aerodynamic coefficient is calculated easily by multiplying the value of the slope by the value of the parameter. For example, if the slope of the curve relating the coefficient of lift to the angle of attack is given as C , then the lift coefficient can be determined for a given angle of attack by $C_L = C_L \alpha$. When the parameter is an angular rate, the derivative is made nondimensional by taking it with respect to the nondimensional velocity parameter $\omega d / (2V)$ * in which ω represents an angular rate. For example, the pitch damping derivative is given by

$$C_{m_q} = \frac{\partial C_m}{\partial \left(\frac{\omega d}{2V} \right)}, \text{ rad}^{-1} (\text{deg}^{-1}) \quad (5-9)$$

where

C_m = aerodynamic pitch moment coefficient about center of mass, dimensionless

C_{m_q} = pitch damping derivative relative to pitch rate q , rad⁻¹ (deg⁻¹)

d = aerodynamic reference length of body, m

q = pitch component of angular rate vector ω expressed in body coordinate system, rad/s (deg/s)

V = speed of a body, speed of air relative to a body, magnitude of velocity vector V , m/s.

See Refs. 4 and 5 for justification of this formulation.

5-2.2 DRAG COEFFICIENTS

As an example of the calculation of aerodynamic forces, Fig. 5-1(A) shows a disk in a flow stream that is perpendicular to the surface of the disk with air density ρ and relative velocity V . The aerodynamic drag on the disk is given by Eq. 5-4. If the surface area of the disk is selected as the reference area, the value of the drag coefficient C_D in incompressible flow has been determined experimentally to be approximately 1.17 at a Reynolds number of 10^6 (Ref. 6). If an aerodynamically shaped nose and tail are added to the disk forming a body with a length-to-diameter ratio of about 12 (Fig. 5-1(B)), the drag coefficient is reduced to about 0.1 for similar flow conditions and the same reference area (Ref. 6). Thus the drag force on the streamlined body is less than one-tenth that on the disk of the same diameter. If the dimensions of the body are doubled (quadrupling the cross-sectional area), the force coefficient C_D is unchanged (neglecting small Reynolds number effects), but the aerodynamic drag D is quadrupled.

As atmospheric air passes around a body with a blunt rear end, the pressure of the air immediately behind the body is reduced. One of the components of drag, called base drag, is caused by this reduced pressure acting on the area of the rear end, or base, of the missile, as indicated in Fig. 5-2. After burnout of the rocket motor, atmospheric pressure acts on the entire base area as shown in Fig. 5-2(A). During the time the rocket motor is burning, the area of the exit plane of the rocket nozzle fills with propellant exhaust gases; therefore, the atmospheric pressure acts only on that portion of the missile base area that does not include the nozzle exit area, as shown in Fig. 5-2(B), and the base drag is consequently reduced. The typical flight of a simulated missile

*The nondimensional velocity parameter $\omega d / (2V)$ represents the angle in radians of the helix described by a point located at radius $d/2$ from the axis of a rotating body. The air striking the surface at this angle creates the angular damping moment. Since the selection of the reference length d is arbitrary, the value of d must be stated in order for a stated value of C_{m_q} to be meaningful. (Refs. 3 and 4)

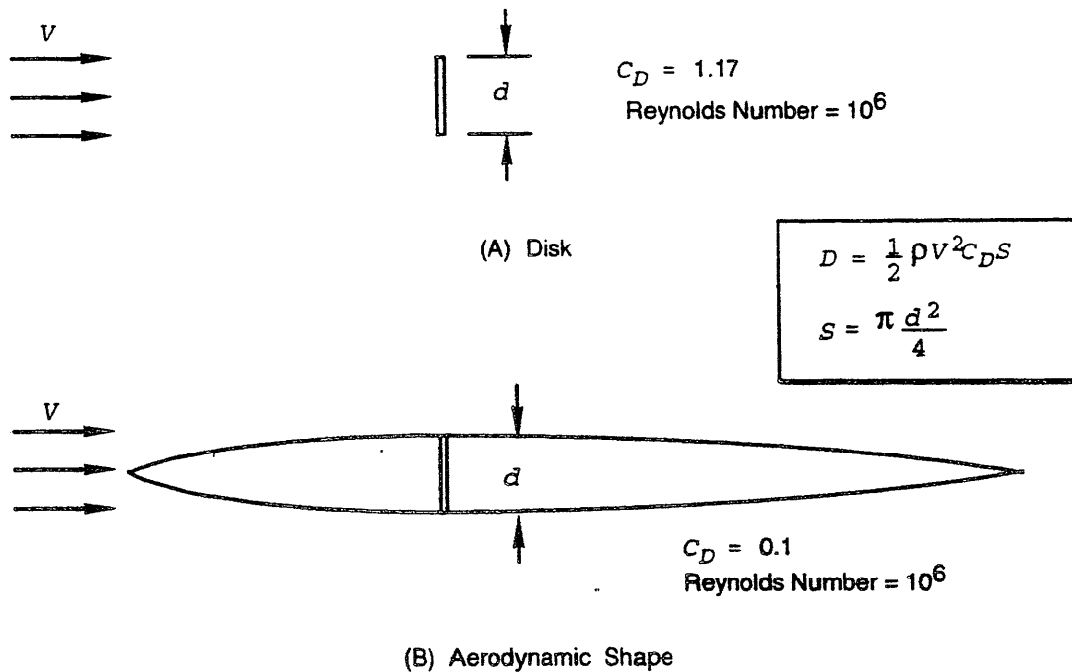


Figure 5-1. Comparison of Drag on a Disk and an Aerodynamic Shape

includes both power-on and power-off phases; therefore, drag characteristics for both phases must be provided. The drag coefficient for a typical, generic surface-to-air missile at zero angle of attack and zero control-surface deflection (zero lift) is shown as a function of Mach number in Fig. 5-3 for both power-on and power-off conditions.

If control surfaces are deflected and the missile rotates to an attitude having an angle of attack the drag increases. This increment of increase is called drag-due-to-lift. A typical relationship between drag and lift, called the drag polar, is shown in Fig. 5-4. In general, this relationship can be represented by a polynomial equation of the form

$$C_D = C_{D0} + kC_L^x, \text{ dimensionless} \quad (5-10)$$

where

- C_D = aerodynamic drag coefficient, dimensionless
- C_{D0} = zero-lift drag coefficient, dimensionless
- C_L = aerodynamic lift coefficient, dimensionless
- k = constant depending on body shape and flow regime, dimensionless
- x = exponent depending on body shape and airflow regime, dimensionless.

The second term on the right is called the induced drag

coefficient, or drag-due-to-lift coefficient. In subsonic flow there are many vehicle configurations for which the drag coefficient is a quadratic function of the lift coefficient ($x = 2$) for some portion of the lift coefficient curve. Also, for thin-winged configurations operating at moderately supersonic speeds (typical of most surface-to-air missiles), the approximation $x = 2$ can be used, as in the subsonic case. Engineering practice often is to use the quadratic approximation at transonic speeds also, even though this is not fully justified from a theoretical standpoint. For thin-winged configurations that operate in the hypervelocity domain, the approximation $x = 3/2$ is appropriate (Ref. 7). For most surface-to-air missile flight simulations, the quadratic form of the parabolic polar ($x = 2$) is applicable.

Although missile drag at a given angle of attack is slightly affected by the angle of control-surface deflection, this effect is often considered to be negligible (Ref. 7) When it is not considered to be negligible, the additional drag due to control-surface deflection can be taken into account by Eq. 5-10 with the addition of an extra term of the form - in which is the effective control-surface deflection angle and $C_{D\delta}$ is the slope of the C_D versus δ curve, assuming linearity.

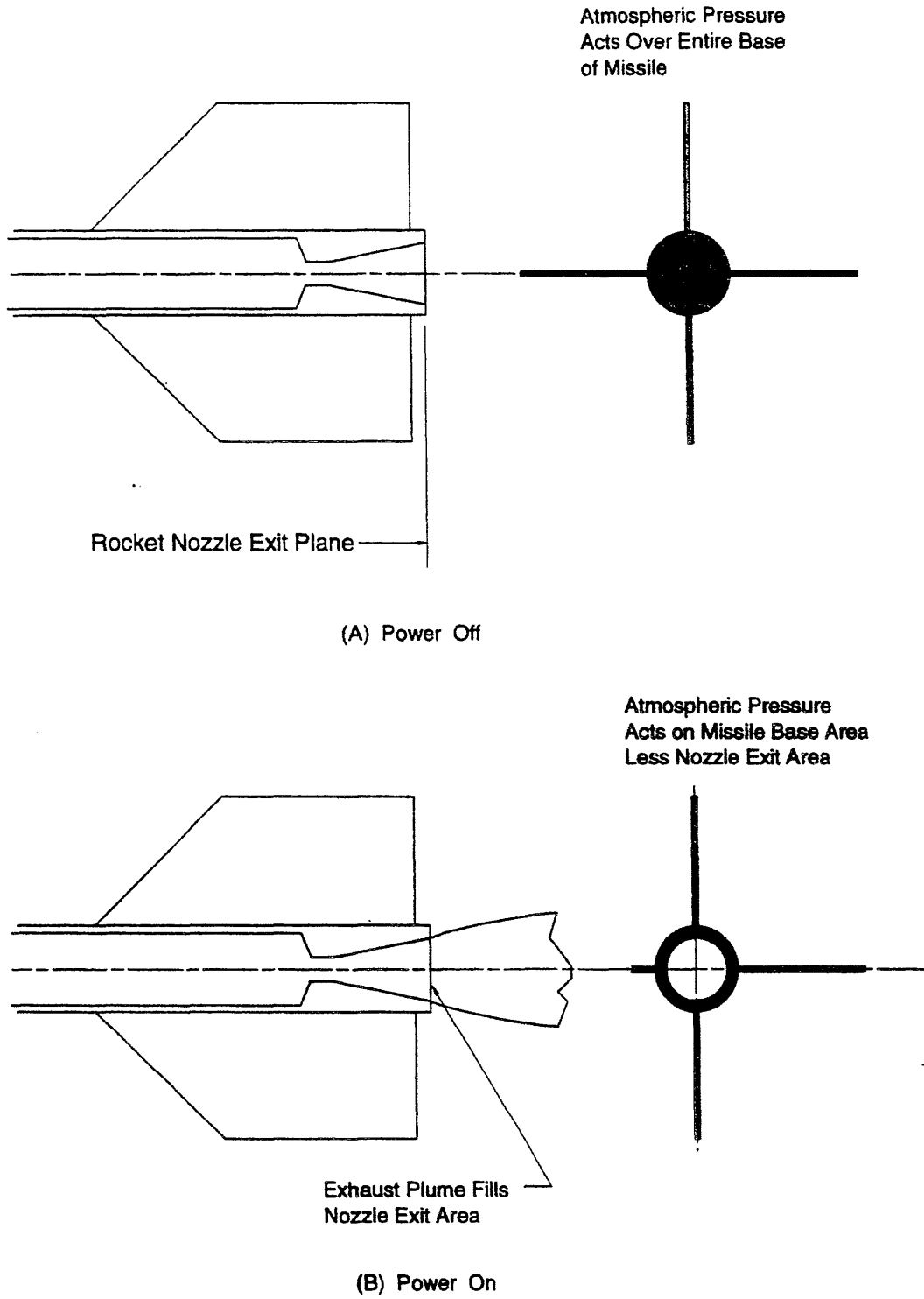


Figure 5-2. Effect of Rocket Plume on Base Drag

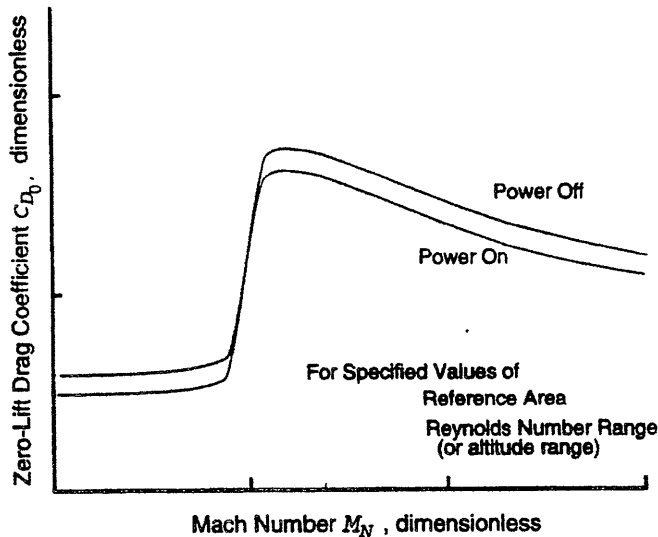
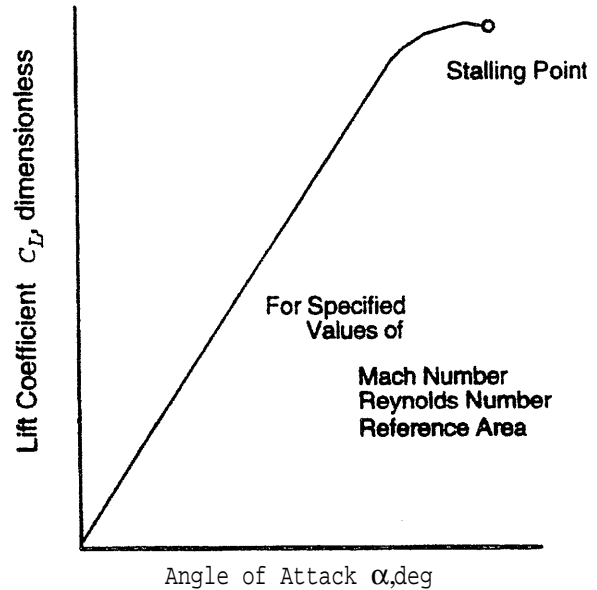


Figure 5-3. Zero-Lift Drag Coefficient



5-5. Coefficient of Lift Versus Angle of Attack

attack. This allows the lift coefficient at a given angle of attack to be calculated using

where

- C_L = aerodynamic lift coefficient, dimensionless
- $C_{L\alpha}$ = slope of curve formed by lift coefficient C_L versus angle of attack a $\text{rad}^{-1}(\text{deg}^{-1})$
- α = angle of attack in pitch plane, rad (deg).

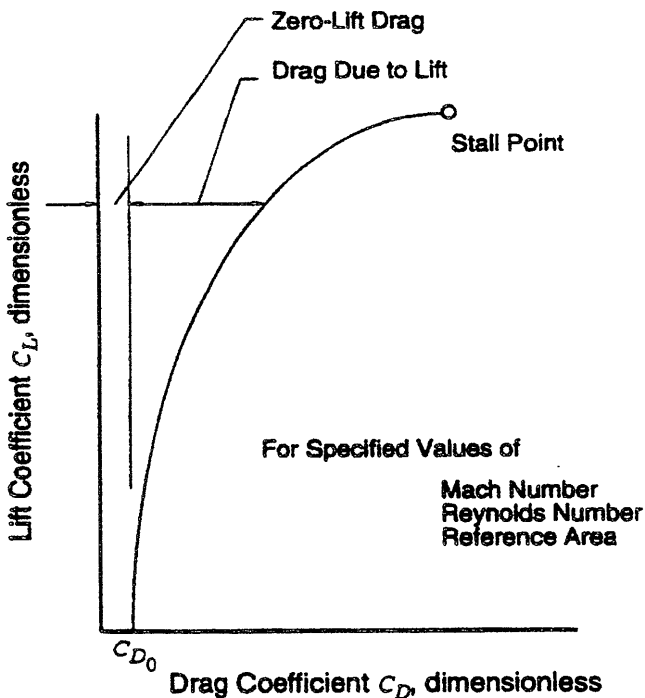


Figure 5-4. Drag Polar

5-2.3 LIFT COEFFICIENTS

The lift is the primary force that causes a missile to maneuver. Lift is considered to be a desirable quantity, whereas drag is an undesirable quantity because it expends missile energy. Unfortunately, lift is bought at the expense of additional drag, as shown in Eq. 5-10 and Fig. 5-4. The lift force is generated by the combined effects of airflow over all the surfaces of the missile including the body.

Fig. 5-5 shows a typical plot of lift coefficient as a function of angle of attack. Over a large portion of the lift curve, the lift coefficient is approximately linear with angle of

At high angles of attack, flow separation from the body causes the lift coefficient to vary in a nonlinear manner, depending on the Reynolds number. As the angle of attack is increased, the lift coefficient finally reaches a maximum value called the stall point. Generally, missiles are not designed to operate at angles of attack near or above the stall point. If the simulated missile is expected to operate at angles of attack above the linear region, however, a table of the nonlinear coefficients is used in place of Eq. 5-11. Alternatively, additional terms in powers of α are added to Eq. 5-11 to make it a better fit to the empirical data. When data are available, terms may also be added to account for the increment of lift produced by control-surface deflections δ . **These terms have the form $C_{L\delta}\delta$, in which $C_{L\delta}$ is the derivative of C_L with respect to δ . The slopes $C_{L\alpha}$ and $C_{L\delta}$ are functions of Mach number and maybe supplied to the simulation in tabular form.**

5-2.4 MOMENT COEFFICIENTS

The moments exerted by aerodynamic forces on a missile are calculated by the moment coefficients C_m , C_n , and C_y for roll, pitch, and yaw, respectively. The moment coefficients for a given missile are primarily functions of Mach number, angle of attack, and control-surface deflections. An acrody-

dynamic moment on a symmetrical configuration is generated by the resultant aerodynamic force acting with a lever arm relative to the axis of rotation. This moment usually is approximated by the normal force acting at the center of pressure with a lever arm equal to the distance between the center of mass and the center of pressure. For asymmetrical configurations, e.g., a missile with deflected control surfaces, an additional moment can be caused by forces that are equal in magnitude but opposite in direction—therefore not included in the resultant force—and whose lines of action are not colinear.

Calculations of aerodynamic moments are based on moment coefficients derived from wind tunnel tests. Fig. 5-6 shows a typical set of moment coefficient curves for various control-surface deflection angles. The indicated moment reference station is the point on the missile, sometimes called the aerostation, about which the moments were measured in the wind tunnel. Moment coefficient curves vary with Mach number therefore, tabular data based on figures similar to Fig. 5-6 are usually input to a flight simulation for several different Mach numbers. The moment coefficients illustrated in Fig. 5-6 represent only the static component of the total instantaneous moment coefficient. In addition, the dynamic damping components, discussed in par. 5-3, are supplied in the form of the dynamic derivatives $C_{m\dot{q}}$ and $C_{m\dot{\alpha}}$ as functions of Mach number.

The moments in Eqs. 4-46 are about the instantaneous center of mass of the missile. As previously stated however, moment coefficients derived from analytical calculations or from wind tunnel data are specified with respect to some reference moment station. The reference moment station is often located at the center of mass of the missile after motor burnout but before motor burnout the missile center of mass changes position with time because of the mass redistribution that occurs when propellant burns and is expelled. Therefore, it is necessary to correct the moment coefficient

to make it relative to the instantaneous center of mass.

Equations for calculating this correction for the pitching and yawing moment coefficients dynamic components are

$$\left. \begin{aligned} C_m &= C_{m_{ref}} - C_{N_z} \frac{x_{cm} - x_{ref}}{d} + \frac{d}{2V} (C_{m_q} + C_{m_{\dot{\alpha}}}) q, \\ C_n &= C_{n_{ref}} + C_{N_y} \frac{x_{cm} - x_{ref}}{d} + \frac{d}{2V} (C_{n_r} + C_{n_{\dot{\beta}}}) r, \end{aligned} \right\} \text{dimensionless} \quad (5-12)$$

where

- C_{m_q} = pitch damping derivative relative to pitch rate q , $\text{rad}^{-1} (\text{deg}^{-1})$
- $C_{m_{ref}}$ = pitching moment coefficient about reference moment station, dimensionless
- $C_{m_{\dot{\alpha}}}$ = pitch damping derivative relative to angle of attack rate $\dot{\alpha}$ (slope of curve formed by C_m versus $\dot{\alpha}$), $\text{rad}^{-1} (\text{deg}^{-1})$
- C_{N_y} = coefficient corresponding to component of normal force on y_b -axis, dimensionless
- C_{N_z} = coefficient corresponding to component of normal force on z_b -axis, dimensionless
- C_{n_r} = yaw damping derivative relative to yaw rate r , $\text{rad}^{-1} (\text{deg}^{-1})$
- $C_{n_{ref}}$ = yawing moment coefficient about reference moment station, dimensionless
- $C_{n_{\dot{\beta}}}$ = yaw damping derivative relative to angle-of-sideslip rate $\dot{\beta}$, $\text{rad}^{-1} (\text{deg}^{-1})$
- d = aerodynamic reference length of body, m
- q = pitch component of angular rate vector ω expressed in body coordinate system, rad/s (deg/s)

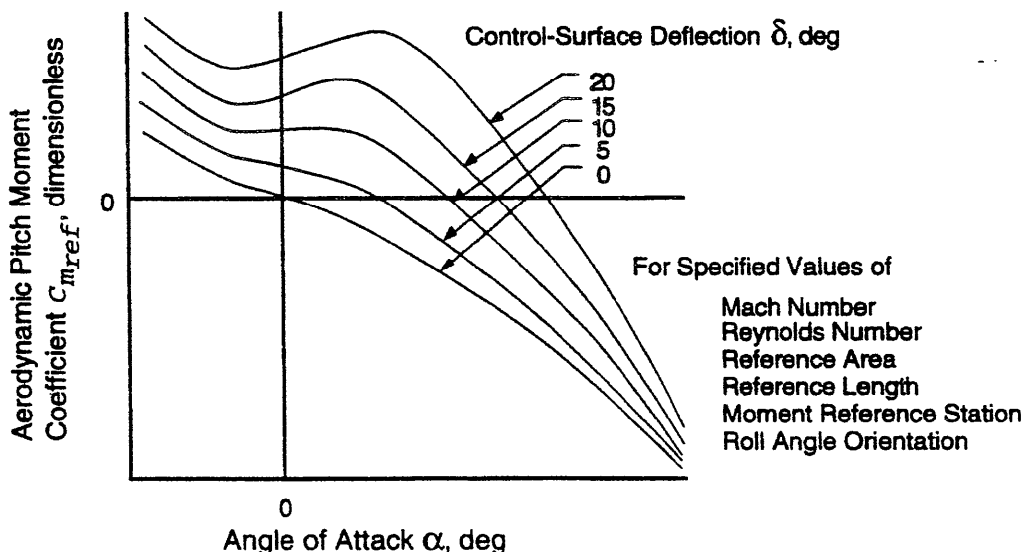


Figure 5-6. Moment Coefficient Versus Angle of Attack (Ref.9)

r = yaw component of angular rate vector w expressed in body coordinate system, rad/s (deg/s)
 V = speed of body, speed of air relative to body, magnitude of velocity vector V , m/s
 x_{cm} = instantaneous distance from missile nose to center of mass, m
 r_{ref} = distance from missile nose to reference moment station, m.

The instantaneous location of the center of mass x_{cm} depends on the shape and burning characteristics of the propellant grain. This parameter usually is given as a function of time for a given missile and can be input to the simulation in tabular form or as an equation that approximates the experimental or analytically estimated data. The damping terms in Eq. 5-12 are not corrected from the reference moment station to the instantaneous center of mass. Although this constitutes an approximation, these terms are usually neither critical enough nor defined accurately enough to justify correction.

At large angles of attack the curve of aerodynamic pitching and yawing moment coefficients as a function of angle of attack may be very nonlinear. This nonlinearity relates to the fact that large angles of attack can cause the missile tail to move out of the downwash field of the forward components of the missile, cause a large increase in the tail efficiency, and cause a large increase in the slopes of the pitching and yawing moment curves (Ref. 8).

The pitching and yawing moment characteristics are essentially the same in missiles with cruciform symmetry, i.e., $C_{m\alpha} = C_{m\alpha}$. The aerodynamic moment coefficients $C_{m\alpha}$ and $C_{m\delta}$ may be input to a missile flight simulation in the form of extensive tables with interpolation among entries for angle of attack Mach number, control-surface deflection angle, and possibly altitude (which affects Reynolds number). The manner in which the aerodynamic moment coefficients are included in a particular simulation depends on the computing equipment and on the level of detail required by the simulation users to simulate angular motion. A less cumbersome, but also less detailed, approach is to input relatively smaller tables of the pitching moment derivatives $C_{m\alpha}$, $C_{m\delta}$, $C_{n\alpha}$, and $C_{n\delta}$ as functions of Mach number. The aerodynamic moment coefficient in the pitch direction is then given by

$$C_{m_{ref}} = C_{m\alpha} \alpha + C_{m\delta} \delta_p, \text{ dimensionless} \quad (5-13)$$

where

$C_{m_{ref}}$ = pitching moment coefficient about reference moment station, dimensionless
 $C_{m\alpha}$ = slope of curve formed by pitch moment coefficient C_m versus angle of attack α , rad⁻¹(deg⁻¹)
 $C_{m\delta}$ = slope of curve formed by pitch moment coefficient

C_m versus control-surface deflection δ_p , rad⁻¹(deg⁻¹)

α = angle of attack in pitch plane, rad (deg)
 δ_p = angle of effective control-surface deflection in the pitch direction, rad (deg).

The assumption that the variations of C_m with respect to α and δ_p are linear can often be justified and thus permit the simplified approach given by Eq. 5-13. For example, the C_m curves are usually relatively linear at angles of attack near the trim angle of attack i.e., on the axis where $C_m = 0$ in Fig. 5-6, and deviations of the missile from the trim condition are likely to be small at least for some missiles (Ref. 9). Eq. 5-13 can be made nonlinear to match wind tunnel data better by the addition of terms in powers of α and δ_p .

Similarly, the aerodynamic moment coefficient in the yaw direction $C_{n_{ref}}$ is given by

$$C_{n_{ref}} = C_{n\beta} \beta + C_{n\delta} \delta_y, \text{ dimensionless} \quad (5-14)$$

where

$C_{n_{ref}}$:= yaw moment coefficient about reference moment station, dimensionless

$C_{n\beta}$:= slope of curve formed by yaw moment coefficient C_n versus angle of sideslip β , rad⁻¹(deg⁻¹)

$C_{n\delta}$ = slope of curve formed by yaw moment coefficient C_n versus effective control-surface deflection δ_y , rad⁻¹(deg⁻¹)

β := angle of sideslip (angle of attack in yaw plane), rad (deg)

δ_y := angle of effective control-surface deflection in the yaw direction, rad (deg).

Many missiles are designed to prevent the aerodynamic roll moment L_r , or at least to reduce it to a minimum. For example, the autopilot of a missile containing a roll-rate gyro can sense missile roll rate and issue control commands to null it. Some missiles have control tabs called rollerons that use gyroscopic moments produced by missile roll to adjust the tab automatically in a direction control the roll. Other missiles are designed to roll continuously. For slender missiles it has been estimated that if the missile roll rate is less than about 20 revolutions per second, the gyroscopic effects are small enough to be neglected (Ref. 10). In this case the terms involving the roll rate p in Eqs. 4-46 can be eliminated. If the roll rate is not considered to be negligible, it is calculated by integrating Eqs. 4-46. These equations involve the roll moment L_r , the aerodynamic contribution of which is calculated from the roll moment coefficient C_l by using Eq. 5-6. The roll moment coefficient is a function of Mach number, control-surface deflection angle, roll rate, and missile speed. One method of calculating the roll moment coefficient is to use two derivatives— $C_{l\delta}$ and C_{lp} . The first derivative accounts for the effective control-surface deflection angle δ_r , and the second accounts for the

damping produced by the roll rate p . The expression for C_l is

$$C_l = C_{l\delta} \delta_r + \frac{d}{2V} (C_{lp} p),$$

dimensionless (5-15)

where

C_l = aerodynamic roll moment coefficient about center of mass, dimensionless

C_{lp} = roll damping derivative (Subpar. 5-2.2.4), rad^{-1} (deg^{-1})

$C_{l\delta}$ = slope of curve formed by roll moment coefficient C_l versus effective control-surface deflection δ_r , rad^{-1} (deg^{-1})

d = aerodynamic reference length of body, m

p = missile roll rate, rate (deg/s)

V = speed of a body, speed of air relative to body, magnitude of velocity vector V , m/s

δ_r = effective control-surface deflection angle corresponding to roll, rad (deg).

5-3 AERODYNAMIC STABILITY DERIVATIVES

In early conceptual design and feasibility studies of a new missile, before extensive aerodynamic data become available, estimated stability derivatives are often used to generate aerodynamic coefficients. After detailed aerodynamic data become available, however, the preferred method may be to use extensive tabular data directly. The power of modern computers makes it practical to enter the aerodynamic coefficients derived from wind tunnel data directly as functions of three or four variables and never go through the process of developing stability derivatives. This decreases the amount of work required to use the wind tunnel data and it makes the process of solving the aerodynamic responses more obvious to the analyst. The discussion of stability derivatives in the subparagraphs that follow is particularly applicable to simulations that employ stability derivatives in lieu of direct tabular data but it is also important to the understanding of missile stability and the interpretation of aerodynamic literature.

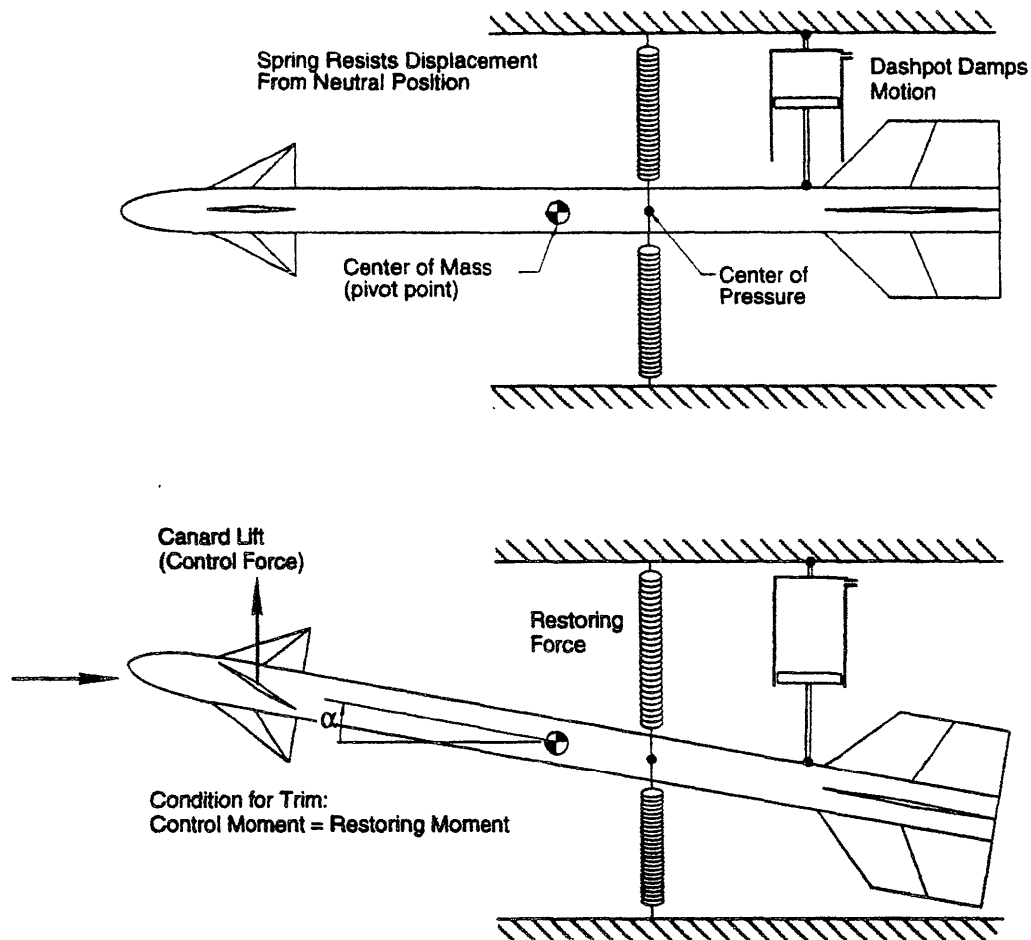
Aerodynamic stability derivatives are classed as static derivatives and dynamic derivatives (Ref. 11). The static derivatives arise from the instantaneous orientation of the airframe with respect to the relative wind and include such derivatives as $C_{L\alpha}$ and $C_{m\alpha}$. The dynamic derivatives arise from the motion (velocities) of the airframe and include such derivatives as $C_{m\dot{\alpha}}$ and $C_{m\dot{\beta}}$. These particular dynamic derivatives partly define the pitch and yaw damping characteristics of a missile, i.e., the tendency of an oscillation in angle of attack to die out with time. Aerodynamic damping is caused by aerodynamic forces that result from the angular rate of the missile and that act on the missile with a lever arm about the center of mass.

Aerodynamic stability is illustrated in Fig. 5-7 by a spring and dashpot analogy (Ref. 3). The net aerodynamic restoring moments are illustrated by the springs placed at the center of pressure, and the dashpot represents the aerodynamic damping due to angular motion. The greater the angle of body rotation about its center of mass, the greater is the restoring moment. Furthermore, if the spring is placed farther aft of the center of mass where it provides a greater static margin, a given angle of attack produces a greater restoring moment. When a control surface is deflected, the force on the control surface produces a moment on the missile, which is resisted by the restoring moment of the spring. The angle of attack that the body will assume for a given control-surface deflection depends on the magnitude of force on the control surface and its distance from the center of mass compared with the restoring moment produced by the body as the angle of attack is increased (spring force multiplied by the static margin in meters). Increasing the static stability decreases the angle of attack that the body will assume due to a given control-surface deflection and therefore decreases the resultant normal force or lateral acceleration (maneuverability) of the missile. Increasing the rotational damping of the missile (larger dashpot) slows the angular rate of response (rate of buildup of angle of attack) to deflection of the control fin and reduces, or prevents, overshoot beyond the trim angle of attack. Too much damping can contribute to increased miss distance against maneuvering targets, whereas too little damping can cause instability.

Depending on the application, there are 30 to 50 stability derivatives used in detailed analytical analyses of stability and control of aerodynamic vehicles. Small changes in the values of some of the stability derivatives can produce pronounced effects on the airframe response to control. Typically, only a few of the more important derivatives are used in missile flight simulations unless the purpose of the simulation is a very detailed analysis of the stability and control characteristics. Only the derivatives most commonly used in missile flight simulations are discussed here.

5-3.1 LIFT CURVE SLOPE

The notation $C_{L\alpha}$ is employed to indicate the derivative $\frac{\partial C_L}{\partial \alpha}$, the slope of the coefficient of lift versus the angle of attack curve with all other parameters held constant. This derivative is commonly known as the "lift curve slope", and it depends on missile configuration and Mach number. When the angle of attack of the airframe is increased, the lift force increases more or less linearly until stall occurs. The derivative $C_{L\alpha}$ is, therefore, always positive in sign at angles of attack below the stall point. A high value of $C_{L\alpha}$ is desirable because a given lift force can be attained at a lower angle of attack than with low $C_{L\alpha}$ and, therefore, with less drag since drag increases with angle of attack.



From "Aerodynamics, Propulsion, Structures and Design Practice" by E.A. Bonney, M. J. Zucrow, and C. W. Besserer, Principles of Guided Missile Design, Edited by G. Merrill, D. Van Nostrand Company, Inc., Princeton, NJ. Reprinted with permission. Copyright © 1956.

Figure 5-7. Spring Analogy for Stability (Ref. 3)

5-32 STATIC PITCH STABILITY DERIVATIVE

The notation C_m is used for the derivative $\partial C_m / \partial \alpha$, the longitudinal static stability derivative. This derivative describes the rate of change of pitching moment coefficient with angle of attack. When the angle of attack of the airframe increases from the equilibrium condition, the increased lift on the tail causes a negative pitching moment about the center of mass of the airframe. Simultaneously, the increased lift on the forward part of the body and any forward fins (canards) causes a positive pitching moment about the center of mass. These contributions are combined to establish the derivative C_m (Ref. 11). A negative value of C_m is necessary for static stability. If C_m relative to the center of mass is positive, the airframe is statically unstable. This derivative is the most important from the standpoint of longitudinal stability and control of the missile. The derivative C_m is a major factor in establishing the dynamic response time of the missile, i.e., the time it takes the missile to achieve a commanded maneuver. This derivative should be small in magnitude for quick response but should not be permitted to become positive.

5-3.3 DYNAMIC STABILITY DERIVATIVES

The notation C_m is given to the derivative

$$\frac{\partial C_m}{\partial \left(\frac{qd}{2V} \right)}$$

This derivative represents the rate of change of the missile pitching moment coefficient with angular velocity in pitch q with angle of attack α held constant. It is known as the pitch damping derivative because it is usually negative and therefore represents resistance to rotation in pitch (Ref. 5). As the vehicle experiences a positive rotation in pitch about its center of mass, the effective angle of attack of the tail fins increases not only because of the change in orientation of the missile longitudinal axis, but also because of the change in direction of the relative wind on the tail caused by the angular rotation. The increment in angle of attack caused by angular rate causes an additional component of lift force to be developed on the tail, and thus increases the negative pitching moment on the vehicle. If aeroelastic effects are

important, an additional contribution to C_{mq} may be produced. At flight speeds for which aeroelastic effects are insignificant, the sign of C_{mq} is always negative, except in missiles designed to be aerodynamically unstable, with stability provided by the autopilot. If the flight speed is sufficiently high for aeroelastic effects to be significant, the sign of C_{mq} can be positive or negative depending on the nature of the aeroelastic effects (Ref. 11). The derivative C_{mq} is very important in pitch dynamics because it contributes a major portion of the damping of the airframe response to commands. The derivative C_{mq} is dimensionless (per radian) when q has dimensions of rad/s.

The notation C_{mq} represents the derivative

$$\frac{\partial C_m}{\partial \left(\frac{\dot{\alpha} d}{2V} \right)},$$

the rate of change of pitching moment coefficient with rate of change of angle of attack. This derivative arises from a "plunging" type of motion along the z-axis in which the angle of pitch θ remains constant. The derivatives owe their existence primarily to the fact that the pressure distribution on a wing or tail does not adjust itself instantaneously to its equilibrium value when the angle of attack is suddenly changed. The calculation or measurement of this effect involves unsteady flow. For low-speed flight C_{mq} is determined mostly by this aerodynamic lag effect and its sign is negative. In high-speed flight however, C_{mq} depends also on aeroelastic effects, and its sign can be either positive or negative (Ref. 11). A negative value of this derivative contributes to the damping of the airframe response to commands. Normally, C_{mq} is significantly smaller than $C_{m\dot{\alpha}}$, and the corresponding components of $\dot{\alpha}$ and q are comparable in size. In addition, the sum of C_{mq} and $C_{m\dot{\alpha}}$ is more easily extracted from test data than the individual values (Ref. 12). Therefore, it is customary to combine these damping terms as $(C_{mq} + C_{m\dot{\alpha}})$ multiplied by q (Ref. 9). The derivative C_{mq} is dimensionless (per rad) when q has dimensions of rad/s.

5-3.4 ROLL STABILITY DERIVATIVES

The notation $C_{l\delta}$ is used for the derivative $\frac{\partial C_l}{\partial \delta}$. It is the change in roll moment coefficient with respect to variations of control-surface deflection. When the direction of the effective control-surface deflection causes a positive roll moment, $C_{l\delta}$ is positive.

The notation C_{lp} is used for

$$\frac{\partial C_l}{\partial \left(\frac{pd}{2V} \right)}$$

which represents the change in roll moment coefficient with respect to changes in roll rate (Ref. 4), and it is known as the roll damping derivative. When the airframe rolls at an angular rate p , a roll moment opposing the rotation is produced by the angular rate of the wings and fins. As wings and fins rotate about the longitudinal axis of the missile, individual components of angles of attack of these surfaces are produced. The resulting lifts on the surfaces are in directions that oppose the rotation. The term $pd/2V$ is the nondimensional rolling parameter.

5-4 DETERMINATION OF AERODYNAMIC COEFFICIENTS

In a missile design the choice of autopilot gains depends heavily on the estimated aerodynamic characteristics, if realized in flight, uncertainties in these characteristics can cause autopilot instability and excessive miss distance. One means for dealing with aerodynamic uncertainty is to keep autopilot gains low; however, if autopilot gains are kept sufficiently low to avoid regions of instability caused by aerodynamic uncertainty, the associated reduction in missile response will also result in a large miss distance. Therefore, accurate determination of aerodynamic coefficients and derivatives is essential to meet design requirements employing high autopilot gains (Ref. 13).

The aerodynamic coefficients used in missile flight simulations are obtained from a number of sources and largely depend on the maturity of the particular missile development program. In early phases, before wind tunnel or flight test data are available, aerodynamic coefficients are determined by analytical predictions and by estimates based on previous experience with similar body shapes and flow conditions. As the missile development program progresses, wind tunnel tests are made, and aerodynamic coefficient predictions are upgraded accordingly. Finally, when flight-test data become available, aerodynamic coefficients are fine-tuned based on flight-test results. These estimates and measurements of aerodynamic data are typically made by the contractors that develop missiles and are normally made available to appropriate Government laboratories.

Aerodynamic data appear in the literature with many assumptions that are not always clearly stated; therefore, special attention must be paid in the use of these data in missile simulations to ensure their applicability. Examples of some of the "traps" to be avoided are

1. Reference area and reference length not defined
2. Data applicable to restricted regions of Mach number
3. Data applicable to restricted regions of Reynolds number
4. Data applicable to only small angles of attack
5. Data applicable to only one type of aerodynamic force
6. Data applicable to only two-dimensional flow.

5-4.1 ANALYTICAL PREDICTION

The aerodynamic performance of a missile is the result of the interactions among an extremely complex set of factors. There are literally dozens of factors that must be considered in the analytical prediction of aerodynamic coefficients. Some are more important than others, and some apply only to certain types of flow characteristics. These factors mostly concern the shape of the body, the relative motion of the air with respect to the body, and the characteristics of the flow. Discussions of these factors can be found in Refs. 1, 4, 6, and 14.

Analytical methods of determining aerodynamic coefficients usually are categorized according to the various air-flow regimes based on Mach number in combination with specified ranges of Reynolds number. Typically, a method that gives good predictions for one flow regime is not applicable to the other regimes.

Analytical techniques involving combinations of theory and test data are relatively well developed in the subsonic and supersonic regimes. Transonic aerodynamic characteristics, however, are particularly difficult to predict analytically. Although transonic theory gives good results in a few extremely simple configurations, mathematical difficulties have limited its application (Ref. 14).

In hypersonic flow shock waves lie close to the body and cause a strong interaction between the boundary layer and the shock wave, which exerts an important influence on the flow field. The boundary layer in hypersonic flow maybe 10 to 100 times thicker than at lower speeds; consequently, a drastic change in the effective body shape results: The air-flow sees the shape of the body as including the boundary layer. This change in effective shape in turn brings about a change in the shape of the nose shock wave. High-temperature gas effects become evident at hypersonic speeds, and the flow becomes essentially nonlinear. Analytical methods of predicting aerodynamic coefficients in hypersonic flow are given in Ref. 14.

Analytical aerodynamic performance prediction is still very much an art. Methodologies for the analytical prediction of aerodynamic characteristics from subsonic through hypersonic forms of flow developed as the need arose. Analytical methods usually are composed of a combination of theory based on approximations and experimental data. A method may apply to only a relatively small number of the flow regimes that might be experienced by a missile. Great care must be taken not to extrapolate techniques to conditions that do not meet the flow regimes for which they were developed. The accuracy of the predicted results based on these methods depends largely on the skill and experience of the aerodynamicist.

One of the largest compilations of theoretical and empirical methods for predicting aerodynamic characteristics of bodies is Datcom—shorthand notation for data compendium (Ref. 14)—an effort sponsored by the Air Force Flight Dynamics Laboratory "to provide timely stability and flight

control data and methods for design of manned aircraft, missiles, and space vehicles". Datcom contains a systematic survey of analytical methods used to estimate basic aerodynamic coefficients and aerodynamic stability and control derivatives. It is intended to be used for preliminary design purposes before test data have been acquired. In preparing Ref. 14, the authors attempted to survey all existing generalized methods, and whenever possible they determined the limits of applicability for each method, and the user is cautioned not to extrapolate beyond the stated limits. Datcom has been expanded and coded as a computer program, called Missile Datcom, specifically applicable to missiles (Ref. 15). These practical methods are in general use in applications that require analytical estimates of aerodynamic coefficients.

Theoretical equations for simulating the flow of fluids relative to bodies of arbitrary shape are available, but their complexity has limited their use, except for certain special applications. The general equations that form the starting point for theoretical aerodynamics are called the Navier-Stokes equations (Ref. 16). They are based on Newton's equations applied to an idealized gas combined with equations that specify the conservation of mass and energy, and they include the effects of viscosity and density. In principle, this system of equations is sufficient to define a given flow completely. In practice, the solution of the full Navier-Stokes equations requires computational speed and memory that are only now becoming feasible with the largest and fastest modern computers (Ref. 17). Some of the important simplifications and approximations that are used singly or together to obtain practical solutions for various applications are steady flow, nonviscous flow, incompressible flow, and small-disturbance flow. In the latter approximation the flow is represented by small disturbances from uniform flow. The equations are rewritten in such a way that products and higher powers of the small-disturbance velocities are ignored. This, of course, linearizes the equations for a compressible flow and is therefore called the linear theory. There are numerous other special approximations for special problems. For flow around specific bodies, it is possible to obtain certain important and fundamental results by manipulation and partial solution of the basic equations without actually solving the equations completely (Ref. 16).

The field of computational fluid dynamics has developed sufficiently in recent years to initiate some changes in the traditional methods of estimating aerodynamic characteristics (Ref. 17), and computational aerodynamics is having a profound effect on methods of airborne vehicle design. Both computer power and numerical algorithm efficiency are improving simultaneously with time. Numerical flow simulations have none of the limitations of wind tunnel testing; they have their own—computer speed and memory. These computational limitations, however, are rapidly being overcome by extremely high-speed computers, and in recent years the general complexity of the Navier-Stokes equa-

tions-on which numerical flow simulations are based-has begun to yield under computational attack with the largest current computers.

In the meantime, approximate and empirical analytical techniques provide "ballpark" estimates that are used in preliminary missile design. However, since the accuracy of the estimates is uncertain, aerodynamic estimates are always improved early in the development phase of a missile by wind tunnel tests.

5-4.2 WIND TUNNEL TESTING

Full-scale flight tests are the final proof of the aerodynamic characteristics of a missile design, but substantial experimental verification of missile performance is needed before the expense and risks of flight testing are incurred. Consequently, testing small models of a missile in a wind tunnel to obtain experimental data on aerodynamic forces has become an essential part of missile development because (1) it is a way of obtaining the required information for less expenditure of time and money than in full-scale testing and (2) test conditions can be more easily controlled and measured in a wind tunnel than on a flight-test range.

Basically, a wind tunnel is a channel through which air is blown or drawn. A precise scale model of the missile is mounted on a strut in a test section of the flow channel. Aerodynamic loads on the model are transmitted to the strut and are measured by balances, such as scales or strain gages. The loads measured for any model configuration change if the model size, the model attitude relative to the flow, the speed of the air, or the air density change.

The equations for forces and moments, developed in subpar. 5-2.1, are used to interpret the measured loads on the model in terms of full-scale missile flight in air of different densities and at different speeds. To obtain meaningful values for the lift coefficient for example, the lift force on the model, measured in the wind tunnel, is divided by the product of the dynamic pressure parameter and the reference area of the model to yield the lift coefficient

$$C_L = \frac{L}{0.5\rho V^2 S}, \text{ dimensionless} \quad (5-16)$$

where

- C_L = aerodynamic lift coefficient, dimensionless
- L = magnitude of aerodynamic lift force vector L , N
- S = aerodynamic reference area, m^2
- V = speed of a body, speed of air relative to a body, magnitude of velocity vector V , m/s
- ρ = atmospheric density, kg/m^3 .

This lift coefficient, derived from testing a model, is then substituted into Eq. 5-5-along with the density, velocity, and reference area of the full-scale missile in flight-to

obtain the lift force on the full-scale missile. This lift force applies only to the missile attitude, i.e., angle of attack, at which the model is tested. To find lift forces applicable to different angles of attack, wind tunnel tests are conducted at various angles of attack.

Similarly, the drag coefficient C_D and moment coefficients C_l , C_m , and C_n are determined by measuring the drag force D and the components L_A , M_A , and N_A of the aerodynamic moment vector MA and substituting them, respectively, into

$$\left. \begin{aligned} C_D &= \frac{2D}{\rho V^2 S}, \text{ dimensionless} \\ C_l &= \frac{2L_A}{\rho V^2 S d}, \text{ dimensionless} \\ C_m &= \frac{2M_A}{\rho V^2 S d}, \text{ dimensionless} \\ C_n &= \frac{2N_A}{\rho V^2 S d}, \text{ dimensionless.} \end{aligned} \right\} (5-17)$$

The force or moment coefficients, found at any model attitude in the wind tunnel, apply to the full-scale missile in flight at the same attitude provided the model is geometrically similar to the full-scale missile and that certain flow similarity parameters are matched between the wind tunnel flow and the flow over the actual missile. The two similarity parameters are Reynolds number and Mach number.

A major goal in wind tunnel design is to obtain values of the test Reynolds number, based on the model reference length d as close as possible to the Reynolds number for actual, full-scale missile flight. Since the small size of the model tends to reduce the Reynolds number, the wind tunnel flow is at least partially compensated by pressurizing to increase the density ρ . Because Mach number is even more important in transonic and supersonic flight, the wind tunnel is designed to match the Mach number and then do its best with respect to Reynolds number.

High-speed wind tunnels require very high powers and specialized test section designs. Such tunnels can be subsonic, transonic, supersonic, or hypersonic. Some tunnels are pressurized several times normal sea level atmospheric pressure to increase the density in order to compensate for the small scale of the models (Ref. 1). To avoid the power requirements of continuously running pressurized high-speed tunnels, some tunnels operate for only a short period-of the order of 15 to 30 s-by exhausting the air from a high-pressure tank through an open circuit tunnel. Data can be obtained over a wide range of angles of attack in a single brief run in these intermittent flow or blowdown tunnels with the aid of equipment that automatically

changes the pitch attitude, which changes the angle of attack. The tank is then pumped up for the next run.

Special techniques have been used to measure the stability derivatives associated with missile angular velocities. For example, one method used to measure pitch damping derivatives is to mount the model in a conventional wind tunnel so that the model is allowed to oscillate in pitch. The model is displaced in pitch and oscillates freely; the damping derivative is obtained from the decay of the amplitude of the oscillation. This oscillation technique gives the total damping ($C_{m\dot{\alpha}} + C_{m\dot{\alpha}}$)

Individual values of damping derivatives $C_{m\dot{\alpha}}$ and $C_{m\dot{\alpha}}$ cannot be determined from oscillation tests alone. Therefore, a less conventional wind tunnel design has been used to measure the damping derivative $C_{m\dot{\alpha}}$. In this technique the model is held steady and the airflow follows a curved path in the vicinity of the model (Ref. 11).

Wind tunnel data are not always as accurate as might be desired, and the results must be interpreted by experienced analysts. Some of the major sources of error in conventional wind tunnel testing are:

1. Scale effects due to the low Reynolds number of the test
2. Choking phenomena at high subsonic Mach numbers
3. Inaccurate corrections to the data, such as tare and alignment corrections and wall corrections
4. Mechanical and instrumentation discrepancies involved in the measurement of forces and moments.

It is essential to understand the sources, importance, and correction of errors in interpreting the results of wind tunnel tests. In spite of these qualifications, wind tunnel testing is a powerful and indispensable tool (Ref. 11).

5-4.3 FLIGHT TESTING

Flight tests examine the entire missile system in a fully operational context (Ref. 18). A typical missile flight-test program proceeds through a number of phases from development to final verification of the principle of operation of the guidance system. The major objectives of flight testing are to verify the aerodynamic performance of the missile and to improve the estimates of aerodynamic coefficients (Ref. 5). Postflight analyses focus on the comparison of predicted versus measured flight values, with refinement of the simulation models as a goal (Ref. 19).

Flight tests are preplanned to include extreme maneuvers at low and high altitudes to test the control system, aerodynamics, and structural design of the missile to the limits of prescribed system performance. If the simulation output matches the flight-test output for a given set of flight conditions, the conditions are said to be in the "neighborhood of validity" of the simulation. When a region of flight-test conditions is reached in which flight-test data do not exist or in which they differ significantly from the simulation output, these conditions are said to be outside the neighborhood of

validity of the simulation model. Further flight testing is then required in this region if it is feasible (Ref. 18),

Aerodynamic forces usually cannot be measured directly in a flight-test missile but are inferred from measurements of translational and rotational accelerations. Ref. 13 describes a method used to extract aerodynamic coefficients from flight-test data. The method is based on a computer program called Aerodynamic Analysis of Flight-Test Data (AAFTD). The program uses all pertinent telemetry and radar measurements to solve the appropriate equations that yield aerodynamic characteristics. In addition, a six-degree-of-freedom simulation is used to reconstruct each flight-test trajectory, evaluate candidate changes in the coefficients computed by AAFTD, and adjust these changes to match overall flight characteristics better. Results from these programs are employed to update the aerodynamic model for the missile. The measured flight parameters selected for use in estimating aerodynamic characteristics are listed in Table 5-1. All of these parameters are functions of missile aerodynamic characteristics.

TABLE 5-1. SELECTED FLIGHT-TEST PARAMETERS FOR ESTIMATING AERODYNAMIC CHARACTERISTICS

Range, altitude, cross-range	Pitch, yaw, axial accelerations
Velocity components	Actual and command fin positions
Body pitch, yaw, roll rates	Seeker roll rate
Seeker pitch and yaw attitudes	Pitch, yaw, roll integrated position
Seeker roll position	Autopilot roll command

The sequence of computations is

1. Simulate the trajectory using the six-degree-of-freedom program and all known postflight data.
2. Identify the differences between simulated and measured parameters.
3. Calculate the partial derivatives of each measured parameter with respect to each aerodynamic parameter in the model.
4. Compute the changes in aerodynamic parameters required to minimize observed differences by using a least squares technique.
5. Evaluate the significance of each solution, and relate it to stored data points in the aerodynamic model. (In some instances, the indicated changes may be unreasonable because observed differences are caused by sources other than aerodynamics.)

5-5 ATMOSPHERIC PROPERTIES

Aerodynamic forces depend on certain properties of the atmosphere among other factors. As shown in Eq. 5-1, the basic atmospheric property needed to calculate aerody -

dynamic force in incompressible flow is the density ρ . To calculate aerodynamic forces under conditions of compressible flow, the speed of sound V_s in ambient air is also required. Atmospheric pressure is required for rocket thrust calculations and for calculating the dynamic pressure parameter calculations using Eq. 3-5. The atmospheric dynamic viscosity γ is needed to calculate Reynolds number if Reynolds number is a parameter in the simulation. Pressure, density, speed of sound, and viscosity are functions of altitude. More precisely, density varies with atmospheric pressure and temperature according to the equation of state for air the speed of sound and viscosity vary with temperature only. Atmospheric data are usually supplied to a missile flight simulation in the form of tabulated data as functions of altitude. The simulation has provisions for table lookup of atmospheric data corresponding to the altitude of the simulated missile at each computational step.

Sometimes kinematic viscosity γ/ρ is provided as a convenience in calculating Reynolds number, which then becomes

$$\text{Reynolds number} = \frac{Vd}{\nu}, \text{ dimensionless (5-18)}$$

where

- d = aerodynamic reference length, m
- V = speed of body, speed of air relative to body, magnitude of velocity vector V, m/s
- ν = atmospheric kinematic viscosity, m^2/s .

Since meteorological conditions constantly vary, there is no "normal" atmosphere. However, a representative set of conditions, called a standard atmosphere, has been defined for use in analyses (Ref. 1). The values of the parameters in the standard atmosphere are adjusted over time as better measurements and understanding of the atmosphere are obtained. In addition to the standard atmosphere certain variations in atmospheric conditions have been adopted to define a standard hot day, a standard cold day, and so forth. To simulate missile flight to match actual flight-test data it is common practice to use actual meteorological measurements taken at the test range within hours or minutes of the flight.

Some simulations contain curve-fit equations that approximate the tabular standard atmospheric data without the need for a table lookup procedure. Equations are also available for adjusting the atmospheric data for nonstandard conditions. For example, if the pressure and temperature at only the launch altitude are measured at the time of an actual flight test, the standard atmospheric properties can be adjusted by these equations at all altitudes to be more or less consistent with the conditions measured at the surface of the earth.

Several definitions of altitude are used in connection with atmospheric properties. The most obvious is the geometric altitude, which is the physical altitude in meters above sea level. The second definition is derived from the fact that the

atmosphere at the time of any given flight test almost certainly will not conform exactly to a standard atmosphere. For example, the air density experienced in a flight test at a given geometric altitude will correspond to a slightly different altitude in the standard atmosphere table. The standard altitude corresponding to the ambient density actually experienced is called the density altitude. Since the aerodynamic forces acting on a body are direct functions of air density, the behavior of the body is strongly influenced by the density altitude. However, viscous effects and Mach number effects, which depend on temperature, may not exactly match the standard values at the density altitude. A third altitude is the pressure altitude, the altitude on a standard day for which the pressure is equal to the actual ambient pressure. Barometric altimeters operate by sensing pressure and therefore are calibrated to read pressure altitude. Pressure altitude, density altitude, and temperature are related through the thermodynamic equation of state for air.

Details of atmospheric modeling and a table of atmospheric pressure, density, speed of sound, and viscosity as functions of geometric altitude are given in Appendix B.

5-6 MISSILE AERODYNAMIC FORCE AND MOMENT EQUATIONS

The equations for calculating aerodynamic forces and moments, required as inputs to the equations of motion in Chapter 4, are summarized here. The equations for the aerodynamic coefficients are based on the assumptions that lift is linear with angle of attack the lift versus drag relationship conforms to a parabolic polar, and moment coefficients are linear with respect to the various parameters that affect them. If more realistic, nonlinear aerodynamic data are available and necessary to the objectives of the simulation they should be input to the simulation in tabular form. Table lookup then replaces the equations for aerodynamic coefficients. As an alternative, the equations presented here can be modified by adding nonlinear terms, e.g., powers of α and δ , as curve fits to the nonlinear data.

5-6.1 FORCES AND MOMENTS

Equations for calculating aerodynamic forces and moments follow:

$$D = 0.5\rho V^2 C_D S, \text{ N} \quad (5-4)$$

$$L = 0.5\rho V^2 C_L S, \text{ N} \quad (5-5)$$

$$L_A = 0.5\rho V^2 C_{l_s} S d, \text{ N}\cdot\text{m} \quad (5-6)$$

$$M_A = 0.5\rho V^2 C_{m_s} S d, \text{ N}\cdot\text{m} \quad (5-7)$$

$$N_A = 0.5\rho V^2 C_{n_s} S d, \text{ N}\cdot\text{m} \quad (5-8)$$

where

- C_D = aerodynamic drag coefficient, dimensionless
 C_L = aerodynamic lift coefficient, dimensionless
 C_l = aerodynamic roll moment coefficient about center of mass, dimensionless
 C_m = aerodynamic pitch moment coefficient about center of mass, dimensionless
 C_n = aerodynamic yaw moment coefficient about center of mass, dimensionless
 D = magnitude of aerodynamic drag force vector D , N
 d = aerodynamic reference length of body, m
 L = magnitude of aerodynamic lift force vector L , N
 L_A, M_A, N_A = components of aerodynamic moment vector M_A , expressed in body coordinate system (roll, pitch, and yaw, respectively), Nzm
 S = aerodynamic reference area, m²
 V = speed of body, speed of air relative to body, magnitude of velocity vector V , m/s
 ρ = atmospheric density, kg/m³.

5-6.2 COEFFICIENTS

Equations for calculating aerodynamic coefficients by employing stability derivatives and a parabolic drag polar follow

$$C_D = C_{D0} + kC_L^2, \text{ dimensionless (Eq. 5-10)} \\ \text{with } x = 2$$

$$C_L = C_{L\alpha}\alpha, \text{ dimensionless (5-11)}$$

$$C_l = C_{l\delta} \delta_r + \frac{d}{2V} (C_{l_p} p), \text{ dimensionless (5-15)}$$

$$C_{m_{ref}} = C_{m\alpha}\alpha + C_{m\delta}\delta_p, \text{ dimensionless (5-13)}$$

$$C_{n_{ref}} = C_{n\beta}\beta = C_{n\delta}\delta_y, \text{ dimensionless (5-14)}$$

where

- C_D = aerodynamic drag coefficient dimensionless
 C_{D0} = zero-lift drag coefficient dimensionless
 C_L = aerodynamic lift coefficient dimensionless
 $C_{L\alpha}$ = slope of curve formed by lift coefficient C_L versus angle of attack α , rad⁻¹ (deg⁻¹)
 C_l = aerodynamic roll moment coefficient about center of mass, dimensionless
 C_{l_p} = roll damping derivative, rad⁻¹ (deg⁻¹)
 $C_{l\delta}$ = slope of curve formed by roll moment coefficient C_l versus control-surface deflection δ_r , rad⁻¹ (deg⁻¹)

- $C_{m_{ref}}$ = pitching moment coefficient about reference moment station, dimensionless
 $C_{m\alpha}$ = slope of curve formed by pitch moment coefficient C_m versus angle of attack α , rad⁻¹ (deg⁻¹)
 $C_{m\delta}$ = slope of curve formed by pitch moment coefficient C_m versus control-surface deflection δ_p , rad⁻¹ (deg⁻¹)
 $C_{n_{ref}}$ = yawing moment coefficient about reference moment station, dimensionless
 $C_{n\beta}$ = slope of curve formed by yawing moment coefficient C_n versus angle of sideslip β , rad⁻¹ (deg⁻¹)
 $C_{n\delta}$ = slope of curve formed by yawing moment coefficient C_n versus control-surface deflection δ_y , rad⁻¹ (deg⁻¹)
 d = aerodynamic reference length of body, m
 k = constant depending on body shape and flow regime, dimensionless
 p = missile roll rate, rad/s (deg/s)
 V = speed of a body, speed of air relative to a body, magnitude of velocity vector V , m/s
 α = angle of attack in pitch plane, rad (deg⁻¹)
 β = angle of sideslip (angle of attack in yaw plane), rad (deg)
 δ_p = angle of effective control-surface deflection in the pitch direction, rad (deg)
 δ_r = effective control-surface deflection angle corresponding to roll, rad (deg)
 δ_y = angle of effective control-surface deflection in the yaw direction, rad (deg).

If the aerodynamic moment reference station is different from the instantaneous station of the center of mass, the pitch and yaw moment coefficients are corrected by using

$$C_m = C_{m_{ref}} - C_{N_z} \frac{x_{cm} - x_{ref}}{d} + \frac{d}{2V} (C_{m_q} + C_{m_{\dot{\alpha}}}) q, \\ \text{dimensionless}$$

$$C_n = C_{n_{ref}} + C_{N_y} \frac{x_{cm} - x_{ref}}{d} + \frac{d}{2V} (C_{n_r} + C_{n_{\dot{\beta}}}) r, \\ \text{dimensionless}$$

(5-12)

where

- aerodynamic pitch moment coefficient about center of mass, dimensionless
 pitch damping derivative relative to pitch rate q , rad⁻¹ (deg⁻¹)
 pitching moment coefficient about reference moment station, dimensionless
 pitch damping derivative relative to angle of attack rate $\dot{\alpha}$ (slope of curve formed by C_m versus α), rad⁻¹ (deg⁻¹)

C_{N_y} = coefficient corresponding to component of normal force on yb-axis, dimensionless	coefficient C_a versus control-surface deflection δ_p , $\text{rad}^{-1} (\text{deg}^{-1})$
C_{N_z} = coefficient corresponding to component of normal force on zb-axis, dimensionless	C_{n_r} = yaw damping derivative relative to yaw rate r , $\text{rad}^{-1} (\text{deg}^{-1})$
C_n = aerodynamic yaw moment coefficient about center of mass, dimensionless	$C_{n_{\dot{\beta}}}$ = yaw damping derivative relative to angle-of-sideslip rate $\dot{\beta}$, $\text{rad}^{-1} (\text{deg}^{-1})$
C_{n_r} = yaw damping derivative relative to yaw rate r , $\text{rad}^{-1} (\text{deg}^{-1})$	$C_{n_{\delta}}$ = slope of curve formed by yaw moment coefficient C_n versus control-surface deflection δ_y , $\text{rad}^{-1} (\text{deg}^{-1})$.
$C_{n_{ref}}$ = yawing moment coefficient about reference moment station, dimensionless	
$C_{n_{\dot{\beta}}}$ = yaw damping derivative relative to angle-of-sideslip rate $\dot{\beta}$, $\text{rad}^{-1} (\text{deg}^{-1})$	
d = aerodynamic reference length of body, m	
q = pitch component of angular rate vector w expressed in body coordinate system, $\text{rad/s} (\text{deg/s})$	
r = yaw component of rate vector w expressed in body coordinate system $\text{rad/s} (\text{deg/s})$	
V = speed of body, speed of air relative to a body, magnitude of velocity vector V , m/s	
x_{cm} = instantaneous distance from missile nose to center of mass, m	
x_{ref} = distance from missile nose to reference moment station, m.	

5-6.3 SIMPLIFICATIONS

In three-degree-of-freedom simulations the moment equations-Eqs. 5-6, 5-7, 5-8, 5-12, 5-13, 5-14, and 5-15 are not required. In five-degree-of-freedom simulations the equations for the aerodynamic pitch and yaw moments are included but not the equations for roll moments. Six-degree-of-freedom simulations use the equations for all three aerodynamic moment components, L_a , M_a , and N_a .

If the missile has cruciform symmetry, the yawing moment derivatives are equal in magnitude to the pitching moment derivatives:

$$\left. \begin{aligned} C_{n_{\dot{\beta}}} &= C_{m_{\dot{\alpha}}}, \text{rad}^{-1} (\text{deg}^{-1}) \\ C_{n_{\delta}} &= C_{m_{\delta}}, \text{rad}^{-1} (\text{deg}^{-1}) \\ C_{n_r} &= C_{m_q}, \text{rad}^{-1} (\text{deg}^{-1}) \\ C_{n_{\dot{\beta}}} &= C_{m_{\dot{\alpha}}}, \text{rad}^{-1} (\text{deg}^{-1}) \end{aligned} \right\} (5-19)$$

where

- C_{m_q} = pitch damping derivative relative to pitch rate q , $\text{rad}^{-1} (\text{deg}^{-1})$
- $C_{m_{\alpha}}$ = slope of curve formed by pitch moment coefficient C_m versus angle of attack α , $\text{rad}^{-1} (\text{deg}^{-1})$
- $C_{m_{\dot{\alpha}}}$ = pitch damping derivative relative to angle of attack rate $\dot{\alpha}$ (slope of curve formed by C_m versus $\dot{\alpha}$), $\text{rad}^{-1} (\text{deg}^{-1})$
- $C_{m_{\delta}}$ = slope of curve formed by pitch moment coefficient

Cruciform symmetry also makes it possible to simplify calculations of forces and moments by employing a body reference frame that is defined as the one in Fig. 3-1(B), except it is rolled about the x_b -axis so that the y_b -axis coincides with the y_w -axis of the wind coordinate system. In this body system the total angle of attack is expressed by α since the angle of sideslip β is equal to zero. Therefore, the lift and drag lie in the $x_b z_b$ -plane, and moments caused by the angle of attack are about the y_b -axis. If a yawing moment exists, it is produced only by deflection of control surfaces. Lift and drag are easily transformed to normal force and axial force in this body frame by applying Eqs. 4-13 and 4-14. Whether or not this particular body system is a significant simplification depends largely on the formulation of the control channels. For example, if pitch and yaw control channels are defined relative to the regular, nonrolling body coordinate system, vectors may have to be transformed between the regular body coordinate system and the one rolled with the wind system; this adds complication.

5-7 ROLLING AIRFRAME CONSIDERATIONS

In general, anything that affects the symmetry of a missile during lateral maneuvers at large angles of attack is apt to produce rolling moments. Under a condition of unequal maneuvers in the pitch and yaw planes, the pattern of lift at the tips and roots of fins becomes asymmetrical and thereby produces rolling moments. Likewise, the lift on opposite fins—one of which is in the lee of the body—is asymmetrical and produces rolling moments. Fin sweepback and flow separation effects on opposite fin panels can cause asymmetrical lift on the fins and thus create a rolling moment (Ref. 3). For the most part these rolling moments are unintentional and undesirable because they can cause maneuvers to be executed in the wrong roll plane as a result of lags in the guidance and control systems. In some missiles the guidance and control concepts are based on a rolling airframe, and roll is intentionally induced by canting the fins. In missiles that are not designed to roll, the aerodynamic configuration is designed to minimize roll moments to the extent possible, and some missiles use special devices to sense and control roll rates to keep them to a minimum.

When a missile airframe rolls slowly about its longitudinal axis, the roll can often be neglected in a flight simulation. When the roll is fast enough to be significant, the

simulation can often be simplified by a body reference frame that does not roll; the roll dynamics are included in the equations of motion as if the entire mass of the missile were an internal rotor.

Since the lift coefficient varies with the roll orientation of the fins relative to the plane of the missile maneuver, the lift coefficient is often averaged over all roll angles. Also, since control-surface deflection angles are changed as a function of roll angle, average deflections rather than peak deflections are needed for calculations that are based on effective fin deflections.

5-7.1 ROLLING REFERENCE FRAMES

The equations of motion-Eqs. 4-37 and 4-46-are expressed in a body reference frame that is fixed to the missile and rolls with it at the instantaneous roll rate p . It is often convenient however, to use a nonrolling body reference frame, even if the missile is spinning, and this is made possible by the cruciform symmetry of typical surface-to-air missiles (Ref. 12). Because of this symmetry, the specific roll attitude of the missile is not important to the dynamic and aerodynamic behaviors of the missile. The body reference frame can then be treated as nonrolling, and the gyroscopic effects of the missile roll rate are taken into account by treating the entire mass of the missile as being contained in an internal, spinning rotor. The nonrolling body reference frame has its x-axis in common with that of the rolling body reference frame, but it differs from the rolling frame in that its y-axis is always horizontal and its xz-plane is always vertical. The use of the nonrolling body frame is permissible provided that (1) the moment of inertia parameters in the nonrolling frame are constant with respect to missile roll angle, (2) the aerodynamic derivatives are constant with respect to roll angle and equal to their counterparts in the axes that are fixed to the missile, and (3) the roll rate of the missile is assumed to be constant. These requirements are approximately met in a missile with cruciform symmetry and for which the roll rate changes slowly relative to the simulation integration time step.

The technique, then, for treating a rolling, cruciform missile by means of a nonrolling reference frame is to

1. Assume all the mass of the missile is contained in an internal rotor. Then in Eq. 4-50 I'_x, I'_y, I'_z -the moments of inertia of the assumed internal rotor-are equal to the actual moments of inertia of the missile (including rotor) I_x, I_y, I_z , respectively.

2. Let the angular rate vector of the assumed rotor Ω equal the angular rate vector w of the actual simulated missile, and let p_0 = the constant or nearly constant roll rate of the missile. Then the roll rate of the rotor $p' = p_0$, and the pitch and yaw rates of the rotor are equal to the respective rates of the missile body, i.e., $q' = q$ and $r' = r$. Since the body reference frame is assumed to be nonrolling, $p = 0$.

Substituting in Eqs. 4-50 and letting $I_x = I_y = J$ (because of cruciform symmetry) gives

$$\left. \begin{aligned} \dot{p} &= 0, \text{ rad/s}^2 \text{ (deg/s}^2\text{)} \\ \dot{q} &= (M - p_0 r I_x) / J, \text{ rad/s}^2 \text{ (deg/s}^2\text{)} \\ \dot{r} &= (N + p_0 q I_x) / J, \text{ rad/s}^2 \text{ (deg/s}^2\text{)} \end{aligned} \right\} \text{ (5-20)}$$

where

I_x = moment of inertia of missile about the x_b -axis
kg-m²

$J = I_x = I_y$ for symmetrical missile, kg-m²

M = pitch component of total moment vector M ,
expressed in body coordinate system, N-m

N = yaw component of total moment vector M
expressed in body coordinate system, N-m

$\dot{p}, \dot{q}, \dot{r}$ = the components of the angular acceleration of
the missile measured with respect to the $x_b, y_b,$
and z_b -axes, respectively, rad/s² (deg/s²)

p_0 = constant or nearly constant roll rate of missile,
rad/s (deg/s)

q = pitch component of angular rate vector w
expressed in body coordinate system, rad/s
(deg/s)

r = yaw component of angular rate vector w
expressed in body coordinate system rad/s
(deg/s).

5-7.2 NEGLECTING LOW ROLL RATES

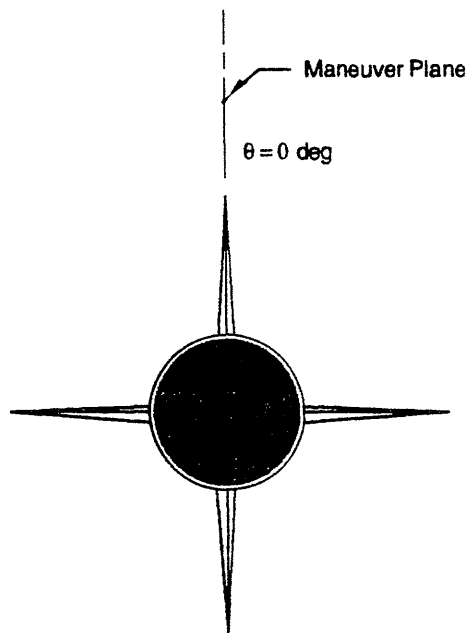
When the actual missile roll rate is known to be small enough to have a negligible effect on the missile guidance and dynamics, Eqs. 4-45 can be simplified considerably by setting $p = p_0$ and letting $I_y = I_z = J$. Then Eqs. 4-45 become

$$\left. \begin{aligned} \dot{p} &= 0, \text{ rad/s}^2 \text{ (deg/s}^2\text{)} \\ \dot{q} &= M/J, \text{ rad/s}^2 \text{ (deg/s}^2\text{)} \\ \dot{r} &= N/J, \text{ rad/s}^2 \text{ (deg/s}^2\text{)}. \end{aligned} \right\} \text{ (5-21)}$$

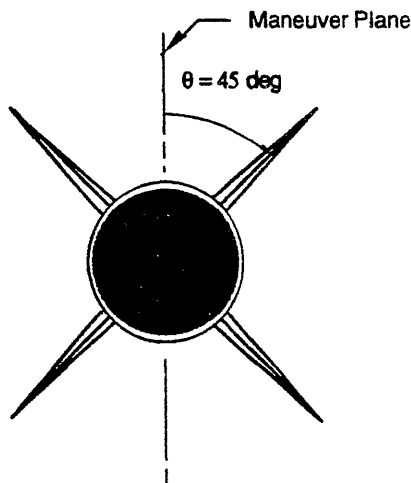
5-7.3 AVERAGING AERODYNAMIC COEFFICIENTS

As a missile rolls with respect to the plane containing the total angle of attack, the flow over the surfaces varies as a function of the roll angle; thus the aerodynamic force characteristics of the entire missile are caused also to vary with roll angle. For example, consider a missile maneuver in a vertical plane. When the missile roll orientation is such that one set of wings and/or fins lies in the maneuver plane (Fig. 5-8(A)), the lift (or normal force) coefficient and moment coefficient are different than when the missile is rotated with neither set of fins in the maneuver plane (Fig. 5-8(B)).

If all roll coupling effects could be accurately modeled in a flight simulation so that the instantaneous roll angle θ could be predicted, then all the aerodynamic coefficients



(A) Fins in Maneuver Plane



(B) Fins 45 deg Relative to Maneuver Plane

Figure 5-8. Fin Rotation Relative to Plane of Missile Maneuver

could conceptually be applied as functions of the instantaneous roll angle. In general, however, this is not necessary or even practical. One method of handling this problem in a simulation is to average the aerodynamic coefficients over all roll angles. Typically, wind tunnel data are measured with one set of fins in the same plane as the angle of attack— $\theta = 0$ deg for an angle of attack in the xz -plane and with the body rotated such that the plane of the angle of attack is halfway between the sets of fins ($\theta = 45$ deg). Common practice is to prepare aerodynamic coefficient input data by averaging the values at the two roll angles. Some missiles, however, have a preferred roll orientation in

a maneuver (Ref. 9), and if this orientation is known for the missile being simulated, the average should be weighted toward the preferred roll angle.

5-7.4 MAGNUS EFFECT

If a spinning missile flies in such a way that the axis of rotation is at an angle to the flight path, i.e., it has an angle of attack, the missile experiences an additional lift force, called the Magnus force, in a direction perpendicular to the plane in which the velocity vector and the rotational axis lie. The Magnus force depends on the roll rate p and on the total angle of attack. At low roll rates the Magnus force may be insignificant however, in simulating missiles with high roll rates, it may be necessary to include the Magnus force and the associated moment in the equations of motion (Refs. 12 and 20). The Magnus effect is not normally included in most simulations (Ref. 9), and equations for the Magnus force are not included in this handbook.

5-7.5 MODULATION OF FIN DEFLECTION ANGLE

As a missile rolls, the deflection angle δ of a given control surface must be modulated, i.e., adjusted in magnitude, at the missile roll rate in order to produce an aerodynamic force in a given direction. For this reason the deflection angle of a given surface can be represented as a sinusoid. This variation should be taken into account when calculating aerodynamic coefficients based on the control-surface deflection angle. A common procedure is to use the average fin deflection over a revolution of the missile. Based on the assumption that the control-surface deflection angle is modulated sinusoidally as the missile rotates, Ref. 10 gives the instantaneous component of deflection angle of a given fin in a given direction, e.g., they-direction, as

$$\delta_y = \frac{\delta_{peak}}{2} [1 + \cos(2\phi)], \text{ rad (deg)} \quad (5-22)$$

where

δ_{peak} = peak fin deflection during revolution of missile, rad (deg)

δ_y = angle of effective control-surface deflection in the yawing direction, rad (deg)

ϕ = missile roll angle, rad (deg).

The value of the component of fin deflection in the y -direction averaged over an entire revolution is then

$$\delta_{y_{avg}} = \frac{\delta_{peak}}{2}, \text{ rad (deg)}$$

where

$\delta_{y_{avg}}$ = average fin deflection component in y -direction, rad (deg).

This average fin deflection angle $\delta_{y_{avg}}$ is substituted into equations when a value of δ_y is required

REFERENCES

1. R. S. Shevell, *Fundamentals of Flight*, Prentice-Hall, inc., Englewood Cliffs, NJ, 1983.
2. Richard W. Kolk, *Modern Flight Dynamics*, Prentice-Hall, Inc., Englewood Cliffs, NJ, 1961.
3. E. A. Bonney, M. J. Zucrow, and C. W. Besserer, "Aerodynamics, Propulsion, Structures and Design Practice", *Principles of Guided Missile Design*, G. Merrill, Ed., D. Van Nostrand Company, Inc., Princeton, NJ, 1956.
4. C. D. Perkins and R. E. Hage, *Airplane Performance Stability and Control*, John Wiley & Sons, Inc., New York, NY, 1949.
5. B. Etkin, *Dynamics of Flight--stability and Control*, John Wiley & Sons, Inc., New York NY, 1982.
6. S. F. Werner, *Fluid-Dynarnic Drag*, Hoerner Fluid Dynamics, Brick Town, NJ, 1965.
7. A. Miele, *Flight Mechanics, Volume 1, Theory of Flight Paths*, Addison-Wesley Publishing Company, Inc., Reading, MA, 1962.
8. J. J. Jerger and G. Merrill, Eds., "Systems Preliminary Design", *Principles of Guided Missile Design*, D. Van Nostrand Co., Inc., Princeton, NJ, 1960.
9. W. G. Younkin, *Studies of the Sidewinders 1C Aerormechanics, Part 2, Dynamics (U)*, NAVWEPS Report 6596 Part 2, NOTS TP 2482, US Naval Ordnance Test Station, China Lake, CA, June 1964 (downgraded to UNCLASSIFIED 1973).
10. R. E. Gould and M. D. Sevachko, *An Aerodynamics Model for Guided Missiles*, DELEW-M-TR-82-36, Electronic Warfare Laboratory, Office of Missile Electronic Warfare, white Sands Missile Range, NM, November 1982.
11. *Dynamics of the Airframe*, BU AER Report AE-61-4II, Bureau of Aeronautics, Navy Department Washington, DC, 1952.
12. Bernard Etkin, *Dynamics of Flight, Stability and Control*, John Wiley and Sons, Inc., New York, NY, 1959.
13. T. R. Driscoll and H. F. Eckenroth, "Flight Test Validation of the Patriot Missile Six-Degree-of-Freedom Aerodynamic Simulation Model", *Automatic Control Theory and Applications* 7, No. 1 (January 1979).
14. R. D. Finck, *USAF Stability and Control Datcom*, AFWAL TR-83-3848, prepared by McDonnell Aircraft Company for Flight Control Division, Air Force Flight Dynamics Laboratory, Wright-Patterson Air Force Base, OH, April 1978.
15. K. D. Bruns, M. E. Moore, S. L. Stoy, S. R. Vukelich, and W. B. Blake, *MISSILE DATCOM User's Manual*, Final Report for Period May 1987-April 1991, WL-TR-91-3039, Control Dynamics Branch, Flight Control Division, Flight Dynamics Directorate, Wright Laboratory, Wright-Patterson Air Force Base, OH, April 1991.
16. A. E. Puckett and S. Ramo, *Guided Missile Engineering*, McGraw-Hill, New York, NY, 1959.
17. Dean R. Chapman, "Computational Aerodynamics Development and Outlook", *AIAA Journal* 17, No. 12 (December 1979).
18. D. C. Montgomery and R. G. Conard, "Comparison of Simulation and Flight-Test Data for Missile Systems", *Simulation* 34, No. 2 (February 1980).
19. T. R. Driscoll and H. F. Eckenroth, "Hybrid Simulation-Key to Successful Flight-Test Program*", *Simulation* 26, No. 1 (January 1976).
20. C. P. Schneider, "Applications to Missile Dynamics", AGARD Lecture Series No. 18, MBB-UA-553/80, Advisory Group for Aerospace Research and Development, North Atlantic Treaty Organization, Neuilly sur Seine, France, 1980.

BIBLIOGRAPHY

AERODYNAMICS

- Jerry M. Allen and A. B. Blair, "comparison of Analytical and Experimental Supersonic Aerodynamic Characteristics of a Forward Control Missile", *Journal of Spacecraft* 19, No. 2 (March-April 1982).
- J. J. Bertin and M. L. Smith, *Aerodynamics for Engineers*, Prentice-Hall, Inc., Englewood Cliffs, NJ, 1979.
- C. W. Besserer and G. Merrill, Eds., "Missile Engineering Handbook", *Principles of Guided Missile Design*, D. Van Nostrand Company, Inc., Princeton, NJ, 1958.
- A. F. Donovan and H. R. Lawrence, Eds., *Aerodynamic Components of Aircraft at High Speeds*, Princeton University Press, Princeton, NJ, 1967.
- L. E. Ericsson and J. P. Reding, "Dynamic Simulation Through Analytic Extrapolation", *Journal of Spacecraft and Rockets* 19, No. 2 (March/April 1982).
- D. I? Hoerner and H. V. Borst, *Fluid-Dynamic Lift*, Hoerner Fluid Dynamics, Brick Town, NJ, 1975.
- E. R. C. Miles, *Supersonic Aerodynamics, A Theoretical Introduction*, Dover Publications, Inc., New York, NY, 1950.
- SAMS Surface-to-Air Missile Simulation Computer Program, Analyst Manual, Vol. 1, Basic Methodology, Flight Dynamics Laboratory, US Air Force Wright Aeronautical Laboratories, US Air Force Systems Command, Wright-Patterson Air Force Base, OH, January 1983.
- W. M. Swanson, "The Magnus Effect: A Summary of Investigations to Date", *Journal of Basic Engineering*, 461 (September 1961).
- Robert Wesley Truitt, *Hypersonic Aerodynamics*, The Roland Press Company, New York, NY, 1959.

FLIGHT TEST

- F. M. Belrose and Alfred M. Baird, The Role of Simulation in High-Technology Missile Applications, Technical Report RD-CR-83-23, US Army Missile Command, Redstone Arsenal, AL, April 1983.

ROLLING AIRFRAME

- J. Shinar, "Divergence Range of Homing Missiles", Israel Journal of Technology 14, (May 1976).

WIND TUNNELS

- R. Smelt, "The Role of Wind Tunnels in Future Aircraft Development", Eleventh ICAS Congress, Lisbon, Portugal, 10-16 September 1978.

CHAPTER 6

MISSILE PROPULSION

The equations of motion given in Chapter 4 need as inputs the force vector F_p and moment vector M_p contributed by the missile propulsion system. This chapter briefly describes various types of missile propulsion systems and gives the detailed methodology for determining these force and moment vectors at each computational time step for solid propellant rocket motors. Consideration is given to the effects of initial propellant grain temperature, ambient atmospheric pressure, changes in mass and moments of inertia, and tube launch.

6-0 LIST OF SYMBOLS

- A_e = exit area of rocket nozzle, m^2
 F_p = instantaneous thrust vector, N
 F_p = magnitude of instantaneous thrust force, N
 $F_{p_{ref}}$ = magnitude of reference-thrust force, N
 $F_{p_{yb}}$
 $F_{p_{zb}}$ = components of thrust vector F_p expressed in the body coordinate system, N
 I_{sp} = specific impulse of propellant, N·s/kg
 M_p, N_p = components of propulsion moment vector M_p expressed in body coordinate system (roll, pitch and yaw, respectively), N·m
 l_p = distance from center of mass to nozzle, m
 M_p = thrust (propulsion) moment vector, N·m
 m = instantaneous missile mass, kg
 m_0 = missile mass at time of launch, kg
 P_a = instantaneous ambient pressure, Pa
 P_{ref} = reference ambient pressure, Pa
 t = time since ignition, s
 y_b, z_b = coordinates of the body coordinate system
 γ_1 = angle measured from x_b -axis to projection of thrust vector F_p on $x_b y_b$ -plane, rad
 γ_2 = angle measured from projection of thrust vector F_p on $x_b y_b$ -plane to the thrust vector F_p , rad

6-1 INTRODUCTION

In general, a missile propulsion system, regardless of the type, produces thrust by burning propellant and expelling the exhaust products through a nozzle, as dimmed in subpars. 2-2.5 and 4-4.2. In addition to generating thrust, expulsion of burned propellant products reduces the missile mass, shifts the position of the center of mass, and reduces the moments of inertia.

This chapter describes methods for handling the propulsion system characteristics in a flight simulation. The end result is the method of calculating the force and moment

components that are applied to the missile by the propulsion system.

6-2 TYPES OF PROPULSION

Several different types of motors have been used or investigated for propelling surface-to-air missiles; however, solid propellant rocket motors are used in all current US Army surface-to-air missiles. In accordance with the stated objectives of this handbook, methods for simulating solid propellant rocket motors are given in detail; however, only brief descriptions of air-augmented rockets, liquid propellant rockets, turbojet engines, and ramjet engines are given.

6-2.1 SOLID PROPELLANT ROCKET MOTOR

For a solid propellant rocket motor, the major portion of the thrust force, the momentum component, depends only on the design of the propellant grain and is not affected by the missile speed or altitude. In contrast, the pressure component of thrust is affected by the instantaneous ambient atmospheric pressure acting on an area equivalent to the exit area of the rocket nozzle. The fact that the histories of the major thrust components of solid rockets are essentially fixed by the design of the solid propellant grain becomes important in computer simulation of their flight. The thrust history of a given motor design is constant from one simulated flight to the next, except for the effects of the initial temperature of the propellant grain, ambient pressure, and roll rate. Often the effects of temperature and roll rate can be neglected, so only the variation of ambient pressure remains to be taken into account during a simulated flight.

Depending on the maturity of the motor design, the thrust history of a given rocket motor is determined by either analytical calculations or tests of full-scale motors. The thrust measured for a captive motor, i.e., one attached to a test stand, is the same as the thrust that would be delivered to a missile in flight under the same ambient pressure conditions and with the same initial grain temperature. Analytical calculations vary in detail, but the most accurate predictions are based on complex computer analyses that account for the various chemical, thermodynamic, and fluid dynamic interactions within the combustion chamber and nozzle of the rocket motor. Once the thrust history is known, how-

ever, the details of how the thrust is generated are not important to a missile flight simulation and are almost never included.

In addition to the thrust history, histories of the mass of the missile and the distribution of mass are needed. The missile mass at any instant in time is used in the simulation to calculate missile acceleration (Eqs. 4-37). The mass distribution is defined by the location of the center of mass and the moments of inertia. The center of mass is used to calculate the aerodynamic moments (Eqs. 5-12), and the moments of inertia are used to calculate the rotational response of the missile (Eqs. 4-45). Methods used to model solid propellant rocket motors in missile flight simulations are given in par. 6-3.

6-2.2 AIR-AUGMENTED ROCKET MOTOR

Air-augmented rocket motors have air inlet systems that capture atmospheric air and mix it with exhaust gases of the rocket. Transfer of some of the kinetic and chemical energy from the rocket exhaust to the captured air, including secondary burning, results in an increase in total momentum exchange across the propulsion unit and gives a significant increase in thrust. The extent of the net thrust increase over the added drag of the inlets depends on system design and operating flight conditions (Ref. 1). Variations in the properties of the ambient atmospheric air and the airspeed during flight must be taken into account in simulations of air-augmented rocket propulsion systems.

6-2.3 LIQUID PROPELLANT ROCKET MOTOR

Liquid propellant rocket motors use a liquid fuel and a liquid oxidizer--each carried onboard in separate containers (Ref. 2). The propellants are metered into a combustion chamber in which high-temperature, high-pressure gases are generated and exhausted through a nozzle to produce thrust. Flight simulations of missiles that use liquid propellants are essentially the same as simulations of missiles that use solid propellants unless the potential for throttle control is exploited in the design of the liquid system.

6-2.4 TURBOJET ENGINE

Vehicles that employ turbojet engines carry the propellant fuel onboard and use atmospheric air as the oxidizer. Air enters a diffuser and compressor section of the engine where it is compressed to high pressure. The compressed air is heated by combustion of the fuel in a combustion chamber and allowed to expand through a turbine that drives the air compressor. From the turbine the high-energy air and products of combustion are expanded and ejected to the atmosphere through a nozzle at the rear of the unit (Ref. 2). Performance of a turbojet engine is a function of throttle control setting, Mach number, and ambient atmospheric

properties--all of which must be taken into account in flight simulations employing turbojet engines.

6-2.5 RAMJET ENGINE

A ramjet engine is similar in principle to the turbojet engine except that the air entering the engine is compressed entirely by passing it through diffusers, i.e., trading velocity for pressure, rather than by a mechanical compressor. As the flight speed increases, the ram air pressure increases and provides increased thrust. A ramjet engine will not operate at zero speed and must therefore be boosted to operating speed by some other means of propulsion, such as a rocket booster (Ref. 2). Mach number and atmospheric properties must be taken into account in simulations of ramjet engine operation.

6-3 SIMULATION OF THRUST AND MASS PARAMETERS

Since the basic performance of a given solid propellant rocket essentially is fixed by its design, the basic motor performance will be the same for all simulated flights, as mentioned in subpar. 6-2.1. The only variations in solid rocket performance from one simulated flight to the next are caused by any difference in the initial temperature of the propellant grain, changes in the ambient atmospheric pressure as the missile changes altitude, and sometimes roll rate.*

Inputs to the simulation that describe the propulsion system of a solid propellant missile consist simply of histories of thrust, mass parameters, i.e., mass, center of mass, and moments of inertia and the exit area of the rocket nozzle. Thrust is generally supplied as an input table based on a reference atmospheric pressure. During the simulated flight, the thrust obtained from the thrust table at each time step is corrected for the ambient atmospheric pressure based on the instantaneous missile altitude (subpar. 6-3.2). If the mass is not supplied in the form of a time history, it can be calculated based on the thrust history and an input value of specific impulse I_{sp} (subpar. 6-3.3). The exit area is the cross-sectional area of the rocket nozzle at the point where the exhaust gas exits from the nozzle.

The center of mass and the moments of inertia are not needed in three-degree-of-freedom simulations because the rotational motion of the missile is not calculated explicitly.

6-3.1 GRAIN TEMPERATURE

If the effects of different initial temperatures of the propellant grain are important to the objectives of the simulation, different thrust tables corresponding to the initial temperatures of interest are usually supplied. Fig. 2-25 illustrates different thrust histories that correspond to different grain temperatures. In most applications of missile flight simulations, the initial temperature of the propellant grain is

*Simulation of the effects of roll rate on the propulsion system is beyond the scope of this handbook.

not an issue because it affects the total impulse-integral of thrust multiplied by time-by only a few percent, and only a single reference-thrust history corresponding to an average initial grain temperature is input to the simulation.

6-3.2 REFERENCE CONDITIONS

The equation for correcting the reference thrust for instantaneous ambient atmospheric pressure is

$$F_p = F_{p_{ref}} + (p_{ref} - p_a) A_e, \text{ N} \quad (6-1)$$

where

- A_e = exit area of rocket nozzle, m^2
- F_p = magnitude of instantaneous thrust force, N
- $F_{p_{ref}}$ = magnitude of reference-thrust force, N
- p_a = instantaneous ambient pressure, Pa
- p_{ref} = reference ambient pressure, Pa.

Reference thrust $F_{p_{ref}}$ is the calculated or measured thrust of the rocket motor operating in a reference ambient pressure p_{ref} . The reference pressure for surface-to-air missile applications is almost always standard sea level pressure. However, it is sometimes zero (vacuum), and occasionally it is some intermediate pressure. The reference pressure on which a given reference-thrust history is based must always be stated.

6-3.3 MASS CHANGE

The change in mass of the missile during flight is determined by the propellant mass flow rate, i.e., the momentum component of thrust and therefore does not vary from one flight profile to another for a given missile design. If the mass history of the motor is not provided in the propulsion system data set, it can be calculated using

$$m = m_0 - \frac{1}{I_{sp}} \int_0^t F_{p_{ref}} dt, \text{ kg}$$

where

- $F_{p_{ref}}$ = magnitude of the reference-thrust force, N
- I_{sp} = specific impulse of propellant, N·s/kg
- m = instantaneous missile mass, kg
- m_0 = missile mass at time of launch, kg
- t = time since ignition, s.

In Eq. 6-2 the specific impulse I_{sp} must be based on the same reference pressure as the reference thrust. A single average value of delivered I_{sp} usually is provided for a boost-glide motor; however, for a boost-sustain motor two different average values of delivered I_{sp} are needed—one for the boost phase and one for the sustain phase. Since the instantaneous mass does not depend on the ambient pressure, the mass can be precalculated as a function of time by using Eq. 6-2 and input to the simulation as a table; however, it is often calculated within the simulation. Likewise, for five- or six-degree-of-freedom simulations, the instantaneous location of the center of mass and the pitching and rolling moments of inertia can be precalculated or calculated within the simulation.

6-3.4 TUBE LAUNCH

Tube-launched missiles that are shoulder-fired are ejected from the tube by an ejection charge as described in subpar. 2-2.5.2. The dynamics of the acceleration of the missile within the tube usually are not simulated since they are essentially the same for every firing. Instead the velocity imparted to the missile by the ejection charge is used as the initial velocity of the missile with the simulation beginning after the missile has cleared the tube. The initial mass of the missile, then, does not include the mass of the ejection charge.

6-4 PROPULSION FORCE AND MOMENT VECTORS

In most missiles the magnitude of the thrust F_p , calculated by Eq. 6-1, is directed along the x_b -axis (the missile centerline). Then, the components of the thrust vector F_p , expressed in the body reference frame are

$$\left. \begin{aligned} F_{p_{x_b}} &= F_p, \text{ N} \\ F_{p_{y_b}} &= 0, \text{ N} \\ F_{p_{z_b}} &= 0, \text{ N} \end{aligned} \right\} \quad (6-3)$$

where

- F_p = magnitude of instantaneous thrust force, N
- $F_{p_{x_b}}, F_{p_{y_b}}, F_{p_{z_b}}$ = components of thrust vector F_p , expressed in the body coordinate system, N.

If the line of thrust is misaligned from the missile axis by angles γ_1 and γ_2 , as shown in Fig. 6-1(A), the components of the thrust vector are given by

$$\left. \begin{aligned} F_{p_{x_b}} &= F_p \cos \gamma_2 \cos \gamma_1, \text{ N} \\ F_{p_{y_b}} &= F_p \cos \gamma_2 \sin \gamma_1, \text{ N} \\ F_{p_{z_b}} &= -F_p \sin \gamma_2, \text{ N} \end{aligned} \right\} \quad (6-4)$$

where

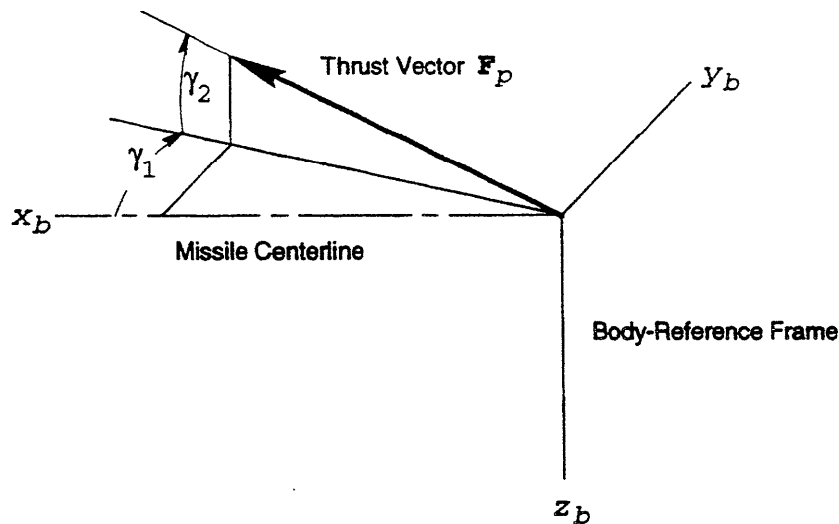
- γ_1 = angle measured from x_b axis to projection of thrust vector F_p on xby_b -plane rad
- γ_2 = angle measured from projection of thrust vector

F_p on xby_b -plane to the thrust vector F_p , rad.
The components of the moment vector M_p are given by

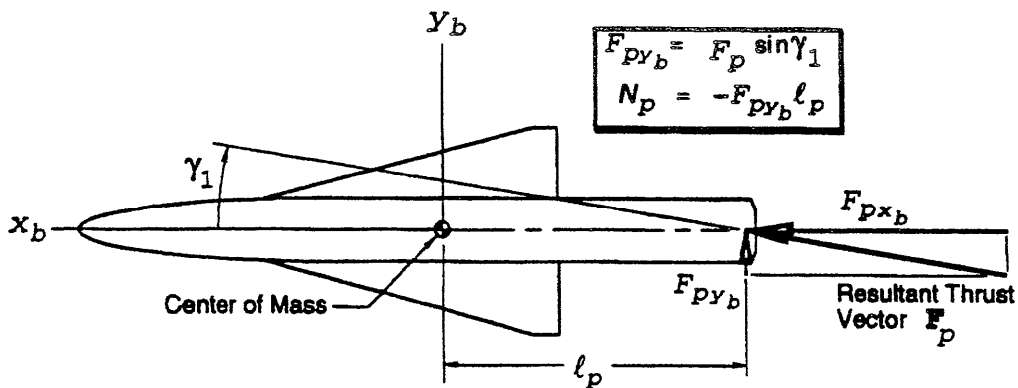
$$\left. \begin{aligned} L_p &= 0, \text{ N} \cdot \text{m} \\ M_p &= F_{p_{z_b}} \ell_p, \text{ N} \cdot \text{m} \\ N_p &= -F_{p_{y_b}} \ell_p, \text{ N} \cdot \text{m} \end{aligned} \right\} \quad (6-5)$$

where

- N_p = components of propulsion moment vector M_p expressed in body coordinate system (roll, pitch, and yaw, respectively), $\text{N} \cdot \text{m}$
- ℓ_p = distance from center of mass to nozzle, m.



(A) Thrust Vector Direction Relative to Body-Reference Frame



(B) Moment Produced by Thrust Vector

Figure 6-1. Thrust Force and Moment

Fig. 6-1 (B) illustrates a thrust vector that is misaligned with the missile axis in only the x-y plane, i e., $\gamma_2 = 0$.

The force and moment vectors produced by the propulsion system are applied in a flight simulation by substitution into Eqs. 4-37 and 4-46.

REFERENCES

1. E. A. Mossman, R. L. Chapman, and R. C. Rozycki, Analytical and Experimental Investigation of Air-Augmented Rockets to Determine Thrust Minus Drag, Quarterly Progress Report, 1 April-30 June 1966, AFRPL-TR-66-193, Air Force Rocket Propulsion Laboratory, Research and Technology Division, Air Force Systems Command, Edwards Air Force Base, CA, August 1966.
2. E. A. Bonney, M. J. Zucrow, and C. W. Besserer, "Aerodynamics, Propulsion, Structures and Design Practice", Principles of Guided Missile Design, G. Merrill, Ed., D. Van Nostrand Company, Inc., Princeton, NJ, 1956.

CHAPTER 7

MISSILE AND TARGET MOTION

This chapter describes mathematical techniques employed in missile flight simulations to calculate the motion of both the missile and the airborne target. Methods of combining the gravitational, aerodynamic, and propulsive forces (described in Chapters 4, 5, and 6) with the vehicle equations of motion (described in Chapter 4) are presented. Variations in the methodology for treating different numbers of degrees of freedom are described; and the equations for simulating simple target evasive maneuvers are given. A method of calculating the closest approach vector and the time of closest approach is provided.

7-0 LIST OF SYMBOLS

\mathbf{A}	= axial force vector; N	C_{lp}	= roll damping derivative relative to roll rate p , $\text{rad}^{-1} (\text{deg}^{-1})$
$\dot{\mathbf{A}}_a$	= rate of change of achieved-lateral-acceleration vector m/s^3	$C_{l\delta}$	= slope of curve formed by roll moment coefficient C_l versus effective control-surface deflection for roll δ_r , $\text{rad}^{-1} (\text{deg}^{-1})$
\mathbf{A}_a	= achieved-lateral-acceleration vector, m/s^2	C_m	= aerodynamic pitch moment coefficient about center of mass, dimensionless
\mathbf{A}_c	= commanded-lateral-acceleration vector, m/s^2	C_{mq}	= pitch damping derivative relative to pitch rate q , $\text{rad}^{-1} (\text{deg}^{-1})$
\mathbf{A}_T	= total acceleration vector of target, m/s^2	C_{mref}	= pitching moment coefficient about reference moment station, dimensionless
A	= magnitude of aerodynamic axial force vector A , N	$C_{m\alpha}$	= slope of curve formed by pitch moment coefficient C_m versus angle of attack α , $\text{rad}^{-1} (\text{deg}^{-1})$
A_c	= magnitude of commanded-lateral-acceleration vector m/s^2	$C_{m\dot{\alpha}}$	= pitch damping derivative relative to angle of attack rate $\dot{\alpha}$ (slope of curve formed by C_m versus α), $\text{rad}^{-1} (\text{deg}^{-1})$
A_e	= rocket nozzle exit area, m^2	$C_{m\delta}$	= slope of curve formed by pitch moment coefficient C_m versus effective control-surface deflection for pitch δ_p , $\text{rad}^{-1} (\text{deg}^{-1})$
A_{max}	= magnitude of maximum lateral acceleration, m/s^2	C_N	= aerodynamic normal force coefficient dimensionless
A_T	= magnitude of total acceleration vector A_T of target, m/s^2	C_{Ny}	= coefficient corresponding to component of normal force on y_b -axis, dimensionless
A_{Tach}	= magnitude of achieved flight path acceleration of target, m/s^2	C_{Nz}	= coefficient corresponding to component of normal force on z_b -axis, dimensionless
A_{TC}	= commanded target maneuver acceleration, m/s^2	$C_{N\alpha}$	= slope of curve formed by normal force coefficient C_N versus angle of attack α , $\text{rad}^{-1} (\text{deg}^{-1})$
A_z	= azimuth angle measured from x_b -axis to projection of vector R_b on x_y -plane, $\text{rad} (\text{deg})$	C_n	= aerodynamic yaw moment coefficient about center of mass, dimensionless
B and C	= intermediate variables used in the calculation of C_l , dimensionless	C_{nr}	= yaw damping derivative relative to yaw rate r , $\text{rad}^{-1} (\text{deg}^{-1})$
C_A	= aerodynamic axial force coefficient, dimensionless	C_{nref}	= yaw moment coefficient about reference moment station, dimensionless
C_D	= aerodynamic drag coefficient, dimensionless		
C_{D0}	= zero-lift drag coefficient, dimensionless		
C_L	= aerodynamic lift coefficient, dimensionless		
$C_{L\alpha}$	= slope of curve formed by lift coefficient C_L versus angle of attack α , $\text{rad}^{-1} (\text{deg}^{-1})$		
C_l	= aerodynamic roll moment coefficient about center of mass, dimensionless		

- $C_{n\beta}$ = slope of curve formed by yawing moment coefficient C_n versus angle of sideslip β , rad^{-1} (deg^{-1})
 $C_{n\dot{\beta}}$ = yawing damping derivative relative to angle of sideslip rate $\dot{\beta}$, rad^{-1} (deg^{-1})
 $C_{n\delta}$ = slope of curve formed by yaw moment coefficient C_n versus effective control-surface deflection for yaw δ_y , rad^{-1} (deg^{-1})
D = aerodynamic drag force vector, N
D = magnitude of aerodynamic drag force vector D, N
d = aerodynamic reference length of body, m
E ℓ = elevation angle measured from projection of line-of-sight vector R_i on xy plane to the vector R_y , rad (deg)
F_A = resultant aerodynamic force vector, N
F_g = gravitational force vector, including effects of earth rotation, N
F_p = total instantaneous thrust force vector, N
F_{Axb}, F_{Ayb}, F_{Azb} = components of aerodynamic force vector F_A expressed in the body coordinate system, N
F_{gxb}, F_{gyb}, F_{gzb} = component of gravitational force vector F_g expressed in the body coordinate system, N
F_{gxe}, F_{gye}, F_{gze} = components of gravitational force vector F_g expressed in the earth coordinate system, N
F_p = magnitude of total instantaneous thrust force vector F_p , N
F_{pref} = reference thrust force, N
F_{pxb}, F_{pyb}, F_{pzb} = components of thrust vector F_p expressed in the body coordinate system, N
g = acceleration due to gravity, m/s^2
g₀ = acceleration due to gravity at earth surface (nominally 9.8 m/s^2), m/s^2
h = altitude above mean sea level, m
I_{sp} = specific impulse of propellant, N-s/kg
I_x, I_y, I_z = moments of inertia (diagonal elements of inertia matrix when products of inertia are zero), $\text{kg}\cdot\text{m}^2$
k = constant in induced drag coefficient, dimensionless
L = aerodynamic lift force vector, N
L, M, N = components of total moment vector **M** expressed in body coordinate system (roll, pitch, and yaw, respectively), $\text{N}\cdot\text{m}$
L_A, M_A, N_A = components of aerodynamic moment vector **MA** expressed in body coordinate system (roll, pitch, and yaw, respectively), $\text{N}\cdot\text{m}$
L_p, M_p, N_p = components of propulsion moment vector **M_p** expressed in body coordinate system (roll, pitch, and yaw, respectively), $\text{N}\cdot\text{m}$
L = magnitude of aerodynamic lift force vector L, N
ℓ = distance from center of mass to nozzle, m
M = total moment vector acting on a body, $\text{N}\cdot\text{m}$
M_A = aerodynamic moment vector, $\text{N}\cdot\text{m}$
M_d = miss distance vector at time of closest approach, directed from missile to target, m
M_p = thrust (propulsion) moment vector, $\text{N}\cdot\text{m}$
m = instantaneous mass of missile, kg
m₀ = mass at time of launch, kg
N = aerodynamic normal force vector, N
N = magnitude of aerodynamic normal force vector N, N
n_g = load factor in units of g, dimensionless
n_{gmax} = specified maximum load factor in units of g to be applied during maneuver, dimensionless
P_M = position vector of missile, m
P_T = position vector of target, m
P_{T0} = initial position vector of target, m
P_d = period of target weave maneuver, s
P_k = kill probability, dimensionless
p, q, r = components of angular rate vector **w** expressed in body coordinate system (roll, pitch, and yaw, respectively), rad/s (deg/s)
 $\dot{p}, \dot{q}, \dot{r}$ = components of angular acceleration **$\dot{\omega}$** expressed in body coordinate system (roll, pitch, and yaw respectively). rad/s^2 (deg/s^2)
p_a = ambient atmospheric pressure, Pa
p_{ref} = reference ambient pressure, Pa
Q = dynamic pressure parameter, Pa
R = range vector from missile center of mass to target center of mass, m
R_{earth} = line-of-sight vector from missile to target expressed in earth coordinates, m
R_t = line-of-sight vector from target to missile expressed in target coordinate system, m
R_e = radius of the earth, m

R_{tx}, R_{ty}, R_{tz}	= components of line-of-sight vector R , expressed in target coordinate system, m		center of mass V_c , m/s
S	= aerodynamic reference area, m ²	$V_{T/M}$	= magnitude of velocity vector of the center of mass of the target relative to the center of mass of the missile $V_{T/M}$, m/s
$[T_{b/e}]$	= transformation matrix from earth to body coordinates, dimensionless	W	= weight vector, N
$[T_{t/e}]$	= transformation matrix from earth to target coordinates, dimensionless	W	= weight, N
t	= simulated time, s	x_{cm}	= instantaneous distance from nose to center of mass, m
(t)	= indicates that the associated variable is calculated at the current calculation time	x_{ref}	= distance from missile nose to the reference moment station, m
$(t-\Delta t)$	= indicates that the associated variable is calculated at the previous calculation time	α	= angle of attack rad (deg)
t_{ca}	= time of closest approach, s	α_t	= total angle of attack rad (deg)
t_{mi}	= time since initiation of the maneuver, s	β	= angle of sideslip (angle of attack in yaw plane), rad (deg)
u_{A_c}	= unit vector in direction of lateral-acceleration-command vector A_c , dimensionless	γ_1	= angle measured from x_b -axis to projection of thrust vector F_p on $x_b y_b$ -plane, rad (deg)
u_{ct}	= unit vector in direction of missile centerline axis, dimensionless	γ_2	= angle measured from projection of thrust vector F_p on $x_b y_b$ -plane to the thrust vector F_p , rad (deg)
u_{V_M}	= unit vector in direction of velocity of missile center of mass V_M , dimensionless	Δt	= computation time step, s
$u_{V_{T/M}}$	= unit vector in direction of relative velocity vector $V_{T/M}$, dimensionless	δ	= general, or effective, angular deflection of control surface relative to body, rad (deg)
u, v, w	= components of absolute linear velocity vector V_M expressed in body coordinate system, m/s	δ_p	= effective control-surf' deflection causing pitching moment, rad (deg)
$\dot{u}, \dot{v}, \dot{w}$	= components of linear acceleration expressed in body coordinate system, m/s ²	δ_r	= effective control-surface deflection causing rolling moment, rad (deg)
V	= absolute linear velocity vector of a body, m/s	δ_y	= effective control-surface deflection causing yawing moment, rad (deg)
\dot{V}_M	= acceleration vector of missile center of mass, m/s	ζ	= damping ratio of a second-order system, dimensionless
V_M	= absolute velocity vector of missile center of mass (equivalent to the vector V for a general body), m/s	θ	= Euler angle rotation in elevation (pitch angle), rad (deg)
V_T	= velocity vector of target center of mass, m/s	ρ	= atmospheric density, kg/m ³
$V_{T/M}$	= velocity vector of the center of mass of the target relative to the center of mass of the missile, m/s	τ	= time constant (time to achieve 63% of a step command in a first-order system), s
V	= speed of a body, speed of air relative to a body, magnitude of velocity vector V , In/s	ϕ	= Euler angle rotation in roll (roll angle), rad (deg)
V_M	= magnitude of velocity vector of the center of mass of the missile V_M , m/s	ϕ_T	= target aircraft bank angle (Euler roll angle of the target coordinate system relative to the earth coordinate system), rad (deg)
V_T	= magnitude of velocity vector of target	ψ	= Euler angle rotation in azimuth (heading angle), rad (deg)
		$\dot{\psi}, \dot{\theta}, \dot{\phi}$	= rates of change of Euler angles in heading, pitch, and roll, respectively, rad/s (deg/s)
		ω	= angular rate vector of rotating reference frame relative to inertial frame, rad/s

ω_T = angular rate vector of target flight path,
rad/s (deg/s)

ω_n = undamped natural frequency of a
second-order system, rad/s (deg/s)

7-1 INTRODUCTION

Missile and target motions are calculated in a simulation by means of the equations of motion given in Chapter 4 by using values of the various forces acting on the vehicle. Methods of determining the values of the gravitational, aerodynamic, and propulsive forces for substitution into these equations of motion are given in Chapters 4, 5, and 6. The equations of motion apply to any flying vehicle including the missile and the target. Integration of the differential equations of motion yields the translational and rotational velocity and position histories of a vehicle throughout the simulated flight. The equations are usually simplified for calculating target motion and may also be simplified for calculating missile motion, depending on the objectives of the simulation.

Vehicle translational and rotational equations of motion are usually solved in the body coordinate system if the simulation has five or six degrees of freedom. In simulations with three degrees of freedom, rotational motion is not calculated explicitly, and the translational equations of motion are most conveniently solved in the earth reference frame.

With three degrees of freedom, missile angular motion about the pitch axis is calculated implicitly for use in calculating the angle of attack. The use of a second-order transfer function is a convenient method of incorporating realistic missile angular response characteristics into a three-degree-of-freedom simulation. Simulations that calculate pitch and yaw rotational motion implicitly as opposed to including them in the basic equations of motion have been called pseudo-five-degree-of-freedom simulations.

In simulating the motion of the target, the objective is to provide the means to study missile flight response to target flight characteristics. These target flight characteristics may extend from straight and level flight to complex evasive maneuvers. Target position relative to the missile is used in a simulation to calculate missile guidance system responses; target angular attitude relative to the missile is used to calculate target signature, which depends on the relative aspect.

7-2 COORDINATE SYSTEMS

As discussed and illustrated in Chapters 3 and 4, flight simulations use different coordinate systems to express different kinds of vectors. Typically, vehicle motion is measured relative to the earth; therefore, the output position and velocity vectors are usually in the earth coordinate system (Fig. 3-1(C)). The calculation of positions and velocities, however, involves various applied forces, which are sometimes difficult to handle mathematically in the earth coordi-

nate system. As previously discussed, aerodynamic forces result directly from the relative wind; therefore, aerodynamic force vectors are most easily defined by expressing them in the wind coordinate system, i.e., wind reference frame, (Fig. 3-1 (F)). Also, since the rotational inertial properties of the vehicle are most easily defined relative to principal body axes, the body coordinate system (i.e., body reference frame) is used to calculate changes in vehicle attitude. Equations for transforming vectors from one coordinate system to another are given in Appendix A.

For simulations with six degrees of freedom, the equations of motion are usually expressed in the body coordinate system. Force and moment vectors that are determined in other coordinate systems are transformed to the body coordinate system for use in the equations of motion. The first integration of the equations of motion yields the vehicle translational and rotational velocities expressed in the body coordinate system. Usually the velocities and other vectors in the equations of motion are then transformed to the earth system for the second integration to yield vehicle position and attitude in the earth coordinate system.

For simulations with only three degrees of freedom, the equations of motion are usually expressed directly in the earth coordinate system for both integrations. Since rotational motion is not calculated explicitly, the need to express the equations of motion in body coordinates is eliminated. Aerodynamic forces, determined in the wind system and propulsive forces, determined in the body system are transformed to the earth system before substitution into the equations of motion.

7-3 MISSILE MOTION

The simulation of missile motion usually begins at the instant the missile leaves the launcher and ends at the time of closest approach to the target. Although the miss distance is the final measure of merit of missile flight performance, the details of missile motion throughout the flight are often of equal interest to the user of the simulation.

7-3.1 INITIAL CONDITIONS

The equations of motion can be solved by starting at any point in the flight provided that all the conditions describing the state of the missile at that point of time are known. Since the initial motion of the missile relative to the launcher is essentially the same for all flights, this quantity can be pre-calculated and supplied as an input to the simulation in the form of initial missile velocity.

When the rocket motor or ejection charge is ignited, the missile begins to travel along the launch rail or in the launch tube. The forward missile hangars or supports reach the end of the launcher and are the first portions of the missile to become unsupported. With the forward portion of the missile unsupported while the rear portion is still supported by the launcher, the force of gravity causes a downward rotation of the missile. The angular rate of the launcher is imparted to the missile, and as the missile leaves the

launcher, the dynamics of the rotating launcher acting on the rear of the missile while the forward part is unsupported imparts an angular velocity to the missile (Ref. 1). These are called tip-off effects, as discussed in subpar. 2-4.1.

For many applications of missile flight simulations, the detailed angular rates imparted to the missile at launch are considered to be of minor importance, and the transition from fully supported to completely airborne is not included in the simulation. Instead the simulation is started at the instant the missile becomes fully unsupported, and the initial conditions are those conditions that would exist at that instant. If determining missile performance in the early part of its flight is an important objective of the simulation, however, these angular rates must be either precalculated and input to the simulation or calculated by a tip-off routine within the simulation.

7-3.2 MISSILE FLIGHT

A simulation computes missile flight parameters by using numerical methods to solve the equations of motion at sequential, simulated time points. The interval between successive calculation times is very small, usually 0.1 s or less, depending on the frequency content of the missile motions being simulated. The results at any given calculation time depend on the results from the previous calculation time. Thus all the parameters that affect the control and the flight of the missile are updated and substituted into the equations of motion at each successive computation time to generate the history of missile motion.

Because the five- or six-degree-of-freedom models and the three-degree-of-freedom models differ considerably in complexity, they are discussed separately.

7-3.2.1 Six Degrees of Freedom

In six-degree-of-freedom models, rotational motions about all three missile axes are simulated, and the translational equations-expressed in body axes-include terms that account for the rotating body reference frame.

7-3.2.1.1 Translational Equations

The translational equations of motion, expressed in the body reference frame and including the appropriate aerodynamic, propulsive, and gravitational forces, are given in Chapter 4 and are repeated here for convenience:

$$\left. \begin{aligned} \dot{u} &= \frac{F_{A_{x_b}} + F_{p_{x_b}} + F_{g_{x_b}}}{m} - (qw - rv), \text{ m/s}^2 \\ \dot{v} &= \frac{F_{A_{y_b}} + F_{p_{y_b}} + F_{g_{y_b}}}{m} - (ru - pw), \text{ m/s}^2 \\ \dot{w} &= \frac{F_{A_{z_b}} + F_{p_{z_b}} + F_{g_{z_b}}}{m} - (pv - qu), \text{ m/s}^2 \end{aligned} \right\} \quad (4-37)$$

where

$F_{A_{x_b}}, F_{A_{y_b}}, F_{A_{z_b}}$ = components of aerodynamic force vector F_A expressed in the body coordinate system, N

$F_{g_{x_b}}, F_{g_{y_b}}, F_{g_{z_b}}$ = components of gravitational force vector F_g expressed in the body coordinate system, N

$F_{p_{x_b}}, F_{p_{y_b}}, F_{p_{z_b}}$ = components of thrust vector F_p expressed in the body coordinate system, N

m = instantaneous missile mass, kg

p, q, r = components of angular rate vector ω expressed in the body coordinate system, (roll, pitch and yaw, respectively), rad/s

u, v, w = components of absolute linear velocity vector V_a expressed in the body coordinate system, m/s

$\dot{u}, \dot{v}, \dot{w}$ = components of linear acceleration expressed in the body coordinate system, m/s^2 .

7-3.2.1.1.1 Aerodynamic Force

The method used to calculate the components of aerodynamic force for substitution into Eq. 4-37 depends largely on the form of the available aerodynamic data set. If extensive tables of the coefficients of the normal-force (pitch and yaw components) and axial force are available as functions of Mach number, angle of attack, angle of sideslip, and control-surface deflection components, table lookup procedures are used to obtain aerodynamic force coefficients directly. The resulting force coefficients are employed to calculate the aerodynamic force components using

$$\left. \begin{aligned} F_{A_{x_b}} &= -0.5\rho V_M^2 C_{A_x} S \\ F_{A_{y_b}} &= 0.5\rho V_M^2 C_{N_y} S \\ F_{A_{z_b}} &= 0.5\rho V_M^2 C_{N_z} S \end{aligned} \right\}, \text{ N} \quad (7-1)$$

where

- C_A = aerodynamic axial force coefficient, dimensionless
- C_N = aerodynamic normal force coefficient, dimensionless
- C_{N_y} = coefficient corresponding to component of normal force on y_b -axis, $C_N \frac{-v}{\sqrt{v^2 + w^2}}$, dimensionless
- C_{N_z} = coefficient corresponding to component of normal force on z_b -axis, $C_N \frac{w}{\sqrt{v^2 + w^2}}$, dimensionless
- S = aerodynamic reference area, m^2
- V_M = magnitude of velocity vector of the center of mass of the missile V_n , m/s
- ρ = atmospheric density kg/m^3 .

Note that a positive axial force is equivalent to a negative force component F_{ax} .

If the given aerodynamic data are supplied in a less convenient form, as is often the case, appropriate transformations among lift, drag, normal force, and axial force (Eqs. 4-13 and 4-14) maybe required. If extensive tables of aerodynamic force coefficients are not available, as in the early stages of development of a missile concept, advantage may be taken of the fact that the force coefficients usually are approximately linear in the regions of most interest, and much smaller tables of coefficient derivatives, discussed in par. 5-2, are used.

The angle of attack and angle of sideslip, required for table lookup of the coefficients, are calculated using

$$\left. \begin{aligned} \alpha &= \text{Tan}^{-1}\left(\frac{w}{u}\right) \\ \beta &= \text{Sin}^{-1}\left(\frac{v}{V_M}\right) \end{aligned} \right\}, \text{ rad (deg)} \quad (7-2)$$

where

- u, v, w = components of absolute linear velocity vector V_n , expressed in the body coordinate system, m/s
- V_M = magnitude of velocity vector of the center of mass of the missile V_n , m/s
- α = angle of attack, rad (deg)
- β = angle of sideslip, rad (deg).

These definitions of α and β result in algebraically positive (+) angles when the respective lateral components w and v of velocity V_n are positive. However, the corresponding normal force components F_{ax} and F_{ax} = in negative directions. Thus either the tabulated aerodynamic coefficients must follow the same convention, i.e., positive angles of attack and sideslip correspond to negative normal force coefficients, or as is often done, the algebraic signs in Eqs.

7-1 or 7-2 are adjusted appropriately to produce the proper force directions.

An alternative and often used equation for calculating the angle of sideslip is

$$\beta = \text{Tan}^{-1}\left(\frac{v}{u}\right), \text{ rad (deg)}. \quad (7-3)$$

For small angles the angles of sideslip calculated by Eqs. 7-2 and 7-3 are essentially equivalent.

The control-surface deflections, required as arguments in the table lookup of aerodynamic force coefficients, are obtained from the output of the guidance and control calculations discussed in Chapter 8.

7-3.2.1.1.2 Propulsive Force

The components of propulsive force expressed in the body reference frame are calculated by using

$$\left. \begin{aligned} F_{p_{x_b}} &= F_p \cos \gamma_2 \cos \gamma_1, \text{ N} \\ F_{p_{y_b}} &= F_p \cos \gamma_2 \sin \gamma_1, \text{ N} \\ F_{p_{z_b}} &= -F_p \sin \gamma_2, \text{ N} \end{aligned} \right\} \quad (6-4)$$

where

- F_p = magnitude of total instantaneous thrust force vector F_p , N
- $F_{p_{x_b}}, F_{p_{y_b}}, F_{p_{z_b}}$ = components of thrust vector F_p , expressed in the body coordinate system, N
- γ_1 = angle measured from x_b -axis to projection of thrust vector F_p on $x_b y_b$ -plane, rad (deg)
- γ_2 = angle measured from projection of thrust vector F_p on $x_b y_b$ -plane to the thrust vector F_p , rad.

The magnitude of the thrust force F_p is calculated by

$$F_p = F_{p_{ref}} + (p_{ref} - p_a)A_e, \text{ N} \quad (6-1)$$

where

- A_e = rocket nozzle exit area, m^2
- $F_{p_{ref}}$ = reference thrust force, N
- p_a = ambient atmospheric pressure, pa
- p_{ref} = reference ambient pressure, Pa.

The atmospheric pressure p_a corresponds to the current altitude of the missile and temperature of the air, and the value of $F_{p_{ref}}$ corresponds to the current simulated time in the reference thrust table. If the missile does not use thrust vector control and no errors in thrust alignment are being simulated, the thrust deflection angles γ_1 and γ_2 , usually are equal to zero. The parameters $F_{p_{x_b}}, F_{p_{y_b}}$, and $F_{p_{z_b}}$ the

components of the propulsive force to be substituted into Eqs. 4-37.

7-3.2.1.1.3 Gravitational Force

The gravitational force expressed in earth coordinates is given by

$$\left. \begin{aligned} F_{g_{x_e}} &= 0, N \\ F_{g_{y_e}} &= 0, N \\ F_{g_{z_e}} &= mg, N \end{aligned} \right\} \quad (7-4)$$

where

$F_{g_{x_e}}, F_{g_{y_e}}, F_{g_{z_e}}$ = components of gravitational force vector F_g expressed in the earth coordinate system, N
 g = moderation due to gravity, m/s^2
 m = instantaneous mass of missile, kg.

The dependence of the acceleration due to gravity on the altitude of the missile is given by

$$g = g_0 \left[\frac{R_e^2}{(R_e + h)^2} \right], m/s^2 \quad (4-29)$$

where

acceleration due to gravity, m/s^2
 g_0 = acceleration due to gravity at earth surface (nominally $9.8 m/s^2$), m/s^2
 h = altitude above mean sea level, m
 R_e = radius of the earth, m.

The acceleration due to gravity at sea level g_0 is selected from Table 4-2 for the appropriate latitude or is set to an average value of $9.8 m/s^2$. The altitude h in Eq. 4-29 is the current altitude of the missile above sea level. Often g is approximated by g_0 in a simulation regardless of altitude because of the relatively small variation of g with altitude.

The gravitational force expressed in body coordinates is calculated by multiplying Eqs. 7-4 by the matrix in Appendix A that transforms a vector from the earth frame to the body frame:

$$\begin{bmatrix} F_{g_{x_b}} \\ F_{g_{y_b}} \\ F_{g_{z_b}} \end{bmatrix} = [T_{b/e}] \begin{bmatrix} F_{g_{x_e}} \\ F_{g_{y_e}} \\ F_{g_{z_e}} \end{bmatrix}, N \quad (7-5)$$

where

$[T_{b/e}]$ = transformation matrix from earth to body coordinates.

The terms $F_{g_{x_b}}$, $F_{g_{y_b}}$, and $F_{g_{z_b}}$ are the components of the gravitational force to be substituted into Eqs. 4-37.

7-3.2.1.1.4 Translational and Angular Rates

The translational velocity components u , v , and w as well as the corresponding acceleration components are evaluated by the simultaneous solution of Eqs. 4-37. The rotational velocity components p , q , and r required for substitution into Eqs. 4-37, are obtained from the simultaneous solution of Eqs. 4-46, as described in par. 7-3.2.1.2.

7-3.2.1.1.5 Mass

The value of missile mass m for substitution into Eqs. 4-37 and Eq. 7-4, is the value determined by table lookup as a function of the current simulation time, or, as an alternative, m can be calculated within the simulation, by using

$$m = m_0 - \frac{1}{I_{sp0}} \int_0^t F_{p_{ref}} dt, kg \quad (6-2)$$

where

$F_{p_{ref}}$ = reference thrust force, N
 I_{sp} = specific impulse of propellant $N \cdot s/kg$
 m_0 = missile mass of the missile at time zero (i.e., at the time of launch), kg
 t = simulated time, s.

This completes the description of variables for substitution into Eqs. 4-37 to calculate translational motion.

7-3.2.1.2 Rotational Equations

The rotational equations of motion expressed in the body reference frame for simulations with six degrees of freedom are

$$\left. \begin{aligned} \dot{p} &= [L_A + L_P - qr(I_z - I_y)] / I_x, rad/s^2 (deg/s^2) \\ \dot{q} &= [M_A + M_P - rp(I_x - I_z)] / I_y, rad/s^2 (deg/s^2) \\ \dot{r} &= [N_A + N_P - pq(I_y - I_x)] / I_z, rad/s^2 (deg/s^2) \end{aligned} \right\} \quad (4-46)$$

where

L_A, M_A, N_A = components of aerodynamic moment vector M_A expressed in body coordinate system (roll, pitch, and yaw, respectively), $N \cdot m$
 L_P, M_P, N_P = components of propulsion moment vector M_p expressed in body coordinate system (roll, pitch, and yaw, respectively), $N \cdot m$

I_x, I_y, I_z = moments of inertia (diagonal elements of inertia matrix when products of inertia are zero), kg-m²
 p, q, r = components of angular rate vector w expressed in the body coordinate system (roll, pitch, and yaw, respectively), rad/s (deg/s)
 $\dot{p}, \dot{q}, \dot{r}$ = components of angular acceleration $\dot{\omega}$ expressed in body coordinate system (roll, pitch, and yaw, respectively) rad/s²(deg/s²).

7-3.2.1.2.1 Aerodynamic Moment

The components of aerodynamic moment, for substitution into Eqs. 4-46, are given by

$$L_A = 0.5\rho V_M^2 C_l S d, \text{ N}\cdot\text{m} \quad (5-6)$$

$$M_A = 0.5\rho V_M^2 C_m S d, \text{ N}\cdot\text{m} \quad (5-7)$$

$$N_A = 0.5\rho V_M^2 C_n S d, \text{ N}\cdot\text{m} \quad (5-8)$$

where

C_l = aerodynamic roll moment coefficient about center of mass, dimensionless
 C_m = aerodynamic pitch moment coefficient about center of mass, dimensionless
 C_n = aerodynamic yaw moment coefficient about center of mass, dimensionless
 d = aerodynamic reference length of body, m
 L_A, M_A, N_A = components of aerodynamic moment vector MA expressed in body coordinate system (roll, pitch, and yaw), respectively, N·m
 S = aerodynamic reference area m²
 V_M = magnitude of velocity vector of the center of mass of the missile, V_m, m/s
 ρ = atmospheric density, kg/m³.

The aerodynamic moment coefficients are obtained from

$$C_l = C_{l\delta} \delta_r + \frac{d}{2V_M} (C_{lp} p), \text{ dimensionless} \quad (5-15)$$

$$\left. \begin{aligned} C_m &= C_{m_{ref}} - C_{N_z} \frac{x_{cm} - x_{ref}}{d} + \frac{d}{2V_M} (C_{mq} + C_{m\dot{\alpha}}) q \\ C_n &= C_{n_{ref}} + C_{N_y} \frac{x_{cm} - x_{ref}}{d} + \frac{d}{2V_M} (C_{nr} + C_{n\dot{\beta}}) r \end{aligned} \right\} \text{dimensionless} \quad (5-12)$$

where

C_l = aerodynamic roll moment coefficient about center of mass, dimensionless
 C_{lp} = roll damping derivative relative to roll rate p, rad⁻¹ (deg⁻¹)
 $C_{l\delta}$ = slope of curve formed by roll moment coefficient C_l versus control-surface deflection rad⁻¹ (deg⁻¹)
 C_m = aerodynamic pitch moment coefficient about center of mass, dimensionless
 $C_{m_{ref}}$ = pitching moment coefficient about reference moment station, dimensionless
 C_{mq} = pitch damping derivative relative to pitch rate q, rad⁻¹ (deg⁻¹)
 $C_{m\dot{\alpha}}$ = pitch damping derivative relative to angle of attack rate a (slope of curve formed by C_m versus a), rad⁻¹ (deg⁻¹)
 C_{N_y} = coefficient corresponding to component of normal force on yb-axis, dimensionless
 C_{N_z} = coefficient corresponding to component of normal force on zb-axis, dimensionless
 C_n = aerodynamic yaw moment coefficient about center of mass, dimensionless
 C_{nr} = yaw damping derivative relative to yaw rate r, rad⁻¹ (deg⁻¹)
 $C_{n_{ref}}$ = yawing moment coefficient about reference moment station, dimensionless
 $C_{n\dot{\beta}}$ = yaw damping derivative relative to angle of sideslip rate β , rad⁻¹ (deg⁻¹)
 d = aerodynamic reference length of body, m
 p, q, r = components of angular rate vector w expressed in body coordinate system (roll, pitch, and yaw, respectively), rad/s
 V_M = magnitude of velocity vector of the center of mass of the missile V_m, m/s
 x_{cm} = instantaneous distance from missile nose to center of mass, m
 x_{ref} = distance from missile nose to reference moment station, m
 δ_r = effective control-surface deflection causing rolling moment, rad (deg).

As discussed in subpar. 5-2.4, the moment coefficients may be input to the flight simulation in the form of tables. In this case C_{m_{ref}} and C_{n_{ref}} are obtained by table lookup based on the current control-surface deflection angles δ_p and δ_y . However, if the moment derivatives are to be employed m

lieu of extensive moment coefficient tables, these reference moment coefficients are obtained using

$$C_{m_{ref}} = C_{m_{\alpha}} \alpha + C_{m_{\delta}} \delta_p, \text{ dimensionless (5-13)}$$

$$C_{n_{ref}} = C_{n_{\beta}} \beta + C_{n_{\delta}} \delta_y, \text{ dimensionless (5-14)}$$

where

$C_{m_{ref}}$ = pitching moment coefficient about reference moment station (This is the static value normally measured in the wind tunnel.), dimensionless

$C_{m_{\alpha}}$ = slope of curve formed by pitch moment coefficient C_m versus angle of attack α , rad^{-1} (deg^{-1})

$C_{m_{\delta}}$ = slope of curve formed by pitch moment coefficient C_m versus control-surface deflection for pitch δ_p , rad^{-1} (deg^{-1})

$C_{n_{ref}}$ = yawing moment coefficient about reference moment station, dimensionless

$C_{n_{\beta}}$ = slope of curve formed by yawing moment coefficient C_n versus angle of sideslip β , rad^{-1} (deg^{-1})

$C_{n_{\delta}}$ = slope of curve formed by yaw moment coefficient C_n versus effective control-surface deflection for yaw δ_y , rad^{-1} (deg^{-1})

α = angle of attack rad (deg)

β = angle of sideslip, rad (deg)

δ_p = effective control-surface deflection causing pitching moment, rad (deg)

δ_y = effective control-surface deflection causing yawing moment, rad (deg).

Attention must be given to the algebraic signs of α and β used in Eqs. 5-13 and 5-14 to ensure correct directions of the aerodynamic moments. (See related discussion for force equations in subpar. 7-3.2.1.1.1) For example, see Eqs. 12-41. The control-surface deflections δ_p and δ_y , in the pitch and yaw planes, respectively, are outputs from the guidance and control routines. The pitch moment derivatives— $C_{m_{\alpha}}$, $C_{m_{\delta}}$, and $(C_{m_{\alpha}} + C_{m_{\dot{\alpha}}})$ —are obtained by table lookup as functions of Mach number. For cruciform missile configurations the derivatives in the yaw plane— $C_{n_{\beta}}$, $C_{n_{\delta}}$, and $(C_{n_{\beta}} + C_{n_{\dot{\beta}}})$ —are equal to the respective derivatives in the pitch plane. The location of the center of mass x_{cm} can be calculated from an integration of thrust, or it can be obtained by table lookup as a function of time. The coefficients $C_{m_{\alpha}}$ and $C_{n_{\beta}}$ are the normal force coefficients that correspond to the components of normal force in the yb- and zb-directions, respectively,

$$\left. \begin{aligned} C_{N_y} &= \frac{F_{A_{yb}}}{0.5\rho V_M^2 S} \\ C_{N_z} &= \frac{F_{A_{zb}}}{0.5\rho V_M^2 S} \end{aligned} \right\}, \text{ dimensionless (7-6)}$$

where

C_{N_y} = coefficient corresponding to component of normal force on yb-axis, dimensionless

C_{N_z} = coefficient corresponding to component of normal force on zb-axis, dimensionless

$F_{A_{yb}}$ = y-component of aerodynamic force vector F_A expressed in the body coordinate system, N

$F_{A_{zb}}$ = z-component of aerodynamic force vector F_A expressed in the body coordinate system, N

S = aerodynamic reference area, m^2

V_M = magnitude of velocity vector of the center of mass of the missile V_m , m/s

ρ = atmospheric density, kg/m^3 .

The normal force components $F_{A_{yb}}$ and $F_{A_{zb}}$ are obtained from Eq. 7-1.

7-3.2.1.2.2 Propulsive Moment

For most applications the moment produced by the propulsion system will be zero. To simulate missiles that do experience a moment generated by the propulsive thrust the components of that moment are calculated by using

$$\left. \begin{aligned} L_p &= 0 \\ M_p &= F_{p_{zb}} \ell_p \\ N_p &= -F_{p_{yb}} \ell_p \end{aligned} \right\}, \text{ N}\cdot\text{m} \quad (6-5)$$

where

$F_{p_{yb}}$ = y-component of thrust vector F_p expressed in the body coordinate system, N

$F_{p_{zb}}$ = z-component of thrust vector F_p expressed in the body coordinate system, N

L_p, M_p, N_p = components of propulsion moment vector M_p expressed in body coordinate system (roll, pitch and yaw, respectively), $\text{N}\cdot\text{m}$

ℓ_p = distance from center of mass to rocket nozzle, m.

The distance ℓ_p is calculated using the current value of the instantaneous distance from missile nose to center of mass x_{cm}

7-3.2.1.2.3 Moments of Inertia

The moments of inertia I_x , I_y and I_z are obtained by table lookup as functions of time.

This completes the description of variables for substitution into Eqs. 4-46 to calculate the rotational motion.

7-3.2.1.3 Euler Angles

Missile attitude is required for a number of simulation functions including the calculation of angle of attack, seeker gimbal angles, fuze look-angles, and warhead spray pattern. In simulations with five or six degrees of freedom, the missile attitude is calculated directly by integrating the set of equations that define Euler angle rates, i.e.,

$$\left. \begin{aligned} \dot{\theta} &= p + (q \sin \phi + r \cos \phi) \tan \theta, \text{ rad/s (deg/s)} \\ \dot{\phi} &= q \cos \phi - r \sin \phi, \text{ rad/s (deg/s)} \\ \dot{\psi} &= (q \sin \phi + r \cos \phi) / \cos \theta, \text{ rad/s (deg/s)} \end{aligned} \right\} \quad (4-51)$$

where

θ : = Euler angle rotation in elevation (pitch angle), rad (deg)

ϕ : = Euler angle rotation in roll (roll angle), rad (deg)

$\dot{\psi}, \dot{\theta}, \dot{\phi}$: = rates of change of Euler angles in heading, pitch, and roll, respectively, rad/s (deg/s)

p, q, r : = components of angular rate vector w expressed in body coordinate system (roll, pitch, and yaw, respectively), rad/s.

7-3.2.2 Five Degrees of Freedom

A five-degree-of-freedom simulation uses the same equations as a simulation having six degrees of freedom (subpar. 7-3.2.1), except that the roll rate p is set equal to zero and the rolling moment L is not calculated.

7-3.2.3 Three Degrees of Freedom

In a three-degree-of-freedom simulation, the angular rate of the body reference frame at any given instant of time is considered to be zero in the equations of motion. Since rotating reference frames are therefore not involved, the terms containing angular rates in Eqs. 4-37 are dropped and thus allow the translational equations of motion to be simplified to the vector equation

$$\dot{\mathbf{V}}_M = \frac{\mathbf{F}_A + \mathbf{F}_p + \mathbf{F}_g}{m}, \text{ m/s}^2 \quad (7-7)$$

where

\mathbf{F}_A : = resultant aerodynamic force vector, N

\mathbf{F}_g : = gravitational force vector including effects of earth rotation, N

\mathbf{F}_p : = total instantaneous thrust force vector, N

m : = instantaneous mass of missile, kg

$\dot{\mathbf{V}}_M$: = acceleration vector of missile center of mass, m/s.

The vectors in Eq. 7-7 are typically expressed in the earth reference frame.

Since rotational motion is not calculated explicitly in simulations with three degrees of freedom, the whole process of calculating fin deflections, rotational rates, and rotational angles is bypassed for the most part. In this type of simulation, it is assumed that the missile control system operates properly to deflect fins as necessary to achieve the angles of attack and therefore to achieve the lift forces required to produce the maneuver acceleration commanded by the guidance system (except when limited by maximum angle of attack maximum fin angle, etc.).

7-3.2.3.1 Aerodynamic Force

Although missile angular motion is not calculated explicitly in three-degree-of-freedom simulations, it is usually necessary to estimate the angle of attack for use in other calculations, e.g., in calculating the drag due to lift using Eqs. 5-10 and 5-11.

7-3.2.3.1.1 Instantaneous Response

In simulations in which missile response time-i.e., time to achieve commanded maneuver acceleration-is not critical, it is assumed that the missile responds instantaneously to commands from the autopilot, which cause the missile to be always in a trimmed condition. That is, the missile angle of attack at any given instant of time is the one that produces the current commanded maneuver acceleration; there is no transition.

As shown in Chapter 8, the practical implementation of proportional navigation in an actual missile often causes the commanded acceleration to be in a direction normal to the missile centerline rather than normal to the flight path as is the case with pure proportional navigation. Eqs. 7-8 through 7-14 apply to this situation-commanded acceleration is normal to the missile centerline. In simulations with different objectives, it may be required that the commanded acceleration be normal to the missile velocity vector. Eqs. 7-15 through 7-17 apply to this application-commanded acceleration is normal to the missile velocity vector.

In either case the trim angle of attack for three-degree-of-freedom simulations is calculated by first calculating the lateral force (normal force or lift force) required to achieve the commanded maneuver acceleration and then calculating the angle of attack required to achieve that lateral force. The order of first calculating the lateral force and then the angle of attack is reversed from the order of events in actual flight in which an angle of attack leads to a lateral force.

In three-degree-of-freedom simulations in which the commanded lateral acceleration is perpendicular to the missile centerline, the normal force is calculated directly from the commanded maneuver acceleration by using

$$\mathbf{N} = m\mathbf{A}_c, \text{ N} \quad (7-8)$$

where

- A_c = commanded-lateral-acceleration vector (normal to missile centerline in this application), m/s^2
 m = instantaneous missile mass, kg
 N = aerodynamic normal force vector, N.

Eq. 7-8 gives the normal force vector that is required to produce the commanded-lateral-acceleration vector A_c . It is assumed that the missile responds as necessary (within any stated limits) to achieve this normal force. The commanded-lateral-acceleration vector A_c is obtained from the guidance law as described in Chapter 8.

The normal force coefficient C_N is

$$C_N = \frac{N}{QS}, \text{ dimensionless} \quad (7-9)$$

where

- C_N = aerodynamic normal force coefficient dimensionless
 N = magnitude of normal force vector N, N
 Q = dynamic pressure parameter, Pa
 S = aerodynamic reference area, m^2 .

Assuming that the normal force derivative $C_{N\alpha}$ is available, usually as a function of Mach number, it can be used to find the total angle of attack (the angle between the missile velocity vector and the missile centerline axis) by using

$$\alpha_t = \frac{C_N}{C_{N\alpha}}, \text{ rad (deg)} \quad (7-10)$$

where

- $C_{N\alpha}$ = slope of curve of normal force coefficient C_N versus angle of attack α , $\text{rad}^{-1}(\text{deg}^{-1})$
 α_t = total angle of attack, rad (deg).

The aerodynamic force F_a for substitution into Eq. 7-7 can be determined using either axial force and normal force components or lift and drag components. The normal force vector N is already known from Eq. 7-8. If tables of axial force coefficient C_A are available, they can be used to calculate axial force vector A ; then the total aerodynamic force vector F_a is immediately determined as the vector sum of the normal force vector N and the axial force vector A .

If the available aerodynamic tables are not sufficiently complete for looking up either C_A or the combination of C_L and C_D , the lift and drag forces can be calculated by assuming a parabolic drag polar, which is discussed in subpar. 5-2.2. With this assumption the lift coefficient C_L can be derived as a function of the normal force coefficient C_N , total angle of attack α_t , and zero-lift drag coefficient C_{D0} as

$$\left. \begin{aligned} C_L &= \frac{-B + \sqrt{B^2 - 4C}}{2} \\ B &= \frac{1}{k \tan \alpha_t} \\ C &= \frac{1}{k} \left(C_{D0} - \frac{C_N}{\sin \alpha_t} \right) \end{aligned} \right\}, \text{ dimensionless (7-11)}$$

where

- B and C = intermediate variables used in the calculation of C_L
 C_{D0} = zero-lift drag coefficient dimensionless
 C_L = aerodynamic lift coefficient, dimensionless
 C_N = aerodynamic normal coefficient, dimensionless
 k = constant in induced drag coefficient, dimensionless
 α_t = total angle of attack, rad (deg).

The magnitude of the aerodynamic drag is then calculated using

$$C_D = C_{D0} + kC_L^2, \text{ dimensionless} \quad (5-10)$$

with $x = 2$

$$D = 0.5\rho V_M^2 C_D S, \text{ N} \quad (5-4)$$

where

- C_D = aerodynamic drag coefficient dimensionless
 C_{D0} = zero-lift drag coefficient dimensionless
 C_L = aerodynamic lift coefficient, dimensionless
 D = magnitude of aerodynamic drag force vector D, N
 k = constant in induced drag coefficient, dimensionless
 S = aerodynamic reference area, m^2
 V_M = magnitude of velocity vector of the center of mass of the missile V_M , m/s
 ρ = atmospheric density, kg/m^3 .

The lift force is calculated by

$$L = 0.5\rho V_M^2 C_L S, \text{ N} \quad (5-5)$$

where

- C_L = aerodynamic lift coefficient, dimensionless
 L = magnitude of aerodynamic lift force vector L, N
 S = aerodynamic reference area, m^2
 V_M = magnitude of velocity vector of the center of mass of the missile V_M , m/s
 ρ = atmospheric density, kg/m^3 .

Since the drag force D is by definition directed opposite the velocity vector V_M and lift is by definition perpendicular to the velocity vector and lies in the plane formed by the velocity vector and the normal force vector, the aerodynamic force vector F_A (for substitution into Eq. 7-7) is given by

$$F_A = L \text{Norm}[(\mathbf{u}_{V_M} \times \mathbf{N}) \times \mathbf{u}_{V_M}] - D\mathbf{u}_{V_M}, \text{ N} \quad (7-12)$$

where

D = magnitude of aerodynamic drag force vector D , N

F_A = resultant aerodynamic force vector, N

L = magnitude of aerodynamic lift force vector L , N

\mathbf{N} = aerodynamic normal force vector, N

\mathbf{u}_{V_M} = unit vector in direction of velocity of missile center of mass V_M , dimensionless

$\text{Norm} []$ = indicates argument is normalized by dividing by its magnitude.

All vectors in Eq. 7-12 are in earth frame coordinates.

The vector direction of the missile centerline axis is altered by changes in the angle of attack, and in most flight simulations this vector is needed to calculate the seeker gimbal angle and also for warhead and fuzing considerations if they are included in the simulation. The missile centerline axis vector is determined from the angle of attack by using the missile velocity vector and the commanded acceleration vector to give it the proper direction, i.e.,

$$\mathbf{u}_{cl} = \text{Norm}(\mathbf{u}_{V_M} + \mathbf{u}_{A_c} \sin \alpha_t), \text{ dimensionless} \quad (7-13)$$

where

\mathbf{u}_{A_c} = unit vector in direction of lateral-acceleration-command vector A_c (normal to missile centerline), dimensionless

\mathbf{u}_{cl} = unit vector in direction of missile centerline axis, dimensionless

\mathbf{u}_{V_M} = unit vector in direction of velocity of missile center of mass V_M , dimensionless

α_t = total angle of attack, rad (deg)

$\text{Norm} ()$ = indicates argument is normalized by dividing by its magnitude.

The unit velocity vector \mathbf{u}_{V_M} and unit acceleration command vector \mathbf{u}_{A_c} are given by

$$\left. \begin{aligned} \mathbf{u}_{V_M} &= \frac{\mathbf{V}_M}{V_M} \\ \mathbf{u}_{A_c} &= \frac{\mathbf{A}_c}{A_c} \end{aligned} \right\}, \text{ dimensionless} \quad (7-14)$$

where

\mathbf{A}_c = commanded-lateral-acceleration vector, m/s^2

A_c = magnitude of commanded-lateral-acceleration vector \mathbf{A}_c , m/s^2

\mathbf{V}_M = absolute velocity of missile center of mass, m/s

V_M = magnitude of velocity vector of the center of mass of the missile \mathbf{V}_M , m/s .

This concludes the discussion of instantaneous response for simulations in which the commanded lateral acceleration is perpendicular to the missile centerline.

As mentioned earlier in this paragraph, in some simulations the calculated maneuver acceleration vector A_c is perpendicular to the tangent to the missile flight path (missile velocity vector) rather than to the missile centerline. Since the component of aerodynamic force perpendicular to the velocity vector is lift instead of normal force, certain equations must be redefined for these simulations. Instead of calculating normal force as in Eq. 7-8, lift should be calculated directly by using

$$\mathbf{L} = m\mathbf{A}_c, \text{ N} \quad (7-15)$$

where

\mathbf{A}_c = commanded-lateral-acceleration vector (normal to velocity vector in this application), m/s^2

\mathbf{L} = aerodynamic lift force vector, N

m = current missile mass, kg.

Eq. 7-15 gives the lift force vector that is required to produce the commanded-lateral-acceleration vector A_c . It is assumed that the missile responds as necessary (within any stated limits) to achieve this lift force. Instead of calculating total angle of attack at by Eq. 7-10, it is calculated by using

$$\alpha_t = \frac{L}{QSC_{L\alpha}}, \text{ rad (deg)} \quad (7-16)$$

where

$C_{L\alpha}$ = slope of curve formed by lift coefficient C_L versus angle of attack α , $\text{rad}^{-1} (\text{deg}^{-1})$

L = magnitude of aerodynamic lift force vector \mathbf{L} , N

Q = dynamic pressure parameter, Pa

S = aerodynamic reference area, m^2

α_t = total angle of attack, rad (deg).

In order to calculate the total aerodynamic force vector F_a , the lift vector calculated by Eq. 7-15-is used directly in Eq. 7-12 in lieu of the triple product. Also, instead of calculating the missile centerline vector by Eq. 7-13, it is calculated by using

$$\mathbf{u}_{ct} = \mathbf{u}_{V_M} \cos \alpha_t + \mathbf{u}_{A_c} \sin \alpha_t, \text{ dimensionless (7-17)}$$

where

\mathbf{u}_{A_c} = unit vector in direction of lateral-acceleration-command vector \mathbf{A}_c (normal to missile centerline), dimensionless

\mathbf{u}_{ct} = unit vector in direction of missile centerline axis, dimensionless

\mathbf{u}_{V_M} = unit vector in direction of velocity of missile center of mass \mathbf{V}_M , dimensionless

α_t = total angle of attack, rad (deg).

7-3.2.3.1.2 Second-Order Response

Even if the angular response time of the missile is important to the purpose of the simulation, it still may be possible to represent the missile motion with sufficient accuracy by a three-degree-of-freedom simulation in which the rotational degrees of freedom are calculated implicitly. A commonly employed approach is to assume that the transient rotational behavior of the missile conforms to a second-order dynamic system characterized by a natural frequency ω_n and a damping ratio ζ . To use this approach, ω_n and ζ for the missile being simulated must be known a priori or assumed. Let \mathbf{A}_a be the achieved-lateral-acceleration vector that results as the missile responds to the commanded-lateral-acceleration vector \mathbf{A}_c commanded by the guidance system. If a second-order response is assumed, this transient vector can be approximated in a digital simulation by (Ref. 2)

$$\begin{aligned} \dot{\mathbf{A}}_a(t) &= \dot{\mathbf{A}}_a(t - \Delta t) + \omega_n^2 [\mathbf{A}_c - \mathbf{A}_a(t - \Delta t)] \Delta t \\ &\quad - 2\omega_n \Delta t \zeta \dot{\mathbf{A}}_a(t - \Delta t), \text{ m/s}^3 \\ \mathbf{A}_a(t) &= \mathbf{A}_a(t - \Delta t) + \dot{\mathbf{A}}_a(t) \Delta t, \text{ m/s}^2 \end{aligned} \quad (7-18)$$

where

\mathbf{A}_a = achieved-lateral-acceleration vector, m/s^2
 $\dot{\mathbf{A}}_a$ = rate of change of achieved-lateral-acceleration vector, m/s^3
 \mathbf{A}_c = commanded-lateral-acceleration vector, m/s^2
 (t) = indicates that the associated variable is calculated at the current calculation time
 $(t - \Delta t)$ = indicates that the associated variable was calculated at the previous calculation time
 Δt = computation time step, s
 ζ = damping ratio of a second-order system, dimensionless

The natural frequency is the frequency at which the missile would oscillate about the pitch or yaw axis if given an initial angle of attack with no damping. The damping ratio is the ratio of the actual amount of damping to the amount of damping that causes zero overshoot, i.e., aperiodic motion, in responding to a step command. These parameters vary as functions of dynamic pressure parameter Q . The lateral acceleration, the natural frequency, and the damping are important parameters that influence the magnitude of the miss distance in engagements against maneuvering targets.

More exact integration techniques than those expressed by Eq. 7-18-discussed in Chapter 10-can be used to solve the second-order response equation. However, the assumption of a second-order transfer function is an approximation, and more accurate integration may be unwarranted.

In a three-degree-of-freedom simulation that employs a second-order-response transfer function, the normal force vector in Eq. 7-8-or the lift vector in Eq. 7-15-is calculated by using the current value of the achieved acceleration $A_s(t)$ in place of the commanded acceleration A_c . Also a unit vector in the direction of $A_s(t)$ must be used in place of \mathbf{u}_{A_c} in Eq. 7-13 or 7-17. Otherwise, the equations used to determine the aerodynamic force for second-order response simulations are the same as those for instantaneous response simulations.

7-3.2.3.2 Propulsive Force

For three-degree-of-freedom simulations, the thrust usually is assumed to act along the body centerline axis, and thus no moment is produced. The magnitude of the thrust is calculated by using Eq. 6-1, and its direction is given by the unit centerline axis vector \mathbf{u}_{ct} (Eq. 7-13 or 7-17). Thus the propulsive force F_p is given by

$$\mathbf{F}_p = F_p \mathbf{u}_{ct}, \text{ N} \quad (7-19)$$

where

\mathbf{F}_p = total instantaneous thrust force vector, N
 F_p = magnitude of total instantaneous thrust force vector \mathbf{F}_p , N
 \mathbf{u}_{ct} = unit vector in direction of missile centerline axis, dimensionless.

7-3.2.3.3 Gravitational Force

In a three-degree-of-freedom simulation the components of the gravitational force vector \mathbf{F}_g are obtained directly from Eqs. 7-4.

$$\mathbf{F}_g = \begin{bmatrix} 0 \\ 0 \\ mg \end{bmatrix}, \text{ N} \quad (7-20)$$

where

- F_g = gravitational force vector, including effects of earth rotation, N
 g = acceleration due to gravity, m/s²
 m = instantaneous mass of missile, kg.

Since these components are already expressed in earth coordinates, there is no need for a coordinate frame transformation.

This completes the description of variables for substitution into Eq. 7-7 to calculate vehicle motion with three degrees of freedom.

7-4 TARGET MOTION

In general, the equations of motion that describe the flight of a missile are equally applicable to an airborne target; however, the equations used to calculate target motion in a missile flight simulation are usually greatly simplified. The flight performance of the target is generally not an issue except to ensure that the simulated target motion is realistic enough to meet the objectives of the particular missile flight simulation. For example, if the objective of the simulation is to calculate the maximum defended area covered by a particular surface-to-air missile, straight, constant-speed target flight paths may be sufficient. At the other extreme, however, if the performance of the missile is to be studied when it engages a particular type of aircraft as it performs specified evasive maneuvers, a much more detailed model of the target is required.

7-4.1 STRAIGHT, CONSTANT-SPEED FLIGHT

When the simulated target is to fly a straight, constant-speed flight path, the target position vector at time t is calculated by using

$$\mathbf{P}_T = \mathbf{P}_{T0} + \mathbf{V}_T t, \text{ m} \quad (7-21)$$

where

- \mathbf{P}_T = position vector of target, m
 \mathbf{P}_{T0} = initial position vector of target, m
 t = simulated time, s
 \mathbf{V}_T = velocity vector (assumed constant) of target center of mass, m/s.

The initial position vector and the constant velocity vector of the target are input to the simulation. Constant speed climbs or dives with straight flight paths are modeled, using Eq. 7-21, by directing the input velocity vector along the path of the desired climb or dive.

7-4.2 MANEUVERING FLIGHT

When an aircraft is flown through defended airspace, the pilot may perform evasive maneuvers to make it more difficult for defensive gunfire or missiles to intercept his aircraft. If the pilot is aware that he is being engaged by a

particular type of missile, he may perform evasive maneuvers prescribed for use against that particular type of missile. To be most effective, the timing and direction-or directions of compound maneuvers-may be important. The magnitudes of the accelerations of evasive maneuvers are particularly important. When a pilot is not aware of a specific engagement by defensive fire, he may perform a more or less continuous series of maneuvers, called jinking, while flying through known defended regions. Other examples of target maneuvers that might be included in a missile flight simulation are terrain-following and terrain-avoidance flight paths or map-of-the-earth flight paths flown by helicopters for concealment.

Usually, the fidelity required to model the target flight path is insufficient to warrant the use of sophisticated numerical integration techniques for solving the equations of motion. The improved Euler method (Chapter 10) is commonly used to update target position and velocity from one calculation time to the next (Ref. 3). By employing this method, the target position is updated by using

$$\mathbf{P}_T(t) = \mathbf{P}_T(t - \Delta t) + \mathbf{V}_T(t - \Delta t) \Delta t + \frac{\mathbf{A}_T \Delta t^2}{2}, \text{ m} \quad (7-22)$$

where

- \mathbf{A}_T = total acceleration vector of target, m/s²
 \mathbf{P}_T = position vector of target, m
 \mathbf{V}_T = velocity vector of target, m/s
 (t) = indicates that the associated variable is calculated at the current calculation time
 $(t - \Delta t)$ = indicates that the associated variable was calculated at the previous calculation time
 Δt = computation time step, s.

The velocity vector $\mathbf{V}_T(t)$ at the end of the current calculation interval is given by

$$\mathbf{V}_T(t) = \mathbf{V}_T(t - \Delta t) + \mathbf{A}_T \Delta t, \text{ m/s.} \quad (7-23)$$

The target acceleration vector \mathbf{A}_T for substitution into Eqs. 7-22 and 7-23 is calculated by using

$$\mathbf{A}_T = \boldsymbol{\omega}_T \times \mathbf{V}_T(t - \Delta t), \text{ m/s}^2 \quad (7-24)$$

where

- $\boldsymbol{\omega}_T$ = the angular rate vector of the target flight path, rad/s (deg/s).

The method of calculating the flight path angular rate vector varies depending on the type of target maneuver. The flight path angular rate vector for controlling target maneuvers can be input as a constant or as a tabular function of time, or it can be calculated within the simulation. Equations for calculating the angular rate vector for target turns and jinking

flight paths in horizontal planes are given in the paragraphs that follow. Equations for maneuver components in the vertical plane or more complicated flight paths are beyond the scope of this handbook.

To calculate the angular rate vector that will produce the desired maneuver, a mathematical relationship between that vector and the desired maneuver is needed. Before describing this relationship, a parameter called load factor, commonly used to describe the magnitudes of vehicle maneuvers, is discussed.

7-4.2.1 Load Factor

When applied to coordinated aircraft maneuvers, no sideslip, the load factor is equal to the ratio of the lift to the weight of the aircraft (Ref. 4):

$$n_g = \frac{L}{W}, \text{ dimensionless} \quad (7-25)$$

where

L = magnitude of aerodynamic lift force vector L ,
N

n_g = load factor in units of g , dimensionless

W = weight, N.

Since $W = mg$, the maneuver load factor n_g is equivalently expressed as the ratio of the lift acceleration (the component of acceleration caused by the lift force a_{lift}) to the acceleration due to gravity g :

$$n_g = \frac{L}{mg} = \frac{a_{lift}}{g}, \text{ dimensionless} \quad (7-26)$$

where

$a_{lift} = \frac{L}{m}$ = component of aircraft acceleration
caused by the lift force, m/s^2

g = acceleration due to gravity, m/s^2

m = instantaneous mass of missile, kg.

Thus the maneuver load factor is the lift acceleration expressed in units of the acceleration due to gravity (called g 's). A 2- g maneuver has a lift acceleration equal to twice the acceleration due to gravity. In straight and level flight the lift must equal the weight to give a load factor of 1 g .

The magnitudes of target maneuvers are usually specified in terms of the load factor; however, the actual acceleration of a vehicle needed by a flight simulation must also include the 1- g downward acceleration of gravity.

7-4.2.2 Horizontal Turns

In a horizontal turn, bank angle ϕ_T is a function of only the load factor. Given the load factor, the bank angle can be calculated by using

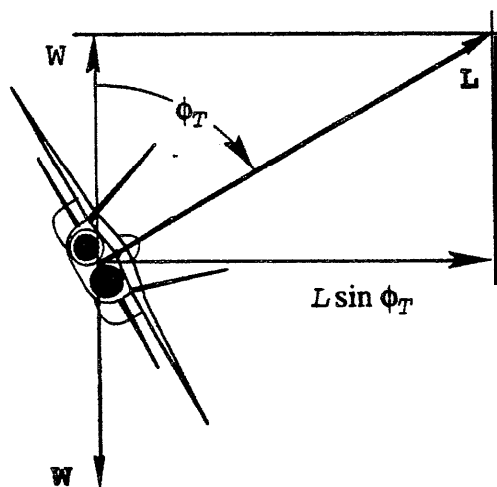
$$\phi_T = \text{Cos}^{-1}\left(\frac{1}{n_g}\right), \text{ rad} \quad (7-27)$$

where

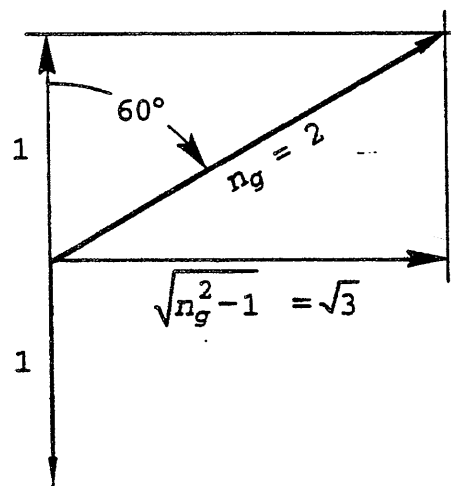
ϕ_T = target aircraft bank angle (Euler roll angle of

the target coordinate system relative to the earth coordinate system), rad (deg).

Fig. 7-1(A) shows an airplane performing a coordinated, horizontal turn with a load factor of 2 g . The bank angle for a 2- g , horizontal turn is 60 deg regardless of speed. The vertical component of the lift vector L is exactly equal and opposite to the airplane weight; otherwise, the airplane would not remain in the horizontal plane. The horizontal component of the lift vector L produces a lateral acceleration that causes the flight path to turn. The 2- g load factor vector is directed along the lift vector, as shown in Fig. 7-1(B). The gravitational component is 1 g directed vertically downward. The vector sum of these two accelerations—due



(A) Force Vectors



NOTE: Magnitude of acceleration vectors expressed in units of g

(B) Acceleration Vectors

Figure 7-1. Forces and Accelerations in Horizontal, 2- g Turn

to lift and gravity—is the total acceleration vector, which has a magnitude of $\sqrt{3}$ directed horizontally toward the center of the turn.

For horizontal, constant-speed, coordinated turns, the magnitude of the total acceleration of the aircraft can be calculated for any given load factor by using

$$A_T = g\sqrt{n_g^2 - 1}, \text{ m/s}^2 \quad (7-28)$$

where

A_T = magnitude of total acceleration vector A_T for target, m/s^2 .

For horizontal turns the angular rate vector ω_T for use in Eq. 7-24 is given by (Ref. 4)

$$\omega_T = \begin{bmatrix} 0 \\ 0 \\ A_T \\ \frac{V_T}{V_T} \end{bmatrix}, \text{ rad/s} \quad (7-29)$$

where

A_{Tc} = commanded target maneuver acceleration, m/s^2

V_T = magnitude of target velocity vector V_T , m/s .

A positive value of A_{Tc} produces right-hand turns; a negative value produces left-hand turns.

If changes in speed are desired during the turn, the magnitude of target velocity V_T is varied accordingly.

7-4.2.3 Weaves in Horizontal Plane

Although pilots employ different types of jinking maneuvers, one that is commonly employed in simulations is a simple weaving flight path in a horizontal plane.

7-4.2.3.1 Cosine Weave

The weaving flight path can be modeled as a cosine curve by calculating the maneuver acceleration as a function of time by using

$$A_{Tc} = A_{max} \cos\left(\frac{2\pi}{P_d} t_{mi}\right), \text{ m/s}^2 \quad (7-30)$$

where

A_{max} = magnitude of maximum maneuver acceleration, m/s^2

A_{Tc} = commanded target maneuver acceleration, m/s^2

P_d = period of target weave maneuver, s

t_{mi} = time since initiation of the maneuver, s.

If horizontal, coordinated maneuvers are assumed, the maximum

maneuver acceleration for substitution into Eq. 7-30 is calculated by using

$$A_{max} = g\sqrt{n_{gmax}^2 - 1}, \text{ m/s}^2 \quad (7-31)$$

where

n_{gmax} = specific maximum load factor in units of g to be applied during the maneuver, dimensionless.

The maximum load factor and the period of the maneuver are set by inputs to the simulation. The time in. in Eq. 7-30 is calculated as the difference between current simulation time t and the time when the maneuver was initiated. The maneuver initiation time may be input, or it can be calculated within the simulation as a function of the engagement, such as the time when the missile reaches a specified range from the target.

At each computation time the instantaneous maneuver acceleration A_{Tc} is substituted into Eq. 7-29 to determine the instantaneous angular rate vector ω_T of the flight path, which in turn is substituted into Eq. 7-24 to yield the instantaneous target acceleration vector A_T . The target acceleration vector A_T is then substituted into Eqs. 7-22 and 7-23 to give the position and velocity of the target at the end of the current computation interval.

7-4.2.3.2 Circular-Arc Weave

A jinking flight path that employs the maximum load factor a greater percentage of the time is similar to the cosine weave except each alternating segment of the flight path is a circular arc rather than a cosine curve. The maneuver acceleration for the circular arc weave is calculated at each computation time by using

$$A_{Tc} = A_{max} \text{sgn} \left[\cos\left(\frac{2\pi}{P_d} t_{mi}\right) \right], \text{ m/s}^2 \quad (7-32)$$

where $\text{sgn} []$ indicates the algebraic sign. (+ or -) of the argument dimensionless. The maximum maneuver acceleration for substitution into Eq. 7-32 is calculated using Eq. 7-31

As it stands, Eq. 7-32 introduces discontinuities in the target acceleration at each switch in flight-path direction, i.e., at each change in sign. In reality, to switch from a maneuver toward, for example, the left to one toward the right, the airplane must roll from a left-bank angle to a right-bank angle, which takes a finite time. Such unrealistic discontinuities are not permissible in missile flight simulations that calculate miss distance because the miss distance could be significantly affected by them. One method of remedying this problem is to pass A_{Tc} through a first-order transfer function (low-pass filter) before using it in Eq. 7-29. In a digital simulation, this transfer function is given by (Ref. 3)

$$A_{T_{ach}}(t) = A_{T_{ach}}(t - \Delta t) \exp\left(-\frac{\Delta t}{\tau}\right) + A_{T_c} \left[1 - \exp\left(-\frac{\Delta t}{\tau}\right) \right], \text{ m/s}^2 \quad (7-33)$$

where

$A_{T_{ach}}$ = magnitude of achieved flight path acceleration of target, m/s^2

A_{T_c} = commanded flight path acceleration given by Eq. 7-32

Δt = computation time step, s

(t) = indicates that the associated variable is calculated at the current calculation time

$(t - \Delta t)$ = indicates that the associated variable was calculated at the previous calculation time

τ = time constant (time to achieve 63% of a step command in a first-order system), s.

The variable A_{ach} is then employed in Eq. 7-29 in place of A_{T_c} . The time constant is selected and input by the user of the simulation to give a realistic representation of the time it takes the target to switch maneuver directions.

7-4.2.4 Roll Attitude

The roll attitude (bank angle) of the target is often required in a simulation to determine the attitude of the target reference frame. When the instantaneous load factor for a coordinated maneuver in a horizontal plane is known, Eq. 7-27 can be used to calculate the roll angle. When the load factor varies, e.g., when the maneuver acceleration is calculated using Eq. 7-30 or Eq. 7-33, however, a convenient method used to calculate the instantaneous roll angle, without having to calculate the instantaneous load factor, is given by

$$\phi_T = \text{Tan}^{-1} \left(\frac{A_{T_{ach}}}{g} \right) \text{sgn}(A_{T_{ach}}), \text{ rad (deg)} \quad (7-34)$$

where

ϕ_T = target aircraft roll angle, rad (deg)

$A_{T_{ach}}$ = magnitude of achieved flight path acceleration, m/s^2

g = acceleration due to gravity, m/s^2

$\text{sgn}()$ = indicates the algebraic sign (+ or -) of the argument, dimensionless.

If the first-order transfer function is not used, e.g., when the cosine weave is simulated, A_{ach} in Eq. 7-34 is equal to Arc.

7-5 RELATIVE MISSILE-TARGET GEOMETRY

The relative range vector R is the vector extending from the position of the missile center of mass to the position of the target center of mass. The relative range vector is identical to the line-of-sight vector from the missile to the target if the distances from the missile seeker to the missile center of mass and the distance from the track point to the target center of mass are neglected. Calculations of seeker tracking and of miss distance depend on the relative range vector.

The relative attitude, or aspect angle defined in terms of Az and El , of the target with respect to the missile is the angular orientation of the target as viewed along the line-of-sight vector.

7-5.1 RELATIVE POSITION

The position of the target relative to the missile is defined by the relative range vector R , which is calculated in the earth coordinate frame by using

$$\mathbf{R} = \mathbf{P}_T - \mathbf{P}_M, \text{ m} \quad (7-35)$$

where

\mathbf{P}_M = position vector of missile, m

\mathbf{P}_T = position vector of target, m

\mathbf{R} = range vector from missile to target, m.

In simple simulations in which perfect seeker track is assumed, the angular rate of the seeker is set equal to the angular rate of R , and the angle between R and the missile centerline axis is the seeker gimbal angle.

7-5.2 RELATIVE ATTITUDE

The relative target attitude is the orientation of the target as viewed from the missile. One use of the relative target attitude in a flight simulation is to calculate the signature of the target as viewed by the missile seeker. The relative target attitude is usually defined by two polar angles Az and El , which give the relative azimuth and elevation of the line of sight from the target to the missile, i.e., -of the negative range vector. Although there is no standardized definition, Az is often measured, as a positive rotation about the target z -axis, and El is the angle between the target xy -plane and the line of sight from the target to the missile, the polarity of which is shown in Fig. 7-2. With this definition the relative target attitude when the missile is directly ahead of the target is $Az = 0$ and $El = 0$. Values of Az are usually stated between 0 and 360 deg (or 0 to 180 and 0 to -180 deg); values of El are between +90 and -90 deg.

The relative target attitude is calculated by first transforming the line-of-sight vector R into the target reference frame and then reversing its direction, i.e.,

$$\mathbf{R}_t = -[T_{te}] \mathbf{R}_{earth}, \text{ m} \quad (7-36)$$

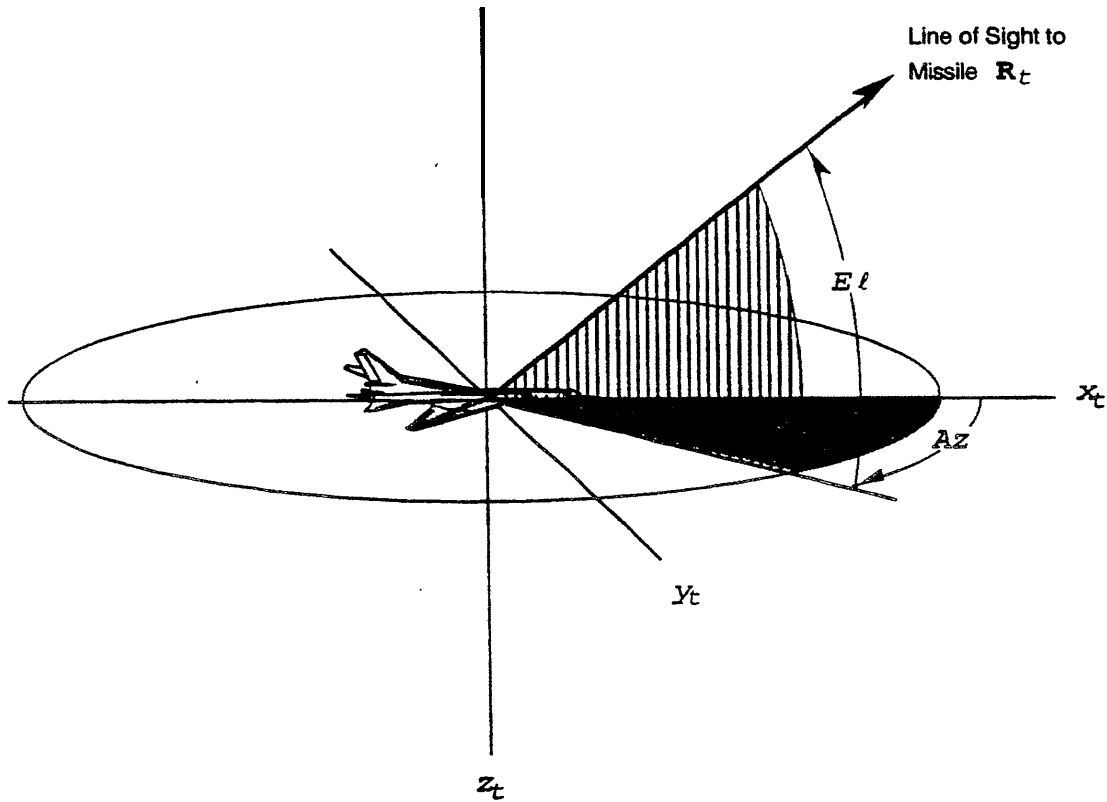


Figure 7-2. Relative Attitude of Target

where

R_{earth} = line-of-sight vector R from missile to target expressed in earth coordinates, m

R_t = line-of-sight vector from target to missile expressed in target coordinates, m

$[T_{e}]$ = transformation matrix from earth to target coordinates, dimensionless.

E_l = elevation angle measured from projection of line-of-sight vector R_t on $x_t y_t$ -plane to the vector R_t , rad (deg)

$R_{tx_t}, R_{ty_t}, R_{tz_t}$ = components of line-of-sight vector R_t expressed in target coordinate system, m.

The relative attitude is calculated by using

$$\left. \begin{aligned} Az &= \text{Tan}^{-1} \left(\frac{R_{ty_t}}{R_{tx_t}} \right) \\ El &= \text{Tan}^{-1} \left(\frac{-R_{tz_t}}{\sqrt{R_{tx_t}^2 + R_{ty_t}^2}} \right) \end{aligned} \right\}, \text{ rad (deg) (7-37)}$$

where

Az = azimuth angle measured from x_t -axis to projection of vector R_t on $x_t y_t$ -plane, rad (deg)

In simulations having a ground-based target tracker, the target attitude relative to this tracker also is determined by Eqs. 7-36 and 7-37, in which the variable R_{earth} is now defined as the vector from the ground-based tracker to the target.

7-5.3 MISS DISTANCE

One of the primary measures of merit of missile flight performance is the achieved miss distance. Missile kill probability is a function of many factors-including miss distance, fuze characteristics, warhead characteristics, and target vulnerability. Acceptable miss distance (sufficiently small) is the first criterion of a successful engagement because the fuze and warhead must be delivered relatively close to the target in order to perform their functions. Because of the complexities and uncertainties involved in predicting fuze and warhead performance and target vulner-

ability, these secondary functions are often considered separately from missile flight function.

Miss distance is usually defined as the closest approach of some point on the missile—usually the missile center of mass—to some point on the target—often the target center of mass. Sometimes miss distance is measured relative to the fuzing point on the target or to the point being tracked by the seeker; however, these points are not always well defined in a simulation, e.g., when there are multiple fuzing and/or tracking points within the target scene.

When miss distance is defined as the closest approach of the missile center of mass to the target center of mass, the closest approach occurs when the range vector R reaches a minimum. As the missile approaches the target, the range rate, i.e., rate of change of the magnitude of R , is negative, i.e., the range is becoming shorter. At the next computation time after closest approach occurs, the range begins to increase, thus the range rate becomes positive. This change in sign-of the range rate is a convenient indicator that the closest approach has occurred. At each computation time a test is made in the simulation to determine whether the range rate has become positive. When a positive range rate is detected, simulation logic causes computation of the missile flight to cease, and the flight simulation program branches into a routine that calculates the miss distance.

There are other possible causes of positive range rates. For example, a missile that is launched vertically against low-altitude targets will have a Positive range rate until the missile flight path turns toward the target. Another example occurs early in the flight of a missile launched against an outgoing target, when the target is faster than the missile. In

such cases logic must be included to prevent this positive range rate early in the flight from indicating that the closest approach has been reached.

The closest approach of the missile to the target usually occurs between the last two discrete computation times in digital simulations, as shown in Fig. 7-3; thus a way of pinpointing the closest approach between the last two computation times is needed. The usual assumption is that the computation interval is short enough that any changes in target and missile velocities between the time of closest approach and the last computation time can be neglected. The velocity vector of the target relative to the missile at the last computation time is calculated, and the target is backed up along the relative path to find the point of closest approach. The path of the target relative to the missile is defined as the straight line that passes through the target position at the last computation time and has the direction of the relative velocity vector.

The relative velocity vector is calculated by taking the difference between the target and missile velocity vectors at the last computation time, i.e.,

$$\mathbf{V}_{T/M} = \mathbf{V}_T - \mathbf{V}_M, \text{ m/s} \quad (7-38)$$

where

\mathbf{V}_M = velocity of missile relative to earth, m/s

\mathbf{V}_T = velocity of target relative to earth, m/s

$\mathbf{V}_{T/M}$ = velocity vector of target center of mass relative to missile center of mass, m/s.

Normalizing the relative velocity vector $\mathbf{V}_{T/M}$ gives the unit vector $\mathbf{u}_{V_{T/M}}$ which has the direction of the relative velocity

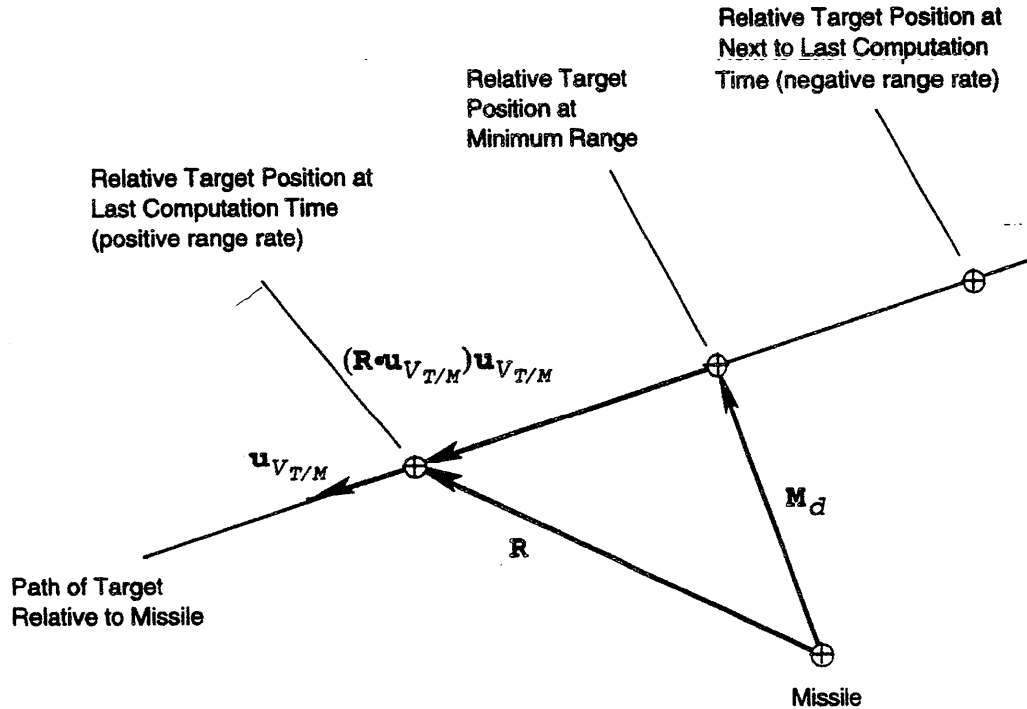


Figure 7-3. Miss Distance Vector Diagram

vector and can therefore be used to define the direction of the relative flight path.

The miss distance vector is approximated as the component of R that is perpendicular to the relative flight path at the last computation time. The time of the closest approach is approximated by calculating the time it takes the target to travel along the relative flight path from the point of closest approach to the final target position and then subtracting this calculated time from the time of the last computation (Ref. 3). Thus

$$\mathbf{M}_d = \mathbf{R} - (\mathbf{R} \cdot \mathbf{u}_{V_{T/M}}) \mathbf{u}_{V_{T/M}}, \text{ m} \quad (7-39)$$

and

$$t_{ca} = t - \frac{(\mathbf{R} \cdot \mathbf{u}_{V_{T/M}})}{V_{T/M}}, \text{ s} \quad (7-40)$$

where

- \mathbf{M}_d = miss distance vector at time of closest approach directed from missile to target, m
- \mathbf{R} = range vector, m
- $\mathbf{u}_{V_{T/M}}$ = unit vector in direction of relative velocity vector $\mathbf{V}_{T/M}$, dimensionless
- t_{ca} = time of closest approach, s
- t = simulation time, s
- $V_{T/M}$ = magnitude of velocity vector of center of mass of target relative to center of mass of missile $\mathbf{V}_{T/M}$, m/s.

The symbol \cdot indicates the vector dot product. All variables on the right-hand sides of Eqs. 7-39 and 7-40 are evaluated at the last computation time.

Because of the dominant effect of miss distance on kill probability P_k , curves of kill probability versus miss distance are sometimes used in conjunction with missile flight simulations to estimate the probability that the target would have been killed, given the miss distance calculated by the simulation (Fig. 7-4). Users of such curves should understand that the curves are necessarily based on assumptions regarding the factors that affect kill probability and that such assumptions are not always stated.

These neglected factors mainly affect how well the missile fuze is able to perform its function and how well the warhead is able to perform its function. For an actual engagement the probability that the target is killed depends on the fine structure of the warhead energy distribution, the fine structure of the structural and component vulnerabilities of the target, and the precise relative positions and attitudes of the missile and target at the instant of warhead detonation. Since the precise conditions in the endgame of an actual engagement are affected by factors not usually simulated in a flight simulation, e.g., random variations in atmospheric conditions along the missile trajectory, random warhead fragment trajectories, and random factors affecting fuze operation, such detailed analyses are usually left to simulations dedicated to studies of warhead and fuze operation.

The band of values of miss distance between "sure-kill" and "sure-safe" is usually relatively narrow. (Often the precisions of a flight simulation and of the kill-probability-versus-miss-distance curve are considered insufficient for reliable estimation of differences in kill probability within this band. In these cases a single miss distance criterion is often used that is usually based on the miss distance for a kill probability of 50%. This criterion is called the lethal radius. Simulated engagements that result in miss distances

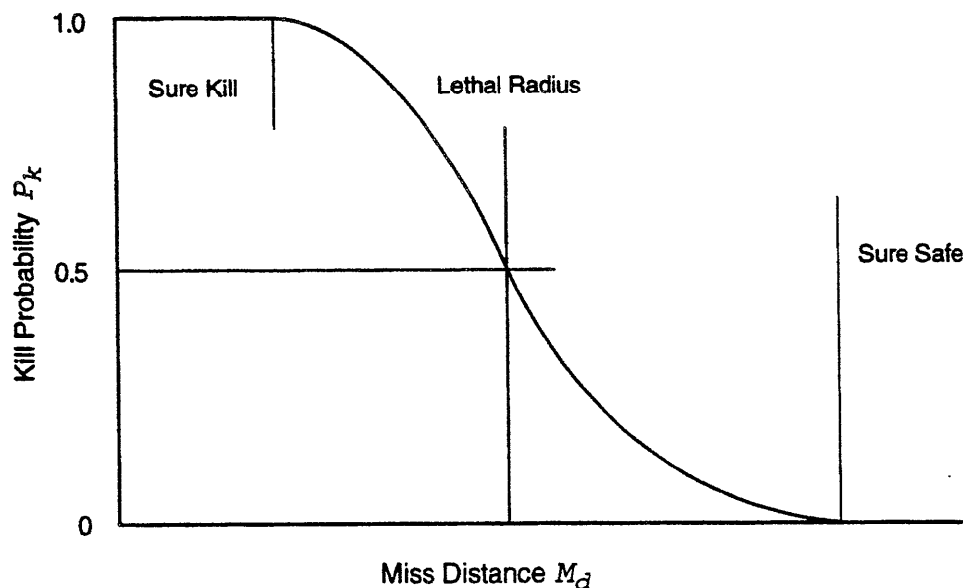


Figure 7-4. Typical Dependence of P_k on Miss DM.ante

smaller than the lethal radius are considered to be successful kills, and those with miss distances greater than the lethal radius are considered to be unsuccessful misses. Gross criteria such as the lethal radius are useful in studies of the relative effectiveness of alternative missile designs and of countermeasures, but they should not be considered to give accurate estimates of the actual effectiveness of a given missile under precisely defined conditions.

REFERENCES

1. J. E. Cochran, Jr. and J. R. Beaty, Simulation of the Flight of a Short Range Air Defense System Rocket Before Radar Acquisition, Final Report, US Army Research Office, Engineering Experiment Station, Auburn University, Auburn, AL, April 1977.
2. J. Malick (personal communication, documented in unpublished paper), "Missile Engagement Simulation Model", by G. A. Branch, SRI International, Menlo Park, CA, November 1983.
3. M. A. Garcia, A Simple Analytical Model of an Air-to-Air Guided Missile for Rapid Flight Simulation, Technical publication TP-72-7, Naval Missile Center, Point Mugu, CA., 17 February 1972.
4. R. S. Shevell, Fundamentals of Flight, Prentice-Hall, Inc., Englewood Cliffs, NJ, 1983.

BIBLIOGRAPHY

COORDINATE FRAMES

- L. D. Duncan, Coordinate Transformations in Trajectory Simulations, Atmospheric Sciences Laboratory, White Sands Missile Range, NM, February 1966.

SIMULATING VEHICLE MOTION

33. L. Byrum and G. E. Russell, "General Airframe Dynamics of a Guided Missile", Journal of The Aeronautical Sciences, 534-40 (August 1955).
- P. N. Jenkins, Missile Dynamics Equations for Guidance and Control Modeling and Analysis, Technical Report RG-84-17, Guidance and Control Directorate, US Army Missile Laboratory, US Army Missile Command, Redstone Arsenal, AL, April 1984.
- A. B. Markov, A Nonlinear Six-Degree-of-Freedom Ballistic Aerial Target Simulation Model, Vol. 1, Theoretical Development, Suffield Memorandum No. 1081, PCNNO.21V10, Defence Research Establishment Suffield, Ralston, Alberta, Canada, February 1984.
- C. P. Schneider, "Application to Missile Dynamics", AGARD Lecture Series No. 18, MBB-UA-553/80, Advisory Group for Aerospace Research and Development, North Atlantic Treaty Organization, Neuilly sur Seine, France, 1980.

CHAPTER 8

GUIDANCE AND CONTROL MODELING

Methods of simulating the guidance and control functions of a missile are described in this chapter. Since simulation methodology depends on the type of missile guidance system being simulated and on the objectives of the simulation itself, specific computational methods are given to meet different modeling requirements. The guidance and control functions considered are seekers, guidance processors, autopilots, and control systems.

Methods of modeling optical and radio frequency (RF) seekers are given for a wide range of fidelity levels. Lower levels of seeker fidelity are represented by perfect tracking and by accurate tracking but with a time lag. An intermediate fidelity seeker model-useful for analyzing the effects of multiple track points within the seeker field of view-is described. And for simulations that require the highest seeker fidelity, employment of actual missile seeker hardware in the simulation loop is described.

Equations are presented for modeling the guidance system processor at various levels of fidelity for both missile borne and ground-based target trackers. The types of guidance laws considered are proportional navigation, command, and command to line of sight. A method of employing a transfer function to simulate the control system response to guidance commands is described.

Missile hardware-in-the-loop simulations are discussed for two basic approaches to hardware substitution-missile seeker in the loop and missile electronics in the loop. Also employment of actual missile autopilot and control system hardware in the simulation loop is described. A checklist of special considerations of laboratory procedures for using hardware in the simulation loop is provided.

8-0 LIST OF SYMBOLS

\mathbf{A}_c = commanded-lateral-acceleration vector, m/s^2	\mathbf{g}_n = vector of component of acceleration due to gravity normal to missile flight path, m/s^2
A_c = magnitude of commanded-lateral-acceleration vector \mathbf{A}_c , m/s^2	K_s = servo system gain, s^{-1}
A_{C_c} = Coriolis term in acceleration command, m/s^2	k_1 = guidance proportionality constant, $(m/s^2)/rad$
$A_{c_{yb}}$ = component of commanded-lateral-acceleration vector \mathbf{A}_c on y-axis of body frame, m/s^2	k_2 = guidance proportionality constant, $(m/s^2)/(rad/s)$
$A_{c_{zb}}$ = component of commanded-lateral-acceleration vector \mathbf{A}_c on z-axis of body frame, m/s^2	k_3 = guidance proportionality constant, dimensionless
\mathbf{d}_1 = distance vector from missile center of mass to seeker, m	NR = navigation ratio, dimensionless
\mathbf{d}_2 = distance vector from target center of mass to tracking point, m	NR_{eff} = effective navigation ratio, dimensionless
\mathbf{e} = vector of error in missile position relative to the guideline, m	\mathbf{P}_B = position vector of a point on the guideline at the point of intercept with the error vector \mathbf{e} , m
$\dot{\mathbf{e}}$ = vector rate of change of error vector \mathbf{e} , m/s	\mathbf{P}_M = position vector of missile, m
e = magnitude of missile position error relative to the guideline, m	\mathbf{P}_T = position vector of target, m
\dot{e} = magnitude of rate-of-change vector $\dot{\mathbf{e}}$, m/s	p_c = commanded roll rate, rad/s
$G(s)$ = control system transfer function, dimensionless	\mathbf{R} = range vector from missile center of mass to target center of mass, m
G_d = seeker discriminator gain function, dimensionless	R = magnitude of range vector \mathbf{R} from missile center of mass to target center of mass, m
G_l = overall autopilot lateral channel gain, $rad/(m/s^2)$	s = Laplace variable
G_r = overall autopilot roll channel gain, $rad/(rad/s)$	t = simulated time, s
$G_s(M, h)$ = system gain as a function of Mach number and altitude, $(m/s^2)/(rad/s)$	(t) = indicates that the associated variable is calculated at the current calculation time
\mathbf{g} = acceleration due-to-gravity vector, m/s^2	$(t-\Delta t)$ = indicates that the associated variable was calculated at the previously calculation time
	\mathbf{u}_{A_c} = unit vector in direction of commanded-lateral-acceleration vector \mathbf{A}_c , dimensionless
	\mathbf{u}_c = unit vector in the direction of the component of the Coriolis acceleration command that is perpendicular to the missile centerline, dimensionless

\mathbf{u}_{cl} = unit vector in the direction of the centerline axis of the missile, dimensionless
 \mathbf{u}_e = unit vector in the direction of the component of \mathbf{e} that is perpendicular to the missile centerline, dimensionless
 $\mathbf{u}_{\dot{e}}$ = unit vector in the direction of the component of $\dot{\mathbf{e}}$ that is perpendicular to the missile centerline, dimensionless
 \mathbf{u}_{gl} = unit vector that represents the direction of the guideline, dimensionless
 \mathbf{u}_{PM} = unit vector in direction of missile position vector \mathbf{P}_M , dimensionless
 \mathbf{u}_{PT} = unit vector in direction of target position vector \mathbf{P}_T , dimensionless
 \mathbf{u}_{sa} = unit vector in direction of seeker boresight axis, dimensionless
 \mathbf{u}_{VM} = unit vector in direction of velocity of missile center of mass \mathbf{V}_M , dimensionless
 \mathbf{V}_{Bperp} = component of velocity of Point B perpendicular to the guideline, m/s
 \mathbf{V}_M = velocity vector of missile center of mass relative to earth, m/s
 \mathbf{V}_{Mperp} = component of missile velocity vector \mathbf{V}_M perpendicular to the guideline, m/s
 \mathbf{V}_T = velocity vector of target center of mass relative to earth, m/s
 \mathbf{V}_{TIM} = velocity vector of center of mass of target relative to center of mass of missile, m/s
 V_c = closing speed, m/s
 V_M = magnitude of velocity vector of center of mass of missile \mathbf{V}_M , m/s
 W_f = seeker response weighting function, dimensionless
 y_b, z_b = subscripts indicating components in body reference frame, dimensionless
 α_t = total angle of attack, rad (deg)
 $\dot{\gamma}$ = angular rate of the flight path, rad/s (deg/s)
 Δt = computation time step, s
 δ = achieved control-surface deflection angle, rad
 $\dot{\delta}$ = angular rate of control-surface deflection, rad/s
 δ_c = commanded control-surface deflection angle, rad
 δ_i = deflection angle of i th control surface, $i = 1, 2, 3, 4$, rad
 $\delta(s)$ = Laplace transform of achieved control-surface deflection, rad
 $\delta_c(s)$ = Laplace transform of commanded control-surface deflection, rad
 ϵ = tracking error angle (angle between line of sight to target and seeker boresight axis), rad (deg)
 ζ = damping ratio of a second-order system, dimensionless
 λ = gimbal angle, rad (deg)
 σ = line-of-sight vector from seeker to tracking point, m

σ = magnitude of the line-of-sight vector σ from seeker to tracking point, m
 τ = time constant (time to achieve 63% of a step command in a first-order system), s
 τ_1 = time constant for seeker dynamics, s
 τ_2 = time constant for signal processing and autopilot, s
 ϕ = missile roll angle, rad (deg)
 ω_{ach} = achieved angular rate vector of the seeker boresight axis, rad/s (deg/s)
 ω_c = commanded seeker tracking rate vector, rad/s (deg/s)
 ω_f = final processed seeker rate signal vector, rad/s (deg/s)
 ω_{gl} = angular rate vector of the guideline, rad/s (deg/s)
 ω_σ = angular rate vector of the line of sight from the seeker to the tracking point, rad/s (deg/s)
 ω_{max} = maximum angular track rate capability of seeker, rad/s (deg/s)
 ω_n = undamped natural frequency of a second-order system, rad/s (deg/s)
 ω_σ = magnitude of angular rate vector ω_σ of the line of sight to the target, rad/s (deg/s)

8-1 INTRODUCTION

This chapter presents the equations for modeling the seeker, autopilot, and control functions in a missile flight simulation and describes the substitution of guidance and control hardware within the simulation loop. As discussed in Chapter 2, the target track sensor (seeker for homing missiles) senses electromagnetic radiation generated by the target or reflected from it. This radiation is processed by the missile guidance system to determine the acceleration commands required to maneuver the missile to intercept the target. The autopilot interprets the acceleration command signals generated by the guidance processor to determine which control surfaces to deflect and how large a deflection is required. Control-surface deflection commands are passed to the control system where power is applied to the actuators to deflect the control surfaces.

In five- and six-degree-of-freedom missile flight simulations, these control-surface deflections are needed in the aerodynamics equations (described in Chapter 5) to calculate the aerodynamic forces and moments applied to the missile. For three-degree-of-freedom simulations in which control-surface deflections are not calculated explicitly the autopilot and control systems of the missile are assumed to operate properly, and missile motion is calculated based on the commanded-lateral-accelerations, as described in Chapter 7.

Almost all missiles that have seekers employ proportional navigation, which depends on the angular tracking rate of the seeker head. Simple guidance models track only a single point-target; equations used to calculate the angular

rate of the seeker head for such models are given in subpars, 8-2.1.1 and 8-2.1.2. To evaluate the effects of multiple targets or a target consisting of multiple points, a more complex seeker model is required. A model with intermediate fidelity, which can respond to multiple objects within the field of view (FOV), is described in subpar. 8-2.1.3.

Classical proportional navigation rarely is implemented exactly, particularly in a homing missile system, because it requires the missile velocity vector, which usually is not available onboard. Closing velocity may be available onboard missiles with radio frequency (RF) seekers, and its use in implementing the guidance law in place of the inertial velocity of the missile changes the effective navigation ratio. In missiles with infrared (IR) seekers the navigation ratio may be established intrinsically by the electrical, mechanical, and aerodynamic design of the seeker and control system rather than by setting a gain in the autopilot. In this case the effective navigation ratio may vary with Mach number and altitude.

Missile systems may employ guidance laws other than proportional navigation. The equations used to calculate beam-rider or command-t-line-of-sight guidance are presented in subpar. 8-2.4.3.

Actual missile hardware components are often employed within a simulation loop to ensure accurate representation of guidance and control components and to eliminate the need for validating very complex mathematical models of the components. Employment of hardware-in-the-loop is divided into two general categories, i.e., missile-seeker-in-the-loop simulations and missile-seeker-electronics-in-the-loop simulations. A missile-seeker-in-the-loop simulation uses an actual hardware seeker and generates physical electromagnetic radiation for the seeker to view. A missile-seeker-electronics-in-the-loop simulation employs hardware of the guidance and control electronic circuits but does not generate actual physical radiation. Instead, the target scene is prerecorded in the field and presented to the hardware circuits electronically. Methods for employing missile hardware-in-the-loop are presented in par. 8-4.

8-2 GUIDANCE MODELING

The degree of fidelity needed in guidance system modeling differs among applications because of the wide variety of uses of missile flight simulations. A high-fidelity mathematical simulation of a guidance system can require an extremely complex computer program. For this reason, actual hardware sometimes is substituted for mathematical modeling of guidance system components. In simulations that require less fidelity in the guidance model, it may be adequate to assume that the guidance law is implemented perfectly by the missile guidance system, i.e., that the seeker measurements are assumed to be accurate with no lags and that guidance processing, autopilot functions, and control system functions are performed perfectly. Between the assumption of perfect guidance and the employment of

actual missile hardware, there is a wide range of possible levels of sophistication of guidance system modeling. Representative levels of modeling are presented in the subparagraphs that follow.

8-2.1 SEEKER MODELING

As discussed in Chapter 2, seekers are basically of two types-optical and radio frequency. The guidance law employed in most applications of missile seekers is some form of proportional navigation (subpar. 2-3.2.4). To implement proportional navigation in a missile, the seeker measures the angular rate of the line of sight from the missile to the target. Since the seeker tracks the target, the angular rate of the seeker boresight axis is used as a measure of the angular rate of the line of sight. In a simulation of missile flight the intermediate details of how the seeker tracks and how the measurement is made are not necessary for predicting flight performance if the accuracy and the timeliness of this measurement are known and included in the simulation. It is only when the use of a simulation includes evaluations of the performance of the seeker itself that the seeker functions must be modeled in detail. In simulations requiring only low-fidelity seeker models, the equations that describe IR and RF seekers are similar and in some cases may be identical. When intermediate levels of seeker-model fidelity are required, the models of IR and RF seekers may still be much alike. For example, differences in the accuracy and timeliness of the measurements of different types of seekers can be expressed in similar mathematical structures through limits, gains, time constants, and functional relationships. On the other hand, very high-fidelity mathematical simulations of seekers require models that include a large amount of detail in the areas of electromagnetic sensing and signal processing. As such, a high-fidelity model of an IR? seeker would be very different from a high-fidelity model of an RF seeker.

8-2.1.1 Perfect Seeker

When the details of the operation of the seeker are not important to the objectives of a simulation, a simplified seeker model can be employed. A common assumption in this case is that the seeker is perfect. A perfect seeker would always track the target accurately with no time lags. The advantage of such a seeker model in a simulation is that it is easy to model and requires minimal computation time. Such a model is adequate, for example, for simulations employed to determine general missile kinematic launch boundaries but not for evaluating countermeasures.

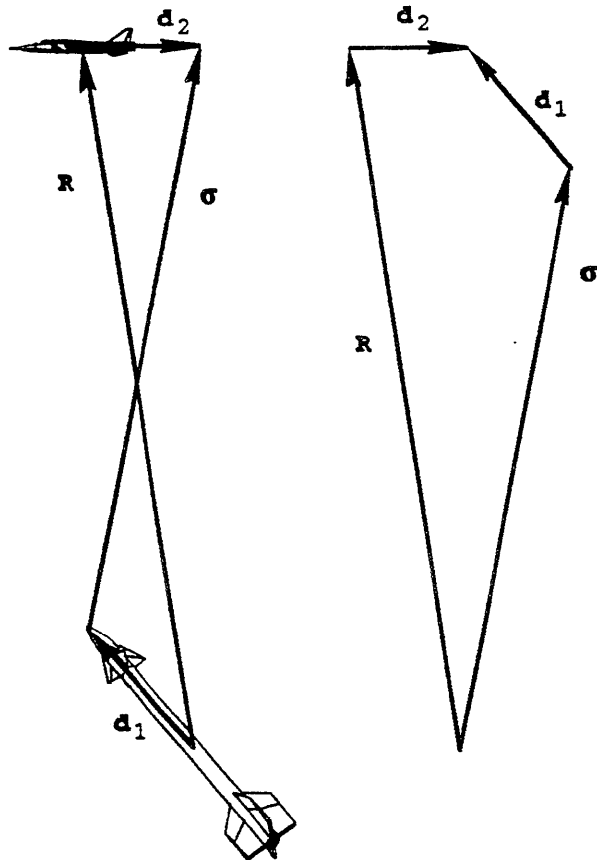
In a perfect-seeker model the boresight axis of the seeker is always directed along the line of sight from the seeker to the target. Therefore, the measured angular rate is always accurate and equal to the angular rate of the line of sight. The relatively short distance from the missile center of mass to the seeker head often is considered to be negligible and is not always included in the geometric calculations. Like-

wise, the distance of the tracking point on the target from the center of mass of the target is often considered negligible; thus the line-of-sight vector σ from the seeker to the tracking point on the target can be approximated by the range vector R . In simulations in which the displacements of the seeker and/or the tracking point from the respective centers of mass are to be accounted for, the line-of-sight vector must be redefined by accounting for the displacement vectors, as shown in Fig. 8-1. In this case the line-of-sight vector σ is given by

$$\sigma = R - d_1 + d_2, m \quad (8-1)$$

where

- d_1 = distance vector from missile center of mass to seeker, m
- d_2 = distance vector from target center of mass to tracking point, m
- R = range vector from missile center of mass to target center of mass, m
- σ = line-of-sight vector from seeker to tracking point, m.



(A) Geometrical Relationships (B) Vector Diagram

Figure 8-1. Relationship Between Range Vector and Line of Sight to Tracking Point

The angular rate vector of the line of sight is given by

$$\omega_{\sigma} = \frac{(\sigma \times V_{T/M})}{\sigma^2}, \text{ rad/s} \quad (8-2)$$

where

- $V_{T/M}$ = velocity vector of center of mass of target relative to center of mass of missile, m/s
- σ = line-of-sight vector from seeker to tracking point, m
- σ = magnitude of the line-of-sight vector σ from the seeker to the tracking point, m
- ω_{σ} = angular rate vector of the line of sight from the seeker to the tracking point, rad/s.

Eq. 8-2 is based on the assumption that the angular rates of the missile and target about their respective centers of mass contribute only negligible amounts to ω_{σ} . The most convenient reference frame for evaluating Eq. 8-2 is the guidance frame. If sufficient accuracy is obtained by assuming that d_1 and d_2 are negligible relative to the range vector, R and R can be substituted for σ and σ , respectively, in Eq. 8-2.

The range vector R for substitution into Eq. 8-1 (or Eq. 8-2 where applicable) is calculated by Eq. 7-35, repeated here for convenience:

$$R = P_T - P_M, m \quad (7-35)$$

where

- P_M = position vector of the missile, m
- P_T = position vector of the target, m.

The relative velocity vector $V_{T/M}$ is given by

$$V_{T/M} = V_T - V_M, \text{ m/s} \quad (7-38)$$

where

- V_M = velocity vector of missile center of mass relative to earth, m/s
- V_T = velocity vector of target center of mass relative to earth, m/s
- $V_{T/M}$ = velocity vector of the center of mass of the target relative to center of mass of the missile, m/s.

If perfect tracking is assumed, the angular rate vector of the seeker head ω_{σ} constitutes the seeker measurement used to calculate the missile commanded-lateral-acceleration vector A . (See Eq. 8-8.)

An actual seeker head is mechanically limited in its angular displacement relative to the missile centerline. If the relative position of the target moves beyond the angular hits of the seeker, the seeker can no longer track it, and large errors occur in the measurement of the line-of-sight rate. When an IR seeker strikes the gimbal stops, i.e., reaches its limiting angular displacement, the spinning head-acting as

a gyro-goes out of control and loses track on the target never to regain it. In simple models common practice is to terminate the computer run if the seeker gimbal angle—the angle between the missile centerline and the boresight axis of the seeker—reaches its maximum value, which is an input to the program. The gimbal angle λ is calculated at each integration step by using

$$\lambda = \text{Cos}^{-1}(\mathbf{u}_{sa} \cdot \mathbf{u}_{ct}), \text{ rad (deg)} \quad (8-3)$$

where

\mathbf{u}_{ct} = unit vector in direction of the centerline axis of the missile, dimensionless

\mathbf{u}_{sa} = unit vector in direction of the boresight axis of the seeker, dimensionless

λ = gimbal angle, rad (deg).

In seeker models with perfect tracking, the unit-seeker-axis vector \mathbf{u}_{sa} , for substitution into Eq. 8-3, is calculated by normalizing the line-of-sight vector σ . The unit-centerline vector \mathbf{u}_{ct} is calculated by using Eq. 7-13:

$$\mathbf{u}_{ct} = \text{Norm}(\mathbf{u}_{VM} + \sin(\alpha_t)\mathbf{u}_{Ac}), \text{ dimensionless} \quad (7-13)$$

where

\mathbf{u}_{Ac} = unit vector in direction of commanded-lateral-acceleration command vector \mathbf{A}_c (normal to the missile centerline), dimensionless

\mathbf{u}_{ct} = unit vector in direction of the missile centerline axis, dimensionless

\mathbf{u}_{VM} = unit vector in direction of velocity of missile center of mass \mathbf{V}_M , dimensionless

α_t = total angle of attack, rad (deg)

$\text{Norm}()$ = indicates argument is normalized by dividing by its magnitude.

In simulations using simple seeker models, the computer run may be terminated also if the magnitude of the angular line-of-sight rate ω_σ exceeds a maximum angular tracking rate ω_{max} because this also would cause the actual seeker to lose target track. The limiting angular rate can be a constant input value, or it can be tabulated as a function of signal strength to represent more accurately the angular rate limits of IR seekers.

8-2.1.2 Accurate Tracking With Time Lag

In an actual missile, torquing moments are applied to the seeker head to cause the seeker boresight axis to follow the line of sight to the target. A small but finite time is required for the signal processing that determines the required direction and magnitudes of these moments, for the application of the moments, and for the response of the seeker head. In addition, as the seeker head responds, a signal proportional

*Although the treatment of the time lags produced in the guidance processor and autopilot logically fit in subpars, 8-2.2, "Guidance Processor Modeling", and 8-2.3, "Autopilot Modeling", these lags are introduced here in the "Seeker Modeling" paragraph because their treatment is parallel with and closely associated with the time lag produced in the seeker.

to the seeker head angular rate must be generated and processed by the guidance system and autopilot to generate control-surface deflection commands. This introduces additional time lags.* One step toward a more realistic seeker simulation is to incorporate these time lags into the equations for a perfect seeker. A common method of including such lags is to treat the seeker head rotation, guidance processor, and autopilot as a series of first-order dynamic systems with appropriate time constants. These could be lumped into a single system with an equivalent time constant, except that the seeker pointing direction is needed in the simulation, and this pointing direction at any given instant is independent of subsequent guidance processor and autopilot time lags. Therefore, one approach is to employ a time constant τ_1 to represent all the lags associated with seeker head rotation and a second time constant τ_2 to represent the remaining time lags associated with guidance processing and the autopilot. Thus the commanded seeker head angular rate vector ω_c is passed through a first-order digital filter with time constant T_1 to yield the achieved seeker head angular rate ω_{ach} . If no rate bias (discussed in subpar. 8-2.1.3) is employed, the commanded seeker head angular rate ω_c is identical to the line-of-sight angular rate ω_σ . Fig. 8-2 illustrates the response of a first-order seeker to a step command. In turn, the achieved angular rate ω_{ach} of the seeker is passed through a similar digital filter with time constant T_2 to yield the final processed tracking rate signal vector ω_f . The first-order filter equations for calculating these responses are

$$\left. \begin{aligned} \omega_{ach}(t) &= \omega_{ach}(t - \Delta t) \exp(-\Delta t/\tau_1) \\ &\quad + \omega_c [1 - \exp(-\Delta t/\tau_1)], \text{ rad/s (deg/s)} \\ \omega_f(t) &= \omega_f(t - \Delta t) \exp(-\Delta t/\tau_2) \\ &\quad + \omega_{ach} [1 - \exp(-\Delta t/\tau_2)], \text{ rad/s (deg/s)} \end{aligned} \right\} \quad (8-4)$$

where

(t) = indicates that the associated variable is calculated at the current calculation time

$(t - \Delta t)$ = indicates that the associated variable was calculated at the previous calculation time

Δt = computation time step, s

τ_1 = time constant for seeker dynamics, s

τ_2 = time constant for signal processing and autopilot, s

ω_{ach} = achieved angular rate vector of the seeker boresight axis, rad/s

ω_c = commanded seeker tracking rate vector, rad/s

ω_f = final processed seeker rate signal vector, rad/s (deg/s).

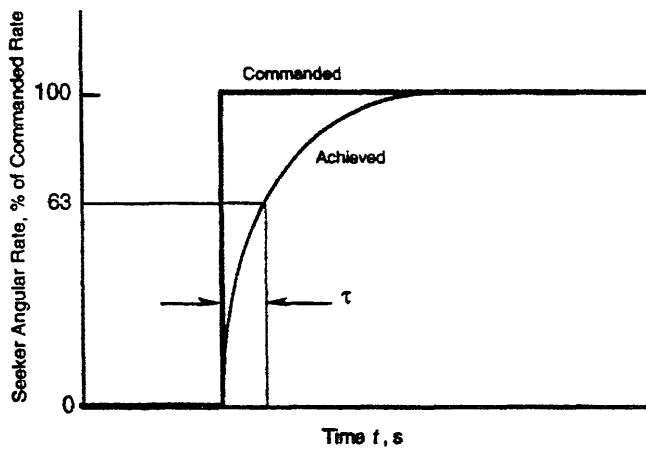


Figure 8-2. Response of First-order Seeker to Step Command

The final processed seeker rate signal vector w_f is employed in the guidance equations to calculate the commanded-lateral-acceleration vector A_c .

The values of the time constants in Eqs. 8-4 are selected to produce simulated seeker and guidance processor time lags that approximate those of the actual missile system.

8-2.1.3 Intermediate-Fidelity Seeker Model

To study the effects of multiple targets, such as decoys, that are within the field of view of the seeker or a single target with distributed tracking points, such as RF glint points or multiple IR sources, a more sophisticated seeker model is required. Very sophisticated seeker models have been developed for use in seeker design analyses; however, their complex setup procedure, their long computer running time, and their uniqueness to specific seeker designs make them unacceptable for use in generalized studies that involve large numbers of computer runs. Such sophisticated models of specific seeker designs are outside the scope of this handbook.

Seeker models of intermediate fidelity fill the gap between the simple seeker models and the very sophisticated seeker models or the use of seeker hardware in the simulation. Simple seeker models have been enhanced to allow multiple targets and multipoint targets by letting the position of the single tracking point be calculated by using weighted averages of the signal strengths of the individual radiating points. For example, one type of model is constructed such that the point tracked by the seeker is the centroid of the powers of all the radiating points within the field of view of the seeker. Fig. 8-3 shows the tracking point of a centroid tracker for an example case in which the signal strength of the decoy is four times that of the target. Although a number of studies of countermeasures effectiveness employ some type of centroid model, such models lack the fidelity required to analyze the effects of detailed seeker characteristics that are important when multiple sources of radiation are present within the FOV.

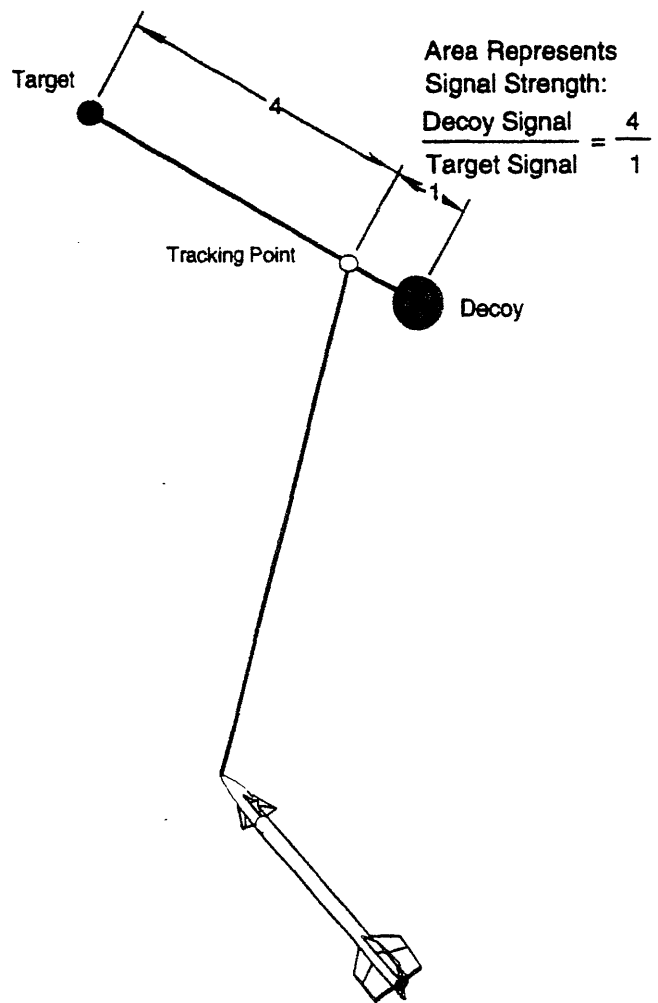


Figure 8-3. Tracking Point of Centroid Tracker

As countermeasures and counter-countermeasures become more sophisticated a more thorough understanding of their effects on various types of missile seekers is needed. Thus it is necessary to ensure that seeker models used in studies of countermeasures are responsive to subtle differences in timing, geometry, and signal characteristics of all signal sources within the field of view. One type of seeker model that fulfills this requirement aggregates many of the complex features of the seeker into simple tabular functions that are input to the simulation. These functions are calibrated to yield results representative of the performance of a given actual seeker operating with multiple signal sources. The fact that many complicated functions are aggregated reduces computer running time while at the same time retains a considerable degree of fidelity relative to the actual seeker that it represents.

Facilities that use these aggregated seeker models typically develop their models to emphasize whatever considerations are important to their particular applications. One such model has been used extensively to investigate general countermeasure and counter-countermeasure concepts (Ref. 1). The approach used in this model is to process all the sig-

nals within the FOV of the seeker to determine the instantaneous seeker tracking command. Each signal source contributes a weighted fraction of the overall command depending on its signal strength and its position within the seeker FOV. In an actual seeker, signal sources near the boresight axis of the seeker usually cause a commanded seeker tracking rate that is approximately proportional to the off-boresight angle, i.e., the angle between the line of sight to the target and the seeker boresight axis. The response of an actual seeker to signal sources that are farther from the boresight axis, i.e., larger off-boresight angle, depends on the particular seeker design-e.g., the reticle design in IR spin-scan seekers; the reticle design and the fraction of time that the signal is within view for IR conical scan seekers; and the beam shape, squint angle, and side-lobes in RF seekers.

To account for these variations in seeker responses, the seeker model uses two tabular functions that are part of the input characteristics for the particular seeker being modeled. These functions are called the discriminator gain function and the response weighting function.

The discriminator gain function accounts for the nominal gain designed into the seeker to relate the commanded tracking rate to the boresight tracking error, i.e., the off-boresight angle. For an IR seeker this is called the static-gain curve. In an RF seeker it is similar to the sum-channel curve. The response weighting function accounts for all other factors that affect the relationship between the commanded seeker tracking rate and the position of the signal source within the seeker FOV. For an IR seeker, for example, the effects of special reticle pattern shapes to aid in discriminating decoys are included in the weighting function. The weighting function for an RF seeker resembles a difference-channel curve. Thus rather than model the detailed reticle and scanning characteristics of an IR seeker, its response characteristics are aggregated into the discriminator gain function and the response weighting function. Similarly, for an RF seeker aggregated tabular functions representing that particular seeker's characteristics are used in place of modeling the radar beam shapes and positions. Typical discriminator gain curves and response weighting functions are illustrated in Fig. 8-4. The discriminator gain function G_d and response weighting function W_f are given as functions of the normalized boresight error. The boresight angular error ϵ is normalized by dividing it by one-half the FOV of the seeker, i.e., $FOV/2$. Thus the normalized boresight error has a value of zero for an object at the center of the FOV of the seeker (on the boresight axis) and a value of one for an object at the outer edge of the FOV.

All calculations in this particular seeker model are based on vectors expressed in the earth reference frame. Although the model could be formulated to use the more sophisticated numerical integration techniques described in Chapter 10, great utility and sufficient fidelity for many applications have been obtained by using the simple integration tech-

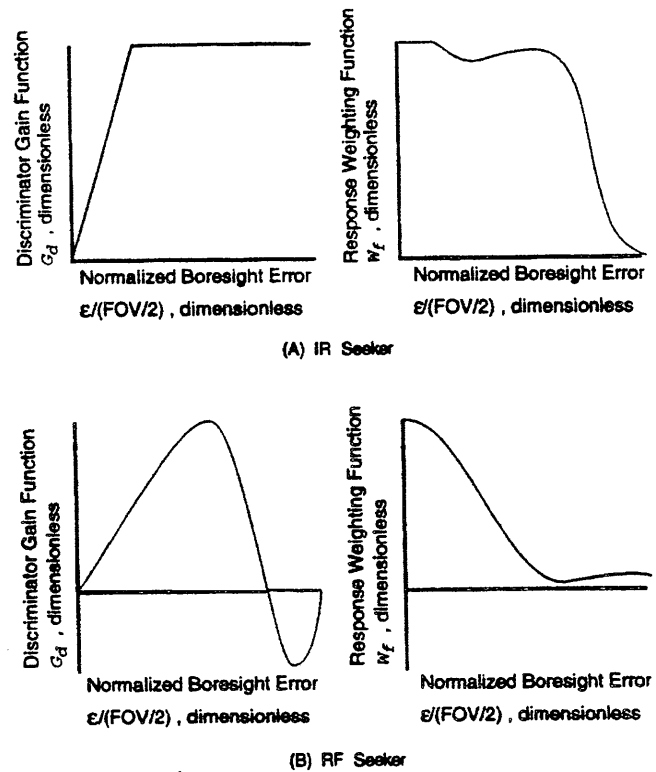


Figure 8-4. Typical Discriminator Gain and Seeker Weighting Functions

nique in which the seeker head angular rate is assumed to be constant from the beginning to the end of an incremental computation time step.

As the target-moves angularly relative to the missile seeker, the seeker boresight pointing direction must be rotated in order to track the target. At any given instant the angular tracking rate required to correct the boresight pointing direction-the commanded tracking rate-depends on the relative signal strengths and positions of all the signal sources within the seeker FOV. In the simulation model the commanded tracking rate w_c emerges in the form of a vector that gives the magnitude and direction of the commanded rate of change of the seeker pointing direction. In an actual IR seeker the commanded tracking rate is in the form of the seeker head gyro torquing voltage. In an RF seeker it may be in the form of seeker head actuator commands or array phasing commands.

In the model the magnitude and direction of the commanded tracking rate vector is based on a signal-sum vector that accounts for the contributions of all the signal sources within the instantaneous FOV of the seeker. The magnitude of the signal-sum vector is the summation of the products of the discriminator gain, weighting function, and signal intensity of each individual signal source; the direction of the signal-sum vector is the vector summation of the component tracking rate directions contributed by each individual signal source. Thus the signal-sum vector accounts for the

intensity, signal attenuation, and position of each signal source within the seeker FOV. The signal intensity of each individual source is established by inputs and may be controlled by simulation logic depending on factors such as range to the target, time, or relative aspect.

Some IR missiles bias the commanded seeker tracking rate to cause the seeker to track ahead of the IR source, which typically is the exhaust plume of the target, as shown in Fig. 8-5. This is called rate bias, and it is implemented by adding a commanded tracking rate component in the direction that causes the seeker boresight axis to rotate toward alignment with the missile axis. That is, rate bias reduces the seeker gimbal angle. (The seeker gimbal angle is defined in subpar. 8-2.1.1.)

As discussed in subpar. 8-2.1.2, a time lag exists between the commanded tracking rate and the achieved tracking rate that is caused by seeker rotational dynamics, and an additional time lag results from signal processing in the guidance and autopilot systems. As with the simple guidance models, these lags can be simulated in a digital model with intermediate fidelity by passing the commanded tracking rate w_c through a pair of digital, first-order lag (low-pass) filters in series (Eqs. 8-4) with appropriate time constants to represent mechanical and signal processing lags. The achieved seeker tracking rate vector w_{ach} is assumed to act during the current computation time step and is employed to find the new boresight axis vector at the end of the time step. The final processed seeker rate signal vector m_i from

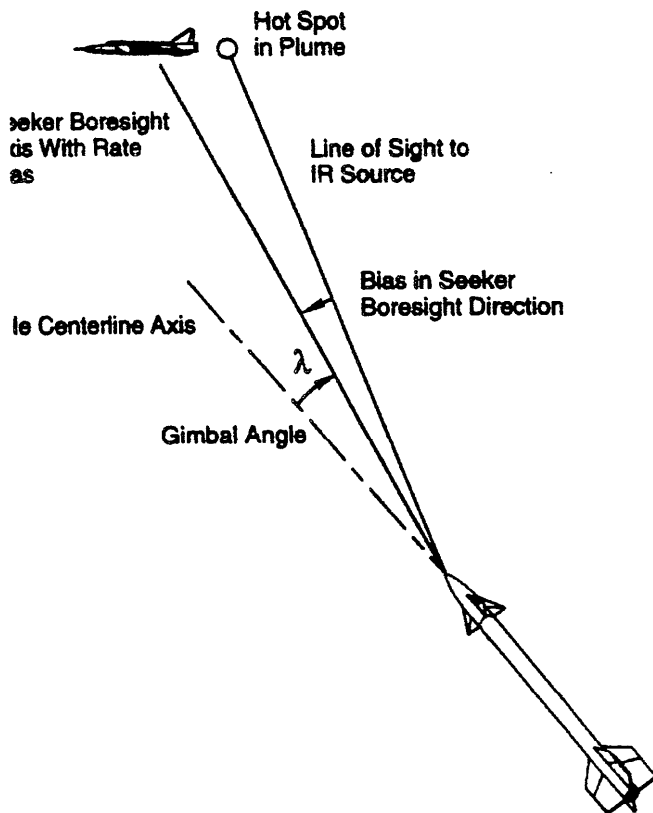


Figure 8-5. Effect of Rate Bias

Eqs. 8-4 is employed in Eq. 8-10 or 8-13 to calculate the missile lateral acceleration command A_C .

8-2.2 GUIDANCE PROCESSOR MODELING

The angular tracking rate of the seeker head is the primary information needed to implement proportional navigation.

Guidance information is processed in different ways in different missiles to determine steering commands. Equations are given here for general simulations that employ the proportional navigation guidance law.

8-2.2.1 Perfect Guidance

In a simple simulation, when perfect guidance is assumed, the missile is assumed to maneuver as required to comply exactly with the guidance law. For the moment consider the case when the target and missile velocity vectors are coplanar. Then classical proportional navigation requires the angular rate of the required flight path, i.e., the angular rate of the missile velocity vector, to be

$$\dot{\gamma} = NR\omega_\sigma, \text{ rad/s (deg/s)} \quad (8-5)$$

where

NR = navigation ratio, dimensionless

$\dot{\gamma}$ = angular rate of the flight path, rad/s (deg/s)

ω_σ = magnitude of angular rate vector ω_σ of the line of sight to the target, rad/s (deg/s).

For the missile flight path to have an angular rate of $\dot{\gamma}$, kinematics shows that the acceleration of the missile normal to the flight path must be equal to $\dot{\gamma}V_M$. Then an ideal implementation of proportional navigation requires that the magnitude of the acceleration normal to the flight path be

$$A_c = NR\omega_\sigma V_M, \text{ m/s}^2 \quad (8-6)$$

where

A_c = magnitude of commanded-lateral-acceleration vector A_c , m/s^2

NR = navigation ratio, dimensionless

V_M = magnitude of velocity vector of center of mass of missile V_M , m/s

ω_σ = magnitude of angular rate vector ω_σ of the line of sight to the target, rad/s .

Some missiles include a gravity compensation term in the guidance processing. In general, gravity exerts a force on the missile with components of gravity in directions along the missile flight path and perpendicular to it. Since missiles are usually controlled by means of aerodynamic lift and lift is perpendicular to the flight path—only that component of gravity that is perpendicular to the flight path can be compensated by the guidance system. The component of the

acceleration of gravity normal to the flight path is calculated in a simulation by using

$$\mathbf{g}_n = \mathbf{g} - (\mathbf{u}_{V_M} \cdot \mathbf{g})\mathbf{u}_{V_M} \text{ m/s}^2 \quad (8-7)$$

where

- \mathbf{g} = acceleration due-to-gravity vector, m/s^2
- \mathbf{g}_n = vector of component of acceleration due to gravity normal to missile flight path, m/s^2
- \mathbf{u}_{V_M} = unit vector in direction of velocity of missile center of mass \mathbf{V}_M , dimensionless.

In the general case, when target and missile velocities are not coplanar, the line-of-sight angular rate vector $\boldsymbol{\omega}_\sigma$ is not perpendicular to the missile flight path. Since aerodynamic lift is perpendicular to the flight path, the missile maneuver can respond only to that component of the line-of-sight-rate vector that is perpendicular to the missile velocity vector. The vector product $(\boldsymbol{\omega}_\sigma \times \mathbf{V}_M)$ gives the correct component of $\boldsymbol{\omega}_\sigma$ multiplied by \mathbf{V}_M and has the proper direction for the commanded acceleration. putting A_c (Eq. 8-6) in vector form and adding a component of acceleration opposite the perpendicular component of gravity give the general equation for the commanded maneuver acceleration for "perfect" guidance in three-dimensional space:

$$\mathbf{A}_c = NR(\boldsymbol{\omega}_\sigma \times \mathbf{V}_M) - \mathbf{g}_n, \text{ m/s}^2 \quad (8-8)$$

where

- \mathbf{A}_c = commanded-lateral-acceleration vector, m/s^2
- \mathbf{g}_n = vector of component of acceleration due to gravity normal to missile flight path, m/s^2
- NR = navigation ratio, dimensionless
- \mathbf{V}_M = missile velocity vector, m/s
- $\boldsymbol{\omega}_\sigma$ = angular rate vector of the line-of-sight vector from the seeker to the tracking point, rad/s .

Since the ideal maneuver-acceleration-command vector is in the lift direction, A_c is substituted into Eq. 7-15 to determine the required lift force for three-degree-of-freedom simulations.

8-2.2.2 Practical Proportional Navigation

In a practical application of proportional navigation, the actual angular line-of-sight rate w_σ is replaced by the processed-seeker-head-angular-rate signal w_f . In addition, the missile velocity vector \mathbf{V}_M usually is not known onboard the actual missile, and thus makes it impossible to implement Eq. 8-8 directly. Various methods have been employed for approximating proportional navigation in a practical seeker when \mathbf{V}_M is not available. Two such methods are described—one for missiles having RF sensors that can measure closing speed and one for IR seekers that cannot.

8-2.2.2.1 Missiles With RF Seekers

Radio frequency systems have the potential to measure the magnitude of the closing velocity, i.e., magnitude of the velocity of the missile relative to the target, and missiles with RF seekers sometimes implement Eq. 8-8 approximately by substituting the closing speed, i.e., the magnitude of the closing velocity V_c for that of the missile velocity \mathbf{V}_M . The closing speed is calculated by using

$$V_c = -\frac{\mathbf{R} \cdot \mathbf{V}_{T/M}}{R}, \text{ m/s} \quad (8-9)$$

where

- \mathbf{R} = range vector from missile center of mass to target center of mass, m
- R = magnitude of range vector \mathbf{R} from missile center of mass to target center of mass, m
- V_c = closing speed, m/s
- $\mathbf{V}_{T/M}$ = velocity vector of center of mass of target relative to center of mass of missile, m/s .

This takes care of the magnitude of the velocity vector to be used in Eq. 8-8, but the direction of the velocity vector must also be approximated. The usual approximation is to substitute the missile axis for the direction of the missile velocity vector in the guidance equation. The missile axis and the velocity vector coincide when the angle of attack α is zero, and the error in the approximation is small for usual angles of attack.

A practical implementation of proportional navigation for RF seekers is obtained, then, by employing the processed seeker angular rate as a measure of the line-of-sight angular rate, substituting closing speed for missile speed, and using the missile centerline axis to approximate the direction of the missile velocity. The equation for simulating this implementation is

$$\mathbf{A}_c = NR(\boldsymbol{\omega}_f \times V_c \mathbf{u}_{cl}), \text{ m/s}^2 \quad (8-10)$$

where

- \mathbf{A}_c = commanded-lateral-acceleration vector, m/s^2
- NR = navigation ratio, dimensionless
- \mathbf{u}_{cl} = unit vector in direction of missile centerline axis, dimensionless
- V_c = closing speed, m/s
- $\boldsymbol{\omega}_f$ = final processed seeker rate signal vector, rad/s .

The gravity compensation term has not been included here; many surface-to-air missiles have no onboard instruments to measure the direction of gravity. For applications that do compensate for gravity, the gravity term can be added as in Eq. 8-8, with \mathbf{g}_n calculated by using \mathbf{u}_{cl} in place of \mathbf{u}_M in Eq. 8-7.

The effect of substituting the direction of the missile axis vector for the direction of the missile velocity vector is that the acceleration command vector, determined by Eq. 8-10, becomes perpendicular to the missile axis rather than perpendicular to the missile flight path as required by pure proportional navigation. Thus the component of aerodynamic force required to produce the commanded acceleration is a normal force rather than lift. Therefore, the commanded-lateral-acceleration vector A_C calculated by Eq. 8-10 should be substituted into Eq. 7-8 to calculate the required normal force for three-degree-of-freedom simulations. For five- and six-degree-of-freedom simulations, the components of A_C are substituted into Eqs. 8-15 and 8-14, respectively.

If the practical implementation of proportional navigation is compared with ideal proportional navigation, the major difference (aside from the dynamic and processing lags) is that the navigation ratio NR has been replaced by an effective navigation ratio NR_{eff} . To show this difference, again consider the coplanar case, and assume that $\omega_f = \omega_\sigma$. Then Eq. 8-10 can be written as the scalar equation

$$A_c = NR\omega_\sigma V_c, \text{ m/s}^2 \quad (8-11)$$

or

$$A_c = NR \frac{V_c}{V_M} \omega_\sigma V_M, \text{ m/s}^2 \quad (8-12)$$

where

- A_c = magnitude of the commanded-lateral-acceleration vector A_c , m/s^2
- NR = navigation ratio, dimensionless
- V_c = closing speed, m/s
- V_M = magnitude of missile velocity (speed) along flight path, m/s
- ω_σ = magnitude of angular rate vector ω_σ of the line of sight to the target, rad/s .

By comparing Eq. 8-12 with Eq. 8-6, it is shown that when V_c is substituted for V_n , the effective navigation ratio NR_{eff} is equal to $NR(V_c/V_n)$ (Ref. 2).

8-2.2.2.2 Missiles With IR Seekers

Missiles with IR seekers typically do not contain instrumentation to measure missile velocity, and they have no means by which to measure closing velocity. Conceptually, an a priori estimate of missile speed as a function of time could be used in place of the actual missile speed V_n to implement proportional navigation in a missile; however, such a priori information is not generally programmed into a guidance processor. Instead this information is taken into account implicitly in the design of the guidance and control components to give an approximation of proportional navigation. That is, the relationships among the missile components are designed without the expense and complexity of an explicit guidance processor to cause the missile flight path angular rate to be approximately proportional to the

seeker angular rate. The approximation is made as good as is reasonably feasible within the design constraints of simplicity and cost. Thus the essence of proportional navigation is implemented in a very simple way, with no guidance computer and only minimal signal processing.

The result is that a guidance law very close to ideal proportional navigation is mechanized in the actual missile, except that the navigation ratio varies with Mach number and altitude, depending on the specific design of the control system and on the aerodynamics of the missile. The designs of the missile subsystems are planned to give navigation ratios as close as possible to the desired ratio within the Mach number regions that are most critical. Atypical curve of navigation ratio versus Mach number at a given altitude for a small IR missile is shown in Fig. 8-6 (Ref. 3).

The navigation ratio multiplied by the velocity is called the system gain. The system gain is a steady state lateral acceleration that the actual missile achieves per unit of seeker angular rate. Fig. 8-7 shows typical system gain

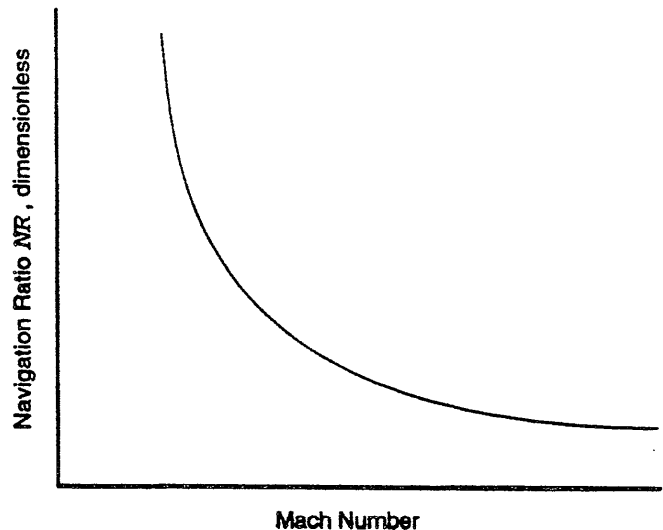


Figure 8-6. Navigation Ratio Achieved by Typical IR Missile Design

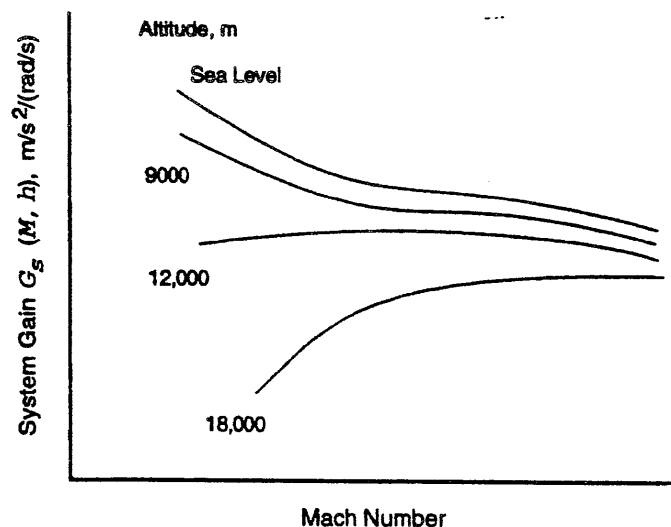


Figure 8-7. System Gain for Typical IR Missile

curves as functions of Mach number and altitude. These curves are constructed by actual measurements of accelerations and of seeker angular rates in flight tests or by very detailed analyses (or simulations) of the missile guidance, control, and aerodynamics. Multiplying the system gain by the seeker angular rate yields the steady state lateral acceleration of the missile. System gain curves are useful in less detailed missile flight simulations because they contain a great deal of a priori information about how the missile performs that need not be recalculated every time the simulation is run. System gain curves are input to the simulation as lookup tables. Actually the system gain also varies depending on the weight and center of mass, and if a very accurate simulation of system gain during the motor burn period is needed, additional system gain curves that cover the burn period must be included in the system gain tabular data for interpolation.

For three-degree-of-freedom simulations using tabular system gain input tables, the commanded-lateral-acceleration vector A_c is calculated by using

$$A_c = G_s(M,h)(\omega_f \times u_{V_M}), m/s^2 \quad (8-13)$$

where

A_c = commanded-lateral-acceleration vector, m/s^2

$G_s(M,h)$ = system gain as a function of Mach number and altitude, $(m/s^2)/(rad/s)$

u_{V_M} = unit vector in the direction of the velocity of the missile center of mass V_M , dimensionless

ω_f = final processed seeker rate signal vector, rad/s .

Published system gain data for existing missiles are sometimes presented in units of acceleration g per degree per second $g/(deg/s)$ in which case the units must be converted before substitution into Eq. 8-13. The acceleration vector A_c calculated by Eq. 8-13 is perpendicular to the missile velocity vector and should therefore be substituted into Eq. 7-15 to calculate the aerodynamic lift.

To simulate the guidance process when the system gain curves are not known requires detailed simulation of the entire guidance and control sequence of events-horn the seeker output through the control servos and fin deflections to the aerodynamic response. An often-selected alternative is to substitute as much of the actual system hardware as is feasible in place of mathematical modeling.

8-2.3 AUTOPILOT MODELING

As discussed in Chapter 2, an actual autopilot in a missile has two basic functions-to ensure stable flight and to translate the guidance law into control-surface deflection commands. Missiles that are designed with conservative (relatively large) static margins and whose normal flight profiles do not include large angles of attack-conditions in which aerodynamics typically become very nonlinear-do

not require much stabilization by an autopilot. This is especially true when torque-balance servos are used because they tend to compensate for changes in dynamic pressure by automatically adjusting the magnitudes of the control-surface deflections and thus remove that burden from the autopilot. In some missiles any needed autopilot functions are included within the design of the seeker and control system. At the other extreme are missiles that depend on complex autopilots to ensure flight stability under widely varying flight conditions and highly nonlinear aerodynamic characteristics.

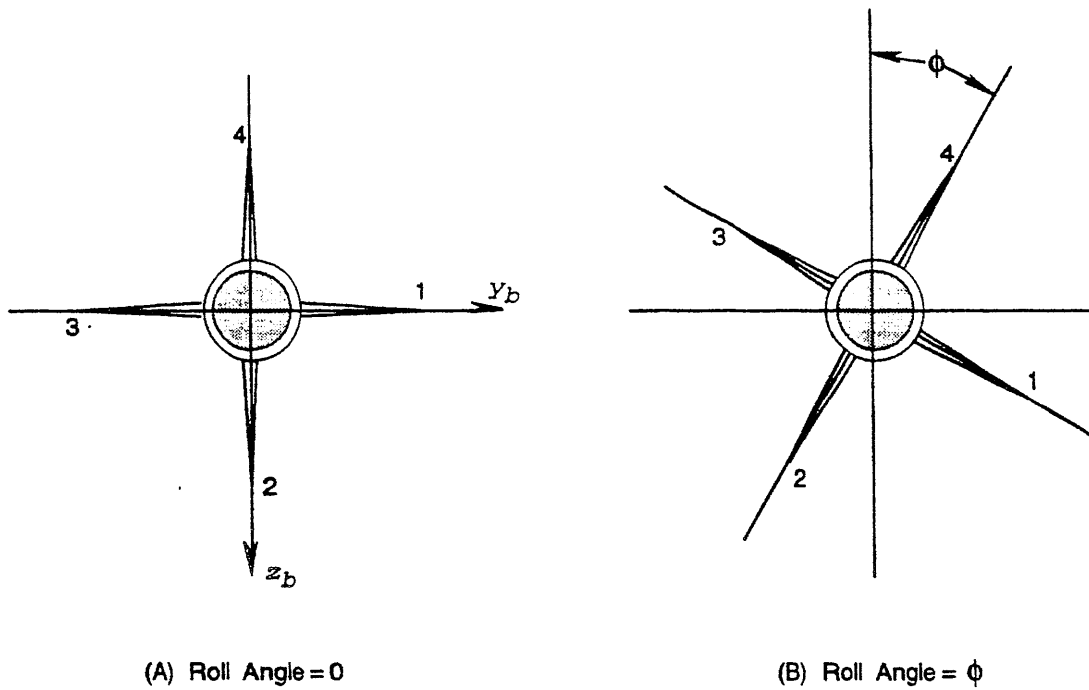
For six-degree-of-freedom simulations in which missile roll is calculated, the autopilot model distributes the control-surface commands to the appropriate control surfaces as the missile rolls. In addition, depending on the design of the missile being simulated and on the objectives of the simulation, the autopilot model may scale and limit the guidance commands for the structural integrity and stability of the missile and provide feedback loops to ensure that the commands are being accurately executed. Digital technology and microprocessors are used in modern autopilot development; they make simulation difficult and increase simulation run times. Autopilot simulations for such applications are very specialized and complex and are beyond the scope of this handbook. There is strong motivation in cases requiring high-fidelity autopilot simulations to use autopilot hardware within the simulation as a substitution for mathematical modeling (Ref. 4).

Equations for simple mathematical models of autopilots applicable to six-, five-, and three-degrees of freedom are provided in the subparagraphs that follow. It is assumed that the missile has four control surfaces in a cruciform pattern and that commanded control-surface deflections are proportional to commanded lateral accelerations for maneuver commands and proportional to commanded roll rates for roll commands.

8-2.3.1 Six Degrees of Freedom

Since control-surface deflections are included in the calculations in five- and six-degree-of-freedom simulations, a method to distribute the maneuver commands to the proper control surfaces is needed. Six-degree-of-freedom autopilots have two lateral channels that process yaw and pitch commands and a roll channel that processes roll commands.

In a full six-degree-of-freedom simulation, the initial roll orientation of the missile (zero roll angle) is the orientation at the time of first motion. A common numbering system for the four control surfaces is shown in Fig. 8-8. Roll angles are calculated relative to the initial orientation throughout the simulated flight. If it is assumed that the simulated body reference frame does not roll with the missile, the control-surface deflection commands-calculated in that nonrolling frame-must be further resolved according to the instantaneous roll angle to determine the magnitude and direction of rotation for each individual fin.



View Looking Forward

Figure 8-8. Numbering Convention for Control Surfaces (Adapted from Ref. 5)

If the missile contains a roll-control channel in the autopilot, the four fins may operate independently and thus allow differential fin deflections to produce rolling moments. In that case, since each fin is controlled individually, it is convenient to define a consistent convention for the positive direction of the deflection of any given fin. A fin

deflection is commonly assumed to be positive if the fin rotation is clockwise when viewed looking outward along the axis of the fin as shown in Fig. 8-9 (Ref. 5). If it is assumed that the control surfaces are located ahead of the missile center of mass (canards), the individual fin deflection angles are given in nonrolling body frame coordinates

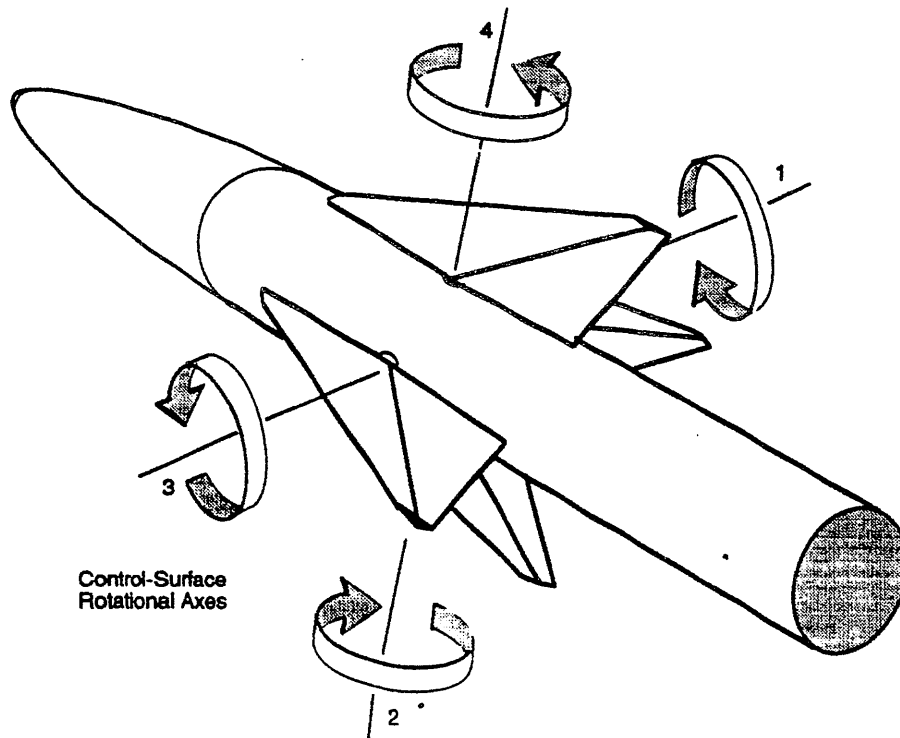


Figure 8-9. Convention for Direction of Control-Surface Rotation

by

$$\left. \begin{aligned} \delta_1 &= G_\ell \left(A_{c_{y_b}} \sin \phi - A_{c_{z_b}} \cos \phi \right) - G_r p_c, \text{ rad} \\ \delta_2 &= G_\ell \left(A_{c_{y_b}} \cos \phi + A_{c_{z_b}} \sin \phi \right) - G_r p_c, \text{ rad} \\ \delta_3 &= -G_\ell \left(A_{c_{y_b}} \sin \phi - A_{c_{z_b}} \cos \phi \right) - G_r p_c, \text{ rad} \\ \delta_4 &= -G_\ell \left(A_{c_{y_b}} \cos \phi + A_{c_{z_b}} \sin \phi \right) - G_r p_c, \text{ rad} \end{aligned} \right\} \quad (8-14)$$

where

$A_{c_{y_b}}, A_{c_{z_b}}$ = components of commanded-lateral-acceleration vector A_c on y-axis and z-axis, respectively, of body frame, m/s^2

G_ℓ = overall autopilot lateral-channel gain, $rad/(m/s^2)$

G_r = overall autopilot roll-channel gain, $rad/(rad/s)$

p_c = commanded roll rate, rad/s

δ_i = deflection angle of i th control surface, $i = 1, 2, 3, 4$, rad

ϕ = missile roll angle, rad (deg).

The overall autopilot gains G_ℓ and G_r can be simple input curves of gain as a function of dynamic pressure, or they can be the output of a more complex autopilot model in the simulations. The commanded roll rate p_c can be input as a constant, or it can be calculated by a model of the autopilot roll channel.

Eqs. 8-14 reflect the fact that the convention selected for specifying control-surface deflections causes negative deflections to produce a positive missile roll about the body frame x-axis. Some missiles use only one pair of control surfaces to control roll, for example, Surfaces 1 and 3, so the roll terms ($G_r p_c$) are eliminated from the equations for δ_2 and δ_4 .

Eqs. 8-14 are made applicable to missiles with control surfaces aft of the missile center of mass (tail control) by reversing the algebraic signs of G_ℓ in each of the four equations. The signs of G_r do not change.

8-2.3.2 Five Degrees of Freedom

Since missile roll is not simulated in five-degree-of-freedom simulations, the axes of Fins 1 and 3 are assumed to remain always horizontal. The guidance-maneuver-command vector A_c is resolved into y- and z-components in the body reference frame. The z-component is applied to control Surfaces 1 and 3, and they-component is applied to Surfaces 2 and 4. The control-surface deflection equations are derived from Eqs. 8-14 by setting the roll angle and the commanded roll rate to zero and assuming that Surfaces 1 and 3 are mechanically linked as well as Surfaces 2 and 4.

These simplified equations are

$$\left. \begin{aligned} \delta_1 &= G_\ell A_{c_{z_b}}, \text{ rad} \\ \delta_2 &= G_\ell A_{c_{y_b}}, \text{ rad} \\ \delta_3 &= -\delta_1, \text{ rad} \\ \delta_4 &= -\delta_2, \text{ rad} \end{aligned} \right\} \quad (8-15)$$

where

$A_{c_{y_b}}, A_{c_{z_b}}$ = components for commanded-lateral-acceleration vector A_c on y-axis and z-axis, respectively, of body frame, m/s^2

G_ℓ = overall autopilot lateral-channel gain, $rad/(m/s^2)$

δ_i = deflection angle of i th control surface, $i = 1, 2, 3, 4$, rad .

8-2.3.3 Three Degrees of Freedom

For three-degree-of-freedom simulations any autopilot functions relating to flight stability are taken into account by the assumption that the missile responds properly to acceleration commands. In this case the autopilot is simulated only by including in Eqs. 7-18 any effects that the autopilot has on the natural frequency and on the damping ratio ζ of the missile response characteristics, and by including a limit on the commanded acceleration. The effects of the autopilot on w_a and ζ must be known a priori from estimates or data obtained by analysis or testing.

The acceleration limit can be a simple tabular input as a function of Mach number and altitude. Such a table is constructed from a priori information or estimates for the missile being simulated. An angle of attack limit may be superimposed in addition to the acceleration limit to eliminate any possibility of unrealistic angles of attack at low dynamic pressures.

If the commanded-lateral-acceleration vector A_c , commanded by the guidance, exceeds the allowable tabulated acceleration limit, this limit is used. Likewise, if the angle of attack that results from performing the commanded lateral acceleration exceeds the maximum allowable angle of attack this maximum angle of attack is used. If the angle of attack does reach its limiting value, the commanded lateral acceleration must be readjusted to conform to that angle of attack under the existent instantaneous flight conditions.

8-2.4 GROUND-BASED GUIDANCE MODELING

As discussed in subpar. 2-3.1.1, parts of the guidance systems of some missiles are located on the ground. Flight simulations for missiles that have ground-based guidance are essentially the same as flight simulations for missiles that have airborne guidance except that in some cases steering commands are directed to the autopilot from the ground

instead of from a seeker and different guidance laws may be employed.

8-2.4.1 Semiactive Homing

A surface-to-air, semiactive homing system (subpar. 2-3.1.2.2) requires a target illuminator on the ground. The seeker on the missile tracks the power reflected from the target in the same way as a passive homing system. Except for considerations of signal strengths and Doppler effects, which are outside the scope of this handbook, simulating the flight of missiles that employ semiactive homing is the same as simulating the flight of missiles that employ active or passive homing.

8-2.4.2 Command

The simulation of command guidance depends on the particular guidance law employed. If proportional navigation is used by the command system, ground-based computers-combined with ground-based target and missile trackers-determine the line-of-sight vector from the missile to the target and calculate the angular rate w_i . This angular rate is then processed in the ground computer through an equation such as Eq. 8-8 to determine the commanded-maneuver-acceleration vector A_c , which is transmitted to the missile. The missile autopilot then determines and distributes control-surface deflection commands to the control system. A missile flight simulation for a missile that employs command proportional navigation uses the same equations that are used for proportional navigation in a homing system except, of course, that missile seeker tracking is not simulated.

8-2.4.3 Beam Rider and Command to Line of Sight

Command-to-line-of-sight guidance is similar to beam-rider guidance, in that both forms attempt to keep the missile within a guidance beam transmitted from the ground. Normally, the guidance beam is aligned with the line of sight from the ground-based target tracker to the target. In some systems, however, the guidance beam does not always point directly toward the target it may be biased forward during the midcourse portion of the engagement to provide a lead angle. In beam-rider guidance the error in the position of the missile relative to the center of the guidance beam is detected by sensors onboard the missile (subpar. 2-3.2.3), and maneuver commands to correct the error are determined onboard. In command-to-line-of-sight guidance the missile position error is detected by sensors on the ground, and guidance maneuver commands are transmitted to the missile from system elements on the ground (subpar. 2-3.1.1.3). The basic equations for missile flight simulations that use these two types of guidance are identical.

As shown in Fig. 8-10, the vector e represents the error in missile position relative to the guidance beam at any given

instant. This error is defined as the perpendicular distance from the missile to the centerline of the guidance beam. The missile guidance commands generated by beam-rider and command-to-line-of-sight systems are proportional to the error vector e and the rate of change of that vector \dot{e} . The proportionality with e causes the missile to be steered toward the center of the guidance beam; the proportionality with \dot{e} provides rate feedback, which causes the missile flight path to maneuver smoothly onto the centerline of the guidance beam without large overshoots.

A third parameter, the Coriolis acceleration A_{cc} , may be included in the guidance equation. This Coriolis acceleration results from the angular rotation of the guidance beam and should not be confused with the Coriolis effects caused by the rotation of the earth. The Coriolis component of missile acceleration is required in order to allow the missile to keep up with the rotating beam as the missile flies out along the beam. In surface-to-air missile applications the angular rate of the guidance beam is typically great enough to cause this parameter to be significant. If the Coriolis term is not included, the missile position lags behind the rotating guidance beam, which results in increased miss distance. This Coriolis acceleration term is included in the guidance loop as a feed-forward term, i.e., it is not affected by feedback loops.

Equations for calculating the guidance parameters e , \dot{e} , and A_{cc} are presented in this paragraph, the method of combining them to form the missile commanded-lateral-acceleration vector AC is given by Eq. 8-21.

For convenience in demonstrating the method of calculating the error vector e , assume the guidance beam transmitter (which may be identical to the target tracker) is located at the origin of the earth coordinate system. Define a unit vector u_g to represent the direction of the guideline, i.e., the centerline of the guidance beam. The error vector e is perpendicular to u_g . The equation for calculating e is

$$e = P_B - P_M, m \quad (8-16)$$

where

e = vector of error in missile position relative to the guideline, m

P_B = position vector of a point located on the guideline at the point of intercept with the error vector e (Point B in Fig.8-10), m

P_M = position vector of the missile, m.

The vector P_B , for use in Eq. 8-16, determines the location of the intersection of the guideline and the error vector e ; it is calculated by

$$P_B = (u_{gt} \cdot P_M)u_{gt}, m \quad (8-17)$$

where

P_B = position vector of a point on the guideline at the point of intercept with the error vector e , m

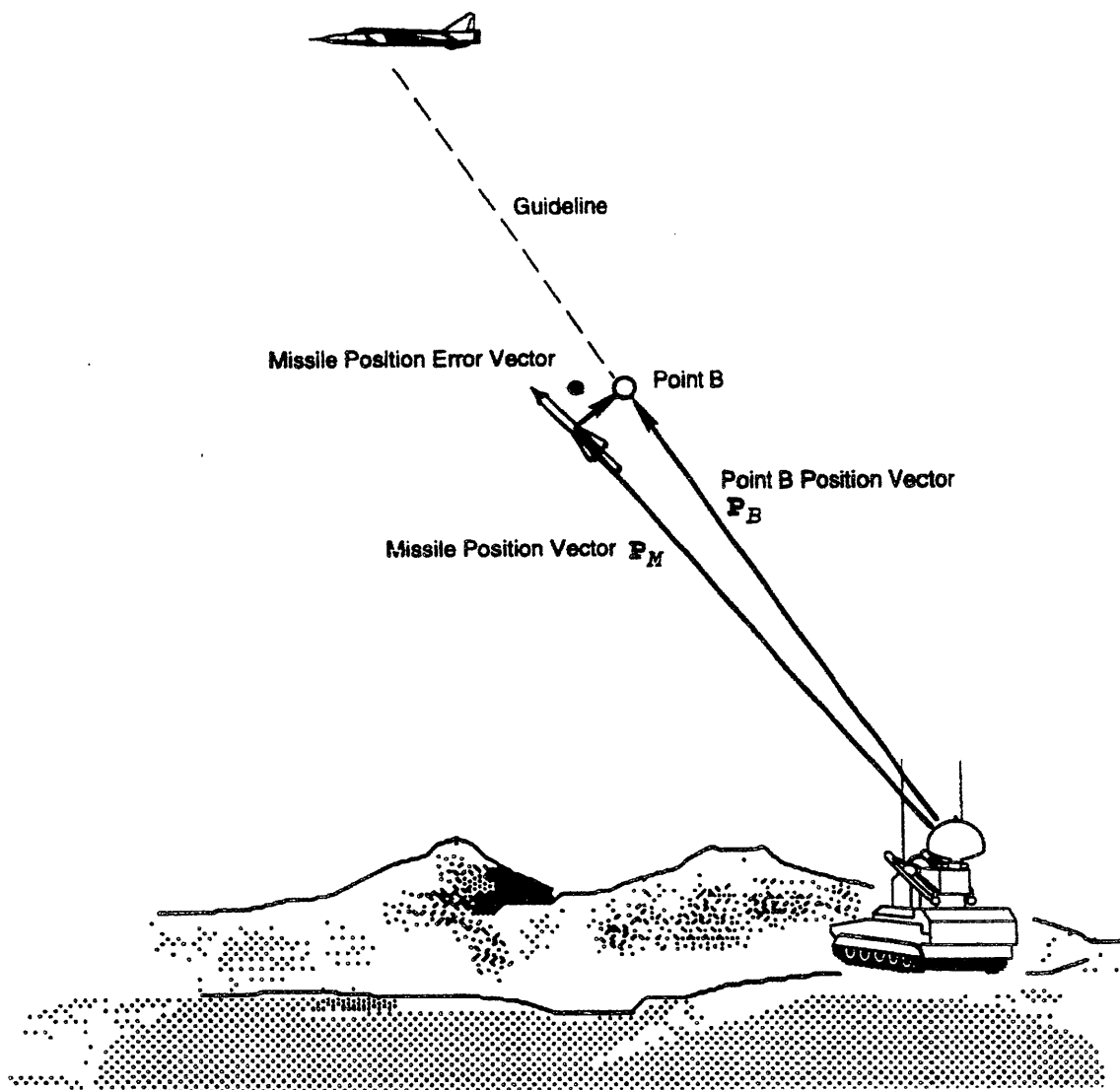


Figure 8-10. Guidance Error for Beam Rider or Command to Line of Sight

\mathbf{P}_M = position vector of missile, m
 \mathbf{u}_{gl} = unit vector that represents the direction of the guideline, dimensionless.

The error rate vector $\dot{\mathbf{e}}$ is calculated as the difference between the component of missile velocity \mathbf{V}_M perpendicular to the guideline and the component of the velocity of Point B perpendicular to the guideline. This component of the velocity of Point B is produced by the angular motion of the guideline as it tracks (or leads) the target. The error rate vector $\dot{\mathbf{e}}$ is given by

$$\dot{\mathbf{e}} = \mathbf{V}_{B_{perp}} - \mathbf{V}_{M_{perp}}, \text{ m/s} \quad (8-18)$$

where

$\dot{\mathbf{e}}$ = vector rate of change of error vector \mathbf{e} , m/s
 $\mathbf{V}_{M_{perp}}$ = component of missile velocity vector \mathbf{V}_M perpendicular to the guideline, m/s

$\mathbf{V}_{B_{perp}}$ = component of velocity of Point B perpendicular to the guideline, m/s.

The components of velocities, for substitution into Eq. 8-18, are calculated by using

$$\left. \begin{aligned} \mathbf{V}_{M_{perp}} &= (\mathbf{u}_{gl} \times \mathbf{V}_M) \times \mathbf{u}_{gl}, \text{ m/s} \\ \mathbf{V}_{B_{perp}} &= \omega_{gl} \times \mathbf{P}_B, \text{ m/s} \end{aligned} \right\} \quad (8-19)$$

where

\mathbf{u}_{gl} = unit vector that represents the direction of the guideline, dimensionless
 $\mathbf{V}_{B_{perp}}$ = component of velocity of Point B perpendicular to the guideline, m/s
 \mathbf{V}_M = velocity vector of missile center of mass relative to earth, m/s

$V_{M_{perp}}$ = component of missile velocity vector V_M perpendicular to the guideline, m/s
 ω_{gt} = angular rate vector of the guideline, rad/s.

The Coriolis acceleration term A_c is calculated using

$$A_{C_c} = \text{Mag}[\omega_{gt} \times (V_M \cdot u_{g\ell})u_{g\ell}], \text{ m/s}^2 \quad (8-20)$$

where

A_{C_c} = Coriolis term in acceleration command, m/s^2
 u_{gt} = unit vector that represents the direction of the guideline, dimensionless
 V_M = velocity vector of missile center of mass relative to earth, m/s
 ω_{gt} = angular rate vector of the guideline, rad/s
 $\text{Mag}[\]$ = the magnitude of the argument vector.

The dot product in Eq. 8-20 gives the component of missile velocity along the guideline; thus the term in square brackets is one-half the Coriolis acceleration vector.

Finally, using the terms calculated in Eqs. 8-16, 8-18, and 8-20, the commanded-lateral-acceleration vector, to guide the missile onto the centerline of the guide beam, is given by

$$A_c = k_1 e u_e + k_2 \dot{e} u_{\dot{e}} + k_3 A_{C_c} u_c, \text{ m/s}^2 \quad (8-21)$$

where

A_c = commanded-lateral-acceleration vector, m/s^2
 A_{C_c} = Coriolis term in acceleration command, m/s^2
 e = magnitude of missile position error relative to centerline of guidance beam, m
 \dot{e} = magnitude of rate-of-change vector \dot{e} , m/s
 k_1 = guidance proportionality constant, $(\text{m/s}^2)/\text{m}$
 k_2 = guidance proportionality constant, $(\text{m/s}^2)/(\text{m/s})$
 k_3 = guidance proportionality constant, dimensionless
 u_c = unit vector in the direction of the component of the Coriolis acceleration command that is perpendicular to the missile centerline, dimensionless
 u_e = unit vector in the direction of the component of e that is perpendicular to the missile centerline, dimensionless
 $u_{\dot{e}}$ = unit vector in the direction of the component of \dot{e} that is perpendicular to the missile centerline, dimensionless.

The missile lateral acceleration commands are constrained to be in directions perpendicular to the missile centerline. The unit vectors u_e , $u_{\dot{e}}$, and u_c , for use in Eq. 8-21, are defined to meet this constraint by

$$\left. \begin{aligned} u_e &= \text{Norm} [e - (e \cdot u_{c\ell}) u_{c\ell}], \text{ dimensionless} \\ u_{\dot{e}} &= \text{Norm} [\dot{e} - (\dot{e} \cdot u_{c\ell}) u_{c\ell}], \text{ dimensionless} \\ u_c &= \text{Norm} (\omega_{g\ell} \times u_{c\ell}), \text{ dimensionless} \end{aligned} \right\} \quad (8-22)$$

where

e = vector of error in missile position relative to the guideline, m
 \dot{e} = vector rate of change of error vector e , m/s
 u_c = unit vector in the direction of the component of the Coriolis acceleration command that is perpendicular to the missile centerline, dimensionless
 $u_{c\ell}$ = unit vector in the direction of the centerline axis of the missile, dimensionless
 u_e = unit vector in the direction of the component of e that is perpendicular to the missile centerline, dimensionless
 $u_{\dot{e}}$ = unit vector in the direction of the component of \dot{e} that is perpendicular to the missile centerline, dimensionless
 ω_{gt} = angular rate vector of the guideline, rad/s (deg/s)
 $\text{Norm}[\]$ = indicates argument is normalized by dividing by its magnitude.

In five-or six-degree-of-freedom simulations the missile commanded-lateral-acceleration vector A_c is transformed into the missile body coordinate system and substituted into Eq. 8-14 or 8-15 to calculate control-surface deflections. In three-degree-of-freedom simulations A_c is substituted directly into Eq. 7-18 to calculate the achieved lateral acceleration of the missile.

All of the parameters used in the simulation to calculate the missile acceleration command (Eq. 8-21) may not be available to the guidance system of an actual beam-rider or command-to-line-of-sight missile. Therefore; care must be taken to distinguish which parameters in the simulation are simply representations of the physics of the engagement and which can actually be known within the missile guidance system of the particular missile system being simulated. For example, the missile velocity V_M , required to determine the Coriolis acceleration term A_c , may not be known accurately onboard a beam-rider missile. In this case it may be necessary to use an approximate value within the actual guidance system in order to take advantage of the Coriolis feed-forward term. The approximate value should, of course, also be employed in the simulation.

8-2.4.4 Track Via Missile

In track-via-missile guidance relative target position and rate measurements are made onboard the missile and transmitted to the ground computer for processing. Maneuver

acceleration commands are transmitted back to the missile, which executes the maneuver. Assuming that proportional navigation is the guidance law employed, track-via-missile guidance modeling for a missile flight simulation is the same as the modeling described for homing guidance in subpars. 8-2.1,8-2.2, and 8-2.3.

8-3 CONTROL SYSTEM MODELING

As does the simulation of other missile subsystems, the simulation of the control subsystem varies in detail, depending on simulation objectives. For example, since three-degree-of-freedom simulations do not calculate control-surface deflections, they have no need for a control system model except to account for the time lag contributed to the guidance process by the control system. At the other extreme, a simulation designed to study control component interactions with each other and with other missile subsystems may include details such as actuator gas pressures, piston and linkage masses, and control-surface rotational inertia. A control actuator model, described in Ref. 6, contains "servo-valve dynamics and all major nonlinearities pertinent to performance, such as current limits, hinge moment load pressure feed-back and fin deflection limits". A control-surface actuator model, described in Ref. 7, also includes rate limits and the effects of viscous friction, body motion, and Coulomb friction.

The designs of the control system components-power sources, power transmission media, servos, and actuators-of different missiles may vary considerably, but all have a common purpose, i.e., to convert autopilot commands into fin deflections. For many simulation purposes, regardless of the details of the control system design, the control system components can be aggregated and described by a simple control system model that uses transfer functions. The input to the model is the control-surface deflection command; the output is the control-surface deflection achieved. The relationship between the output and the input is defined mathematically by appropriate transfer functions and logical elements such as limits on the magnitudes of control-surface deflections. Transfer functions provide a powerful means of representing the operation of missile control systems in an aggregated form without the need for detailed simulation.

Fig. 8-11 shows example block diagrams for control systems employing open-hop and closed-loop servos. The input to the control system is the commanded control-surface deflection δ_c . The output of the control system is the achieved control-surface deflection δ . The transfer function is $G(s)$, where s is the Laplace variable. By definition, the transfer function is equal to the ratio of the Laplace transform of the output of the system to the Laplace transform of the input, that is

$$\frac{\delta(s)}{\delta_c(s)} = G(s), \text{ dimensionless} \quad (8-23)$$

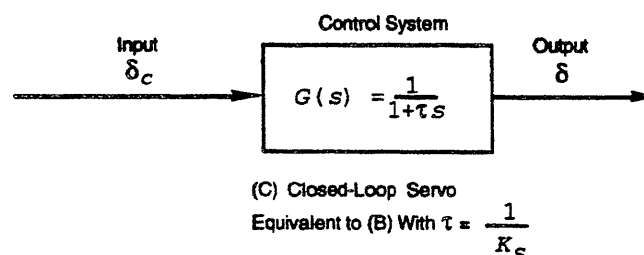
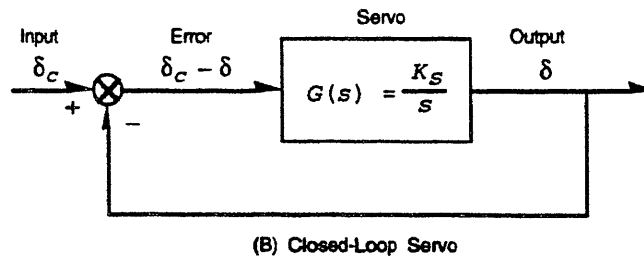
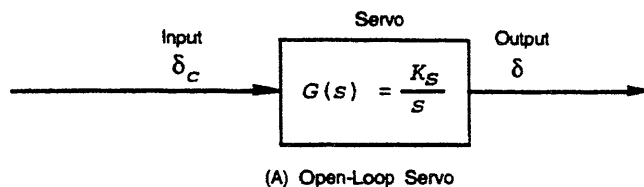


Figure 8-11. Control System Block Diagrams

where

$\delta_c(s)$ = Laplace transform of commanded control-surface deflection, rad (deg)

$\delta(s)$ = Laplace transform of achieved control-surface deflection, rad (deg)

$G(s)$ = control system transfer function, dimensionless.

Thus no matter how complicated the system, if the system transfer function and the input to the system are known, the output can be calculated.

Transfer functions can be obtained for a given control system by two methods (Ref. 8). The first is by computation, i.e., start with the differential equations of the system and solve them for the desired ratio. The second method is by experimental measurement, i.e., use the actual system hardware.

To illustrate the computation of the transfer function of a simple servo, it is assumed that the rate of fin deflection is proportional to the magnitude of the deflection command. The differential equation describing this servo is

$$\dot{\delta} = K_s \delta_c, \text{ rad/s} \quad (8-24)$$

where

K_s = servo system gain, s^{-1}

δ_c = commanded control-surface deflection angle, rad

$\dot{\delta}$ = angular rate of control-surface deflection, rad/s.

The Laplace transform of Eq. 8-24-ignoring initial conditions since the frequency response characteristics do not depend on initial conditions-is

$$s\delta(s) = K_s\delta_c(s). \quad (8-25)$$

Solving for the transfer function gives

$$\frac{\delta(s)}{\delta_c(s)} = \frac{K_s}{s} \text{ (open loop)}. \quad (8-26)$$

Therefore, the transfer function $G(s)$ is equal to K_s/s (Ref. 9), as shown in Fig. 8-11(A) for a control system consisting of only the servo with no feedback.

Fig. 8-11(B) shows the block diagram of a closed-loop control system in which the fin deflection achieved is fed back and compared with the input. For this case the input to the control servo is the difference between the output and the input to the control system. In this block diagram of the control system, only the servo is represented by a transfer function.

By a derivation similar to that given for the open-loop system the transfer function for the entire closed-loop control system, not just the servo as in Fig. 8-11(B), is determined to be

$$G(s) = \frac{1}{1 + \tau s} \text{ (closed loop)} \quad (8-27)$$

where

$\tau = 1/K_s$, control system time constant (time to achieve 63% of a step command), s.

Fig. 8-11(C) illustrates the use of a single transfer function to represent the control system that consists of both the servo and the feedback loop. Fig. 8-11(C) is mathematically equivalent to Fig. 8-11(B).

The measured transfer functions of actual missile control systems may be considerably more complicated than the examples given here.

8-4 HARDWARE SUBSTITUTION

In studies of the effects of countermeasures on production missiles that use simulation, it is extremely important that the right answers be obtained and the correct conclusions be drawn. These simulation studies must be practical, not just theoretical; they must relate to the actual probability of successful intercepts of targets. The most practical tool for such studies is missile-hardware-in-the-loop simulation (Ref. 10). Missile-hardware-in-the-loop simulation has been used extensively in the determination of the susceptibilities of

missile systems to countermeasures and has also been useful in determining the effectiveness of countermeasure equipment in protecting US aircraft (Ref. 10).

The reason actual missile hardware is used in the simulation loop is its realistic and relatively accurate representation of the key elements of the entire simulation--the missile guidance and control. The use of the actual seeker head and actual signal processing hardware eliminates the difficult task of modeling the nonlinear characteristics of the multiloop missile system mathematically, in particular, defining these characteristics when the missile is subjected to a countermeasures environment (Ref. 11).

In addition to its utility in countermeasures studies, missile-hardware-in-the-loop simulation is also valuable in earlier stages of missile development. Closed-loop operation in a realistic simulation employing missile hardware-in-the-loop provides an opportunity to study the dynamic stability of the hardware system firsthand and under controlled conditions (Ref. 12).

8-4.1 DESCRIPTION OF MISSILE HARDWARE SUBSTITUTION

In a missile-hardware-in-the-loop simulation, components of missile hardware are connected with a computer (or multiple computers) in a closed loop, and the simulation is operated in real time. The hardware provides the actual complex, nonlinear response characteristics of the guidance and control, and the computer simulates the aerodynamic and dynamic response of the missile, which cannot be reproduced by an actual missile in the laboratory. In a typical missile-hardware-in-the-loop simulation, an arrangement of electromagnetic sources provides target and countermeasures stimuli much like those experienced by a missile in an operational environment (Ref. 10).

8-4.1.1 Substituting Missile Hardware

Any of the components of the guidance and control system of a missile may be included as hardware in a simulation. These include the seeker, signal processor, onboard computer, autopilot, and control servos. In most missile-hardware-in-the-loop simulations, however, not all of the guidance and control components are included as hardware. Only those that are critical to the objectives of the simulation are included.

Typically, missile-hardware-in-the-loop simulations are arranged so that any or all of the missile hardware can be removed from the simulation loop and replaced temporarily by mathematical digital or analog models (Ref. 13) that permit simulation checkouts to be performed without the unanticipated effects and uncertainties associated with hardware performance and interfaces. These mathematical models of the components are often simplified versions that permit calculations to be performed in real time for real-time checkout of the simulation.

Two basic modes of missile-hardware-in-the-loop simulation are defined: missile-seeker-in-the-loop simulations and missile-seeker-electronics-in-the-loop simulations. The difference between them depends on the type of hardware components employed.

In many applications sections of actual production missile hardware are used in the simulation as shown in Fig. 8-12. Sometimes, however, especially in the early phases of the development of a missile, actual seeker hardware is not available. In this case prototypes of the actual (or proposed) electronic signal processing circuits are substituted in the simulation, whereas other pertinent seeker functions—such as optical components and gyros for electro-optical (EO) seekers, and antennas, radomes, and rate gyros for RF seekers—are modeled mathematically.

8-4.1.1.1 Missile-Seeker-in-the-Loop Simulation

Missile-seeker-in-the-loop simulation includes an actual physical missile seeker and physical electromagnetic radiation sources that simulate the target, background, and countermeasures for the seeker to view (Ref. 10). Basically, this means that the seeker optics and gyro for IR seekers, or radome, antenna and rate gyros for RF seekers, and all the guidance signal processing are represented in the simulation by the actual missile hardware. For EO missiles the sources of radiation power may include blackbody radiators and arc lamps. These sources produce power in the correct spectral regions and are imaged onto the missile seeker dome by appropriate optical lenses and mirrors (Ref. 14). For RF seekers the scenes are generated by RF antennas and reflectors. The RF power of the various sources that makeup the scene can be processed to give the proper Doppler and other effects, such as scintillation and glint.

The missile-seeker-the-loop simulation mode permits evaluation of actual missile hardware in a realistic environment with the seeker acquiring and tracking real radiation that has the spectral characteristics of real target signatures and that zooms in image size and moves in relation to the seeker boresight axis (Ref. 15).



Figure 8-12. Examples of Production Hardware Employed in Simulation (Ref. 14)

Advantages of missile-seeker-in-the-loop simulation are that optics, gyros, radomes, antenna patterns, and inertial instruments do not have to be modeled mathematically and validated. Thus missile-seeker-in-the-loop simulation provides a high degree of realism and credibility to the simulation. However, complex scenes are precluded by inherent limitations in present-day scene generators. Another disadvantage of missile-seeker-in-the-loop simulation is that actual missile hardware is not always available, particularly during the early development phases of a missile.

8-4.1.1.2 Missile-Seeker-Electronics-in-the-Loop Simulation

The only hardware included in missile-seeker electronics-in-the-loop simulations is electronics. For example, the actual (or an electronic equivalent) seeker electronic processor is included as hardware, but the optics and gyro of the seeker are modeled mathematically. No electromagnetic radiation is generated in a missile-seeker-electronics-in-the-loop simulation because there is no physical seeker to sense it. Instead the target, background, and countermeasures scene is prerecorded and played back as electronic signals to a missile-seeker-electronics-in-the-loop simulation by a special electronic scene simulator. The electronic scene simulator is capable of recording real scene data obtained by field measurements of actual targets against actual backgrounds and with actual countermeasures (Ref. 14). The scene signals, played back to the seeker electronics in the simulation, appear as they would if they were coming from the seeker detector itself.

Missile-seeker-electronic packaging provides special breakout points in their circuits that permit monitoring of various signals and also permit subcomponents (seeker detector, gyro torquer, guidance filter's, etc.) to be bypassed and the corresponding mathematical models inserted in their places (Ref. 12). The electronics are typically arranged on circuit cards in a chassis suitable for mounting in a rack. This configuration provides a multitude of test points not accessible for monitoring when the complete seeker guidance and control assembly is used and allows easier evaluation of seeker performance during the simulation. Also the lower density packaging affords better cooling for the electronics than is possible with production packaging.

The major advantage of the missile-seeker-electronics-in-the-loop simulation mode over the missile-seeker-in-the-loop mode is the complexity and authenticity with which the target and countermeasures scene can be simulated and presented to the missile guidance electronics. This capability is essential for a realistic evaluation of imaging and pseudoimaging seekers that scan target and countermeasures scenes. Another important advantage is that electronics are easily modified for parameter optimization and design tradeoff studies early in a missile system development cycle. A significant advantage in the cost and scheduling of computer runs is elimination of a cooling period,

which is required in the missile-seeker-in-the-loop mode between each simulated flight to prevent the seeker from overheating (Ref. 14).

8-4.1.2 Positioning Missile Hardware

In missile-seeker-in-the-loop simulations, it is essential that the seeker boresight axis have the angular freedom of motion it would have in an actual flight. In addition, the proper angular positions and rates between the hardware seeker boresight axis and the hardware missile body axis should be maintained, and if missile roll is included in the simulation, the hardware missile body should be rolled at the simulated rates. To permit the guidance and control hardware to experience physically the simulated angular rates, at least the section of missile hardware containing the seeker is mounted on a missile-positioning unit (MPU), also called a rotational motion simulator, or a flight table (Ref. 16). Dynamic inputs to the MPU, originating from a real-time dynamic simulation, enable hardware components mounted on the MPU to experience real-world rotational rates and angular positions during a simulated flight (Ref. 17).

The MPU supports and rotates the missile hardware about three rotational axes--yaw, pitch, and roll. When a missile is rolled during the simulation run, electrical slip rings are used to provide electrical power to the seeker, to allow monitoring, and to make available selected functions and signals from the hardware--such as the control-surface deflection commands--for use in the simulation. Cryogenic cooling of an IR seeker detector is provided by routing inert gas from a large, external tank through high-pressure plumbing to the missile seeker mounted in the MPU. This capability eliminates the need to mount a cryogenic reservoir directly on the MPU and thus reduces the mass loading on the MPU and the need for frequent recharging of a smaller reservoir. The MPU is servo driven, usually electro-hydraulic, and receives its angular position and rate commands from the solution of the rotational equations of motion in the flight simulation. Thus the missile hardware experiences the rotational motion predicted by the mathematical simulation.

8-4.1.3 Closing the Loop With Missile Hardware

In a missile-seeker-in-the-loop simulation, the missile hardware seeker detects the radiation emitted from the sources in the scene simulation, performs the target tracking internally to the hardware, and processes the seeker signals, and thus generates electronic commands to the missile control surfaces. This electronic signal is sent by hardwire to the computer where mathematically simulated control surfaces respond to the command. Based on simulated control-surface motion and on the missile aerodynamic characteristics, the missile flight is simulated in the computer by using the equations of motion. Inputs to the MPU are derived from the calculated Euler angles (Ref. 12), which define missile attitude, and the MPU updates the attitude of the missile hardware. In the computer the simulated target position is compared with the simulated missile position to obtain line-of-sight angles. Electrical commands based on the calculated line-of-sight angles are sent to the target scene simulator, which updates the target and countermeasures positions in the scene. The signatures of targets, decoys, and jammers, stored in computer memory as functions of aspect angle, are used to compute the new radiation characteristics of each of the components in the scene. Finally, the hardware seeker responds to the updated scene, and thus the simulation loop is closed.

The sequence is similar in a missile-seeker-electronics-in-the-hop simulation except that preprocess scene data are supplied directly to the hardware electronics by a target image simulator. The hardware electronics responds to the scene data by providing signals to the mathematical model to rotate the simulated seeker head and to deflect the simulated control surfaces. The simulation of missile and target positions and attitudes and the calculation of new line-of-sight angles proceed as in a missile-seeker-in-the-loop simulation. Finally, the target image simulator responds to the new range and line-of-sight data with a new set of preprocessed scene data which is sent to the hardware electronics, and thus the simulation loop is closed.

Fig. 8-13 shows the simulation loop in--block diagram form for the missile-seeker-in-the-loop mode, and Fig. 8-14 shows the loop for the missile-seeker electronics-in-the-loop mode.

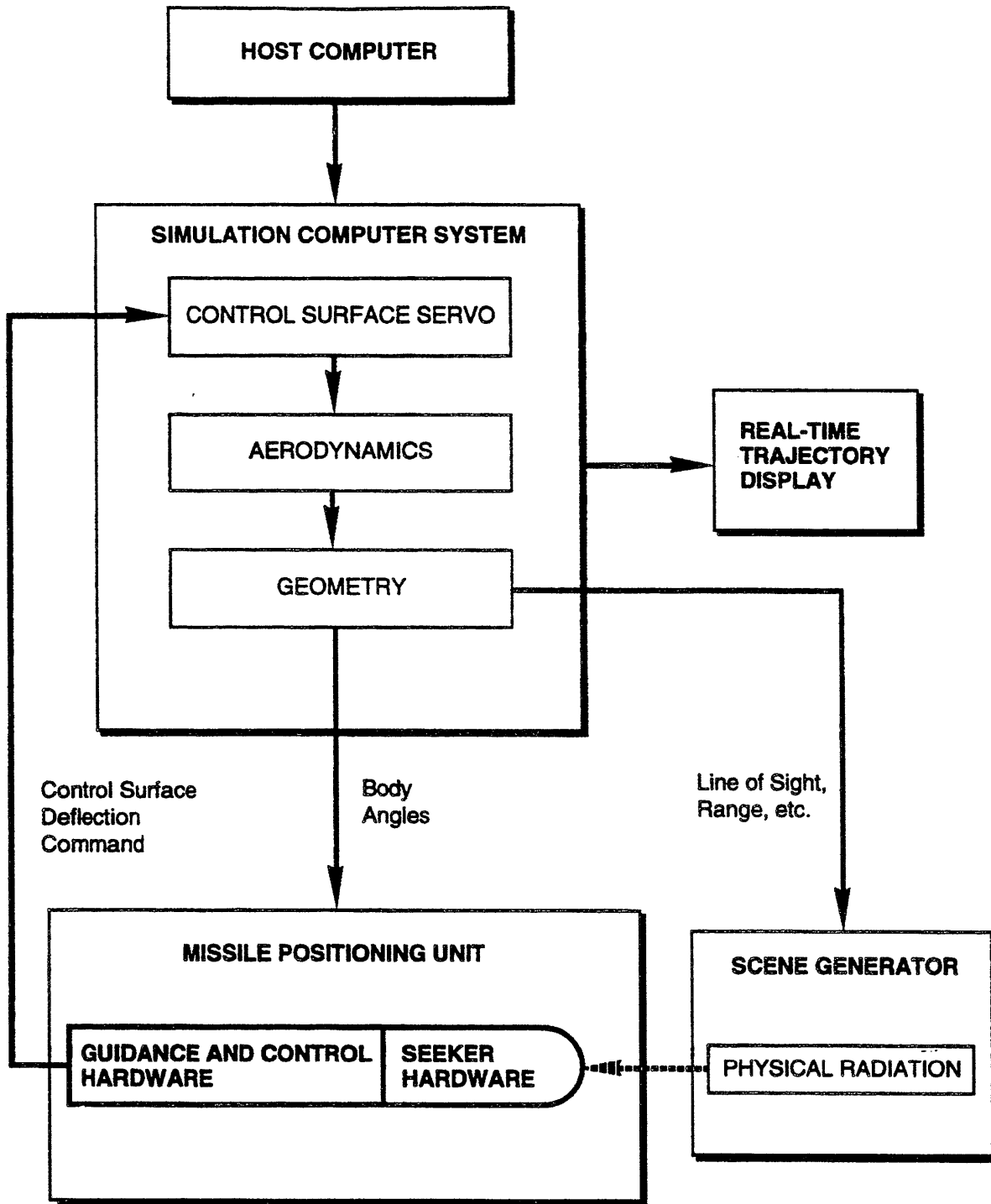


Figure 8-13. Flight Simulation Employing Actual Missile Seeker in the Loop (Ref. 14)

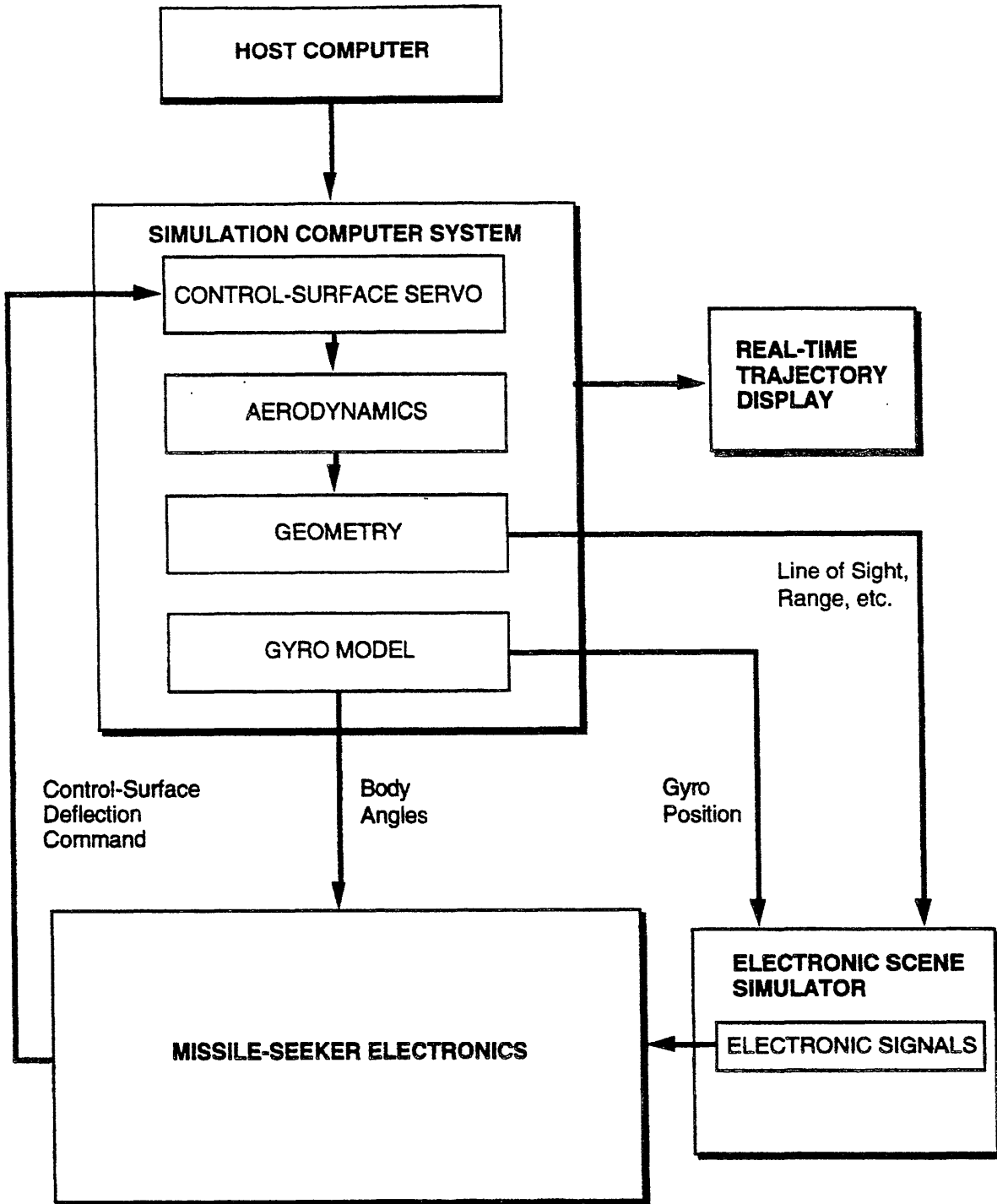


Figure 8-14. Flight Simulation Employing Seeker Electronics in the Loop (Ref. 14)

8-4.2 SEEKER HARDWARE SUBSTITUTION

To evaluate the effects of countermeasures on missile performance, it is particularly important that the missile seeker be accurately represented in a simulation because countermeasures usually act on the missile seeker. Therefore, to ensure an accurate representation of the seeker, actual seeker hardware often is employed in a simulation in place of a mathematical model.

8-4.3 AUTOPILOT HARDWARE SUBSTITUTION

Since the autopilot functions for some missiles are incorporated into the seeker electronics and into the design of the control system, there is no separate autopilot hardware to substitute in flight simulations of these missiles. Some other missiles have relatively simple autopilots that can be adequately simulated by relatively simple mathematical models. Even when a missile has a complicated autopilot, a simple representation in a flight simulation by transfer functions is adequate for many applications.

On the other hand, using breadboard autopilot hardware in the simulation loop can be a very effective design tool during development of a missile that requires a complex autopilot. The trend toward digital autopilots amplifies the importance of using autopilot hardware in missile flight simulations. Digital autopilot performance is difficult and expensive to verify by mathematical simulation because of the small time steps required to simulate the digital effects of the onboard computer. Checkout and validation of complex microprocessor-based subsystems require exercising hundreds or thousands of logic path possibilities. To solve this problem, actual microprocessor-based digital autopilot (DAP) hardware is used in the simulation loop, with realistic interfacing to other systems, to simulate real-time trajectories. In this way both the actual flight microprocessor hardware and the actual software can be tested in the laboratory under controlled conditions (Ref. 4).

8-4.4 CONTROL HARDWARE SUBSTITUTION

In many applications the control servos are simulated mathematically in response to control-surface deflection commands from either a hardware or a simulated autopilot. Sometimes, however, actual hardware control servos are employed in the simulation. In an actual missile in flight, control servos operate against the control-surface hinge moments produced by air loads on the surface. Therefore, accurate operation of a hardware control servo actuator in a simulation requires some method of simulating the aerodynamic load against which it can operate. Mechanical springs are typically used for this purpose (Ref. 12). The resulting control-surface deflections are measured and sent to the computer simulation where they are used to calculate the aerodynamic response of the missile.

REFERENCES

1. J. Malick and W. F. H. Ring, SRI International (private communication), Information documented in Missile Seeker Model (unpublished) by G. A. Branch, prepared for SRI International, Menlo Park, CA, 30 October 1984.
2. J. Gonzalez, "New Methods in the Terminal Guidance and Control of Tactical Missiles", Guidance and Control for Tactical Guided Weapons With Emphasis on Simulation and Testing, AGARD Lecture Series No. 101, Advisory Group for Aerospace Research and Development, North Atlantic Treaty Organization, Neuilly sur Seine, France, May 1979.
3. W. G. Younkin, Unpublished notes on Chaparral performance characteristics, US Naval Ordnance Test Station, China Lake, CA, Undated.
4. W. V. Albanes, J. T. Bosley, and J. B. Meadows, "Verification of Digital Autopilot Microprocessor Hardware and Software via Hardware-in-the-Loop Simulation", Proceedings of the Tenth Annual Pittsburgh Conference, Modeling and Simulation, Vol. 10, Part 5, University of Pittsburgh, Pittsburgh, PA, April 1979, pp. 1815-20, Instrument Society of America, Research Triangle Park, NC.
5. P. Garnell, Guided Weapon Control Systems, 2nd Ed., Royal Military College of Science, Shrivenham, Swindon, England, Brassey's Defence Publishers, London England, 1987.
6. T. R. Driscoll and H. F. Eckenroth, "Hybrid Simulation-Key to Successful Flight-Test Program", Simulation 26,34 (January 1976).
7. W. Read and J. Sheehan, "AMRAAM System Simulation, A Detailed Design and Performance Evaluation Tool", Electronic Progress 22,34 (Winter 1980).
8. H. S. Seifert and K. Brown, Ballistic Missile and Space Vehicle System, John Wiley & Sons, Inc., New York NY, 1961.
9. J. J. Jerger and G. Merrill, Eds., "Systems Preliminary Design", Principles of Guided Missile Design, D. Van Nostrand Co., Inc., Princeton, NJ, 1960.
10. T. A. Atherton, "A Missile Flight Simulator for Infrared Countermeasures Investigations", Proceedings of the Society of Photo-Optical Instrumentation Engineers, Optics in Missile Engineering, SPIE Vol. 133, Los Angeles, CA, 1978, pp. 103-5, Society of Photo-Optical Instrumentation Engineers, Bellingham, WA.
11. A. M. Baird, R. B. Goldman, N. C. Randall, W. C. Bryan, F. M. Belrose, and W. C. Holt, Verification and Validation of RF Environmental Models-Methodology Overview, Technical Report RD-81-2, US Army Missile Command, Redstone Arsenal, AL, October 1980.
12. H. L. Pastrick, C. M. Will, Jr., L. S. Isom, A. C. Jolly, L.

- H. Hazel, R. J. Vinson, and J. Mango, "Recent Experience in Simulating Missile Flight Hardware in Terminal Homing Applications", Proceedings of the Society of Photo-Optical Instrumentation Engineers, Optics in Missile Engineering, SPIE Vol. 133, Los Angeles, CA, 1978, pp. 108-15, Society of Photo-Optical Instrumentation Engineers, Bellingham, WA.
13. G. M. Griner and L. Hazel, "Implementation and Validation of an AD-10 Multiprocessor in a Hardware-in-the-Loop Missile Simulation", Summer Computer Simulation Conference, Toronto, Ontario, Canada, July 1979, p. 37, Simulation Council, La Jolla, CA.
 14. G. H. Johnson, Electro-Optical Countermeasures Simulation Facility, Office of Missile Electronic Warfare, White Sands Missile Range, NM, Undated.
 15. D. J. Strittmatter, "A Seasonal Approach to Missile Target Simulators", Proceedings of the Society of Photo-Optical Instrumentation Engineers, Optics in Missile Engineering, SPIE Vol. 133, Los Angeles, CA, January 1978, pp. 83-95, Society of Photo-Optical Instrumentation Engineers, Bellingham, WA.
 16. H. L. Pastrick, L. S. Isom, C. M. Will, and R. J. Vinson, L. H. Hazel, "Monte Carlo Model Requirements for Hardware-in-the-Loop Missile Simulations", Proceedings of the 1976 Summer Computer Simulation Conference, Washington, DC, July 1976, pp. 112-17, Simulation Council, La Jolla, CA.
 17. D. W. Sutherlin, "On an Application of Hybrid Simulation to Antiradiation Missiles", Proceedings of the 1976 Summer Computer Simulation Conference, Washington, DC, July 1976, pp. 1.07-11, Simulation Council, La Jolla CA.
- G. A. Branch, Biased Proportional Navigation, (Unpublished Notes), 16 October 1988.
- R. H. Delano, "A Theory of Target Glint or Angular Scintillation in Radar Tracking", Proceedings of the IRE, December 1953, pp. 1778-84, Institute of Electrical and Electronics Engineers, Inc., New York, NY. (IEEE was formerly IRE.)
- R. E. Dickson, Optimum Intercept Law: Part II, Report No. RD-TR-62-12, US Army Missile Command, Redstone Arsenal, AL, September 1988.
- G. W. Egbert, Command Guidance of BRV Interceptors, McDonnell Douglas Astronautics Company-West, Santa Monica, CA, Undated.
- R. Goodstein, "Guidance Law Applicability for Missile Closing", Guidance and Control of Tactical Missiles, AGARD Lecture Series No. 52, Advisory Group for Aerospace Research and Development, North Atlantic Treaty Organization, Neuilly sur Seine, France, May 1972.
- W. Hofmann and D. Joos, "Missile Guidance Techniques", Guidance and Control for Tactical Guided Weapons With Emphasis on Simulation and Testing, AGARD Lecture Series No. 101, Advisory Group for Aerospace Research and Development North Atlantic Treaty Organization, Neuilly sur Seine, France, May 1979.
- A. S. Locke, "Guidance", Principles of Guided Missile Design, D. Van Nostrand Co., Inc., Princeton, NJ, 1955.
- S. A. Murtaugh and H. E. Criel, "Fundamentals of Proportional Navigation", IEEE Spectrum, 75-85 (December 1966).
- F. W. Nesline and P. Zarchan, "A New Look at Classical vs Modern Homing Missile Guidance", J. Guidance and Control 4, No. 1, AIAA 79-1727R (January-February 1981).
- F. W. Nesline and P. Zarchan, Missile Guidance Design Tradeoffs for High-Altitude Air Defense, Raytheon Company, Missile Systems Division, Bedford, MA 1982.
- F. W. Nesline, "Missile Guidance for Low-Altitude Air Defense", J. Guidance and Control 2, No. 4, Article No. 78-1317,283-9 (July-August 1979).

BIBLIOGRAPHY

AUTOPILOT SIMULATION

- M. L. Butler and H. L. Pastrick "Digital Autopilot Design and Evaluation for FAMMS (Future Army Modular Missile System)", Proceedings of the 1983 American Control Conference, San Francisco, CA, June 1983, pp. 1062-7, American Automatic Control Council, Northwestern University; Evanston, IL.
- P. Garnell, Guided Weapon Control Systems, 2nd Ed., Royal Military College of Science, Shrivenham, Swindon, England, Brassey's Defence Publishers, London, England, 1987.
- R. J. Heaston and C. W. Smoots, introduction to Precision-Guided Munitions, Vol. 1: Tutorial, GACIAC HB-83-01, Guidance and Control Information Analysis Center, IIT Research Institute, Chicago, IL, May 1983.

GUIDANCE SIMULATION

- F. P. Adler, "Missile Guidance by Three-Dimensional Proportional Navigation", J. Applied Physics 27, 500-7 (May 1956).

TRANSFER FUNCTIONS

- J. A. Aseltine, Transform Methods in Linear System Analysis, McGraw-Hill Book Company, Inc., New York, NY, 1958.
- W. L. Brogan, Modern Control Theory, 2nd Ed., Prentice-Hall, Inc., Englewood Cliffs, NJ, 1985.
- H. Chestnut and R. W. Mayer, Servomechanisms and Regulating System Design, Vol. 1, John Wiley & Sons, Inc., New York, NY, 1951.
- R. N. Clark, introduction to Automatic Control Systems, John Wiley & Sons, Inc., New York, NY, 1962.

- V. Del Toro and S. R. Parker, Principles of Control Systems Engineering, McGraw-Hill Book Company, New York, NY, 1960.
- B. Etkin, Dynamics of Flight-Stability and Control, John Wiley & Sons, Inc., New York, NY, 1982.
- M. F. Gardner and J. L. Barnes, Transients in Linear Systems, Vol. 1, John Wiley & Sons, Inc., New York, NY, 1942.
- P. Garnell, Guided Weapon Control Systems, 2nd Ed., Royal Military College of Science, Shrivenham, Swindon, England, Massey's Defence Publishers, London, England, 1987.
- J. J. Jerger and G. Merrill, Eds., "Systems Preliminary Design", Principles of Guided Missile Design, D. Van Nostrand Co., Inc., Princeton, NJ, 1960.
- R. W. Kolk, Modern Flight Dynamics, Prentice-Hall, Inc., Englewood Cliffs, NJ, 1961.
- Problem Solver in Automatic Control Systems/Robotics, Research and Education Association, New York, NY, 1983.
- H. S. Seifert and K. Brown, Ballistic Missile and Space Vehicle System, John Wiley & Sons, Inc., New York NY, 1961.
- J. M. Smith, Mathematical Modeling and Digital Simulation for Engineers and Scientists, John Wiley & Sons, Inc., New York, NY, 1987.
- H. S. Tsien, Engineering Cybernetics, McGraw-Hill Book Company, Inc., New York, NY, 1954.

CHAPTER 9

SCENE SIMULATION

Requirements for simulating target scenes are described in this chapter. Three types are addressed: mathematical scenes for purely mathematical flight simulations, physical scenes for simulations that use seeker hardware in the simulation loop, and electronic scenes for simulations that use seeker electronic hardware in the simulation loop. Methods and equipment used to simulate the scene elements—target, background, and countermeasures—are described for both optical and radio frequency (RF) sensors.

9-1 INTRODUCTION

Missile seekers receive electromagnetic radiation from targets, backgrounds, and countermeasures, all of which have characteristics that can be sensed by the seeker. These characteristics include radiation parameters and patterns, as well as physical motions relative to the missile and to other components of the scene. The signal intensities of targets are different from those of decoys, and signal intensities vary as functions of aspect, range (distance), atmospheric characteristics, and, in some cases, time. In addition, optical signals have properties such as wavelength and spatial distribution, and radio frequency (RF) signals have properties such as phase and Doppler effects. The combination of all electromagnetic signals received by the seeker at any instant of time constitutes a target scene.

An actual physical scene—viewed by a target tracker—is composed of electromagnetic radiation that is radiated by or reflected from the various objects within the field of view; and target trackers sense this radiation within relatively narrow wavelength bands. The characteristics of the radiation emitted by the target within the wavelength band of the tracker constitute the target signature for that tracker. To track a target, a seeker must discriminate target signals from background and countermeasures signals; it strives to accomplish this on the basis of the differences among the characteristics of the various signals.

One primary objective of many missile flight simulations is to test the ability of the seeker to perform this discrimination. To meet this objective, a simulated scene must be provided that closely approximates the "real-life" scene; the suitability of this simulated scene to the detailed, specific objectives is critical. Many forms of scene simulations are possible, and the choice depends on the objectives of the missile flight simulation. If a simulation is completely mathematical, i.e., no missile hardware is included in the simulation, a mathematical scene is required; if an actual hardware seeker is employed in a simulation loop, a physical scene must be presented for the seeker to view; and if missile seeker electronic hardware is employed in a simulation loop, but not the actual radiation sensor, a scene in the form of electronic signals must be provided. This chapter discusses the techniques used to generate mathematical, physical, and electronic scenes.

Whatever scene simulation concept is being developed,

consideration must be given to the many parameters that characterize actual scenes. These considerations include radiometric parameters, such as spectral distributions and atmospheric transmission; physical parameters, such as shapes, sizes, and locations; dynamic parameters, such as angular rates and closing rates; background parameters, such as sky, clouds, sun, and terrain; and countermeasures parameters, such as decoys and jammers (Ref. 1). The ideal is to present the scene to the flight simulation exactly as it would be viewed by the sensor in an actual missile engagement. Constraints of time and cost however, require compromises, which must be balanced carefully to meet the objectives successfully.

If a scene simulation includes actual physical radiation, the means of simulating the scene vary considerably, depending on whether an electro-optical (EO) or RF seeker is employed in the flight simulation. EO radiation is generated by blackbodies and arc lamps, and the radiation is attenuated, shaped, and directed by optical elements such as filters, apertures, mirrors, and telescopes. RF radiation is generated by RF generators, processed electronically, and transmitted from antennas. The RF seeker and RF scene simulation antennas are enclosed together in a shielded chamber designed to cause the radiation of the scene to behave as it would in free space. Various types of special equipment for simulating EO and RF scenes have been developed; examples are described.

9-2 SCENE ELEMENTS

There may be three different types of electromagnetic signal sources in a scene—targets, background, and countermeasures. Generally, the signals presented to the missile seeker have relative motion with respect to each other and to the seeker. The intensity of radiation reaching the seeker from any given source depends on the characteristics of the source object and on the attenuation of the signal as it travels from the source to the seeker. Characteristics of scene elements are discussed in this paragraph; techniques for representing the scene elements in a scene simulation are discussed later in this chapter.

9-2.1 TARGET

Targets for surface-to-air missiles vary in physical size and configuration from very small, slender targets, such as

cruise missiles, to very large, extended targets, such as bombers. Target speeds vary from zero, for hovering helicopters, to supersonic, for high-speed airplanes. Targets may travel straight, constant-speed flight paths, or they may perform evasive maneuvers expressly designed to cause the missile seeker to lose its track on the target or at least to cause a large miss distance. There may be one or more than one target within the seeker field of view at any given time, or if the seeker loses track, no targets are within the field of view.

When a target is viewed by a seeker from long range, it appears essentially as a point source. As the range from the missile to the target decreases, the target appears larger and huger until it finally fills the field of view of the seeker. Depending on the application, a target is represented in a scene simulation by a single point source, an area of radiation having a definable shape, or a number of discrete point sources.

Many seekers function most effectively when the image appears as a point source. The growth of the relative size of the target image as the missile approaches the target can affect the ability of a seeker to track accurately. For example, an EO seeker using a reticle (subpar. 2-2.1.1.1) modulates the target signal by alternately allowing the target signal to reach the detector and blocking it from the detector. This passing and blocking of the signal is accomplished by the transparent and opaque areas of the reticle through which the signal must pass to reach the detector. When the target image is smaller than the individual transparent and opaque areas, the entire image is essentially contained within only one element of the reticle pattern at any given instant, as shown in Fig. 9-1(A). In this case the modulation of the target signal by the reticle is easily processed to furnish the relative position of the target within the field of view. However, when the target image becomes large enough to cause target radiation to pass through more than one transparent region at the same time, as shown in Fig. 9-

1(B), accurate signal processing is more difficult.

Although signal processing for RF seekers is entirely different from that for EO seekers, RF seekers also experience increased tracking errors when the angular size of the target becomes significant relative to the size of the seeker field of view. These RF tracking errors are caused by the wandering of the apparent center of target radiation relative to the physical target center and this causes the seeker to adjust its pointing direction constantly.

The characteristics of the electromagnetic signals radiated from a target or reflected by it constitute the target signature. The parameters of target signatures include the signal strength and spectral properties of the radiation and the effects of aspect angle and time on the target signal. For a given seeker only those target signature characteristics that are detectable by that particular seeker are of interest; therefore, typical target signatures are applicable only within given frequency band limits, which must be specified for the signature to be meaningful.

9-2.1.1 Electro-Optical Signatures

As discussed in subpar. 2-2.1.1, the sources of EO radiation emitted from the target are the propulsion system, i.e., engine exhaust plume and hot tailpipe, the aircraft surface, i.e., heating by aerodynamics, solar energy, and thermal energy generated by internal components, and reflected energy, i.e., solar or laser illumination.

Since these various EO radiation sources have different temperatures, the predominant wavelengths of the respective radiated power fall into different wavelength bands of the EO spectrum. Typical seeker detectors are sensitive to only certain portions of the spectrum; therefore, not all of the EO power emanating from a target is detected by any given seeker. An example of the spatial distribution of an infrared (IR) signature in the azimuth plane of a typical target and in the wavelength band of a typical EO seeker is given in Fig. 2-4.

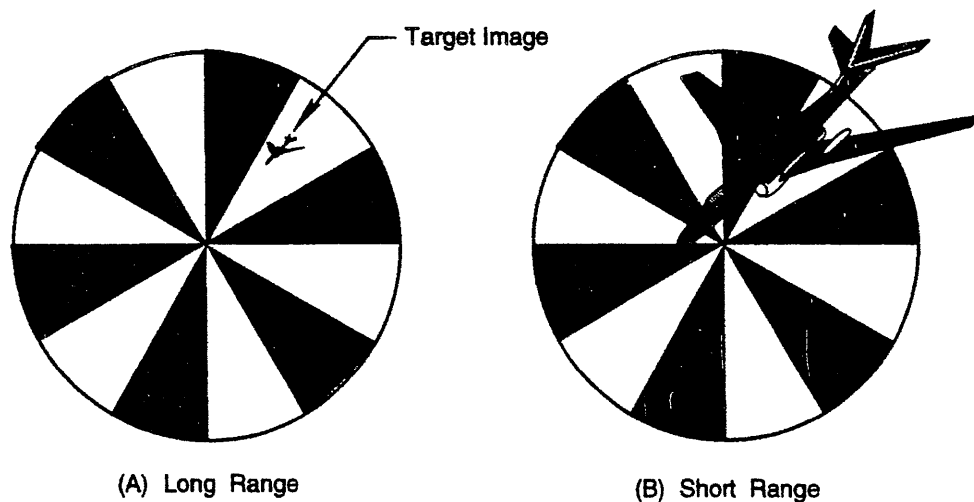


Figure 9-1. Size of Target Relative to Reticle Pattern

Very high temperatures are required to radiate significant amounts of energy in the ultraviolet (UV) region of the spectrum; therefore, only small amounts of UV energy are generated by the target. The UV energy from sunlight is reflected from both the target and the sky background, and the W energy density from the sky may be greater or less than that reflected from the target. When the target W reflection is less than that of the background, the target appears to a UV detector as a hole in the relatively uniform radiation pattern of the sky background. In either case the W contrast of the target relative to the background can be employed by certain missile seekers that are designed to detect it.

EO power emitted from one target component can be masked by other target components. For example, much of the power of the exhaust plume is not visible to a seeker from the head-on direction because the power is masked by the airplane structure.

Variations in the IR signature of a target occur when the engine power setting of the target is changed because (1) changing the power setting changes the amount of power in the exhaust plume and (2) the resulting change in speed affects the aerodynamic heating of the surfaces of the aircraft. Sun glint from various surfaces of the target aircraft may affect the performance of an EO seeker.

9-2.1.2 Radio Frequency Signatures

Radio frequency radiation can be generated by electronic equipment onboard the target or it can be generated by an illuminator radar and reflected by the target.

When a complex target, such as an aircraft, is illuminated by an RF wave, power is dispersed in all directions from multiple points on the target. The apparent distribution of the radiating points of the target and the intensity of the target signal vary nonlinearly with respect to range and aspect angle (Ref. 2). The spatial distribution of power reflected from the target depends on the size, shape, and composition of the target and on the frequency and nature of the incident radiation wave.

The intensities of the RF signatures of targets are characterized by a parameter called the scattering cross section. The power reflected from a radar target in a particular direction can be expressed as the product of an effective area and an incident radiation power density. In general, that effective area is the scattering cross section of the target. Because scattered radiation fields depend on the attitude at which the target is presented to the incident wave, the scattering cross section fluctuates as the relative attitude changes. Thus the scattering cross section is not a constant but strongly depends on the aspect angles of the target relative to both the illuminator and the receiver radars. For directions other than back toward the illuminating radar, the scattering cross section is called the bistatic cross section, and when the direction is back toward the illuminating radar, it is called the backscattering cross section or simply the radar cross section (RCS) (Ref. 3). A typical RF signature in the azimuth plane of an airplane is shown in Fig. 9-2.

The amplitude of the echo signal from a complex target may vary over wide limits as the aspect changes. If this variation in signal amplitude occurs during the observation time

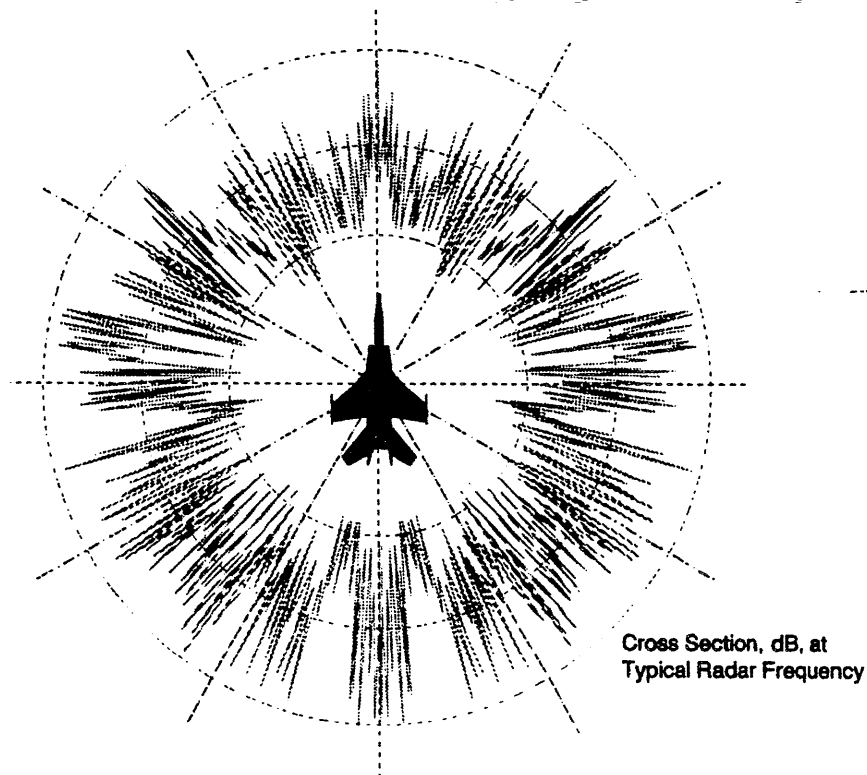


Figure 9-2. Typical Radar Cross Section in Azimuth Plane of Target

of a conical scan tracker, i.e., one revolution of the antenna beam, tracking errors are introduced that increase missile miss distance. The monopulse radar, on the other hand, determines the angular tracking error on the basis of a single pulse, and its tracking accuracy is not affected by changes in signal amplitude with time (Ref. 4).

At long range the receiver of the scattered RF energy views the target as essentially a single-point scatterer. At shorter ranges the apparent center of reflection might not correspond to the target center. Changes in the target aspect with respect to the radar can cause the apparent center of radar reflections to wander from one point to another. In fact, it need not be confined to the physical extent of the target and may be off the target a significant fraction of the time. This aimpoint wander, called glint, is perceived by the seeker as target motion and is a particularly important parameter in investigations of the miss distance of missiles with RF seekers. These angle fluctuations affect all tracking radars whether conical scan, sequential lobing, or monopulse (Ref. 4).

9-2.2 SCENE BACKGROUND

Seekers view targets against a background of EO and RF radiation scatterers that may fill the entire seeker field of view. There must be contrast between the target and the background for the seeker to be able to discriminate the target signal from background signals.

The various types of background that affect the operation of EO seekers are sky, haze, clouds, sun, and surface of the earth (terrain or sea). EO seeker performance is also affected by the intersections of different backgrounds, such as the horizon or cloud edges.

Radio frequency seeker performance is affected by scattered RF radiation, called clutter, reflected from scatterers in the sky or the surface of the earth. Since the velocity of the target relative to the seeker is generally different from the velocity of the background scatterers relative to the seeker, the Doppler frequency of the target is generally different from that of the clutter. Continuous-wave or pulse-Doppler radars can often discriminate between targets and clutter based on this difference in Doppler frequencies. Radio frequency seeker performance is also affected by the phenomenon of multipath. Multipath occurs when targets are close to the surface of the earth and signals can reach the seeker by a direct path, i.e., target to seeker, and by a reflected path, i.e., target to earth to seeker. The target signals that reach the seeker by reflection from the earth contain components of angle, range, and Doppler frequency shift that are different from those of the direct-path signals; this causes the seeker tracking to be faulty unless these multipath signals can be discriminated.

9-2.3 COUNTERMEASURES

Countermeasures are used by target aircraft or by other sources, such as standoff jammers to reduce the probability that a missile can successfully engage its target. A num-

ber of different types of countermeasures are employed, among which are vehicle signature suppression, target evasive maneuvers, jamming, and decoys. Each is discussed in the subparagraphs that follow.

9-2.3.1 Signature Suppression

The reduction of the signatures of vehicles is included in a general class of technology referred to as low-observables techniques (Ref. 5). The specifications of essentially all modern combat aircraft require signature suppression. The signature of a vehicle is suppressed in the design of the vehicle by judicious selection of the vehicle shape and of the materials from which it is fabricated. Materials that reduce reflected RF energy by absorbing a portion of it are referred to as radar-absorbent materials (RAM). The vehicle configuration and materials are designed to minimize the reflection of RF radiation and to minimize and mask IR radiation. The target signal intensities in a scene simulation are adjusted to account for the effects of signature suppression.

9-2.3.2 Evasive Maneuvers

Target maneuvers are portrayed in a scene simulation by causing the simulated target signal to move relative to the seeker in the same angular relationship as an actual maneuvering target. The parameters of target motion are calculated in the flight simulation as described in par. 7-4 and are passed to the scene simulation for control of the position and aspect of the simulated target. Target maneuvers may include some general form of jinking, such as a weave, or a specific maneuver in response to an individual missile engagement.

9-2.3.3 Jamming

IR jamming typically takes the form of a modulated IR signal generated by a jammer located on the target. The modulation is designed to confuse the seeker signal processing. RF jamming signals are emitted within the frequency band of the RF seeker and are designed to overpower the target signal with noise or to confuse or mislead the RF signal processor. Jamming is introduced in scene simulations by including simulated or physical radiation sources that have the appropriate characteristics of jammers.

9-2.3.4 Decoys

Active decoys are IR and RF energy sources intended to attract the missile seeker from the target. Expendable decoys are typically ejected from dispensers onboard the target aircraft. The separation of decoys from the target is accelerated by the combined forces of aerodynamic drag and gravity. The initial direction and speed of ejection and the aerodynamic characteristics of the decoy determine its trajectory relative to the target aircraft. Decoys also may be towed by the target aircraft.

The signal strength of a decoy is usually designed to be considerably greater than the signal strength of the target; this causes the missile to track closer to the decoy. If the

angular separation of the target and decoy as viewed by the missile seeker exceeds the field of view of the seeker, then at most only one of the two sources can be in the field of view. The missile may track the decoy and allow the target to escape from the field of view.

Since active or semiactive RF missile seekers depend on the target being illuminated with RF energy, passive RF decoys that reflect the illumination energy are possible. Passive RF decoys include chaff and towed RF reflectors. Active RF decoys receive the signal from an illuminating radar and retransmit it in a form and with sufficient energy to divert the missile seeker from the target.

The design and development of missile seekers and target decoys are dynamic processes in which seekers that can recognize and reject decoy signatures are continuously being developed, and improved decoys to counter these advanced seekers are being developed.

A decoy is represented in a scene simulation by a radiation source that provides the proper signal strength, spectral characteristics, spatial characteristics, and relative motion as functions of time. This radiation source may be mathematical or physical, depending on whether the seeker in the simulation is mathematical or physical hardware.

Decoy trajectories, relative to the target, are input to the simulation as function tables or are calculated by the flight simulation computer. When decoy trajectories are calculated, simplified equations of motion employing three degrees of freedom usually are used. Typically, decoys have poor aerodynamic shapes that cause them to tumble. Since the drag coefficient at any instant depends on the angle of attack at that instant, the usual procedure is to use an average drag coefficient that provides a reasonable match with observed flight-test trajectories.

The times for decoy ejection and the decoy trajectory parameters are passed from the simulation computer to the scene simulator (physical or mathematical) in which the decoy signal is generated and given the required motion relative to the missile seeker. The intensities of decoys as functions of time and the attenuation of decoy signals are also controlled by the flight simulation computer, and appropriate parameters are passed to the scene simulation for control of the intensities of decoy signals presented to the simulation seeker.

9-2.4 ATMOSPHERIC AND RANGE EFFECTS

EO signals can be greatly attenuated by the atmosphere, depending on the wavelength of the radiation and on the composition of the atmosphere. The attenuation of EO radiation by the atmosphere is illustrated in Fig. 2-3, which shows windows of low attenuation within specified wavelength bands.

As discussed in subpar. 2-2.1.2, certain radio frequency signals are relatively unaffected by atmospheric attenuation. For example, as shown in Fig. 2-11, the two-way attenuation of RF signals with frequencies between 1 and 10 GHz

is about 0.02 to 0.06 dB/nmi in a standard atmosphere at sea level, and these attenuation values continue to decrease as the altitude increases. The attenuation caused by rain becomes increasingly important as the radar frequency increases above about 3 GHz (Ref. 5); however, if the objectives of an RF missile flight simulation do not specifically include a study of the effects of atmospheric attenuation, these effects usually can be neglected.

Both EO and RF signals are attenuated by range. Signal strengths are measured as power density (W/m^2), and as the radiation wave propagates from its source or a reflection point, the surface area of the spherical wave front expands by an amount proportional to the square of the range, i.e., the square of the radius of the spherical front. The spread of a given quantity of power over this increased wave front area causes the power density to be reduced by amounts that are inversely proportional to the square of the range.

One method for calculating the combined atmospheric and range attenuation of EO radiation is to attenuate the signal by $1/R^n$, where R is range and n depends on the atmospheric conditions. Detailed computer programs are available to calculate atmospheric transmission of EO radiation, but these are rarely embedded in flight simulations.

RF signals that reach the seeker by reflection from the target are attenuated by $1/(R_1^2 R_2^2)$, where R_1 is the range from the signal source (illuminator) to the target, and R_2 is the range from the target to the seeker. RF signals that reach the seeker by a direct path from the source-active RF decoy, jammer, or signals generated by the target are attenuated by $1/R_3^2$, where R_3 is the range from the active RF source to the missile seeker.

9-3 METHODS OF SCENE SIMULATION

Because missile flight simulations have different objectives, several techniques for simulating target scenes have been developed. Scene simulation techniques that meet certain flight simulation objectives, particularly those requiring hardware-in-the-loop, are complicated and expensive to implement and operate. Other scene simulation techniques that meet the objectives of less demanding flight simulations are simple, and their cost is minimal. No single scene simulation technique meets the needs of all possible flight simulation objectives. Each technique has advantages and disadvantages that must be considered during selection of a scene simulation technique for a particular application.

Three basic methods used to simulate scenes are (1) mathematically, for use with seekers that are simulated mathematically, (2) physically, for use with hardware seekers in the simulation loop, which use actual sources that generate signals with proper spectral characteristics to represent the target, background, and countermeasures, and (3) electronically, for use with hardware seeker electronics in the simulation loop, which employ scenes generated electronically,

9-3.1 MATHEMATICAL SCENE SIMULATION

When seeker hardware is not used, the scene must be generated mathematically. The items usually simulated in a mathematical scene simulation are targets, jammers, and decoys. To reduce the computational requirements, these are often represented in a flight simulation by mathematical points that represent the relative positions of the centers of mass of the objects. Associated with each point is a signal strength that depends on parameters such as aspect, time, and attenuation. Targets are sometimes represented by a composite of several points in order to be more realistic when the target angular size increases enough to have a significant effect on seeker tracking. Mathematical simulations of RF targets sometimes include multiple radiating points with random positions and intensities to represent the effects of glint. The statistical distributions of the relative positions and intensities of the glint points are chosen to be representative of field measurements. When random parameters are employed to simulate glint, a simulation must be run repeatedly in Monte Carlo fashion to obtain statistically significant results.

The backgrounds of scenes also can be represented mathematically as composites of points, but this is seldom done because of the computing time required to process detailed scenes, such as clouds or terrain.

The equations for mathematically simulating the motion of targets are given in pars. 7-4 and 7-5. The motion of standoff jammers is calculated by the same equations. The motion of free-fall decoys is usually calculated by equations such as Eq. 7-7 in which the aerodynamic force is represented as pure drag and the propulsive force is zero. The signal strengths of the various objects in the mathematical scene are based on inputs of target signatures, jammer and decoy characteristics, and atmospheric characteristics and on parameters calculated within the simulation such as aspects and ranges.

Mathematical scenes are quick to prepare, they can be modified easily, and the costs of preparation and operation are small compared with the generation of physical scenes. Since the frequency content of the sensor signals is usually high, many time samples must be taken (small computation time steps) to model the physical devices adequately. This usually causes the computational requirements to be high, which is a major disadvantage of mathematical scenes.

9-3.2 PHYSICAL SCENE SIMULATION

When actual hardware seeker heads are used in simulations, sources of physical signals must be provided to represent the scene. The physical signals in a scene must be given the proper motions relative to the seeker head as the simulated engagement progresses, and physical source intensities and sizes must be adjusted as the simulated missile approaches the simulated objects in the scene.

The advantage of physical scene generation is that the use of an actual missile seeker eliminates the difficult task of

mathematically modeling and validating the seeker and signal processing functions (Ref. 2).

The disadvantages of physical scene generation include (1) long lead times for design and development and (2) high developmental and operating costs. The major disadvantage is that the state of the art of physical scene generation equipment is inadequate to generate a complex scene. These disadvantages restrict the use of physical scene generation to applications that do not require simulation with detailed scenes. When a hardware seeker is employed in the simulation, however, there is no alternative; physical radiation must be generated for the target scene.

9-3.2.1 Electro-Optical

The signals of EO scenes are generated by laboratory equipment designed to produce physical EO radiation with proper spectral characteristics. The general basic requirements for simulating EO scenes are (Ref. 2)

1. Simulation of multiple radiating objects
2. Modulation of EO power from sources with varying modulation parameters
3. Variation of radiation intensity and color between sources
4. Simulation of dynamic separation between sources
5. Simulation of dynamic variation of target image size
6. Simulation of dynamic intensity changes as a function of closing range.

The equipment used to simulate EO scenes includes sources of EO radiation (blackbodies and arc lamps) used to simulate the signatures of targets, flares, jammers, and backgrounds. This equipment may contain electronically controlled servomechanisms that simulate the apparent angular motion of objects in the scene relative to the missile, the intensity of the radiation reaching the seeker, and the apparent sizes of the objects. Servo-controlled filters may be employed to vary the intensity of the target and decoy signals. Electronic commands sent from the computer to the variable apertures and filters produce the computed target sizes and effective irradiances. By means of appropriate optical elements, the combined scene—including targets, background, and countermeasures—may be brought together and presented to the hardware missile seeker (Ref. 6).

9-3.2.2 Radio Frequency

When RF missile seeker heads are used in missile flight simulations, signals that generate scenes are produced by physical RF radiation generators. These generators produce radiation with the proper radiation frequency spectral characteristics, signal return delays, waveforms, and Doppler effects.

The RF environment that must be considered during design of a scene simulation is the composite of all RF signals that stimulate the missile antenna during flight. It includes target scattering returns, clutter, multipath, and

electronic countermeasures signals. During a simulation RF signals are generated in real time and transmitted to the seeker mounted on a three-axis flight table (missile-positioning unit (MPU)). To exercise the missile seeker hardware properly during simulation, the signals presented to the seeker by the environmental models ideally should be indistinguishable from those encountered during actual combat flight. Because of incomplete knowledge of the physical phenomena involved and constraints in time and budgets, this goal is often only partially realized (Ref. 7).

Different levels of detail are appropriate for RF environmental models, depending on the simulation objectives. To determine acquisition range, for example, a simple point target may suffice, but to determine end-game seeker performance in the presence of countermeasures, a realistic extended target model is required.

When the target scene is represented by physical RF radiation, an actual RF seeker looks into an anechoic chamber containing the elements that generate the scene (Ref. 8). If the missile seeker is active, it emits a burst of RF energy. The simulated target receives the burst converts it to a synthesized return, and reradiates it to the seeker, which acquires and tracks it. If the seeker is semiactive, radar pulses are radiated by the simulated target as if it had been illuminated by an illuminator radar. Multiple radiation sources may be included in the RF scene simulation to represent multiple targets and countermeasures.

9-3.3 ELECTRONIC SCENE SIMULATION

Electronic scene simulation methods have been developed to provide additional detail in the target scene not currently achievable with physical scene simulations. Electronic scenes are generated by measurements in the field, using an imaging radiometer, of actual scenes composed of targets, backgrounds, and countermeasures. The measured data are stored for subsequent use in missile flight simulations that employ seeker electronics in the simulation loop. After off-line processing by a host computer, the electronic scene data are passed into a target image simulator (TIS) described in subpar. 9-4.1.2. The TIS forms sequential matrices of electronic scene elements that are appropriate to the instantaneous seeker fields of view of the seeker being simulated. These sequential electronic scenes are passed into the hardware seeker electronics with appropriate timing so that the signals entering the seeker electronics closely approximate the signals that would have been generated by an actual seeker detector viewing the same scene in the field.

The major advantage of electronic scene simulation for the seeker-electronics-in-the-loop mode over physical scene generation for the seeker-in-the-loop mode is that signals from actual scenes are presented to the missile seeker electronics. This is essential for a realistic evaluation of imaging and pseudoimaging seekers (Ref. 6). The major disadvantage of electronic scene generation is the specialized equipment required.

9-4 EQUIPMENT FOR SCENE SIMULATION

The development of scene simulations for use with missile guidance hardware in a missile flight simulation requires very specialized laboratory equipment, and often the equipment used in a given missile flight simulation is unique, having been developed to meet the particular objectives of that simulation. Also the scene simulation equipment used for EO scenes is very different from equipment employed to simulate RF scenes.

9-4.1 ELECTRO-OPTICAL SCENES

Various special kinds of EO equipment have been developed or adapted to generate scenes for hardware-in-the-loop simulations. The UV/IR scene generator, target image simulator, and unique decoy generator are three examples. Each is discussed in the subparagraphs that follow.

9-4.1.1 Ultraviolet-infrared Scene Generator (VIRSG)

9-4.1.1.1 Components and Operation

The UVIRSG is a collection of controlled EO sources used to model targets, decoys, jammers, and backgrounds (Ref. 9). Physical EO radiation, generated by the UVIRSG, is used to excite the hardware detectors in an actual missile seeker, which is mounted on an MPU. The UVIRSG can simulate one target, two decoys, and one jammer simultaneously in both UV and IR wavelength bands, as well as provide a uniform W background to model the sky.

The UVIRSG is contained in two bays, one with three IR source assemblies and the other with three UV source assemblies (Fig. 9-3). For each spectral band the target and colocated jammer are produced in one source assembly, and a decoy is produced in each of the two other source assemblies. In addition, each UV source assembly contains a background source to permit simulation of targets and decoys with either positive or negative contrast with respect to the background. The IR bay contains a blackbody for the target and a xenon lamp for the jammer and each decoy. Each UV source assembly contains one xenon lamp to represent the target decoy, or jammer and an additional xenon lamp for the UV background.

The emissions from each target and decoy source pass through a variable aperture that controls the size of the image viewed by the missile seeker. The target image is square with the diagonals positioned horizontally and vertically. Target image sizes range from 0.05 deg to 3.0 deg. As viewed by the missile seeker, the UV background is 9.0 deg in diameter (nonvariable) and has a uniform intensity. There is no IR background. The emissions from each target and decoy source also pass through servo-controlled circular variable neutral density (CVND) filters to control the intensity of the signals.

In each bay of the UVIRSG are a telescope section and beam-steering mirrors used to position the signals in azi-

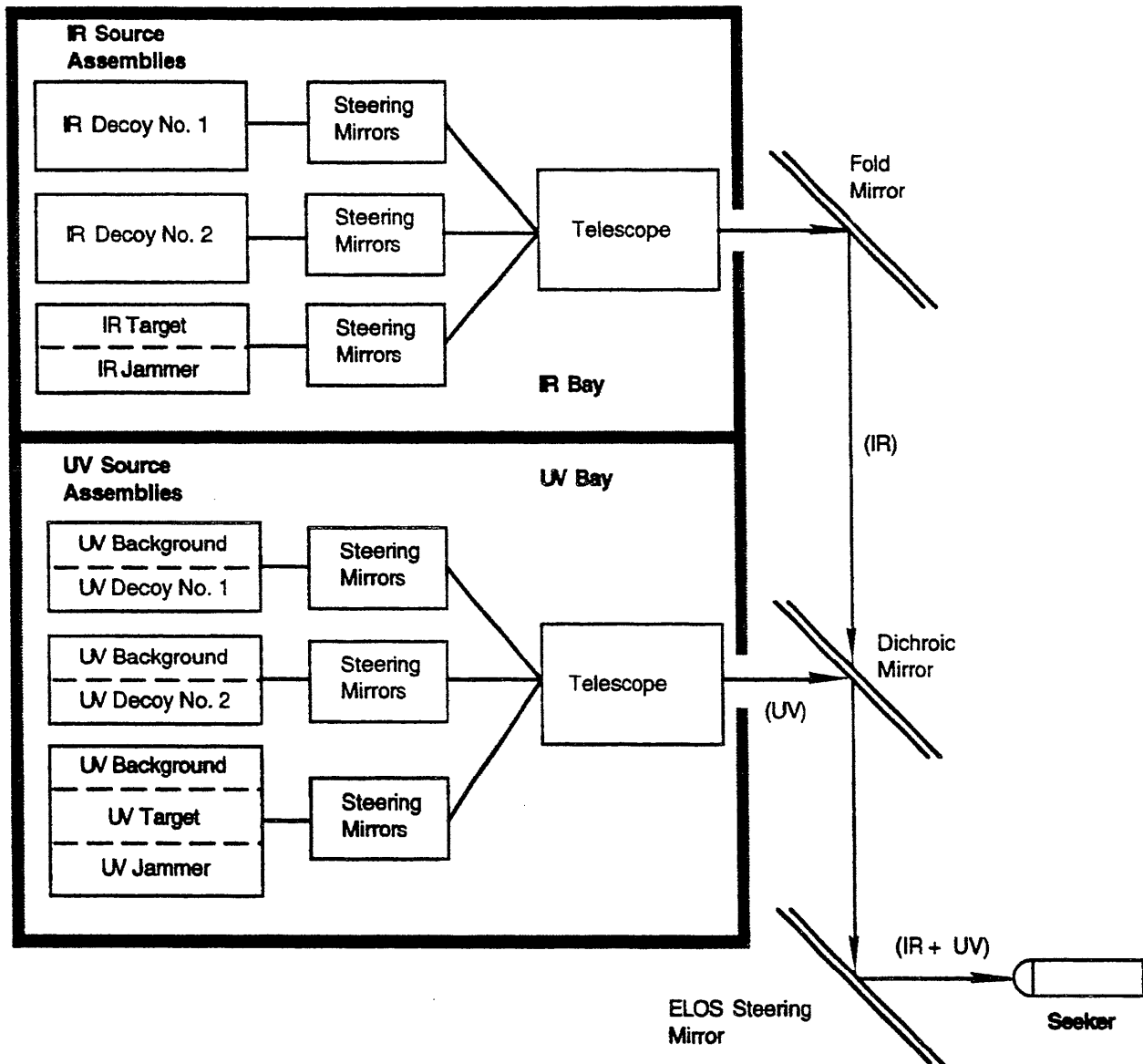


Figure 9-3. Ultraviolet-Infrared Scene Generator Configuration (Adapted from Ref. 9)

azimuth and elevation. In the IR bay the IR energy that represents the target and jammer is combined with the energy from each of the IR decoy sources and is magnified by the telescope. The UV bay is similarly arranged; energy from the various UV sources is combined and then magnified by a telescope. The IR and UV telescope outputs are combined by a dichroic beam splitter and directed in a collimated beam to the missile seeker head (Ref. 9).

Each source in each bay can be steered independently in both azimuth and elevation. The steering mirrors are servo controlled and thus permit angular changes to be made in the line of sight between the radiation sources and the seeker. Computer-generated commands based on the relative target-missile geometry are used to maintain the appropriate line-of-sight angles and angular rates during a simulated missile fright. Each orthogonal steering mirror unit can provide ± 6 deg of angular separation in both azi-

imuth and elevation for each decoy and target source. This feature permits decoys to separate from targets independently.

Although the UV and IR steering mirrors can move scene objects in both azimuth and elevation with respect to the missile seeker, the principal motion in elevation is performed by the elevation line-of-sight (ELOS) steering mirror, which can rotate the entire combined UV and IR scene ± 20 deg in elevation. Similarly, the UVIRSG is mounted on a computer-controlled azimuth rate table that rotates the entire scene ± 50 deg and provides the principal motion of the scene in azimuth.

Thirty different computer-controlled servomechanisms are contained in the UVIRSG to control the size, intensity, and direction of the radiation from each of the 11 radiation sources. When a simulated missile narrowly misses its target, extremely high angular rate commands are generated;

all electromechanical servomechanisms are limited in velocity to prevent damage when such commands occur. Over 300 optical elements are employed to generate, filter, image, magnify, direct, and combine the EO radiation into a target scene (Ref. 9).

The W and IR signatures of targets, decoys, and jammers are stored in computer memory as functions of appropriate parameters, such as aspect angle or time. The apertures, filters, mirrors, and the azimuth table are controlled by outputs from routines in the flight simulation computer that calculate relative geometry, signature data, and size and effective irradiance for each object in the scene.

Calibration equipment for the scene generator includes a dual-spectral-band alignment tool to verify the positions of the various radiation sources and a dual-band radiometer for intensity measurements. The system alignment tool allows source positions to be verified within ± 0.05 deg in both spectral bands (Ref. 6).

9-4.1.1.2 Targets

Infrared energy for targets is emitted from a 1500-K blackbody. This energy is filtered, attenuated, field stopped, and combined with the IR jammer energy. Similarly, the UV target energy is emitted from a 400-W arc lamp, combined with its background energy, filtered attenuated, field stopped, and combined with the UV jammer energy. Each UVIRSG target signal reaching the seeker is a composite of IR radiation generated in the IR bay and UV radiation generated in the UV bay. Each of the combined UV and IR target sources has five computer inputs to control IR target size, UV target size, IR target intensity, UV target intensity, and UV background intensity (Ref. 9).

9-4.1.1.3 Decoys

UVIRSG contains four independent decoy source assemblies—two identical IR units and two identical W units. Infrared energy that represents a decoy is emitted from an 800-W arc lamp, the UV energy for a decoy is emitted from a 400-W arc lamp, and the UV background energy associated with each UV decoy source is also emitted from a 400-W arc lamp. For each decoy, the size, shape, position, and positive or negative UV contrast generation are the same as those described for the target sources (Ref. 9).

9-4.1.1.4 Jammers

The energy for the IR jammer source is delivered by an 800-W arc lamp. A 350-W arc lamp is used to provide the W energy for the jammer. Jammers appear to the missile seeker as small emitters with an angular size of less than 0.1 deg located at the center of the combined W and IR target. Jammer simulations must be capable of generating specified waveforms. Therefore, before the energy from jammer lamps is combined with the W and IR energy of the target, it is transmitted through EO crystal modulators. The jammer energy is electronically modulated by any arbitrary time-varying waveform through application of a high-voltage

field with the desired waveform across the modulation crystals. The magnitude and waveform of the high-voltage field are controlled by either a computer or an external signal generator (Ref. 9).

9-4.1.2 Target Image Simulator

9-4.1.2.1 Components and Operation

The target image simulator is an assemblage of digital, electronic equipment that generates target and countermeasure scenes for missile flight simulations that employ hardware missile-seeker electronic signal processors in the simulation loop. The TIS accepts "real-world" scene data from actual scenes composed of targets, background, and countermeasures (Refs. 6 and 9). The scene data are obtained by field measurements of radiation intensity made with an imaging radiometer.

The TIS presents to the hardware signal processor (seeker electronics) the same signals that would be generated by the detector of an actual EO seeker viewing the same scene. Target and background data can be measured separately by the imaging radiometer, therefore, a target scene measured at one location can be simulated with a background measured at a different location. For example, targets measured against a clear sky can be simulated with background of a cloudy sky (Ref. 9).

Before scene data are entered into the TIS processor for use during the simulated missile flight the data are preprocessed off-line by a host computer that convolves the raw field-measured image data with the instantaneous field of view of the simulated seeker. Once the scene is configured and entered into the TIS by the host computer, the TIS becomes a stand-alone device.

In the TIS a scene is described by a matrix of elements (up to 256 x 256). Each element is described by up to eight bits allowing the scene to be quantized into 256 intensity levels (Ref. 6). The TIS stores up to twelve "snapshots" of the target scene. The host computer can update the TIS memory without interrupting the simulation; therefore, more than twelve scenes can be used in one simulated missile flight.

Each scene in the TIS represents a target at a particular range and aspect angle relative to the missile. If the aspect angle history of the target is known a priori, each scene is prepared by using the appropriate combination of aspect angle and range. This makes it possible for the TIS to interpolate between scenes and thereby between ranges and aspect angles during real-time simulated flight. If variations in the aspect angle are not sufficiently known a priori, the modeler can use one of two techniques to account for aspect angle variations—iterative modeling and updating on the fly.

9-4.1.2.2 Iterative Modeling

In iterative modeling an initial functional relationship is assumed between the target aspect angle and range. This relationship is entered into the TIS, and a trial run of the

simulated engagement is made. The aspect-angle-versus-range history that results from the simulated flight is then compared with the assumed history. If the assumed relationship does not match the relationship developed by the flight, the process is repeated using the output aspect-angle-versus-range history as the assumed one for generating scenes for the next trial simulation run. This procedure is repeated until an acceptable match is achieved.

9-4.1.2.3 Updating on the Fly

Implementation of the updating-on-the-fly technique requires storage of a large number of scenes in the host computer; each of these scenes is based on a particular range and aspect angle. For each computation time step, a pair of scenes selected from memory is interpolated by the TIS to produce a scene that corresponds to the range and aspect angle of the target at that step. Interpolated scenes must be available to the simulation in real time. Therefore, the scenes to be interpolated must be loaded into the TIS before the aspect angle for a given step is available from the simulation; this requires that the next aspect angle be predicted. While the TIS is producing an interpolated scene for a given time step, the host computer predicts the next aspect angle that will occur and selects from its memory another scene that can be interpolated with the last selected scene to produce one that matches the predicted aspect angle for the next step. The newly selected scene is loaded into TIS memory and is ready to be interpolated to form the next scene in time for the next step. The success of this technique depends on the speed of the TIS and the host computer.

Updating on the fly can also be used to expand the number of scenes the TIS can contain; the host computer acts as a virtual memory for the TIS (Ref. 9).

9-4.1.3 Unique Decoy Generator

The unique decoy generator (UNDEGE) is an extremely fast and powerful collection of digital hardware used to simulate decoys in a seeker-electronics-in-the-hop missile simulation that employs the TIS. In conjunction with a host computer, the decoy generator calculates the instantaneous position and intensity of flares and inserts this information into the target scene of the TIS. The decoy generator receives inputs, such as time, relative target position, seeker boresight direction, and range, from the simulation computer. The output of UNDEGE is an analog voltage corresponding to the seeker detector signals (before attenuation by range) that would be generated if the actual missile seeker were viewing the modeled scene of actual decoys (Refs. 6 and 9).

Flare position data relative to the point of ejection from the target and intensity data as functions of time are stored on disk files that are accessed in a nonreal-time fashion and stored in tables in the UNDEGE before a simulated flight is made. In some applications the same flare table can be employed for numerous flares because the trajectories of all the flares (of a given type) relative to a constant-speed target

are identical except for displacements in time. During the simulated flight the UNDEGE calculates the projected flare displacement angles from the target and looks up the flare intensity from data in the flare table.

In its basic configuration the decoy generator can model up to 62 flares simultaneously and accommodate flare ejection rates up to 20 per second. Each flare is modeled as a circular shape of arbitrary size with a variable intensity gradient across the extent of the flare (Ref. 6).

9-4.2 RADIO FREQUENCY SCENES

In the simulation of physical RF scenes (environments), any RF signals generated for the scene must behave as if they were in free space, i.e., signals must be prevented from reflecting from walls and equipment in the simulation laboratory. In addition, extraneous RF signals that could affect the performance of the missile seeker must be shielded from the seeker. These requirements generally are met by containing the scene signals and the missile seeker within an enclosed metal chamber that blocks external radiation from entering and that has internal surfaces covered with materials that absorb RF energy rather than reflect it. Such an enclosure is a shielded anechoic chamber as shown in Fig. 9-4.

Radiation signals are transmitted from an antenna array on one side of the chamber to a guidance sensor (RF seeker) projected through an aperture on the opposite side of the chamber (Ref. 10). A tight RF seal is maintained between the flight table containing the missile seeker and the wall of the anechoic chamber. This seal ensures that the large amounts of RF power transmitted within the chamber are confined—a requirement necessary to ensure the safety of personnel and to prevent external power from entering the anechoic chamber and contaminating the free space environment (Ref. 8).

9-4.2.1 Simulation Equipment

In general, each flight simulation facility that employs RF hardware in the missile flight simulation designs its own scene simulation system. The Radio Frequency Simulation System (RFSS) at the US Army Missile Command, Redstone Arsenal, AL, (Refs. 7 and 10) is an example of special equipment used to generate RF scenes. The RFSS can simulate in real time any RF guidance mode. The simulation includes coherent and noncoherent signals for active, semi-active, passive, command, beam-rider, and track-via-missile systems.

The RFSS target simulator consists of 550 antennas located on the concave side of a metal, dish-shaped surface that has a spherical radius of curvature of approximately 12.2 m (40 ft) and a diameter of 10.1 m (33 ft). The array can either transmit RF signals dynamically controlled in relative angular position or receive RF signals over a field of view of approximately 0.73 rad (42 deg) as viewed by a sensor mounted on a flight table. The location of the apparent source of RF signals can be regulated to within 0.3 mr.

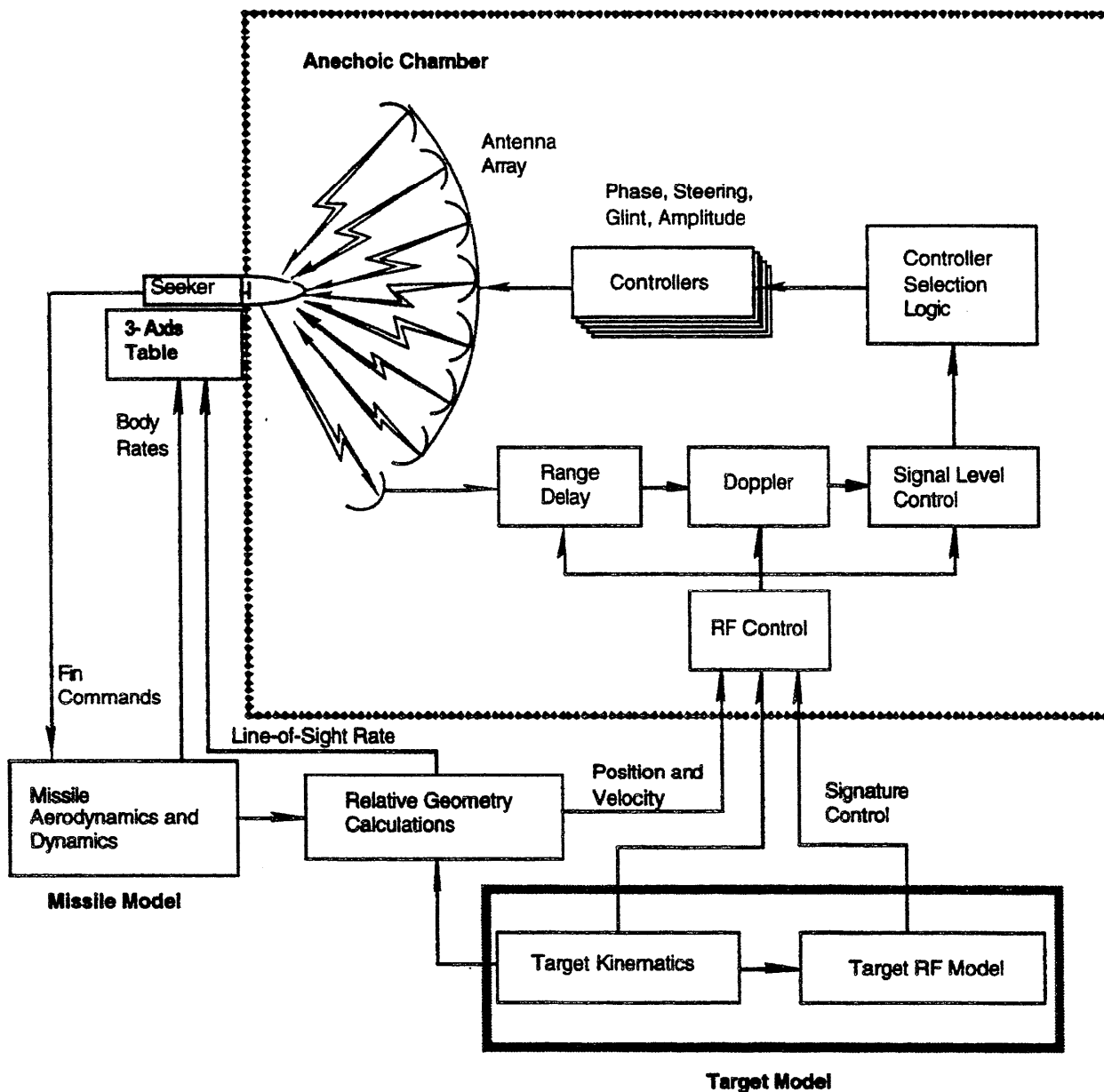


Figure 9-4. Typical RF Scene Simulation Configuration (Adapted from Ref. 9)

The RFSS operates over a frequency range of 2 to 18 GHz. Target position is updated at 1- μ s intervals with error standard deviations of 0.3 m within the 2- to 12-GHz band and 1.0 m within the 12- to 18-GHz band. The 550 antennas are divided into two arrays—a main target array of antennas and an electronic countermeasures (ECM) array of 16 antennas uniformly distributed among the 534 target antennas (Ref. 10). The target array generates sources of radiation that can represent up to four independently controllable, complex target signals. Any of the radiated signals can be used as a source of radiation simulating self-screening jammers. When a semiactive missile that has a rear-facing antenna to receive reference signals from the target illuminator, subpar. 2-3.1.2.2, is simulated, the RFSS supplies the rear reference signal to the missile.

9-4.2.2 Levels of Fidelity

The general approach to environmental modeling that uses the RFSS involves forming hierarchies of generic models for each RF environment element (Ref. 7). These hierarchies—which exist for targets, clutter, jet engine modulation, propeller and helicopter blade modulation, multipath, and chaff—range from simple to complex with corresponding ranges of applicability and realism. The hierarchies are generic in the sense that their formulation is driven by specific databases that are generated empirically or analytically and that are appropriate for both the missile system being tested and the target or threat vehicle being simulated.

The target model hierarchy, for example, consists of four levels of complexity:

1. Isotropic Scatterer Model
2. Empirical Scatterer Model
3. Statistical Model
4. Deterministic Multiple Scatterer Model.

The simplest, the Isotropic Scatterer Model, consists of a point reflector located at the target centroid with a fixed radar cross section (RCS). The Empirical Scatterer Model allows slow variation of both the target RCS (amplitude scintillation) and apparent angular position (glint or bright-spot wander) as a function of aspect angle. The Statistical Model has the capabilities of the Empirical Scatterer Model, and, in addition, it allows rapid variation of amplitude with aspect angle (high-frequency amplitude scintillation) and variations of angular glint components that are either aspect or aspect-rate dependent. The final and most realistic member of the hierarchy, the Deterministic Multiple Scatterer Model, treats the target as a collection of point scatterers. Each scatterer can have aspect-dependent amplitude and phase-scattering properties, and the total target return can be computed as the coherent superposition of the returns from the individual scatterers illuminated by a radar transmitter. This results in the seeker receiving signals that have realistic amplitude scintillation and angle glint.

Each of these environmental models is driven by an empirical or semiempirical database, and the extent to which a particular model realistically represents the radar signature of a particular target or threat vehicle depends largely on the quality and completeness of the database.

REFERENCES

1. D. J. Strittmatter, "A Seasoned Approach to Missile Target Simulators", Proceedings of the Society of Photo-Optical Instrumentation Engineers, Optics in Missile Engineering, SPIE Vol 133, Los Angeles, CA, January 1978, pp. 83-95, Society of Photo-optical Instrumentation Engineers, Bellingham, WA.
2. T. A. Atherton, "A Missile Flight Simulator for Infrared Countermeasures Investigations", Proceedings of the Society of Photo-Optical Instrumentation Engineers, Optics in Missile Engineering, SPIE Vol 133, Los Angeles, CA, January 1978, pp. 103-5, Society of Photo-Optical Instrumentation Engineers, Bellingham, WA.
3. E. F. Knott, J. F. Shaeffer, and M. T. Tuley, Radar Cross Section, Its Prediction, Measurement and Reduction, Artech House, Inc., Dedham, MA, 1985.
4. M. I. Skolnik, Introduction to Radar Systems, 2nd Ed., McGraw-Hill Book Company, New York, NY, 1980.
5. D. C. Schleher, Introduction to Electronic Warfare, Artech House, Dedham, MA, 1986.
6. G. H. Johnson, Electm-Optics! Countermeasures Simulation Facility, Office of Missile Electronic Warfare, White Sands Missile Range, NM, Undated.
7. A. M. Baird, R. B. Goldman, N. C. Randall, W. C.

Bryan, F. M. Belrose, and W. C. Holt, Verification and Validation of RF Environmental Models—Methodology Overview, Technical Report RD-81-2, US Army Missile Command, Redstone Arsenal, AL, October 1980.

8. M. E. Sisle and E. D. McCarthy, "Hardware-in-the-Loop Simulation for an Active Missile", Simulation 39, 159-67 (November 1982).
9. M. D. Sevachko et al, "Scene Generation for Real-Time Missile Flight Test", Aerospace Simulation III 19, The Society for Computer Simulation International (3-5 February 1988).
10. D. W. Sutherlin, "On an Application of Hybrid Simulation to Antiradiation Missiles", Proceedings of the Summer Computer Simulation Conference, Washington, DC, July 1976, pp. 107-11, Simulation Council, La Jolla, CA.

BIBLIOGRAPHY

SCENE SIMULATION

- P. C. Gregory, "Testing of Missile Guidance and Control Systems", Guidance and Control for Tactical Guided Weapons With Emphasis on Simulation and Testing, AGARD-LS-101, Advisory Group for Aerospace Research and Development North Atlantic Treaty Organization, Neuilly sur Seine, France, May 1979.
- H. L. Pastrick, L. S. Isom, C. M. Wall, R. J. Vinson, and L. H. Hazel, "Monte Carlo Model Requirements for Hardware-in-the-Loop Missile Simulations", Proceedings of the 1976 Summer Computer Simulation Conference, Washington, DC, 1976, pp. 112-7, Simulation Council, La Jolla, CA.

TARGET SIGNATURE

- D. K. Barton, Radar Systems Analysis, Prentice Hall, Inc., Englewood Cliffs, NJ, 1964.
- R. H. Delano, "A Theory of Target Glint or Angular Scintillation in Radar Tracking", Proceedings of the IRE, December 1953, pp. 1778-84, Institute of Electrical and Electronics Engineers, Inc., New York, NY. (IEEE was IRE.)
- P. Garnell, Guided Weapon Control Systems, 2nd Ed., Royal Military College of Science, Shrivenham, Swindon, England, Brassey's Defence Publishers, London, England, 1987.
- E. F. Knott, J. F. Shaeffer, and M. T. Tuley, Radar Cross Section, Its Prediction, Measurement and Reduction, Artech House, Inc., Dedham, MA, 1985.
- F. W. Nesline, and P. Zarchan, Missile Guidance Design Tradeoffs for High-Altitude Air Defense, Raytheon Company, Missile Systems Division, Bedford, MA, 1982.
- M. Skolnik, Radar Handbook, McGraw-Hill Book Company, New York, NY, 1970.

CHAPTER 10 IMPLEMENTATION

To this point the handbook has focused on the equations and algorithms that must be programmed for a computer to construct a missile flight simulation. This chapter addresses (1) selection of a computer system suitable for implementing the equations and algorithms, (2) selection of a computer language to develop the simulation, (3) application of numerical techniques required for digital solutions, and (4) special instructions to operate missile flight simulations that contain missile hardware in the simulation loop.

10-0 LIST OF SYMBOLS

a_i and b_i = constants in transfer function
 F = magnitude of force, N
 $f(t)$ = vector of functions of time t
 $G(t, y)$ = vector of functions of t and y
 $G(s)$ = transfer function
 $G(\Delta)$ = function of the reciprocal of the z -transform
 $H_1 = G(t_n, y_n)$
 $H_2 = G(t_n + 1/2 T, y_n + 1/2 T H_1)$
 $H_3 = G(t_n + 1/2 T, y_n + 1/2 T H_2)$
 $H_4 = G(t_n + T, y_n + T H_3)$
 m = mass, kg
 n = index for identifying a particular computation step, dimensionless
 s = Laplace transform variable
 T = length of computation step (sampling interval), s
 T_n = integration step size of the n th step, s
 t = independent variable, e.g., time
 t_n = value of independent variable at beginning of step n
 t_{n+1} = value of independent variable at beginning of step $(n + 1)$
 v = magnitude of velocity (speed), m/s
 x = magnitude of displacement, m
 $x(s)$ = Laplace transform of input
 $x(t)$ = time-domain input of the linear system
 Y = vector of predicted dependent variables
 Y_{n+1} = vector of predicted dependent variables at beginning of step $(n + 1)$
 $Y_{n+1/2}$ = vector of predicted dependent variables at midpoint of step n
 y = vector of dependent variables
 y_n = vector of dependent variables at beginning of step n
 y_{n+1} = vector of dependent variables at beginning of step $(n + 1)$
 y_{n-1} = vector of dependent variables at beginning of step $(n - 1)$

$y(s)$ = Laplace transform of output
 $y(t)$ = time-domain output of a linear system
 z = z -transform variable
 $\Delta = e^{-sT} = z^{-1}$
 ζ = damping ratio, dimensionless
 τ = system time constant, s
 ω_d = damped natural frequency of system, rad/s
 ω_n = undamped natural frequency of system, rad/s

10-1 INTRODUCTION

A number of factors must be considered in the selection of a computer system to implement a missile flight simulation and these factors must be reevaluated often in light of the rapid advancements in computer technology. Depending on the objectives of the simulation, special computational equipment may be needed to meet the computational speed requirements, particularly if the simulation includes hardware-in-the-loop. Simulations that must calculate the high-frequency characteristics of seekers, actuators, or control-surface deflections in real time are especially demanding of computational speed. The primary objective in the selection of a computer system is to satisfy simulation requirements with the least cost. Secondary objectives that reinforce the main objective are ease of implementation, setup and operation, and support by the manufacturer.

Those simulation developers who have the luxury of choice regarding the computer system to be used for their simulation must choose one that will satisfy the computation and memory requirements of the simulation. Otherwise, it may be necessary to relax the simulation objectives to allow implementation of the simulation on available computational equipment. If the simulation must supply outputs at the same rate as the components of the actual missile, i.e., real-time simulation, speciality multiprocessor or high-speed, high-cost supercomputers may be required. These uncommon computers often require their own specialized software, and users must consider issues in the selection of these machines that are different from the issues in selecting the general-purpose digital machines used in most computer applications.

The main considerations in choosing a computer language to develop a missile flight simulation are compatibil-

ity with the host processor, ability to achieve processing speed requirements, ease of use, and ease of modification. Early flight simulations were sometimes written in assembly language because of its efficiency; however, modern, efficient compilers of high-level languages greatly ease the programming burden and approach the speeds of assembly language. FORTRAN is the most widely used language for simulation and other scientific applications; however, more-structured languages, such as PASCAL, C, and Ada, are also suitable for missile simulations that can run on general-purpose digital computers. As previously stated, specialized computers may require their own specialized software.

The differential equations used to model missile flight are sets of nonlinear differential equations with time-varying coefficients that cannot be solved analytically. Therefore, to implement the solutions to these equations on digital computers, numerical methods must be employed in which algebraic difference equations are used to simulate the differential equations. Several standard methods of numerical integration are discussed in par. 10-4.

Although transfer functions can be solved digitally by any numerical integration method, the fact that they correspond to linear differential equations with constant coefficients allows special techniques to be applied. Tustin's method is a popular technique in which the Laplace transfer variable s is replaced by a particular z -transform function. The result is a simple algebraic difference equation for a given transfer function. Another method used to solve transfer functions digitally is based on a recently developed root-matching procedure in which the roots of the difference equation are matched to the roots of the differential equation being simulated. Since the roots are matched, the difference equation cannot become unstable-provided the differential equation is stable-regardless of the integration step size. Details of these methods of digital solution of transfer functions are given.

here are many special considerations in the development and operation of flight simulations that employ hardware-in-the-hop. These considerations deal mainly with ensuring that the hardware is operating properly and safely and that the interfaces with the computer system are correct. Special instructions for operating hardware-in-the-loop simulations are given.

10-2 SELECTION OF COMPUTERS

When selecting a computer system for missile simulations, the overall objective is to select one that will satisfy the simulation objectives with minimal cost. Considerations that go into the choice are

1. Accuracy
2. Processing speed
3. Ease of programming and ability to use standard languages and other available software
4. Continuing support by the manufacturer

5. Rapid setup of simulation runs and ease of operation

6. Cost.

(Memory size usually is not an issue in missile simulation; the computational deficiency most often encountered is insufficient computer processing speed to satisfy intensive calculation requirements.) Computer capability is advancing so rapidly that the most cost-effective choice for executing missile simulations must be reevaluated whenever a computer purchase is contemplated.

Many developers will neither be able nor need to acquire a special computer, or computer system, to execute their missile simulations. Several simulation objectives-discussed in pars. 3-2 and 3-4-require only simplified, e.g., three degrees of freedom, missile models or those that do not have to execute in real time. These models will run easily on the widely available, faster personal computers and workstations. Also developers may not have a budget available for the sole purpose of executing missile simulations and may have to be satisfied with existing computer resources.

At the other extreme are simulations that are required to be complex, accurate models of missile performance and must be executed in real time to support hardware-in-the-loop and countermeasures environments. For these applications a developer may be assigned a budget to procure a laboratory facility that includes a computer system to support the real-time computational needs.

Executing a six-degree-of-freedom model in real time places a large burden on digital computational equipment. Unlike many algebraic equations that can be solved directly in closed form, simultaneous differential equations for translational (Eqs. 4-37) and rotational (Eqs. 4-46) motion and other elements of missile dynamics must be solved by numerical integration methods (See par. 10-4.). To obtain high-fidelity solutions, the integration step size must be small enough to include the highest frequency effects that must be modeled, and the solutions must be computed for each small step. Small step size contributes greatly to the computational burden. For digital computers the higher the frequency of the process being modeled, the greater the processing speed required to maintain the same accuracy level as for lower frequency processes (Ref. 1). If the frequency of the modeled process is low enough or the computer fast enough, the programmer can choose an integration step size small enough that the model accuracy obtained will be no less than the precision of the digital computer. As the frequency of the modeled process increases to the point at which reduction in the integration step size is not allowed because real-time simulation execution constraints cannot be satisfied the accuracy begins to degrade.

In the past, analog computers provided real-time solutions when digital computers were unable to perform at the required rate of speed. Analog computers were ideally suited to solving simultaneous differential equations

because the use of feedback loops in linear circuits eliminates the need for the computation-intensive integration calculations required on digital computers. Traditionally, however, analog computers

1. Were difficult to program using a patch panel to link manually the circuit components required for each simulation model

2. Had difficulty providing the accuracy desired

3. Had limited elements to model complex systems

4. Were difficult to calibrate and setup for runs.

Hybrid computers then evolved that combined both digital and analog processors to connect some of the deficiencies encountered in the use of analog computers alone. The patch panel was replaced with digital means to control and set up analog processors, which permitted digital programming. Digital control of the analog processor resulted in accurate calibration and faster setup and indirectly in greatly increased accuracy. The digital processor was also used to execute some of the slower running parts of the simulation, so the analog components were reserved for the higher speed requirements.

If a new laboratory facility is planned, given current 1994 computer technology, the most cost-effective approach to solving highly accurate missile simulations in real time or faster for testing hardware-in-the-loop is to use configurations of multiple digital processors. Solving the simultaneous differential equations associated with six-degree-of-freedom missile models can be accomplished more cheaply and easily by performing the integrations in parallel whether analog or digital computers are used. Because of the type of problem missile simulation presents, a number of inexpensive processors working in parallel can surpass the speed of single multimillion-dollar supercomputers. This type of advantage over supercomputers is only readily realizable for those problems that can take advantage of parallel computation.

Since the speeds of multiprocessor computers have increased to the point at which they can handle high-frequency missile components in real time for reasonable cost, they have essentially replaced analog computers for performing missile simulations. This was a natural evolution when the difficulties of operating analog and hybrid computers and the reasonable cost of the digital processors of today are considered.

For established, real-time hardware-in-the-loop missile simulation laboratories, there may be neither a need nor a budget to upgrade to new computational equipment even where older analog equipment may still be in use. In these laboratory situations it may be more convenient and cost-effective to supplement existing digital computers with analog integrators and other analog components to model a limited number of missile components with high-frequency processes.

For a new, all-digital computer facility the main difficulty

today because of multiple products of different types and quality is integrating the processors, software, and interface devices for analog sensors and other equipment into a cost-effective simulation system. The developer of a simulation laboratory for real-time, hardware-in-the-loop evaluation may choose to assemble a multiprocessor system from commercial components, to select and develop software to operate the computer equipment, and to assemble a set of analog-to-digital and digital-to-analog converter boards to interface with hardware-in-the-loop, or the developer may turn to commercial companies that provide this service. Applied Dynamics International (ADI) and Electronic Associates, Incorporated,* (EM) have been building computer systems for many years to solve missile simulations and other dynamic applications of simultaneous differential equations. Both companies have "turnkey" products that not only achieve the necessary speeds at reasonable cost by using parallel architecture but also provide custom software and other amenities that make simulation development much easier.

ADI produces the Applied Dynamics Real-Time Station (AD RTS), the hardware architecture of which is based on the open-architecture Versa Module Eurocard (VME) bus for internal communications. Connected to the bus is a variety of processors-some optional-with different functions. The VME bus Interact Manager (VIM) communicates with workstations on a local area network so that simulations can be setup and executed remotely from the network. A Communications Processor (COP) synchronizes and optimizes communications on the bus. One or more Compute Engines (CEs), which use the Motorola MC88110 microprocessors, are available to perform the nonhardware-in-the-loop portions of the simulation. One or more Parallel Intelligent Resources (PIRs) each provides access to multiple interfaces of different types. A PIR provides the following interfaces: analog (digital-to-analog and analog-to-digital), digital (bidirectional interface with control lines), serial (up to eight RS 422/RS 485 serial ports operating at data rates up to 1 Mbit/s on each connection), and specialized circuits (e.g., waveform generators, programmable resistive devices, or transition interval measurement devices that can be used to emulate transducers or other functions). Other VME bus-compatible devices can be connected and used.

EAI produces the Starlight computer, which is divided into two main parts: the Digitally Implemented Analog Computer (DIAC) and the VME Ancillary Multiprocessor (VAMP). The Starlight computer connects by Ethernet to any X-based workstation with the Silicon Graphics Indigo as a default. If the workstation is connected to a network, network operation of Starlight is possible. The VAMP, which is based on the VME bus, provides the interface to the workstation with its host central processing unit (CPU) based on the Motorola 68040. The VAMP also optionally processes user-written FORTRAN, C, or Ada language code

*The use of company names does not constitute an endorsement by the US Government.

sequentially (as opposed to parallel execution in the DIAC). The DIAC is designed and built by EAI and uses up to four arithmetic computation modules (ACMS) to perform numerical integration to solve the simultaneous differential equations constituting the simulation model. The ACM uses the Texas Instruments SN74ACT8847 32-bit math processor. The DIAC uses the EAI-designed Starbus for internal communications, which can support a maximum sustained rate of 80 Mbyte/s. The DIAC can also have optional interface modules connected to the Starbus: analog interface modules (AIMs) with 16 analog-to-digital and 16 digital-to-analog converters for hardware-in-the-loop interfaces, digital interface modules (DIMs) with 32 discrete input and 32 discrete output bits, and processor interface modules (PIMs) with 4K by 32-bit, dual-ported memory for interface with external processors that may be part of the simulation.

There may be instances in which compromises must be made in the simulation model to satisfy processing requirements. It is important to make these compromises with minimal impact on the missile simulation objectives. Previous chapters of this handbook discuss numerous simplifications and approximations that preserve some level of fidelity in the missile simulation.

The missile simulation developer must thoroughly understand the objectives to prevent a mismatch between these objectives and the computer system used. Particularly important is the selection of computer power (which equates to cost). It is essential to guard against acquiring unnecessary computer power to model seekers or actuators if the simulation objective can be satisfied by using transfer functions or actual hardware-in-the-loop to approximate or directly represent these processes. For example, a missile system manufacturer may not require the processing power necessary to model high-frequency seeker processes when constructing a test bed for the developed missile because hardware-in-the-loop will be used for the seeker (Ref. 2). If it is important however, to analyze different types of realistic countermeasure environments not modeled accurately by hardware scene simulators and the only way to assess the seeker response to the mathematical scene is to create a mathematical model of the seeker (Ref. 3), it would be a mistake to procure a computer system incapable of simulating the high-frequency processes that need to be evaluated and to assume that simplifying approximations are acceptable.

10-2.1 ASSESSING COMPUTER PROCESSING SPEED (BENCHMARKS)

Digital computer speeds expressed in normalized operations per second (NOPS), millions of instructions per second (MIPS), or millions of floating point operations per second (MFLOPS) can be deceiving and should be considered to be only estimates. The set of machine executable instructions varies from one computer type to another and causes variation in execution speed from one computer to

another for the same high-level program, e.g., FORTRAN. Compiler efficiency differs among computers for the same high-level language and from compiler to compiler on the same machine. These variations in compiler efficiency create differences in execution speed. Variation in the speed of machine executable arithmetic operations can also cause significant variations in execution speed for different programs, depending on the mix of arithmetic instructions. For example, if one computer is slower at adding but faster at multiplying than another, it may execute programs rich in multiplications faster than the other but execute programs that are addition intensive more slowly.

Attempts have been made to establish representative mixes of instructions, called benchmarks, that are more representative of computer processing capability. One example is the classic whetstone mix; many computers were rated by the number of whetstones per second. Other benchmark are dhrystone, SPECint92, SPECfp92, SPECrate_int92, SPECrate_fp92, AIM II, AIM XII, AIM Milestone, SPEC SDM, TPC-A, TPC-B, TPC-C, Linpack, and CPU2 (Refs. 4 and 5). Benchmarks can also be seriously misleading in the same way that average performance may never be representative of any given situation (Refs. 6 through 9). The only way to be sure that a particular computer and compiler can execute a particular algorithm or function in the time required is to construct a benchmark with a representative instruction mix for that application or to create the code and then compile and execute it on the computers under consideration for acquisition. These test programs should consist of the most demanding portions of the missile simulation, if not the entire missile simulation.

10-2.2 EXAMPLE SIMULATION COMPUTER FACILITY (Ref. 3)

The US Army Research Laboratory Simulation Facility at White Sands Missile Range, NM, illustrates the use of multiple computers to satisfy specific missile simulation objectives. (Other hardware in the facility is discussed in a previous chapter.) The laboratory configuration of this computer supports two modes or levels of missile hardware in the simulation loop. The missile-seeker-in-the-loop mode includes a complete missile guidance assembly or seeker, i.e., gyro/optics and signal processing electronics. The combination target and countermeasures scene is produced by a scene generator that contains actual electro-optical sources, i.e., blackbodies and arc lamps. These sources produce energy in the correct spectral region and are imaged on the missile seeker dome via appropriate optical lenses and mirrors. The second mode, termed missile-seeker-electronics-in-the-loop mode, incorporates only the signal processing electronics of the missile guidance assembly and thus necessitates the modeling of the gyro/optics or seeker head in the computer. The target and countermeasures scene for the missile-seeker-electronics-in-the-loop mode is produced by a special electronic scene simulator that is capable

of accepting real scene data obtained by field measurements of targets, background, and countermeasures.

The simulation computer system consists of an ADI AD-100 computer hosted by a DEC AXP 4000-610 and a hybrid computer consisting of an EAI Model 7800 analog computer and an EAI Pacer 100 digital computer. The 7800 is a 100-V machine-consisting of 78 summer/integrators, 30 inverting amplifiers, 36 multipliers, and 6 resolvers-used to simulate the high-frequency seeker responses in the missile-seeker-electronics-in-the-loop mode. The EAI Pacer 100 provides for computer control of the analog computer and is slaved to the AXP 4000-610. The AD-100 is used to generate the missile aerodynamic functions for solution of axial and lateral accelerations as well as for the integrations, multiplications, and summations required for the translational and rotational equations of motion for the target and missile. The AD-100 also solves the missile target geometric equations. Peripheral and input/output devices for the simulation computer system include control terminals, real-time display units, two eight-channel strip chart recorders, a line printer, and various disk drives.

10-2.3 SECONDARY CONSIDERATIONS

Although processing capability and cost are primary considerations, secondary considerations can also affect the choice of a computer. If several computer choices are equivalent in terms of processing speed (or at least satisfy the simulation objectives) and cost, other factors such as memory capacity, word length, hardware reliability, and manufacturer support can influence the decision to purchase.

Advances in computer technology have essentially eliminated memory capacity as an issue for missile simulation; memory is now much less costly than it was, and the 32-bit or longer word lengths found on most of the faster computers permit sufficient memory addressing for this application. Nevertheless, estimates should be made of the amount of memory required per processor in a multiprocessor system. Estimates can be made based on the memory required for compiled benchmarks including any actual simulation coding available. Care should be exercised in evaluating virtual memory computers with their "unlimited" memory because these machines are automatically loading and reloading memory from the available storage devices during execution when the complete program code will not fit in the available actual memory. The processes of loading and reloading can slow program execution speed significantly and therefore should be considered in the evaluation.

The word length used by a digital computer determines the parameter resolution that can be achieved in the missile simulation. More specifically, the number of bits used in the mantissa for floating point operations defines the range between the most and least significant bits. This range is adequate for most missile simulation requirements, even for the typical 32-bit word processors (6 or 7 decimal digit range). Many computers use much larger word sizes. Dou-

ble-precision (two-word) arithmetic operations are available on most computers; however, substantially more processing time is required for each operation compared with single precision. Therefore, use of this feature must be carefully evaluated when considering processing speed. Estimates of the largest and smallest magnitudes for all of the important variables of the simulation should be determined to make sure that the computer system will have sufficient word length to achieve the necessary parameter resolution. Rounding errors are also a consideration (See par. 10-4.).

Software development also can greatly influence operating costs. As computer hardware has evolved toward major increases in processing capability, the decrease in hardware cost has been equally significant. The lower hardware costs plus the increases in model complexity have resulted in a major percentage of computer costs being attributable to software. Programming a simulation on multiple processors of different types presents programming difficulties. Therefore, the simulation developer should (1) become familiar with all software that will be required on the computers considered for acquisition, (2) determine which high-level languages can be used to embed program modules in the computer system software provided by the manufacturer, and (3) estimate the time required for program development and maintenance.

Reliability of the hardware and support by the manufacturer are also key considerations in computer acquisition. Hardware downtime can be costly, particularly with respect to delays in ongoing analyses or simulation development. It is also important to have access to spare parts and repair service. If the computer model acquired is discontinued or the manufacturer goes out of business, the simulation developer may be in a difficult position. Therefore, evaluation of manufacturer support should be part of an acquisition decision.

Setup time for computer runs can significantly reduce the time available to use the simulation for analysis. For example, if multiple runs must be made to compute miss distance statistics-which are required if random variables in the scene or elsewhere are modeled-and variations in several parameters are required to complete an analysis, hundreds or even thousands of runs may be necessary. (If excessive numbers of runs are expected for simulations not exercising hardware-in-the-loop, the simulation may need to execute in faster than real time to satisfy the time requirements for analysis completion.) It may not be feasible to conduct this number of runs if the setup time for each run is inordinately long. Therefore, calibration and software compiling and loading time at the start of the run should be determined as part of an acquisition evaluation of a particular computer.

Data analysis time can be markedly reduced if the software and hardware tools are available to manipulate the outputs from the simulation runs. Most useful are hard copy plotting and interactive graphics capabilities. Disk or other storage for easy access and software for manipulation of data are important for computing statistics and identifying

data for plotting. Graphics and data manipulation capabilities provided by the computer manufacturer or available from third-party vendors should be investigated for any computer system to be acquired and the use of peripheral devices should be planned for the facility to be developed. Most computers now have standard interface ports-parallel and serial, e.g., RS-232-for attachment of peripheral devices. It is important to have enough ports for all of the peripheral devices planned for the system.

10-3 SELECTION OF COMPUTER LANGUAGES

The computer language chosen to develop the missile simulation should be (1) compatible with the processing speed required and (2) as easy as possible to use. In addition to these high-priority requirements, it is desirable that the language be widely used to ensure a large pool of potential programmers and to increase the chances that the simulation will run on other computer systems if that need is anticipated. Selection of a language is not as critical for simulations that do not need to execute in real time or faster and can execute on general-purpose digital computers. For real-time execution of a missile simulation, the developer may not have much choice of the computer languages and operating software used because of the requirement to solve simultaneous differential equations at high speed on specialized computers that use their own specialized compilers.

Early in computer development high-speed simulations were programmed in assembly language because the programmers could use the high correlation between assembly and machine instructions to produce efficient code, i.e., code with the minimum number of instructions for a particular model. The burden was placed on the programmers to reach maximum available speed through clever use of the assembly/machine instructions. Higher level languages removed most of this burden from the programmers when compilers for these languages began to approach the efficiency achievable with assembly language programs.

The most widely used language for simulation and other scientific application is FORTRAN. Assembly routines are still embedded within FORTRAN programs primarily for real-time processing of data inputs or outputs. FORTRAN lacks the capability to do the efficient bit manipulations that are usually required for packing and unpacking data during high-rate communications, so assembly language is often still used for those functions to achieve maximum processing speed.

In the many years that FORTRAN has been used, the language has been made more structured to allow more methodical and error-free programming. Minimizing the cost of software maintenance requires that programs be structured to use many short modules, each of which has as little effect as possible on other modules, in order to minimize debugging time when changes are required. The responsibility to construct structured programs in FOR-

TRAN lies with the programmer. High-level languages developed later-e.g., PASCAL, C, and Ada-force the programmer to use more structure and also may provide more programming power and flexibility. Any of these languages are suitable for missile simulations that can run on general-purpose digital computers. Most often FORTRAN is selected because of its wide use. FORTRAN and Ada are the principal Government-approved languages.

While the capability of general-purpose programming languages was evolving, special languages for simulation were developed for general-purpose digital computers. These languages, such as General-Purpose Simulation System (GPSS) and SIMSCRIPT, were designed to make it easier for the programmers to develop a simulation by developing high-level instructions peculiar to simulation problems and performing bookkeeping operations, such as automatically keeping track of simulated time. Unfortunately, these languages were primarily aimed at queuing models not applicable to missile simulation. In addition, the price for programmer convenience was a decrease in execution speed.

Analog computers required a different type of compiler. Originally, analog computers were programmed by manually wiring analog components together through a patch panel. After automatic control of analog devices was introduced, a compiler called Automatic Programming and Scaling of Equations (APSE) was developed in the late 1960s, which extended FORTRAN as a basis to allow specification of differential equations (Ref. 10). By the use of this compiler, the generated program could be targeted to different analog computers.

With support by the US Government the APSE compiler was improved to become a Program Generation System (PGS), which was capable of providing automatic setup, checkout, and operation of analog processors. This system became the Extended Continuous System Simulation Language (ECSSL), which included an online interpreter called HYTRAN. The interpreter accepted object code and performed setup and checkout of the parallel analog processor. Later versions of ECSSL were capable of providing interactive analog program operation including graphic display and recording of results.

Multiprocessor systems have additional major programming problems. Most compilers are designed to execute a program on only one processor, and several processors of different types require that the programmer determine which code is to be executed in which processor, or the compiler must make that decision. Because of the programming difficulties encountered with multiprocessor systems, the simulation developer is constrained at present to use the software developed for these systems. At the same time, the manufacturers of these specialized languages and compilers are attempting to make simulation development much easier than would otherwise be the case in this environment.

ADI provides several different types of software with the

AD RTS. COSIM is ADI's scheduling, synchronization, and communications-control software. It is used to manage data flow and to coordinate and synchronize the parallel processors. COSIM also includes an extensive run-time library to operate various interfaces provided by the hardware. ADSIM is a simulation language compiler specifically directed toward real-time environments. COSIM enables programs to execute a mixture of ADSIM, FORTRAN, or C languages on single or multiple CEs. Alternatively, models programmed graphically using the Boeing EASY 5x software can be linked to the appropriate interfaces and run-time tools by COSIM. EASY 5x has a graphical user interface (GUI), which replaces code writing effort with simple icons that represent various system components or mathematical operators. ADI also provides SIMplot to assist plotting of simulation results.

EAI developed the Starlight Interactive Simulation Language (SISL) to program the parallel part of the simulation. SISL conforms to Continuous System Simulation Language (CSSL) (predecessor of ECSSL) specifications developed originally for analog computers. SISL enables the simulation developer to begin with the simultaneous, coupled differential equations, which compose the simulation. The Starlight compiler then maps the SISL source directly into parallel machine code without the intermediate step of converting the code into sequentially executed FORTRAN or C. EAI claims that this direct efficient conversion is one of the key reasons the Starlight computer can perform simulations at high speeds. Standard compilers may be used for user-supplied FORTRAN, C, or Ada source code, which is independently linked to the DIAC to be executed along with the compiled and linked SISL code by the Starlight Executive (SX).

10-4 TECHNIQUES

In general, the differential equations encountered in missile flight simulations cannot be solved by classical analytical methods. Digital computer solutions require numerical methods. A large number of numerical integration methods have been developed, and discussions in the literature are sometimes confusing because terminology is not standardized (Ref. 11). Although some of the numerical integration methods are convenient for other computational purposes, they are not suitable for simulation.

Numerical methods used to solve differential equations usually involve replacing a differential equation by a number of algebraic equations, called difference equations, in such a way that the solution of the difference equations approximates the solution of the differential equation. Since they are algebraic, the difference equations are readily solved by digital computers. These numerical procedures

start with the initial conditions and solve the difference equations at successive discrete time steps.

Some numerical integration methods employ difference equations that can be solved explicitly, whereas others use difference equations that require an iterative procedure for solution and therefore are called implicit methods. Numerical integration methods are further divided into one-step and multistep types. A one-step integration method uses the value of the dependent variable only at the current integration step to calculate the value at the succeeding step. A multistep integration method uses values of the dependent variable at the current integration step and also at one or more preceding steps. One-step difference equations are self-starting, and multistep processes depend on a self-starting method to calculate the first few integration intervals. Examples of self-starting (one-step), explicit methods are Euler's method and the Runge-Kutta method. The improved Euler method is an example of a one-step, implicit method. Examples of multistep, implicit methods are Milne's method and the Adams methods.

The choice of the applicable numerical integration methods to employ in a simulation depends largely on the run-time and accuracy requirements of the simulation, although ease of implementation often is also a major factor. The most accurate methods often require more computer time to process the equations. Each of the methods has advantages and disadvantages, which are discussed later (Ref. 12).

Three general types of errors—rounding errors, truncation errors, and stability errors—can occur in applying difference equations for the solution of differential equations. Stability errors may be triggered by the buildup of rounding and truncation errors. Rounding errors occur because a digital computer can accommodate only a limited number of significant figures. A rounding error at any step in the computation propagates to the next step and is combined with the rounding error of that step. The amount of the rounding error at each step is difficult to predict. Truncation errors occur because in general the discrete nature of difference equations cannot exactly duplicate continuous differential equations. Truncation errors depend only on the type of difference equation used and are independent of the method or computing equipment used to solve the equation. Instabilities can arise from the difference equations, even when the differential equations being simulated are stable, because the difference equations are not always matched dynamically with the differential equations. These instabilities can result in spurious solutions that do not correspond to solutions of the differential equations (Ref. 12), and if not recognized as such, they can lead to serious errors in conclusions drawn from the results of a simulation.

10-4.1 NUMERICAL SOLUTION OF DIFFERENTIAL EQUATIONS

Any normal* system of differential equations can be written as a first-order normal system, which in vector notation has the form

$$\frac{dy}{dt} = \mathbf{G}(t, y) \quad (10-1)$$

where

$\mathbf{G}(t, y)$ = vector of functions of t and y
 t = independent variable, e.g., time
 y = vector of dependent variables.

The general solution of the set of differential equations represented by Eq. 10-1 is given by

$$y = f(t) \quad (10-2)$$

where

$f(t)$ = vector of functions of time t .

Eq. 10-2 is subject to the initial conditions $y = y_0$ at $t = t_0$.

Eq. 10-1 is solved numerically by substituting one or more difference equations in place of each differential equation. In general, the difference equations cannot be solved directly at any particular value of t . Instead the value of y is calculated sequentially, point by point, beginning at the initial values and continuing at intervals of the independent variable t until the solution has been extended over the required range of t (Ref. 13). The value of the dependent variable at each succeeding computation step is based on the value of that variable at one or more preceding steps.

Methods of numerical integration are divided into explicit and implicit types. Each type is discussed in the paragraphs that follow.

10-4.1.1 Explicit Methods

In an explicit method the value of the dependent variable y_{n+1} is determined explicitly at step $n+1$ in terms of the independent variable t_{n+1} and of the values of the dependent variable at one or more preceding time steps.

The Euler method and the Runge-Kutta method are examples of explicit numerical processes.

10-4.1.1.1 Euler Method

The Euler method is based on a difference equation having the form

$$y_{n+1} = y_n + \mathbf{G}(t_n, y_n)T_n, \text{ for } n = 0, 1, 2, \dots \quad (10-3)$$

*Any ordinary differential equation that has the form

$$\frac{d^n y}{dx^n} = G\left(x, y, \frac{dy}{dx}, \dots, \frac{d^{n-1} y}{dx^{n-1}}\right)$$

where

$\mathbf{G}(t_n, y_n)$ = vector of functions of t and y

n = index for identifying a particular computation step, dimensionless

T_n = integration step size for the n th step, s

y_n = vector of dependent variables at beginning of step n

y_{n+1} = vector of dependent variables at beginning of step $(n+1)$.

Starting with the value y_0 , Eq. 10-3 is used to calculate y_n successively at the points $n = 1, 2, \dots$

For example, consider the differential equation that describes Newton's second law for an application with constant force and constant mass

$$\frac{d^2 x}{dt^2} = \frac{F}{m}, \text{ m/s}^2 \quad (10-4)$$

where

F = magnitude of force, N

m = mass, kg

t = time, s

x = magnitude of displacement, m.

Writing Eq. 10-4 as a system of first-order equations in the form of Eq. 10-1 gives

$$\left. \begin{aligned} \frac{dv}{dt} &= \frac{F}{m}, \text{ m/s}^2 \\ \frac{dx}{dt} &= v, \text{ m/s} \end{aligned} \right\} \quad (10-5)$$

where

v = magnitude of velocity (speed), m/s.

Thus the vector y is defined in this case as

$$y = \begin{bmatrix} v \\ x \end{bmatrix} \quad (10-6)$$

and the vector G as

$$G = \begin{bmatrix} \frac{F}{m} \\ v \end{bmatrix}. \quad (10-7)$$

Then at the beginning of step n , the vectors y and G have values given by

$$\mathbf{y}_n = \begin{bmatrix} v_n \\ x_n \end{bmatrix} \quad (10-8)$$

$$\mathbf{G}(t_n, \mathbf{y}_n) = \begin{bmatrix} \frac{F}{m} \\ v_n \end{bmatrix}. \quad (10-9)$$

Substituting Eqs. 10-8 and 10-9 into Eq. 10-3 and assuming a constant time step—allowing the subscript n to be dropped from the time step—gives the system of difference equations

$$\begin{aligned} v_{n+1} &= v_n + \frac{F}{m}T, \text{ for } n = 0, 1, 2, \dots \\ x_{n+1} &= x_n + v_n T \end{aligned} \quad (10-10)$$

where

T = length of computation time step, s.

Solving Eq. 10-10 algebraically yields an approximate solution to Eq. 10-4 and gives values of v and x at successive time steps. The value of t at the beginning of time step n is given by

$$t = nT, \text{ s.} \quad (10-11)$$

The Euler method, also called simple rectangular integration, introduces a truncation error at each step, as shown in Fig. 10-1. As the time step T becomes sufficiently small, the error becomes insignificant. Reducing the time step to the extremely short times required for great accuracy, however, increases the computation time and can introduce a significant rounding error, depending on the word length of the

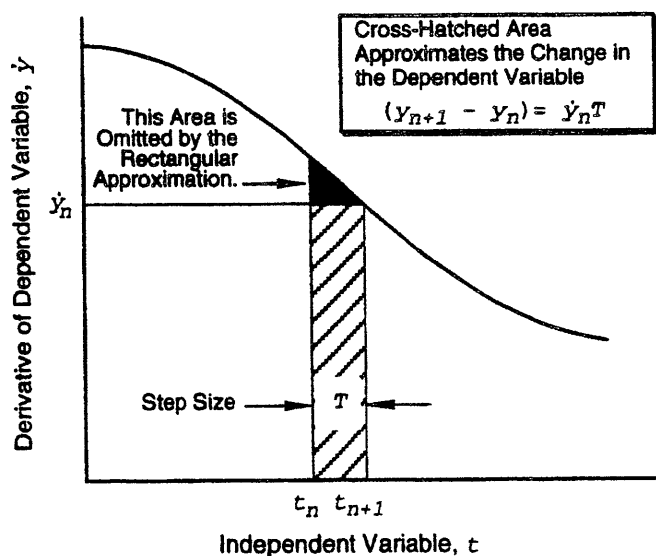


Figure 10-1. Truncation Error in Euler Method

digital computer employed. The Euler method is seldom used in simulations because of these difficulties (See the improved Euler method in subpar. 10-4.1.2.1.). The Euler method is presented here as a basis for later discussions of other numerical integration methods that permit the size of the integration interval T to be increased and the integration accuracy to be improved.

10-4.1.1.2 Runge-Kutta Method

The Runge-Kutta method and its variations are very popular in missile flight simulations. The method provides good accuracy, is simple to program, requires minimum storage, and is stable under most circumstances with integration intervals of reasonable size (Refs. 10 and 14). The basic derivation of the method involves a summation of terms, the number of which is arbitrary. The most common form of the method is based on the summation of four terms; consequently, it is referred to as the fourth-order Runge-Kutta method. Also in the derivation of the method are certain arbitrary constants. In the fourth-order Runge-Kutta method, the most frequently selected arbitrary constants lead to a set of difference equations of the form

$$\mathbf{y}_{n+1} = \mathbf{y}_n + \frac{T}{6} (\mathbf{H}_1 + 2\mathbf{H}_2 + 2\mathbf{H}_3 + \mathbf{H}_4) \quad (10-12)$$

where

$$\mathbf{H}_1 = \mathbf{G}(t_n, \mathbf{y}_n)$$

$$\mathbf{H}_2 = \mathbf{G}(t_n + 1/2 T, \mathbf{y}_n + 1/2 T\mathbf{H}_1)$$

$$\mathbf{H}_3 = \mathbf{G}(t_n + 1/2 T, \mathbf{y}_n + 1/2 T\mathbf{H}_2)$$

$$\mathbf{H}_4 = \mathbf{G}(t_n + T, \mathbf{y}_n + T\mathbf{H}_3)$$

\mathbf{y}_n = vector of dependent variables at beginning of step n

\mathbf{y}_{n+1} = vector of dependent variables at beginning of step $(n + 1)$.

Eq. 10-12 is applicable to sets of first-order differential equations that have the form of Eq. 10-1.

There are also Runge-Kutta methods that involve more than four steps; however, they are rarely used in simulation applications because the small improvement in accuracy generally does not justify the increase in execution time (Ref. 11).

Although the Runge-Kutta method involves fairly simple equations, it has certain disadvantages:

1. If a function G is complicated, evaluation of the H terms at each computation step can be time-consuming.
2. The method will calculate a solution across points of discontinuity, giving erroneous results without giving any indication that this has been done.
3. There is no readily obtainable error analysis.

The lack of any error analysis for the fourth-order Runge-Kutta method can be partially compensated by using certain rules of thumb. One such rule of thumb (Ref. 12) is that if the numerical value of the quantity

$$\left| \frac{H_2 - H_3}{H_1 - H_2} \right|$$

where

$$\begin{aligned} H_1 &= \text{magnitude of vector } \mathbf{H}_1 \\ H_2 &= \text{magnitude of vector } \mathbf{H}_2 \\ H_3 &= \text{magnitude of vector } \mathbf{H}_3 \end{aligned}$$

becomes larger than a few hundredths at any point t_n , the step size T should be decreased.

10-4.1.2 Implicit Methods

The equations for implicit methods of numerical integration are in a form that cannot be solved explicitly for y_{n+1} . An implicit solution to such equations generally can be found by iterative calculations. In practice, instead of performing many iterations to solve the equations accurately for y_{n+1} , the same accuracy is obtained with much less effort by employing a smaller computation step size and performing only one or two iterations (Ref. 12). These implicit methods are called predictor-corrector methods.

10-4.1.2.1 One-Step Processes

One-step difference equations determine the value of the dependent variable at step $(n+1)$ in terms of its value only at the preceding step n . Thus, to start the calculations of a one-step method, the initial value of the dependent variable is used as the preceding value to calculate the first step. Since only one preceding value of the dependent variable is used, one-step methods are called self-starting.

The two explicit methods described in subpar. 10-4.1.1, the Euler method and the Runge-Kutta method, are both one-step processes and are, therefore, self-starting. The improved Euler method and the modified Euler method are examples of implicit methods that also use a one-step process.

10-4.1.2.1.1 Improved Euler Method

The improved Euler method is implemented by a set of predictor equations and a set of corrector equations (Ref. 12). Again, consider the general normal system of first-order differential equations given by Eq. 10-1

$$\frac{dy}{dt} = \mathbf{G}(t, \mathbf{y}) \quad (10-1)$$

where

$$\begin{aligned} \mathbf{G}(t, \mathbf{y}) &= \text{vector of functions of } t \text{ and } \mathbf{y} \\ t &= \text{independent variable, e.g., time} \\ \mathbf{y} &= \text{vector of dependent variables.} \end{aligned}$$

The Euler method, Eq. 10-3, gives a good first approximation and is employed as the predictor equation for the improved Euler method:

$$\mathbf{Y}_{n+1} = \mathbf{y}_n + \mathbf{G}(t_n, \mathbf{y}_n)T \quad (10-13)$$

where

T = length of computation time step, s

\mathbf{Y}_{n+1} = vector of predicted dependent variables at beginning of step $(n+1)$.

The corrector equation is

$$\mathbf{Y}_{n+1} = \mathbf{y}_n + [\mathbf{G}(t_{n+1}, \mathbf{Y}_{n+1}) + \mathbf{G}(t_n, \mathbf{Y}_n)] \frac{T}{2} \quad (10-14)$$

The vector \mathbf{Y}_{n+1} of predicted values of the dependent variable is calculated by using Eq. 10-13 and substituting into Eq. 10-14 to solve for the corrected dependent variable vector \mathbf{y}_{n+1} . The term $\mathbf{G}(t_{n+1}, \mathbf{Y}_{n+1})$ is simply the function \mathbf{G} , defined by Eq. 10-1, evaluated at time t_{n+1} and using the value of the predicted dependent variable \mathbf{Y}_{n+1} . In preparation for the next computation step, $\mathbf{G}(t_{n+1}, \mathbf{Y}_{n+1})$ is calculated by substituting the value of \mathbf{Y}_{n+1} , calculated by Eq. 10-14, into the function \mathbf{G} .

Eq. 10-14 is based on the trapezoidal integration equation. This equation is similar to rectangular integration (the Euler method) except that the value of \mathbf{G} used is based on the mean of the value of \mathbf{G} at the beginning of the step and the predicted value of \mathbf{G} at the end of the step.

As an example, again consider the system of equations that describes Newton's second law, assuming constant force and constant mass, as given by Eqs. 10-5

$$\left. \begin{aligned} \frac{dv}{dt} &= \frac{F}{m}, \text{ m/s}^2 \\ \frac{dx}{dt} &= v, \text{ m/s} \end{aligned} \right\} \quad (10-5)$$

where

$$\begin{aligned} F &= \text{magnitude of force, N} \\ m &= \text{mass, kg} \\ t &= \text{time, s} \\ v &= \text{magnitude of velocity (speed), m/s} \\ x &= \text{magnitude of displacement, m.} \end{aligned}$$

As in Eq. 10-9, the function \mathbf{G} at step n is given by

$$\mathbf{G}(t_n, \mathbf{y}_n) = \begin{bmatrix} \frac{F}{m} \\ v_n \end{bmatrix} \quad (10-15)$$

Substituting Eq. 10-15 into Eq. 10-13 yields the predictor

$$\mathbf{Y}_{n+1} = \begin{bmatrix} v_n + \left(\frac{F}{m}\right)T \\ x_n + v_n T \end{bmatrix} \quad (10-16)$$

The values of the functions $\mathbf{G}(t, \mathbf{Y})$ needed to solve Eq. 10-14 for this example are given by

$$\mathbf{G}(t_n, \mathbf{Y}_n) = \begin{bmatrix} \frac{F}{m} \\ \mathbf{v}_n \end{bmatrix} \quad (10-17)$$

and

$$\mathbf{G}(t_{n+1}, \mathbf{Y}_{n+1}) = \begin{bmatrix} \frac{F}{m} \\ \mathbf{v}_{n+1} \end{bmatrix}. \quad (10-18)$$

Substituting into Eq. 10-14 yields the corrected values of the dependent variables

$$\mathbf{y}_{n+1} = \begin{bmatrix} \mathbf{v}_{n+1} = \left(\frac{F}{m} + \frac{F}{m}\right) \frac{T}{2} \\ \mathbf{x}_n + (\mathbf{v}_{n+1} + \mathbf{v}_n) \frac{T}{2} \end{bmatrix}. \quad (10-19)$$

Eq. 10-19 simplifies to

$$\mathbf{v}_{n+1} = \mathbf{v}_n + \frac{F}{m} T, \text{ m/s} \quad (10-20)$$

$$\mathbf{x}_{n+1} = \mathbf{x}_n + \mathbf{v}_n T + \frac{1}{2} \frac{F}{m} T^2, \text{ m.} \quad (10-21)$$

These are the one-dimensional equations of motion of a mass with constant acceleration F/m over the time period T . Even when the acceleration is variable with time, the assumption that the acceleration changes in steps and is held constant over the duration of each incremental time step is sufficiently accurate for many applications. The improved Euler method, Eqs. 10-20 and 10-21, was used in Chapter 7 to calculate target motion by using Eqs. 7-22 and 7-23 and is often used in three-degree-of-freedom simulations to solve the equations of motion of the missile.

10-4.1.2.1.2 Modified Euler Method

There are at least two different numerical integration methods in the literature referred to as modified Euler methods. One method is similar to the Euler method (subpar. 10-4.1.1.1) except that the modified method attempts to average out the truncation error at step n by integrating from $(n-1)$ to $(n+1)$ at each step; thus it is a multistep method. It can be shown, however, that when this particular method is used in a simulation of a component in a feedback loop, an unstable solution always results (Ref. 11); therefore, the method should not be used for missile flight simulations.

A more useful one-step method also identified as the modified Euler method, begins by using the predictor equation for only half of a time-step interval and then processes the second half of the interval by using the corrector equation. Thus the predicted value of G is at the middle of the integration interval. The predictor and corrector equations for the modified Euler method are given by

$$\mathbf{Y}_{n+1/2} = \mathbf{y}_n + \mathbf{G}(t_n, \mathbf{y}_n) \frac{T}{2} \quad (10-22)$$

where

$\mathbf{G}(t_n, \mathbf{y}_n)$ = vector of functions of t_n and \mathbf{y}_n

T = length of computation time step, s

$\mathbf{Y}_{n+1/2}$ = vector of predicted dependent variables at midpoint of step n

\mathbf{y}_n = vector of dependent variables at beginning of step n

and

$$\mathbf{y}_{n+1} = \mathbf{y}_n + \mathbf{G}(t_{n+1/2}, \mathbf{Y}_{n+1/2}) \frac{T}{2}. \quad (10-23)$$

When applied to the particular differential equation described by Eq. 10-4, this modified Euler method yields the same results as the improved Euler method, i.e., Eqs. 10-20 and 10-21.

10-4.1.2.2 Multistep Processes

A k -step difference equation employs the values of the dependent variable at the first k preceding steps. For example, a four-step difference equation-not to be confused with fourth-order Runge-Kutta-determines the value of y_{n+1} by using values of y_n, y_{n-1}, y_{n-2} , and y_{n-3} . Because of the need for multiple preceding values of the dependent variable, multistep difference equations are not self-starting, and some auxiliary method is required to determine the preceding values (Ref. 12). Atypical approach is to use a one-step method, such as the Runge-Kutta method to calculate the first n values of the dependent variable and then to switch to the multistep method.

10-4.1.2.2.1 Milne Method

The Milne method requires multiple previous values of the dependent variable to solve the difference equations representing the differential equations; therefore, it is a multistep method. The derivation of the Milne method is parallel to that of the improved Euler method, except that the well-known trapezoidal rule is used in the improved Euler method, whereas the Simpson rule, instead of the trapezoidal rule, is used in the Milne method (Ref. 12).

The predictor equation for the Milne method is (Ref. 15)

$$\mathbf{Y}_{n+1} = \mathbf{y}_{n-3} + [2\mathbf{G}(t_n, \mathbf{y}_n) - \mathbf{G}(t_{n-1}, \mathbf{y}_{n-1}) + 2\mathbf{G}(t_{n-2}, \mathbf{y}_{n-2})] \frac{4T}{3}, \quad (10-24)$$

and the Milne corrector equation is

$$\mathbf{Y}_{n+1} = \mathbf{y}_{n-1} + [\mathbf{G}(t_{n+1}, \mathbf{Y}_{n+1}) + 4\mathbf{G}(t_n, \mathbf{Y}_n) + \mathbf{G}(t_{n-1}, \mathbf{Y}_{n-1})] \frac{T}{3}. \quad (10-25)$$

These equations use four previously calculated values of the dependent variable to find the succeeding value. Other forms of the Milne method are possible. For example, see

Ref. 11 for Milne equations that use only two previously calculated values of the dependent variable and Ref. 15 for Milne equations that use six previous values of the dependent variable. Ref. 15 also gives special Milne equations that are applicable to second- and third-order differential equations.

Since the Milne method is a multistep process requiring previous values of the dependent variable, it is not self-starting. A one-step method, such as the Euler method, the improved Euler method, or the Runge-Kutta method, is required to calculate the values of the dependent variables for the first few computation steps.

Although it is not as popular as the Adams methods for application to missile flight simulations, the Milne method gives a perspective of the relationships among the various numerical integration methods. Other predictor-corrector methods differ from the improved Euler method and the Milne method only with respect to the polynomial interpolation equations from which the predictor and corrector equations are derived.

10-4.1.2.2.2 Adams Methods

The Adams-Bashforth equations are a family of methods often used as predictors. A commonly used predictor equation is the fourth-order Adams-Bashforth equation, which is given by

$$\mathbf{Y}_{n+1} = \mathbf{y}_n + \frac{T}{24}(55\mathbf{G}_n - 59\mathbf{G}_{n-1} + 37\mathbf{G}_{n-2} - 9\mathbf{G}_{n-3}) \quad (10-26)$$

where

$$\begin{aligned} \mathbf{G}_n &= \mathbf{G}(t_n, \mathbf{y}_n) \\ \mathbf{G}_{n-1} &= \mathbf{G}(t_{n-1}, \mathbf{y}_{n-1}); \text{ etc} \\ T &= \text{length of computation step, } s \\ \mathbf{Y}_{n+1} &= \text{vector of predicted dependent variables at} \\ &\quad \text{beginning of step } (n+1) \\ \mathbf{y}_n &= \text{vector of dependent variables at beginning of} \\ &\quad \text{step } n. \end{aligned}$$

This equation is most frequently used in conjunction with the Adams-Moulton corrector equation, which is given by

$$\mathbf{y}_{n+1} = \mathbf{y}_n + \frac{T}{24}(9\mathbf{G}_{n+1} + 19\mathbf{G}_n - 5\mathbf{G}_{n-1} + \mathbf{G}_{n-2}) \quad (10-27)$$

where the function G now depends on the predicted variable Y , i.e., $G_n = G(t_n, Y_n)$, $G_{n-1} = G(t_{n-1}, Y_{n-1})$, etc.

In simulations that require real-time operations, computation time is typically reduced by using the second-order Adams-Bashforth predictor in place of the fourth-order Adams-Bashforth predictor given in Eq. 10-26. This method is known as AB2; it is just a predictor method, i.e., a corrector is not used. The second-order Adams-Bashforth equation is

$$\mathbf{y}_{n+1} = \mathbf{y}_n + 0.5T(3\mathbf{G}_n - \mathbf{G}_{n-1}). \quad (10-28)$$

The Adams equations are more accurate than the Euler equations and are comparable in accuracy to the Runge-Kutta method but require about half as much computation (Ref. 10). In predictor-corrector methods the difference between the predicted and corrected values is one measure of the error being made at each computation step and therefore can be used to control the step size employed at the integration (Ref. 16). Predictor-corrector methods, however, are not self-starting, and unlike the Runge-Kutta method, they cannot be easily used alone with a variable time step. These difficulties frequently are alleviated in practice by using the Runge-Kutta method to obtain the starting values and also to compute the solution for the first few computation steps after the step size has been changed or after a discontinuity has been encountered.

Another difficulty with predictor-corrector methods is that, in some cases, they are subject to certain types of instabilities that do not occur when the Runge-Kutta method is used. Numerical instability in a simulation usually is considered to be the unbounded compounding of numerical error that results from either a truncation or rounding error or a combination of the two. One approach to resolving a truncation error is to reduce the step size of the simulation until the numerical integration process is stable and then test the process to determine whether at the small step size a rounding error introduces a significant error in the simulation. One particular type of instability manifests itself first by creating an error that is larger than expected and then by increasing this error even more when an attempt is made to reduce it by decreasing the step size. A more detailed discussion of this instability is given in Ref. 17.

The tendency of multistep methods to become numerically unstable under certain conditions can lead to disastrous results; therefore, these methods should not be used indiscriminately (Ref. 10). In many applications involving complicated equations, however, the predictor-corrector methods can result in a considerable savings of computer time over the Runge-Kutta method (Ref. 12). Another important advantage of multistep methods is that with little additional computation they provide automatic monitoring of the accuracy, which can be used as a basis for deciding whether the step size is too small, too large, or about right (Ref. 10).

A number of special forms of various numerical integration methods are available for specific use with higher order differential equations. For general-purpose computing these special methods are not very useful for solving differential equations; however, for the special cases in which they are applicable, these methods reduce the number of calculations required for numerical evaluation (See, for example, Refs. 15 and 18.). Ref. 19 contains a discussion of higher order methods and variable step size methods that attempt to select an optimum integration step,

10-4.1.3 Modern Numerical Integration Methods

The dynamical system problems presently being faced are forcing classical numerical methods to their limits and leading to numerical instabilities of such drastic extent that very small step sizes are required to stabilize digital simulations. This leads to costly simulation at best and inaccurate simulation at worst—due to the propagation of rounding errors.

A digital simulation is, in itself, a discrete dynamic system. It can be filtered, tuned, stabilized, controlled, analyzed, and synthesized in the same manner as any discrete system. This viewpoint broadens the scope of numerical methods and mathematical modeling techniques applicable to simulation. This applies not only to the classically developed methods previously discussed but to all of those developed from the viewpoints of sampled-data theory and discrete system theory. This broadening of applicability has led to the development of new simulation methods that have no classical counterparts (Ref. 15).

Modern numerical methods that simulate the motion of continuous systems accurately and efficiently in both the time and frequency domains date back only to 1959, and most of the methods for simulating nonlinear processes were developed in the early and mid 1970s (Ref. 15).

One type of modern numerical integrator is based on matching the roots of the difference equation to the roots of the differential equation it simulates. Since the dynamics of a continuous system are completely characterized by its roots and final value, it is appropriate to make the roots and final value of the simulating difference equations match those of the system being simulated. If a system of difference equations is synthesized having poles, zeros, and final value that match those of the continuous system these equations will accurately simulate the continuous system. Difference equations generated in this manner are intrinsically stable if the system they are simulating is stable regardless of the step size.

Another type of modern numerical integrator is based on tunable digital filters whose phase and amplitude characteristics can be varied to control integration error. Turnability in both the time domain and frequency domain has no counterpart in classical numerical integration. These numerical integrators, however, reduce to certain classical integration equations when phase-shift errors are introduced. This leads to an interesting corollary that large classes of classical numerical integrators are actually the same integrator, differing only by the amount of integrand phase shift (Ref. 15).

Significant advances in techniques for evaluating nonlinear equations of motion have been developed recently, by using piecewise linear difference equations in which the Jacobian of the differential equation plays a key role (Ref. 15). If the simulation involves many state vectors, however, a major difficulty can arise because these techniques require the inversion of a Jacobian matrix at each computational time step.

The details of these methods are too extensive to be included in this handbook; however, a complete discussion of a number of methods of synthesizing and applying modern numerical integration techniques is given in Ref. 15. See also Refs. 20 through 23 for discussions of the application of numerical methods to state-space equations. Although future surface-to-air missile simulations will include applications of these modern methods, there is no universal method that solves every problem. When choosing a method or methods, the user must evaluate the advantages and disadvantages of the different methods in terms of their application to the particular problem (Ref. 15).

10-4.1.4 Applications

Missile flight simulations require the simultaneous solution of several differential equations at each time step. For example, in a six-degree-of-freedom simulation, the equations of missile motion form a set of six differential equations (Eqs. 4-37 and 4-46) containing many cross connections among them. Integration of these six equations yields the velocity components of the missile. A second integration of each equation is required to solve for the displacement components; thus the number of equations to be solved doubles. The cross couplings among all of these equations are handled by applying the numerical integration procedures to the separate equations in parallel. That is, the first iteration of a numerical procedure is applied to all of the differential equations, the next iteration is applied to all of the equations, and so on, until all of the iterations for a given computational time step are completed.

The particular numerical method to employ in a given simulation depends largely on the requirements for accuracy and computation speed. Different methods in a given application behave differently. The numerical analyst must be constantly alert to indications that a numerical integration algorithm is not functioning properly (Ref. 10). The most useful comparison of the various methods of numerical integration is based on their performance, on an experimental basis, in the actual simulation being considered (Ref. 11).

Present general practice is to use a simple, straightforward, fast-running method, such as the improved or modified Euler methods for applications that do not require great accuracy. Many simulations for general systems studies of proposed or hypothetical missiles or of foreign missiles based on uncertain intelligence data often fall in this category because the uncertainties in the input parameters that describe the missile make great computational accuracy unwarranted. Also the miss distance calculated by a simulation of a guided missile is likely to be affected only insignificantly by small errors introduced through numerical integration methods. The reason for this low sensitivity to errors induced by the numerical integration method is that the simulated closed-loop guidance system generates control commands based on the sum of the simulated missile heading error plus any heading errors induced by computa-

tional errors. Thus the effect of computational errors on miss distance is reduced because the simulated missile attempts to "steer out" the computationally induced errors as well as the simulated heading errors.

The Runge-Kutta method often is employed in simulations that require computational accuracy but do not require great computational speed. Although speed of computation is almost always desirable, it is often sacrificed for programming ease and the fewer computational stability problems of the Runge-Kutta method.

Applications that require both accuracy and computational speed generally use a predictor-corrector method, such as the Adams equations. Attention must be given to ensure that the numerical method is stable and that the frequency response of the method adequately represents that of the actual dynamic system being modeled. A self-starting method, such as Runge-Kutta is employed to start the calculation for these multistep methods and to restart the calculation when discontinuities are encountered.

At present the trend is toward all-digital simulation, even for applications that are required to run in real time. It can be expected that the high-fidelity, fast computational speed, and lack of computational stability problems of some of the modern numerical integration methods will permit the methods to be used to simulate many or all of the missile functions presently performed by analog simulations. For example, IBM claims that difference equations derived by a new method that they have developed can be used to simulate linear or nonlinear, continuous or sampled-data control systems (Ref. 24). They suggest that the accuracy of very high-speed difference equation techniques can surpass much of the analog simulation work.

10-4.2 DIGITAL SOLUTION OF TRANSFER FUNCTIONS

A transfer function corresponds to a linear differential equation with constant coefficients; therefore, any method of numerically integrating differential equations can be used to evaluate transfer functions. For example, the Runge-Kutta method often is used in simulations to solve transfer function equations. However, because of the linear, time-invariant properties of transfer functions, special techniques can be used for their solution, and in general, no exploitation of these properties is possible with the general numerical integration methods. A number of special techniques for digital solution of transfer functions have been developed. The more important of these methods are ascribed to Blum, Boxer-Thaler, Tustin, and Madwed-Truxal. The Tustin method of evaluating transfer functions is one of the simplest to apply once a necessary set of constants has been determined and was judged "probably the best, overall" by one investigator (Ref. 14).

10-4.2.1 The Tustin Method

Digital simulation of continuous systems at discrete time intervals falls within the general class of sampled data systems. A form of transformation calculus known as z-transform theory was developed specifically for treating sampled data systems (Ref. 25). The substitution method used to simulate transfer functions derives difference equations by substituting a z-transform function for the s^{-1} in the Laplace transfer function of the system to be simulated and inverting the resulting z-domain transfer function, i.e., finding the inverse z-transformation, into a difference equation. The well-known Tustin method is based on such a z-transform substitution. This method leads to relatively stable, although not necessarily highly accurate, difference equations for simulating the transfer functions of continuous processes (Ref. 15).

The z-transform variable z is related to the Laplace transform variables by the identity

$$z = e^{sT} \quad (10-29)$$

where

s = Laplace transform variable

T = sampling interval, s

z = z-transform variable.

In nearly all practical applications, the inverse of z , i.e., e^{-sT} is most useful; therefore, the operator Δ is defined as

$$\Delta = e^{-sT} = z^{-1}. \quad (10-30)$$

The Tustin method employs z-transforms to define a recursion difference equation that is used to solve a transfer function. In this method a transfer function $G(s)$ is transformed to $G(\Delta)$ by making the substitution

$$s = \frac{2}{T} \frac{(1-\Delta)}{(1+\Delta)}. \quad (10-31)$$

The resulting function $G(\Delta)$ is simplified to the form

$$G(\Delta) = \frac{a_0 + a_1\Delta + a_2\Delta^2 + \dots + a_m\Delta^m}{1 - b_1\Delta - b_2\Delta^2 - \dots - b_m\Delta^m} \quad (10-32)$$

where

a_i and b_i = constants that depend on the particular transfer function being modeled.

The corresponding recursion equation

$$y_n = a_0x_n + a_1x_{n-1} + \dots + a_mx_{n-m} + b_1y_{n-1} + b_2y_{n-2} + \dots + b_my_{n-m} \quad (10-33)$$

where

$x = x(t)$ = time-domain input of the linear system
 $y = y(t)$ = time-domain output of the linear system.

The recursion equation is used in a simulation at each computation step n to find the output y resulting from the input x .

As an example, consider the transfer function given in Eq. 8-29.

$$\frac{y(s)}{x(s)} = G(s) = \frac{1}{1 + \tau s} \quad (8-29)$$

where

$G(s)$ = transfer function
 s = Laplace transform variable
 $x(s)$ = Laplace transform of input
 $y(s)$ = Laplace transform of output
 τ = system time constant, s.

To solve the transfer function of Eq. 8-29 by the Tustin method, the constants a and b_1 in Eq. 10-33 must be determined. First, substitute Eq. 10-31 into Eq. 8-29 and arrange the resulting equation in the form of Eq. 10-32, giving

$$G(\Delta) = \frac{\left(\frac{T}{2\tau} \right) + \left(\frac{T}{2\tau} \right) \Delta}{1 - \left(\frac{1 - \frac{T}{2\tau}}{1 + \frac{T}{2\tau}} \right) \Delta} \quad (10-34)$$

By inspection of Eq. 10-34, the constants in Eq. 10-33 are determined to be

$$a_0 = \left(\frac{\frac{T}{2\tau}}{1 + \frac{T}{2\tau}} \right); a_1 = \left(\frac{\frac{T}{2\tau}}{1 + \frac{T}{2\tau}} \right); b_1 = \left(\frac{1 - \frac{T}{2\tau}}{1 + \frac{T}{2\tau}} \right) \quad (10-35)$$

As an example, suppose that the time constant t is given as 0.5 s, and the simulation time step T has been chosen as 0.1 s. A common rule of thumb for applying numerical methods is that the computational time step should be no greater than about one-tenth the system time constant. Here we use a time step only one-fifth the time constant in order to evaluate the method under less than ideal conditions. Evaluating Eqs. 10-35 and substituting into Eq. 10-33 yields

the Tustin recursion equation for evaluating the transfer function of Eq. 8-29 for given t and T

$$y_n = 0.090909x_n + 0.090909x_{n-1} + 0.8181818y_{n-1} \quad (10-36)$$

Fig. 10-2(A) shows the response of the transfer function to a step input command applied at time zero. Each plotted point was calculated in sequence using Eq. 10-36.

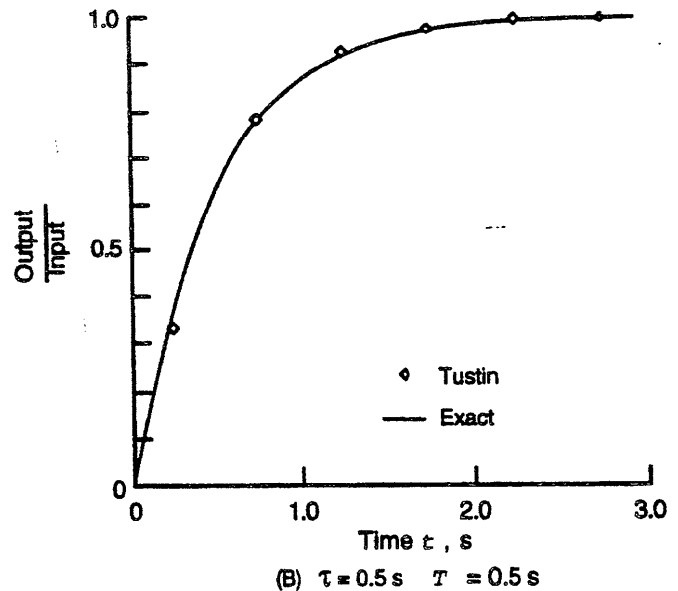
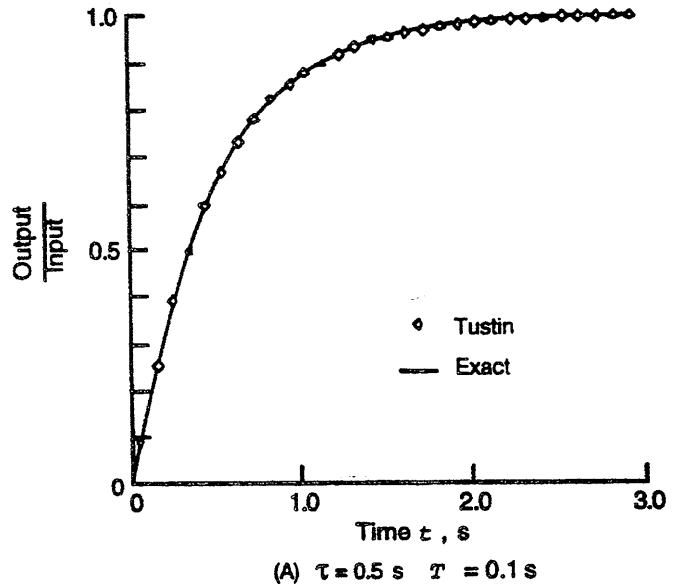


Figure 10-2. Response of First Order Transfer Function to Step Input Calculated by Tustin Method

Since the particular transfer function of Eq. 8-29 is a relatively simple one, it can be solved exactly by analytical methods when the input commands are simple. The exact solution can then be used as a reference for measuring the accuracy of numerical methods used to solve that particular transfer function. When the input is a unit step, the exact solution of the transfer function of Eq. 8-29 is given by

$$y(t) = 1 - \exp(-t/\tau) \quad (10-37)$$

where

- t** = time since application of the step command, s
 $y(t)$ = time-domain output of a linear system
 τ = system time constant, s.

Comparison of the numerical solution with the exact solution in Fig. 10-2(A) shows excellent agreement. Even when the time step is increased to be equal to the system time constant and this increase often produces extremely erroneous results in numerical methods, the Tustin method performs remarkably well for this example as shown in Fig. 10-2(B).

In any numerical method, the simulation developer must determine the actual timing of the sequence of solution values in order to compare them with a true continuous-time check case. Engineers and programmers often overlook this problem of timing and try to compare continuous and discrete computing processes at time nT instead of recognizing that numerical integration is an approximation process (Ref. 15), and adjustments in the timing sequence may be necessary because of the discrete nature of the time samples.

For example, in the digital application of the unit step function, the unit step command is represented digitally by the sequence ..0,0,1,1,1, The step command clearly originates during the interval of time between the last "0" and the first "1" but exactly where within that interval is uncertain. One reasonable assumption would be that the step originates at the instant of time corresponding to the first "1"; however, to obtain the results shown in Fig. 10-2 by using the Tustin method, an assumption is required that the step originated halfway between the last "0" and the first "1". In this case time t is calculated by

$$t = nT - T/2, s \quad (10-38)$$

where

- n** = index for identifying a particular time step, dimensionless
 T = length of computation time step, s
 t = independent variable, s.

Refs. 14 and 15 contain discussions of zero-order and first-order hold functions designed to improve the timing representation of digital data that simulate continuous systems and that are employed in hybrid simulations to convert digital data to analog signals.

10-4.2.2 Root-Matching Method

As discussed in subpar. 10-4.1.2, root-matching methods are employed to form a difference equation with the same dynamic characteristics as the differential equation that describes the continuous system being simulated. This objective is achieved by a difference equation that (Ref. 15)

1. Has poles and zeros that match those of the differential equation
2. Has a final value that matches the final value of the differential equation
3. Is phase adjusted to best match the response of the discrete system with the response of the continuous system.

To develop a root-matching difference equation for a transfer function, follow the algorithm:

1. Determine the Laplace transform of the transfer function.
2. Map the s-plane poles and zeros into the z-plane by using the relationship

$$z_{pole} = \exp(s_{pole}T); z_{zero} = \exp(s_{zero}T).$$

3. Form a transfer function polynomial in z with the poles and zeros determined in Step 2.
4. Determine the final values of the unit step response of the continuous system and the unit step response of the discrete system, and match the final values by introducing a constant in the transfer function generated in Step 3.
5. Add additional zeros to the transfer function of the discrete system until the order of the denominator of the discrete system matches the order of the numerator of the discrete system.
6. Inverse z-transform the z-transfer function developed in Step 5 to form the simulating difference equation.

The root-matching method is applicable only when the conditions that follow are met. The system 'must

1. Be linear
2. Possess a Laplace transformation
3. Be asymptotically stable and satisfy the final value theorem*, and the final value must be nonzero.

The difference equation generated in this manner is not only stable but accurate. That is, the solution to the homogeneous difference equation exactly matches the homogeneous solution to the differential equation, and the difference equation will exactly compute the sequence of sampled values of the homogeneous solution of the continu-

*Final Value Theorem (Ref. 10): If $f(t)$ is z-transformable, $Zf(t) = F(z)$, and if $F(z)$ contains no poles on or outside the unit circle, then

$$\lim_{t \rightarrow \infty} f(t) = \lim_{n \rightarrow \infty} f(nT) = \lim_{z \rightarrow 1} \left\{ \frac{z-1}{z} F(z) \right\}$$

ous process. It will also exactly compute the sequence of solutions of the continuous system to unit step forcing functions. It follows then that the difference equation can be used to simulate accurately the response of the continuous system to an arbitrary forcing function provided that the forcing function is sampled often enough to extract the highest frequency components that are important to the simulation (Ref. 15).

Applying the previous steps to the first-order transfer function of Eq. 8-29 leads to the root-matched difference equation

$$y_n = \exp(-T/\tau) y_{n-1} + [1 - \exp(-T/\tau)] x_n \quad (10-39)$$

Fig. 10-3(A) compares the results of Eq. 10-39 for a unit step input to the exact results calculated by Eq. 10-37. The conditions are the same as those for Fig. 10-2(A). That is, the system time constant $\tau = 0.5$ s, and the computational step size $T = 0.1$ s. The match is perfect; the root-matching method gives results identical to the exact solution. In fact, the match is perfect no matter how large the step size is; for example, Fig. 10-3(B) shows a perfect match when the step size is equal to the system time constant. Furthermore, no shift in the time scale is necessary for Fig. 10-3, i.e., time is calculated as $t = nT$.

Another important example of the root-matching method is the solution of transfer functions for second-order systems. The transfer function of a second-order system is given by

$$\frac{y(s)}{x(s)} = \frac{\omega_n^2}{s^2 + 2\zeta\omega_n s + \omega_n^2} \quad (10-40)$$

where

- s = Laplace transform variable
- $x(s)$ = Laplace transform of input
- $y(s)$ = Laplace transform of output
- ζ = damping ratio, dimensionless
- ω_n = undamped natural frequency of system, rad/s.

If the six steps outlined previously are followed, the root-matched difference equation for digital solution of the second-order transfer function is determined to be (Ref. 15)

$$y_n = Ay_{n-1} - By_{n-2} + (1 - A + B)x_n, \quad (10-41)$$

where

$$A = 2\exp(-\zeta\omega_n T) \cos(\omega_n T \sqrt{1 - \zeta^2})$$

$$B = \exp(-\zeta\omega_n T).$$

Since root-matched difference equations are stable-provided the system they are simulating is stable-no matter what the step size, numerical-method stability considerations need not be considered in the selection of a step size for a simulation that employs the root-matching method. The primary criterion that remains for selecting the step size is to ensure that the simulated system responds properly to the highest frequency of interest within the objectives of the simulation. Shannon's theorem states that if a continuous function $f(t)$ is band limited at w_c Hz, i.e., has no frequency components higher than w_c , the minimum sampling rate that completely determines the function $f(t)$ is $2w_c$ samples per second (Refs. 15 and 26). If the function is sampled at a rate $1/T$ less than $2w_c$, a phenomenon called "aliasing", or "frequency foldback", occurs in which the high-frequency components of the continuous-function spectrum are erro-

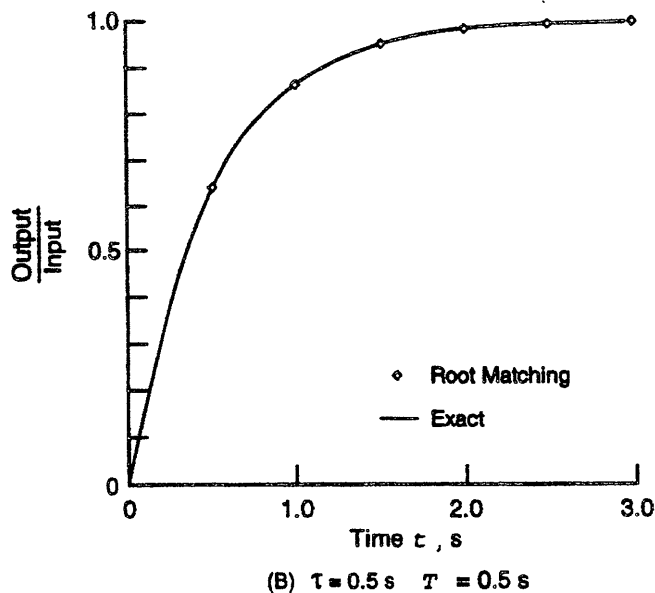
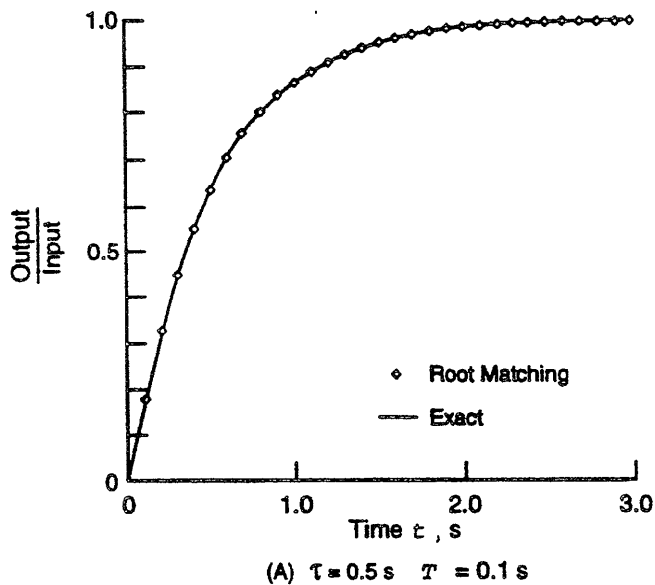


Figure 10-3. Response of First-Order Transfer Function to Step Input Calculated by Root-Matching Method

neously folded back and appear, along with the low-frequency components, within the band $0 - 1/(2T)$ Hz of the discrete-function spectrum.

Since most functions encountered in simulations are not band limited, i.e., there are no bounds on the highest frequency they may contain, the minimum rate at which functions should be sampled is 5 to 10 times the highest frequency of interest (Ref. 15).

For example, in simulating a second-order system, it seems prudent to set the step size small enough to excite the resonant frequency of the system. The damped natural frequency of a second-order system is given by

$$\omega_d = \omega_n \sqrt{1 - \zeta^2}, \text{ rad/s} \quad (10-42)$$

where

ζ = damping ratio, dimensionless

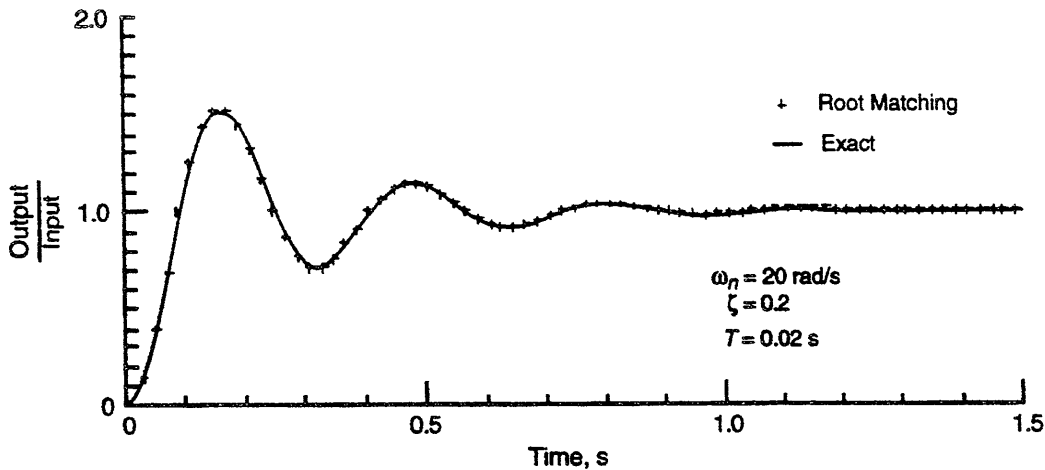
ω_d = damped natural frequency of system, rad/s

ω_n = undamped natural frequency of system, rad/s.

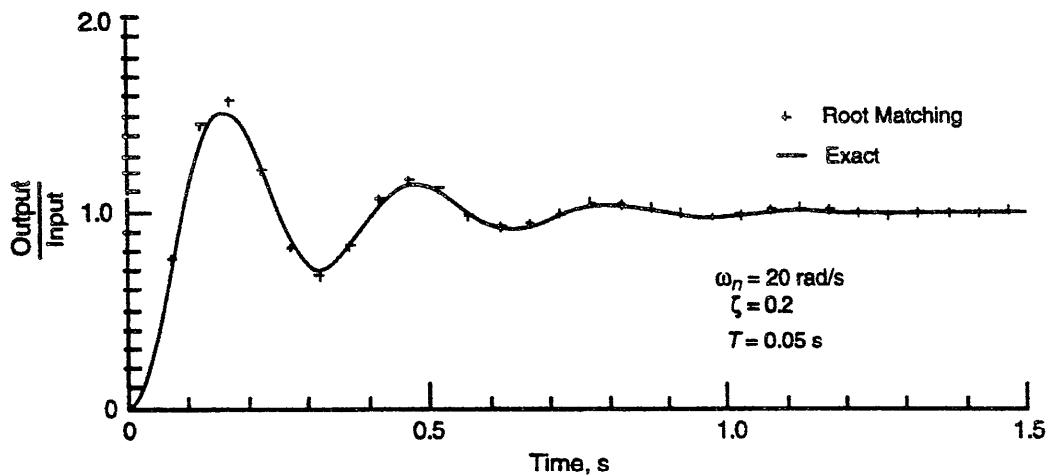
Adopting the criterion that the sampling rate (near midpoint of range of minimum rates given in Ref. 15) must be at least seven times the highest frequency of interest, the step size T that should be selected for this application is

$$T \leq \frac{2\pi}{7\omega_d}, \text{ s.} \quad (10-43)$$

Fig. 10-4 shows the solution of a second-order transfer function for a step input. The plotted points were calculated by the root-matching method that employs Eq. 10-41, and



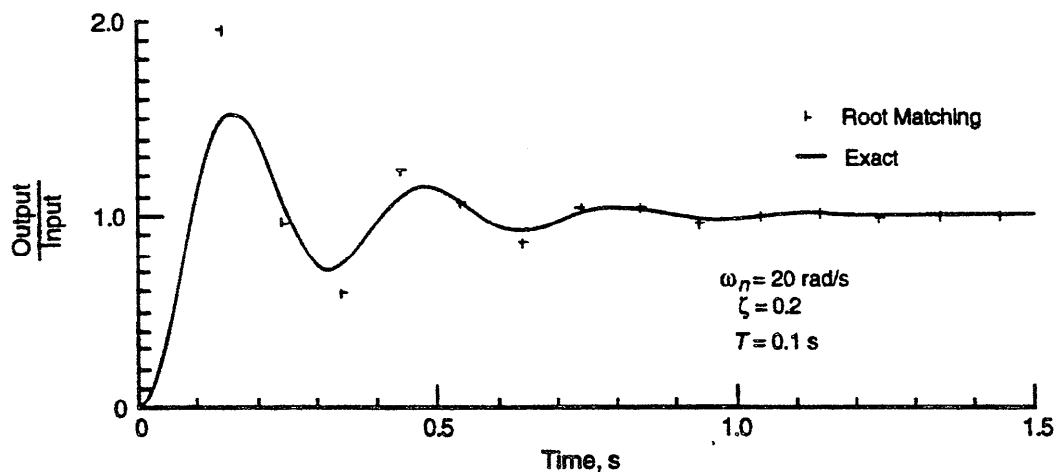
(A) $\frac{\text{Number of Computation Points}}{\text{Period of Damped Oscillations}} = 16$



(B) $\frac{\text{Number of Computation Points}}{\text{Period of Damped Oscillations}} = 6$

Figure 10-4. Response of Second-Order Transfer Function to Step Input Calculated by Root-Matching Method

(cont'd on next page)



$$(C) \frac{\text{Number of Computation Points}}{\text{Period of Damped Oscillations}} = 3$$

Figure 10-4. (cont'd)

the continuous curve was calculated by using the exact equation for the response of a second-order system to a step command (Ref. 27). The example case shown is for a second-order system with an undamped natural frequency $\omega_n = 20$ rad/s and a damping ratio $\zeta = 0.5$. In Fig. 10-4(A) the time step $T = 0.02$ s; this gives a sampling rate of about 16 times the damped natural frequency. At this sampling rate the root-matching difference equation gives good results. When the sampling rate is reduced to about six times the damped natural frequency, the aliasing effect begins to introduce errors as shown in Fig. 10-4(B). At a sampling rate of only three times the damped natural frequency, the aliasing error is pronounced, as shown in Fig. 10-4(C).

To obtain the match between the difference equation solutions and the exact solution, shown in Fig. 10-4, the time after initiation of the step input is calculated by $t = nT + (\sqrt{2}-1)T$ assuming $n = 0$ at the instant the step is initiated

10-4.3 SPECIAL INSTRUCTIONS FOR HARDWARE-IN-THE-LOOP SIMULATIONS

Hardware-in-the-loop simulations require a number of special instructions to ensure proper operation of the hardware components and to prevent them from being damaged. Examples of these instructions are (Ref. 28)

1. Ensure that the scene is correct, e.g., check the decay deployment times relative to the launch time.
2. Input the proper motion parameters to the launcher, including any pointing errors.
3. Allow time for the power supply to energize.
4. Allow time for the detector of an IR seeker to cool.
5. Ensure the proper initial automatic gain control (AGC) setting.
6. Ensure that the gyro is running at the proper speed.
7. Start the simulation a few seconds before seeker

lock-on to prevent the sensor from observing infinite simulated accelerations.

8. Allow sufficient time between sequential runs to permit the hardware to cool.

Special considerations in the design of hardware-in-the-loop simulations include

1. The requirements of real-time execution necessitate careful allocation of time for the digital calculations.
2. Typically, the simulation is tested by using mathematical models of all components to ensure proper real-time operation before hardware is substituted in the simulation loop (Ref. 29).
3. In a hybrid computer a method may be needed to compensate for the time lags associated with analog-to-digital and digital-to-analog conversions (Ref. 30). One method is linear extrapolation-based on derivatives-into the next time frame.
4. To be useful, a simulation must provide flexibility in its operation and easy access to system elements so that system parameters and their values can be varied and the phenomena associated with guidance and control can be studied
5. The simulation must permit a high sampling rate, i.e., short time between successive runs, to permit economical use of Monte Carlo methods to account for statistical variations.

REFERENCES

1. R. M. Howe, "Analog vs Digital Computers: Quantitative Speed Comparison Revisited", Applied Dynamics International, Ann Arbor, MI, Undated.
2. M. E. Sisle and E. D. McCarthy, "Hardware-in-the-Loop Simulation for an Active Missile", Simulation 39, No. 5, 159-67 (November 1982).
3. G. H. Johnson, "Electro-Optical Countermeasures Sim-

- ulation Facility", Office of Missile Electronic Warfare, White Sands Missile Range, NM, Undated.
4. "A Briefing on Benchmarks", Digital News & Review 9, No. 24,23 (21 December 1992).
 5. B. Case, "Updated SPEC Benchmarks Released", Microprocessor Report 6, No. 12, 14-9 (16 September 1992).
 6. M. Barber, "The Trouble With Benchmarks", Microprocessor Report 6, No. 10, 14-7 (29 July 1992).
 7. R. Glidewell, "A Guide to Smart Benchmark Management", Corporate Computing 1, No. 1,275-9 (June-July 1992).
 8. M. Sister, "The Trouble With Benchmarks", Microprocessor Report 6, No. 7, 3,(27 May 1992).
 9. "SPECmark Inflation", Microprocessor Report 5, No. 23,3 (18 December 1991).
 10. A. Ralston, Ed., Encyclopedia of Computer Science and Engineering, 2nd Ed., Van Nostrand Reinhold, New York, NY, 1983, pp. 697-8.
 11. R. J. Kochenburger, Computer Simulation of Dynamic Systems, Prentice-Hall, Inc., Englewood Cliffs, NJ, 1972.
 12. Advanced Methods for Solving Differential Equations, Research and Education Association, New York, NY, 1982.
 13. C. R. Wylie, Jr., Advanced Engineering Mathematics, McGraw-Hill Book Company, Inc., New York, NY, 1951.
 14. W. D. Fryer and W. C. Schultz, A Survey of Methods for Digital Simulation of Control Systems, CAL Report No. XA-1681-E-1, Cornell Aeronautical Laboratory, Inc., Buffalo, New York, NY, July 1964.
 15. J. M. Smith, Mathematical Modeling and Digital Simulation for Engineers and Scientists, 2nd Ed., John Wiley & Sons, Inc., New York NY, 1987.
 16. R. W. Hamming, Numerical Methods for Scientists and Engineers, McGraw-Hill Book Company, Inc., New York NY, 1962.
 17. S. D. Conte and C. de Boor, Elementary Numerical Analysis-An Algorithmic Approach, McGraw-Hill Book Company, Inc., New York, NY, 1965.
 18. K. Arbenz and A. Wohlhauser, Advanced Mathematics for Practicing Engineers, Artech House, Inc., Norwood, MA, 1986.
 19. C. W. Gear, Numerical Initial Value Problems in Ordinary Differential Equations, Prentice-Hall, Inc., Englewood Cliffs, NJ, 1971.
 20. P. S. Maybeck, Stochastic Models, Estimation, and Control, Volume 1, Academic Press, Inc., Orlando, FL, 1979.
 21. A. Gelb, Ed., Applied Optimal Estimation, The M. I. T. Press, Massachusetts Institute of Technology, Cambridge, MA, 1974.
 22. W. L. Brogan, Modern Control Theory, 2nd Ed., Prentice-Hall, Inc., Englewood Cliffs, NJ, 1985.
 23. J. A. Folck, SAMS Surface-to-Air Missile Simulation Computer Program, Analyst Manual, Vol 1, Basic Methodology, Flight Dynamics Laboratory, US Air Force Wright Aeronautical Laboratories, US Air Force Systems Command, Wright-Patterson Air Force Base, OH, January 1983.
 24. An introduction to Real-Time Digital Flight Simulation, IBM Data Processing Application, IBM Technical Publications Department, White Plains, NY, Undated.
 25. J. A. Aseltine, Transform Methods in Linear System Analysis, McGraw-Hill Book Company, Inc., New York, NY, 1958.
 26. C. E. Shannon, "Communications in the Presence of Noise", Proceedings of the IRE, January 1949, Institute of Electrical and Electronics Engineers, Inc., New York, NY. (IEEE was IRE)
 27. V. Del Torro and S. R. Parker, Principles of Control Systems Engineering, McGraw-Hill Book Company, Inc., New York NY, 1960.
 28. M. D. Sevachko and R. E. Gould, (personal communication), Electronic Warfare Laboratory, Office of Missile Electronic Warfare, White Sands Missile Range, NM, November 1982.
 29. H. L. Pastrick, C. M. Will, Jr., L. S. Isom, A. C. Jolly, L. H. Hazel, R. J. Vinson, and J. Mango, "Recent Experience in Simulating Missile Flight Hardware in Terminal Homing Applications", Proceedings of the Photo-Optical Instrumentation Engineers, Optics in Missile Engineering, SPIE Vol. 133, Los Angeles, CA 1978, pp. 108-15, Society of Photo-Optical Instrumentation Engineers, Bellingham, WA.
 30. H. L. Pasterick, W. H. Holmes et al, "Real-Time Hybrid Hardware-in-the-Loop Simulation of a Terminal Homing Missile", Proceedings of the 1973 Summer Computer Simulation Conference, Montreal, Canada, July 1973, Simulation Council, La Jolla, CA.

BIBLIOGRAPHY

NUMERICAL METHODS

- L. E. Barker, Jr., R. L. Bowles, and L. H. Williams, Development and Application of a Local Linearization Algorithm for Integration of Quaternion Rate Equations in Real-Time Flight Simulation Problems, NASA TN-D-7347, National Aeronautics and Space Administration, Washington, DC, December 1973.
- M. E. Fowler, "A New Numerical Method for Simulation", Simulation 4,324-30 (1965).
- F. W. Hamming, Numerical Methods for Scientists and Engineers, 2nd Ed., McGraw-Hill Book Company, Inc., New York. NY, 1973.

- M. L. James, G. M. Smith, and J. C. Woford, Applied Numerical Methods for Digital Computation With FORTRAN, International Textbook Co., Scranton, PA, 1967.
- H. R. Martins, "A Comparative Study of Digital Integration Methods", Simulation VII, 87-96 (February 1969).
- W. E. Milne, Numerical Solution of Differential Equations, John Wiley & Sons, Inc., New York, NY, 1953.
- A. Ralston and P. Rabinowitz, A First Course in Numerical Analysis, 2nd Ed., McGraw-Hill Book Company, Inc., New York, NY, 1978.
- J. M. Smith, "Recent Developments in Numerical Integration", Journal of Dynamic Systems, Measurement, and Control (March 1974).
- A. Tustin, "A Method Analyzing the Behavior of Linear Systems in Terms of Time Series", Journal I.E.E.E. 94, Part II-A (May 1947).
- R. M. Howe, "The Role of Modified Euler Integration in Real-Time Simulation", Proceedings of the SCS Multi-conference on Aerospace Simulation III, Vol. 19, April 1988.

CHAPTER 11

VERIFICATION AND VALIDATION

This chapter gives an overview of the processes required to ensure that a simulation represents actual missile performance to an acceptable level of confidence. Usage of the terms associated with verification and validation within the simulation community are discussed; and the need to tailor the validation effort to meet simulation objectives is emphasized, A range of possible methods of validating simulations is presented.

11-1 INTRODUCTION

The users of a missile flight simulation must have confidence that the simulation results are meaningful and that the simulation output is representative of actual missile performance (Ref. 1). It is essential that the models of the missile system, subsystems, and physical environment have a demonstrable correspondence with the system, subsystem, or environment being modeled. This confidence is gained through the processes of verification and validation. Verification ensures that the computer program operates correctly according to the conceptual model of the missile system. Validation determines the extent to which the simulation is an accurate representation of the real world.

Most if not all, flight simulations contain approximations and consequently are not expected to be perfect representations of the actual missile system over all flight conditions. One of the objectives of validation is to determine the flight conditions for which the simulation does accurately represent the actual missile. As discussed in Chapter 3, different levels of fidelity are required in simulations; the extent and nature of validation processes are largely determined by the fidelity requirements. In particular, it must be demonstrated that the missile performance functions most critical to the simulation objectives are simulated to an acceptable degree of fidelity. The limits of acceptability can be relatively wide for less critical parameters and narrower for more critical ones (Ref. 1).

Validation is performed by comparing simulation output with flight-test and laboratory data obtained under similar flight conditions. Various methods are used to make these comparisons; they range from visual comparison of plotted data overlays to sophisticated statistical and spectral analyses.

Missile flight simulations are often developed progressively as the missile system is developed. As new and better data on the actual system become available, the simulation model is updated, and the validation of the model is extended to include the update.

As discussed in Chapter 3, modern weapons development management and test philosophies depend heavily on missile flight simulation experiments in lieu of flight testing. As confidence in the flight simulation of a missile increases, dependence on costly and time-consuming flight tests can be reduced.

11-2 VERIFICATION

Verification is the process of confirming that the conceptual description and specifications of the model of a missile system and the environment have been accurately translated into an operational program and that calculations made with this program use the correct input data (Ref. 2). Verification evaluates the extent to which sound and established software engineering techniques' have been employed in the development of the simulation (Ref. 3).

Verification is basically a debugging process to ensure that logic sequences are operating as intended, that the program accurately reflects the model equations, that interfaces with hardware components are handled properly, and that modeled system and subsystem characteristics are consistent with the conceptual model descriptions and specifications.

Formal verification programs have three basic stages:

1. Review of model design requirements
2. Verification of model implementation
3. Periodic calibration and diagnostic maintenance.

During review of the design requirements, checks are made to see that the mathematical model meets the requirements agreed upon by the simulation customer and the simulation developer. Verification of the model implementation ensures that the mathematical model is correctly implemented and, if the model must operate in real time, that real-time operation is correct. Calibration and diagnostic maintenance are routine tests made daily or weekly during simulation operations to check that the models continue to function properly.

Methods of verification include inspecting the computer program and design documentation, comparing with other simulations, testing individual simulation modules against known or reasonable standards, and ensuring that all logic branches are tested for accuracy. The overall simulation is verified by demonstrating the correct interfaces among independently verified component models. If verification testing reveals that a particular simulation design objective is not met, corrective action is taken—correcting program errors, improving the model, or relaxing the design specification if it is demonstrated to be overly ambitious (Ref. 1).

11-3 VALIDATION

Model validation addresses the issue of how accurately the model reflects reality. It is the process of confirming that the simulation of the missile system and the environment is applicable to its intended use by demonstrating an acceptable correspondence between the computational results of the model and data obtained from tests of the actual system (Ref. 4) or other reliable sources. Validation methods include expert consensus, comparison with historical results, comparison with test data, peer review, and independent review (Ref. 3). When available, the most reliable method of validation is comparison of simulation predictions with actual observed characteristics of the missile system, which are normally obtained through flight tests and laboratory tests as required or available (Ref. 1). Simulation validity implies that a set of input conditions to the model will produce outputs that agree within defined limits with those produced by the actual missile system when it is exposed to the same conditions.

Philosophies of validation concepts from the points of view of the pure rationalist, empiricist, and absolute pragmatist are discussed in Ref. 5. Arguments and controversy among the points of view are usually over matters of emphasis and degree, and most experimenters incorporate ideas from all three points of view into what might be called a utilitarian approach as described in the paragraphs that follow.

11-3.1 LEVELS OF CONFIDENCE

Verification and validation can be viewed as building a pyramid of confidence in the predictions made by a simulation as illustrated in Fig. 11-1 (Ref. 6). As new scenarios are introduced, sensitivity analyses performed, models improved, and simulation predictions validated with flight-test data and other independent analyses, the knowledge base of the pyramid is broadened, and higher levels of confidence are reached over a period of time. In general, the cost and effort required to validate a simulation depend on its complexity and the level of confidence required. A simulation that is validated only to the level required by the specific application is a tool that provides design and management data at each level of missile system development at minimum cost.

The concept of validity is one of degree; it is not a binary decision variable. Tests with ever increasing levels of sophistication and expense can be devised which will improve model credibility (Ref. 5); however, a point is reached at which these increased efforts have diminishing returns, as illustrated conceptually in Fig. 11-2. Total confidence can never be achieved because not all possible scenarios and contingencies can be explored in validation testing. There will always be uncertainties, such as unknown sensor bias and errors in measured flight-test data that can never be resolved completely; therefore, simulation data will never match flight-test data precisely. Seldom, if ever, will validation result in proof that a simulation is a totally correct or true model of the real process (Ref. 7), but an iterative validation program carried out over a period of time reduces risk and uncertainty to an acceptable level (Ref. 6).

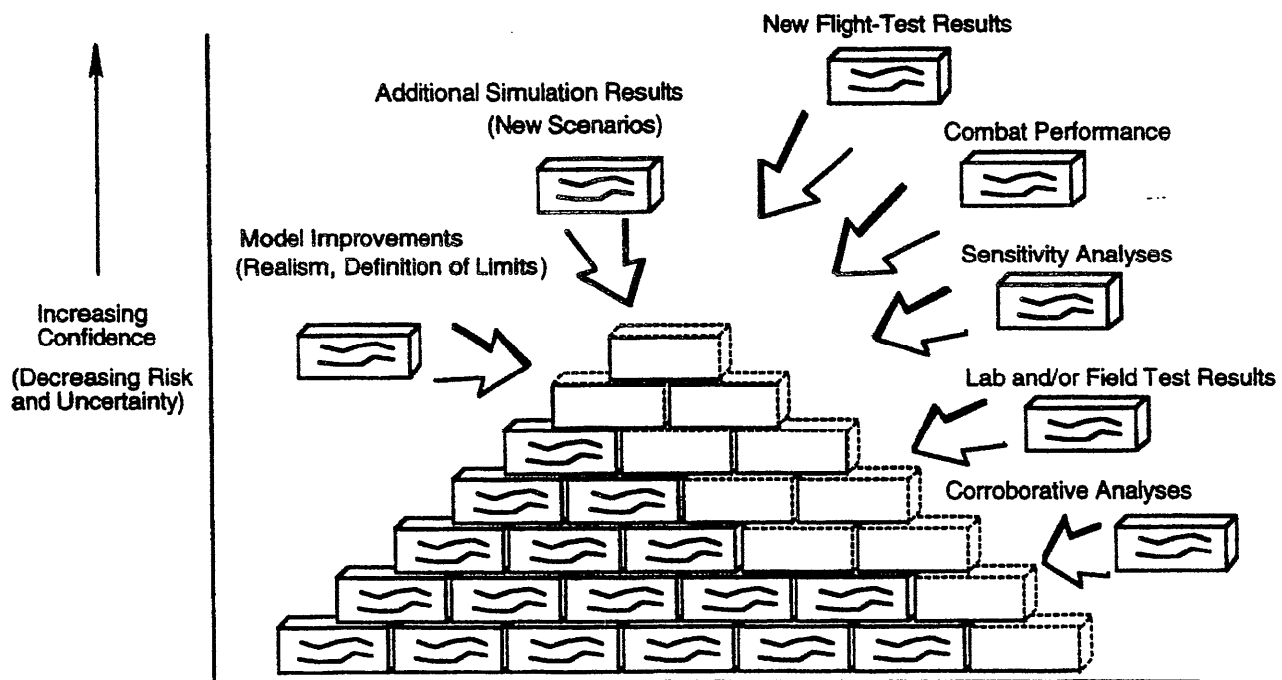


Figure 11-1. Validation—Building a Pyramid of Confidence (Ref. 6)

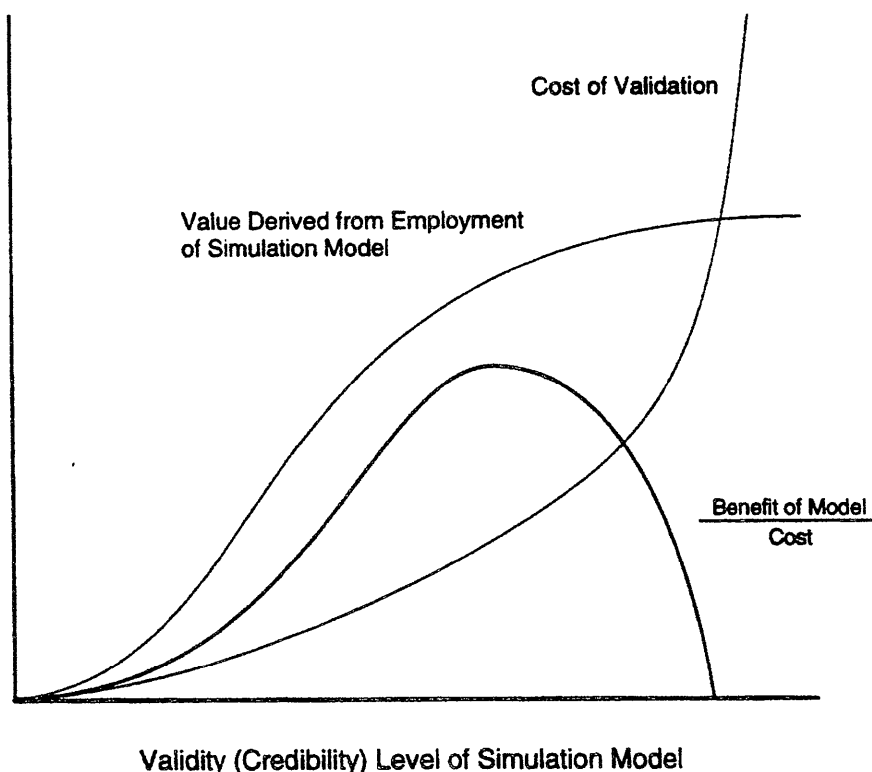


Figure 11-2. Effect of Model Validity Level on Benefit-to-Cost Ratio

11-3.2 COMPARISON WITH TEST RESULTS

The parameters to be compared depend on the purpose and objectives of the simulation, but in general, they include parameters that will reveal the validity of the

1. Simulated thrust and aerodynamics
2. Dynamic response characteristics of the simulated control system and airframe
3. Simulated mechanization of the guidance system
4. Simulated seeker performance.

Examples of parameters that can be compared to reveal the adequacy of a simulation are kinematic boundary, acquisition boundary, flight path history, velocity history, response to maneuver commands, lateral accelerations, roll rate, control-surface position, system gain, natural frequency, static gain, achieved navigation ratio, signal processing, automatic gain control, seeker tracking rate, control servo responses, miss distance, etc. Much insight into the overall validity of a missile flight simulation can be gained simply by comparing fin deflection commands because essentially they reflect the responses of all other missile functions (Ref. 1).

Many techniques are available to analyze the performance of a simulation relative to missile flight-test data. The techniques range from very sophisticated statistical analyses to simple nonstatistical visual comparisons of plotted simulation and flight-test output data. Each technique is discussed in the paragraphs that follow.

11-3.2.1 Statistical Methods

Many of the parameters employed in a validation process vary with time throughout the flight and, therefore, are expressed as functions of time, i.e., they are expressed as mathematical time series. Differences in phase angle, gain, and frequency of oscillation usually have specific meaning to the missile designer, who would like to know whether such differences are present (Ref. 8). Statistical procedures used to compare phase differences, gain differences, and frequency differences are presented in Ref. 9. The use of spectral analysis to compare simulated parameters expressed as time series with flight-test parameters expressed as time series is described in Ref. 8. The method is illustrated by several numerical examples in which control-surface command data generated by simulations and by flight tests are compared and evaluated, and confidence intervals are constructed. In Ref. 10 the model is extended to cross-spectral analysis, and additional illustrations of the application of these methods are given.

Statistical techniques available for testing the "goodness of fit" of simulation model data include analysis of variance, chi-square test factor analysis, Kolmogorov-Smirnov tests, nonparametric tests, regression analysis, and spectral analysis (Ref. 11). Discussions of these methods are given in Refs. 12 through 15.

Frequently, comparison of simulated results with test results is hampered by a paucity of test results in compari-

son' with an abundance of simulation results. A technique for quantitative evaluation of the degree to which the model of the system predicts the performance of the red system is called Bayesian Updating, in which test data can be examined in terms of the probabilities they derive from one of several hypothesized model formulations. As more test data become available, the probability distribution that represents the best estimate of real system performance is updated by using a specific procedure. In the Bayesian Updating process, the probability of correct choice among the alternative hypothesized assumptions is increased as more and higher quality test data become available. The procedure does as much as is possible, consistent with the available data it is quantitative and permits sensitivity analysis with respect to the assumptions (Ref. 1).

11-3.2.2 Nonstatistical Methods

When the evidence is of such a nature that objective validation techniques (also called, formal techniques) are not applicable or are difficult to apply; subjective (informal) validating procedures—which are generally nonstatistical—can be used.

The most common nonstatistical method of comparison is to plot as time series the parameters from a simulation run and a corresponding flight test and to, overlay the plots. The analyst determines subjectively (or with simple quantitative measures) whether the outputs from, the simulation agree acceptably with the flight-test results. The difficulties with this approach are that it does not quantify the risk associated with the design and that different analysts may arrive at different conclusions.

Another nonstatistical procedure is Theil's inequality coefficient. Although this procedure is more quantitative than the visual comparison method, there is no simple distribution theory for Theil's inequality coefficient, and so no statistical statements can be made about a time series (Ref. 8). Theil's inequality coefficient method is described in Ref. 16, and examples of application of the method are given in Ref. 4. Ref. 17 suggests an extension of Theil's inequality coefficient method that combines the comparisons of a number of different functions by employing weighting factors that describe the importance, of each function in the intended application of the simulation and thus gives a single number to describe the overall comparison of all the time series tested.

11-3.2.3 Model Calibration

When a simulation is first run for conditions that duplicate those of a particular flight test, the simulated results may not match the flight-test results with acceptable fidelity. These observations of minor differences between actual and predicted characteristics indicate that the model needs further refinement. Such refinement may be as simple as adjustment (calibration) of parameters to cause the simulated flight to match the actual flight. Any parameter adjust-

ments must of course be reasonable and consistent with all available information on the missile system. Ref. 18 describes a method of extracting aerodynamic parameters from flight-test data to refine the aerodynamics parameters of the model. (See subpar. 5-4.3.)

11-3.2.4 Neighborhood of Validity

Flight tests are characterized by a set of flight conditions, such as type of target, altitude, range, type of maneuver, and environmental factors. Since approximations employed in simulations may be good approximations under some flight conditions and poor approximations under others, a necessary element of validation is to define those conditions under which the simulation model meets its objectives. The set of conditions under which the simulation meets its objectives is called the neighborhood of validity of the simulation. Within the neighborhood of validity, simulation may be substituted for flight testing. When a region of flight conditions is simulated in which neither flight tests nor laboratory tests exist as a basis of comparison or in which these test results differ significantly from the results of the simulation, the simulated flight is outside the neighborhood of validity of the simulation model, and the simulation results cannot be used with high confidence. If the questionable region of flight conditions is important, further flight testing in this region may be justified if it is feasible, or additional laboratory tests and analyses may be required to improve confidence in the simulation.

11-3.3 SCENE VALIDATION

Validation of environmental models (scenes) can involve both direct measurements of the simulated environment and indirect measurements of the effect of the environment on a test seeker that incorporates target detection, discrimination, and location logic. A test seeker used to validate a scene can be of generic design or a version of the seeker under evaluation. Data on the adequacy of previously developed and tested models are also valuable for determining the adequacy of a new environmental model. Thus a number of data acquisition and analysis activities can generate data for the validation of the environmental model (Ref. 1).

11-4 ACCREDITATION

Accreditation is the acceptance by the simulation customer (or his delegates) that the verification and validation processes provide sufficient evidence that the computer model is adequate for the purpose for which it is intended. It is based on experience and expert judgment at a management level of responsibility (Ref. 3). Depending on the requirements of the application sponsor, accreditation can be as simple and informal as a verbal briefing to (and acceptance by) the simulation customer describing the verification and validation procedures that have been performed, or it can be as complete and formal as a fully documented written description of these procedures with evaluation of verifica-

cation and validation evidence by a specially appointed accreditation working group.

11-5 SELECTION OF METHODS

The selection of verification and validation methods should be considered carefully; no one method is best. Decisions on the methods and data that are actually specified for validating a simulation are based on balancing the cost of testing against the cost of an incorrect inference if the simulation is wrong (Ref. 7). Such decisions depend on what can be accomplished within reasonable time, cost, and technical feasibility constraints. In many cases relatively simple validation procedures suffice.

It is the joint responsibility of the customer, or user, and the simulation developer during the coordinating and planning stage of simulation development to agree not only on the model specifications that satisfy the customer's test objectives and that can be implemented in the simulation (Ref. 1) but also on the methods and data to be employed in verification and validation. A simple declaration that a simulation must be verified and validated is insufficient. Often, users of simulation results are not fully aware of the implications of the various imperfections and approximations in the simulations, and as a result, decisions are made based on simulated results that are outside the range of validity of the simulation. Therefore, it is important that as much detail as possible be discussed and agreed upon early in simulation planning concerning the levels of verification and validation to be performed.

REFERENCES

1. A. M. Baird, R. B. Goldman, N. C. Randall, W. C. Bryan, F. M. Belrose, and W. C. Holt Verification and Validation of RF Environmental Models-Methodology Overview, Technical Report RD-81-2, US Army Missile Command, Redstone Arsenal, AL, October 1980.
2. Technical Committee on Model Credibility, Society of Computer Simulation (SCS), "Terminology of Model Credibility", *Simulation*, 103-4 (March 1979).
3. AR 5-11, Army Model and Simulation Management Program, 10 June 1992.
4. N. A. Kheir and W. M. Holmes, "On Validating Simulation Models of Missile Systems", *Simulation* 30, No. 4, 117-28 (April 1978).
5. R. E. Shannon, *Systems Simulation: The Art and Science*, Prentice-Hall, Inc., Englewood Cliffs, NJ, 1975.
6. M. M. Rea, A. M. Baird, D. W. Batchelder, F. M. Belrose, and W. C. Holt, *Missile System Simulation at the Advanced Simulation Center*, Technical Report RD-82-11, Systems Simulation and Development Directorate, Advanced Simulation Center, US Army Missile Laboratory, US Army Missile Command, Redstone Arsenal, AL, 25 January 1982.

7. R. L. Van Horn, "Validation of Simulation Results", *Management Science* 17, No. 5 (January 1971).
8. D. C. Montgomery and R. G. Conard, "Comparison of Simulation and Flight-Test Data for Missile Systems", *Simulation* 34, No. 2, 63-72 (February 1980).
9. W. A. Fuller, *Introduction to Statistical Time Series*, John Wiley & Sons, Inc., New York, NY, 1976.
10. D. C. Montgomery and L. Greene, "Methods for Validating Computer Simulation Models of Missile Systems", *Journal of Spacecraft and Rockets* 20, No. 3, 272-78 (May-June 1983).
11. N. A. Kheir, "A Validation Procedure for Missile-Systems Simulation-Models", *Proceedings of the Seventh Annual Pittsburgh Conference, Modeling and Simulation*, Vol. 7, Part 1, Pittsburgh, PA, April 1976, pp. 534-39.
12. G. A. Mihram, *Simulation: Statistical Foundations and Methodology*, Academic Press, Inc., New York, NY, 1972.
13. C. A. Bennett and N. L. Franklin, *Statistical Analysis in Chemistry and the Chemical Industry*, Second Edition, John Wiley & Sons, Inc., New York, NY, 1961.
14. T. H. Naylor and J. M. Finger, "Verification of Computer Simulation Models", *Management Science* 14, No. 2, B-92-B-101 (October 1967).
15. G. S. Fishman and P. J. Kiviat, "The Analysis of Simulation-Generated Time Series", *Management Science* 13, No. 7, 525-57 (March 1967).
16. H. Theil, *Economic Forecasts and Policy*, North-Holland Publishing Co., Amsterdam/London, 1970.
17. W. E. Schrank and C. C. Holt, "Critique of: Verification of Computer Simulation Models", *Management Science* 14, No. 2, B-104-B-106 (October, 1967).
18. T. R. Driscoll and H. F. Eckenroth, "Flight-Test Validation of the Patriot Missile Six-Degree-of-Freedom Aerodynamic Simulation Model", *Automatic Control Theory and Applications* 7, No. 1, 8-15 (January 1979).

BIBLIOGRAPHY

VERIFICATION AND VALIDATION

- F. M. Belrose and A. M. Baird, *The Role of Simulation in High-Technology Missile Applications*, Technical Report RD-CR-83-23, US Army Missile Command, Redstone Arsenal, AL, April 1983.
- R. M. Cyert, "A Description and Evaluation of Some Firm Simulations", *Proceedings of IBM Scientific Computing Symposium Simulation Models and Gaming*, IBM Processing Division, White Plains, NY, 1966.
- G. S. Fishman, "problems in the Statistical Analysis of Simulation Experiments: The Comparison of Means and the Length of Sample Records", *Communications of the ACM* 10, No. 2, 94-9 (February 1967).

MIL-HDBK-1211(MI)

- J. W. Forrester, Industrial Dynamics, M. I. T. Press, Cambridge, MA, 1961.
- G. M. Jenkins, "General Considerations in the Analysis of Spectra", Technometrics 3, No. 2, 133-66 (May 1961).
- T. H. Naylor, J. L. Balintfy, D. S. Burdick, and K. Chu, Computer Simulation Techniques, John Wiley & Sons, Inc., New York, NY, 1966.
- H. Theil, Applied Economic Forecasting, Rand McNally and Co., Chicago, IL 1966.
- M. R. Wigan, "The Fitting, Calibration, and Validation of Simulation Models", Simulation, 188-92 (May 1972).

CHAPTER 12

SIMULATION SYNTHESIS

Equations and procedures for modeling the various subsystems of missile flight have been presented in previous chapters. This chapter employs an example to illustrate how the level of detail in a simulation is selected to satisfy simulation objectives, and to show how to synthesize a complete flight simulation by combining the subsystem models.

12-0 LIST OF SYMBOLS

\mathbf{A}_c = commanded-lateral-acceleration vector, m/s^2	C_n = yawing moment coefficient about center of mass, dimensionless
A = aerodynamic axial force, N	C_{nr} = yaw damping coefficient relative to yaw rate r , $rad^{-1} (deg^{-1})$
A_{cxb} = i -component of \mathbf{A}_c expressed in body coordinate system, m/s^2	C_{nref} = aerodynamic yaw moment coefficient with respect to reference moment station, dimensionless
A_{cyb} = j -component of \mathbf{A}_c expressed in body coordinate system, m/s^2	$C_{n\beta}$ = yaw moment derivative relative to angle of sideslip (slope of C_n versus β curve), $rad^{-1} (deg^{-1})$
A_{czb} = k -component of \mathbf{A}_c expressed in body coordinate system, m/s^2	$C_{n\dot{\beta}}$ = yaw damping derivative relative to angle-of-sideslip rate $\dot{\beta}$, $rad^{-1} (deg^{-1})$
A_e = exit area of rocket nozzle, m^2	$C_{n\delta}$ = yaw moment derivative relative to control-surface deflection angle (slope of C_n versus δ_y curve), $rad^{-1} (deg^{-1})$
A_p = actuator piston area, m^2	$c\theta$ = $\cos \theta$
C_D = aerodynamic drag coefficient, dimensionless	$c\psi$ = $\cos \psi$
C_{D0} = zero-lift drag coefficient, dimensionless	D = aerodynamic drag force, N
$C_{H\alpha_f}$ = partial derivative of fin moment coefficient with respect to fin angle of attack, rad^{-1}	d = aerodynamic reference length, m
C_L = aerodynamic lift coefficient, dimensionless	d_f = aerodynamic reference length of control surface (fin), m
$C_{L\alpha}$ = slope of curve formed by lift coefficient C_L versus angle of attack α , rad^{-1}	$DSET$ = flag used to control equations to be evaluated in subroutine DERIVS
C_m = pitching moment coefficient about center of mass, dimensionless	DTR = $\pi/180$, factor for converting degrees to radians
C_{mq} = pitch damping derivative relative to pitch rate q , $rad^{-1} (deg^{-1})$	F_{Axb} = x_b -component of aerodynamic force in body coordinate system, N
C_{mref} = aerodynamic pitch moment coefficient with respect to reference moment station, dimensionless	F_{Ayb} = y_b -component of aerodynamic force in body coordinate system, N
$C_{m\alpha}$ = pitch moment derivative relative to angle of attack (slope of curve formed by C_m versus α), $rad^{-1} (deg^{-1})$	F_{Az_b} = z_b -component of aerodynamic force in body coordinate system, N
$C_{m\dot{\alpha}}$ = pitch damping derivative relative to angle-of-attack rate $\dot{\alpha}$, $rad^{-1} (deg^{-1})$	$F_{g_{xb}}$ = i -component of gravitational force on the missile in body coordinate system, N
$C_{m\delta}$ = pitch moment derivative relative to control-surface deflection (slope of C_m versus δ_p curve), $rad^{-1} (deg^{-1})$	$F_{g_{yb}}$ = j -component of gravitational force on the missile in body coordinate system, N
C_{N_y} = aerodynamic coefficient corresponding to the component of normal force on the y_b -axis, dimensionless	$F_{g_{zb}}$ = k -component of gravitational force on the missile in body coordinate system, N
C_{N_z} = aerodynamic coefficient corresponding to the component of normal force on the z_b -axis, dimensionless	$F_{g_{x_e}}$ = i -component of gravitational force on the missile in earth coordinate system, N
	$F_{g_{y_e}}$ = j -component of gravitational force on the missile in earth coordinate system, N

F_{gz_e} = k -component of gravitational force on the missile in earth coordinate system, N	N = aerodynamic normal force, N
F_p = magnitude of thrust force, N	N_A = aerodynamic moment in yaw plane, N-m
$F_{p_{ref}}$ = magnitude of reference-thrust force, N	NR = nominal navigation ratio, dimensionless
$F_{p_{xb}}$ = i -component of thrust force vector in body coordinate system, N	P_M = position vector of missile in earth coordinate system, m
$F_{p_{yb}}$ = j -component of thrust force vector in body coordinate system, N	P_T = position vector of target in earth coordinate system, m
$F_{p_{zb}}$ = k -component of thrust force vector in body coordinate system, N	$P_M(i)$ = i -component of missile position vector P_M in earth coordinate system, m
G_n = gain factor relating angle of attack of control surface to acceleration command per unit dynamic pressure parameter, $(\text{rad}\cdot\text{Pa})/(\text{m/s})^2$	$P_M(j)$ = j -component of missile position vector P_M in earth coordinate system, m
G_p = gain factor relating actuator piston pressure to acceleration command, $\text{Pa}/(\text{m/s}^2)$	$P_M(k)$ = k -component of missile position vector P_M in earth coordinate system, m
$G_s(M, h)$ = system gain as a function of Mach number and altitude, m/s	$P_T(i)$ = i -component of target position vector P_T in earth coordinate system, m
g = acceleration due to gravity, m/s^2	$P_T(j)$ = j -component of target position vector P_T in earth coordinate system, m
H = Δt , factor for use in Runge-Kutta Subroutine RK4	$P_T(k)$ = k -component of target position vector P_T in earth coordinate system, m
HH = $H/2$, factor for use in Runge-Kutta Subroutine RK4	$\dot{P}_M(i)$ = i -component of rate of change vector of missile position P_M , m/s
$H6$ = $H/6$, factor for use in Runge-Kutta Subroutine RK4	$\dot{P}_M(j)$ = j -component of rate of change vector of missile position P_M , m/s
h = altitude of missile above sea level, m	$\dot{P}_M(k)$ = k -component of rate of change vector of missile position P_M , m/s
I = instantaneous moment of inertia about y - and z -axes (pitch and yaw), $\text{kg}\cdot\text{m}^2$	p, q, r = components of missile inertial angular rate vector in body coordinate system, rad/s
I_{bo} = moment of inertia about y - and z -axes at burnout, $\text{kg}\cdot\text{m}^2$	P_a = ambient pressure at altitude h , Pa
I_{sp} = specific impulse, $\text{N}\cdot\text{s}/\text{kg}$	P_{act} = actuator pressure, Pa
I_0 = moment of inertia about y - and z -axes at launch, $\text{kg}\cdot\text{m}^2$	P_{act1} = actuator pressure for the pitch channel, Pa
k = constant used to calculate induced drag coefficient, dimensionless	P_{act2} = actuator pressure for the yaw channel, Pa
L = aerodynamic lift force, N	P_{ref} = reference ambient pressure, Pa
L_{arm} = bell crank lever arm, m	Q = dynamic pressure parameter, Pa
$LFLAG$ = logical flag to indicate gimbal angle has exceeded its limit, dimensionless	\dot{q} = pitch component of angular acceleration $\dot{\omega}$ expressed in body coordinate system, rad/s^2
M_d = miss distance vector in earth coordinate system, m	R = range vector from missile to target in earth coordinate system, m
M_A = aerodynamic moment in pitch plane, N-m	R = magnitude of range vector R from missile to target in earth coordinate system, m
M_f = aerodynamic moment on control surface about hinge line, N-m	$RFLAG$ = logical flag to indicate that seeker angular rate has exceeded its limit, dimensionless
M_H = hinge moment applied to control surface by actuator, N-m	RTD = $180/\pi$, factor for converting radians to degrees
M_N = Mach number, dimensionless	\dot{r} = yaw component of angular acceleration $\dot{\omega}$ expressed in body coordinate system, rad/s^2
m = instantaneous missile mass, kg	S = missile aerodynamic reference area, m^2
m_{bo} = missile mass at burnout, kg	S_f = aerodynamic reference area of control surface (fin), m^2
m_0 = missile mass at launch, kg	$s\theta$ = $\sin \theta$
	$s\psi$ = $\sin \psi$

$[T_{b/e}]$ = earth-to-body coordinate system transformation matrix, dimensionless	$V_M(k)$ = k -component of missile velocity vector \mathbf{V}_M , m/s
$[T_{e/b}]$ = body-to-earth coordinate system transformation matrix, dimensionless	V_s = speed of sound, m/s
t = simulation time, s	$V_T(i)$ = i -component of target velocity vector \mathbf{V}_T in earth coordinate system, m/s
(t) = indicates value at beginning of current time step, s	$V_T(j)$ = j -component of target velocity vector \mathbf{V}_T in earth coordinate system, m/s
$(t+\Delta t)$ = indicates value at beginning of first succeeding time step, s	$V_T(k)$ = k -component of target velocity vector \mathbf{V}_T in earth coordinate system, m/s
$(t-\Delta t)$ = indicates value at beginning of first preceding time step, s	V_{TM} = magnitude of velocity vector of target relative to missile in earth coordinate system, m/s
t_{bo} = time of burnout, s	x_{cm} = instantaneous distance from missile nose to center of mass, m
t_{ca} = time of closest approach, s	x_{cm0} = distance from missile nose to center of mass at launch, m
t_{gon} = time to initiate guidance, s	x_{cmbo} = distance from missile nose to center of mass at burnout, m
t_{max} = maximum time of flight, s	x_{ref} = distance from missile nose to reference moment station, m
t_{nr} = time for buildup of navigation ratio, s	$Y(i)$ = input array of Runge-Kutta Subroutine RK4
\mathbf{u}_{ct} = unit missile centerline axis vector in earth coordinate system, dimensionless	$YOUT$ = output array of Runge-Kutta Subroutine RK4
\mathbf{u}_R = unit range vector from missile to target in earth coordinate system, dimensionless	α = angle of attack of missile, rad
\mathbf{u}_{sa} = unit vector along seeker boresight axis, dimensionless	α_f = angle of attack of control surface (fin), rad
\mathbf{u}_{V_M} = unit vector of missile velocity, dimensionless	α_{fp} = commanded angle of attack of pitch-channel control surface (fin), rad
$\mathbf{u}_{V_{TM}}$ = unit vector in direction of velocity of target relative to missile in earth coordinate system, dimensionless	α_{fpa} = achieved angle of attack of pitch-channel control surface (fin), rad
$u_{ct}(i)$ = i -component of \mathbf{u}_{ct} in earth coordinate system, dimensionless	α_{fy} = commanded angle of attack of yaw-channel control surface (fin), rad
$u_{ct}(j)$ = j -component of \mathbf{u}_{ct} in earth coordinate system, dimensionless	α_{fya} = achieved angle of attack of yaw-channel control surface (fin), rad
$u_{ct}(k)$ = k -component of \mathbf{u}_{ct} in earth coordinate system, dimensionless	α_t = total angle of attack (angle between missile velocity vector and missile centerline axis), rad
u, v, w = components of missile inertial velocity vector \mathbf{V}_M in body coordinate system, m/s	β = angle of sideslip of missile, rad
$\dot{u}, \dot{v}, \dot{w}$ = components of linear acceleration expressed in body coordinate system, m/s ²	Δt = integration time step, s
\mathbf{V}_M = missile inertial velocity vector in earth coordinate system, m/s	δ_{max} = maximum control-surface (fin) deflection angle relative to the missile, rad
\mathbf{V}_T = target inertial velocity vector in earth coordinate system, m/s	δ_p = pitch-channel control-surface deflection relative to missile, rad
\mathbf{V}_{TM} = velocity vector of target relative to missile in earth coordinate system, m/s	δ_y = yaw-channel control-surface deflection relative to missile, rad
V = magnitude of $\mathbf{V}_M = V_M$, m/s	θ = Euler angle rotation in elevation (pitch), rad (deg)
V_c = missile-to-target closing speed, m/s	$\dot{\theta}$ = angular rate of Euler angle rotation in elevation (pitch), rad/s (deg/s)
V_M = magnitude of missile inertial velocity, m/s	λ = seeker gimbal angle (angle between missile centerline axis and seeker boresight axis), rad
$V_M(i)$ = i -component of missile velocity vector \mathbf{V}_M , m/s	
$V_M(j)$ = j -component of missile velocity vector \mathbf{V}_M , m/s	

- λ_{max} = maximum gimbal angle of seeker, rad (deg)
 ρ = atmospheric density at altitude h , kg/m³
 σ = line-of-sight vector from seeker to track point on target, m
 σ = magnitude of line-of-sight vector σ , m
 τ_1 = seeker tracking loop time constant, s
 τ_2 = seeker signal processing time constant, s
 τ_3 = combined autopilot and control servo time constant, s
 ϕ = Euler angle rotation in roll, rad (deg)
 $\dot{\phi}$ = angular rate of Euler angle rotation in roll, rad/s (deg/s)
 ψ = Euler angle rotation in azimuth (heading), rad (deg)
 $\dot{\psi}$ = angular rate of Euler angle rotation in yaw, rad/s (deg/s)
 ω_{ach} = achieved seeker-head angular rate vector, rad/s
 ω_f = final processed tracking-rate-signal vector, rad/s
 ω_σ = angular rate vector of the line-of-sight vector σ , rad/s
 $\omega_{s,max}$ = maximum angular tracking rate of seeker boresight axis, rad/s (deg/s)

12-1 INTRODUCTION

The earlier chapters of this handbook described missile systems and methods used to simulate the various missile subsystems. The purpose of this chapter is to show how to synthesize a simulation by using the information provided in the earlier chapters. An example of a relatively simple digital flight simulation of a generic surface-to-air missile is used to illustrate the principles involved.

12-2 EXAMPLE SIMULATION

As discussed in Chapters 1 and 3, missile flight simulations are developed to fulfill various objectives, and the details of the simulation depend largely on those objectives. In the development of the example simulation, objectives are selected that lead to a simulation sophisticated enough to illustrate the principles but not so complicated that clarity is sacrificed.

12-2.1 SCENARIO

The objectives of the example simulation are derived from the following hypothetical scenario. A new surface-to-air missile system is to be developed. The time is early in the development process. The missile configuration is still in the conceptual phase, and a missile flight simulation is needed to evaluate various design alternatives. Aerodynamic data are available for missiles that are generally similar to the proposed configurations, but only limited wind tunnel data are available for the specific configurations

to be modeled. No flight-test data are yet available. The autopilot and control systems have not been defined in detail, but general transfer functions are available for the types of systems that are likely to be developed for this missile. The seeker design requirements have not been completed, but tentative seeker characteristics have been estimated.

12-2.2 OBJECTIVES

In the scenario described in subpar. 12-2.1, the overall objective of the proposed simulation is that it be adequate to investigate the gross effects of different missile design alternatives on missile system performance. Thus the simulation should be constructed so that the missile and subsystem characteristics in it are easy to change.

Since the basic purpose of a surface-to-air missile is to defend surface-based assets from air attack a major performance measure of alternative missile designs is the size and shape of the engagement boundary that can be achieved under various conditions of target signal strength, speed, altitude, and evasive maneuver. In general, engagement boundaries are determined by missile parameters, such as thrust and aerodynamic drag, and by seeker characteristics, such as lock-on range, tracking rate limit, and gimbal angle limit. Therefore, parameters that represent these missile characteristics will be included in the simulation.

Since the missile configuration has not yet been frozen, the characteristics of the dynamic response of the missile that result from different conjunctions constitute a major issue to be investigated by using the simulation. The simulation must have at least five degrees of freedom in order for the dynamic response characteristics of preliminary missile designs to be studied. It is anticipated that the missile motion in roll about its longitudinal axis will be sufficiently controlled so that the roll degree of freedom need not be simulated at this point in the development. It is assumed that the missile will have cruciform symmetry.

Since the detailed seeker requirements have not yet been established, the simulation will not be used to investigate missile performance against countermeasures; therefore, a simple seeker model will suffice for the early objectives of the simulation. For example, representing the seeker and signal processing by a simple low-pass digital filter with appropriate time constant and limits will provide the necessary guidance signal and permit investigation of the effects of tracking rate and gimbal angle limits on the engagement boundary. As more definitive seeker data become available, more sophisticated seeker models can be included in the simulation.

Items and their resulting impacts on the design of the simulation that will not be addressed are the following:

1. Control system detailed design. The control system can be simulated by a transfer function.
2. Autopilot detailed design. The autopilot can be simulated by a transfer function.

3. Aerodynamic flow-field interactions. These will be considered later in the missile development phase when wind-tunnel test data become available. Simple linear approximations of aerodynamic characteristics are adequate for the initial simulation. This means that the validity of the model is limited to relatively small angles of attack because of the nonlinear nature of aerodynamic parameters at large angles of attack.

4. Seeker detailed design. The seeker specifications for performance in countermeasure environments are being

developed by a separate effort; therefore, the simulated seeker model need only provide a tracking signal and an indication when seeker limits are exceeded.

12-2.3 PROGRAM STRUCTURE

The structure of the example computer program for simulating missile flight is illustrated in Fig. 12-1. The detailed equations and procedures to implement the blocks in the diagram are given in the paragraphs that follow.

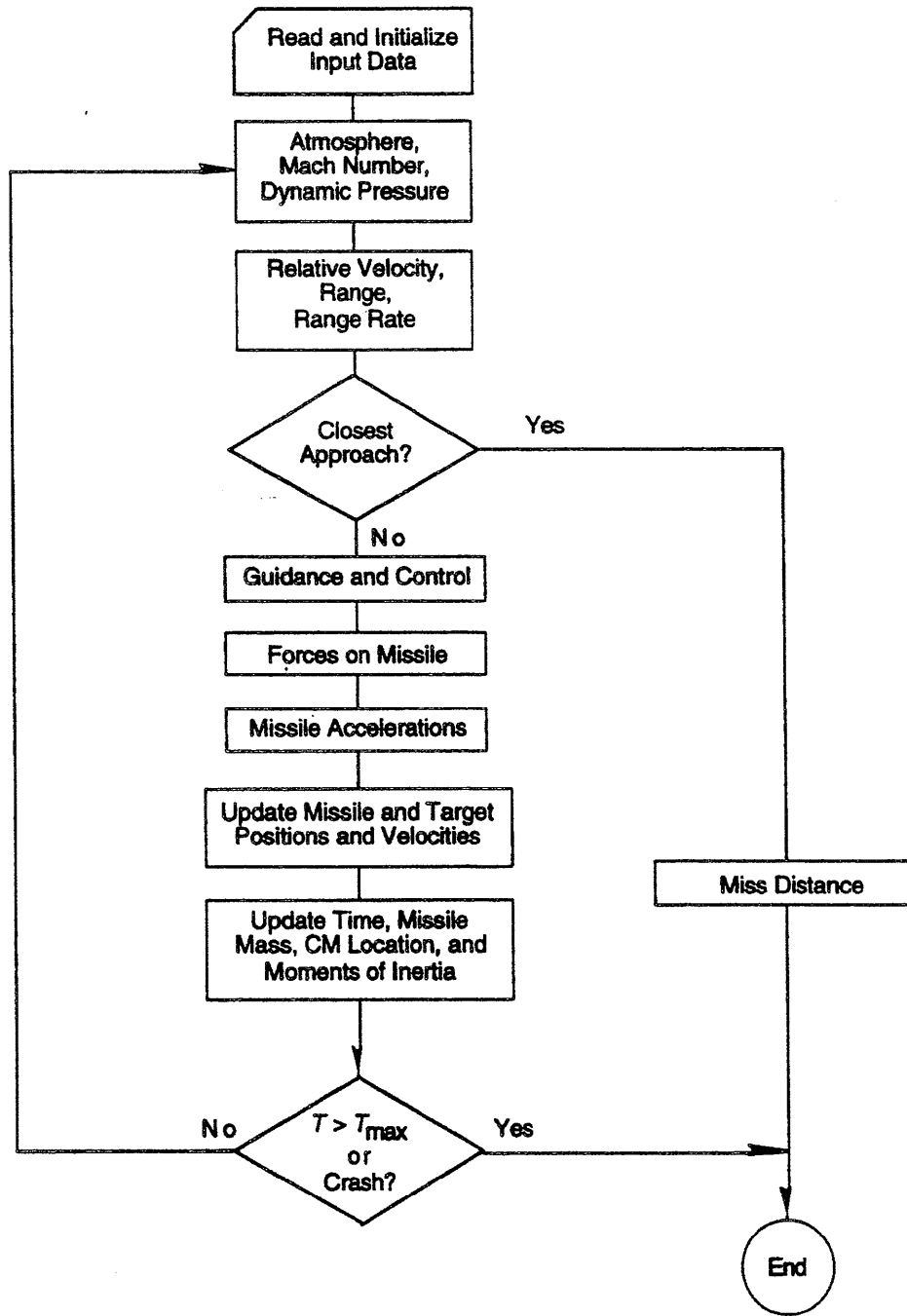


Figure 12-1. Typical Top-Level Flow Diagram for a Flight Simulation

12-2.4.2 Propulsion

For purposes of illustration it is assumed that a particular missile configuration is to be investigated. The missile configuration to be studied is controlled by torque-balanced canard control surfaces, and the canards and stabilizing tail fins are arranged in a cruciform configuration. The description of the missile required for the simulation model is given by the inputs to the simulation in the paragraphs that follow.

12-2.4.1 Mass

$m_0 = 85.0$	missile mass at launch, kg
$m_{bo} = 57.0$	missile mass at burnout, kg
$I_0 = 61.0$	moment of inertia about y- and z-axes at launch, $\text{kg}\cdot\text{m}^2$
$I_{bo} = 47.0$	moment of inertia about y- and z-axes at burnout, $\text{kg}\cdot\text{m}^2$
$x_{cm0} = 1.55$	distance from nose to center of mass at launch, m
$x_{cmbo} = 1.35$	distance from nose to center of mass at burnout, m.

TIME	REFERENCE THRUST $F_{p_{ref}}, \text{N}$
0.0	0
0.01	450
0.04	17,800
0.05	23,100
0.08	21,300
0.10	20,000
0.20	18,200
0.30	17,000
0.60	15,000
1.00	13,800
1.50	13,300
2.50	13,800
3.50	14,700
3.80	14,300
4.0	12,900
4.1	11,000
4.3	7,000
4.5	4,500
4.7	2,900
4.9	1,500
5.2	650
5.6	0
100.00	0

$t_{bo} = 5.6$	time of burnout, s
$p_{ref} = 101,314$	reference ambient pressure, Pa
$A_e = 0.011$	exit area of rocket nozzle, m^2
$I_{sp} = 2224$	specific impulse, N-s/kg.

12-2.4.3 Aerodynamics

$S = 0.0127$	missile aerodynamic reference area, m^2
$d = 0.127$	aerodynamic reference length, m
$x_{ref} = 1.35$	distance from missile nose to reference moment station, m

COEFFICIENT	MACH NUMBER M_n , dimensionless					
	0.0	0.8	1.14	1.75	2.5	3.5
C_{D0}	0.8	0.8	1.2	1.15	1.05	0.94
$C_{L\alpha}$	38.0	39.0	56.0	55.0	40.0	33.0
$C_{m\alpha}$	-160.0	-170.0	-185.0	-235.0	-190.0	-150.0
$C_{m\delta}$	180.0	250.0	230.0	130.0	80.0	45.0
$C_{m_q} + C_{m\dot{\alpha}}$	-6,000	-13,000	-16,000	-13,500	-10,000	-6,000
k	0.0255	0.0305	0.0361	0.0441	0.0540	0.0665

where

C_{D0} = zero-lift drag coefficient, dimensionless
 $C_{L\alpha}$ = slope of curve formed by lift coefficient C_L versus angle of attack α , rad^{-1} (deg^{-1})
 C_{mq} = pitch damping derivative relative to pitch rate q , rad^{-1} (deg^{-1})
 $C_{m\alpha}$ = pitch moment derivative relative to angle of attack (slope of curve formed by C_m versus α , rad^{-1} (deg^{-1})
 $C_{m\dot{\alpha}}$ = pitch damping derivative relative to angle-of-attack rate $\dot{\alpha}$, rad^{-1} (deg^{-1})
 $C_{m\delta}$ = pitch moment derivative relative to control-surface deflection (slope of curve formed by pitch moment coefficient C_m versus control-surface deflection δ_p), rad^{-1} (deg^{-1})
 k = constant used to calculate induced drag coefficient, dimensionless.

12-2.4.4 Seeker

$\tau_1 = 0.01$ seeker tracking loop time constant, s
 $\tau_2 = 0.01$ seeker signal processing time constant, s
 $\omega_{smax} = 25.0$ maximum angular tracking rate of seeker boresight axis, deg/s
 $\lambda_{max} = 40.0$ maximum gimbal angle of seeker, deg.

12-2.4.5 Autopilot

$t_{gon} = 0.5$ time to initiate guidance, s
 $\tau_3 = 0.04$ combined autopilot and control servo time constant, s
 $\delta_{max} = 20$ maximum control-surface (fin) deflection angle relative to the missile, deg
 $NR = 4.0$ nominal navigation ratio, dimensionless
 $G_n = 250.0$ gain factor relating angle of attack of control surface to acceleration command per unit dynamic pressure parameter, $(\text{rad}\cdot\text{Pa})/(\text{m/s})^2$
 $t_{nr} = 1.0$ time for buildup of navigation ratio, s.

12-2.4.6 Program Control

Input data that describe the initial positions and speeds of the missile and target are likely to be changed for each simulated flight. This information is included in the program control data. The initial missile speed is assumed to apply the instant the missile leaves the launcher. The direction of missile velocity will be calculated in the fire-control routine. For the example simulation, the target flies a straight, constant-speed flight path; therefore, target control parameters are not needed.

$P_M(i) = 0$ missile initial position coordinates, m
 $P_M(j) = 0$
 $P_M(k) = 0$
 $V_M = 30$ magnitude of missile initial velocity, m/s
 $t_{max} = 60$ maximum time of flight, s
 $P_T(i) = 4000$ target initial position coordinates, m
 $P_T(j) = 1000$
 $P_T(k) = -3000$
 $V_T(i) = -250.0$ target initial velocity components, m/s
 $V_T(j) = 0.0$
 $V_T(k) = 0.0$
 $\Delta t = 0.005$ integration time step, s.

12-2.4.7 Constants

$g = 9.80665$ acceleration due to gravity, m/s^2
 $\pi = 3.141592654$ Pi, dimensionless
 $DTR = \pi/180$ factor for converting degrees to radians
 $RTD = 180/\pi$ factor for converting radians to degrees
 $H = \Delta t$ for use in Subroutine RK4
 $HH = H/2$ for use in Subroutine RK4
 $H6 = H/6$ for use in Subroutine RK4.

12-2.5 INITIALIZATION

Before entering the computation loop, time is set to zero, and flags and physical parameters are given their initial values.

$t = 0$ initial simulation time, s
 $LFLAG = \text{false}$ logical flag to indicate that gimbal angle has exceeded its limit, dimensionless
 $RFLAG = \text{false}$ logical flag to indicate that seeker angular rate has exceeded its limit, dimensionless
 $m = m_0$ missile mass at launch, kg
 $I = I_0$ moment of inertia about y- and z-axes at launch, $\text{kg}\cdot\text{m}^2$
 $x_{cm} = x_{cm0}$ distance from missile nose to center of mass at launch, m.

12-2.6 FIRE CONTROL

The initial missile pointing direction and angular rates are calculated in the fire-control block. For the example simulation, a simple algorithm is employed in which the missile is pointed directly at the target at the instant of launch, and missile angular rates at launch are assumed to be negligible.

The unit vector u_r in the direction from the missile to the target is calculated by normalizing the range vector R ,

which is calculated by using

$$\mathbf{R} = \mathbf{P}_T - \mathbf{P}_M, \text{ m} \quad (7-35)$$

where

\mathbf{P}_M = position vector of missile in earth coordinate system, m

\mathbf{P}_T = position vector of target in earth coordinate system, m

\mathbf{R} = range vector from missile to target in earth coordinate system, m.

The missile inertial velocity vector \mathbf{V}_M and the unit missile centerline vector \mathbf{u}_{ct} are aligned with the range vector \mathbf{R} by

$$\mathbf{V}_M = V_M \mathbf{u}_R, \text{ m/s} \quad (12-1)$$

$$\mathbf{u}_{ct} = \mathbf{u}_R, \text{ dimensionless} \quad (12-2)$$

where

\mathbf{u}_{ct} = unit missile centerline axis vector in earth coordinate system, dimensionless

\mathbf{u}_R = unit range vector from missile to target in earth coordinate system, dimensionless

\mathbf{V}_M = missile inertial velocity vector in earth coordinate system, m/s

V_M = magnitude of missile inertial velocity, m/s.

The initial Euler angles are based on the initial missile centerline vector

$$\psi = \text{Tan}^{-1} \left(\frac{u_{ct}(j)}{u_{ct}(i)} \right), \quad (12-3)$$

$$\theta = \text{Tan}^{-1} \left(-u_{ct}(k) / \sqrt{u_{ct}(i)^2 + u_{ct}(j)^2} \right), \quad (12-4)$$

rad (deg)

$$\phi = 0, \text{ rad (deg)} \quad (12-5)$$

where

$u_{ct}(i)$ = i -component of \mathbf{u}_{ct} in earth coordinate system, dimensionless

$u_{ct}(j)$ = j -component of \mathbf{u}_{ct} in earth coordinate system, dimensionless

$u_{ct}(k)$ = k -component of \mathbf{u}_{ct} in earth coordinate system, dimensionless

θ = Euler angle rotation in elevation (pitch), rad (deg)

ϕ = Euler angle rotation in roll, rad (deg)

ψ = Euler angle rotation in azimuth (heading), rad (deg).

The initial missile inertial velocity vector \mathbf{V}_M expressed in earth coordinates is transformed into body coordinates using the earth-to-body reference frame transformation

matrix given in subroutine TBE (subpar. 12-2.18.4)

$$\begin{bmatrix} u \\ v \\ w \end{bmatrix} = [T_{b/e}] \mathbf{V}_M, \text{ m/s} \quad (12-6)$$

where

$[T_{b/e}]$ = transformation matrix (earth to body coordinates), dimensionless

u, v, w = components of missile inertial velocity vector \mathbf{V}_M in body coordinate system, m/s

\mathbf{V}_M = missile inertial velocity vector in earth coordinate system, m/s.

Since the initial angular rates of the missile are assumed to be negligible, they and the angle-of-attack components are initialized to zero by

$$\begin{bmatrix} p \\ q \\ r \end{bmatrix} = 0, \text{ rad/s (deg/s)} \quad (12-7)$$

$$\alpha = 0, \text{ rad (deg)} \quad (12-8)$$

$$\beta = 0, \text{ rad (deg)} \quad (12-9)$$

$$\alpha_t = 0, \text{ rad (deg)} \quad (12-10)$$

where

p, q, r = components of missile inertial angular rate vector in body coordinate system, rad/s (deg/s)

α = angle of attack, rad (deg)

α_t = total angle of attack, rad (deg)

β = angle of sideslip, rad (deg).

The computer program routines for reading the input data, initializing variables, and calculating fire-control parameters are entered by the program only once for a given simulated flight. The routines described in the paragraphs that follow, however, are entered repeatedly as required to calculate the parameters needed at each iterative time step.

12-2.7 ATMOSPHERE

The label "START" is placed in the simulation at this point to mark the beginning of each time step.

For the example simulation, it is assumed that the missile altitude at the launch position is at sea level; therefore, missile altitude above sea level, for use in the atmosphere tables, is given by

$$h = -P_M(k), \text{ m} \quad (12-11)$$

where

h = altitude of missile above sea level, m
 $P_M(k)$ = k -component of missile position vector
 P_M in earth coordinate system, m.

A table lookup procedure is used to find the atmospheric density ρ , atmospheric pressure p , and the speed of sound V_s . Since the missile being simulated is relatively small and will not reach altitudes at which Reynolds number effects must be included, the atmospheric viscosity is not required.

Missile Mach number M_N is calculated by using

$$M_N = \frac{V_M}{V_s}, \text{ dimensionless} \quad (12-12)$$

where

M_N = Mach number, dimensionless
 V_M = magnitude of missile inertial velocity, m/s
 V_s = speed of sound, m/s.

The dynamic pressure parameter Q is calculated using

$$Q = 0.5\rho V_M^2, \text{ Pa} \quad (3-6)$$

where

Q = dynamic pressure parameter, Pa
 V_M = magnitude of missile inertial velocity, m/s
 ρ = atmospheric density, kg/m³.

12-2.8 RELATIVE POSITION AND VELOCITY

The velocity vector $V_{T/M}$ of the target relative to the missile is calculated by using

$$V_{T/M} = V_T - V_M, \text{ m/s} \quad (7-38)$$

where

V_M = missile inertial velocity vector in earth coordinate system, m/s
 V_T = target inertial velocity vector in earth coordinate system, m/s
 $V_{T/M}$ = velocity vector of target relative to missile in earth coordinate system, m/s.

The unit vector $u_{T/M}$ is calculated by normalizing the vector $V_{T/M}$.

Although the range vector was originally calculated in subpar. 12-2.6, the equation must occur again at this point for subsequent loops of the simulation,

$$R = P_T - P_M, \text{ m} \quad (7-35)$$

where

P_M = position vector of missile in earth coordinate system, m
 P_T = position vector of target in earth coordinate system, m

R = range vector from missile to target in earth coordinate system, m.

The unit range vector u_R is obtained by normalizing R , and the range magnitude R is determined by calculating the magnitude of the vector R .

The closing speed V_c -negative of range rate-is calculated by using

$$V_c = -u_R \cdot V_{T/M}, \text{ m/s} \quad (12-13)$$

where

u_R = unit range vector from missile to target in earth coordinate system, dimensionless
 V_c = missile-to-target closing speed
 $V_{T/M}$ = velocity vector of target relative to missile in earth coordinate system, m/s.

12-2.9 TEST CLOSING SPEED

If the missile overtakes the target, the closing speed goes to zero at the instant of closest approach and changes signs as the missile continues past the target. The closing speed also switches signs in a tail-chase engagement if the missile slows to a speed less than that of the target so that the range begins to increase as the target pulls away. This switch in signs is used as an indicator to terminate the simulated flight.

Thus, if the algebraic sign of V_c becomes negative, the program branches to Subroutine MISDIS (subpar. 12-2.18.3), in which the closest approach distance is calculated and the simulated flight is terminated.

12-2.10 SEEKER

The seeker tracking point is assumed to be the center of mass of the target and although a first-order lag in the tracking rate is introduced later, the small angular deviation of the seeker boresight-axis vector from the line of sight to the tracking point is not calculated. Also the displacement of the physical position of the seeker from the missile center of mass is considered negligible for this application. Therefore, the seeker line-of-sight vector σ is assumed to be identical with the range vector R ,

$$\sigma = R, \text{ m} \quad (12-14)$$

where

R = range vector from missile to target in earth coordinate system, m
 σ = line-of-sight vector from seeker to track point on target, m.

The seeker boresight-axis vector u_{sa} has the direction of the line-of-sight vector σ , i.e.,

$$u_{sa} = \frac{\sigma}{\sigma}, \text{ dimensionless} \quad (12-15)$$

where

\mathbf{u}_{sa} = unit vector along seeker boresight axis, dimensionless
 σ = magnitude of line-of-sight vector σ , m.

The seeker gimbal angle is calculated using

$$\lambda = \text{Cos}^{-1}(\mathbf{u}_{sa} \cdot \mathbf{u}_{ct}), \text{ rad} \quad (8-3)$$

where

\mathbf{u}_{ct} = unit missile centerline axis vector in earth coordinate system, dimensionless
 \mathbf{u}_{sa} = unit vector along seeker boresight axis, dimensionless
 λ = seeker gimbal angle (angle between missile centerline axis and seeker boresight axis), rad.

If the absolute value of λ is greater than λ_{max} LFLAG is set. LFLAG is used to terminate guidance if the seeker gimbals strike their limits.

The angular rate of the line-of-sight vector ω_{σ} is calculated by using

$$\omega_{\sigma} = \frac{(\sigma \times \mathbf{V}_{T/M})}{\sigma^2}, \text{ rad/s} \quad (8-2)$$

where

$\mathbf{V}_{T/M}$ = velocity vector of target relative to missile in earth coordinate system, m/s
 σ = magnitude of line-of-sight vector σ , m
 σ = line-of-sight vector from seeker to track point on target, m
 ω_{σ} = angular rate vector of the line-of-sight vector, rad/s.

The angular rate of the seeker head lags the angular rate of the line-of-sight vector. This lag is taken into account in calculating the guidance commands; however, for this application it is not considered important that the boresight-axis vector (Eq. 12-15) incorporates this lag. This lag is assumed to be represented by a first-order transfer function, as discussed in subpars. 8-2.1.2 and 10-4.2.2, and the seeker-head rate is calculated by using

$$\omega_{ach}(t) = \omega_{ach}(t - \Delta t) \exp(-\Delta t/\tau_1) + \omega_{\sigma} [1 - \exp(-\Delta t/\tau_1)], \text{ rad/s} \quad (8-4)$$

where

(t) = indicates value at beginning of current time step, s
 $(t - \Delta t)$ = indicates value at beginning of first preceding time step, s
 Δt = integration time step, s

τ_1 = seeker tracking loop time constant, s
 ω_{ach} = achieved seeker-head angular rate vector, rad/s.

If the magnitude of $w_{ach}(t)$ exceeds the maximum angular rate ω_{max} of the seeker boresight axis, RFLAG is set.

There are assumed to be delays involved in processing the seeker-head angular rate signal. The filtered seeker-head angular rate signal is given by

$$\omega_f(t) = \omega_f(t - \Delta t) \exp(-\Delta t/\tau_2) + \omega_{ach} [1 - \exp(-\Delta t/\tau_2)], \text{ rad/s} \quad (8-4)$$

where

τ_2 = seeker signal processing time constant, s
 ω_f = final processed tracking-rate-signal vector, rad/s.

12-2.11 GUIDANCE AND CONTROL

Guidance is not initiated until a short time t_{gn} after launch in order to permit the missile to gain enough speed so that it can be controlled. After time t_{gn} , the autopilot bases the missile maneuver commands on the achieved seeker-head angular rate vector w_{ach} , and the control system responds to autopilot commands by deflecting the control surfaces. If the seeker gimbals should strike their limits, the guidance is turned off, or if the seeker tracking rate exceeds the capability of the seeker ω_{max} , target tracking is assumed to be lost and the simulated flight is terminated.

12-2.11.1 Test for Active Guidance

If t is less than t_{gn} the commanded-lateral-acceleration vector A_x , pitch control fin deflection angle δ_p , and yaw control fin deflection angle δ_y , are set to zero.

If LFLAG is set indicating the gimbal angle has reached its limit, then the fin deflections δ_p and δ_y are assumed to retain the values reached at the time the gimbal angle limit is reached. This assumption may be modified as better data become available on the behavior of the seeker, autopilot, and control system when the seeker gimbal strikes the stops.

If RFLAG is set indicating that the required tracking rate exceeds the limit of the seeker, the run is terminated. Even in cases when the tracking rate does not reach its limit during the main portion of the flight it probably becomes rate limited during the last few integration time steps when the missile passes close to the target. Therefore, to prevent termination of the simulated flight before the closest approach distance is attained, the flight is allowed to continue for an additional fraction of a second after reaching the rate limit.

12-2.11.2 Autopilot

If guidance has been initiated and no seeker limits have been encountered, the maneuver acceleration command is calculated based on the proportional navigation guidance

law. It is assumed for simplicity and minimal cost that the missile will be designed to approximate proportional navigation by making the control-surface actuator pressures proportional to the maneuver acceleration commands, which in turn are proportional to the seeker angular rate signal ω_f . The control fins achieve the angles of attack that cause the aerodynamic hinge moments on the control surfaces to balance the hinge moments generated by actuator pressures, as discussed in subpar. 2-2.3.5.

In the actual missile the distribution of the pressure between the pitch and yaw channels is determined directly by circuitry between the seeker head torquing coils and the control servos without ever determining an actual maneuver-acceleration command. In the simulation, however, a convenient method for calculating this pressure distribution to the actuators is by means of a theoretical commanded-lateral-acceleration vector A_c . Since the missile velocity vector and the direction of gravity are not known onboard the missile, Eq. 8-13 is approximated by

$$A_c = G_s(M,h)(\omega_f \times u_{ct}), \text{ m/s}^2 \quad (12-16)$$

where

- A_c = commanded-lateral-acceleration vector, m/s^2
- $G_s(M,h)$ = system gain as a function of Mach number and altitude, m/s
- u_{ct} = unit missile centerline axis vector in earth coordinate system, dimensionless
- ω_f = final processed tracking-rate-signal vector rad/s .

In Eq. 12-16 the filtered (processed) seeker-head rate signal of approximates the actual line-of-sight rate, and the missile centerline vector u_{ct} approximates the direction of V_n . It is assumed that the detailed relationships among the guidance processing circuits, control system, and aerodynamics—which work together to form the system gain $G_s(M,h)$ --have not yet been completely defined. To initiate the study of potential missile subsystem configurations, it is assumed that the subsystem relationships are perfect in the sense that the system gain $G_s(M,h)$ is always equal to the product of NR and the instantaneous velocity V_n . With this assumption the achieved navigation ratio is equal to the desired navigation ratio NR. This allows exploration in a controlled way of the effects of changes in the navigation ratio on the performance of the missile. As the subsystems become better defined, more accurate representations of the system gain will be employed in the simulation.

The vector representing the commanded-lateral-acceleration vector A_c is transformed to the body reference frame by

$$\begin{bmatrix} A_{c_{xb}} \\ A_{c_{yb}} \\ A_{c_{zb}} \end{bmatrix} = [T_{b/e}] A_c, \text{ m/s}^2 \quad (12-17)$$

where

- A_c = commanded-lateral-acceleration vector, m/s^2
- $A_{c_{xb}}$ = i -component of A_c expressed in body coordinate system, m/s^2
- $A_{c_{yb}}$ = j -component of A_c expressed in body coordinate system, m/s^2
- $A_{c_{zb}}$ = k -component of A_c expressed in body coordinate system, m/s^2
- $[T_{b/e}]$ = earth-to-body coordinate transformation matrix, dimensionless

by using the earth-to-body reference frame transformation matrix $[T_{b/e}]$ given in Subroutine TBE (subpar. 12-2. 18.4).

12-2.11.3 Control System

The actuator piston pressure for Control Surfaces 1 and 2 are given by

$$\left. \begin{aligned} p_{act_1} &= -G_p A_{c_{zb}}, \text{ Pa} \\ p_{act_2} &= G_p A_{c_{yb}}, \text{ Pa} \end{aligned} \right\} \quad (12-18)$$

where

- G_p = gain factor relating actuator piston pressure to acceleration command, $\text{Pa}/(\text{m/s}^2)$
- p_{act_1} = actuator pressure for the pitch channel, Pa
- p_{act_2} = actuator pressure for the yaw channel, Pa.

In true proportional navigation the component $A_{c_{zb}}$ of the acceleration command, which is directed along the missile centerline axis, has a value of zero. Because of the approximations in Eq. 12-17, however, the calculated value of $A_{c_{xb}}$ may have a small finite value, which should be ignored.

Since this missile employs a torque balance servo, the actuator piston pressure—commanded by the autopilot—determines a fin angle of attack the resulting fin deflection angle relative to the missile depends on the angle of attack of the missile at that time. For a given actuator pressure p_{act} , the actuator hinge moment M_H is

$$M_H = p_{act} A_p L_{arm}, \text{ N}\cdot\text{m} \quad (12-19)$$

where

- A_p = actuator piston area, m^2
- L_{arm} = bell crank lever arm, m
- M_H = hinge moment applied to control surface by actuator, $\text{N}\cdot\text{m}$

The hinge moment M_h is balanced by an aerodynamic moment M_f on the control surface about the hinge axis, given by

$$M_f = C_{H\alpha_f} \alpha_f Q S_f d_f, \text{ N}\cdot\text{m} \quad (12-20)$$

where

- $C_{H\alpha_f}$ = partial derivative of fin moment coefficient with respect to fin angle of attack, rad^{-1}
 d_f = aerodynamic reference length of control surface (fin), m
 M_f = aerodynamic moment on control surface (fin) about hinge line, N·m
 Q = dynamic pressure parameter, Pa
 S_f = aerodynamic reference area of control surface (fin), m^2
 α_f = angle of attack of control surface (fin), rad.

The fin angle of attack α_f that causes the two moments to be balanced is determined by equating the moments in Eqs. 12-19 and 12-20 and solving for α_f , i.e.,

$$\alpha_f = \frac{P_{act} A_p L_{arm}}{C_{H\alpha_f} Q S_f d_f}, \text{ rad.} \quad (12-21)$$

Since most of the details of the control fin shape and control servos of the missile design are still to be determined, it is convenient at this stage of the missile development to combine several of the parameters that may change from one alternative missile configuration to the next but do not vary during any given simulated flight. Therefore,

$$G_n = \frac{G_p A_p L_{arm}}{C_{H\alpha_f} S_f d_f}, (\text{rad}\cdot\text{Pa})/(\text{m/s}^2) \quad (12-22)$$

where

- G_n = gain factor relating angle of attack of control surface to acceleration command per unit dynamic pressure parameter, $(\text{rad}\cdot\text{Pa})/(\text{m/s}^2)$.

Combining Eqs. 12-18, 12-21, and 12-22, the control-surface angles of attack that result from the actuator pressures commanded by the autopilot are

$$\alpha_{fp} = \frac{-G_n A_{c_{y_b}}}{Q}, \text{ rad (deg)} \quad (12-23)$$

and

$$\alpha_{fy} = \frac{G_n A_{c_{y_b}}}{Q}, \text{ rad} \quad (12-24)$$

where

- α_{fp} = commanded angle of attack of pitch-channel control surface, rad
 α_{fy} = commanded angle of attack of yaw-channel control surface, rad.

12-2.11.4 Autopilot and Control System Lag

The dynamic response of the combination of the autopilot and the control system is assumed to be described by a first-order system with time constant t_3 . The achieved angles of attack of the fins will lag those given in Eqs. 12-23 and 12-24 as given by

$$\left. \begin{aligned} \alpha_{f_{pa}}(t) &= \alpha_{f_{pa}}(t - \Delta t) \exp(-\Delta t/\tau_3) \\ &\quad + \alpha_{fp} [1 - \exp(-\Delta t/\tau_3)], \text{ rad} \\ \alpha_{f_{ya}}(t) &= \alpha_{f_{ya}}(t - \Delta t) \exp(-\Delta t/\tau_3) \\ &\quad + \alpha_{fy} [1 - \exp(-\Delta t/\tau_3)], \text{ rad} \end{aligned} \right\}$$

(Derived from Eq. 10-39)

where

- $(t - \Delta t)$ = indicates value at beginning of preceding time step, s
 Δt = integration time step, s
 α_{fp} = commanded angle of attack of pitch-channel control surface (fin), rad
 α_{fy} = commanded angle of attack of yaw-channel control surface (fin), rad
 $\alpha_{f_{pa}}$ = achieved angle of attack of pitch-channel control surface, rad
 $\alpha_{f_{ya}}$ = achieved angle of attack of yaw-channel control surface, rad
 τ_3 = combined autopilot and control servo time constant, s.

12-2.11.5 Fin Angle of Incidence

The angles of incidence of the control fins, i.e., the fin deflection angles relative to the missile body, depend on the fin angles of attack and on the missile body angles of attack and sideslip. The fin angles of incidence are calculated by using

$$\delta_p = \alpha_{f_{pa}} - \alpha, \text{ rad} \quad (12-25)$$

$$\delta_y = \alpha_{f_{ya}} - \beta, \text{ rad} \quad (12-26)$$

where

- α = angle of attack of missile, rad
- β = angle of sideslip of missile, rad
- δ_p = pitch-channel control-surface deflection relative to missile, rad
- δ_y = yaw-channel control-surface deflection relative to missile, rad.

The absolute values of δ_p and δ_y are tested against the maximum fin deflection angle δ_{max} ; if the absolute value of a fin angle of incidence exceeds δ_{max} , it is reset to δ_{max} and retains its original sign.

12-2.12 AERODYNAMICS

It is assumed that aerodynamic force coefficient data are supplied in terms of lift and drag. The calculated lift and drag forces are therefore transformed to axial force and normal force in order to be applicable to the body reference frame used for solving the equations of motion.

12-2.12.1 Lift and Drag

C_{D0} as a function of Mach number M_0 is obtained by table lookup. If the total angle of attack is used, the aerodynamic lift coefficient C_L is then calculated by

$$C_L = C_{L\alpha} \alpha_t, \text{ dimensionless} \quad (5-11)$$

where

- C_L = aerodynamic lift coefficient, dimensionless
- $C_{L\alpha}$ = slope of curve of lift coefficient C_L versus angle of attack α , rad^{-1}
- α_t = angle between missile velocity vector and missile centerline axis, rad.

The total drag coefficient is calculated by using

$$C_D = C_{D0} + kC_L^2, \text{ dimensionless} \quad (5-10 \text{ with } x = 2)$$

where

- C_D = aerodynamic drag coefficient, dimensionless
- C_{D0} = zero-lift drag coefficient, dimensionless
- C_L = aerodynamic lift coefficient, dimensionless
- k = constant used to calculate induced drag coefficient, dimensionless.

The aerodynamic drag D and lift L forces are calculated by using

$$\left. \begin{aligned} D &= Q C_D S, \text{ N} \\ L &= Q C_L S, \text{ N} \end{aligned} \right\} \text{ (Derived from 5-4 and 5-5)}$$

where

- C_D = aerodynamic drag coefficient, dimensionless
- C_L = aerodynamic lift coefficient, dimensionless
- D = aerodynamic drag force, N
- L = aerodynamic lift force, N
- Q = dynamic pressure parameter, Pa
- S = missile dynamic reference area, m^2 .

12-2.12.2 Axial Force and Normal Force

Drag and lift are transformed to axial force A and normal force N by using

$$\left. \begin{aligned} A &= D \cos \alpha_t - L \sin \alpha_t, \text{ N} \\ N &= D \sin \alpha_t + L \cos \alpha_t, \text{ N} \end{aligned} \right\} \text{ (4-13 and 4-14)}$$

where

- A = aerodynamic axial force, N
- N = aerodynamic normal force, N
- α_t = total angle of attack (angle between missile velocity vector and missile centerline axis), rad.

Axial force A is, by definition, directly opposite the x_b -axis. Substituting A for $0.5\rho V_M^2 C_A S$ in Eq. 7-1 gives

$$F_{Ax_b} = -A, \text{ N} \text{ (Derived from 7-1)}$$

where

- F_{Ax_b} = x_b -component of aerodynamic force in body coordinate system, N.

The normal force vector can be defined in body frame coordinates by using

$$\left. \begin{aligned} F_{Ay_b} &= N \left(-v / \sqrt{v^2 + w^2} \right), \text{ N} \\ F_{Az_b} &= N \left(-w / \sqrt{v^2 + w^2} \right), \text{ N} \end{aligned} \right\} \text{ (12-27)}$$

where

- F_{Ay_b} = y_b -component of aerodynamic force in body coordinate system, N
- F_{Az_b} = z_b -component of aerodynamic force in body coordinate system, N
- N = aerodynamic normal force, N
- v = y_b -component of missile velocity in body coordinate system, m/s

w = z_b -component of missile velocity in body coordinate system, m/s.

Coefficients corresponding to the components of the normal force in the y_b - and z_b -axes are calculated by

$$\left. \begin{aligned} C_{N_y} &= \frac{F_{A_{y_b}}}{QS}, \text{ dimensionless} \\ C_{N_z} &= \frac{F_{A_{z_b}}}{QS}, \text{ dimensionless} \end{aligned} \right\} \text{ (Derived from 7-6)}$$

where

C_{N_y} = aerodynamic coefficient corresponding to the component of normal force on the y_b -axis, dimensionless

C_{N_z} = aerodynamic coefficient corresponding to the component of normal force on the z_b -axis, dimensionless

Q = dynamic pressure parameter, Pa

S = missile aerodynamic reference area, m^2 .

12-2.12.3 Aerodynamic Moments

Since the missile is assumed to have cruciform symmetry, let

$$\left. \begin{aligned} C_{n_\beta} &= C_{m_\alpha}, \text{ rad}^{-1} (\text{deg}^{-1}) \\ C_{n_\delta} &= C_{m_\delta}, \text{ rad}^{-1} (\text{deg}^{-1}) \\ C_{n_r} &= C_{m_q}, \text{ rad}^{-1} (\text{deg}^{-1}) \\ C_{n_{\dot{\beta}}} &= C_{m_{\dot{\alpha}}}, \text{ rad}^{-1} (\text{deg}^{-1}) \end{aligned} \right\} \text{ (5-19)}$$

where

C_{m_q} = pitch damping coefficient relative to pitch rate q , $\text{rad}^{-1} (\text{deg}^{-1})$

C_{m_α} = pitch moment derivative relative to angle of attack (slope of curve formed by C_m versus α curve), $\text{rad}^{-1} (\text{deg}^{-1})$

$C_{m_{\dot{\alpha}}}$ = pitch damping derivative relative to angle-of-attack rate $\dot{\alpha}$, $\text{rad}^{-1} (\text{deg}^{-1})$

C_{m_δ} = pitch moment derivative relative to control-surface deflection (slope of C_m versus δ_p curve), $\text{rad}^{-1} (\text{deg}^{-1})$

C_{n_r} = yaw damping coefficient relative to yaw rate r , $\text{rad}^{-1} (\text{deg}^{-1})$

C_{n_β} = yaw moment derivative relative to angle of sideslip (slope of C_n versus β curve) $\text{rad}^{-1} (\text{deg}^{-1})$

$C_{n_{\dot{\beta}}}$ = yaw damping derivative relative to angle-of-sideslip rate $\dot{\beta}$, $\text{rad}^{-1} (\text{deg}^{-1})$

C_{n_δ} = yaw moment derivative relative to control-surface deflection angle (slope of C_n versus δ_y curve), $\text{rad}^{-1} (\text{deg}^{-1})$.

It is assumed that C_m was measured in a wind tunnel or estimated with the control surfaces set at zero angles of incidence and that C_m represents the additional component of aerodynamic moment on the missile contributed by deflection of a control surface away from zero angle of incidence. Then the pitch and yaw components of the aerodynamic moment about the moment reference station are calculated by using

$$C_{m_{ref}} = C_{m_\alpha} \alpha + C_{m_\delta} \delta_p, \text{ dimensionless} \quad (5-13)$$

$$C_{n_{ref}} = C_{n_\beta} \beta + C_{n_\delta} \delta_y, \text{ dimensionless} \quad (5-14)$$

where

$C_{m_{ref}}$ = aerodynamic pitch moment coefficient with respect to reference moment station, dimensionless

C_{m_α} = pitch moment derivative relative to angle of attack (slope of curve formed by C_m versus α), $\text{rad}^{-1} (\text{deg}^{-1})$

C_{m_δ} = pitch moment derivative relative to control-surface deflection (slope of C_m versus δ_p curve), $\text{rad}^{-1} (\text{deg}^{-1})$

C_n = yawing moment coefficient about center of mass, dimensionless

$C_{n_{ref}}$ = aerodynamic yaw moment coefficient with respect to reference moment station, dimensionless

C_{n_β} = yaw moment derivative relative to angle of sideslip (slope of C_n versus β curve), $\text{rad}^{-1} (\text{deg}^{-1})$

C_{n_δ} = yaw moment derivative relative to control-surface deflection angle (slope of C_n versus δ_y curve), $\text{rad}^{-1} (\text{deg}^{-1})$

α = angle of attack of missile, rad (deg)

β = angle of sideslip of missile, rad (deg)

δ_p = pitch-channel control-surface deflection relative to missile, rad (deg)

δ_y = yaw-channel control-surface deflection relative to missile, rad (deg).

The reference moment coefficients are corrected to relate to the current center of mass, and the damping terms are included by using

$$\left. \begin{aligned}
 C_m &= C_{m_{ref}} - C_{N_z} \left(\frac{x_{cm} - x_{ref}}{d} \right) \\
 &\quad + \frac{d}{2V} (C_{m_q} + C_{m_{\dot{\alpha}}}) q, \\
 &\text{dimensionless} \\
 C_n &= C_{n_{ref}} + C_{N_y} \left(\frac{x_{cm} - x_{ref}}{d} \right) \\
 &\quad + \frac{d}{2V} (C_{n_r} + C_{n_{\dot{\beta}}}) r, \\
 &\text{dimensionless}
 \end{aligned} \right\} (5-12)$$

where

- C_m = pitching moment coefficient about center of mass, dimensionless
- $C_{m_{ref}}$ = aerodynamic pitch moment coefficient with respect to reference moment station, dimensionless
- C_{m_q} = pitch damping derivative relative to pitch rate q , $\text{rad}^{-1} (\text{deg}^{-1})$
- $C_{m_{\dot{\alpha}}}$ = pitch damping derivative relative to angle-of-attack rate $\dot{\alpha}$, $\text{rad}^{-1} (\text{deg}^{-1})$
- C_{N_y} = aerodynamic coefficient corresponding to the component of normal force on the y_b -axis, dimensionless
- C_{N_z} = aerodynamic coefficient corresponding to the component of normal force on the z_b -axis, dimensionless
- C_n = yawing moment coefficient about center of mass, dimensionless
- C_{n_r} = yaw damping coefficient relative to yaw rate r , $\text{rad}^{-1} (\text{deg}^{-1})$
- $C_{n_{ref}}$ = aerodynamic yaw moment coefficient with respect to reference moment station, dimensionless
- $C_{n_{\dot{\beta}}}$ = yaw damping derivative relative to angle-of-sideslip rate $\dot{\beta}$, $\text{rad}^{-1} (\text{deg}^{-1})$
- d = aerodynamic reference length, m
- q = pitch component of angular rate vector ω expressed in body coordinate system, $\text{rad/s} (\text{deg/s})$
- r = yaw component of angular rate vector ω expressed in body coordinate system, $\text{rad/s} (\text{deg/s})$
- V = magnitude of missile inertial velocity vector V_M in earth coordinate system, m/s
- x_{cm} = instantaneous distance from missile nose to center of mass, m
- x_{ref} = distance from missile nose to reference moment station, m.

The aerodynamic moments in the pitch and yaw planes are

calculated using

$$M_A = Q C_m S d, \text{ N}\cdot\text{m} \quad (\text{Derived from 5-7})$$

$$N_A = Q C_n S d, \text{ N}\cdot\text{m} \quad (\text{Derived from 5-8})$$

where

M_A = aerodynamic moment in pitch plane, N·m

N_A = aerodynamic moment in yaw plane, N·m

Q = dynamic pressure parameter, Pa

S = missile aerodynamic reference area, m^2 .

12-2.13 PROPULSION

The input thrust table is used to look up the thrust $F_{p_{ref}}$ corresponding to the reference atmospheric pressure as a function of time. The thrust is corrected for the ambient atmospheric pressure p_a by

$$F_p = F_{p_{ref}} + (p_{ref} - p_a) A_e, \text{ N} \quad (6-1)$$

where

A_e = exit area of rocket nozzle, m^2

F_p = magnitude of thrust force, N

$F_{p_{ref}}$ = magnitude of reference thrust force, N

p_a = ambient pressure at altitude h , Pa

p_{ref} = reference ambient pressure, Pa.

The thrust is assumed to be aligned with the missile longitudinal axis; therefore,

$$\left. \begin{aligned}
 F_{p_{x_b}} &= F_p, \text{ N} \\
 F_{p_{y_b}} &= 0, \text{ N} \\
 F_{p_{z_b}} &= 0, \text{ N}
 \end{aligned} \right\} (6-3)$$

where

$F_{p_{x_b}}$ = i -component of thrust force vector in body coordinate system, N

$F_{p_{y_b}}$ = j -component of thrust force vector in body coordinate system, N

$F_{p_{z_b}}$ = k -component of thrust force vector in body coordinate system, N.

The line of action of the thrust is assumed to pass through the missile center of mass; therefore, the propulsion system contributes no moments on the missile body.

12-2.14 GRAVITY

The standard value of the acceleration due to gravity is used, and since the missile configurations being simulated will operate at relatively low altitude, no correction for the radial distance from the center of the earth is made. Thus the gravitational force in earth coordinates is

$$\left. \begin{aligned} F_{g_{x_e}} &= 0, \text{ N} \\ F_{g_{y_e}} &= 0, \text{ N} \\ F_{g_{z_e}} &= mg, \text{ N} \end{aligned} \right\} \quad (7-4)$$

where

$$\begin{aligned} F_{g_{x_e}} &= i\text{-component of gravitational force on the missile in earth coordinate system, N} \\ F_{g_{y_e}} &= j\text{-component of gravitational force on the missile in earth coordinate system, N} \\ F_{g_{z_e}} &= k\text{-component of gravitational force on the missile in earth coordinate system, N} \\ g &= \text{acceleration due to gravity, m/s}^2 \\ m &= \text{instantaneous missile mass, kg.} \end{aligned}$$

The gravitational force is transformed to the body reference frame by using

$$\begin{bmatrix} F_{g_{x_b}} \\ F_{g_{y_b}} \\ F_{g_{z_b}} \end{bmatrix} = [T_{b/e}] \begin{bmatrix} F_{g_{x_e}} \\ F_{g_{y_e}} \\ F_{g_{z_e}} \end{bmatrix}, \text{ N} \quad (7-5)$$

where

$$\begin{aligned} F_{g_{x_b}} &= i\text{-component of gravitational force on the missile in body coordinate system, N} \\ F_{g_{y_b}} &= j\text{-component of gravitational force on the missile in body coordinate system, N} \\ F_{g_{z_b}} &= k\text{-component of gravitational force on the missile in body coordinate system, N} \\ [T_{b/e}] &= \text{earth-to-body coordinate system transformation matrix, dimensionless.} \end{aligned}$$

12-2.15 EQUATIONS OF MOTION

The equations of motion that yield the missile rotational rate and the missile translational velocity are integrated numerically in the body reference frame. These equations of motion are integrated simultaneously along with the Euler angle-rate equations. The resulting missile velocity vector is transformed to the earth reference frame to form the positional differential equations of motion, which are integrated numerically to yield missile position.

12-2.15.1 Rotation, Translation, and Euler Angles

The equations of motion, which are to be integrated simultaneously, are the rotational equations (Eqs. 4-46), the translational equations (Eqs. 4-37), and the Euler equations (Eqs. 4-51). The assumptions for the example simulation permit Eqs. 4-46 to be simplified by setting p , p , M_p , and N_p to zero and I_x to I ; thus

$$\left. \begin{aligned} \dot{q} &= M_A/I, \text{ rad/s}^2 \\ \dot{r} &= N_A/I, \text{ rad/s}^2 \end{aligned} \right\} \quad (12-28)$$

where

$$\begin{aligned} I &= \text{moment of inertia about pitch and yaw axes, kg}\cdot\text{m}^2 \\ M_A &= \text{aerodynamic moment in the pitch plane, N}\cdot\text{m} \\ N_A &= \text{aerodynamic moment in the yaw plane, N}\cdot\text{m} \\ \dot{q} &= \text{pitch component of angular acceleration } \dot{\omega} \text{ expressed in body coordinate system, rad/s}^2 \\ \dot{r} &= \text{yaw component of angular acceleration } \dot{\omega} \text{ expressed in body coordinate system, rad/s}^2. \end{aligned}$$

The translational equations (Eqs. 4-37) are simplified by setting p , $F_{p_{y_b}}$, and $F_{p_{z_b}}$ to zero, giving

$$\left. \begin{aligned} \dot{u} &= \frac{F_{A_{x_b}} + F_{p_{x_b}} + F_{g_{x_b}}}{m} - (qw - rv), \text{ m/s}^2 \\ \dot{v} &= \frac{F_{A_{y_b}} + F_{g_{y_b}}}{m} - ru, \text{ m/s}^2 \\ \dot{w} &= \frac{F_{A_{z_b}} + F_{g_{z_b}}}{m} + qu, \text{ m/s}^2 \end{aligned} \right\} \quad (12-29)$$

where

$$\begin{aligned} F_{A_{x_b}} &= x_b\text{-component of aerodynamic force in body coordinate system, N} \\ F_{A_{y_b}} &= y_b\text{-component of aerodynamic force in body coordinate system, N} \\ F_{A_{z_b}} &= z_b\text{-component of aerodynamic force in body coordinate system, N} \\ F_{g_{x_b}} &= i\text{-component of gravitational force on the missile in body coordinate system, N} \\ F_{g_{y_b}} &= j\text{-component of gravitational force on the missile in body coordinate system, N} \\ F_{g_{z_b}} &= k\text{-component of gravitational force on the missile in body coordinate system, N} \\ F_{p_{x_b}} &= i\text{-component of thrust force vector in body coordinate system, N} \\ q &= \text{pitch component of angular rate vector } \omega \text{ expressed in body coordinate system, rad/s} \\ r &= \text{yaw component of angular rate vector } \omega \text{ expressed in body coordinate system, rad/s} \end{aligned}$$

u, v, w = components of missile inertial velocity vector V_M in body coordinate system, m/s
 $\dot{u}, \dot{v}, \dot{w}$ = components of linear acceleration expressed in body coordinate system, m/s².

The Euler equations (Eqs. 4-51) are simplified by setting p to zero, giving

$$\left. \begin{aligned} \dot{\phi} &= (q \sin \phi + r \cos \phi) \tan \theta, \text{ rad/s} \\ \dot{\theta} &= q \cos \phi - r \sin \phi, \text{ rad/s} \\ \dot{\psi} &= (q \sin \phi + r \cos \phi) / \cos \theta, \text{ rad/s} \end{aligned} \right\} \quad (12-30)$$

where

q = pitch component of angular rate vector ω expressed in body coordinate system, rad/s (deg/s)
 r = yaw component of angular rate vector ω expressed in body coordinate system, rad/s (deg/s)
 θ = Euler angle rotation in elevation (pitch), rad (deg)
 $\dot{\theta}$ = angular rate of Euler angle rotation in elevation (pitch), rad/s (deg/s)
 ϕ = Euler angle rotation in roll, rad (deg)
 $\dot{\phi}$ = angular rate of Euler angle rotation in roll, rad/s (deg/s)
 $\dot{\psi}$ = angular rate of Euler angle rotation in yaw, rad/s (deg/s).

Eqs. 12-28, 12-29, and 12-30 are integrated simultaneously, using the fourth-order Runge-Kutta method. The Runge-Kutta procedure is contained in a subroutine named RK4 (subpar. 12-2.18.1). The values of the dependent variables of the differential equations at the beginning of an integration time step are input to RK4, and the values of these variables at the end of the time step are output. The inputs to Subroutine RK4 are in the form of an array designated the Y-array. The number of elements in the Y-array is equal to the number of differential equations being integrated, and the values of the array elements are equal respectively to the values of the dependent variables of the differential equations. Thus on entering RK4 the Y-array is filled by making the following variable substitutions:

$$\left. \begin{aligned} Y(1) &= q \\ Y(2) &= r \\ Y(3) &= u \\ Y(4) &= v \\ Y(5) &= w \\ Y(6) &= \psi \\ Y(7) &= \theta \\ Y(8) &= \phi \end{aligned} \right\} \quad (12-31)$$

In computer languages such as FORTRAN, these variable substitutions are conveniently made by employing the call-statement argument list.

Subroutine DERIVS (subpar. 12-2.18.2), called by Subroutine RK4, contains two sets of equations. The first set for solution of Eqs. 12-28, 12-29, and 12-30 is selected by setting the flag DSET equal to unity before calling RK4.

The Runge-Kutta procedure employs four steps for each integration time step. Each Runge-Kutta step in RK4 calls the Subroutine DERIVS, which calculates derivatives based on the equations being integrated. The Subroutine DERIVS uses an input array named V, and the values placed in V differ for each of the four Runge-Kutta steps. The output of Subroutine DERIVS is an array named DERIV, which contains the calculated values of the derivatives. The output array DERIV is renamed on each exit from DERIVS for use in the final summation in the fourth step of Subroutine RK4. The output of Subroutine RK4 is an array named YOUT. The array YOUT contains the values of the dependent variables of the differential equations at the end of the integration time step. Thus, at the end of the current time step, i.e., at the beginning of the next time step,

$$\left. \begin{aligned} q &= YOUT(1) \\ r &= YOUT(2) \\ u &= YOUT(3) \\ v &= YOUT(4) \\ w &= YOUT(5) \\ \psi &= YOUT(6) \\ \theta &= YOUT(7) \\ \phi &= YOUT(8) \end{aligned} \right\} \quad (12-32)$$

12-2.15.2 Missile Position

The components of missile velocity obtained by solving Eqs. 12-29 are expressed in the body reference frame, which, in general, is a rotating frame of reference. To use the velocity vector to calculate missile position, the velocity vector (components u , v , and w in body coordinate system)

is transformed to the inertial earth coordinate system by using

$$\mathbf{V}_M = [T_{e/b}] \begin{bmatrix} u \\ v \\ w \end{bmatrix}, \text{ m/s} \quad (12-33)$$

where

$[T_{e/b}]$ = transformation matrix (body-to-earth coordinates), dimensionless.

The unit velocity vector u_{V_M} is calculated by normalizing \mathbf{V}_M .

The differential equations yielding the components of the missile position vector in the earth coordinate system are

$$\left. \begin{aligned} \dot{P}_M(i) &= V_M(i), \text{ m/s} \\ \dot{P}_M(j) &= V_M(j), \text{ m/s} \\ \dot{P}_M(k) &= V_M(k), \text{ m/s} \end{aligned} \right\} \quad (12-34)$$

where

$\dot{P}_M(i)$ = i -component of rate of change vector of missile position \mathbf{P}_M , m/s
 $\dot{P}_M(j)$ = j -component of rate of change vector of missile position \mathbf{P}_M , m/s
 $\dot{P}_M(k)$ = k -component of rate of change vector of missile position \mathbf{P}_M , m/s
 $V_M(i)$ = i -component of missile velocity vector \mathbf{V}_M , m/s
 $V_M(j)$ = j -component of missile velocity vector \mathbf{V}_M , m/s
 $V_M(k)$ = k -component of missile velocity vector \mathbf{V}_M , m/s.

Eqs. 12-34 are integrated numerically by entering Subroutine RK4 with

$$\left. \begin{aligned} Y(1) &= P_M(i), \text{ m} \\ Y(2) &= P_M(j), \text{ m} \\ Y(3) &= P_M(k), \text{ m} \end{aligned} \right\} \quad (12-35)$$

where

$P_M(i)$ = i -component of missile position vector \mathbf{P}_M in earth coordinate system, m
 $P_M(j)$ = j -component of missile position vector \mathbf{P}_M in earth coordinate system, m
 $P_M(k)$ = k -component of missile position vector \mathbf{P}_M in earth coordinate system, m
 $Y(i)$ = input array of Runge-Kutta Subroutine RK4.

The flag DSET is set equal to two in order to select the second set of equations in the Subroutine DERIVS.

On exiting RK4 the missile position vector components are given in earth coordinates by

$$\left. \begin{aligned} P_M(i) &= YOUT(1), \text{ m} \\ P_M(j) &= YOUT(2), \text{ m} \\ P_M(k) &= YOUT(3), \text{ m} \end{aligned} \right\} \quad (12-36)$$

where

$YOUT(i)$ = output array of Runge-Kutta Subroutine RK4.

Assume that the ground level is at sea level. Calculate the altitude of the missile above the ground level by using

$$h = -P_M(k), \text{ m} \quad (12-37)$$

where

h = missile altitude above sea level, m.

12-2.15.3 Target Position

For a target with constant velocity, target position is updated from the position at the beginning of a time step to the position at the end of the time step, i.e., at the beginning of the following time step, by

$$\mathbf{P}_T(t + \Delta t) = \mathbf{P}_T(t) + \mathbf{V}_T(t)\Delta t, \text{ m} \quad (12-38)$$

where

\mathbf{P}_T = position vector of target in earth coordinate system, m

(t) = indicates value at beginning of current time step, s

$(t + \Delta t)$ = indicates value at beginning of first succeeding time step, s

\mathbf{V}_T = target inertial velocity vector in earth coordinate system, m/s

Δt = integration time step, s. ...

12-2.16 UPDATE

Simulated time is updated by using

$$t(t + \Delta t) = t(t) + \Delta t, \text{ s} \quad (12-39)$$

where

t = simulation time, s.

Missile mass is updated by using a difference equation to simulate Eq. 6-2, i.e.,

$$m(t + \Delta t) = m(t) - F_{p_{ref}} \Delta t / I_{sp}, \text{ kg} \quad (12-40)$$

where

$F_{p_{ref}}$ = magnitude of reference-thrust force, N

I_{sp} = specific impulse, N·s/kg
 m = instantaneous missile mass, kg
 (t) = indicates value at beginning of current time step, s
 $(t + \Delta t)$ = indicates value at beginning of first succeeding time step, s
 Δt = integration time step, s.

The inputs for this example simulation include missile mass at launch and at burnout, the thrust profile, and the specific impulse. This combination of variables is redundant, and the input value of specific impulse must be correctly matched to the combination of the thrust profile and the total mass change in order for the mass calculated by Eq. 12-40 at burnout to match the input value m_0 .

Assume that the location of the center of mass varies linearly with the mass. The location of the center of mass x_{cm} is updated by using

$$x_{cm} = x_{cm_0} - (x_{cm_0} - x_{cm_{bo}}) \left(\frac{m_0 - m}{m_0 - m_{bo}} \right), \text{ m} \quad (12-41)$$

where

m = instantaneous missile mass, kg
 m_{bo} = missile mass at burnout, kg
 m_0 = missile mass at launch, kg
 x_{cm} = instantaneous distance from missile nose to center of mass, m
 $x_{cm_{bo}}$ = distance from missile nose to center of mass at burnout, m
 x_{cm_0} = distance from missile nose to center of mass at launch, m.

Assuming that the moment of inertia varies linearly with the mass, the moment of inertia is updated using

$$I = I_0 - (I_0 - I_{bo}) \left(\frac{m_0 - m}{m_0 - m_{bo}} \right), \text{ kg} \cdot \text{m}^2 \quad (12-42)$$

where

I_{bo} = moment of inertia at burnout, $\text{kg} \cdot \text{m}^2$
 I_0 = moment of inertia at launch, $\text{kg} \cdot \text{m}^2$.

Since the unit missile centerline vector coincides with the unit x_c -axis vector, the missile centerline can be updated by using the Euler angles:

$$\mathbf{u}_{cl} = \begin{bmatrix} \cos \theta \cos \psi \\ \cos \theta \sin \psi \\ \sin \theta \end{bmatrix}, \text{ dimensionless} \quad (12-43)$$

where

\mathbf{u}_{cl} = unit missile centerline axis vector in earth coordinate system, dimensionless
 θ = Euler angle rotation in elevation (pitch), rad (deg)
 ψ = Euler angle rotation in azimuth (heading), rad (deg).

The missile angles of attack α and sideslip β are updated by using

$$\left. \begin{aligned} \alpha &= \text{Tan}^{-1} \left(\frac{w}{u} \right), \text{ rad} \\ \beta &= \text{Tan}^{-1} \left(\frac{-v}{u} \right), \text{ rad} \end{aligned} \right\} \quad (12-44)$$

where

u, v, w = components of missile inertial velocity vector \mathbf{V}_M in body coordinate system, m/s
 α = angle of attack of missile, rad (deg)
 β = angle of sideslip of missile, rad (deg).

The negative value of v is required for the calculation of β in order to produce the correct yawing moment. (See discussion in subpar. 7-3.2.1.1.1.)

The total angle of attack α_t is updated by using

$$\alpha_t = \text{Cos}^{-1}(\mathbf{u}_{V_M} \cdot \mathbf{u}_{cl}), \text{ rad} \quad (12-45)$$

where

\mathbf{u}_{cl} = unit missile centerline axis vector in earth coordinate system, dimensionless
 \mathbf{u}_{V_M} = unit vector of missile velocity, dimensionless
 α_t = total angle of attack, rad (deg).

12-2.17 TEST FOR MAXIMUM TIME OR CRASH

If t is greater than t_{max} or h is less than zero, an appropriate message is printed, and the simulation is terminated. Otherwise, the simulation program returns to label START (subpar. 12-2.7) to begin the cycle of calculations for the next time step.

12-2.18 SUBROUTINES

The subroutines that follow are called from the main program.

12-2.18.1 RK4

Subroutine RK4 implements the fourth-order Runge-Kutta method of numerical solution of differential equations by an algorithm patterned after one given in Ref. 1. In the equations that follow each element of the array on the left side of the equal sign is evaluated by employing the

respective elements of the arrays on the right side of the equal sign. The mathematical symbol "*" indicates multiplication.

First Step:

```
SET FLAG DSET
V = Y
CALL DERIVS
DYDX = DERIV
YT = Y + HH * DYDX
```

Second Step:

```
V = YT
CALL DERIVS
DYT = DERIV
YT = Y + HH * DYT
```

Third Step:

```
V = YT
CALL DERIVS
DYM = DERIV
YT = Y + H * DYM
DYM = DYT + DYM
```

Fourth Step:

```
V = YT
CALL DERIVS
DYT = DERIV
YOUT = Y + H6 * (DYDX
+ DYT + 2 * DYM).
```

(12-46)

12-2.18.2 DERIVS

Based on the equations of motion, the Subroutine DERIVS calculates the values of derivatives and assigns them to an array named DERIV. The inputs to Subroutine DERIVS are contained in the V-array, which is filled at each step in Subroutine RK4.

If Subroutine DERIVS is entered with the flag DSET equal to 1, then only Eqs. 12-47 need be evaluated.

$$DERIV(1) = M_A / I$$

$$DERIV(2) = N_A / I$$

$$DERIV(3) = \frac{F_{A_{x_b}} + F_{P_{x_b}} + F_{g_{x_b}}}{m} - [V(1)V(5) - V(2)V(4)]$$

$$DERIV(4) = \frac{F_{A_{y_b}} + F_{g_{y_b}}}{m} - V(2)V(3)$$

$$DERIV(5) = \frac{F_{A_{z_b}} + F_{g_{z_b}}}{m} - V(1)V(3)$$

$$DERIV(6) = \frac{\{V(1) \sin[V(8)]\}}{\cos[V(7)]} + \frac{\{V(2) \cos[V(8)]\}}{\cos[V(7)]}$$

$$DERIV(7) = V(1) \cos[V(8)] - V(2) \sin[V(8)]$$

$$DERIV(8) = \{V(1) \sin[V(8)]\} \tan[V(7)] + \{V(2) \cos[V(8)]\} \tan[V(7)].$$

(12-47)

If DSET = 2, then only Eqs. 12-48 need be evaluated.

$$\left. \begin{aligned} DERIV(1) &= V_M(i), \text{ m/s} \\ DERIV(2) &= V_M(j), \text{ m/s} \\ DERIV(3) &= V_M(k), \text{ m/s} \end{aligned} \right\} (12-48)$$

In simulations in which greater accuracy is required, differential equations describing functions, such as rate of change of missile mass and rate of change of moment of inertia, could be included in the set of differential equations to be solved simultaneously. Thus m and I would be treated as variables in Eqs. 12-47 instead of being held constant over the integration time step. Even greater accuracy could be obtained by including differential equations that describe seeker gimbal angle rates and control-surface deflection rates. In this case aerodynamic forces and moments would have to be reevaluated at each step in RK4.

12-2.18.3 MISDIS

Subroutine MISDIS is called from the routine that tests closing speed, described in subpar. 12-2.9. When the closing speed V_c becomes negative, the program calls Subroutine MISDIS to calculate the distance between the target and the

missile at the instant of closest approach, i.e., the miss distance. The miss distance vector M_d is calculated in MISDIS by using

$$M_d = R - (R \cdot u_{V_{T/M}})u_{V_{T/M}}, m \quad (7-39)$$

where

- M_d = miss distance vector in earth coordinate system, m
 $u_{V_{T/M}}$ = unit vector in direction of velocity of target relative to missile in earth coordinate system, dimensionless
 R = range vector from missile to target in earth coordinate system, m,

and the time t_{ca} of closest approach is calculated by using

$$t_{ca} = t - \frac{(R \cdot u_{V_{T/M}})}{V_{T/M}}, s \quad (7-40)$$

where

- t = simulation time, s
 t_{ca} = time of closest approach, s
 $V_{T/M}$ = magnitude of velocity vector of target relative to missile in earth coordinate system, m/s.

Since variables change quickly during the integration time step in which closest approach occurs, it maybe desirable to refine the endgame conditions by going back to the time just preceding the closest approach, reducing the size of the integration time step, and proceeding until V_c again becomes negative before evaluating Eqs. 7-39 and 7-40.

12-2.18.4 TBE

Subroutine TBE* calculates the transformation matrix $[T_{b/e}]$ for transforming vectors expressed in earth reference coordinates to the body reference coordinates. The earth-to-body transformation matrix is a 3 x 3 matrix given by

$$[T_{b/e}] = \begin{bmatrix} c\theta c\psi & c\theta s\psi & -s\theta \\ -s\psi & c\psi & 0 \\ s\theta c\psi & s\theta s\psi & c\theta \end{bmatrix}, \text{ dimensionless} \quad (12-49)$$

where

- $s\theta = \sin \theta$
 $c\theta = \cos \theta$
 $s\psi = \sin \psi$
 $c\psi = \cos \psi$.

*The notation most often encountered in the literature places the subscript for the destination reference frame first, followed by a slash and the reference frame from which the vector is being transformed. Thus $[T_{b/e}]$ is the transformation matrix that transforms a vector to the body frame from the earth frame.

12-2.18.5 TEB

Subroutine TEB calculates the transformation matrix $[T_{e/b}]$ for transforming vectors expressed in body reference coordinates to the earth reference coordinates. The body-to-earth transformation matrix is the transpose of the earth-to-body transformation matrix given by

$$[T_{e/b}] = \begin{bmatrix} c\theta c\psi & -s\psi & s\theta c\psi \\ c\theta s\psi & c\psi & s\theta s\psi \\ -s\theta & 0 & c\theta \end{bmatrix}, \text{ dimensionless.} \quad (12-50)$$

12-2.19 RESULTS

The equations and procedures described in subpars. 12-2.5 through 12-2.17 were implemented on a digital computer, and results for a simulated flight are given in Figs. 12-2 through 12-11. In this example the target is flying a straight and level path at an altitude of 3 km and a speed of 250 m/s, and the target flight path is offset laterally 1 km from the missile launch site. At the instant of missile launch the target is inbound at a downrange distance of 4 km from the launch site.

The guided missile flight path generated by the simulation passes within a miss distance of 0.01 m of the track point on the target (assumed to be the center of mass of the target). The introduction of countermeasures or noise on the guidance signal would of course cause the miss distance to be increased. The time of flight to intercept is 7.6s.

Fig. 12-2 shows a top view of the engagement. Since the launcher is aimed directly at the target at the time of launch, the proportional navigation guidance causes the missile to turn in a direction to lead the target-as is required to strike a moving target. This missile maneuver is initiated when guidance is turned on (0.5s). At this early time in the flight, the missile speed is slow, which causes the amount of lead, and, therefore, the amount of the maneuver to be overestimated. As the missile gains speed, the missile flight path is corrected, as shown by the slight "s" curvature at the beginning of the missile path in Fig. 12-2.

Fig. 12-3 shows a side view of the engagement projected onto the x_z -pkne. If the missile launch site is considered to be in the plane of the paper, the target flight path is parallel to the plane of the paper and 1 km toward the viewer. The initial missile pull-up, which produces the vertical component of the lead angle, is visible in this view.

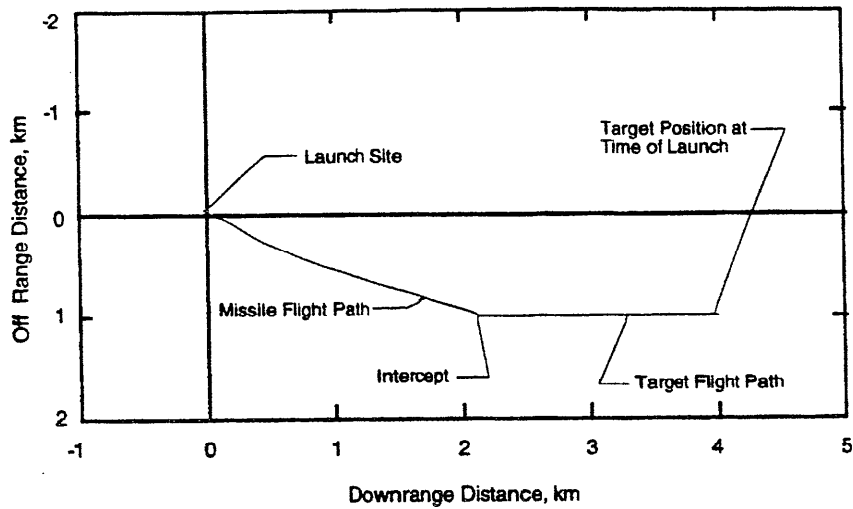


Figure 12-2. Top View of Simulated Engagement

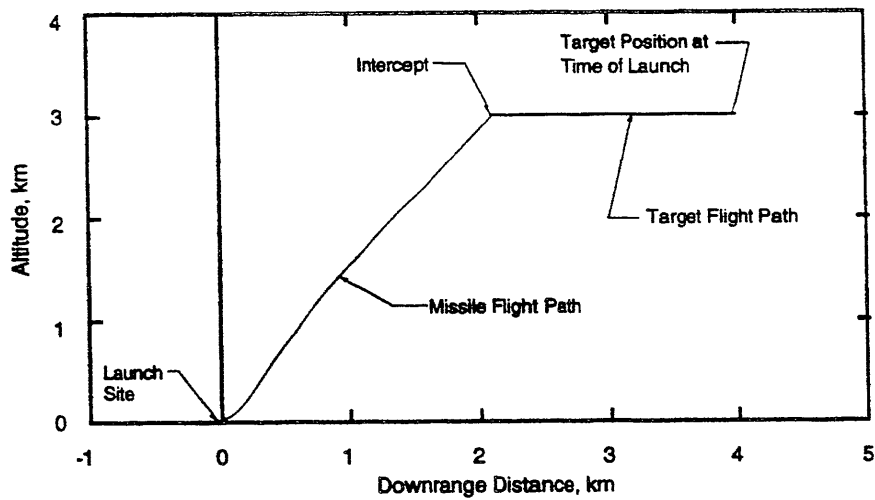


Figure 12-3. Side View of Simulated Engagement xz-Plane

Fig. 12-4 shows the speed history of the missile. The slight perturbation of the speed during the first 2 s is caused by the increased drag that results from the missile maneuvers. The pronounced change in the speed starting about 4 s into the simulated flight is the result of thrust termination.

Fig. 12-5 shows the history of the filtered signal that represents the angular rate of the missile seeker head. Fig. 12-5(A) shows the rate history in the pitch channel, and Fig. 12-5(B) shows the rate history in the yaw channel. The objective of proportional navigation is to cause the missile to fly a path that brings the seeker angular rate to zero. As the missile approaches the target and flies within a fraction of a meter of it, the seeker angular rate suddenly becomes very large, as shown in the figure at a time of 7.6s, the time of intercept.

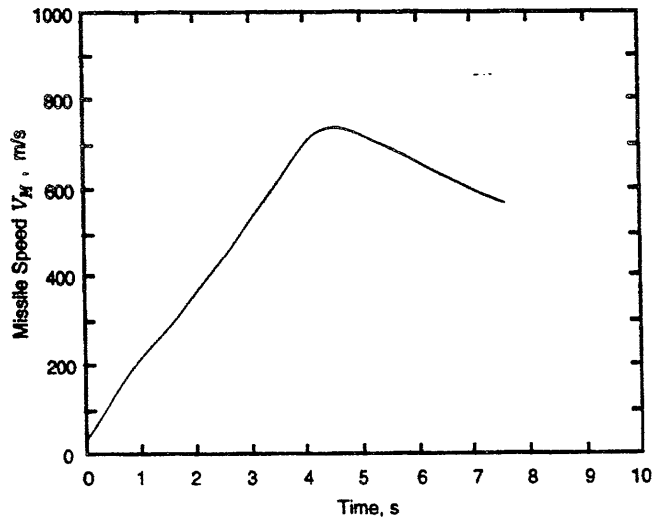


Figure 12-4. Missile Speed History

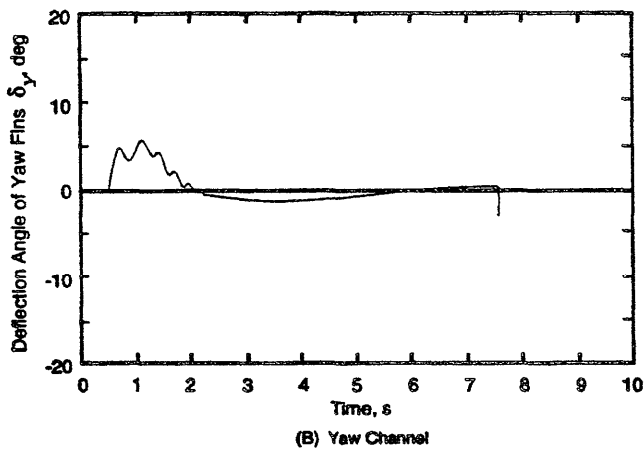
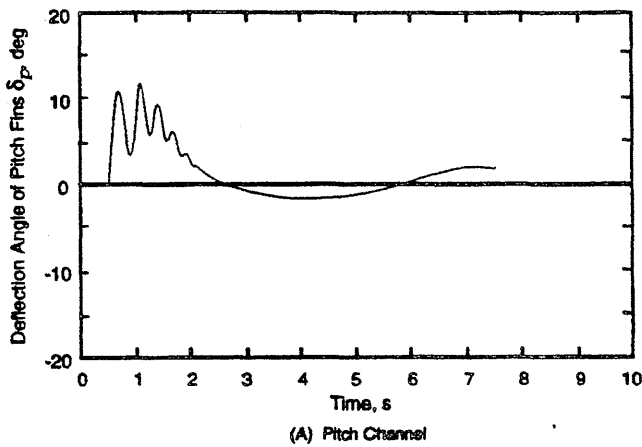


Figure 12-7. Fin Deflection Angle Histories

The pitch and yaw rotational moments on the missile—caused by the combination of fin deflections, the restoring moment from the resulting angle of attack, and the damping effect of the missile angular rate—are shown in Fig. 12-8. The angular motion of the missile is similar to the behavior that would result from the spring analogy illustrated in Fig. 5-7. When the control fins are initially deflected a large moment is generated and the missile rotates and overshoots the trim angle of attack. A restoring moment is generated to rotate the missile back toward the trim condition; this results in an oscillatory motion. The damping moment causes the oscillations to diminish until trim conditions are achieved.

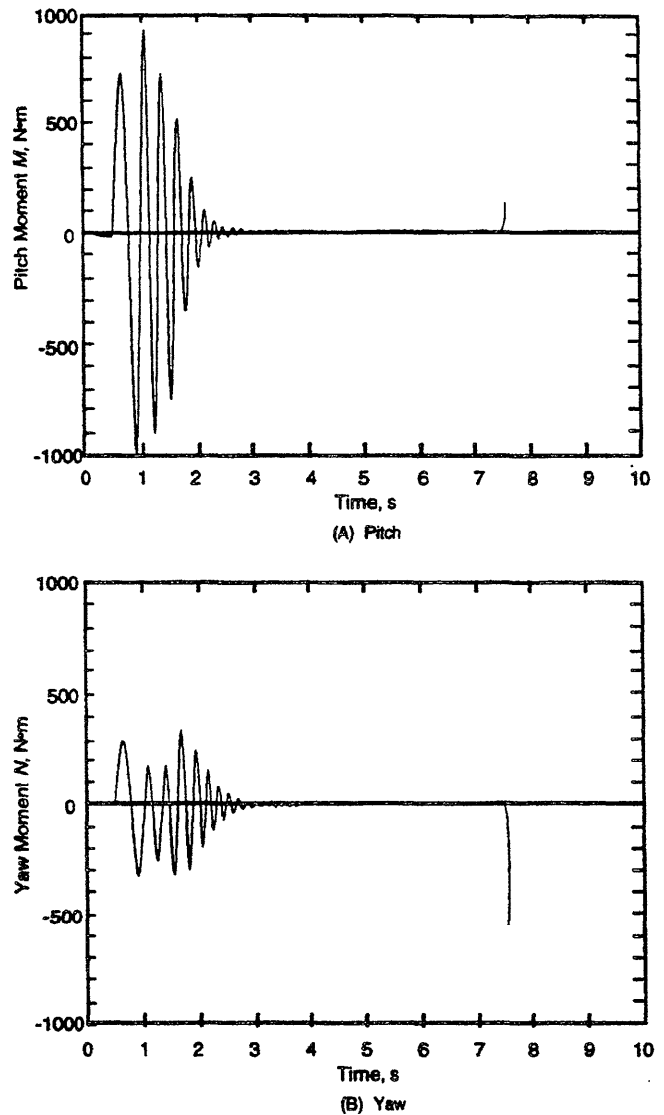
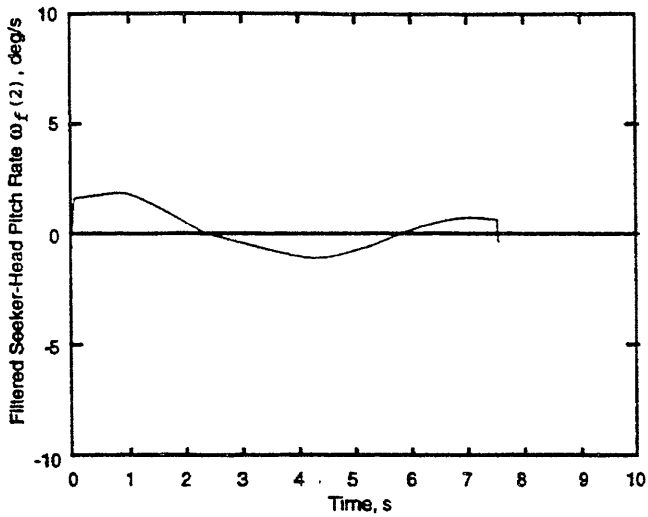
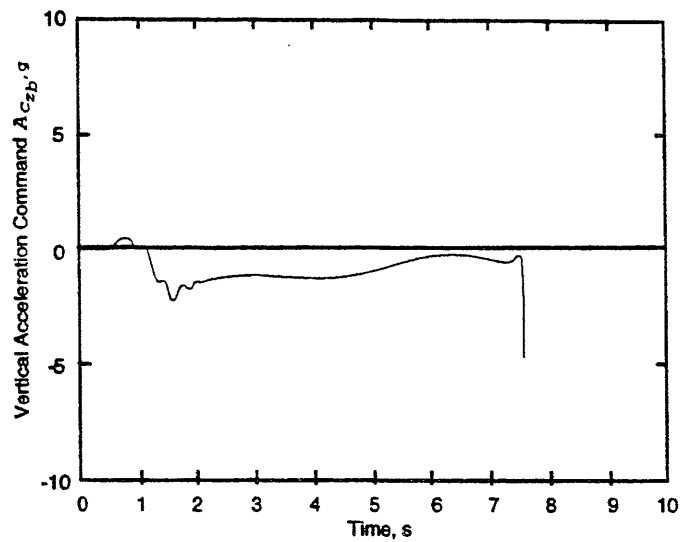


Figure 12-8. Missile Rotational Moment Histories

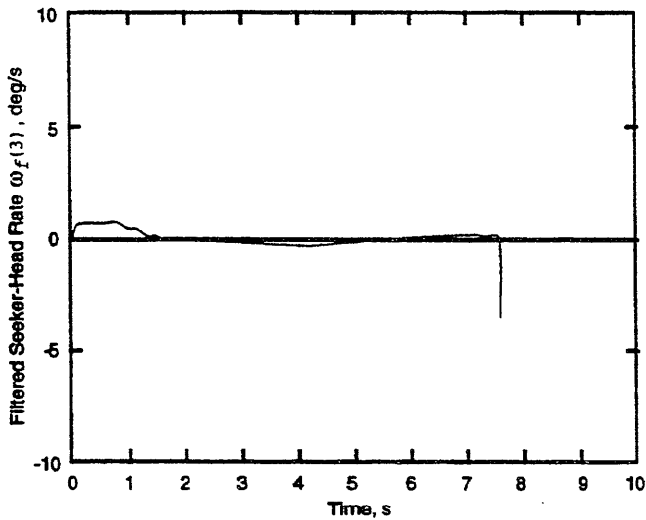
The angle-of-attack and angle-of-sideslip histories that result from the moments applied to the missile are shown in Fig. 12-9. During the half second before guidance is initiated, the angle of attack begins to increase slightly because gravity causes the missile flight path to deviate downward from the direction the missile is initially pointed as it leaves the launcher. The restoring moment, caused by this small angle of attack, rotates the missile downward to point into its relative wind; this reduces the angle of attack essentially to zero by the time guidance is initiated. Fig. 12-10 shows the total combined angle-of-attack history.



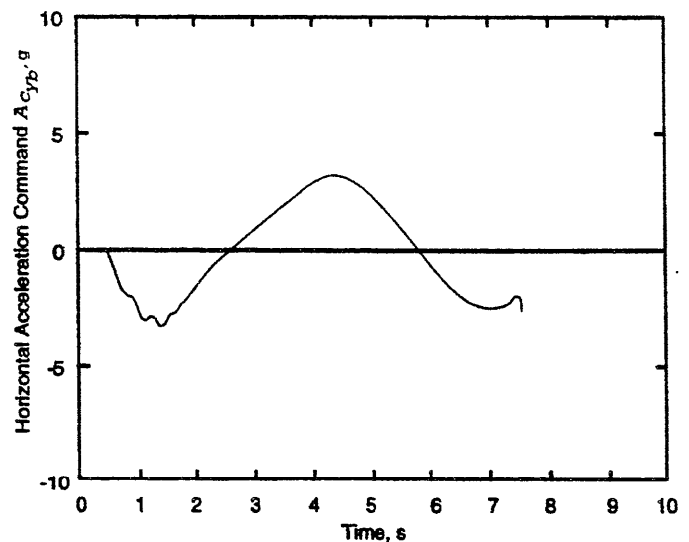
(A) Pitch Channel



(A) Vertical



(B) Yaw Channel



(B) Horizontal

Figure 12-5. Seeker-Head Angular Rate Histories

Figure 12-6. Lateral Acceleration Command Histories

The response of the autopilot to the seeker angular rate signal is to issue actuator pressure commands to deflect the missile control surfaces. Intermediate to issuing these commands, there are implied lateral maneuver acceleration commands that result from the particular implementation of proportional navigation. These lateral maneuver acceleration commands are shown for the pitch and yaw guidance channels in Fig. 12-6. Fig. 12-7 shows the resulting fin deflections.

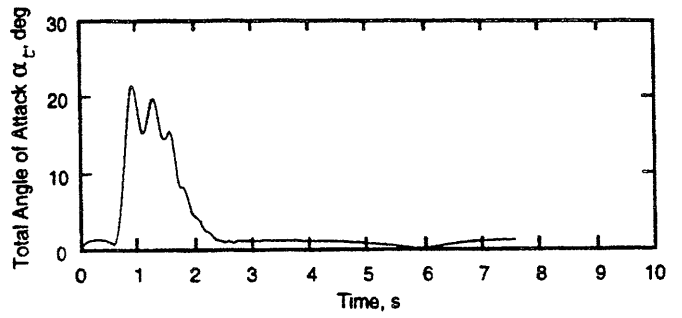
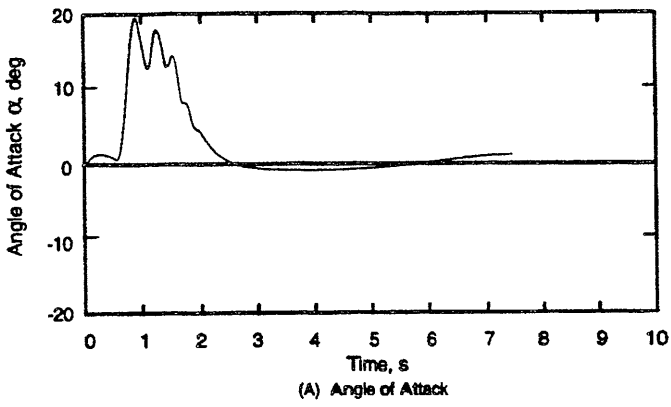


Figure 12-10. Total Angle-of-Attack History

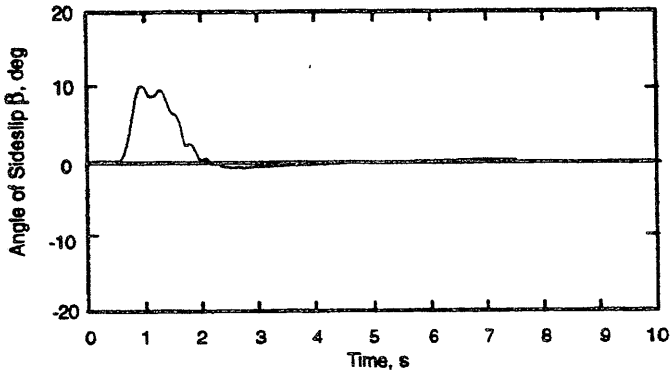


Fig. 12-11 shows the missile angular rate histories q and r about the y_b - and z_b - axes respectively.

Figure 12-9. Angle-of-Attack and Angle-of-Sideslip Histories

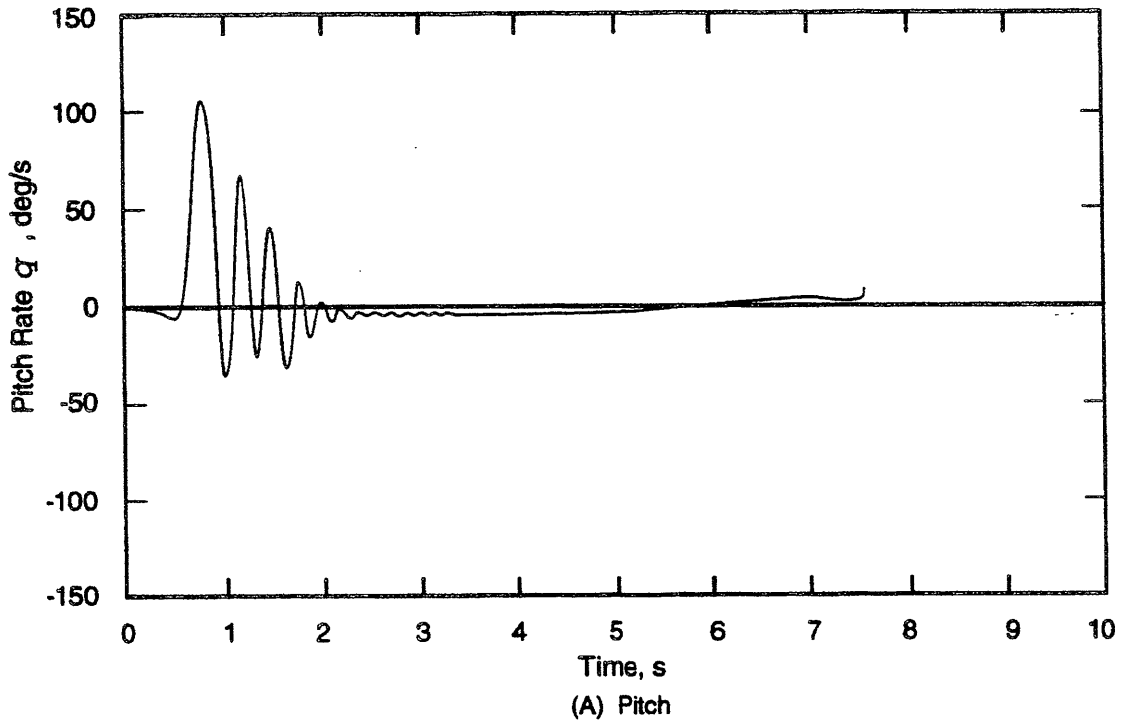


Figure 12-11. Missile Rotational Rate Histories

(cont'd on next page)

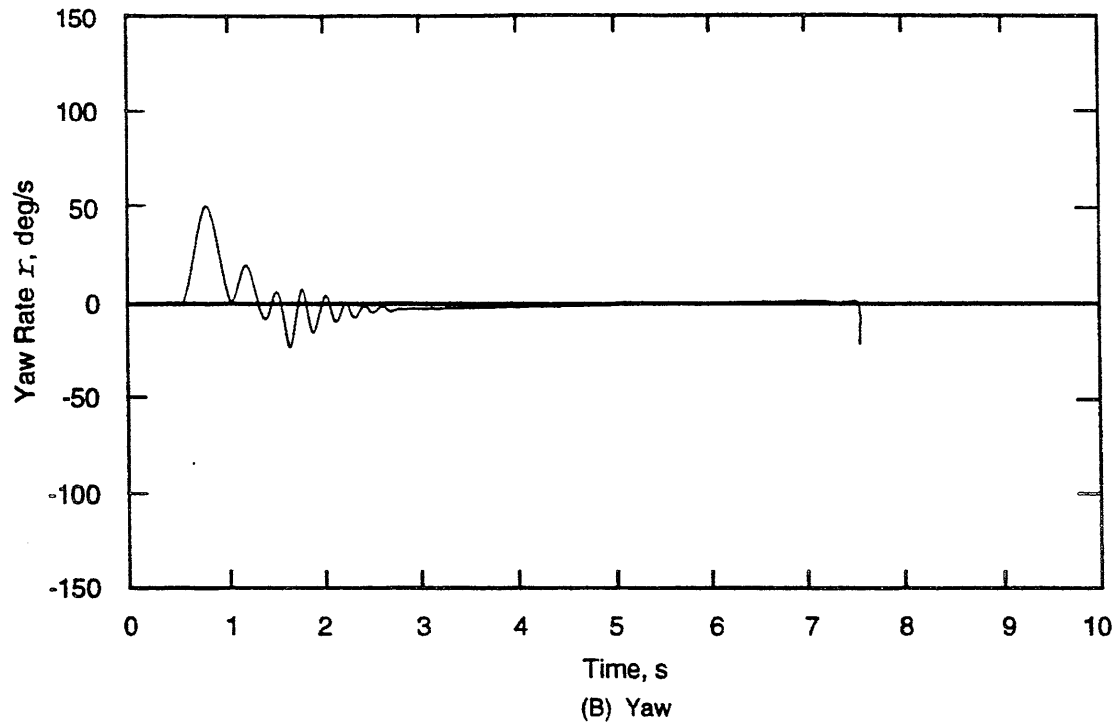


Figure 12-11. (cont'd)

REFERENCE

1. W. H. Press, B. P. Flannery, S. A. Tenkolsky, W. T. Vetterling, Numerical Recipes, The Art of Scientific Computing, Cambridge University Press, Cambridge, MA, 1986.

APPENDIX A

COORDINATE SYSTEMS

A-0 LIST OF SYMBOLS

$C_1 = -v + \sqrt{v^2 + w^2}$, dimensionless
 $C_2 = -w + \sqrt{v^2 + w^2}$, dimensionless
 c = cosine function of an angle (e.g., $c\theta = \cos \theta$), dimensionless
 D = aerodynamic drag force, N
 F_{Ab} = aerodynamic force vector expressed in the body reference frame, N
 F_{Aw} = aerodynamic force vector expressed in the wind reference frame, N
 i, j, k = unit vectors in the direction of the x -, y -, and z -axes respectively, dimensionless
 i_b = unit vector in the direction of the x -axis of body reference frame, dimensionless
 L = aerodynamic lift force, N
 p, q, r = components of angular rate vector ω expressed in body coordinate system (roll, pitch, and yaw respectively), rad/s (deg/s)
 s = sine function of an angle (e.g., $s\theta = \sin \theta$), dimensionless
 $[T_{b/s}]$ = tracker-to-body coordinate transformation matrix, dimensionless
 $[T_{e/b}]$ = body-to-earth coordinate transformation matrix, dimensionless
 $[T_{e/g}]$ = guidance-to-earth coordinate transformation matrix, dimensionless
 $[T_{e/t}]$ = target-to-earth coordinate transformation matrix, dimensionless
 u, v, w = i -, j -, k -components, respectively, of absolute velocity vector V_M expressed in body coordinate system, m/s
 V_M = missile velocity vector, m/s
 V_M = magnitude of missile velocity vector, m/s
 v_b = vector in body coordinate system
 v_e = vector in earth coordinate system
 v_s = vector in tracker coordinate system
 v_t = vector in target coordinate system
 x_b, y_b, z_b = coordinates of a body reference frame
 x_e, y_e, z_e = coordinates of a fixed (earth) reference frame
 x_g, y_g, z_g = coordinates of a guidance reference frame
 x_s, y_s, z_s = coordinates of a tracker (seeker) reference frame
 x_t, y_t, z_t = coordinates of a target reference frame
 x_w, y_w, z_w = coordinates of a wind reference frame

α_t = total angle of attack, rad (deg)
 θ = Euler angle rotation in elevation (pitch) of body frame relative to earth frame, rad (deg)
 θ_g = elevation angle relative to the earth frame of initial range vector from the missile to the target at the instant of launch (or trigger), rad (deg)
 θ_s = Euler angle rotation in the pitch plane of the seeker boresight axis relative to the body frame, rad (deg)
 θ_t = Euler angle rotation in elevation (pitch) of target frame relative to earth frame, rad (deg)
 ϕ = Euler angle rotation in roll of body frame relative to earth frame, rad (deg)
 ϕ_t = Euler angle rotation in roll of target frame relative to earth frame, rad (deg)
 ψ = Euler angle rotation in azimuth (heading) of body frame relative to earth frame, rad (deg)
 ψ_g = azimuth angle relative to earth frame of initial range vector from the missile to the target at the instant of launch (or trigger), rad (deg)
 ψ_s = Euler angle rotation in the yaw plane of the seeker boresight axis relative to the body frame, rad (deg)
 ψ_t = Euler angle rotation in azimuth (heading) of target frame relative to earth frame, rad (deg)

A-1 INTRODUCTION

As described in subpar. 3-3.3, several different coordinate systems are employed in missile flight simulations. Each coordinate system has certain advantages that facilitate mathematical modeling of a particular aspect of missile flight.

A-2 COORDINATE SYSTEM CONVENTIONS

The positive directions of coordinate system axes and the directions of positive rotations about the axes are arbitrary, and different conventions are found in the literature. For applications to missile flight simulations, however, right-handed orthogonal coordinate systems and right-handed rotations are generally employed. In such systems

$$\left. \begin{aligned} \mathbf{i} \times \mathbf{j} &= \mathbf{k} \\ \mathbf{j} \times \mathbf{k} &= \mathbf{i} \\ \mathbf{k} \times \mathbf{i} &= \mathbf{j} \end{aligned} \right\} \quad (\text{A-1})$$

where

i = unit vector in the direction of the x-axis

j = unit vector in the direction of the y-axis

k = unit vector in the direction of the z-axis.

A positive rotation of a coordinate system about a given axis is defined as the direction that the right-hand fingers curl when the thumb is pointed in the direction of the rotational axis. Stated another way, positive rotations are clockwise when viewed from the origin, looking out along the positive direction of the axis. These conventions are illustrated in Fig. A-1.

When Euler angles are employed in the transformation of a vector expressed in one reference frame to the expression of the vector in a different reference frame, any order of the three Euler rotations is possible, but the resulting transformation equations depend on the order selected. The generally accepted order for applications to missile flight simulation is that the first Euler rotation is about the z-axis, the second is about the y-axis, and the third is about the x-axis. With reference to missile body orientation, the resulting order is yaw, pitch, and roll. With reference to geographical orientation, the resulting order is azimuth (heading), elevation (pitch), and roll (bank angle).

A-3 COORDINATE SYSTEM DEFINITIONS

In missile flight simulations it is sometimes advantageous to define special coordinate systems to simplify the equations describing subsystem performance; however, in the majority of cases relatively few coordinate systems are needed. The most common coordinate systems are described in the paragraphs that follow, and equations for the usual transformations between them are given:

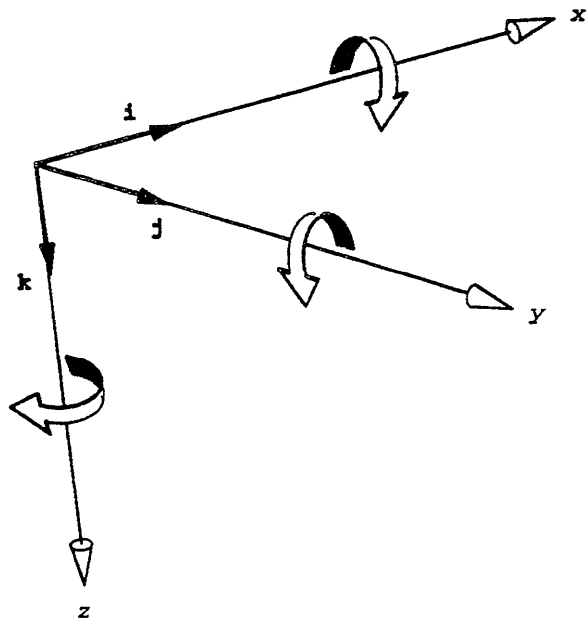


Figure A-1. Coordinate System Conventions

A-3.1 EARTH COORDINATE SYSTEM

For the surface-to-air missile simulations described in this handbook, the earth is considered to be flat and nonrotating, thus avoiding the necessity for calculating the Coriolis accelerations related to the rotation of the earth and the changes in the direction of gravity as the missile moves over the surface of the earth. The earth is also considered to be fixed relative to inertial space, thereby making the earth coordinate frame an absolute (inertial) frame of reference in which Newton's laws apply.

The earth coordinate system is defined by a set of axes x_e , y_e , and z_e , illustrated in Fig. 3-1(C). The x_e - and y_e -axes lie in a horizontal plane, and the z_e -axis is pointed vertically downward. Although the earth coordinated system can be defined with the origin at any convenient location, a common definition places the origin at sea level with the upward extension of the z_e -axis passing through the missile launcher. This causes the magnitude of the negative z -coordinate of the missile position vector at any point in the flight to be equal to the altitude of the missile above sea level, which is the parameter needed to enter atmospheric tables. The azimuthal direction of the x_e -axis is arbitrary. When the simulated flight is to be related to a map, the x_e -axis is often defined as pointing north; this causes the y_e -axis to point east. When the missile simulation is to be employed to calculate launch boundaries, the x_e -axis is commonly pointed in the general downrange direction (the direction from which threats arrive). In applications in which the geographical relationships among different simulated flights are unimportant the x_e -axis is usually oriented so that the target position at the time of missile launch lies in or near the $x_e z_e$ -plane.

The primary purpose of the earth coordinate system is to describe the positions of the missile and target during the engagement and as an inertial frame of reference for application of Newton's laws of motion.

A-3.2 BODY COORDINATE SYSTEM

The body coordinate system is defined by the set of axes x_b , y_b , and z_b , as illustrated in Fig. 3-1(B). The origin of the body coordinate system is located at the instantaneous center of mass of the missile, and the x_b -axis is parallel with the body longitudinal centerline and points toward the nose of the missile. At the instant of launch the y_b -axis of the body coordinate system lies in a horizontal plane, i.e., a plane parallel to the $x_e y_e$ -plane, and is directed to the right as viewed by an observer at the launcher facing in the direction the missile is pointing. The z_b -axis completes the right-handed triad, pointing in a direction below the horizontal.

A body coordinate system can be defined as rolling or nonrolling, causing a distinction to be made in the methods of handling the subsequent directions of the y_b - and z_b -axes during maneuvering flight. At the instant of launch the three axes of a rolling body coordinate system are identical with those of a nonrolling body coordinate system. As the missile body rotates about its three axes during flight, however, the

rolling body coordinate system duplicates the angular motion of the missile about all three axes, whereas the non-rolling body coordinate system duplicates the missile rotational motion only about the pitch and yaw axes. In other words, the rolling body coordinate system behaves as if it were firmly attached to the missile body, and the nonrolling body coordinate system behaves in the same manner except that it does not experience roll about the x_b -axis (missile centerline axis).

The instantaneous angular orientation of the body coordinate system relative to the earth coordinate system is described by the three Euler angles ψ , θ , and ϕ (Fig. 4-2). This orientation is calculated in a simulation by integrating the Euler angle rate equations, Eqs. 4-51. The angular motion of the rolling body coordinate system is calculated using all three components of missile angular rate p , q , and r , whereas to calculate the angular motion of a nonrolling body coordinate system, the value of p , i.e., missile roll rate about its centerline axis, is set to zero.

The rolling body coordinate system is employed in full six-degree-of-freedom simulations and provides the means to calculate the missile roll angle as the missile responds to rolling moments. In simulations that do not require explicit calculation of roll angle, the equations can be simplified by using a nonrolling body coordinate system. In this case missile roll rates may still be calculated by integrating Eqs. 4-46, but the instantaneous roll angle of the missile is never calculated.

The primary importance of the body coordinate system is that it facilitates calculations of body rotational motion since the principal rotational axes of the body are aligned with the axes of the coordinate system (subpar. 4-5.2). The body coordinate system is also used to calculate the direction of the thrust force and any moments on the body caused by thrust misalignment.

A-3.3 WIND COORDINATE SYSTEM

The wind coordinate system is defined by the set of axes x_w, y_w , and z_w . If there is no atmospheric air movement (wind) relative to the inertial earth coordinate system, the x_w -axis is parallel with and in the same direction as the missile inertial velocity vector. Thus the total inertial velocity vector has no components on the y_w - and z_w -axes. The roll orientation of the y_w - and z_w -axes can be defined to suit the needs of the particular application.

For example, a convenient orientation of the wind reference frame relative to the body reference frame is illustrated in Fig. 3-1(F). To achieve this orientation, the wind coordinate system is rolled about the x_w -axis such that the missile centerline axis (x_b -axis) lies in the $x_w z_w$ -plane. Thus the plane of the total angle of attack, i.e., the plane formed by the missile centerline axis and the missile inertial velocity vector, coincides with the $x_w z_w$ -plane; therefore, the total

aerodynamic force vector lies in that plane. The direction of the y_w -axis is defined as the vector cross product ($V_w \times x_b$), as illustrated in Fig. 3-1(F). The z_w -axis completes the right-handed triad.

A-3.4 GUIDANCE COORDINATE SYSTEM

The guidance coordinate system employs the set of axes x_g, y_g, z_g , as illustrated in Fig. 3-1(D). The origin of the guidance coordinate system is located at the center of mass of the missile. The x_g -axis is directed along the initial range vector from the missile to the target at the instant of launch (or trigger). The y_g -axis is horizontal to the right, and the z_g -axis completes the right-handed triad. The guidance coordinate system translates with the missile but has no angular motion.

A-3.5 TRACKER (SEEKER) COORDINATE SYSTEM

The equations in Chapter 8 for simulating seeker performance employ vectors expressed in the earth reference system. In some applications of target tracker simulations, however, calculations relating the signals from several radiating sources within the field of view of the tracker (subpar. 8-2.1.3) may be facilitated by using a tracker coordinate system. One such coordinate system is defined by the set of axes x_s, y_s, z_s , as shown in Fig. 3-1(E). The x_s -axis is aligned with the boresight axis of the seeker. The y_s - and z_s -axes are identical with the y_b - and z_b -axes when the seeker boresight axis is aligned with the missile centerline. Angular displacements of the seeker reference frame from the body reference frame are described by the Euler angles ψ_s in the yaw plane and θ_s in the pitch plane, executed in that order. The seeker coordinate system does not roll relative to the body reference frame.

A-3.6 TARGET COORDINATE SYSTEM

The target coordinate system is the set of axes, x_t, y_t, z_t illustrated in Fig. 3-1(A). The origin is located at the center of mass of the target. The x_t -axis points forward and is parallel with the fuselage reference line of the target aircraft. The z_t -axis is perpendicular to the x_t -axis and points downward when the target aircraft is in normal, level flight. The y_t -axis completes the right-handed triad.

The target coordinate system is used primarily to define the target signature. It is also employed when missile fuzing and warhead performance are included in the simulation.

A-4 COORDINATE SYSTEM TRANSFORMATIONS

In missile flight simulations, vectors expressed in one coordinate system frequently must be transformed into a different coordinate system. Matrix transformation equations for some of the most common transformations are described in the subparagraphs that follow.

A-4.1 BODY TO EARTH

A vector v expressed in the body coordinate system is transformed to the earth coordinate system by the matrix equation:

$$\mathbf{v}_e = [T_{e/b}] \mathbf{v}_b \quad (\text{A-2})$$

where

c = cosine function (e.g., $c\theta = \cos \theta$), dimensionless

s = sine function (e.g., $s\theta = \sin \theta$), dimensionless

$[T_{e/b}]$ = body-to-earth transformation matrix,

$$\begin{bmatrix} c\theta c\psi & s\phi s\theta c\psi - c\phi s\psi & c\phi s\theta c\psi + s\phi s\psi \\ c\theta s\psi & s\phi s\theta s\psi + c\phi c\psi & c\phi s\theta s\psi - s\phi c\psi \\ -s\theta & s\phi c\theta & c\phi c\theta \end{bmatrix},$$

dimensionless

\mathbf{v}_b = vector in body coordinate system

\mathbf{v}_e = vector in earth coordinate system

θ = Euler angle rotation in elevation (pitch) of body frame relative to earth frame, rad (deg)

ϕ = Euler angle rotation in roll of body frame relative to earth frame, rad (deg)

ψ = Euler angle rotation in azimuth (heading) of body frame relative to earth frame, rad (deg).

A-4.2 WIND TO BODY

When the wind coordinate system is defined as in Fig. 3-1(F), the aerodynamic force vector F_{A_i} is expressed in the wind system as

$$\mathbf{F}_{A_w} = \begin{bmatrix} -D \\ 0 \\ L \end{bmatrix} \quad (\text{A-3})$$

where

D = aerodynamic drag force, N (always positive)

\mathbf{F}_{A_w} = aerodynamic force vector expressed in the wind reference frame, N

L = aerodynamic lift force, N (always positive).

The aerodynamic force vector is transformed to the body coordinate system to determine \mathbf{F}_{A_b} by using

$$\mathbf{F}_{A_b} = \begin{bmatrix} c\alpha_i & 0 & s\alpha_i \\ -C_1 s\alpha_i & 0 & C_1 c\alpha_i \\ -C_2 s\alpha_i & 0 & C_2 c\alpha_i \end{bmatrix} \mathbf{F}_{A_w} \quad (\text{A-4})$$

where

$$C_1 = -v + \sqrt{v^2 + w^2}, \text{ dimensionless}$$

$$C_2 = -w + \sqrt{v^2 + w^2}, \text{ dimensionless}$$

$$c\alpha_i = \cos \alpha_i$$

$$s\alpha_i = \sin \alpha_i$$

u, v, w = i, j, k -components, respectively, of absolute velocity vector \mathbf{V}_M expressed in body coordinate system, m/s

V_M = magnitude of missile velocity vector, m/s

$$\alpha_i = \text{Cos}^{-1}\left(\frac{u}{V_M}\right), \text{ total angle of attack, rad (deg).}$$

Eq. A-4 is derived from Eqs. 4-13, 4-14, and 7-1. The matrix in Eq. A-4 applies specifically to the vector F_{A_i} as defined in Eq. A-3; it is not a general transformation matrix.

A-4.3 GUIDANCE TO EARTH

A vector v expressed in the guidance coordinate system is transformed to the earth coordinate system by

$$\mathbf{v}_e = [T_{e/g}] \mathbf{v}_g \quad (\text{A-5})$$

where

$[T_{e/g}]$ = guidance-to-earth coordinate transformation matrix,

$$\begin{bmatrix} c\theta_g c\psi_g & -s\psi_g & s\theta_g c\psi_g \\ c\theta_g s\psi_g & c\psi_g & s\theta_g s\psi_g \\ -s\theta_g & 0 & c\theta_g \end{bmatrix},$$

dimensionless

\mathbf{v}_e = vector in earth coordinate system

\mathbf{v}_g = vector in guidance coordinate system

θ_g = elevation angle relative to the earth frame of initial range vector from the missile to the target at the instant of launch (or trigger), rad (deg)

ψ_g = azimuth angle relative to earth frame of initial range vector from the missile to the target at the instant of launch (or trigger), rad (deg).

A-4.4 TRACKER (SEEKER) TO BODY

A vector v expressed in the seeker coordinate system is transformed to the body coordinate system by

$$\mathbf{v}_b = [T_{b/s}] \mathbf{v}_s \quad (\text{A-6})$$

where

$[T_{b/s}]$ = tracker-to-body coordinate transformation matrix,

$$\begin{bmatrix} c\theta_s c\psi_s & -s\psi_s & s\theta_s c\psi_s \\ c\theta_s s\psi_s & c\psi_s & s\theta_s s\psi_s \\ -s\theta_s & 0 & c\theta_s \end{bmatrix},$$

dimensionless

\mathbf{v}_b = vector in body coordinate system

\mathbf{v}_s = vector in tracker coordinate system

θ_s = Euler angle rotation in the pitch plane of the seeker boresight axis relative to the body frame, rad (deg)

ψ_s = Euler angle of rotation in the yaw plane of the seeker boresight axis relative to the body frame, rad (deg).

A-4.5 TARGET TO EARTH

A vector v expressed in the target coordinate system is transformed to the earth coordinate system by

$$\mathbf{v}_e = [T_{e/t}] \mathbf{v}_t \quad (\text{A-7})$$

where

$[T_{e/t}]$ = target-to-earth coordinate transformation matrix,

$$\begin{bmatrix} c\theta_s c\psi_s & s\phi_s s\theta_s c\psi_s - c\phi_s s\psi_s & c\phi_s s\theta_s c\psi_s + s\phi_s s\psi_s \\ c\theta_s s\psi_s & s\phi_s s\theta_s s\psi_s + c\phi_s c\psi_s & c\phi_s s\theta_s s\psi_s - s\phi_s c\psi_s \\ -s\theta_s & s\phi_s c\theta_s & c\phi_s c\theta_s \end{bmatrix}$$

dimensionless

\mathbf{v}_e = vector in earth coordinate system

\mathbf{v}_t = vector in target coordinate system

θ_s = Euler angle rotation in elevation (pitch) of target frame relative to earth frame, rad (deg)

ϕ_s = Euler angle rotation in roll (bank) of target frame relative to earth frame, rad (deg)

ψ_s = Euler angle rotation in azimuth (heading) of target frame relative to earth frame, rad (deg).

A-5 QUATERNIONS

In 1843 to extend three-dimensional vector algebra to include multiplication and division, Sir William Rowan Hamilton found it necessary to invent an algebra for quadruples of numbers, which he named quaternions (Ref. 1). A quaternion is represented by four numbers written in a definite order. Quaternions can be interpreted geometrically as operators on vectors.

In par. A-2 the transformation of a vector from one coordinate system to another was described by three successive rotations about the three coordinate axes performed in a specified sequence. These Euler rotations lead to the transformation equations described in par. A-4, which employ matrices of direction cosines, the nine elements of which are specified in terms of the Euler rotation angles. As an alternative approach, however, it is possible to rotate from one coordinate frame to another by a single rotation about an appropriately selected axis of rotation (generally, not one of the axes of either reference frame). Thus the alternative approach requires the manipulation of only four parameters—the three coordinates of the axis of rotation plus the angle of rotation. Quaternion algebra can be used to implement such four-element transformations.

Advantages of quaternion transformations over Euler transformations are fewer calculations per transformation, avoidance of singularities that occur in Euler transformations when the pitch angle θ reaches 90 deg, and usually avoidance of computing trigonometric functions. The use of quaternions should be considered for real-time (or faster-than-real-time) applications because of their potential for computational speed advantage over other methods.

REFERENCE

1. L. Brand, Vector and Tensor Analysis, John Wiley & Sons, Inc., New York, NY, 1947.

BIBLIOGRAPHY

COORDINATE TRANSFORMATIONS

- B. L. Byrum and G. E. Russell, "General Airframe Dynamics of a Guided Missile", Journal of the Aeronautical Sciences, 534-40 (August 1955).
- L. D. Duncan, Coordinate Transformations in Trajectory Simulations, DA TASK 1V14501B53A-10, ECOM-5032, Atmospheric Sciences Laboratory, White Sands Missile Range, NM, February 1966.
- H. Goldstein, Classical Mechanics, Second Edition, Addison-Wesley Publishing Company, Inc., Reading, MA, 1980.
- P. N. Jenkins, Missile Dynamic Equations for Guidance and Control Modeling and Analysis, Technical Report RG-84-17, Guidance and Control Directorate, US Army Missile Laboratory, US Army Missile Command, Redstone Arsenal, AL, April 1984.
- R. W. Kolk, Modern Flight Dynamics, Prentice-Hall, Inc., Englewood Cliffs, NJ, 1961.

QUATERNIONS

- L. Brand, Vector and Tensor Analysis, John Wiley & Sons, Inc., New York, NY, 1947.
- J. L. Farrell, Integrated Aircraft Navigation, Academic Press, Inc., New York NY, 1976.
- "Quaternions and Their Geometrical Interpretation", Navy ACMR/I Missile Simulations, Volume I, Appendix A, NADC-74156-50, Revision 1, Naval Air Development Center, Warminster, PA, 1975.
- A. C. Robinson, On the Use of Quaternions in Simulation of Rigid-Body Motion, WADC Technical Report 58-17, Wright Aeronautical Development Center, Wright-Patterson Air Force Base, OH, December 1958.
- C. P. Schneider, "Application to Missile Dynamics", AGARD Lecture Series No. 18, MBB-UA-553/80, Advisory Group for Aerospace Research and Development, North Atlantic Treaty Organization, Neuilly sur Seine, France, 1980.

APPENDIX B

ATMOSPHERIC MODELING

B-0 LIST OF SYMBOLS

- a** = lapse rate, K/m
 g_0 = acceleration due to gravity at earth surface, m/s^2
 (equivalent to N/kg)
 h = altitude for which atmospheric properties are to be
 calculated, m
 h_1 = reference altitude (e.g., sea level or earth surface), m
 p = pressure at altitude h , Pa
 p_b = barometric pressure, Pa
 p_v = vapor pressure of water, Pa
 p_1 = given pressure at altitude h_1 , Pa
 R = gas constant (287.05), N·m/(kg·K)
 r = relative humidity, %
 T = temperature at altitude h , K
 T_c = atmospheric temperature, °C
 T_1 = given temperature at altitude h_1 , K
 V_s = speed of sound at altitude h , m/s
 γ = ratio of specific heats (1.4), dimensionless
 ρ = density at altitude h , kg/m^3
 ρ_m = mixture density, kg/m^3

B-1 INTRODUCTION

The atmosphere interacts with missiles in two basic ways. First, the flow of atmospheric air over the surfaces of the missile produces aerodynamic forces and moments. Second, the ability of the atmosphere to transmit electromagnetic signals impacts on the performance of a missile seeker.

As discussed in par. 5-5, the primary atmospheric properties employed in aerodynamic calculations are density, pressure, and speed of sound. For simulations that calculate Reynolds number, atmospheric viscosity also is required. As discussed in subpars. 2-2.1.1 and 2-2.1.2, the transmissibility of electromagnetic radiation through the atmosphere is largely determined by conditions in the atmosphere, such as water vapor content, carbon dioxide content, smoke, haze, rain, and snow.

Missile flight simulations employ tables or models of the atmosphere to provide values of atmospheric properties at the instantaneous altitude of the missile for each computational cycle.

B-2 SOURCES OF ATMOSPHERE DATA

Sources from which atmospheric data can be selected for aerodynamic calculations include internationally accepted tables for a standard atmosphere, tables based on average local experience at a given test range, tables based on a standard hot day or a standard cold day, a complete set of measurements of atmospheric properties made at the time and location of a specific flight test, or calculations that extrapo-

late atmospheric data from incomplete measurements or estimates. As in other aspects of missile modeling, the source of atmospheric data used in a simulation depends on the objectives of the simulation and the availability of data.

For missile simulations that are not intended to be compared with flight tests, it is not critical that the atmospheric data be precise because in actual operational flight the atmospheric properties will vary from one flight to the next. Missile flight simulation results, however, are often compared with the results of other flight simulations, and the use of a common standard atmosphere facilitates such comparisons.

If a simulated flight is to be compared with flight-test data, actual measured atmospheric conditions at the time of the flight test should be used in the simulation. Often, atmospheric properties are measured throughout the altitude regime of a specific flight test, and extensive measurements are taken immediately before and after the flight. Measurements of temperature and pressure at only the surface of the earth are much less expensive and may be adequate for some applications when they are extrapolated mathematically to other altitudes.

Sources of data for electromagnetic transmission characteristics of the atmosphere include graphs such as Figs. 2-3 and 2-11 and computer programs that are available for predicting the transmission properties of the atmosphere under various conditions (Ref. 1).

B-3 ATMOSPHERIC PROPERTIES

The properties of the US Standard Atmosphere (1976) are described and presented in tabular form in Ref. 2. Table B-1 is an abbreviated table of pressure, density, speed of sound, and kinematic viscosity for geometric altitudes up to 24,000 m.

B-4 MODELING ATMOSPHERIC PROPERTIES

Atmospheric properties are modeled in a typical simulation by including tables of the appropriate atmospheric parameters as functions of altitude. The simulation contains table lookup routines that are exercised at each computational time step to match atmospheric properties with the instantaneous altitude of the missile. Polynomial and exponential curve fits to the data tables are sometimes substituted for the tables to simplify data input and, in some cases, to reduce computation time.

In applications in which measured atmospheric data are available at only one or a few altitudes, the atmosphere is modeled in a flight simulation by using equations that extrapolate or interpolate data according to known principles of atmospheric variation with altitude. These equations

TABLE B-1. PROPERTIES OF US STANDARD ATMOSPHERE (1976)

ALTITUDE, m	PRESSURE, Pa	DENSITY, kg/m ³	SPEED OF SOUND, m/s	KINEMATIC VISCOSITY, m ² /s
0	101,325	1.2250	340.29	1.4607E-5
2,000	79,501	1.0066	332.53	1.7147E-5
4,000	61,660	0.81935	324.59	2.0275E-5
6,000	47,217	0.66011	316.45	2.4161E-5
8,000	35,651	0.52579	308.11	2.9044E-5
10,000	26,499	0.41351	299.53	3.5251E-5
12,000	19,399	0.31194	295.07	4.5574E-5
14,000	14,170	0.22786	295.07	6.2391E-5
16,000	10,352	0.16647	295.07	8.5397E-5
18,000	7,565.2	0.12165	295.07	1.1686E-4
20,000	5,529.3	0.088910	295.07	1.5989E-4
22,000	4,047.5	0.064510	296.38	2.2201E-4
24,000	2,971.7	0.046938	297.72	3.0743E-4

are based on hydrostatic theory, the equation of state for air, and the observed behavior of atmospheric temperature with altitude. For altitudes up to about 11,000 m above sea level, experimental data show that the atmospheric temperature decreases more or less linearly with altitude. This region is called the troposphere. Extending above the troposphere to an altitude of about 21,000 m is an isothermal region known as the stratosphere within which the atmospheric temperature is approximately constant with altitude.

Equations used to extrapolate atmospheric properties are often based on the following simplifying assumptions:

1. The air is dry.
2. The air behaves as a perfect gas.
3. The gravity field is constant.
4. The rate of change of temperature with altitude (lapse rate) is constant within a specified altitude region.

Then, given the conditions at any altitude within the troposphere, for example, and an assumed or measured lapse rate, the atmospheric properties at a higher altitude within the troposphere can be calculated by using

$$T = T_1 + a(h - h_1), \text{ K} \quad (\text{B-1})$$

$$p = p_1 \left(\frac{T}{T_1} \right)^{-\frac{g_0}{aR}}, \text{ Pa} \quad (\text{B-2})$$

$$\rho = \frac{p}{RT}, \text{ kg/m}^3 \quad (\text{B-3})$$

$$V_s = \sqrt{\gamma RT}, \text{ m/s} \quad (\text{B-4})$$

where

- a = lapse rate, K/m
- g_0 = acceleration due to gravity at earth surface, m/s² (equivalent to N/kg)
- h = altitude for which atmospheric properties are to be calculated, m
- h_1 = reference altitude (e.g., sea level or earth surface), m
- p = pressure at altitude h , Pa
- p_1 = given pressure at altitude h_1 , Pa
- R = gas constant (287.05), N·m/(kg·K)
- T = temperature at altitude h , K
- T_1 = given temperature at altitude h_1 , K
- V_s = speed of sound at altitude h , m/s
- γ = ratio of specific heats (1.4), dimensionless
- ρ = density at altitude h , kg/m³.

A typical lapse rate within the troposphere is 0.0065 K/m.

Within the stratosphere the standard lapse rate is assumed to be zero, and Eq. B-2 is replaced by

$$p = p_1 \exp \left[-\frac{g_0}{RT} (h - h_1) \right], \text{ Pa} \quad (\text{B-5})$$

where both subscripted and unsubscripted variables are considered to be within the stratospheric region. Eq. B-3 is used to calculate the density, and Eq. B-4 predicts the speed of sound, which is constant within the stratosphere since the temperature is constant.

The atmosphere is actually a mixture of air and water vapor. The relative amount of water vapor is described by the relative humidity. The total atmospheric pressure (the pressure measured by a barometer) is the sum of the vapor pressure and the air pressure. Also the mixture density is the sum of the mass of air and the mass of water vapor per cubic meter of the mixture. The previous assumption of dry air can be relaxed if the barometric pressure and the relative humidity are known. The mixture density can be calculated by using

$$\rho_m = \frac{(p_b - 0.379 p_v)}{RT}, \text{ kg/m}^3 \quad (\text{B-6})$$

where

p_b = barometric pressure, Pa
 p_v = vapor pressure of water, Pa
 ρ_m = mixture density, kg/m³.

The vapor pressure can be determined directly from a wet-and-dry-bulb hygrometer reading, or it can be calculated using the relative humidity by (Ref. 3)

$$p_v = r[1.286 + 1.694E - 3(1.8T_c + 32)^{2.245}], \text{ Pa} \quad (\text{B-7})$$

where

r = relative humidity, %
 T_c = atmospheric temperature, °C.

The lapse rate a is also affected by nonstandard humidity conditions. Eqs. B-1 through B-5 are made applicable to nonstandard humidity conditions by using a known or estimated lapse rate in Eqs. B-1 and B-2, replacing Eq. B-3 with Eq. B-6, and letting $P = P_m$.

REFERENCES

1. F. X. Kneizys et al, Users Guide to LOWTRAN 7, AFGL-TR-88-0177, US Air Force Geophysics Laboratory, Hanscom Air Force Base, MA, August 1988.
2. US Standard Atmosphere 1976, National Oceanic and Atmospheric Administration, National Aeronautics and Space Administration, and the United States Air Force, 1976.
3. R. E. Gould and M. D. Sevachko, An Aerodynamics Model for Guided Missiles, DELEW-M-TR-82-36, Electronic Warfare Laboratory, Office of Missile Electronic Warfare, White Sands Missile Range, NM, November 1982.

GLOSSARY

A

Absolute Acceleration. Acceleration relative to an inertial reference frame.

Absolute Velocity. Velocity relative to an inertial reference frame.

Accreditation. An official determination by management that a model or simulation is acceptable for a specific purpose.

Aeroelasticity. Elastic deformation of the airframe caused by aerodynamic loads.

Air-Augmented Rocket. Rocket motor that uses captive atmospheric air to increase thrust.

Airframe Damping. The effect of aerodynamic forces that suppress oscillations of the airframe.

Aliasing (Frequency Foldback). Phenomenon that occurs in the discrete sampling of continuous functions when the high-frequency components in the spectrum of the continuous function are erroneously folded back and appear as lower-frequency components in the spectrum of the discrete sample. If the time intervals between samples is H seconds, the highest frequency in the continuous function that can be defined in the sample is $1/(2H)$ Hz (called the Nyquist frequency).

Anechoic Chamber. Enclosed metal chamber that has internal surfaces covered with materials that absorb radio frequency energy rather than reflect it.

Angle of Attack. Angle between missile centerline and velocity vector relative to the air.

Areal Density. Density per unit area.

Aspect Angle. Azimuth and elevation relative to the target of the line of sight between a sensor and the target.

Autopilot Gains. Amplification settings for functions performed by the autopilot.

B

Backscattering Cross Section. Scattering cross section when the aspect of the target relative to the illuminator is the same as that relative to the receiver.

Bayesian Updating. A statistical method by which probabilities are calculated that the observed test data conform to various alternative hypothesized model formulations.

Beam-Rider Guidance. Guidance technique in which the missile flies along a tracking beam from the launcher to the target.

Bistatic Cross Section. Scattering cross section when the aspect of the target relative to the illuminator is different from that relative to the receiver.

Boost-Glide. Propulsion system in which there is no additional thrust after the missile is accelerated to its maximum speed.

Boost-Sustain. Propulsion system in which a small thrust is applied to sustain missile speed after acceleration.

Boresight Axis. Central pointing direction of a device such as a target tracker.

C

Chaff. Small radar reflectors released in huge quantities in the atmosphere to form a cloud that resembles a target or that masks a target.

Clutter. Radar signals reflected from scattering points in the background of a scene.

Command and Control. Personnel, materiel, and procedures used to exercise military force.

Command Guidance. Guidance technique in which maneuver commands are transmitted from an external guidance processor (located on the ground) to the missile.

Command-to-Line-of-Sight Guidance. Guidance technique in which maneuver commands are transmitted to the missile to cause it to fly along the line of sight from the launcher to the target.

Commanded Seeker Tracking Rate. The angular rate that the seeker is commanded to achieve to change its pointing direction.

Compressibility Effects. Characteristics of fluid flow caused by fluid compressibility.

Control Channel. Sequence of guidance and control functions that determine the maneuvering of a missile in a given plane, such as the pitch control channel or the yaw control channel.

Coriolis Acceleration. Acceleration of a body relative to a rotating reference frame caused by a combination of the motion of the reference frame and the motion of the body relative to the reference frame.

Countermeasures. Measures taken by a target to decrease the probability of its being damaged by the missile.

Cross Coupling (aerodynamic). Effect of missile motion about one axis on motion about a different axis.

Cruciform Symmetry. Form of symmetry in which a missile is symmetrical about the longitudinal axis in both the pitch and yaw planes and the missile cross sections in the pitch and yaw planes are identical.

Current Time Point. Instantaneous simulated time at which flight parameters are currently being calculated.

D

Damping Ratio. Ratio of the amount of damping actually present in a system to the amount of damping required to prevent oscillatory motion.

Decoy. Device intended to distract attention (or missile seekers) from the true target.

is perpendicular to the plane formed by the velocity vector and the spin axis.

Midcourse Guidance. Guidance from the end of the launch phase to the beginning of the terminal phase.

Miss Distance. The distance between the missile and the target at the time of closest approach.

Missile Dynamics. The subject dealing with the translational and rotational motions of a missile in response to forces and moments applied to it.

Missile Hardware-in-the-Loop. A type of simulation that includes missile hardware in the simulation loop; both the missile seeker in the loop and missile-seeker electronics in the loop are of this type.

Missile-Seeker Electronics in the Loop. A type of simulation that includes missile-seeker electronics (or its equivalent) in the simulation loop.

Missile Seeker in the Loop. A type of simulation that includes a missile seeker in the simulation loop.

Momentum Thrust. The component of thrust due to the rate of change of momentum of the exhaust gases, as opposed to the pressure thrust.

Motion Simulator. See Flight Table.

Multipath. Radar signals that propagate from the target to the radar receiver by a direct path and by reflections.

N

Nap-of-the-Earth Flight Path. Very low-altitude flight at heights that barely avoid vegetation.

Natural Frequency. Undamped frequency of oscillation of a physical system when perturbed from equilibrium.

Neighborhood of Validity. The region of flight conditions within which the simulation is adequate for its intended purpose.

Neutral Point. Point on the missile about which the aerodynamic moment is independent of the angle of attack.

O

Off-Boresight Angle. The angle between the boresight axis of the seeker and the line of sight to a point in the target scene.

Optical. Pertaining to visible or near-visible light; encompassing the ultraviolet, visible, and infrared spectra (0.1 to 30 μm).

Overshoot. Amount by which response of a controlled system exceeds the command.

P

Predictor-Corrector Method. Method of numerical solution of differential equations by which a solution is obtained by an iterative process in which each iteration improves the accuracy of the solution. This process often consists of an initial approximation that uses a predictor equation and an improved result that uses a corrector equation.

Pressure Thrust. The component of thrust due to the imbalance of atmospheric pressure on the nose of the missile relative to that across the exit plane of the nozzle.

Pseudoforce. An equivalent force that would produce acceleration of masses observed in moving reference frames that are actually the result of the reference frame motion.

R

Ramjet Engine. Jet engine that uses dynamic (ram) pressure to compress atmospheric air.

Range Rate. Rate of change of magnitude of range.

Rate Bias. A bias included in the seeker tracking rate command of some infrared seekers to cause the seeker to track ahead of the unbiased tracking point. If the unbiased tracking point is the target exhaust plume, rate bias forces the seeker to point ahead of the plume in order to track the target itself.

Reference Frame. A coordinate system defined by three orthogonal unit vectors.

Response Weighting Function. Function that accounts for all factors affecting the commanded tracking rate of a seeker except the discriminator gain function. The response weighting function accounts for reticle pattern designs for decoy discrimination with infrared seekers and is similar to the difference pattern curve of radio frequency seekers.

Root Matching. Method of numerical solution of differential equations by which the roots of the numerical differential equations are matched to the roots of the differential equation being solved.

Rounding Errors. Error that occurs in digital computation caused by the finite number of significant digits carried by the computer.

S

Stuttering Cross Section. Measure of the power of radiation scattered from a radar target in a given direction, normalized with respect to the power density of the incident radiation, and further normalized so that the decay due to the spherical spreading of the scattered wave is not a factor in computing the scattering cross section.

Seeker. Target-tracking device mounted onboard a missile.

Seeker Gimbal Angle. The instantaneous angle between the boresight axis of the seeker and the centerline axis of the missile.

Self-Screening Jammer. Target that protects itself from radar detection by emitting jamming signals.

Shock Wave. Thin wave or layer of gas generated by the supersonic movement of gas relative to a body. Upon passing through this wave, the gas experiences abrupt changes in pressure, velocity, density, and temperature.

Simulated Scene. Mathematical, physical, or electronic scene, which may contain targets, background, and

countermeasures intended to be viewed by simulated or hardware seekers in flight simulations.

Simulation Loop. A closed loop in a simulation of a dynamic system. For example, in the guidance and control loop (1) the seeker tracks the relative motion of the target, (2) the resulting seeker motion is employed to generate missile guidance commands, (3) the missile flight path is altered in response to guidance commands, (4) the altered missile flight path causes the motion of the target relative to the missile to change, and (5) the seeker tracks the target to complete the loop.

Solid Propellant Rocket. Rocket motor that uses propellant in solid form.

Specific Impulse. Thrust obtained per unit of gas flow rate or impulse of a unit mass of propellant.

Squint Angle. The angle between the axis of the antenna beam and the boresight axis of a radio frequency seeker. Thus, for a conical scan seeker, squint angle is the angle between the instantaneous beam axis and the axis of beam rotation.

Stability Derivative. Slope of a linearized aerodynamic coefficient or parameter.

Stability Errors. Error in numerical integration caused by an instability in the numerical difference equation used.

Stagnation Point. Theoretical point on a body at which the relative fluid velocity is zero.

Stall Point. Angle of attack at which maximum lift occurs.

Standoff Jammer. Vehicle other than the target that protects the target by emitting jamming signals.

Static Stability. Inherent tendency of a missile to return to its trimmed angle of attack if it is displaced from this angle by an outside force.

T

Target Signature. Spectral, spatial, and intensity characteristics of electromagnetic radiation emitted or reflected by the target.

Terrain-Avoidance Flight Path. Low-altitude flight in which hills are avoided by flying around them.

Terrain-Following Flight Path. Low-altitude flight in which hills are avoided by flying over them.

Theil's Inequality Coefficient Method. A mathematical method used to compare two time series.

Tip-Off Effect. Perturbation of missile flight caused by the rotational moment that exists when the missile is only partially supported by the launcher.

Top-Level Flow Diagram. Computer flow diagrams at the most aggregated level.

Track-via-Missile Guidance. Command guidance employing target position data measured by a target tracker onboard the missile.

Truncation Errors. Error in numerical integration caused by the numerical difference equation not being a perfect simulator of the differential equation being integrated; this error is a function of the integration method used.

Turbojet Engine. Jet engine that uses a gas turbine to compress atmospheric air.

V

Validation. The process of determining the extent to which a model or simulation is an accurate representation of the real world from the perspective of the intended use.

Vector. A mathematical representation of magnitude and direction of quantities such as position, velocity, acceleration, force, and moment.

Verification. The process of determining the extent to which a model or simulation accurately represents the developer's conceptual description and specifications.

W

War Game Model. Computer program used to carry out simulated military exercises.

- Degrees of freedom, 1-4,3-7,3-12,3-13
- Differential equations, 10-7-10-14
errors, 10-7, 10-9, 10-13
numerical solutions of, 10-7, 10-8-10-14
- Digital computers, 1-2--1-3, 1-4
- Digital simulation, 10-13
- Digital solution of transfer functions, 10-14-10-19
- Doppler effect, 2-10
- Drag, 4-10-4-12
example simulation, 12-13
- Drag coefficients, 5-5,5-6-5-8,5-16
- Drag polar, 5-7.5-19
- Dynamic pressure parameter, 5-3-5-4
- Dynamic stability derivatives, 5-13,5-14
- E**
- Earth coordinate system, 3-8,7-4,7-7, 7-12, 7-14,7-17, A-2
- Electro-optical scenes, 9-2-9-3, 9-7-9-10
signatures, 9-1, 9-2-9-3, 9-7-9-10
seekers. See Optical seekers.
- Electronic scene simulation, 9-5,9-7
- Environment, missile, 1-1-1-2
- Equations of motion, 4-34-4, 4-6-4-10, 4-11,4-16-4-21
applications of, 4-12,4-21
example simulation, 12-16-12-18
for a rigid body, 4-4,4-7,4-18-4-20
inputs to, 4-3
outputs, 4-3
rotational, 4-3,4-6,4-9,4-10,4-11, 4-18-4-21
translational, 4-3,4-11,4-16-4-18
- Equipment for scene simulation, 9-7-9-12
- Euler angles, rate of change, 4-21,7-10,7.15
- Euler integration method, 10-7, 10-8-10-9
improved, 10-10-1--11, 10-13
modified, 10-11, 10-13
- Eulerian axes, 4-6
- Evasive maneuvers, of target, 9-4
- Example simulation
initialization, 22-7
input data 12-6-12-7
objectives, 12-4-12-5
program structure, 12-5-12-7
results, 12-21-12-26
scenario, 12-4
seeker, 12-7, 12-10
- Exhaust gases, 4-12, 4-13,4-14
- Explicit numerical integration method, 10-8-10-10
- F**
- Fin deflection angle, modulation of, 5-22
- Fire control, 2-2
example simulation, 12-7-1 2-8
- Fire unit, 2-1,2-2
- Five-degree-of-freedom simulation, 3-13,7-4,7-10
- aerodynamics, 5-20
- guidance and control, 8-10,8-13,8-16
- Fixed earth (inertial) reference frame, 4-5,4-6,4-7,4-9,4-11,4-14,4-18,4-19
- Flight, missile. See Missile motion.
- Flight performance, 2-1
- Flight, target. See Target motion.
- Flight testing, 2-19, 3-1-3-2, 3-3, 3-4, 3-6,5-7,5-14,5-16, 5-17
- Flow regimes, 5-2,5-15
- Force
aerodynamic, 5-2-5-6, 5-9-5-10, 5-12,5-165-18, 5-22,7-4,7-5-7-6,7-10-7-13
gravitational. See Gravitational force.
normal (pressure), 5-2,5-5,5-10,5-21
propulsive, 7-4, 7-6-7-7, 7-9,7-13
tangential (shearing), 5-2,5-4
- Force coefficient, aerodynamic, 5-4,5-5
- Forces and moments, 4-3-4-4,4-10-4-16,4-17, 4-18, 4-20-4-21
aerodynamic, 4-3,4-10-4-13,4-16,4-18, 4-21, 5-2-5-3, 5-5-5-6, 5-16,5-17, 5-18-5-19
components, 5-5-5-6
drag, 4-10-4-12
equations, 5-18-5-19
example simulation, 12-13-12-15
nomenclature, 4-4-45
propulsion, 6-1,6-2-6-5
- Fragment warheads, 2-18
- Friction forces, 5-2
- Fuze, 1-4,2-2,2-15,2-18,2-19
- Fuzing logic, 2-8
- G**
- Gimbal angle, 1-2
limits, 2-3
- Grain temperature, 6-2--6-3
- Gravitational attraction, 4-14
- Gravitational force, 3-5-3-6,4-4,4-10,4-14-4-16, 4-17, 4-21,7-7, 7-13-7-14
- Gravity, example simulation, 12-15-12-16
- Gravity in a rotating earth frame, 4-14-4-16
- Ground-based guidance modeling, 8-13-8-17
- Guidance, 1-1, 1-4, 2-1-2-3, 2-11,2-12,2-24-2-31
active, 2-27
beam-rider, 2-28
command, 2-25
command-to-line-of-sight, 2-25
ground, 2-25-2-27
horning, 2-27
implementation, 2-1, 2-25-2-27
intercept point prediction, 2-28
laws, 2-2, 2-27-2-3 1
modeling, 8-3-8-17
on-board, 2-1,2-27

INDEX

A

- Acceleration, 4-3,4-6,4-7,4-9-4-10, 4-15-4-18, 4-20,4-21
 centrifugal, 4-10, 4-14-4-16
 due to gravity, 4-3, 4-9-4-10, 4-11, 4-14-4-16
 in a rotating frame, 4-9-4-10
 rotational, 4-18-4-20
 Acceleration limit, 8-13
 Accreditation, 11-5
 Achieved tracking rate, 8-8
 Active seeker, 2-8-2-9
 Actuators, 2-15
 Adams numerical integration methods, 10-12
 Aerodynamic Analysis of Flight-Test Data 5-17
 Aerodynamic cross coupling, 1-4
 Aerodynamics, example simulation, 12-6-12-7, 12-13-12-15
 Air-augmented motors, 3-6,62
 Airframe, 1-1, 1-4,2-2, 2-23-2-24
 Altitude, 5-18
 Analog computers, 1-2, 1-3, 1-4
 Analog-to-digital converters, 1-3
 Anechoic chamber, 9-7
 Angle of attack, 5-7,5-9,5-11,5-12,5-13, 5-14,5-18,5-20
 limit, 8-13
 Angular tracking, 2-6,2-10
 Antenna, 2-3,2-8,2-9,2-10
 Atmosphere, 5-17-5-18
 effects on signals, 9-5
 example simulation, 12-8-12-9
 Atmospheric data B-1
 Atmospheric properties, B-1
 Atmospheric transmission windows, 2-3
 Autopilot, 2-1,2-2,2-12,2-13,2-15,2-24,5-11,5-14,8-2,
 8-5,8-8,8-11-8-13,8-14,8-23
 example simulation, 12-7, 12-10-12-11, 12-12
 hardware, 8-23
 Axial force coefficients, 5-5,5-6-5-8,5-16
- B
- Background, scene, 9-4
 Bayesian updating, 11-4
 Beam rider, 2-28
 Beam-rider guidance, 8-14-8-16
 Body coordinate system, 3-8,4-4,4-16,4-21,74, 7-5,7-6,
 7-7,7-10, A-2-A-3
 Body reference frame, 4-4,4-8,4-11,4-16,4-17, 4-19,4-20,
 4-21
 Body-to-earth system transformation, A-4
 Boost glide, 2-21
 Boost sustain, 2-21,2-23
 Boost-glide motor, 6-3
 Boost-sustain motor, 6-3
 Boresight axis, 2-3
 Boresight tracking error, 8-7
- C
- Canard control, 2-14-2-15
 Cartesian coordinates, 4-5
 Clutter, 2-10
 Coefficients, aerodynamic, 5-3-5-12, 5-14-5-17, 5-21
 application of, 5-3-5-6
 averaging, 5-21-5-22
 determination of, 5-14-5-17
 linearity assumption, 5-3,5-6
 moment, 5-4, 5-9-5-12, 5-13, 5-14,5-16,5-1 8-5-22
 prediction, 5-3, 5-15-5- 16
 Command guidance, 2-25,8-14
 Command-to-line-of-sight guidance, 2-25,8-14-8-16
 Commanded tracking rate (seeker), 8-7-8-8
 Compressibility of air, 5-4
 Computer language, 10-6-10-7
 Computer, selection, 10-2-10-6
 Computers, 1-2-1-4
 conical-scan radar, 9-4
 Conical-scan reticle, 2-7
 Conical scanning, 2-10,2-12
 Continuous rod warheads, 2-18
 Continuous wave, 2-10
 Continuous wave radar, 2-10
 Control hardware, 8-23
 Control system, 2-12-2-15
 example simulation, 12-1 1-12-12
 modeling, 8-17-8-18
 Coordinate systems, 4-4, 4-10-4-11, 4-16, 4-21, 7-4, A-1-A-4
 conventions, A-1-A-2
 definitions, A-2-A-3
 role of, 3-8
 transformations, A-3-A-5
 types, 3-8-3-9
 Coriolis acceleration, 4-10,4-15
 Countermeasures, 1-1,2-2,2-19,94-9-5
 Cruciform symmetry, 5-11,5-20,5-21
- D
- Damping derivatives, 5-17
 Datcom, 5-15
 Decoys, 2-8,9-4-9-5
 Degree of fidelity, 8-3, 8-6-8-8

- Degrees of freedom, 1-4,3-7,3-12,3-13
- Differential equations, 10-7-10-14
- errors, 10-7, 10-9, 10-13
 - numerical solutions of, 10-7, 10-8-10-14
- Digital computers, 1-2-1-3, 1-4
- Digital simulation, 10-13
- Digital solution of transfer functions, 10-14-10-19
- Doppler effect, 2-10
- Drag, 4-10-4-12
- example simulation, 12-13
- Drag coefficients, 5-5, 5-6-5-8, 5-16
- Drag polar, 5-7,5-19
- Dynamic pressure parameter, 5-3-5-4
- Dynamic stability derivatives, 5-13,5-14
- E**
- Earth coordinate system, 3-8,7-4,7-7,7-12,7-14, 7-17, A-2
- Electro-optical scenes, 9-2-9-3, 9-7-9-10
- signatures, 9-1, 9-2-9-3, 9-7-9-10
 - seekers. See Optical seekers.
- Electronic scene simulation, 9-5,9-7
- Environment missile, 1-1-1-2
- Equations of motion, 4-34-4,4-6-4-10,4-11, 4-16-4-21
- applications of, 4-12,4-21
 - example simulation, 12-16-12-18
 - for a rigid body, 4-4,4-7, 4-1-4-20
 - inputs to, 4-3
 - outputs, 4-3
 - rotational, 4-3,4-6,4-9,4-10,4-11,4-18-4-21
 - translational, 4-3,4-11, 4-16-4-18
- Equipment for scene simulation, 9-7-9-12
- Euler angles, rate of change, 4-21,7-10,7-15
- Euler integration method, 10-7, 10-8-10-9
- improved, 10-10-10-11, 10-13
 - modified, 10-11, 10-13
- Eulerian axes, 4-6
- Evasive maneuvers, of target, 9-4
- Example simulation
- initialization, 12-7
 - input data, 12-6-12-7
 - objectives, 12-4-12-5
 - program structure, 12-5-12-7
 - results, 12-21-12-26
 - scenario, 12-4
 - seeker, 12-7, 12-10
- Exhaust gases, 4-12,4-13,4-14
- Explicit numerical integration method, 10-8-10-10
- F**
- Fin deflection angle, modulation of, 5-22
- Fire control, 2-2
- example simulation, 12-7-12-8
- Fire unit, 2-1,2-2
- Five-degree-of-freedom simulation, 3-13,7-4,7-10
- aerodynamics, 5-20
 - guidance and control, 8-10,8-13,8-16
- Fixed earth (inertial) reference frame, 4-5,4-6,4-7,4-9,4-11,4-14,4-18,4-19
- Flight, missile. See Missile motion.
- Flight performance, 2-1
- Flight, target. See Target motion.
- Flight testing, 2-19, 3-1-3-2, 3-3,3-4,3-6,5-7,5-14, 5-16, 5-17
- Flow regimes, 5-2,5-15
- Force
- aerodynamic, 5-2-5-6, 5-9-5-10, 5-12,5-16-5-18,5-22,7-4,7-5-7-6,7-10-7-13
 - gravitational. See Gravitational force.
 - normal (pressure), 5-2,5-5,5-10, 5-21
 - propulsive, 7-4,7-6-7-7,7-9,7-13
 - tangential (shearing), 5-2,5-4
- Force coefficient, aerodynamic, 5-4,5-5
- Forces and moments, 4-3-4-4,4-10-4-16,4-17, 4-18, 4-20-4-21
- aerodynamic, 4-3,4-10-4-13,4-16,4-18, 4-21, 5-2-5-3, 5-5-5-6, 5-16,5-17, 5-18-5-19
 - components, 5-5-5-6
 - drag, 4-10-4-12
 - equations, 5-18-5-19
 - example simulation, 12-13-12-15
 - nomenclature, 4-4-4-5
 - propulsion, 6-1,6-2-6-5
- Fragment warheads, 2-18
- Friction forces, 5-2
- Fuze, 1-4,2-2,2-15,2-18,2-19
- Fuzing logic, 2-8
- G**
- Gimbal angle, 1-2
- limits, 2-3
- Grain temperature, 6-243
- Gravitational attraction, 4-14
- Gravitational force, 3-5-3-6,4-4,4-10,4-14-4-16, 4-17, 4-21,7-7,7-13-7-14
- Gravity, example simulation, 12-15-12-16
- Gravity in a rotating earth frame, 4-14-4-16
- Ground-based guidance modeling, 8-13--8-17
- Guidance, 1-1,1-4, 2-1-2-3, 2-11,2-12,2-24-2-31
- active, 2-27
 - beam-rider, 2-28
 - command, 2-25
 - command-to-line-of-sight, 2-25
 - ground, 2-25-2-27
 - homing, 2-27
 - implementation, 2-1, 2-25-2-27
 - intercept point prediction, 2-28
 - laws, 2-2, 2-27-2-31
 - modeling, 8-3-8-17
 - on-board, 2-1,2-27

INDEX

A

Acceleration, 4-3,4-6,4-7,4-9-4-10, 4-15-4-18, 4-20,4-21
 centrifugal, 4-10,4-14-4-16
 due to gravity, 4-3,4-9-4-10,4-11,4-14-4-16
 in a rotating frame, 4-9-4-10
 rotational, 4-18-4-20
 Acceleration limit, 8-13
 Accreditation, 11-5
 Achieved tracking rate, 8-8
 Active seeker, 2-8-2-9
 Actuators, 2-15
 Adams numerical integration methods, 10-12
 Aerodynamic Analysis of Flight-Test Data, 5-17
 Aerodynamic cross coupling, 1-4
 Aerodynamics, example simulation, 12-6-12-7, 12-13-12-15
 Air-augmented motors, 3-6,6-2
 Airframe, 1-1, 1-4,2-2, 2-23-2-24
 Altitude, 5-18
 Analog computers, 1-2, 1-3, 1-4
 Analog-to-digital converters, 1-3
 Anechoic chamber, 9-7
 Angle of attack, 5-7,5-9,5-11,5-12,5-13, 5-14,5-18,5-20
 limit, 8-13
 Angular tracking, 2-6,2-10
 Antenna, 2-3,2-8,2-9,2-10
 Atmosphere, 5-17-5-18
 effects on signals, 9-5
 example simulation, 12-8-12-9
 Atmospheric data, B-1
 Atmospheric properties, B-1
 Atmospheric transmission windows, 2-3
 Autopilot, 2-1,2-2,2-12,2-13,2-15, 2-24,5-11,5-14,8-2,
 8-5,8-8, 8-11-8-13, 8-14,8-23
 example simulation, 12-7, 12-10-12-11, 12-12
 hardware, 8-23
 Axial force coefficients, 5-5,5-6-5-8,5-16

B

Background, scene, 9-4
 Bayesian updating, 11-4
 Beam rider, 2-28
 Beam-rider guidance, 8-14-8-16
 Body coordinate system, 3-8,4-4,4-16,4-21,7-4, 7-5,7-6,
 7-7,7-10, A-2-A-3
 Body reference frame, 4-4,4-8,4-11,4-16,4-17, 4-19,4-20,
 4-21
 Body-to-earth system transformation, A-4
 Boost glide, 2-21

Boost sustain, 2-21,2-23
 Boost-glide motor, 6-3
 Boost-sustain motor, 6-3
 Boresight axis, 2-3
 Boresight tracking error, 8-7

C

Canard control, 2-14-2-15
 Cartesian coordinates, 4-5
 Clutter, 2-10
 Coefficients, aerodynamic, 5-3-5-12, 5-14-5-17,5-21
 application of, 5-3-5-6
 averaging, 5-21-5-22
 determination of, 5-14-5-17
 linearity assumption, 5-3,5-6
 moment, 5-4, 5-9-5-12, 5-13, 5-14,5-16,5-1 8-5-22
 prediction, 5-3,5- 15-5- 16
 Command guidance, 2-25,8-14
 Command-to-line-of-sight guidance, 2-25,8-14-8-16
 Commanded tracking rate (seeker), 8-7-8-8
 Compressibility of air, 5-4
 Computer language, 10-6-10-7
 Computer, selection, 10-2-10-6
 Computers, 1-2-1-14
 conical-scan radar, 9-4
 Conical-scan reticle, 2-7
 Conical scanning, 2-10,2-12
 Continuous rod warheads, 2-18
 Continuous wave, 2-10
 Continuous wave radar, 2-10
 Control hardware, 8-23
 Control system, 2-12-2-15
 example simulation, 12-11-12- 12
 modeling, 8-17-8-18
 Coordinate systems, 4-4, 4-10-4-11, 4-16, 4-21, 7-4, A-1-A-4
 conventions, A-1-A-2
 definitions, A-2-A-3
 role of, 3-8
 transformations, A-3-A-5
 types, 3-8-3-9
 Coriolis acceleration, 4-10,4-15
 Countermeasures, 1-1,2-2,2- 19,94-9-5
 Cruciform symmetry, 5-11,5-20,5-21

D

Damping derivatives, 5-17
 Datcom, 5-15
 Decoys, 2-8,9-4-9-5
 Degree of fidelity, 8-3,8-6-8-8

optimal, 2-30-2-31
 passive, 2-27
 proportional navigation, 2-28-2-30
 pursuit ("hound and hare"), 2-28
 selection of, 2-24-2-25
 semiactive, 2-27
 Guidance and control, example simulation, 12-10-12-13
 Guidance coordinate system, 3-8, A-3
 Guidance processor, 8-2,8-5, 8-8-8-1 1
 Guidance-to-earth system transformation, A-4
 Guidance with IR seeker, 8-3,8-4--8-5,8-7-8-8, 8-10-
 8-11,8-19-8-20
 Guidance with RF seeker, 8-3,8-7-8-8,8-9-8-10, 8-19
 Gyroscopic couples, 4-20
 Gyroscopic moments, 4-204-21

H

Hardware-in-the-loop, 1-4,8-3,8-18-8-23,10-19
 Hardware substitution, 8-18-8-23
 Homing guidance, 2-27
 Homing, semiactive, 8-14

I

Imaging, 2-8
 Implicit (multistep) integration method, 10-7, 10-11-10-12
 Implicit (one-step) integration method, 10-7,10-10-10-11
 Inertial rotor, 4-4,4-21
 Infrared, 2-3
 Infrared seeker. See Seeker, infrared
 Intercept point prediction, 2-28
 Iterative modeling, 9-9-9-10

J

Jamming, 9-4
 Jinking, 7-14-7-17

K

Kill probability. See Lethality.

L

Laser, 2-3
 Lateral acceleration, 2-13-2-14,2-15
 Launch boundary, 2-1-2-2
 Launcher, 2-31
 Lethality, 1-1,2-19-2-20
 Levels of fidelity, 11-1
 simulation, 9-11-9-12
 Lift, 4-10,4-11
 aerodynamic, 2-1, 2-13-2-15
 example simulation, 12-13
 Lift coefficients, 5-5,5-6,5-9,5-16,5-21
 Lift curve slope, 5-12
 Lift versus drag, 5-9,5-18
 Liquid propellant, 2-20,6-2
 Liquid propellant motor, 6-2

M

Mach number, 3-6, 3-7, 3-8,5-2, 5-4, 5-9-5-12, 5-16, 5-
 17,8-10,8-13
 Magnus effect, 5-22
 Man-portable missile systems, 2-1
 Maneuver commands, 2-1
 Maneuvering flight, target, 7-14-7- 17,9-4
 horizontal turns, 7-16
 load factor, 7-15,7-16
 roll attitude, 7-17
 weaves, 7-16-7-17
 Mass change, 6-3
 Mass, missile, 7-7
 Mathematical conventions, missile dynamics, 4-4-4-5
 Mathematical scene simulation, 9-5-9-6
 Milne numerical integration method 10-7, 10-1 1-10-12
 Miss distance, 2-1,2-2,2-27,5-12,5-14, 7-18-7-21
 Missile
 accuracy, 1-1
 aerodynamic cross coupling, 1-4
 control, 1-1, 1-2
 counter-countermeasures, 1-1
 design of, 2-1
 flight, 1-1, 1-2, 1-4
 analysis of, 1-1
 testing, 1-2
 fuzing, 1-1
 gimbal angle, 1-2
 guidance, 1-1, 1-4
 guided, 1-1, 1-4
 laboratory test, 1-2
 lethality, 1-1
 life-cycle, 1-1
 maneuver, 1-1, 1-2
 mathematical model, 1-1, 1-2, 1-4
 model, 1-1
 performance, 1-1, 1-2,1-3
 estimates, 1-2
 measures, 1-1
 position, example simulation, 12-17-12-18
 subsystems, 1-1,1-2, 1-4
 surface-to-air, 1-1, 1-2, 1-3, 1-4,4-16,5-7,5-21
 tracking rate, 1-2
 Missile electronics in the loop, 8-19-8-20
 Missile flight vehicle, 2-1
 Missile motion, 7-4-7-14
 translational and angular rates, 7-7
 Missile seeker in the loop, 8-19
 Missile systems, 2-1-2-3
 aerodynamic forces, 3-4
 description, 2-1-2-2
 equipment, 2-1-2-2
 fin deflections, 3-5,3-7,3-13
 functions, 2-1-2-2
 guidance and control. See Guidance.

life cycle, 3-2
 maneuver command. See Guidance.
 motors, 3-6
 propulsion, 3-6,3-13
 purpose of, 2-1
 thrust. See Propulsion.
 Missile-target geometry, 7-17-7-21
 relative attitude, 7-17-7-18
 relative position, 7-17
 Model
 atmospheric characteristics, 1-1, 1-2
 equations, 1-1, 1-2, 1-4
 mass, 1-1
 mathematical, 1-1, 1-2, 1-4
 seeker, 1-4
 simulation. See Simulation.
 Moment coefficients, 5-4, 5-9-5-12, 5-13, 5-14, 5-16, 5-18-5-22
 Moments of inertia, 4-6,4-7,4-10,4-18,4-19,4-20,4-18, 4-20,7-10
 Moments, See also Forces and moments.
 aerodynamic, 7-8-7-9
 propulsive, 7-9
 Monopulse radar, 9-4
 Monopulse tracking, 2-10,2-12
 Motion, missile. See Missile motion.
 Motion, target. See Target motion.
 Motors, 2-2,2-20-2-23,3-6,5-6, 5-10,6-1-6-2,6-3. See also Propulsion.
 Moving target indicator, 2-10

N

Navier-Stokes equations, 5-15-5-16
 Navigation, proportional, 2-28-2-30,8-2-8-3,8-8, 8-9-8-11,8-14,8-17,12-15
 Navigation ratio (proportionality factor), 2-28,2-30
 Neighborhood of validity, 11-4
 New boresight axis vector, 8-8
 Newton's equations, 5-15
 Newton's laws, 4-4,4-6-49,4-10,4-12,
 Newton's second law, 3-5-3-6,4-6-47
 Nike Ajax, 2-25
 Nike Hercules, 2-25
 Nomenclature, missile dynamics, 4-4-4-5
 Normal force coefficients, 5-5,5-6,5-9,5-16,5-21
 Numerical solution of differential equations, 10-7, 10-8-10-14

O

Off-boresight angle, 8-7
 On-board guidance, 2-1,2-27
 Optical seekers, 2-3-2-8, 8-3, 8-7-8-8, 9-2. See also Seeker, infrared and Radio frequency seekers.
 defined, 2-3
 imaging, 2-8

pseudoimaging, 2-8
 Optimal guidance, 2-30-2-31

P

Passive seeker, 2-8
 Patchboard, 1-2, 1-3
 Payload, 2-1
 Perfect guidance, 8-8-8-9
 Perfect seeker, 8-3-8-5
 Physical laws, 1-1
 Physical scene simulation, 9-5,9-6-9-7
 Positions, relative, example simulation, 12-9
 Predictions, aerodynamic, 5-3, 5-15-5-16
 Products of inertia, 4-18,4-19,4-20,4-21
 propellants, 1-4,4-7-4-12,6-1-6-3
 and missile momentum, 4-12
 grain temperature, 2-22
 Proportional navigation, 2-28-2-30, 8-2-8-3, 8-8, 8-9-8-11,8-14,8-17
 Propulsion. See also Motor.
 example simulation, 12-15
 force and moment vectors, 6-3-6-5
 selection of, 2-22-2-23
 system, 2-20-2-23
 selection of, 2-22
 thrust and mass parameters, 6-1,62-6-3
 Repulsive force, 3-6,4-21
 Propulsive thrust, 4-10,4-124-14
 Pseudo-forces, 4-10
 Pseudoimaging, 2-8
 Pulse Doppler radar, 2-10
 Pulse radars, 2-10

Q

Quaternions, A-5

R

Radars, 2-1, 2-8-2-12, 9-4. See also Radio frequency seekers.
 types, 2-10
 Radiation, optical, 2--3-2-5
 Radio frequency radiation, 2-8-2-12
 attenuation, 2-9
 Radio frequency scenes, 9-10-9-12
 Radio frequency seekers, 2-8-2-10, 8-3, 8-7-8-8. 8-9-8-10,8-19
 defined, 2-8
 error detection, 2-10
 Radio frequency signatures, 9-1,9-3-9-4,9-10-9-12
 Radio Frequency Simulation System, 9-10-9-12
 Radome, 2-11,2-23
 Ram-jet motors, 3-6
 Ramjet engine, 6-2
 Range effects on signals, 9-5
 Rate bias, 8-8

Real-time computation, 1-4
 Reference area, 5-4--5-5,5-14
 Reference conditions, 6-3
 Reference frame, 4-5,4-5,4-6,4-7,4-17, 4-19
 nonaccelerating, 4-4
 relationship between a vector and, 4-4-45, 4-7
 rolling, 5-21
 Reticle, 2-5-2-7
 Reynolds number, 3-7,3-13,5-4,5-14,5-16, 5-17, 5-18
 Rocket motors. See Motors.
 Roland, 2-28
 Roll moment, aerodynamic, 5-5-5-6,5-11,5-20,5-21
 Roll rate, 5-11-5-12, 5-21
 Roll stability derivatives, 5-14
 Rollerons (control tabs), 5-11
 Rolling airframe considerations, 5-20-5-22
 Rolling reference frames, 5-21
 Root-matching method, 10-16-10-19
 Rotating reference frame, 4-7-4-10,4-14-4-16,4-17-4-18
 Rotational equations, 4-3, 4-4, 4-6, 4-9,4-11,4-18-4-21, 7-7-7-10
 Runge-Kutta integration method, 10-7, 10-9-10-10, 10-14
 example simulation, 12-1-7-12-20

S

Scene elements, 9-1-9-5
 Scene generator, 1-3
 Scene simulation, 9-1-9-12
 equipment, 9-7-9-12
 methods, 9-5-9-7
 Seeker, 1-2, 1-3, 1-4, 2-3-2-12, 8-3-8-8, 8-9-8-11, 8-14,8-18-8-20
 example simulation, 12-7, 12-10
 hardware, 8-18,8-23
 infrared, 8-3, 8-4-8-5, 8-7-8-8, 8-10-8-11, 8-19-8-20
 intermediate fidelity, 8-6-8-8
 range, 1-2
 tracking time lag, 8-5-8-6
 types, 2-3-2-10
 Seekers, 2-3-2-12
 Seekers, optical. See Optical seekers.
 Seekers, radio frequency. See Radio frequency seekers.
 Semiactive homing, 8-14
 Semiactive seeker, 2-8
 Sequential lobing, 2-10,2-12
 Sequential lobing radar, 9-4
 Servomotor, 2-15
 Shaped-charge warheads, 2-18
 Shoulder-fired missile, 6-3
 Signal intensity, 8-7-8-8
 Signal processing, 1-4
 Signature suppression, 9-4
 Signatures, 9-2-9-4

Simulation, 4-3-4-4,4-7,4-16,4-19, 6-2-6-5
 action of gravity, 4-16
 aerodynamic force and moment, 3-6-3-7
 aerodynamics, 1-1
 airframe response, 3-5,3-7
 assessing missile performance, 3-3-3-4
 autopilot, 3-5
 autopilot and control, 3-4-3-5
 breadboard, 1-1, 1-4
 complexity, 1-4
 computation, 1-3, 1-4
 computational cycle, 3-10-3-12
 acceleration, 3-12
 atmospheric data, 3-10
 forces, 3-11-3-12
 guidance, 3-11
 moments, 3-11-3-12
 processing, 3-10-3-11
 table lookup, 3-10
 velocity vectors, 3-10-3-11
 coordinate systems, 3-8-3-9
 decoy deployment, 1-1
 decoys, 9-5
 designing and optimizing missiles, 3-3
 desired output, 4-16
 effects of structural deflection, 4-4
 environment, 1-1, 1-2
 equations, 1-1, 1-2, 1-4
 simplifying, 1-4
 equations of motion, 1-1. See also Equations of motion.
 establishing requirements, 3-2-3-4
 example. See Example simulation.
 execution, 3-12-3-13
 near-real time, 3-4
 real time, 3-4,3-12
 fidelity, 3-12-3-13
 fin deflection, 3-7,3-13
 flow diagram, 3-10-3-13
 gimbal angle, 1-2
 guidance, 1-1, 3-4-3-5
 hardware-in-the-loop, 1-4
 hierarchy, 3-3
 hybrid, 1-3
 inputs, 1-2, 1-3,3-1,3-10
 jamming, 9-4
 level of detail, 3-12-3-13. See also Degrees of freedom.
 logic, 1-1
 mathematical, 1-1, 1-2, 1-4
 missile and target motion, 3-5-3-7
 missile flight, 1-1-1-3
 objectives, 1-1, 3-2-3-4, 3-12-3-13
 output, 1-2
 physical, 1-1,1-2, 1-3
 preflight, 3-3
 purpose, 1-1, 9-2, 1-4, 3-2-3-4

- rotation, 3-7, 3-13
 - seeker, 1-2, 1-4,3-13
 - limits, 1-2
 - scene generation, 1-3
 - signature suppression, 9-4
 - sophistication of, 1-2, 1-4
 - subsystems, 1-1
 - target, 9-1-9-4
 - thrust, 1-1
 - tracking rate, 1-2
 - training, 3-4
 - Six-degree-of-freedom simulation, 1-4,3-3,3-7,3-12,3-13, 4-3,4-11,7-4,7-5-7-10
 - aerodynamics, 5-17,5-20
 - guidance and control, 8-10,8-1 1-8-13, 8-16
 - Six degrees of freedom, 4-4,10-13
 - Solid propellant, 2-20,6-1-6-2
 - motors, 2-20-2-22,3-6, 6-1-6-2
 - spartan, 2-25
 - Specific impulse, 2-21
 - Spin-scan reticle, 2-6-2-7
 - Sprint, 2-25
 - Stability derivatives, 5-12-5-1 4
 - Stabilization, 2-3
 - Static pitch stability derivative, 5-13
 - Static stability, 2-23--2-24
 - Static tests, 2-19
 - Surface-to-air missile, 6-1
- T
- Tail control, 2-15
 - Target, 1-1,1-4, 9-1-9-4
 - coordinate system, 3-9, A-3
 - countermeasures, 1-1
 - flight path, 1-1
 - illuminators, 2-27
 - image, 2-3-2-8
 - maneuverability, 1-1
 - models, 1-1, 1-2,9-1 1-9-12
 - motion, 7-4, 7-14-7-17
 - position, example simulation, 12-18
 - reflection of radio frequency radiation from, 2-10-2-11
 - scene generation, 1-3
 - signature, 1-1, 1-2,2-2, 9-2-9-4
 - simulation, 9- 1-9-4
 - speed, 1-1
 - Target Image Simulator, 9-9-9-10
 - Target-to-earth system transformation, A-S
 - Target tracker, model, 3-5. See also Seeker.
 - Target, tracking, 1-1, 1-2
 - Target-missile geometry. See Missile-target geometry.
 - Telescope, 2-5
 - Terminal engagement simulations, 2-19-2-20
 - Tests, 2-19
 - closing speed, example simulation, 12-9
 - maximum time/crash, example simulation, 12-19-12-20
 - Testing. See Wind tunnel testing and Flight testing.
 - Theil's inequality coefficient, 11-4
 - Three-degree-of-freedom simulation, 1-4, 3-7, 3-12, 3-13, 4-3,4-11,6-2,7-4,7-10-7-14
 - aerodynamics, 5-20
 - guidance and control, 8-10,8-13
 - Thrust, 2-20-2-21,4-3,4- 10,4-12-4-14
 - Thrust force, 6-2,6-3
 - Track via missile, 2-25-2-26
 - guidance, 8-16-8-17
 - Tracker (seeker)-to-body system transformation, A-4-A-5
 - Tracker coordinate system, 3-8, A-3
 - Tracking
 - channels, 2-10
 - error, 2-3-2-4, 2-6,2-10-2-12
 - radar, 9-3-9-4
 - rate, 1-2, 8-7-8-8
 - time lag, 8-5-8-6
 - Tracking in angle, 2-10-2-12
 - Tracking in frequency (velocity gating), 2-10
 - Tracking in range (range gating), 2-10
 - Transfer functions, 10-14-10-19
 - Translational equations, 4-3,4- 11,4-16,4-18,7-5-7-7
 - Tube launch, 2-22
 - Tube-launched missile, 6-3
 - Turbojet engine, 6-2
 - Tustin method, 10-14-10-16
 - Two-degree-of-freedom simulation, 3-12
- U
- Ultraviolet, 2-3
 - Ultraviolet-hfrared Scene Generator, 9-7-9-9
 - Unique Decoy Generator, 9-10
 - Updating on the fly, 9-10
- V
- Validation, 11-2-11-5
 - Bayesian updating, 11-4
 - comparison with test results, 11-3
 - levels of confidence, 11-2
 - model calibration, 11-4
 - neighborhood of validity, 11-4
 - nonstatistical methods, 11-4
 - scene, 114
 - statistical methods, 11-3-11-4
 - Theil's inequality coefficient, 11-4
 - Variable mass, 4-12-4-14
 - Velocities, relative, example simulation, 12-9
 - Verification, 11-1
 - Verification and validation
 - accreditation, 11-4
 - selection of methods, 11-5
 - Visible spectrum, 2-3

MIL-HDBK-1211(MI)

W

Wargames, models of, 3-2-3-2
Warhead, 1-1, 1-4,2-2, 2-15-2-19
types, 2-18
Weapons, acquisition of, 3-2
Weaves, 7-16-7-17

Wind coordinate system, 3-8,4-4, 4-10-4-11, 7-4, A-3
Wind reference frame, 4-4, 4-10,4-11
Wind-to-body system transformation, A-4
Wind tunnel testing, 5-3,5-10,5-11,5-12,5-14-5-17,5-22
Wing control, 2-15

SUBJECT TERM (KEY WORD) LISTING

Aerodynamic forces	Missile-target geometry
Boresight axis	Moments of inertia
Coordinate systems	Newton's laws of motion
Coordinate system transformation	Propulsion
Coriolis acceleration	Reynold's number
Degrees of freedom	Rocket motor
Equations of motion	Rotational equations
Euler angles	Scene generation
Forces and moments	Target flight path
Guidance and control	Target model
Mach number	Translational equations
Miss distance	Validation
Missile flight path	

Custodian:
Army-MI

Review activity:
Army-HD

Preparing activity:
Army-MI

(Project 14GPA133)

STANDARDIZATION DOCUMENT IMPROVEMENT PROPOSAL

INSTRUCTIONS

1. The preparing activity must complete blocks 1, 2, 3, and 8. In block 1, both the document number and revision letter should be given.
2. The submitter of this form must complete blocks 4, 5, 6, and 7.
3. The preparing activity must provide a reply within 30 days from receipt of the form.

NOTE: This form may not be used to request copies of documents, nor request waivers, or clarification of requirements on current contracts. Comments submitted on this form do not constitute or imply authorization to waive any portion of the referenced document(s) or to amend contractual requirements.

1. DOCUMENT NUMBER
MIL-HDBK-1211(MI)

2. DOCUMENT DATE (YYMMDD)
950717

3. DOCUMENT TITLE

Missile Flight Simulation, Part One, Surface-to-Air Missiles

4. NATURE OF CHANGE (Identify paragraph number and include proposed rewrite, if possible. Attach extra sheets as needed.)

5. REASON FOR RECOMMENDATION

6. PREPARING ACTIVITY

a. NAME

US Army Missile Command

b. TELEPHONE (Include Area Code)

(1) Commercial

205-995-6125

(2) DSN

645-6125

c. ADDRESS (Include Zip Code)

ATTN: AMSMI-RD-SE-TD-ST
Redstone Arsenal, AL 35898-5270

IF YOU DO NOT RECEIVE A REPLY WITHIN 45 DAYS, CONTACT:

Defense Quality and Standardization Office
5203 Leesburg Pike, Suite 1403, Falls Church, VA 22041-3466
Telephone (703) 756-2340 AUTOVON 289-2340

